



**This electronic thesis or dissertation has been
downloaded from Explore Bristol Research,
<http://research-information.bristol.ac.uk>**

Author:

Mykura, Rory C

Title:

The lithiation–borylation reaction

in situ IR spectroscopy studies & automation on a batch platform

General rights

Access to the thesis is subject to the Creative Commons Attribution - NonCommercial-No Derivatives 4.0 International Public License. A copy of this may be found at <https://creativecommons.org/licenses/by-nc-nd/4.0/legalcode>. This license sets out your rights and the restrictions that apply to your access to the thesis so it is important you read this before proceeding.

Take down policy

Some pages of this thesis may have been removed for copyright restrictions prior to having it been deposited in Explore Bristol Research. However, if you have discovered material within the thesis that you consider to be unlawful e.g. breaches of copyright (either yours or that of a third party) or any other law, including but not limited to those relating to patent, trademark, confidentiality, data protection, obscenity, defamation, libel, then please contact collections-metadata@bristol.ac.uk and include the following information in your message:

- Your contact details
- Bibliographic details for the item, including a URL
- An outline nature of the complaint

Your claim will be investigated and, where appropriate, the item in question will be removed from public view as soon as possible.

**The Lithiation–Borylation Reaction:
In Situ IR Spectroscopy Studies
&
Automation on a Batch Platform**



University of
BRISTOL

Rory Cameron Mykura

University of Bristol

Supervisor: Professor Varinder K. Aggarwal

A dissertation submitted to the University of Bristol in accordance with the requirements for
award of the degree of Doctor of Philosophy in the Faculty of Science

Word Count: 54,763

Abstract

The homologation of boronic esters using lithiated Hoppe-type diisopropylcarbamates and Beak-type 2,4,6-triisopropylbenzoate (TIB) esters represents an efficient process for the formation of carbon–carbon bonds in a highly stereoselective manner. This process is referred to as lithiation–borylation.

Studying this reaction using in situ IR spectroscopy has revealed reaction times for a series of alkyl carbamates and TIB esters. Alkyl TIB esters undergo lithiation faster than their corresponding carbamates, and the lithiated alkyl carbamates undergo faster borylations than the lithiated TIB esters. It is discussed how the size and coordinating ability of each directing group could lead to these differences. Varying solvent has also provided evidence on the factors that affect lithiation and borylation. Using in situ IR spectroscopy, the lithiation–borylation of alkyl TIB esters has been further optimised, where lithiations are now performed in toluene and borylations with the addition of THF.

Boranes, boronic esters and borate esters all react with lithiated TIB esters at a similar rate providing further evidence for a pre-complexation event between the lithium carbenoid and the Lewis basic oxygen atoms. The use of a proximal aromatic group leads to rapid borylations of diamine-ligated lithiated carbenoids, providing further evidence for a cation– π interaction between the aromatic group and lithium atom of the carbenoid. By generating the lithiated species under diamine-free conditions, the effects of various additives have been explored.

In situ IR spectroscopy was then employed to study the lithiation–borylation of a set of *O*-cycloalkyl TIB esters (cyclopropyl through to cyclohexyl). Only the cyclobutyl TIB ester underwent the full process in practical yields. It is described as occupying a “Goldilock’s zone” where the ring is small enough to allow facile deprotonation without decomposition, but large enough to allow 1,2-migration to occur.

The lithiation–borylation reaction has been optimised on a Chemspeed batch automation platform using a model boronic ester. We have shown homologations with either LiCH_2Cl (the Matteson reaction) or a lithiated benzoate (derived from the α -stannyl benzoate) proceed in ~90% yield per step over 2 steps. Set up time for 4 reactions can be as little as 30 minutes with 1 iteration performed per day.

A new automated synthesis of (+)-kalkitoxin analogues was designed. The starting point for the synthesis (a thiazoline bearing boronic ester) was synthesised in the lab in 6 steps starting from protected L-cysteine. The final steps of the total synthesis are Morken amination of a boronic ester, amidation and then methylation of the amide. We have shown the 3-step sequence works well on the automated platform for phenethyl boronic acid pinacol ester (42% over 3 steps) however for a model thiazoline bearing boronic ester the thiazoline undergoes rapid (1 h) isomerization to the thiazole (isolated in 46% over 3 steps) under the basic conditions required for the amination.

Acknowledgements

Firstly, I would like to thank Varinder for teaching me so much during my time in Bristol. I expected to learn lots about chemistry but was not anticipating the level of personal development I would receive in this group. I use Varinder's approaches to problem solving every day and shall continue to use to them.

Thanks to Adam Noble for teaching me so much during my time here and for giving me a confidence boost before my interview for my next position.

Eddie Myers finished as I started however his impact on how I approach chemistry and what areas of chemistry I enjoy has been massive. Thank you for all you taught me while writing and compiling the React-IR project.

A big shout out to Craig Butts who started and developed my interest in both computation and NMR (two areas of chemistry I now really enjoy). I feel very lucky to have been a part of your group and thank you for all you taught me during meetings.

Alex Kovsky without a doubt has been one of the most influential people in my PhD. The amount of practical knowledge Kovy distilled into me is exceptional and I am so grateful for all the time you spent carefully explaining in detail things to me. Kovy also got me back into two hobbies (computers and photography) that I had lost interest in when I started for which I am immensely thankful.

I am thankful to Steve for so many things. Steve has always been best in the group for synthetic methods and tricky synthesis, and I always looked up to him/relied on him for these areas (and ran a lot of questions by him). Thanks so much for getting me into good coffee.

Mio cugino Valerio. You have taught me so much about organisation and computation and these are skills I will take with me for the rest of my life. Thank you for the many laughs, all the hard work and most importantly the beers.

Thanks to the following: Fawcett for teaching me lots when I started (which I still use) and showing me how methodology projects should be run. Bateman for guiding me through lithiation–borylation. Felix for teaching me how metals work (and the importance of hard work). James for everything when we first got that Chemspeed... Sheenagh for making the best TLC stains. Kay for being a fantastic fume hood neighbour. Durga for teaching me so much.

Thanks to my CDT cohort for making that first year so enjoyable and a fantastic holiday. Thank you to the CDT management for everything but mainly making getting that uncertain extension so quick and painless.

I have been lucky to have a great group of housemates and friends during my time in Bristol and I cannot wait to see you all again soon.

Author's Declaration

I declare that the work in this dissertation was carried out in accordance with the requirements of the University's Regulations and Code of Practice for Research Degree Programmes and that it has not been submitted for any other academic award. Except where indicated by specific reference in the text, the work is the candidate's own work. Work done in collaboration with, or with the assistance of, others, is indicated as such. Any views expressed in the dissertation are those of the author.

SIGNED: DATE:.....

Contents

1	Introduction	1
1.1	Directed Lithiation α to Heteroatoms	1
1.1.1	Beak's Dipole-stabilised Carbanions	1
1.1.2	Hoppe's Diisopropylcarbamates	3
1.1.3	Mechanistic Detail and Evidence for a Pre-Complexation event	4
1.2	Homologation of Boronic Esters	7
1.2.1	Substrate Controlled Homologation	8
1.2.2	Reagent Controlled Homologation/Lithiation–Borylation	10
1.2.3	Iterative lithiation–borylation chemistry (assembly–line synthesis)	13
1.3	Optimisation of the Lithiation–Borylation Reaction	18
1.3.1	In situ IR spectroscopy in Lithiation–Electrophilic Trapping Procedures	19
1.4	Aims	23
2	Results and Discussion	24
2.1	Data collection	24
2.2	Initial comparison of directing groups	24
2.3	Effect of steric hindrance at the β position	27
2.4	Effect of solvent	28
2.5	Effect of different organoboron partners	34
2.6	Effect of a proximal aromatic group	37
2.7	Study on tin–lithium exchange and effect of additives on borylation	39
2.8	Applications in the lithiation–borylation of small to medium rings	42
2.8.1	Aims and Introduction	42
2.8.2	Results and Discussion	43
2.8.3	Summary	51
3	Conclusions	53

3.1	Outlook	54
4	Automated synthesis	56
4.1	Introduction	56
4.1.1	Factors required for iterative synthesis	56
4.1.2	Automation in synthesis: literature examples	57
4.1.3	Description of the UOB Chemspeed platform	65
4.2	Results and discussion	67
4.2.1	Early modifications	67
4.2.2	Filtration and Evaporation	69
4.2.3	Matteson homologation	70
4.2.4	Dispensing Tests and Transfer Optimisation	73
4.2.5	Iterative Matteson Reactions	75
4.2.6	Homologation with stannane 41	80
4.3	Summary of optimisation	84
4.4	Applications in the synthesis of kalkitoxin	85
4.4.1	Reactions in parallel	85
4.4.2	(+)-Kalkitoxin	85
4.4.3	Synthesis of boronic ester 126	89
4.5	Final Three Steps	103
4.6	Conclusions	114
4.6.1	Outlook	115
5	Experimental Section	117
5.1	General information	117
5.2	In Situ IR Spectroscopy	120
5.2.1	General Procedures	120
5.2.2	Experimental: Mechanistic Studies	121

5.2.3	Experimental: <i>O</i> -cycloalkyl benzoate/carbamate studies	136
5.2.4	NMR spectra	140
5.2.5	<i>In Situ</i> IR Traces	162
5.3	Automation	179
5.3.1	Chemspeed Platform	179
5.3.2	Experimental	189
5.3.3	NMR Spectra	208
6	References	225

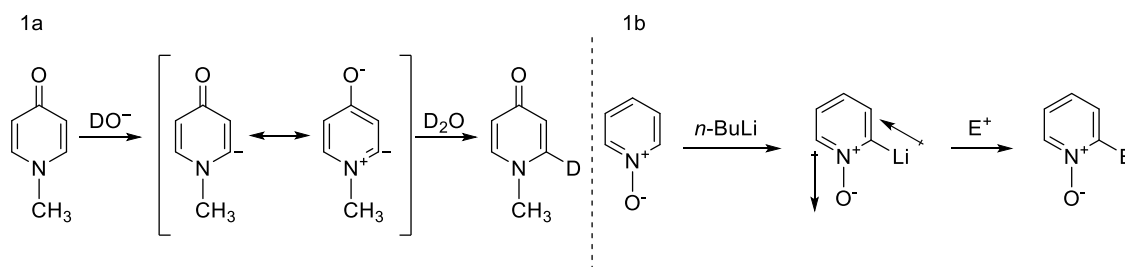
1 Introduction

1.1 Directed Lithiation α to Heteroatoms

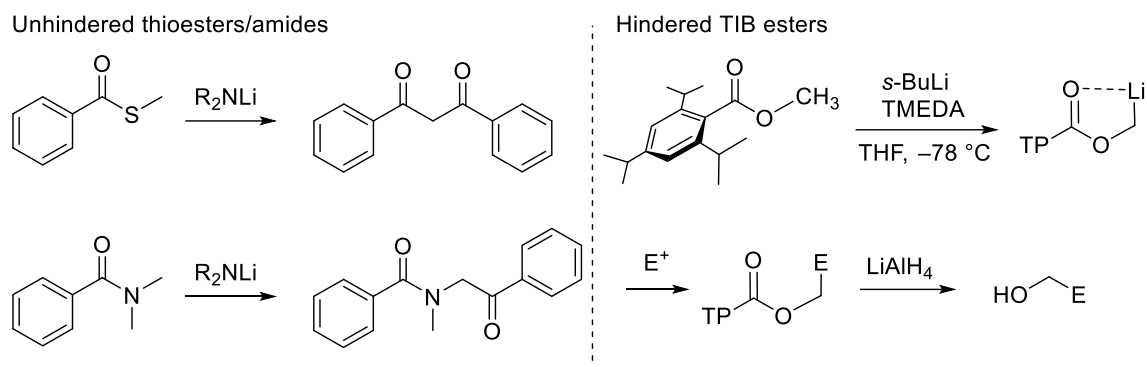
1.1.1 Beak's Dipole-stabilised Carbanions

The concept of a dipole-stabilised carbanion was postulated in the 1960s, with seminal work by Beak, concerning mainly deprotonation/deuteration studies of, for example, *N*-methyl-4-pyridones.¹ These processes were shown to be more facile than expected which was rationalised by postulating greater stability of the anion, by not only inductive effects alone, but also mesomeric stabilisation by an α heteroatom conjugated with an electron withdrawing group (Scheme 1a). With a move to more synthetically useful examples, metalations, and subsequent electrophilic trappings, were demonstrated with pyridine 1-oxides, again going through a postulated dipole-stabilised carbanion (Scheme 1b).²

Beak demonstrated the α -heteroatom metalation of various benzyl thioesters/amides with lithium 2,2,6,6-tetramethylpiperidide (LiTMP), which then reacted with the starting thioester/amide (Scheme 2).³ The equivalent benzoate esters required additional mesomeric stabilisation to undergo metalation under the same reaction conditions; alkyl benzoate esters underwent orthometalation of the phenyl ring.⁴ The difficult lithium proton exchange for alkyl esters, compared to thioesters or amides, is presumably due to the lack of dipole stabilisation provided by the ester group. Several years later, Beak demonstrated the lithiation of methyl 2,4,6-triisopropylbenzoate (TIB) ester, using *sec*-butyllithium (*s*-BuLi) and *N,N,N',N'*-tetramethylethylenediamine (TMEDA).⁵ The bulky isopropyl groups in the 4 and 6 position of the phenyl ring now sufficiently hinder the carbonyl so that the metalated benzoate does not react with the starting benzoate.

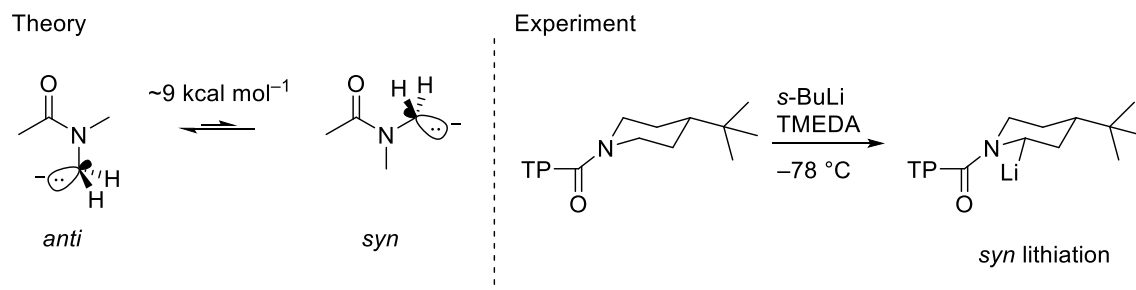


Scheme 1: a) Beak's early example of a deuteration, moving through a dipole-stabilised carbanion; b) an example of lithiation and trapping, the lithiated species is stabilised through the alignment of dipoles shown.



Scheme 2: Unhindered thioesters and amides dimerise upon lithiation, the thioester undergoing rearrangement and thiolate induced cleavage to the observed product, while hindered TIB esters are chemically stable at $-78\text{ }^{\circ}\text{C}$ and cannot dimerise, due to the hindered carbonyl group. TP = 2,4,6-triisopropylphenyl.

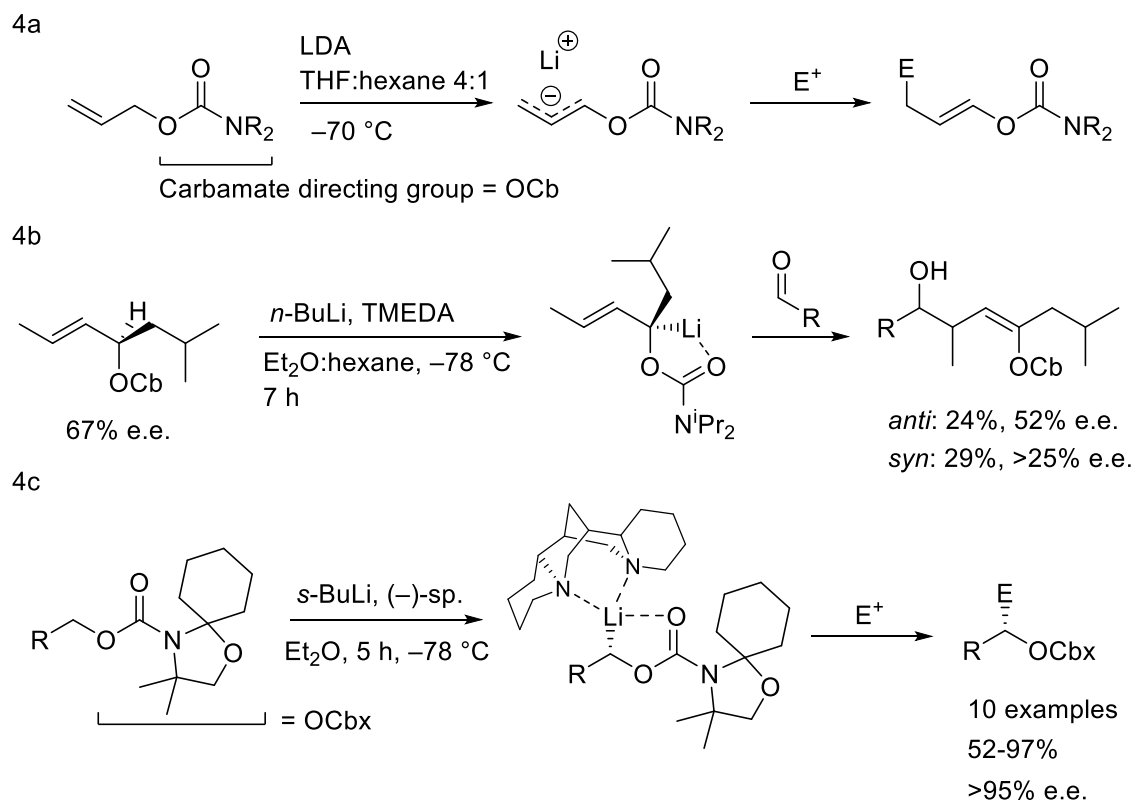
Beak described this advancement as a means to an α -lithioalkyl alcohol synthon, as, after lithiation and trapping with electrophiles, the TIB ester could be cleaved with lithium aluminium hydride to the corresponding alcohol.⁶ To provide more evidence for the dipole stabilisation of a lithium carbanion, Beak performed *ab initio* self-consistent field (SCF) calculations.⁷ These estimated the *anti*-isomer (with respect to the carbanion and carbonyl oxygen, scheme 3) to be $\sim 9\text{ kcal mol}^{-1}$ more stable than the corresponding *syn*-isomer, however, this did not agree with experimental findings, as the lithiation of substituted *N*-(*tert*-butoxycarbonyl)piperidines gave products exclusively from *syn*-lithiation alpha to the nitrogen (Scheme 3). Clearly the calculations performed did not include the lithium ion, and the differences between theory and experiment were attributed to lithium-ion complexation. Later studies showed level of theory to be an important factor.⁸ The idea of having lithium as a strongly complexing ion, or carbonyls as strongly directing groups for lithium, was one that had been discussed in the literature, and is one that became increasing more important for lithiation chemistry.⁹



Scheme 3: Theory predicts the *anti*-isomer to be more stable than the *syn*, but experiment shows a preferential *syn* lithiation. The calculations, presumably, do not account for stabilisation of the *syn* isomer over the *anti*-isomer due to lithium–oxygen coordination. TP = 2,4,6-triisopropylphenyl.

1.1.2 Hoppe's Diisopropylcarbamates

Other variants of α -lithioalkyl synthons were developed, an important example being *N,N*-dialkylcarbamates from the Hoppe group, first documented in 1980 (Scheme 4a).¹⁰ Again, this example can be seen as a dipole-stabilised carbanion, similar to Beak's TIB esters. Early examples from Hoppe had additional mesomeric stabilisation, and were deprotonated with lithium diisopropylamide (LDA) in ethereal/non-polar solvent mixtures.¹⁰ The metallated species did not react with the starting materials, and so could be trapped with several electrophiles. Hoppe also demonstrated the transmetalation of the carbanion from lithium to titanium, which could then undergo homoaldol chemistry with aldehydes and ketones.¹¹ In the search for an enantioselective homoaldol reaction, Hoppe investigated the configurational stability of both the lithium and the titanium carbanions at temperatures under -70 °C. By generating the lithium carbanion from enantioenriched allylic *N,N*-diisopropylcarbamate (Scheme 4b) with *n*-butyllithium (*n*-BuLi) and TMEDA over 7 hours at -78 °C, and then trapping with an aldehyde, Hoppe was able to demonstrate that the deprotonation occurs with retention and that the

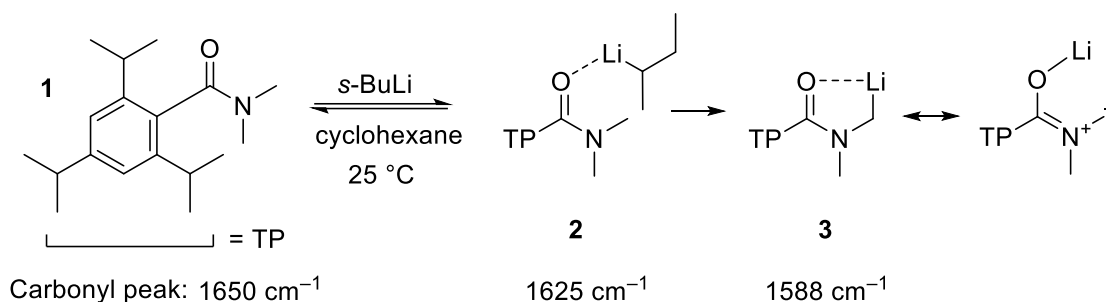


Scheme 4: a) First use of the carbamate directing group. No addition to starting materials was seen when $R \neq \text{Me}$; b) the use of enantiomerically enriched starting materials demonstrates that the lithiation proceeds with retention to give configurationally stable lithiated species c) use of the chiral diamine (-)-sparteine to generate chiral products from prochiral starting materials.

carbanion was configurationally stable under the reaction conditions.^{12,13} This meant the lithium cation must be essentially in a sp^3 hybridised sigma bond to the carbon. A limitation to this methodology was that the carbanion had to be generated from a chiral substrate, which could only be generated in moderate enantiomeric excess (e.e.) by kinetic resolution. To generate the chiral, configurationally stable carbanion from a prochiral substrate would circumvent this limitation, and Hoppe managed to demonstrate this a few years after the discovery of the configurational stability of the carbanions (Scheme 4c).¹⁴ Using the commercially available diamine (-)-sparteine ((-)-sp.) as a ligand for the lithium atom of *s*-BuLi, the base now selectively removed the pro-*S* proton from a number of different carbamates. Instead of the *N,N*-diisopropylcarbamate used in previous work, Hoppe now used a spirocyclic variant, termed Cbx (Scheme 4c), presumably due to an easier removal of the directing group.¹⁵ Beak subsequently demonstrated that the lithiation of *N*-(*tert*-butoxycarbonyl)pyrrolidines occurred enantioselectively using (-)-sparteine, which could then be trapped with electrophiles to give 2-substituted products, with e.e. values ranging from 88 to 95%.¹⁶ Both Hoppe and Beak demonstrated that the trapping with an electrophile could occur with either retention or inversion, through an S_E2 pathway.¹⁴ Beak suggested that electrophiles that could complex to lithium, such as esters, would prefer to trap with retention.¹⁷

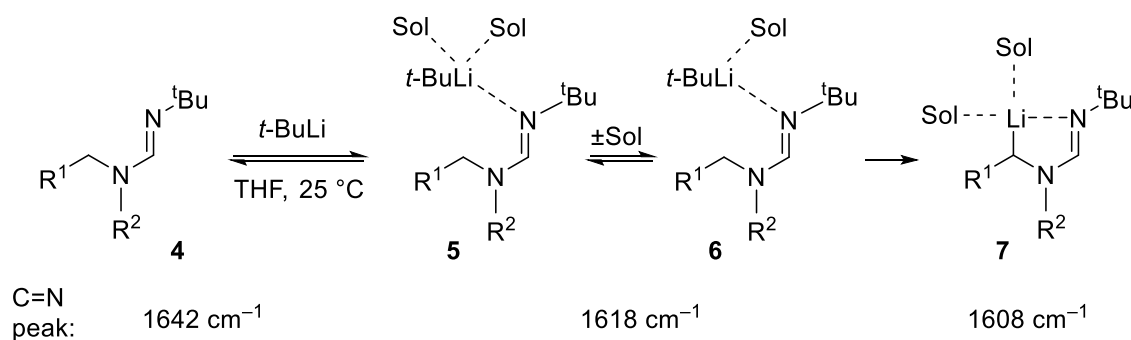
1.1.3 Mechanistic Detail and Evidence for a Pre-Complexation event

The idea of an interaction between the lithium atom of commonly used alkyllithium bases with the carbonyl of the directing group, such as the TIB ester or *N,N*-diisopropylcarbamate, before metalation was discussed by Beak. In early reports of ortho metalations of phenyl rings, evidence for this coordination was provided by crystal structures involving nitrogen non-bonding electron pair coordination to the lithium ion.¹⁸ However, Beak managed to provide evidence of a coordination event along the reaction pathway by using stopped-flow infrared (IR) spectroscopy.¹⁹ This technique allows for rapid mixing of two reactants, then an accurate mixing time, before another rapid transfer to a detector for kinetic analysis, and had been used previously for studies concerning organometal additions and deprotonations.²⁰ Beak's work detailed the lithiation of *N,N*-dimethyl-2,4,6-triisopropylbenzamide **1** (Scheme 5) using *s*-BuLi in non-polar solvents. The reaction shows the IR band of the starting material **1** at 1650 cm^{-1} , and a new band at 1625 cm^{-1} . These both disappear with first order rate constants, with concurrent increase in a band at 1588 cm^{-1} . The new, transient band at 1625 cm^{-1} is the



Scheme 5: Beak's use of stopped flow IR spectroscopy to study the lithiation of benzamide **1** allowed for detection of an intermediate along the reaction pathway. The product was trapped with D_2O to demonstrate that lithiation was occurring *syn* to the carbonyl.

coordination complex **2**, the lower wavenumber in comparison to starting material due to the reduced bond order of the carbonyl upon coordination to lithium. The final band produced with disappearance of the first two is the lithiated complex **3**, the much-reduced wavenumber now due to a strong lithium–oxygen coordination in a five membered chelate. Resonance forms can also be drawn, like Beak proposed for a dipole-stabilised carbanion, where the carbonyl oxygen has a lower bond order due to donation from the nitrogen, leading to a lower carbonyl wavenumber. The group of Meyers also detailed evidence for a pre-lithiated complex (Scheme 6), using a *tert*-butylformamidine substrate **4**.²¹ Upon addition of *tert*-butyllithium (*t*-BuLi) to the substrate, of which the C=N stretch appears at 1642 cm^{-1} in tetrahydrofuran (THF), a new transient peak is observed at 1618 cm^{-1} , with a final band produced at 1608 cm^{-1} . The transient peak can be attributed to the pre-lithiated complex **5/6**, the final band the carbanion **7**. The decrease in wavenumber for each species from the starting material follows the same pattern as for Beak's *N,N*-dimethyl-2,4,6-triisopropylbenzamide **1** (Scheme 5). This example was extremely solvent-dependent; strongly coordinating solvents like dimethoxy ethane (DME) provided almost no lithiated product, while weakly coordinating solvents like diethyl ether (Et_2O) provided high levels of lithiation.



Scheme 6: Meyer's observation of a pre-lithiated species using IR spectroscopy. The solvated pre-lithiated species **5** needs to undergo solvent dissociation to allow lithiation.

Meyers attributed these large solvent effects to the need for solvent to dissociate from the pre-lithiated complex **5**, to form the active complex **6**, before lithiation could occur. Beak and Meyers developed the term Complex Induced Proximity Effects (CIPEs), and have reviewed many examples that followed the rationale of kinetic over thermodynamic deprotonation due to a prior complexation event.²² Further studies into the mechanism of the α -lithiation of carboxamides were performed by Beak, using stopped flow IR spectroscopy.²³ This study demonstrated the difficulty in providing a full kinetic analysis of lithiations using alkyllithium bases with diamines, as the base will be aggregated to various extents, with a number of diamines coordinated to each aggregate, to generate many different active species available for deprotonation. The idea of aggregation of organolithiums in solution is well known, and Beak determined solution structure **8** (Figure 1) for isopropylolithium (*i*-PrLi), a non-diastereomeric substitute for *s*-BuLi, complexed to (-)-sparteine in Et₂O by performing a variety of ¹H, ¹³C and ⁶Li NMR experiments. The structure is described as a heterodimer, with two *i*-PrLi units complexed to one (-)-sparteine ligand and a number of ligated solvent molecules.²⁴ The preference for a heterodimer rather than a homodimer, which would contain two (-)-sparteine molecules, demonstrates the steric bulk of the (-)-sparteine ligand.

Another mechanistic study was performed by Garcia-Rio and co-workers, on the rate-determining step in the benzylic lithiation of carbamates and TIB esters (Figure 2).²⁵ In all experiments they worked under pseudo first order conditions, using a large excess of *n*-BuLi, and in hexane/THF mixtures. They determined that the carbamate had a reactivity over 500 times greater than that of the ester, which was attributed to the more basic carbonyl group present on the carbamate, in comparison to the ester. The rate determining step was determined to be complexation for the non-deuterated ester **9**, and deprotonation

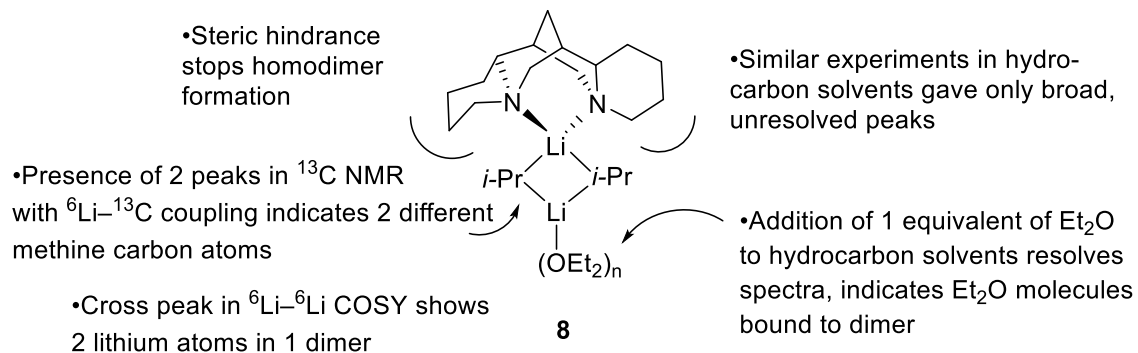


Figure 1: The solution structure determined by Beak and co-workers for *i*-PrLi/(-)-sparteine in Et₂O, which was unlike other simple organolithium/diamine complexes at the time, as they were usually symmetrical homodimers.

for the deuterated ester **9-D** and carbamates **10/10-D**. When moving to solvent mixtures with less THF, they found the rate of lithiation of ester **9** increased. Presumably in THF the active *n*-BuLi dimer is more strongly solvated than in hexane, and so competes with the ester for complexation, and therefore the lithiations are slower in the presence of more THF. The authors did not comment on the effect of changing solvent mixtures on the lithiation of carbamates.

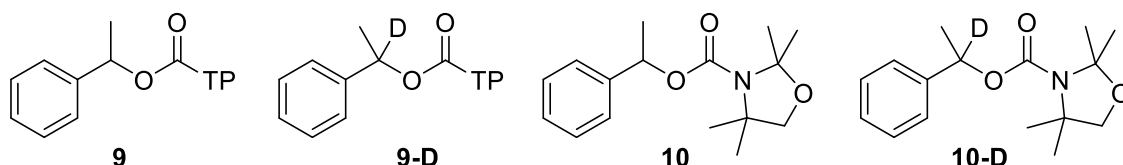
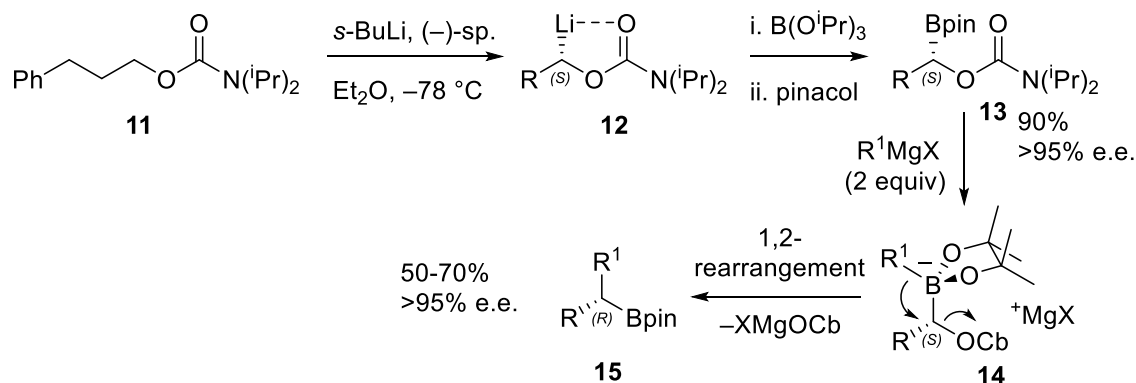


Figure 2: Substrates used in Garcio-Rio's study. Carbamate **10** was found to be over 500 times more reactive than ester **9**. Pre-complexation was rate-limiting for ester **9**, but deprotonation was rate-limiting for **9-D**, **10**, and **10-D**.

1.2 Homologation of Boronic Esters

Hoppe demonstrated the use of his alkyl diisopropylcarbamates, not only as a directing group but also as a leaving group.²⁶ Beak had proposed his TIB esters as α -lithioalkyl alcohol synthons, however Hoppe now changed the paradigm and viewed his carbamates as a lithium carbenoid equivalent. By trapping lithiated carbamate **12** with triisopropyl borate, and then transesterifying to the pinacol ester, Hoppe could isolate α -carbamoyloxy-alkylboronic ester **13** in 90% yield and with >95% e.e. (Scheme 7). He then used a Grignard reagent to transform the Lewis acidic boronic ester to the tetra coordinate, negatively charged boronate complex **14**. This boronate complex is



Scheme 7: Hoppe's homologation of boronic esters, using the carbamate directing group developed in his lab to direct lithiation, but also as a leaving group in 1,2-rearrangement of the boronate complex formed from addition of a Grignard.

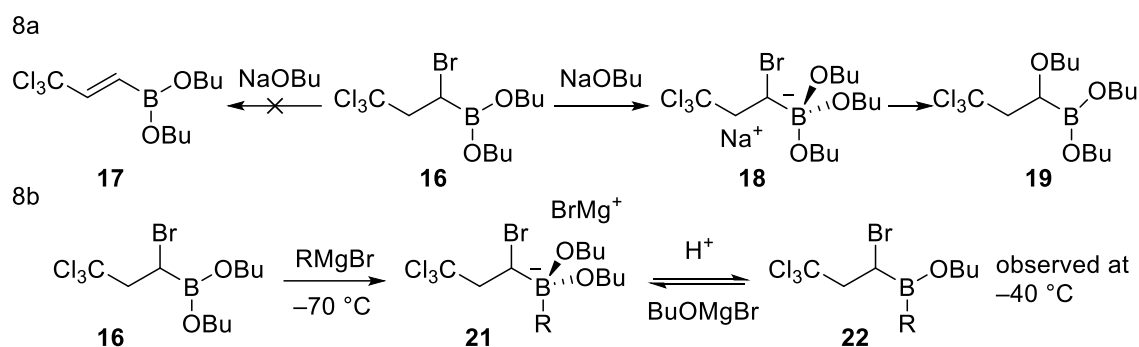
chemically and configurationally stable at $-78\text{ }^{\circ}\text{C}$ but can undergo a 1,2-metalate rearrangement upon warming. This is where the carbon on boron (R^1) migrates to the α -carbon, which is electron deficient due to the carbamate group, expelling the carbamate group and providing the homologated product **15**. It is important to note that the 1,2-rearrangement requires two equivalents of the Grignard reagent, as one equivalent acts as a Lewis acid and increases the leaving group ability of the carbamate group.

The 1,2-metalate rearrangement of boronate complexes (derived from addition of lithium carbenoids to organoboron compounds) is stereospecific with inversion of configuration, with seminal work performed by Matteson. The homologation of organoboron compounds using achiral and chiral metal carbenoids has grown from a simple observation by Matteson to a powerful process used extensively today in methodology and natural product synthesis.

1.2.1 Substrate Controlled Homologation

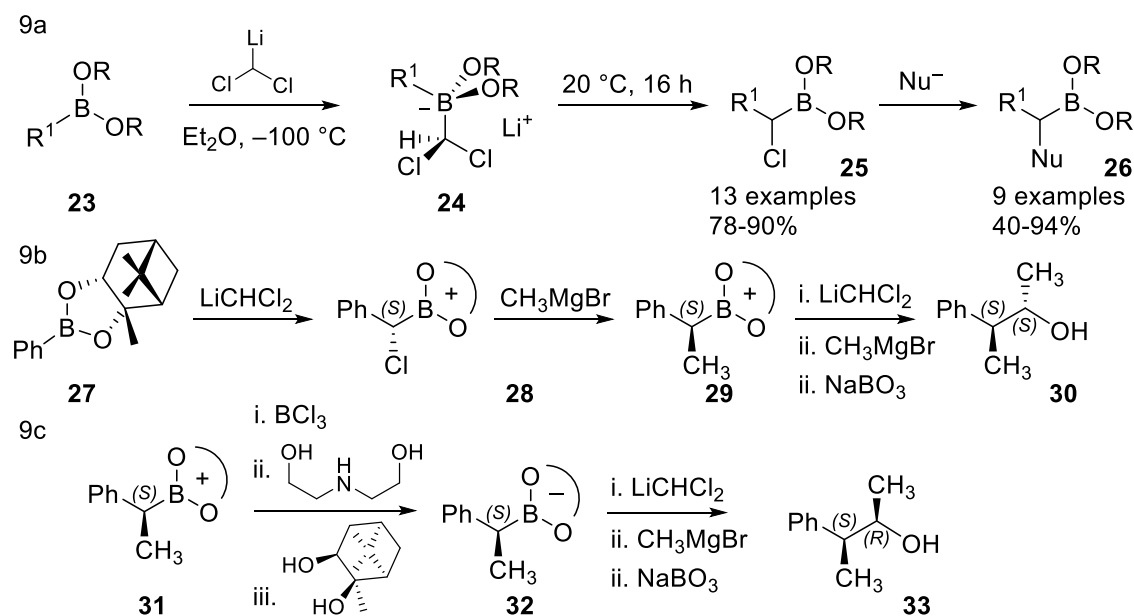
Matteson, in 1963, observed that the addition of sodium butoxide to α -bromo boronic ester **16** did not provide the dehydrobrominated product **17**, but instead the addition product **19** (Scheme 8a).²⁷ The corresponding butyl ester only reacted 0.2–0.3 times as fast as the boronic ester **16**. This discrepancy was rationalised by proposing the reaction preceded through the four coordinate boronate complex **18**, which could then undergo 1,2-metalate rearrangement to expel the bromide anion. The formation of the boronate complex along the reaction pathway was confirmed by reacting boronic ester **16** with a Grignard reagent at low temperature (Scheme 8b). This was then hydrolysed with acid to the boronic ester **22**, while maintaining a low temperature.²⁸ Upon warming, the boronic ester would rearrange back to the boronate complex, and then undergo 1,2-rearrangement.

Fifteen years later, Matteson demonstrated the synthetic utility of these observations, by developing the synthesis of α -chloro boronic esters from the homologation of a boronic ester using (dichloromethyl)lithium (Scheme 9a).²⁹ The lithiated carbenoid was generated from dichloromethane and *n*-BuLi at $-100\text{ }^{\circ}\text{C}$, and adds to the boronic ester at this temperature. The 1,2-metalate rearrangement takes place upon warming to $20\text{ }^{\circ}\text{C}$ for 16 hours. This generated the α -chloro boronic esters, which could be isolated after distillation, and then further reacted with nucleophiles to give products **26**. The process could be applied iteratively, however it would quickly give multiple diastereomers. Matteson solved this problem with the use of a chiral boronic ester, made using a chiral



Scheme 8: a) addition of NaOBu to boronic ester **16** did not provide dehydrobrominated product **17**, instead substitution occurred, through boronate complex **18**; b) evidence for boronate complexes was provided by observation of boronic ester **22** at low temperatures.

diol (Scheme 9b).²⁹ The chiral diol on boron acts as a directing group. This allowed for the stereoselective synthesis of both the (2*S*,3*S*) and (2*R*,3*S*) diastereomers of 3-phenyl-2-butanol (**30** and **33**) from optically pure phenyl boronic (+)-pinanediol ester **27**, with 97% diastereoselectivities in the first step and 92-95% diastereoselectivities in the second. One limitation is that the procedure is under substrate control. Therefore, to swap between forming one diastereomer and the other in this Matteson process, the chiral diol on the boronic ester must be removed and the corresponding stereoisomer installed, adding steps to the synthesis. With only moderate yields and diastereoselectivities for more hindered

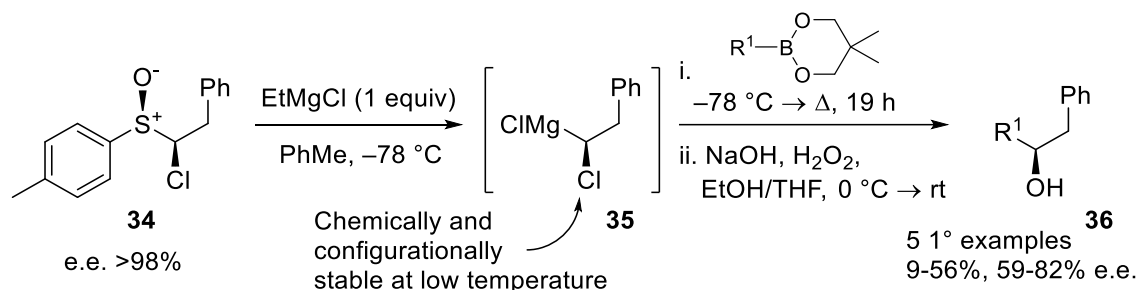


Scheme 9: a) Use of (dichloromethyl)lithium (CHCl_2Li) to generate α -chloro boronic esters **25**, which can then react with nucleophiles (Nu^-) and undergo 1,2-rearrangement to afford boronic esters **26**; b) esterification of a chiral diol onto the boronic ester allows for stereospecific reactions with CHCl_2Li , to generate non-racemic product; c) to change the stereocenter installed, the diol must be transesterified to the enantiomer. The removal of the chiral diol did not proceed under standard acidic conditions, and so was removed with BCl_3 .

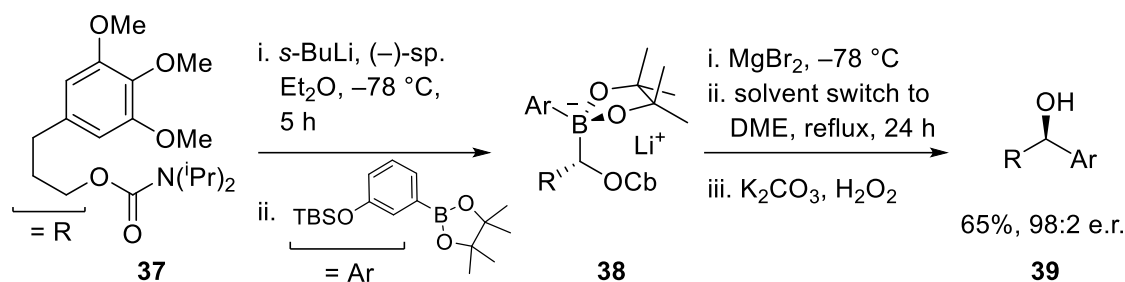
substrates, and the observation that lithium chloride could epimerise α -chloro boronic esters, Matteson tested metal salts capable of binding chloride to catalyse the reaction. Zinc(II) chloride, between 0.5 and 0.65 equivalents, was found to significantly increase the yield and diastereoselectivity of the process, and Matteson applied the methodology to the synthesis of two more natural products.³⁰ Several years later Matteson developed the carbenoid (chloromethyl)lithium, which can be used to insert a methylene group in boronic ester homologations.³¹

1.2.2 Reagent Controlled Homologation/Lithiation–Borylation

Matteson's protocol has a deficiency in that it is substrate controlled, and so requires laborious transesterification of the boronic ester to access alternative diastereoisomers. Hoppe's approach, discussed earlier (beginning of section 1.2), uses (–)-sparteine to stereoselectively install the boronic ester, and so is under reagent control: the use of (+)-sparteine would allow for the synthesis of the other stereoisomer. However, Hoppe's approach (Scheme 7) also has a drawback as it is two steps, the procedure requires the isolation of the enantioenriched boronic ester, then reaction with the Grignard afterwards. In 2006, Blakemore and co-workers published a one-pot homologation procedure, using α -chloro-sulfoxides as their chiral carbenoid reagent (Scheme 10).³² The sulfoxide can undergo exchange with an organomagnesium or organolithium reagent to give α -chloro-metalate species **35**, which is configurationally stable at low temperatures. These add to boronic esters to give boronate complexes, which then undergo 1,2-metallate rearrangement to give the homologated product. Importantly for a one-pot process, the ate complex formed, here a boronate complex, must not undergo 1,2-rearrangement at low temperature or the carbenoid **35** could add again to the boronic ester product, to give over-homologated products. The carbenoid, then, must be both configurationally and

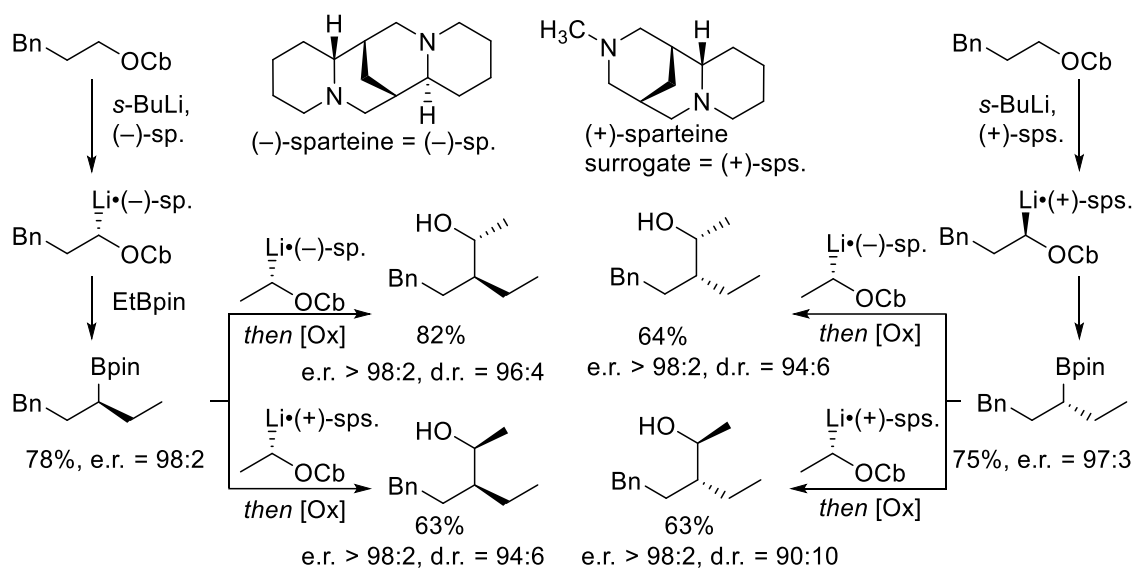


Scheme 10: Blakemore's one-pot procedure for the reagent controlled homologation of boronic esters using α -chloro-sulfoxides. The magnesium carbenoid generated was not nucleophilic enough to add to boronic acid pinacol esters; in subsequent work the lithiated carbenoid was generated using alkylolithiums to achieve this.



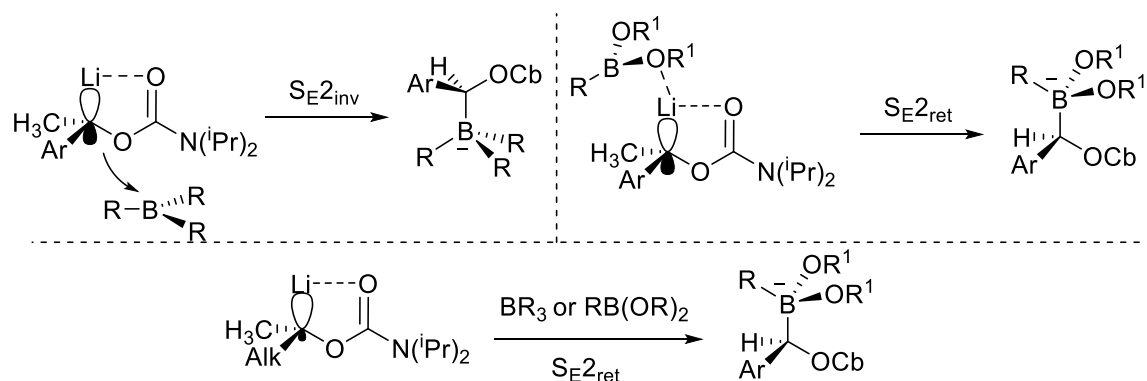
Scheme 11: Kocienski's one-pot lithiation–borylation procedure in the synthesis of (*S*)-(-)-*N*-acetylcolchicol. The addition of MgBr_2 and a harsh reflux was required to achieve the 1,2-rearrangement, which was not required under Hoppe's two step conditions.

chemically stable at low temperature, but any excess carbenoid must degrade upon warming, to ensure no over-homologation after 1,2-rearrangement (Scheme 10). Blakemore's protocol met these requirements and could provide homologated products, from simple α -chloro-sulfoxides and boronic acid neopentyl glycol/catechol esters, in moderate to good yields, with good to high e.e. values. Blakemore refined the process in subsequent years to allow for the conversion of boronic acid pinacol esters, which are easier to handle than the less hindered neopentyl glycol/catechol esters, by transmetallating to the lithium carbenoid instead of magnesium. He was able to demonstrate the synthesis of all four isomers of a stereodiad motif in good diastereomeric ratio (d.r.) and excellent enantiomeric ratio (e.r.).³³ Unfortunately, Blakemore's process can suffer from lower yields and poor d.r. values due to the instability of the α -chloro Mg/Li species. Kocienski demonstrated a one-pot lithiation–borylation procedure in his synthesis of (*S*)-(-)-*N*-acetylcolchicol, using Hoppe's carbamates as a chiral carbenoid (Scheme 11).³⁴ In this example, the migrating group is already installed on the boronic ester (Ar, scheme 11). Once the lithiated carbamate adds to form the boronate complex **38**, the desired group can then migrate. However, now devoid of excess Grignard reagent, Kocienski's process required the addition of MgBr_2 and a solvent swap, then reflux, to allow for 1,2-rearrangement to occur. Aggarwal expanded on this process the following year, with an in-depth study into the use of Hoppe's non-racemic lithiated carbamates as chiral carbenoids for the homologation of boranes and boronic acid pinacol esters.³⁵ Aggarwal had previously demonstrated the use of chiral sulfonium ylides for this process, however due to the slower 1,2-rearrangement of the boronic ester derived ate complex, only boranes, and not boronic esters, could be used.³⁶ The methodology (using chiral lithiated carbamates) was then applied in an iterative process, as the product boronic ester could be isolated and reacted again with another chiral carbenoid (Scheme 12).



Scheme 12: Aggarwal's use of lithiation–borylation in an iterative fashion. The high e.r. value of the lithiation maintains high e.r. and d.r. values over several homologations.

This produced all stereoisomers of 3-ethyl-5-phenylpentan-2-ol with excellent e.r. and d.r. values. This process, termed lithiation–borylation, has been expanded to use many different chiral carbenoids. Secondary benzylic carbamates can be used as they are configurationally stable at low temperature, unlike primary benzylic carbamates.³⁷ Now the lithiated species has a more planar carbanion than seen for alkyl carbamates. This leads to differences in enantioselectivity between boranes and boronic esters (Scheme 13).³⁸ Boronic esters react with retention of stereochemistry, due to a postulated coordination between the Lewis basic pinacol oxygen and the lithium of the carbenoid. Boranes, which are devoid of Lewis basic heteroatoms, now react preferentially with inversion, presumably due to a less sterically hindered pathway. Simple alkyl substrates do not exhibit this difference in enantioselectivity, as the carbanion is located in a strictly

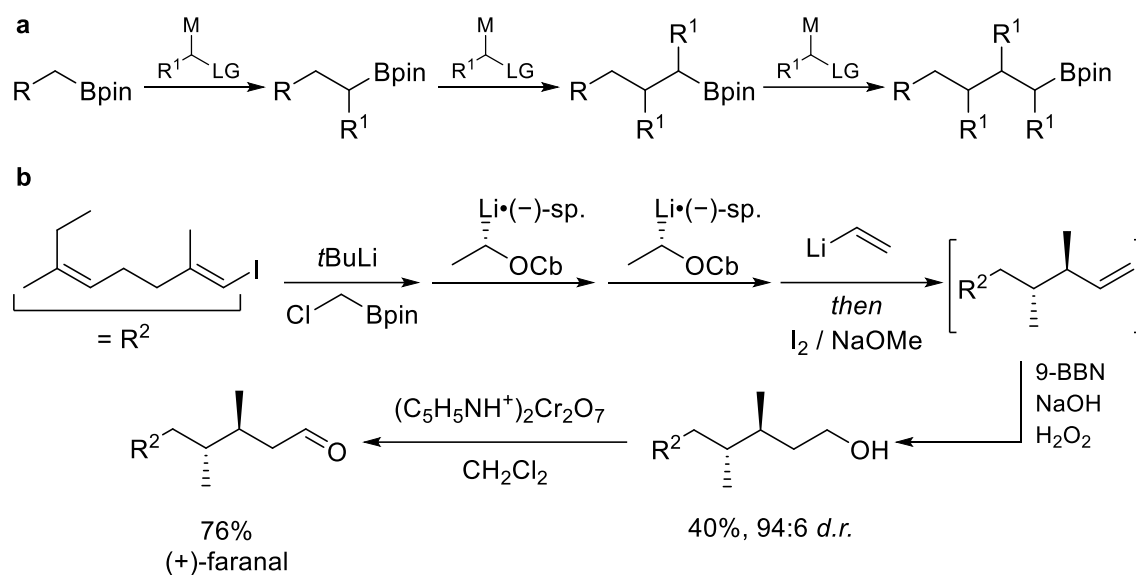


Scheme 13: Lithiation of benzylic carbamates generates an almost planar carbanion, in which the essentially sp^2 hybridised orbital leads to enantiodivergent reactions based on organoboron partner used. The use of alkyl carbamates generates the carbanion in an sp^3 orbital, so this effect is not seen.

sp^3 hybridised orbital, and so there is little electron density opposite to the lithium to allow for a reaction with inversion. Other secondary carbamates with additional stabilisation, for example allylic³⁹ and propargylic,⁴⁰ can also be used. Mesomerically stabilised carbamates such as these usually undergo facile deprotonation, typically in the presence of non-hindered diamines such as TMEDA or under diamine-free conditions. This leads to non-hindered lithiated species that undergo borylation easily. Interestingly, the 1,2-metalate rearrangement of the derived boronate complexes is also more facile than for simple alkyl carbamates. 1,2-Migrations of aryl carbamate derived boronate complexes are typically complete within 2 h at RT, whereas boronate complexes derived from alkyl carbamates require Lewis acids, heating and extended reaction times to undergo full 1,2-migration. Harvey and co-workers were able to corroborate this result computationally.⁴¹ The lithiation–borylation methodology was expanded to the use of Beak’s TIB esters by Aggarwal in 2011, due to the slow 1,2-rearrangement seen with some boronate complexes derived from Hoppe’s carbamates.⁴² The TIB ester is a better leaving group than the carbamate, and so does not usually require $MgBr_2$ or heating in order to complete the rearrangement. Similarly to Hoppe’s carbamates, the lithiated TIB esters can be formed in high e.r. by deprotonation of the TIB ester in the presence of *s*-BuLi/sparteine, adding another lithium carbenoid for use in the homologation of boronic esters. TIB esters have also been shown to promote lithiation (over carbamates) when using dialkyl systems.⁴³ Aggarwal has applied this lithiation–borylation methodology to the synthesis of several natural products.^{44–46}

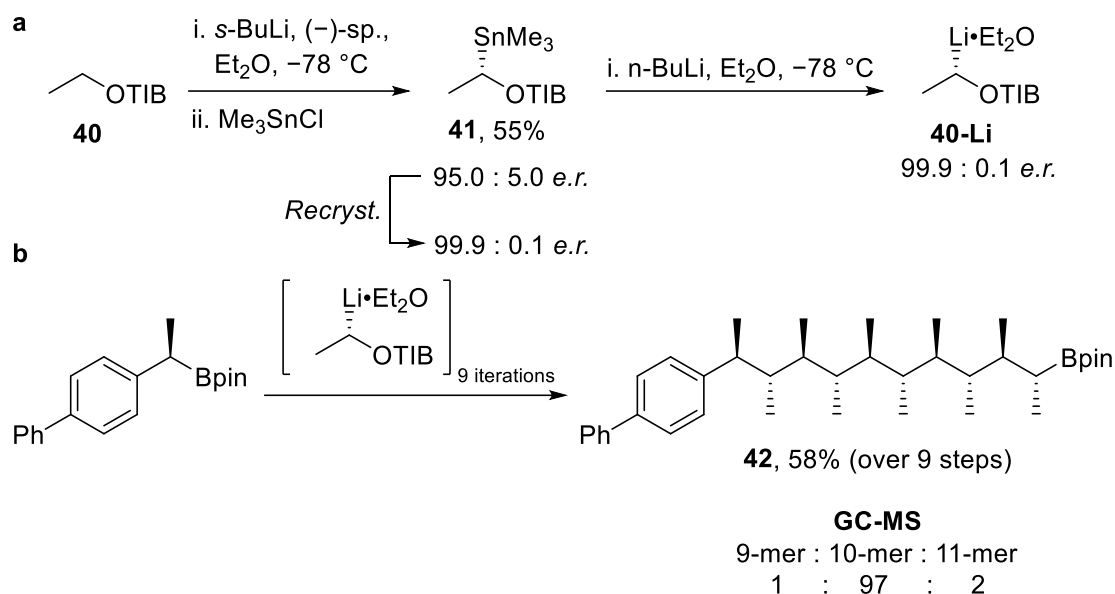
1.2.3 Iterative lithiation–borylation chemistry (assembly–line synthesis)

Lithiation–borylation chemistry can be used in the coupling of two complex fragments (a boronic ester and a carbamate/TIB ester) providing a distinct way to build C–C bonds stereoselectively. This provides a boronic ester product that can be transformed in a variety of ways.⁴⁷ As shown in scheme 14, an interesting transformation is the same lithiation–borylation reaction that has just been applied – however using multiple advanced lithium carbenoid fragments iteratively is unlikely to be desired. Instead, use of smaller lithium carbenoids (or building blocks) in an iterative fashion leads to a powerful process where smaller groups can be inserted along a carbon-chain, with a boronic ester at the head (Scheme 14a). This procedure was applied in the synthesis of the insect pheromone (+)-faranal (Scheme 14b) where four iterative homologations were used to install the central methylated chain of the natural product.



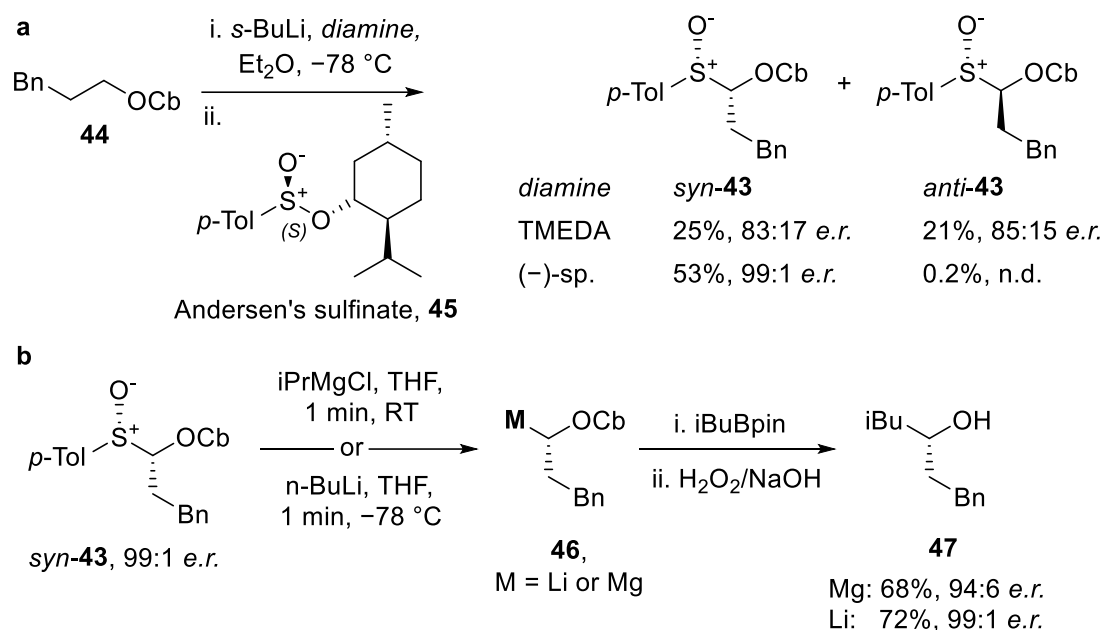
Scheme 14: a) outline of assembly-line synthesis, where a boronic ester chain is grown using metal carbenoids. $M = \text{Li, Mg}$; $\text{LG} = \text{leaving group}$; b) Aggarwal's synthesis of (+)-faranal, which uses a 4-step homologation sequence, including a Zweifel olefination with vinyl lithium.⁴⁸

Unfortunately, iterative use of lithium carbenoids derived directly from sparteine-mediated lithiation (*e.r.* 98:2 to 95:5) will lead to accumulation of many diastereomers, therefore generating impure material. It is important to note that any minor enantiomers will be converted into diastereomers after the reagent controlled homologation, leading to enantioenrichment of the major diastereomer (the Horeau Principle).⁴⁹ To avoid the generation of many diastereomers when performing several iterative homologations, an enantioenrichment step is required of the carbenoid precursor. In 2014, Aggarwal reported such a process, whereby ethyl 2,4,6-triisopropylbenzoate **40** is lithiated in the presence of (+) or (–)-sparteine. This lithiated species can then be trapped with Me_3SnCl to afford the organostannane **41** in good yield and high *e.r.* $\approx 95:5$. Importantly this organostannane is crystalline and can be recrystallized (MeOH) to afford enantiopure product **41**, *e.r.* $> 99.9:0.1$ (Scheme 15a). Treating the stannane with *n*-BuLi stereospecifically reveals the lithium carbenoid, which can then be trapped with a boronic ester to form a boronate complex, which undergoes 1,2-migration (both steps are completely stereospecific). This procedure was performed 9 times iteratively (with an aqueous work-up every 3rd iteration) to afford boronic ester **42**.⁵⁰ Changing the enantiomer of the lithium carbenoid used allowed the synthesis of all-*syn* or *syn-anti* conformers which demonstrate strong conformational control in solution due to the avoidance of *syn*-pentane interactions. Due to the Horeau principle (described above), the final compounds are expected to be isolated as literally one enantiomer.



Scheme 15: a) Use of Beak's 2,4,6-triisopropylbenzoate directing group, coupled with recrystallization of the organostannane intermediate **41**, leads to enantiopure lithium carbenoid **40-Li**; b) lithium carbenoid **40-Li** can be used in iterative homologations to provide highly enantiopure and diastereomerically pure materials, which are conformationally controlled in solution.

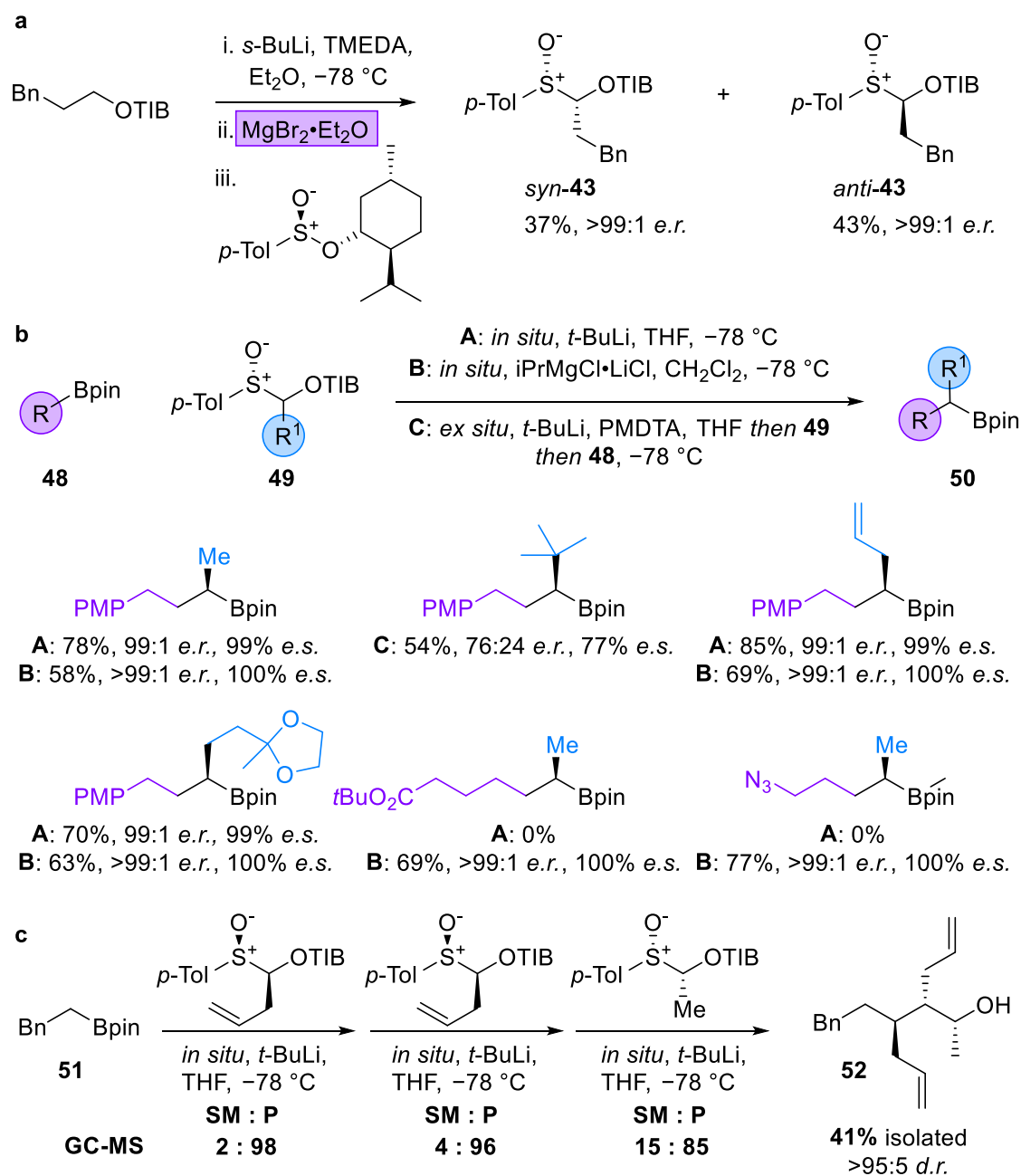
The crystalline nature of organostannane **41** is unfortunately rare and other related α -stannyl benzoates synthesised have been oils, precluding enantioenrichment by recrystallization and therefore limiting their use in lithiation–borylation chemistry. As well as this, Me_3SnCl is toxic and other organotin compounds are either known to be toxic or regarded as toxic.⁵¹ O'Brien and co-workers have demonstrated the generation of α -sulfinyl carbamates **43** from lithiation of carbamate **44** and trapping with Anderson's sulfinate **45** (Scheme 16).⁵² These underwent magnesium–sulfoxide exchange at room temperature in 1 minute to provide the magnesiated species **46**, which could be trapped with electrophiles. Generating the α -sulfinyl carbamate using *s*-BuLi/TMEDA gave only poor *e.r.* values (~85:15) of the *syn*- and *anti*-diastereomers, however generation with *s*-BuLi/sparteine mixtures gave high *e.r.* values (99:1) of one diastereomer (with reduced *e.r.* value of the minor diastereomer). O'Brien then demonstrated these α -sulfinyl carbamates could undergo facile magnesium–sulfoxide (1 min, RT) or lithium–sulfoxide (1 min, $-78\text{ }^\circ\text{C}$) exchange to give the metal carbenoids **46**, which were then trapped with isobutyl boronic acid pinacol ester (among other electrophiles). This gave, after 1,2-migration and oxidation, secondary alcohol **47** with an excellent *e.r.* value (Scheme 16b).



Scheme 16: a) O'Brien's synthesis of α -sulfinyl carbamate **43** in *syn* and *anti* forms, where (-)-sparteine is required for high *e.r.* value of a major diastereomer; b) synthetic application of sulfoxide **43** was shown by metal-sulfoxide exchange to give carbenoids **46**, then trapping with a boronic ester, 1,2-migration and oxidation.

Aggarwal was able to improve and expand on these results in 2017 in an attempt to describe a general way to generate different enantiopure metal carbenoids for boronic ester homologations (Scheme 17).⁵³ Firstly, α -sulfinyl benzoates instead of the corresponding carbamates were targeted, presumably due to the more facile 1,2-migration observed with benzoates.⁴² The same low enantiospecificity was observed when trapping lithiated benzoates with Andersen's sulfinate, however it was found that transmetallating from the lithiated benzoate to the magnesiated benzoate gave complete enantiospecificity (Scheme 17a). This allows the generation of the both the *syn*- and *anti*- diastereomers (usually separable by column chromatography) with high *e.r.* values (typically >98:2 *e.r.*) using TMEDA/*s*-BuLi mixtures, also therefore avoiding the use of sparteine. Various α -sulfinyl benzoates **49** could be prepared and metalated (using conditions to generate either the Li or Mg carbenoids) then trapped with a range of boronic esters **48** to give the homologated products **50** (Scheme 17b). Due to potential acid-base side reactions, three sets of conditions were optimised for different combinations of α -sulfinyl benzoates and boronic esters (conditions **A**, **B** & **C**). This methodology was then further applied in the iterative homologation of phenethyl boronic acid pinacol ester **51** (Scheme 17c) to give alcohol **52** after three homologations and oxidation. The use of the Li carbenoid (instead of Mg) was essential for full conversion in the first two homologations. Unfortunately, the third homologation suffered from lower conversion due to the hindered nature of the

boronic ester. Generating the same lithium carbenoid from organostannane **41** afforded 99% conversion for the same step. This indicates that when boronate complex formation is slow, other deleterious processes can operate under the conditions used for the α -sulfinyl benzoates.



Scheme 17: a) Conditions for the synthesis of α -sulfinyl benzoates with high enantiospecificity; b) selected examples detailing the homologation of boronic esters with metal carbenoids derived from α -sulfinyl benzoates; c) use of the methodology in the iterative homologation of a boronic ester.⁵³

1.3 Optimisation of the Lithiation–Borylation Reaction

Clearly the one-pot homologation of boronic esters using a chiral lithiated carbenoid is a useful but intricate process, and it can be broken down into three key parts:

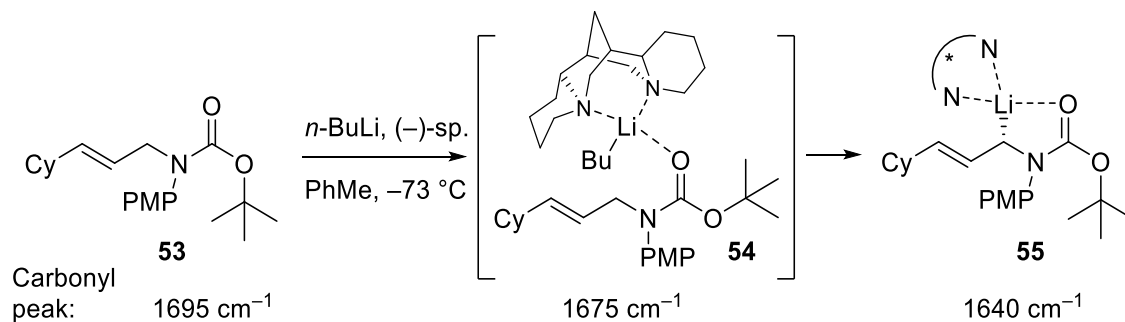
- 1) Generation of the lithiated carbenoid at low temperature, either by deprotonation of a suitable substrate with a directing group, using a suitable organolithium/diamine complex, or tin/sulfoxide–metal exchange;
- 2) Metal–boron exchange with a suitable organoboron partner, also at low temperature to generate a boronate complex; and
- 3) 1,2-rearrangement of this boronate complex, usually at 20 °C or higher and possibly in the presence of a Lewis acid, which expels the directing/leaving group and affords the homologated boronic ester product.

Optimisation of these three steps is non-trivial, as, for example, both lithiation and borylation take place at low temperature and are air sensitive, and each step in the one-pot process will be affected by any changes performed in an earlier step. The lithiation step can be and is most easily monitored by deuteration studies, however this can involve multiple reactions and re-isolation of material for subsequent analysis. Borylation can be monitored by ^{11}B NMR, however, this is rarely done in situ due to the requirement for prohibitively expensive and specialist equipment. The ex situ nature of analysis does therefore mean that inaccuracies will be present, and could dominate, due to the warming of the reaction. For example, lithium–boron exchange can become reversible at temperatures where the 1,2-rearrangement begins to occur. The third step, 1,2-rearrangement, is easier to monitor by ^{11}B NMR as the reaction mixture is no longer cooled or particularly air/moisture sensitive. The products (boronic esters, $\delta \approx 30$ ppm) and starting materials (boronates, $\delta \approx 8$ ppm) have large differences in chemical shift, simplifying analysis. Of course, the starting material boronic ester will usually appear at the same chemical shift as the product boronic ester.

The use of in situ IR spectroscopy has emerged as a powerful technique for the analysis of reactions of this type, as the directing groups commonly used, including benzoates and carbamates, contain a carbonyl group that is involved, and its bond order affected, at all stages along the reaction pathway.

1.3.1 In situ IR spectroscopy in Lithiation–Electrophilic Trapping Procedures

In 1983, Beak demonstrated early use of stopped flow IR spectroscopy in providing evidence for a pre-lithiated species when lithiating *N,N*-dimethyl-2,4,6-triisopropylbenzamide (see scheme 5, section 1.1.3). Almost 20 years later, in 2001, he demonstrated use of in situ IR spectroscopy in a comprehensive study on the lithiation of (*E*)-*N*-Boc-*N*-(*p*-methoxyphenyl)-3-cyclohexylallylamine **53** (Scheme 14).⁵⁴ To begin with, *n*-BuLi (1.2 equiv) was added to a premixed solution of substrate **53** (1 equiv) and (–)-sparteine (1.2 equiv) in toluene at –73 °C. Three major peaks are seen in this reaction sequence, the starting substrate **53** at 1695 cm⁻¹, which decreases upon addition of *n*-BuLi (Figure 3). A peak at lower wavenumber, due to a reduced bond order, forms at 1640 cm⁻¹, which can be attributed to the lithiated species **55**. In this species, the strong lithium to carbonyl oxygen coordination leads to the reduced bond order of the carbonyl group. The third peak, at an intermediate wavenumber of 1675 cm⁻¹, appears rapidly upon the addition of *n*-BuLi, and then decays over time. This can be attributed to the coordination complex **54**, also called the pre-lithiated species, where there is coordination between the lithium cation and carbonyl group, leading to a reduced bond order and, therefore, lower wavenumber. The coordination is not as strong as for the lithiated species **42**, leading to a wavenumber of intermediate magnitude between the starting material and lithiated species. Importantly, the three peaks are sharp signals that are not overlapped, and so reliable information could be obtained from this analysis (Figure 3). Interestingly, Beak noted that the addition of *n*-BuLi in the absence of (–)-sparteine led to only the pre-lithiated complex peak at 1675 cm⁻¹, which was persistent under these diamine free conditions. Upon the addition of (–)-sparteine, the pre-lithiated complex was then converted to the lithiated species **55**. Beak noted that this observation could be used to design a process that is catalytic in (–)-sparteine, however, this would require an electrophile which does not react with free alkylolithiums in solution. The group of



Scheme 18: Wavenumbers observed for the lithiation of carbamate **53** with *n*-BuLi at low temperatures. The wavenumber decreases upon stronger lithium–oxygen coordination.

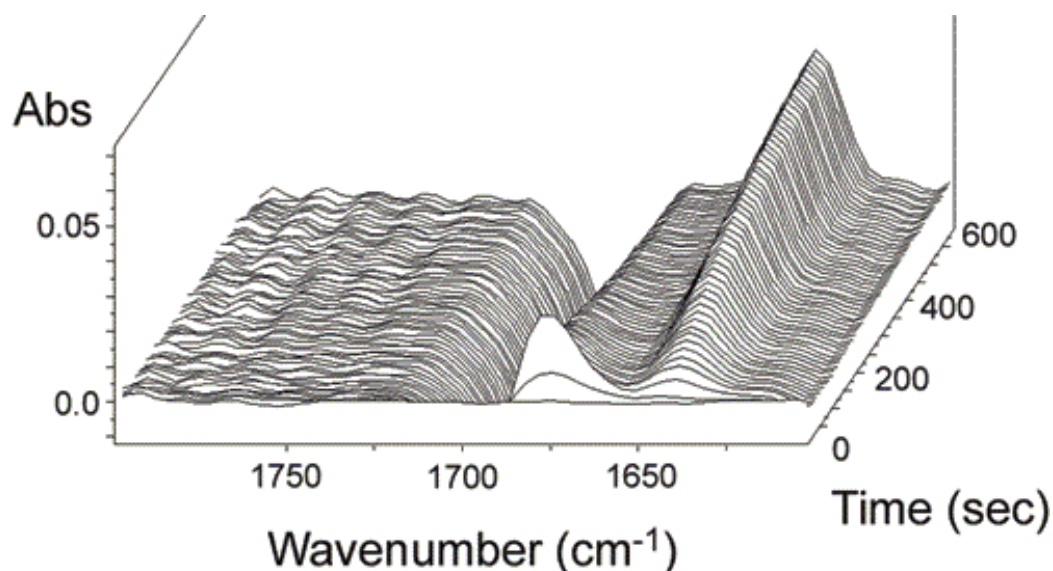
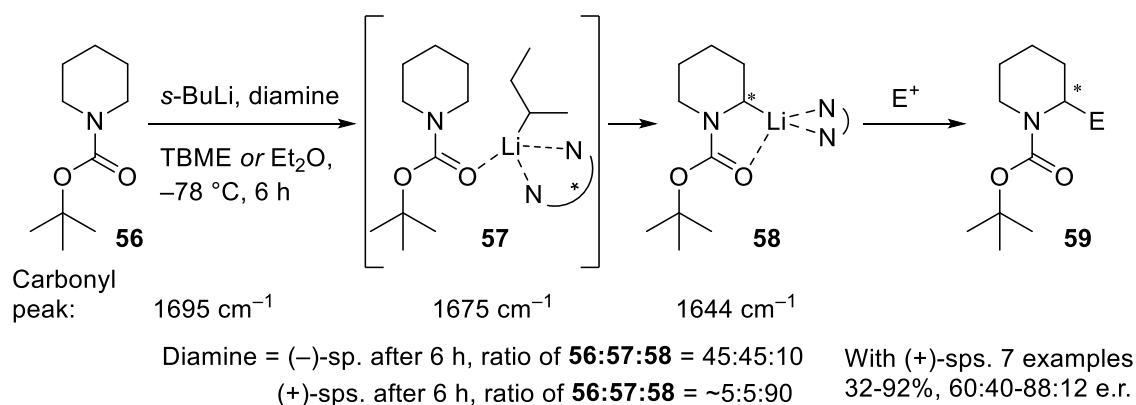


Figure 3: Reproduced from ref⁵⁴. 3D in situ IR trace produced by Beak, for the lithiation of carbamate **53**. Starting material can be seen as the peak that decreases below Abs = 0 at 1695 cm⁻¹, due to the instrument being referenced with the substrate already in solution. The pre-lithiated complex **54** is at 1675 cm⁻¹ and is transient. The lithiated species **55** is observed at the lowest wavenumber of 1640 cm⁻¹.

O'Brien has used in situ IR spectroscopy monitoring to study the lithiation and electrophilic trapping of *N*-Boc piperidine **56** (Scheme 19/figure 5).⁵⁵ This substrate was known to give poor yields (~10%) after lithiation and trapping, and so O'Brien undertook an optimisation using in situ IR monitoring. They applied the known, poor yielding, conditions to the lithiation of piperidine **56**, which used (-)-sparteine. As in Beak's previous work, they observed three different peaks (Scheme 19/figure 4). However, even after 6 hours, the lithiated species **58** was still only a minor component of the reaction. O'Brien then applied modified conditions, using the (+)-sparteine surrogate developed in his lab, and saw a vast improvement in yield after lithiation and trapping (~80%).



Scheme 19: O'Brien's in situ IR optimisation of the lithiation of *N*-Boc-piperidine **56**. By using the (+)-sparteine surrogate ((+)-sps) developed in his lab, they were able to achieve an enantioselective lithiation of the substrate in ~6 h.

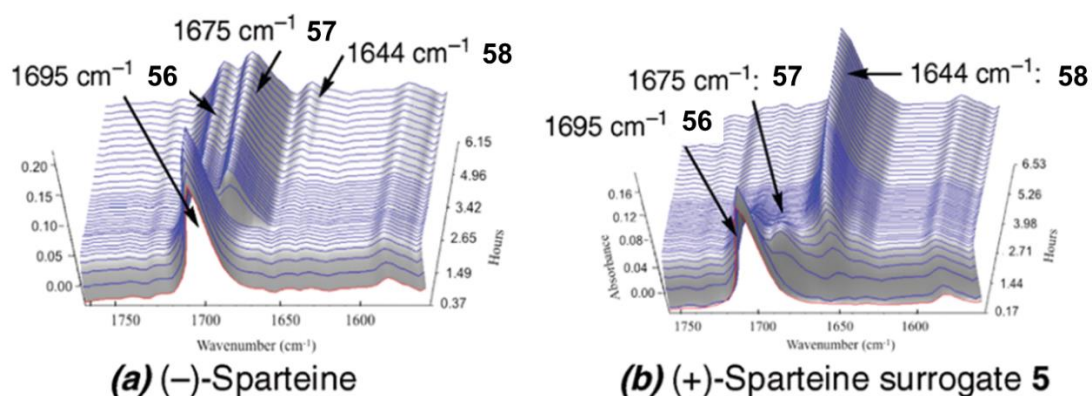
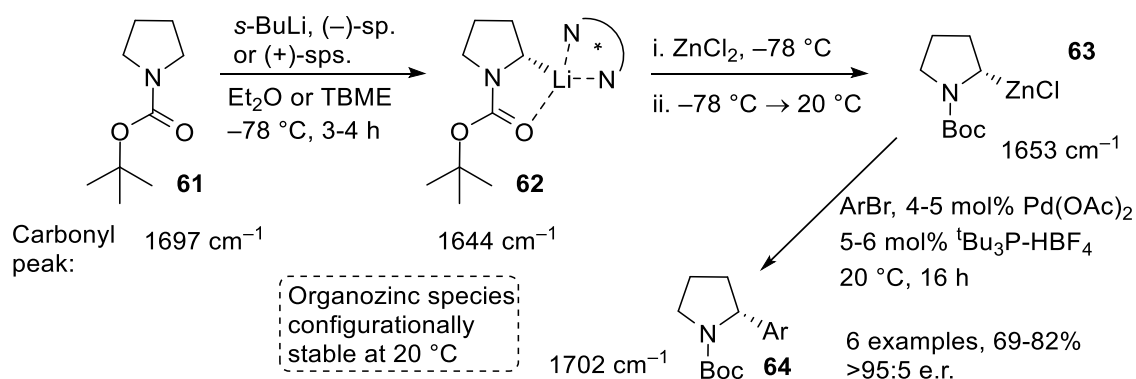


Figure 4: Reproduced from ref⁵⁵. 3D in situ IR traces from O'Brien's *N*-Boc-piperidine optimisation. The trace for the reaction with (-)-sparteine has significantly less lithiated species after 6 hours in comparison with the trace for the (+)-sparteine surrogate.

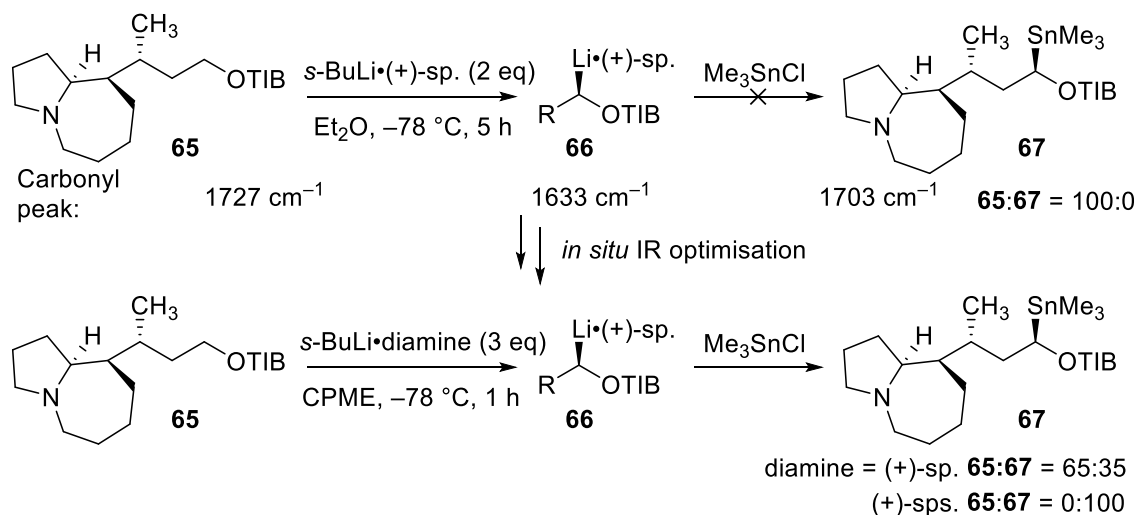
Presumably, the (+)-sparteine surrogate, as a less hindered diamine than (-)-sparteine, promotes a more rapid and facile lithiation due to the less hindered active complex it forms with *s*-BuLi. However, the less hindered diamine should lead to an easier electrophilic trapping, but this was not observed in all cases, and so a diamine-free protocol was developed, by tin–lithium exchange from the corresponding stannane. O'Brien has since expanded this analysis to a series of substrates, usually concerning lithiation and subsequent trapping procedures. One example includes a transmetallation event of a lithiated *N*-Boc pyrrolidine to the corresponding organozinc compound for a Negishi coupling to give α -arylated products **64** (Scheme 16).⁵⁶ As before, the carbonyl peak for the starting substrate **60** can be seen at 1697 cm^{-1} , which is then replaced by a peak at 1644 cm^{-1} upon the addition of *s*-BuLi and (-)-sparteine, corresponding to the lithiated species **61**. The lithiation time was seen to be only 1 hour, not the 5 to 6 hours normally used for this substrate, though the authors use 3–4 h throughout their optimisation. The lithiated species was then transmetallated to the organozinc compound **62** by addition of ZnCl_2 at $-78\text{ }^\circ\text{C}$. The structure **62** drawn in scheme 20 is for simplicity; in solution it would most likely be a mixture of aggregates. Interestingly, the transmetallation did not occur at low temperature, but upon warming to $20\text{ }^\circ\text{C}$. As high e.r. values were observed ($>95:5$) this means the transmetallation must occur below $-60\text{ }^\circ\text{C}$, as the lithiated species are not configurationally stable above $-60\text{ }^\circ\text{C}$, and that the organozinc compound must be configurationally stable at $20\text{ }^\circ\text{C}$. The peak for the organozinc compound was seen at 1653 cm^{-1} , an intermediate wavenumber between starting material and lithiated species, which demonstrates that alternative metalated species can be observed by in situ IR spectroscopy separate from starting materials or



Scheme 20: O'Brien's enantioselective lithiation, subsequent transmetalation with ZnCl_2 and Negishi coupling of *N*-Boc-pyrrolidines. All species carbonyl peaks along the reaction pathway have different wavenumbers, allowing for full analysis of the reaction by *in situ* IR spectroscopy.

lithiated species. The wavenumber of the peak for the organozinc compound is intermediate due to the presence of lithium cations in solution, coordinating to the carbonyl, but more importantly due to the metalate/carbanion character of the carbon bonded to zinc. This negative charge creates an alpha effect,⁵⁷ which pushes more electron density into the carbonyl, lowering the bond order. This alpha effect will have a different magnitude for different metals, depending on their electronegativity.

The Aggarwal group has demonstrated the use of *in situ* IR spectroscopy in the optimisation of the lithiation of TIB ester **65** (Scheme 21) in the total synthesis of (-)-stemaphylline.⁴⁵ The standard conditions for lithiation, *s*-BuLi and (+)-sparteine in Et_2O for 5 h, gave no evidence of lithiation after performing lithiation-trapping studies.



Scheme 21: Use of *in situ* IR in the optimisation of the lithiation of TIB ester **65**. The authors found higher equivalents of *s*-BuLi, a switch to O'Brien's sparteine surrogate and using CPME instead of Et_2O essential for full lithiation.

However, by changing to (+)-sparteine surrogate, a less hindered diamine, and using cyclopentylmethyl ether (CPME) as opposed to Et₂O, full lithiation could be achieved after 1 h at -78 °C. As with the observations by O'Brien, the less hindered nature of the (+)-sparteine surrogate seems to promote a far more active lithiation complex. The lithiated species could then be trapped with Me₃SnCl at -78 °C to give the stannane **67**. The in situ IR spectroscopy studies demonstrated that the trapping occurred as quickly as the electrophile was added. All the species along the reaction pathway exhibit different chemical shifts, the stannane coming at reduced wavenumber to the starting material due to increased metalate character of the α-carbon, generating a greater alpha effect and reducing the bond order of the carbonyl. The authors also demonstrated that upon trapping the lithiated carbenoid **66** with a primary boronic ester, full borylation occurred after 45 minutes as observed by ¹¹B NMR analysis, although in situ IR spectroscopy was not used to monitor this step.

1.4 Aims

As described above, the lithiation–borylation process for stabilised carbamates/benzoates (aryl, for example) is typically facile, with rapid and (usually) high yielding elementary steps (lithiation, borylation, and 1,2-migration).^{38,41} However, when using simple alkyl systems, which provides a more general way to disconnect natural products, for example, the three elementary steps of a lithiation–borylation process are more difficult, and typically require optimisation. This was exemplified in Aggarwal's synthesis of (-)-stemaphylline, where in situ IR spectroscopy was used to optimise a difficult lithiation of an alkyl benzoate.⁴⁵ The main aim of this project was to explore the lithiation and borylation of a series of alkyl carbamates and benzoates using in situ IR spectroscopy, with different solvents, for example, to provide useful data to the chemist in case of troubleshooting.

2 Results and Discussion

2.1 Data collection

Some of the initial results in this section were obtained by Simon Veth and Ana Varela and are noted as such in the table footnotes. As initial work for this project, these results are essential for discussion. This work (sections 2.2–2.6) forms part of a publication: R. C. Mykura, S. Veth, A. Varela, L. Dewis, J. J. Farndon, E. L. Myers, V. K. Aggarwal, *J. Am. Chem. Soc.* **2018**, *140*, 14677-14686.

2.2 Initial comparison of directing groups

The in situ IR spectra for the lithiation and borylation of ethyl carbamate and ethyl TIB ester under standard conditions are shown in figures 5 and 6. Importantly, the spectra demonstrate that the lithiation–borylation reaction can be followed by in situ IR spectroscopy, as the peaks are intense and do not overlap with each other or solvent. The TIB ester shows a carbonyl peak at $\sim 1730\text{ cm}^{-1}$, and the carbamate has a carbonyl peak at 1697 cm^{-1} . These are fully consistent with the wavenumbers seen for the compounds taken on an FT-IR spectrometer, and with previous work on in situ IR spectroscopy from the groups of O'Brien and Aggarwal.^{45,55} The difference in wavenumber between the two substrates reflects the difference in bond order determined by the donation of the nitrogen lone pair on the carbamate into the carbonyl group. Upon the addition of *s*-BuLi (1.2 equiv based on substrate) to the reaction mixture containing substrate and (+)-sparteine (1.2 equiv based on substrate, 1:1 with *s*-BuLi), the peak attributed to the starting materials **68/40** (blue line) decreases in intensity, with an increase in intensity of a peak at reduced wavenumber; 1633 cm^{-1} for the TIB ester **40** and 1616 cm^{-1} for the carbamate

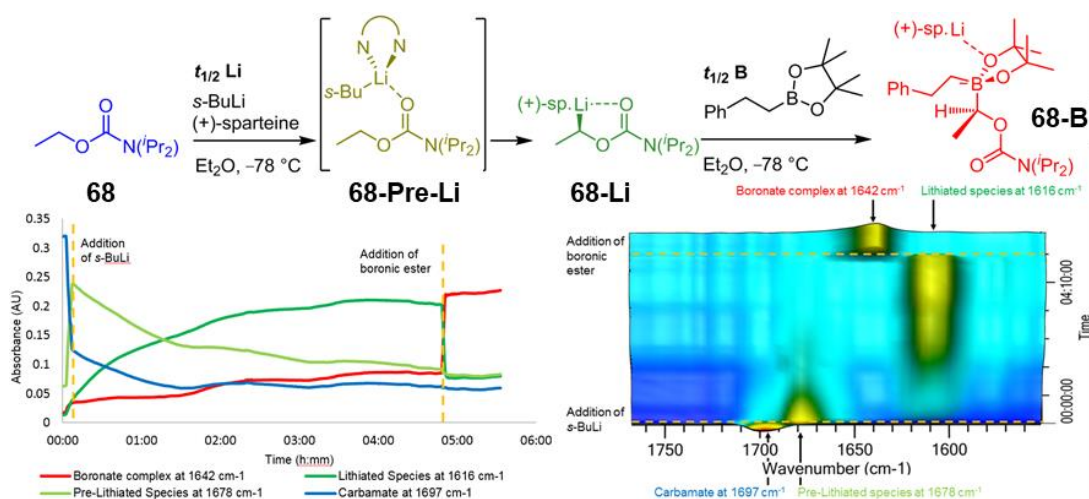


Figure 5: 2D and 3D trace for the lithiation and borylation of ethyl carbamate with phenethylboronic acid pinacol ester.

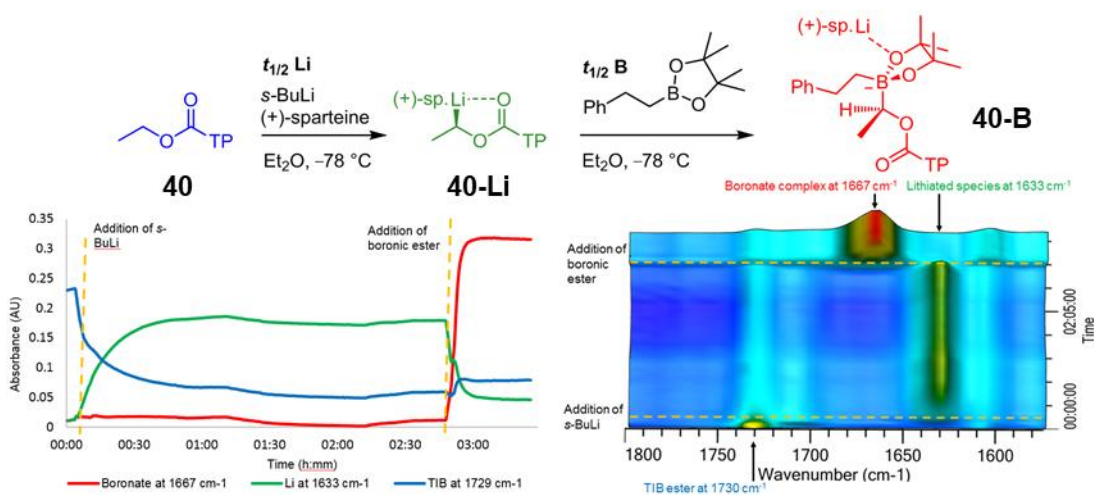


Figure 6: 2D and 3D trace for the lithiation and borylation of ethyl TIB ester with phenethylboronic acid pinacol ester.

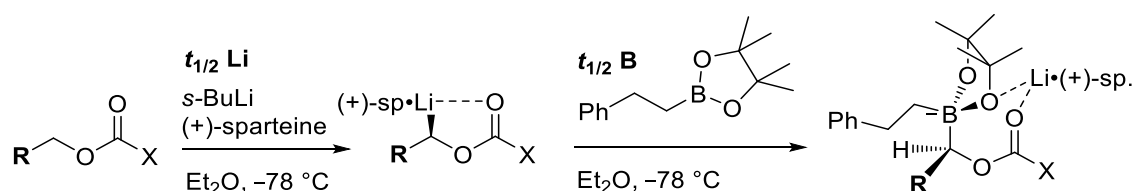
68. This signal at reduced wavenumber can be attributed to the lithiated species **68-Li/40-Li** (dark green line), the reduced wavenumber caused by the strong lithium–oxygen coordination and the alpha effect. The peak for the lithiated species does not change over time, and so the lithiated species must be chemically stable under the reaction conditions for extended periods of time, as expected. The spectra for the two substrates differ upon lithiation, as the carbamate shows another, transient, peak at an intermediate wavenumber of 1678 cm^{-1} (light green line). This can be attributed to the pre-lithiated complex **68-Pre-Li**, which has been observed before by O’Brien for similar substrates.⁵⁵ The TIB ester **40** does not show a pre-lithiated species under these conditions. Presumably, the proton transfer is now rapid enough, compared to the carbamate, that the pre-lithiated species is not formed to a high enough concentration to be detected by the instrument. Once the lithiation has gone to completion, phenethylboronic acid pinacol ester is then added, and the signals for the lithiated species drop, with appearance of a new peak at intermediate wavenumber; 1667 cm^{-1} for the TIB ester and 1642 cm^{-1} for the carbamate. This is the boronate complex **68-B/40-B** (red line), where the lithium carbenoid has undergone lithium–boron exchange. The intermediate wavenumber of the boronate complex is due to the presence of lithium cations in solution, which will most likely still coordinate the carbonyl oxygen, and due to the metalate character of the carbon adjacent to the directing group generating an alpha effect, as seen previously for O’Brien’s organozinc species **63** (Scheme 20, section 1.3.1). Immediate analysis of these two graphs indicates that the ethyl carbamate undergoes proton–lithium exchange at a reduced rate compared to the ethyl TIB ester. It is convenient to express the rate of reaction as a half-life ($t_{1/2}\text{ Li/B}$), referring to the time taken for the peak to reach half of its

maximum intensity. Analysis of figures 5 and 6 produces $t_{1/2} Li = 30$ min for the lithiation of ethyl carbamate and $t_{1/2} Li = 8$ min for ethyl TIB ester. These results, therefore, do not follow the same pattern for the benzylic substrates examined by Garcia-Rio and co-workers, who observed a faster lithiation for benzylic carbamates over TIB esters.²⁵ Thermodynamically, the two sets of substrates (benzylic⁵⁸ and alkyl⁵⁹ carbamates versus benzoates) have similar pK_a values. For benzylic substrates, the lithiation is facile (due to the inherent higher acidity of the benzylic protons), however this inherent acidity is removed for the alkyl systems, such that other factors must dominate (discussed further in section 2.4). The carbamate demonstrates an extremely rapid lithium–boron exchange, in which the carbanion is consumed as quickly as the boronic ester is added, defined as $t_{1/2} B < 0.25$ min, as the instrument scans once every 15 seconds. The TIB ester undergoes a slower, but still rapid, borylation with $t_{1/2} B = 2$ min. The difference in borylation half-lives most likely stems from steric crowding around the lithium carbenoid, the TIB ester generating a more sterically hindered environment than the carbamate. Both substrates then underwent 1,2-rearrangement under standard conditions and the homologated boronic ester products were oxidised (aq. $H_2O_2/NaOH$) to the corresponding alcohols, which were received in moderate yields (44% for carbamate **68** and 45% for benzoate **40**) and with high e.r. values of 98:2 and 95:5 for the carbamate and benzoate respectively, as expected.

During this project, a set of standard conditions were used such that experiments could be compared directly. The substrate (benzoate/carbamate) and diamine (1.2 equiv) are dissolved in the solvent (0.3 M with respect to substrate). The lithiation is performed with *s*-BuLi (1.2 equiv) at -78 °C. Once the lithiation is complete, which is defined as when the absorbance of the peak no longer changes, the boronic ester (1.2 equiv) is added as a 1.0 M solution. The additions are performed manually and dropwise over 3–5 minutes.

2.3 Effect of steric hindrance at the β position

By substituting additional methyl groups at the β position of the substrate, the effect of steric hindrance on lithiation and borylation was explored (table 1). For the series of carbamates, the half-life varies from $t_{1/2} \text{ Li} = 30$ min for ethyl carbamate (entry 1) to $t_{1/2} \text{ Li} = 81$ min for isobutyl carbamate (entry 3), the neopentyl carbamate did not undergo measurable lithiation under these conditions (entry 5). Interestingly, when moving from ethyl to propyl carbamate, entries 1 and 2, the half-life of lithiation does not increase by a significant factor. Moving from the ethyl to propyl substrate for the TIB ester does result in a significant difference in half-life; the TIB ester series demonstrates a doubling of half-life upon addition of each methyl group, entries 6 – 9, from $t_{1/2} = 8$ min for ethyl TIB ester to $t_{1/2} = 94$ min for neopentyl TIB ester. This suggests a more rapid increase in steric environment for the TIB ester than for the carbamate upon addition of a β methyl group, indicating the propyl carbamate can avoid a sterically crowded conformation the TIB ester cannot. This in turn could be due to the more congested environment generated by the isopropyl groups of the TIB ester, which lie orthogonal to the carbonyl group. A popular cyclic carbamate, isobutyl 2,2,4,4-tetramethyloxazolidine-3-carboxylate (Cby, entry 4) was also studied under the same reaction conditions. This substrate demonstrated a lithiation half-life significantly larger than the corresponding diisopropyl carbamate.



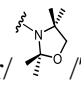
Entry	R/X/Substrate	$t_{1/2} \text{ Li}$ (min)	$t_{1/2} \text{ B}$ (min)	Yield (%)	e.r.
1 ^a	Me/ <i>NiPr</i> ₂ / 68	30	<0.25	44	98:2
2 ^a	Et/ <i>NiPr</i> ₂ / 69	33	<0.25	60	98:2
3 ^a	<i>iPr</i> / <i>NiPr</i> ₂ / 70	81	3	67	98:2
4	 / 71	145	3	28	98:2
5 ^a	<i>t</i> Bu/ <i>NiPr</i> ₂ / 72	-	-	-	-
6 ^a	Me/TP/ 40	8	2	45	95:5
7 ^a	Et/TP/ 73	16	8	77	97:3
8 ^a	<i>iPr</i> /TP/ 74	31	35	66	97:3
9 ^a	<i>t</i> Bu/TP/ 75	94	296	21	99:1

Table 1 Results of increasing steric hindrance at the β -position. Entry 4 = Cby. Yield and e.r. determined after oxidation to the corresponding alcohol (H_2O_2 , NaOH). ^a Reaction performed by S.V./A.V.

The borylation half-lives of the carbamates were rapid across the series, even the slow-to-lithiate Cby group maintained a rapid borylation of $t_{1/2}B = 3$ min (entry 4). The TIB ester was much more sensitive to borylation, the neopentyl variant undergoing an extremely slow borylation of $t_{1/2}B = 296$ min (entry 9). The already hindered and therefore less nucleophilic lithiated TIB ester must be more severely affected by steric factors than the carbamate. That lithium–boron exchange can be so slow in sterically hindered environments is an important observation, and one that should be carefully considered when using lithiation–borylation in synthesis. It is worth noting that the e.r. values for the carbamate series stay constant across the series at 98:2, however for the TIB ester they increase from 95:5 to 99:1 upon increasing steric crowding.

The results above demonstrate that most lithiation–borylation protocols should be reconsidered. The extreme times for lithiation and borylation with some of the more hindered substrates, remembering that the reactions in table 1 use an unhindered, primary boronic ester, demonstrated further the need for an in-depth study into the optimisation of the lithiation–borylation procedure.

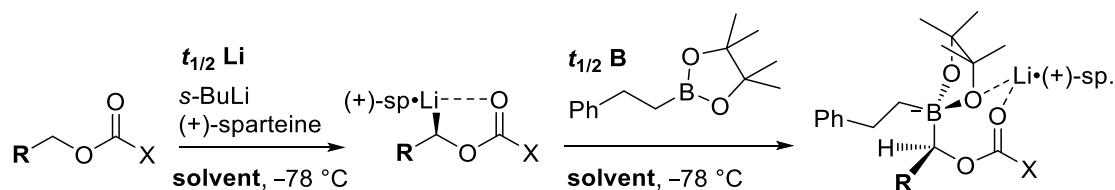
2.4 Effect of solvent

Various solvents are commonly used for the lithiation of Beak's TIB esters and Hoppe's diisopropylcarbamates, usually non-polar, ethereal solvents such as Et₂O, TBME, CPME. THF was used by Beak originally for TIB ester lithiation, however, THF competes with (+)-sparteine for lithium coordination in solution and so leads to reduced e.r. values.^{60,61} CPME has been used previously in the Aggarwal group, as it provides higher yields than other ethereal solvents when lithiating hindered secondary TIB esters, in the presence of 6 equiv. TMEDA at –60 °C.⁴³ In the same report, the authors also note a decreased yield for lithiations with THF/TMEDA, potentially due to over complexation of the alkyllithium base by THF. Most examples of slow trapping/low yielding reactions of lithiated carbanions by electrophiles are usually solved by generating the lithiated species under diamine-free conditions, from a stannane or other precursor that can undergo exchange with alkyllithiums.^{55,62} The non-ligated lithiated species is now less hindered and undergoes faster trapping with an electrophile. However, the use of different solvents has not been explored to facilitate this step, in the same way it has for lithiation.

To study the effect of solvent on lithiation and borylation, the propyl and isobutyl substrates were used due to their longer half-lives, which are easier to measure. Switching

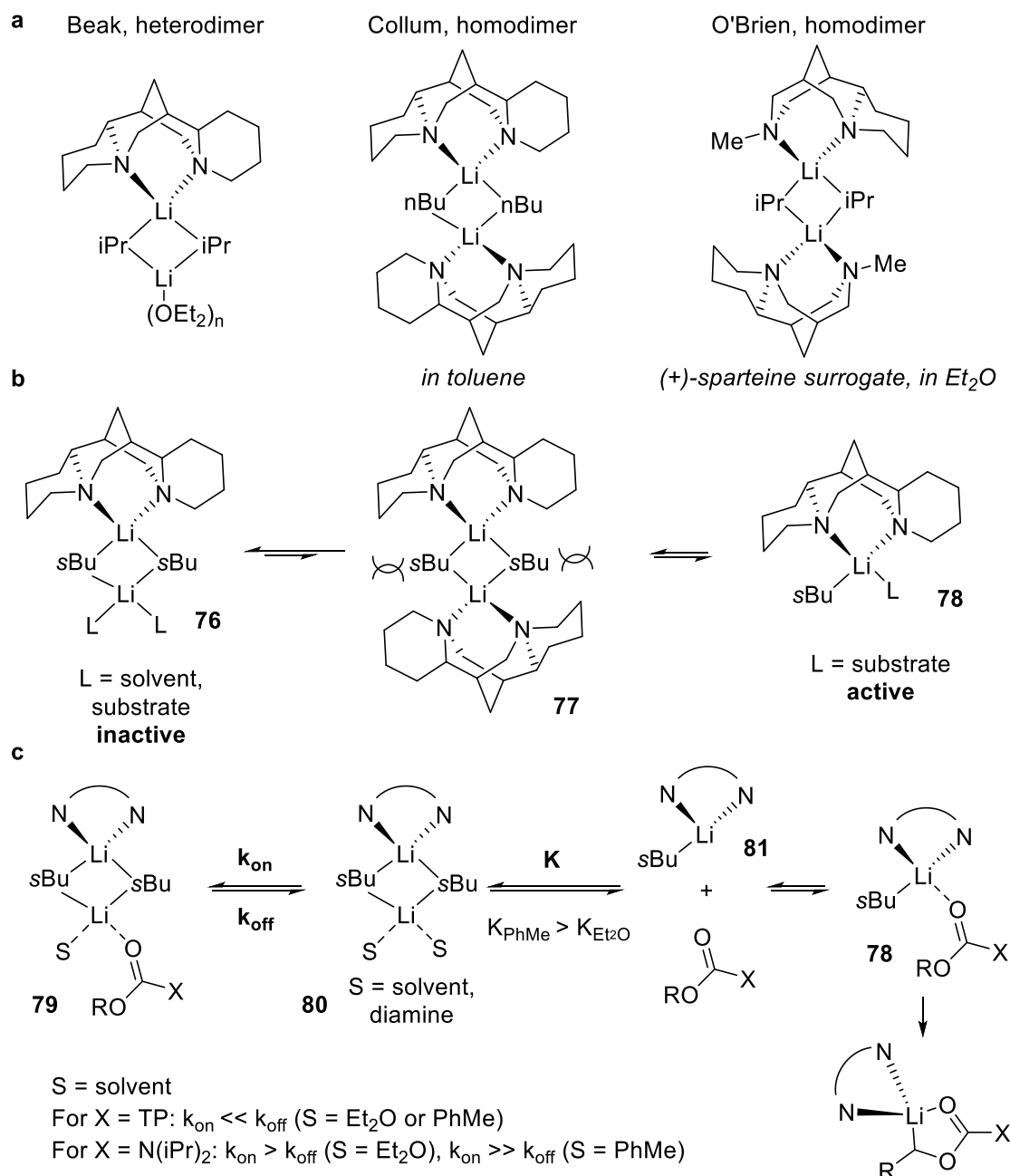
to TBME from Et₂O led to an increase in the lithiation half-lives for both propyl carbamate (entries 1–2, table 2) and propyl/isobutyl TIB ester (entries 4–5/9–10, table 2), to around the same extent. Potentially, this could be due to the more sterically hindered TBME solvent leading to a more sterically hindered active lithiation complex in solution. While hard to rationalise, these data demonstrate TBME should be used only in lithiation–borylation processes where solubility in other ethereal solvents is an issue. The next solvent used for lithiation was toluene, which has been used previously for the lithiation of mesomerically stabilised carbamates by Beak.⁵⁴ The lithiation of propyl and isobutyl carbamate in toluene had a longer half-life compared to those performed over Et₂O (entries 3 and 8), however the corresponding TIB esters demonstrated reduced half-lives (entries 6 and 11).

To attempt to rationalise the differing solvent effect between the two directing groups, their different sizes and coordinating strengths to lithium in solution can be compared. In doing so the differences in reactivity observed more generally between alkyl carbamates and benzoates can be commented on.



Entry	R/X/Substrate	Solvent	$t_{1/2}$ Li (min)	$t_{1/2}$ B (min)
1 ^a	Et/NiPr ₂ / 69	Et ₂ O	33	<0.25
2	Et/NiPr ₂ / 69	TBME	43	<0.25
3	Et/NiPr ₂ / 69	Toluene	66	42
4 ^a	Et/TP/ 73	Et ₂ O	16	8
5	Et/TP/ 73	TBME	26	13
6 ^a	Et/TP/ 73	Toluene	9	501
7 ^a	<i>i</i> Pr/NiPr ₂ / 70	Et ₂ O	145	3.5
8	<i>i</i> Pr/NiPr ₂ / 70	Toluene	195	>50
9 ^a	<i>i</i> Pr/TP/ 74	Et ₂ O	31	35
10 ^a	<i>i</i> Pr/TP/ 74	TBME	52	45
11 ^a	<i>i</i> Pr/TP/ 74	Toluene	15	N.R.

Table 2: Effects of different solvents on lithiation and borylation. The borylation for entry 11 was essentially not observable.. N.R. = not recorded. ^a Reaction performed by S.V/A. V.



Scheme 22: a) solution state structures of various diamine/BuLi complexes; b) our proposed equilibrium between inactive and active *s*-BuLi/diamine complexes, where more strongly coordinating solvents (like Et₂O instead of PhMe) lead to more inactive complex; c) possible equilibria of benzoates and carbamates with *s*-BuLi/diamine complexes.

First, consider the structures of the alkyl lithium/sparteine complexes in solution. Beak and co-workers have shown that *i*-PrLi and (–)-sparteine in Et₂O are present as a 2:1 heterodimer, with a number of coordinated solvent molecules on the non-diamine-ligated lithium (Figure 22a).²⁴ Collum and co-workers have shown less hindered *n*-BuLi to be a homodimer with (–)-sparteine in toluene,⁶³ similarly to O'Brien and co-workers who have shown that the less hindered (+)-sparteine surrogate and *i*-PrLi form a homodimer in Et₂O.⁶¹ The contribution towards stabilisation of the heterodimer **76** (from Beak's study)

by non-polar solvents like toluene is likely to be less than for ethereal solvents, potentially leading to higher concentrations of labile homodimer **77** and/or mono-ligated *s*-BuLi **78** (Figure 22b). Overall, if this equilibrium is operating, this means the coordination between the substrate and *s*-BuLi is likely to be more rapid therefore leading to a faster lithiation.

The large size of the 2,4,6-triisopropylphenyl group ($X = TP$, figure 22c) of the TIB ester likely impedes the formation of stable heterodimers **79** (that is, $k_{on} \ll k_{off}$, figure 22c) which are unable to undergo lithium–proton exchange. Avoiding a high concentration of heterodimer **79** therefore allows formation of active monodentate *s*-BuLi complex **81**, which can then combine with the substrate and form a productive complex **78** for lithium–proton exchange. Importantly, the concentration of monodentate *s*-BuLi **81** (the magnitude of **K**, figure 22c) is greater under the conditions using toluene than Et₂O. This can account for the rapid lithiation of alkyl TIB esters and the reduction in lithiation half-life for them when moving from Et₂O to toluene.

The carbamate ($X = N(i-Pr)_2$), however, with its smaller size and more strongly complexing carbonyl group than the benzoate, presumably rapidly forms stable complexes **79** ($k_{on} > k_{off}$) unable to undergo proton–lithium exchange. These complexes **79** can be thought of as “parasitic-complexes”. This leads to a reduced concentration of monodentate *s*-BuLi and free carbamate, and therefore the rate of “active-complex” formation is reduced. With weakly-coordinating toluene as solvent, the rate of carbamate displacement from the complex is further reduced ($k_{on} \gg k_{off}$). This can account for the slower lithiation of alkyl carbamates and increase in half-life when switching from Et₂O to toluene.

The IR spectrum for the lithiation of the TIB esters in toluene now show “pre-lithiated species” immediately upon addition of substrate (Figure 7), indicating the more rapid coordination of substrate to *s*-BuLi complex. The carbamate shows this peak upon lithiation in Et₂O and toluene, but in toluene the lithiation does not go to completion, that is, the peak for the “pre-lithiated species” remains when the lithiated species peak plateaus. This supports the idea that the species responsible for this peak may be non-productive complexes, unable to undergo lithiation and responsible for longer lithiations seen with carbamates generally.

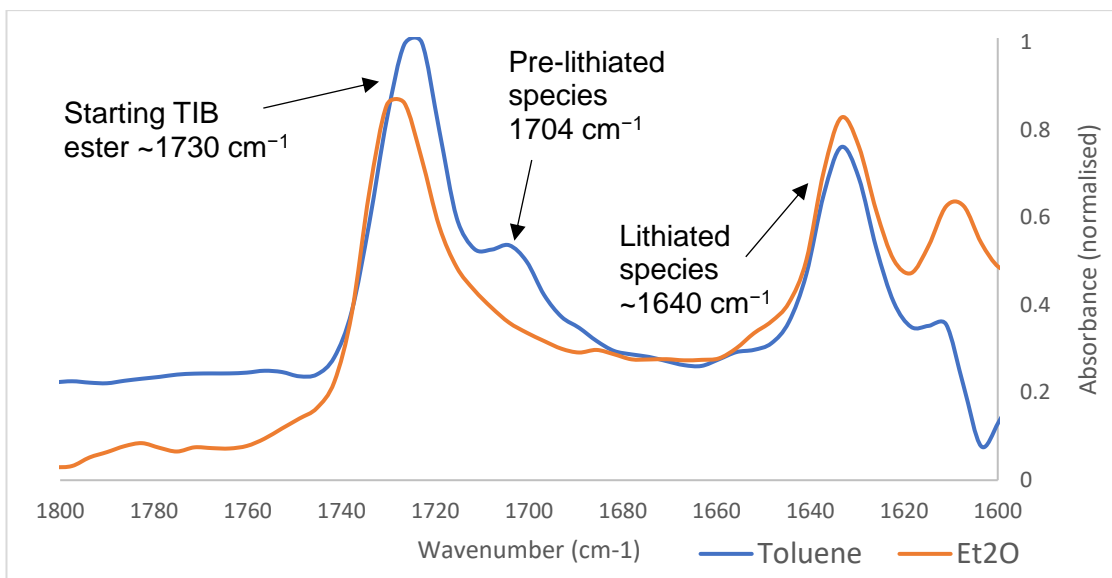
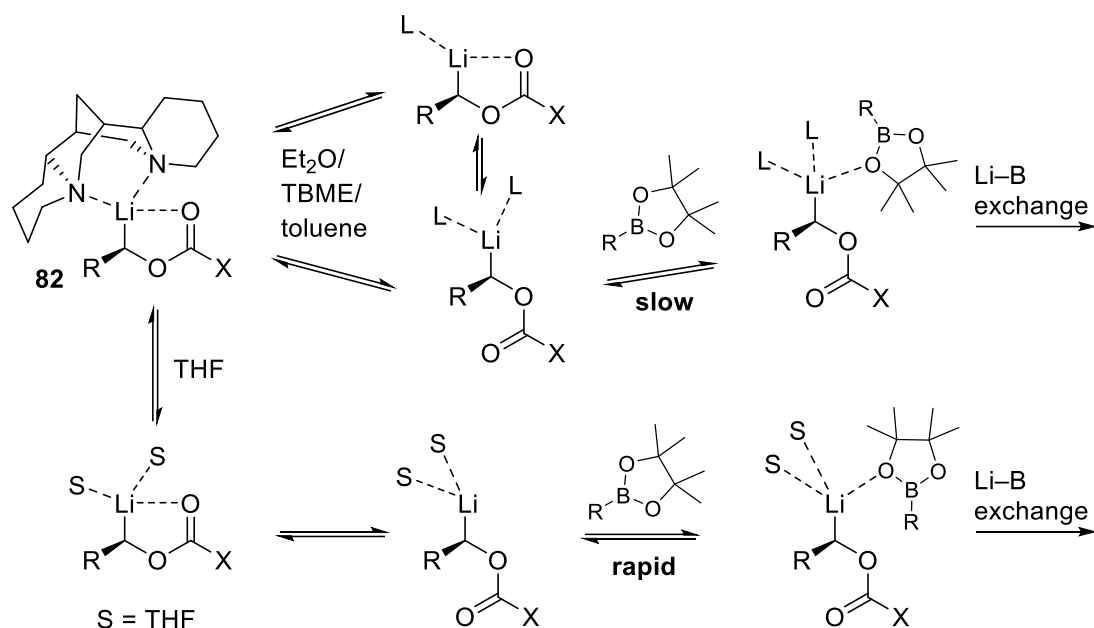


Figure 7: IR spectrum for the lithiation of isobutyl TIB ester **74** in toluene (blue line) and Et₂O (orange line) at 30 minutes. The peaks at ~1730 cm⁻¹ are the starting material, with the pre-lithiated species at 1704 cm⁻¹ for the lithiation in toluene. Lithiated species can be seen at ~1640 cm⁻¹.

Further evidence for these equilibria (Scheme 22c) was found when we performed pseudo 1st order studies under conditions developed by Beak.⁵⁴ Following the reaction by in situ IR spectroscopy, we added ethyl carbamate **68** (0.02 M, 1 equiv.) to a 1:1 mixture of *s*-BuLi:(+)-sparteine (0.69 M, 28 equiv.) in 1:1.5 Et₂O:cyclohexane. Only formation of a species with an IR signal that had been assigned to the “pre-lithiated” complex (1678 cm⁻¹) was observed. The same result was observed with propyl and isobutyl carbamate, although the “pre-lithiated” complexes formed more slowly. Under these conditions, we believe the carbamate is quickly sequestered into complex **79**, as the concentration of the heterodimer **76** (Scheme 22b) is very high, which cannot undergo lithium–proton exchange, supporting the hypothesis. Under the same conditions, ethyl benzoate **40** does undergo lithiation, again supporting the hypothesis that benzoates do not form the same “parasitic complexes” to a large extent. Further discussion of how to study the differences between alkyl benzoates and carbamates is given in the outlook.

The effect of solvent on the borylation step was assessed next (table 2). TBME increased the half-life of borylation of both the propyl and isobutyl TIB esters (entries 5 and 10, table 2), however no effect was seen for the propyl carbamate, which could be due to the quick borylation of this substrate, $t_{1/2} B < 0.25$ min. In all cases, the borylation half-life in toluene was increased by a large factor for both directing groups (entries 3, 6, 8 and 11), the isobutyl TIB ester not undergoing borylation at a measurable rate. This solvent effect can be rationalised by considering the structure of the lithiated species **82** (Scheme 23),



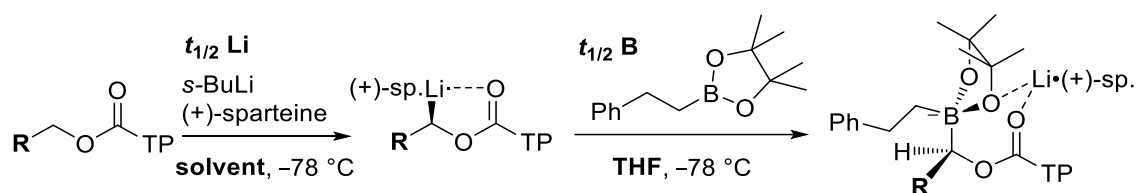
Scheme 23: Diverging fast and slow pathways for the borylation of lithiated carbenoids in poorly coordinating solvents (Et_2O /TBME/toluene) and THF, a strongly coordinating solvent.

which should have the diamine coordinated to the lithium, as lithiations cannot be performed with a sub-stoichiometric amount of diamine. This diamine, especially if it is sterically demanding like sparteine, is likely to hinder the carbanion to a large extent. For lithium–boron exchange to take place, the diamine or carbonyl oxygen is needed to disassociate from the lithium atom to allow for lithium–oxygen coordination (in the case of reactions with boronic esters) and then lithium–boron exchange can occur. This idea of lithium–oxygen pre-coordination is supported by the stereodivergent trapping of benzylic carbamates with either boronic esters or boranes.³⁸

Et_2O , TBME and toluene, as relatively poorly coordinating solvents, are less able to coordinate to the lithium of the carbanion and therefore the lability of ligands on lithium is reduced, leading to a more sterically crowded lithium carbenoid and slower borylation (slow pathway, scheme 23). The disassociation of the carbonyl oxygen of the directing group from the lithium to allow for lithium–boron exchange could also be a valid pathway and is probably likely in these relatively poorly coordinating solvents.

We envisaged replacing the bulky diamine ligand (which can now be removed as the pertinent stereocentre has been set in the lithiation step) with smaller solvent ligands to allow for facile borylation. We used THF as the additive, as THF is known to compete with sparteine for lithium coordination.⁶¹ The addition of THF (0.6 equiv based on substrate) to the borylation of propyl TIB ester resulted in a significant increase in the

rate of borylation (table 3). The addition of the boronic ester as a solution in THF (1.0 M) afforded an extremely rapid borylation, $t_{1/2} B = 2$ min (entry 2, table 3). This was reflected in the borylation of the more sterically hindered substrates, entries 3 and 4. THF can coordinate preferentially over sparteine to the lithium atom of the carbenoid, which leads to labile and not sterically crowded ligands on lithium. The boronic ester can then easily coordinate, to give lithium–boron exchange. Importantly, the e.r. values for these reactions remained unaffected by the addition of the boronic ester in THF, indicating that this modification should become part of most lithiation–borylation protocols.



Entry	R	Solvent A	$t_{1/2}$ Li (min)	$t_{1/2}$ B (min)	e.r.	$t_{1/2}$ B (min) ^b
1 ^a	Me/ 40	Toluene	7	<0.25	95:5	165
2 ^a	Et/ 73	Toluene	9	2	95:5	501
3 ^a	<i>i</i> Pr/ 74	Toluene	15	11	97:3	N.R.
4 ^a	<i>t</i> Bu/ 75	Et ₂ O	78	15	98:2	296

Table 3: Lithiation and borylation half-lives when using toluene/THF conditions ^aReaction performed by S.V./A.V. . ^bThe boronic ester was added as a solution in Solvent A.

2.5 Effect of different organoboron partners

The concept of lithium–boron exchange being preceded by coordination of one of the pinacol oxygens to lithium has been invoked for the stereodivergent trapping of lithiated benzylic carbamates with boranes versus boronic esters (Scheme 13, section 1.2.2).³⁸ The boronic ester coordinates to the lithium ion and so traps with retention, the borane cannot coordinate and so traps with inversion. Boranes are more Lewis acidic than boronic esters, due to the lack of electron donation into their empty *p* orbital, and so are more reactive. However, we were keen to establish whether the lack of Lewis basic pinacol oxygens could lead to lower reactivity than anticipated with a lithium carbenoid, compared to a boronic ester. First, the reaction of tributylborane with isobutyl TIB ester was studied (Figure 8). The isobutyl TIB ester was used due to its easy to measure, relatively long, borylation half-life, compared to carbamates or the less sterically hindered TIB esters. The lithiated species was generated under standard conditions in the presence of *s*-BuLi and (+)sparteine. However, addition of tributylborane (1.0 M solution in Et₂O, 1.2 equiv

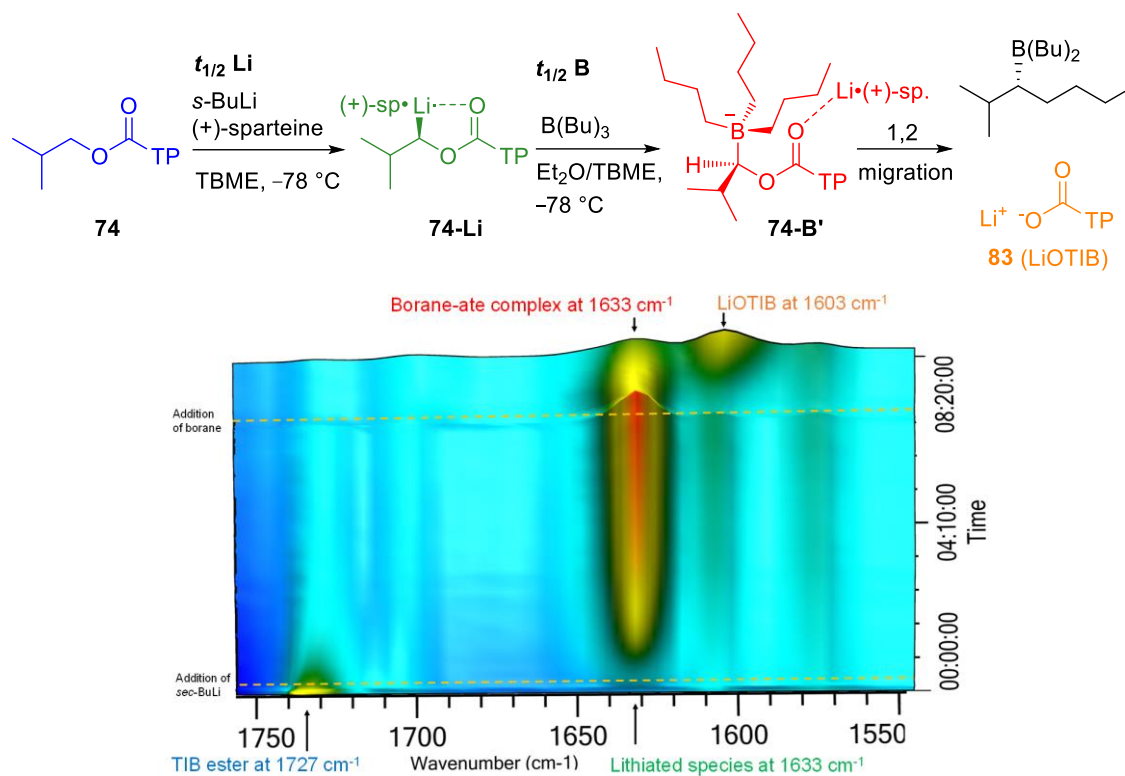
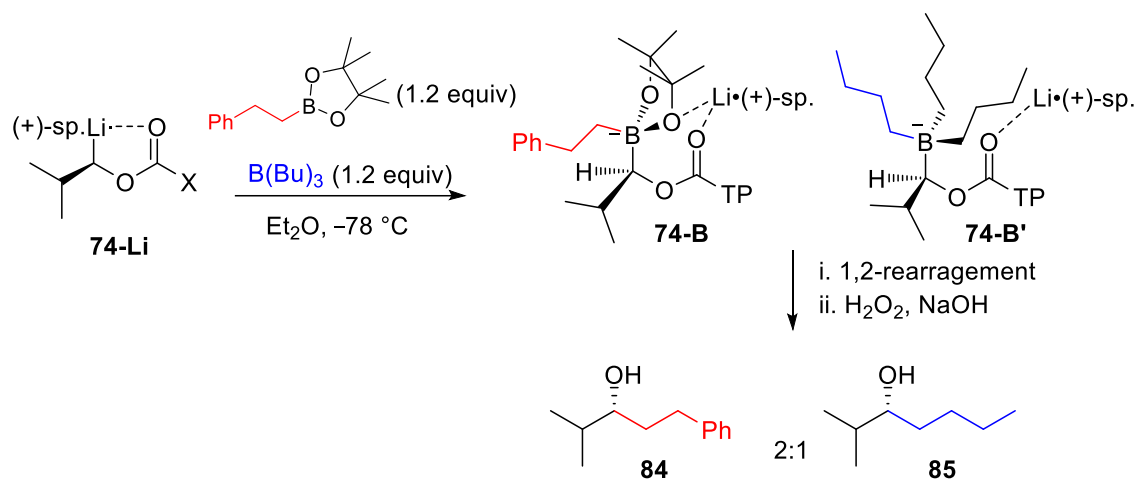


Figure 8: 3D trace of the lithiation and borylation of isobutyl TIB ester with tributylborane.

based on substrate) to a solution of lithiated isobutyl TIB ester **74-Li** did not demonstrate the intermediate peak for the boronate complex usually observed ($\sim 1666\text{ cm}^{-1}$ for a TIB ester). Instead, only a slow decrease in the peak at the wavenumber of the lithiated species was observed, with the appearance of a broad peak at lower wavenumber of $\sim 1600\text{ cm}^{-1}$.

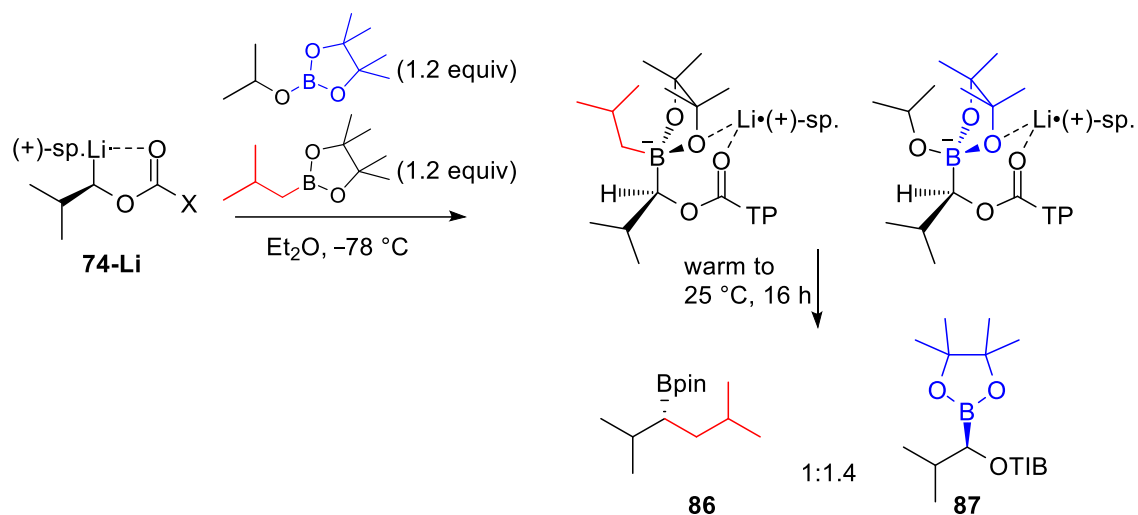
It is apparent that the borane derived boronate complex, or borane-ate complex, **74-B'**, has no additional sites for the associated lithium cation to coordinate to apart from the carbonyl oxygen, and so produces a peak at the same wavenumber as the lithiated species. The boron atom, devoid of electronegative oxygen atoms, could also generate an alpha effect greater in magnitude therefore lowering the bond order of the carbonyl in the borane-ate complex (versus the boronic ester-ate complex). This borane-ate complex is far more reactive than the equivalent boronic ester-ate complex, and undergoes 1,2-rearrangement even at $-78\text{ }^{\circ}\text{C}$, $t_{1/2}$ 1,2-migration = 134 min. This facile 1,2-rearrangement could also be due to the position of the lithium ion, which can only coordinate to the carbonyl group, and the presence of three equivalent migrating groups (compared to a boronic ester which only has one). This means the broad peak at $\sim 1600\text{ cm}^{-1}$ is the lithium salt of the carboxylate leaving group, LiOTIB, **83**. The low wavenumber is to be expected as the carbonyl now has a formal bond order of 1.5. Another experiment demonstrated the 1,2-rearrangement was complete upon warming to



Scheme 24: Competition experiment between phenethyl boronic acid pinacol ester and tributylborane. Ratio is based on isolated yields after chromatography.

room temperature. This overlapping of peaks means that it is difficult to obtain the borylation half-life when trapping with boranes. Instead of in situ IR spectroscopy studies, competition experiments were performed to identify whether the classically less reactive boronic ester could react at a high enough rate to afford product in the presence of the more reactive borane. Rapid addition of a solution of tributylborane (1.2 equiv based on substrate) and phenethyl boronic acid pinacol ester (1.2 equiv based on substrate) in Et₂O (2.0 M with respect to organoboron partners) to a solution of lithiated isobutyl TIB ester, stirring at $-78\text{ }^{\circ}\text{C}$ for 6 hours to ensure full borylation, then overnight at room temperature to ensure full 1,2-rearrangement of the boronic ester-ate complex was performed. After oxidation under standard conditions, with careful exclusion of air to avoid destruction of the homologated borane, the two products were isolated in the ratio 2:1, in favour of the boronic ester derived product (Scheme 24). A similar reaction, with 3-phenylpropyl TIB ester, delivered the two products in a 1:2 ratio, now in favour of the borane derived product.

These competition experiments show that the boronic ester and borane trap with similar rates, even though the boron atom's empty p orbitals have significantly different Lewis acidities. This can be rationalised through the coordination of the Lewis basic pinacol oxygens on the boronic ester prior to lithium–boron exchange, providing a lower energy pathway for the boronic ester and, therefore, similar reaction rates for the boronic ester and borane. Boronic esters are synthetically more useful than boranes as they are mostly stable to air and column chromatography, however for this reason they are viewed as less reactive than boranes. These results show that the boronic ester maintains equivalent



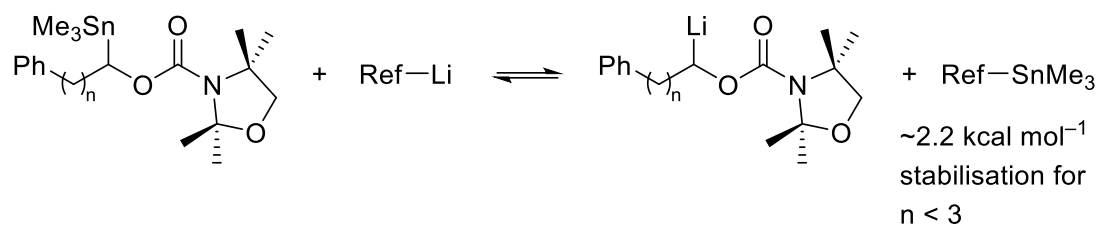
Scheme 25: Competition experiment between isopropoxy borate ester and isobutyl boronic acid pinacol ester. Ratio is based on ^1H NMR analysis of the crude reaction mixture.

reactivity to the borane in the lithiation–borylation reaction, potentially due to a lithium–oxygen coordination.

Next, the borate ester, $\text{B}(\text{OR})_3$, which is less Lewis acidic than the boronic ester, was studied to determine whether the presence of more Lewis basic oxygen sites could promote a more rapid trapping. For this experiment, the commercially available isopropoxy borate ester was used for borylation. A competition experiment, similar to that performed in the borane/boronic ester study, was carried out using the isopropoxy borate ester and isobutyl boronic acid pinacol ester (Scheme 25). After lithiation and borylation, with stirring overnight for full 1,2-rearrangement, the two products could be observed by ^1H NMR analysis of the crude reaction mixture, which gave a ratio of 1:1.4, in favour of the borate ester derived product **66**. These results demonstrate that the presence of Lewis basic oxygen sites on the organoboron partner increases reactivity in the lithiation–borylation reaction, despite the reduction in Lewis acidity, adding evidence towards a prior lithium–oxygen coordination to lithium–boron exchange.

2.6 Effect of a proximal aromatic group

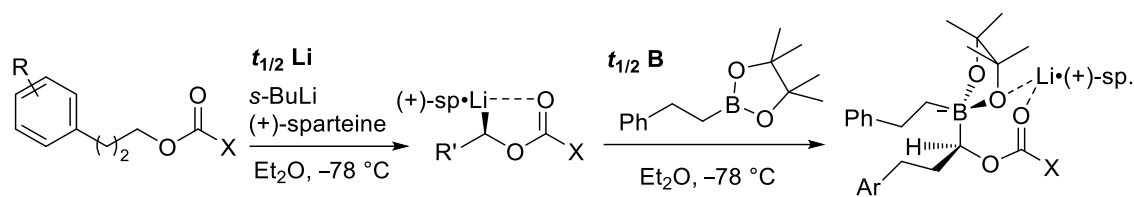
When developing new methodologies in lithiation–borylation chemistry, the 3-phenylpropyl TIB ester or carbamate (**88–91**, see table 4) is often used, as it seems to provide facile lithiation. Sardina and co-workers have shown that presence of a cation– π interaction between the lithium cation of a lithiated carbamate and a proximal phenyl ring or alkene leads to significant stabilisation.⁶⁴ This was measured by the difference in equilibria between a corresponding stannane and reference alkyl lithium, the equilibrium



Scheme 26: The group of Sardina's work on experimentally establishing a cation- π interaction for tethered, proximal aromatic groups. Alkenes also demonstrated the same effect for $n < 3$. The side of the equilibrium is favoured where the lithium ion is bound to the most stable carbanion. Ref-Li = Reference lithiated species.

favours the side where the most stable carbanion is paired with the more electropositive lithium atom (Scheme 26). To investigate whether this interaction could provide significant coordination to lithium to allow for a more facile borylation, through displacement of the diamine ligated to lithium, the 3-phenylpropyl carbamate and TIB ester were prepared and their lithiation and borylation performed under standard conditions. Both substrates exhibited shorter half-lives for lithiation compared to the propyl substrates (entries 1 and 2, table 4 versus entries 2 and 7, table 1).

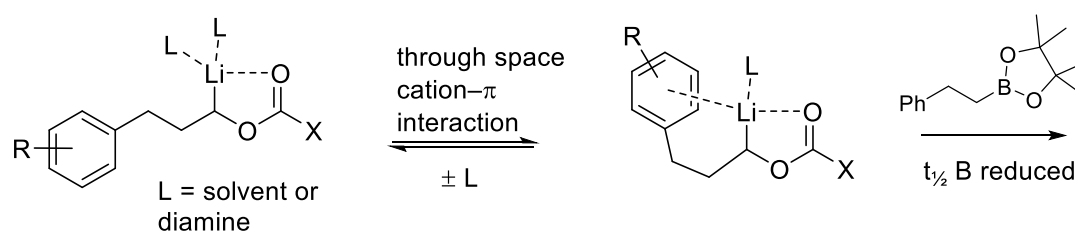
This could be due to a stabilising pre-complexation event, or the presence of a stabilising inductive effect. The electron rich *para*-methoxyphenyl and electron poor 3,5-bis(trifluoromethyl)phenyl examples were prepared, compounds **90** and **91**, respectively. The *para*-methoxyphenyl example, entry 3, underwent lithiation with a similar half-life to the unsubstituted example, $t_{1/2} \text{Li} = 2$ min versus $t_{1/2} \text{Li} = 1$ min. The bis(trifluoromethyl) example, entry 4, underwent an extremely rapid lithiation, $t_{1/2} \text{Li} < 0.25$ min. This could be due to inductive stabilisation by the electron poor phenyl ring, or potentially due to a pre-complexation event, leading to a lower energy pathway to lithiation. The electron poor ring would be expected to exhibit a weaker cation- π interaction, however, the presence of through space lithium-fluorine interactions are known, and it could be this coordination which provides such a rapid lithiation.⁶⁵ Beak and co-workers have shown that 4-phenyl-substituted *N*-Boc piperidine undergoes lithiation more rapidly than unsubstituted *N*-Boc piperidine. This suggests the rate enhancement is through an inductive effect, as the phenyl group in the 4-position should not participate in a productive pre-complexation event.⁶⁶



Entry	R/X/Substrate	$t_{1/2}$ Li (min)	$t_{1/2}$ B (min)	Yield (%)
1	H/NiPr ₂ / 88	5	<0.25	58
2	H/TP/ 89	1	4	67
3	4-OMe/TP/ 90	2	5	58
4	3,5-(CF ₃) ₂ /TP/ 91	<0.25	12	77

Table 4: Half-lives for lithiation and borylation of substrates with a pendant aromatic ring.

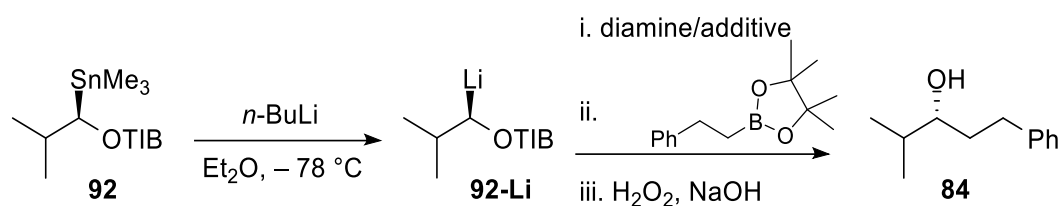
The borylation step proceeded with what appears to follow the trend of inductive stabilisation; the electron poor example having an increased borylation half-life, $t_{1/2} B = 12$ min, compared to the *para*-methoxyphenyl ($t_{1/2} B = 5$ min) and phenyl ($t_{1/2} B = 4$ min) examples, entries 3 & 4. However, the propyl TIB ester **73** would be expected to undergo the quickest borylation, with no inductive stabilisation, but has $t_{1/2} B = 8$ min, placing it in the middle of the series. This demonstrates that, for the borylation of the phenyl and *para*-methoxyphenyl examples **89** and **90**, a through space cation– π interaction is a plausible mechanism for displacing non-labile ligands on the lithium cation, allowing for a more rapid borylation (Scheme 27).



Scheme 27: A plausible through space cation– π interaction displaces ligands on lithium, leading to a more facile lithium–oxygen coordination and borylation.

2.7 Study on tin–lithium exchange and effect of additives on borylation

Lithium carbenoids can be generated from tin–lithium exchange in the absence of a diamine. This leads to a non-ligated lithium cation, which is now not sterically hindered, and can undergo facile lithium–boron exchange. To investigate the time taken for tin–lithium exchange, and to study the borylation step in more detail, the isobutyl stannane **92** was prepared. This was then lithiated using *n*-BuLi (1.2 equiv) in Et₂O, to deliver non-ligated carbenoid **92-Li**, which took 20 minutes (Figure 9). Interestingly, the slope of the



Entry	Diamine/Additive	$t_{1/2} B$	Change in $\nu_{C=O}$
1	None	< 15 s	N/A
2	TMEDA	< 15 s	Intensity increase
3	PMDTA	< 15 s	Intensity increase, + 5 cm^{-1}
4	(+)-sparteine	29 min	Intensity increase, - 5 cm^{-1}

Table 5: Addition of different coordinating tertiary amines to a non-ligated lithiated carbenoid led to changes in the carbonyl wavenumber, demonstrating their coordinating ability.

gradient did not change over the course of the lithiation. This indicates that even as the concentration of the stannane drops over the reaction, the lithiation still happens at a constant rate: the reaction is zero order with respect to substrate. This is most likely due to a slow disassociation of the *n*-BuLi aggregates to an active, lower aggregate, which then quickly undergoes tin–lithium exchange. Addition of the boronic ester as a solution (1.0 M, 1.2 equiv based on substrate) in Et₂O then led to an instantaneous borylation, $t_{1/2} B < 0.25$ min (entry 1, table 5). This confirms that non-diamine ligated carbenoids can undergo rapid borylation. A similar reaction was carried out in toluene, however no tin–lithium exchange occurred, presumably due to the higher order and unreactive *n*-BuLi aggregates persisting in the solvent. The interaction between coordinating diamines/additives and the carbenoid was investigated, by adding the diamines/additives after tin–lithium exchange and before borylation. The addition of TMEDA (1.2 equiv) to a solution of lithiated isobutyl TIB ester (1 equiv), generated from tin–lithium exchange, led to an intensity increase in the band, but no change in wavenumber (entry 2, table 5, and figure 9). As the intensity of an IR band can be reduced by symmetry in a system, the TMEDA could lower the aggregate order of the lithiated carbenoid, leading to a decrease in symmetry and an increase in intensity. Borylation still proceeded as quickly as the boronic ester was added, $t_{1/2} B < 0.25$ min, indicating that TMEDA is a labile ligand on lithium. Another frequently used additive, the triamine *N, N, N', N'', N'''*-pentamethyldiethylenetriamine (PMDTA), was added to a solution of non-ligated lithiated isobutyl TIB ester (entry 3, table 5). This led to an increase in intensity, but also an increase in wavenumber, +5 cm^{-1} , of the carbonyl peak (Figure 10a). As an increase in wavenumber

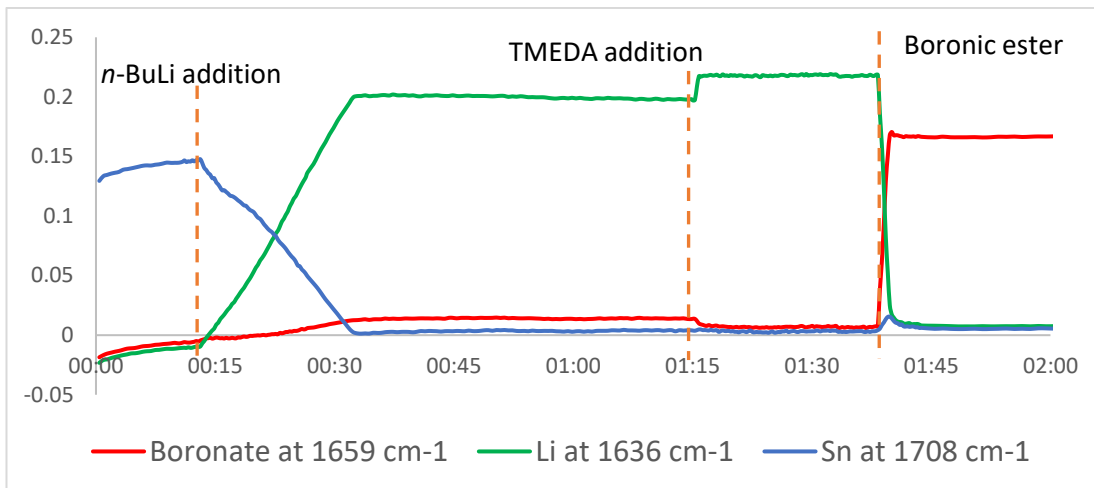
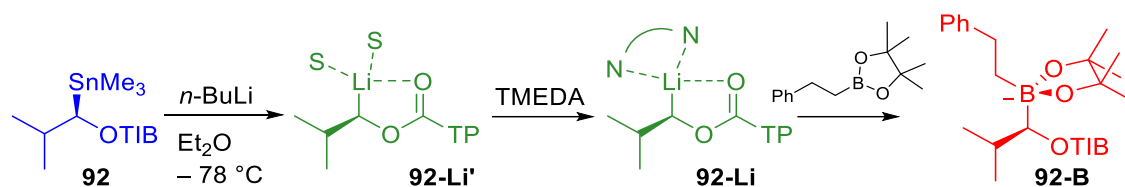


Figure 9: Chart: y-axis = absorbance, x-axis: time (hh:mm). Tin–lithium exchange of stannane **92**, and subsequent addition of TMEDA leading to an intensity increase, presumably due to disaggregation of carbenoid aggregates, and then rapid borylation. For lithiated carbenoid **92-Li'**, S = solvent or another carbenyl. For TMEDA bound species **92-Li**, the TMEDA could either be η_1 or η_3 bound.

is indicative of an increase in bond strength, the triamine ligand most likely satisfies the lithium coordination sphere, leading to a weaker coordination of lithium to the carbonyl oxygen, and therefore a stronger carbonyl bond. However, this change in coordination did not lead to a noticeable change in borylation half-life, and the borylation was complete as soon as the boronic ester addition finished (entry 3, table 5). Finally, the diamine (+)-sparteine was added to the lithiated isobutyl stannane (entry 4, table 5). Again, the increase in IR peak intensity was observed, along with a decrease in the wavenumber of the carbonyl peak (Figure 10b). This demonstrates a weaker carbonyl bond and is most likely due to stronger lithium–oxygen coordination. (+)-Sparteine, as a more sterically demanding ligand than TMEDA or PMDTA, must hinder full solvation of the lithium ion, and so actually increases the coordination to the carbonyl oxygen. This presumably is another factor towards the slow borylation of sparteine-ligated lithium carbenoids. The borylation then proceeded with a half-life of $t_{1/2} B = 29$ min, similar to that of lithiated isobutyl TIB ester generated by deprotonation in the presence of (+)-sparteine ($t_{1/2} B = 35$ min).

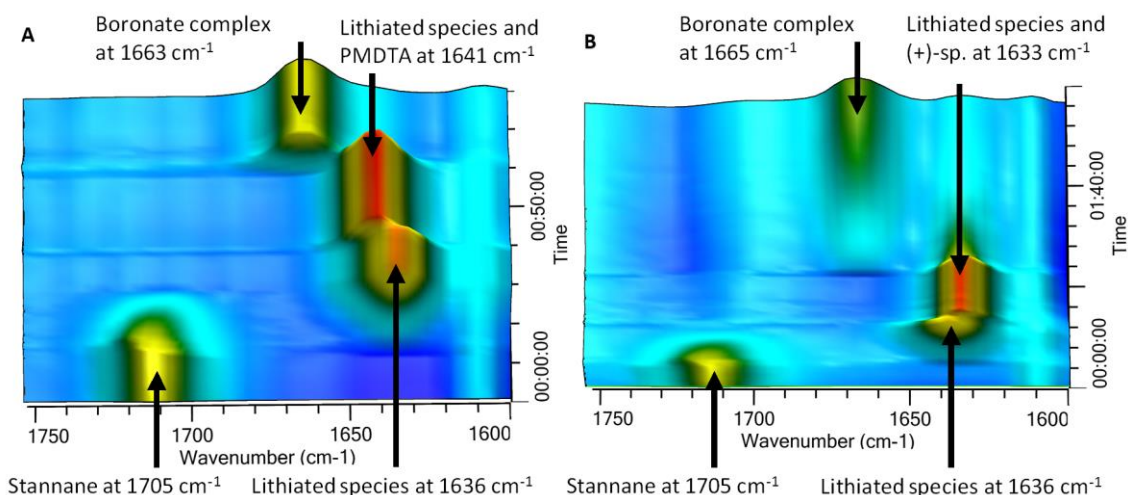


Figure 10: a) Addition of PMDTA to a solution of non-ligated lithiated isobutyl TIB ester leads to an increase in carbonyl bond strength and therefore a higher wavenumber for the lithiated species carbonyl peak; b) Addition of (+)-sparteine leads to a decrease in carbonyl bond strength and therefore a lower wavenumber for the carbonyl peaks.

2.8 Applications in the lithiation–borylation of small to medium rings

The following work (section 2.8) forms part of a publication: R. C. Mykura, P. Songara, E. Luc, J. Rogers, E. Stammers, V. K. Aggarwal, *Angew. Chem. Int. Ed.* **2021**, *60*, 11436–11441.

2.8.1 Aims and Introduction

In situ IR spectroscopy has been shown to be a useful technique for studying the lithiation–borylation of alkyl carbamates and benzoates. We were interested in studying the lithiation–borylation of a range of small to medium cycloalkyl carbamates and benzoates (derived from cyclopropanol through to cyclohexanol). The Aggarwal group has previously demonstrated the lithiation–borylation of acyclic dialkyl substrates.⁴³ In these examples, more forcing conditions ($-60\text{ }^{\circ}\text{C}$, TMEDA (6 equiv)) are required due to the inherent reduced acidity of the dialkyl system, and it was shown that the benzoate (instead of the carbamate) is superior in promoting lithiation in these cases. It was anticipated these conditions, or similar conditions, could be transferred to the cyclic systems on which few studies have been performed, except on systems that are already stabilised by an adjacent benzyl group.^{67,68} This would allow us to prepare a range of 1,1-disubstituted ring systems with a useful boronic ester functional handle for further derivatization, and most likely with complete stereospecificity (as the 1,2-migration of boronic esters is known to be stereospecific). Some fundamental concepts concerning the lithiation–borylation of these cyclic systems could then be explored (Scheme 11).

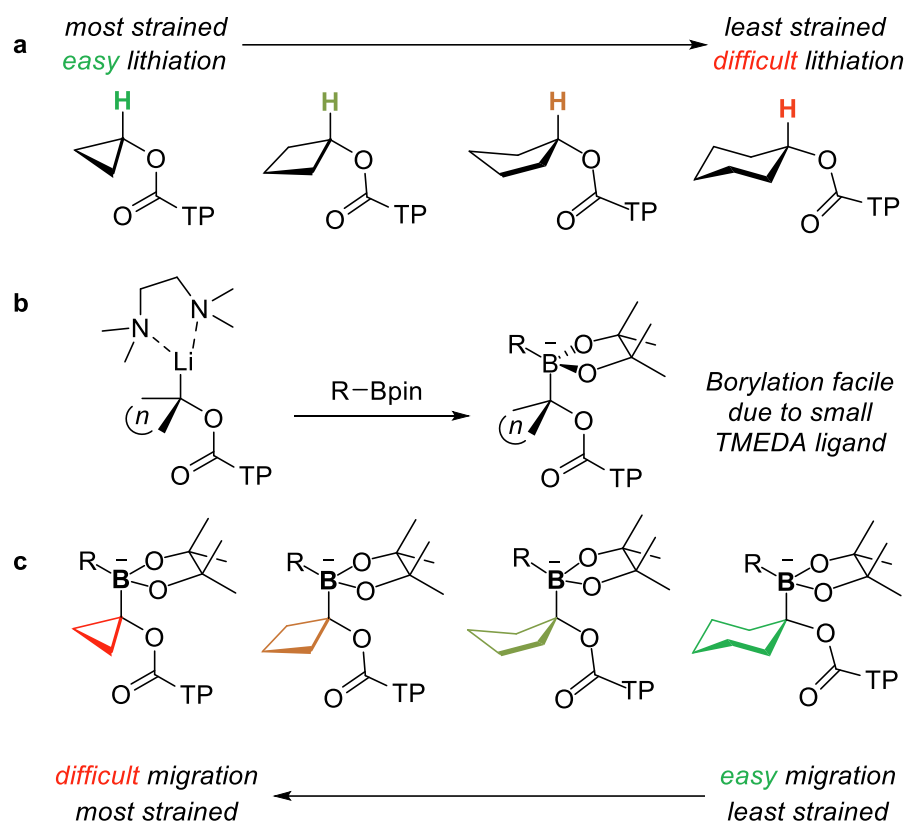
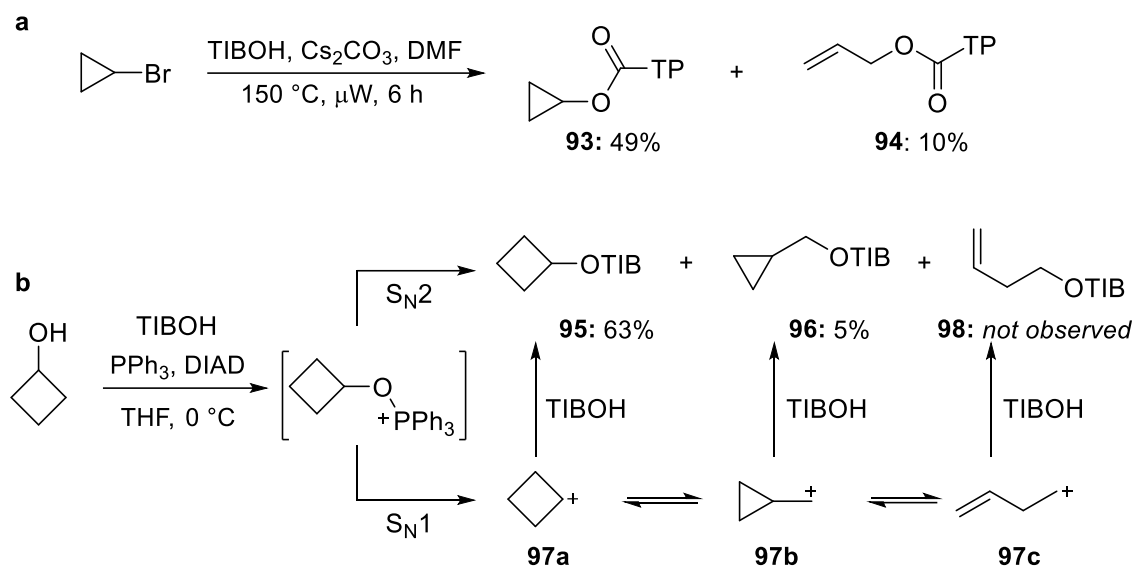


Figure 11: Expected trends for the study. a) Lithiation should be most facile for the smallest ring system; b) borylation should be rapid across the series due to the small TMEDA ligand; c) 1,2-migration should be most difficult for the smallest ring system due to the strain generated in the 1,2-migration.

For example, the smaller ring systems are expected to undergo more rapid lithiation due to a higher amount of s-character in the C–H bonds on the ring (Scheme 11a).⁶⁹ Due to the lack of need for stereoselectivity there was no reason to use sparteine, which is a sterically demanding diamine ligand and would slow borylation. Instead TMEDA was used, which was expected to lead to a fast borylation across the series (Scheme 11b). The final step, 1,2-migration, would show the opposite trend to the lithiation step, that is, the 1,2-migration would become harder with decreasing ring size (Scheme 11c). This is because the transition state for 1,2-migration will become more strained (higher energy) at the carbon centre for the smaller ring systems.

2.8.2 Results and Discussion

The two-medium ring TIB esters, cyclopentyl TIB ester **101** and cyclohexyl TIB ester **104** were made under standard conditions: Mitsunobu reaction with 2,4,6-trisopropyl benzoic acid (TIBOH) and the corresponding alcohol. Cyclopropyl TIB ester **93** was synthesised in moderate yield through an S_N2 reaction between bromocyclopropane and TIBOH (Scheme 28a).



Scheme 28: a) Synthesis of cyclopropyl benzoate; b) synthesis of cyclobutyl benzoate.

Some allyl TIB ester **94** was also observed, presumably due to ring opening of the strained three membered ring, which was separable by column chromatography.

Cyclobutyl TIB ester **95** was made through a Mitsunobu reaction between cyclobutanol and TIBOH but another side product was observed: cyclopropylmethyl TIB ester **96** (Scheme 28b). Once the oxygen of cyclobutanol is activated as per the Mitsunobu reaction, an S_N2 pathway will deliver the product. An S_N1 pathway, however, will provide carbocation **97a**. This is an example of a non-classical carbocation which can be viewed as being in equilibration with cyclopropylmethyl carbocation **97b** (as well as the homoallyl carbocation **97c**).^{70–72} Roberts and co-workers have shown the ratio of products (and therefore the ratio of carbocations at equilibrium) after generation of the non-classical carbocation and trapping is **97a**:**97b**:**97c** \approx 1:0.9:0.1.⁷⁰ In this case, addition of the TIBOH nucleophile will provide again desired product **95** but also the side product **96**. Presumably, under our conditions, S_N2 is the major pathway and S_N1 is the minor pathway, explaining why desired product **95** is the major product, with only minor side product **96** and no observed homoallyl TIB ester **98**. Any attempts to deviate from these conditions led to worse yields of the desired product.⁷³ Homoallyl TIB ester **98** was not separable from the desired product by column chromatography, however it did not interfere with subsequent chemistry.

First, we studied the lithiation–borylation of cyclopropyl TIB ester **93** under the standard condition developed for primary alkyl substrates (Figure 12). The benzoate was dissolved in Et₂O (0.3 M) in the presence of TMEDA (1.2 equiv based on substrate).

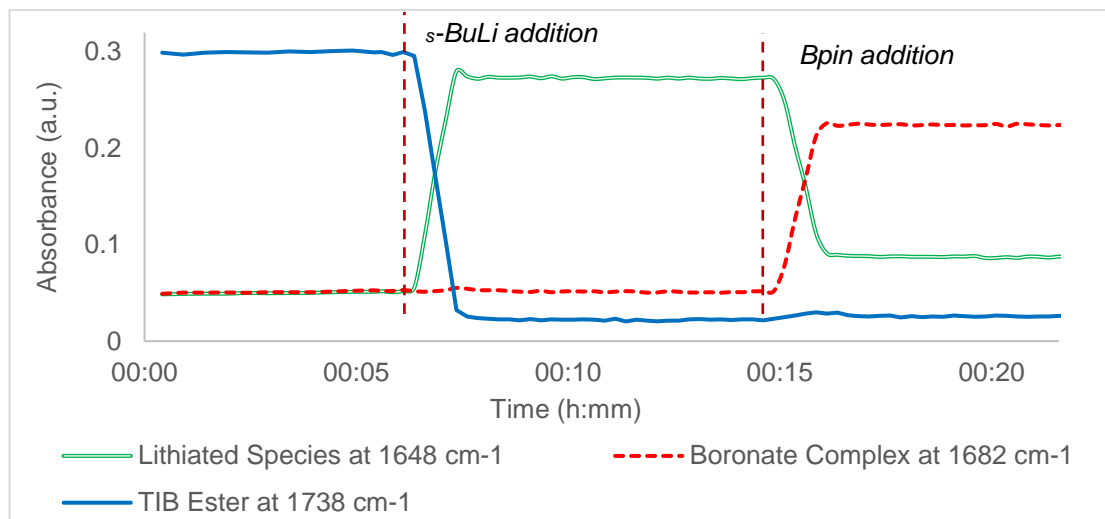
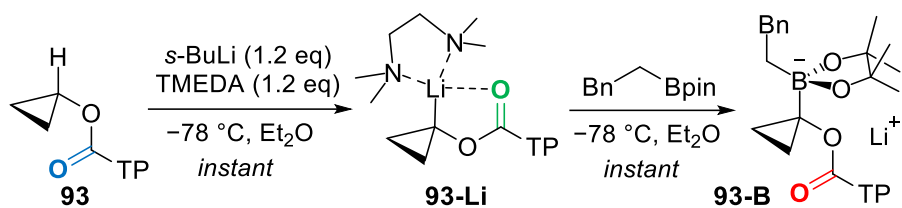
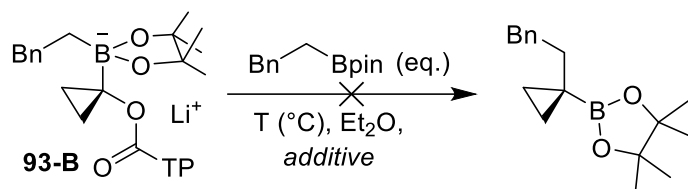


Figure 12: *In situ* IR spectroscopy trace for the lithiation–borylation of cyclopropyl benzoate **93**. Both steps are essentially instantaneous under these conditions.

For cyclopropane **93**, the carbonyl shift is observed at 1738 cm^{-1} , slightly higher than the typical shift of an alkyl benzoate ($\sim 1728\text{ cm}^{-1}$). Upon dropwise addition of *s*-BuLi (1.2 equiv based on substrate) at $-78\text{ }^{\circ}\text{C}$ an immediate decrease in the starting benzoate peak is observed, with concomitant increase in a signal at 1648 cm^{-1} which can be attributed to the lithiated species **93-Li**. Again, the lithiated species is at higher wavenumber than a typical TMEDA ligated lithiated alkyl TIB ester ($\sim 1636\text{ cm}^{-1}$). This essentially instantaneous lithiation demonstrates the high kinetic acidity generated by the strained cyclopropane ring. The intensity of the signal attributed to **93-Li** does not change with time indicating the lithiated species is chemically stable under the reaction conditions, and no other signals were observed to rise or fall during this time. Phenethyl boronic acid pinacol ester (1.2 equiv based on substrate, 1.0 M in Et_2O) was then added dropwise at $-78\text{ }^{\circ}\text{C}$. This resulted in the immediate disappearance of the signal attributed to the lithiated species and increase in a signal at 1682 cm^{-1} , which can be assigned as the boronate complex **93-B**. Again, the signal is at a higher wavenumber in comparison to a typical alkyl boronate complex ($\sim 1666\text{ cm}^{-1}$). The borylation is instant, presumably due to lack of steric hindrance provided by the TMEDA ligand. With such a positive *in situ* IR spectroscopy trace for the cyclopropyl benzoate **93** we did not explore the carbamate.



Entry	Additive	Temperature (°C)	Time (h)	Yield
1	None	40	16	0%
2	CHCl ₃ (solvent swap)	60	16	0%
3	MgBr ₂ •Et ₂ O	40	16	<5%
4	MgBr ₂ /MeOH	50	16	0%
5	Mg(ClO ₄) ₂ /CF ₃ CH ₂ OH	50	16	0%

Table 6: Attempted 1,2-migration of the cyclopropyl boronate complex **93-B** was unsuccessful.

Unfortunately, despite several attempts (table 7), the boronate complex **93-B** did not undergo 1,2-migration. Various Lewis acids were tried, along with solvent switches to higher boiling point apolar solvents (known to help the 1,2-migration of recalcitrant boronate complexes).^{45,74} Only starting material or decomposition was observed. Despite the promising lithiation and borylation steps, the optimisation of this substrate was stopped here. It has been shown that cyclopropyl bromide can be lithiated in the presence of boronic esters, and, after borylation, the boronate complexes (with a much better bromide leaving group) undergo facile 1,2-migration.⁷⁵⁻⁷⁷

Next, attention was turned to cyclobutyl benzoate **95**. Following the same procedure as for the cyclopropyl example **93**, the benzoate can be observed in Et₂O at 1730 cm⁻¹. Upon addition of *s*-BuLi, a new signal is observed at 1637 cm⁻¹ which can be attributed to the lithiated species **95-Li**. The lithiation is no longer instantaneous, however is still rapid and only take ~15 minutes to go to completion. Once formed, the intensity of the signal drops slowly over time, with appearance of a new broad signal at ~1581 cm⁻¹. This broader signal can be assigned as the carboxylate leaving group **83** (LiOTIB). This was previously observed by in situ IR spectroscopy in the 1,2-migration of borane-ate complexes (see figure 8, section 2.5). This indicates lithiated species **95-Li** is not chemically stable at -78 °C and will degrade over time, albeit slowly. Upon addition of phenethyl boronic acid pinacol ester, immediate conversion is seen to the boronate

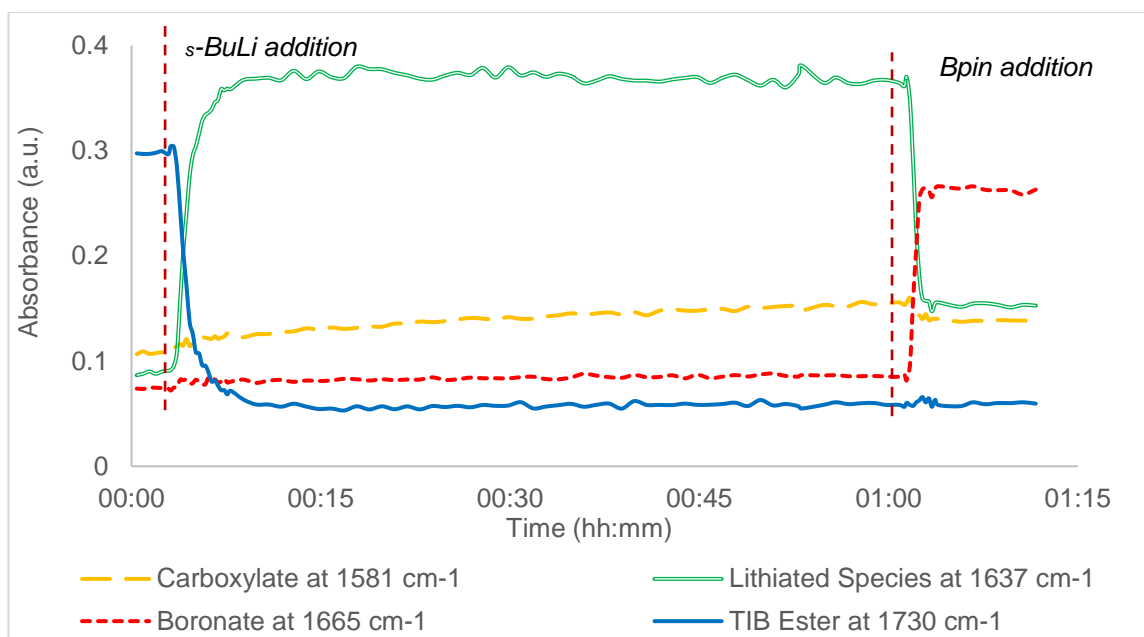
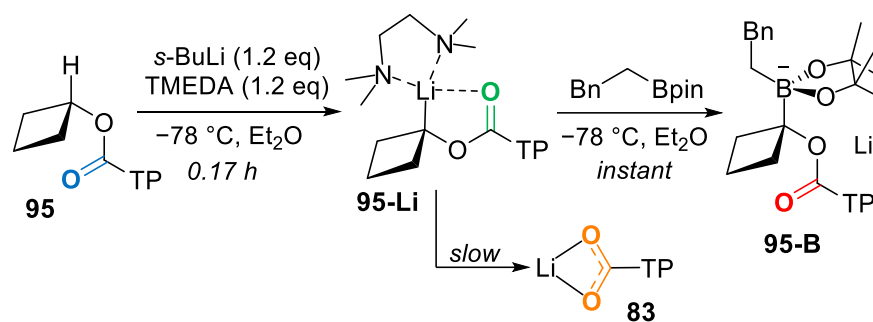
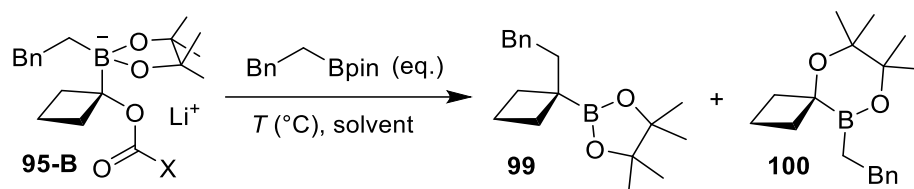


Figure 13: In situ IR spectroscopy trace for the lithiation and borylation of cyclobutyl benzoate **95**. The lithiation is complete within 15 minutes, however lithiated species **95-Li** is not stable under the reaction conditions and slowly decomposes, presumably by α -elimination. Borylation then proceeds instantly to provide boronate complex **95-B**.

complex **95-B** at 1665 cm^{-1} . As with the cyclopropyl example, the lithiated species is not hindered by a large diamine ligand and so borylation is rapid. The 1,2-migration was then studied, and it proceeded even at RT in Et_2O , however the yield was low (entry 1, table 7). The use of MgBr_2 was also trialed, however did not improve yields (entry 3, table 7). Finally, use of a solvent switch to CHCl_3 and heating to $60\text{ }^{\circ}\text{C}$ for 3 h allowed us to obtain the product in high yield (entry 4 table 7).

The use of cyclobutyl bromide or chloride in an analogous procedure to cyclopropyl bromide⁷⁷ (strong base, in situ conditions) only led to poor yields and recovery of boronic ester starting material. This is presumably due to the more rapid rate of α -elimination for the cyclobutyl systems versus the cyclopropyl systems.



Entry	Eq	Solvent	T (°C), t (h)	100 : 99 : 95-B ^a	Yield (%)
1	1.2	Et ₂ O	22, 16	10:70:20	64 ^b (59 ^d)
2	1.2	Et ₂ O	30, 16	10:70:20	67 ^b (53 ^d)
3	1.5	Et ₂ O	40, 16	15:65:25	42 ^{d,c}
4	1.5	CHCl ₃	60, 3	10:90:0	86 ^b (67 ^d)

Table 7: a) The ratio of O-migrated side-product ($\delta \approx 50$ ppm) to C-migrated product ($\delta \approx 32$ ppm) to Boronate complex ($\delta \approx 8$ ppm), ratio determined by ¹¹B NMR; b) crude ¹H NMR yield relative to 1,3,5-trimethoxybenzene; c) 8 equivalents of a 1 M solution of MgBr₂ in MeOH were added to the reaction; d) isolated yield after flash column chromatography.

Cyclopentyl benzoate **101** was tested next (Figure 14). The benzoate was observed at 1725 cm⁻¹ in Et₂O solution, as expected. Upon addition of *s*-BuLi we observed the expected decrease in this signal, however no lithiated species (**101-Li**) was observed at the typical wavenumber. Instead, only a signal at 1585 cm⁻¹ was observed, which we have previously attributed to the carboxylate leaving group LiOTIB **83**. This indicates that the lithiated benzoate undergoes decomposition at a much faster rate than its lithiation. Quenching the reaction after 4 h (when the signals were no longer changing in intensity) with *d*₄-methanol gave a poor recovery (27%) of material with 0% D-incorporation. The half-life of lithiation (*t*_{1/2} Li) was measured as 17 minutes. To compare, isobutyl TIB ester under the same conditions has *t*_{1/2} Li = 17 minutes. One can also observe from the in situ IR spectroscopy trace that the intensity of the benzoate signal does not increase upon the addition of methanol therefore the species generated does not protonate with methanol to a benzoate ester. Lithiated benzoates are known to undergo rearrangement to the α -hydroxy ketone upon warming,⁷⁸ however to receive the carboxylate leaving salt we believe the lithiated cyclopentyl system must undergo rapid α -elimination. Metal carbenoids are known to undergo α -elimination, and classically their stabilities are hard to predict.⁷⁹ However, the high instability of the lithiated cyclopentyl benzoate was surprising given the well-known stability of lithiated benzoates at -78 °C. To stabilise the lithiated species carbamate **102** (made under standard conditions using cyclopentanol

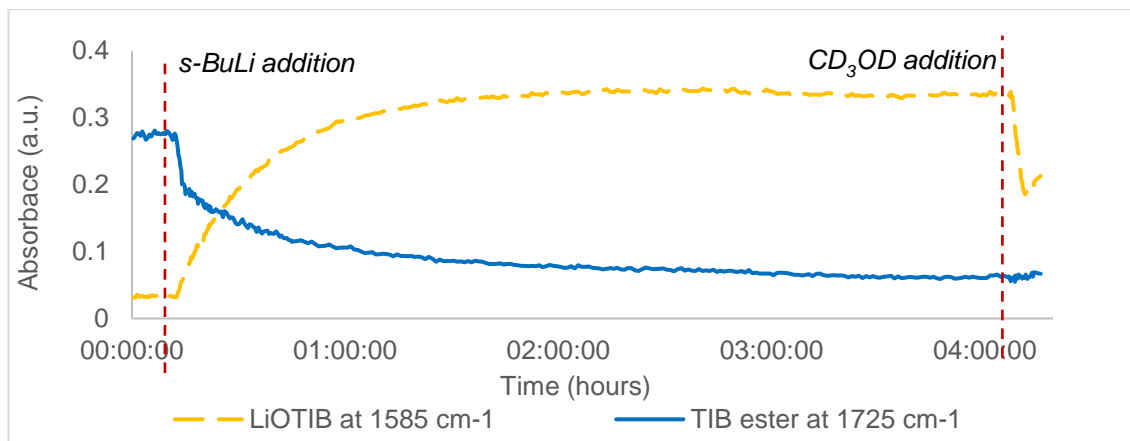
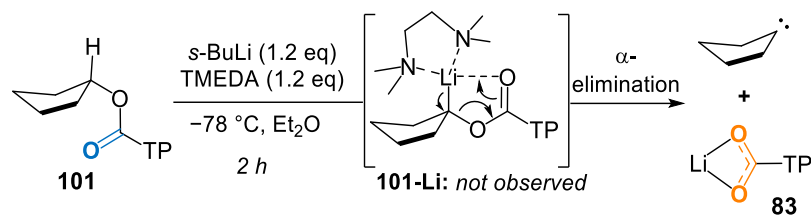


Figure 14: *In situ* IR spectroscopy trace of the lithiation and borylation of cyclopentyl benzoate **101**. No lithiated species is observed however, only immediate decomposition to the carboxylate is seen.

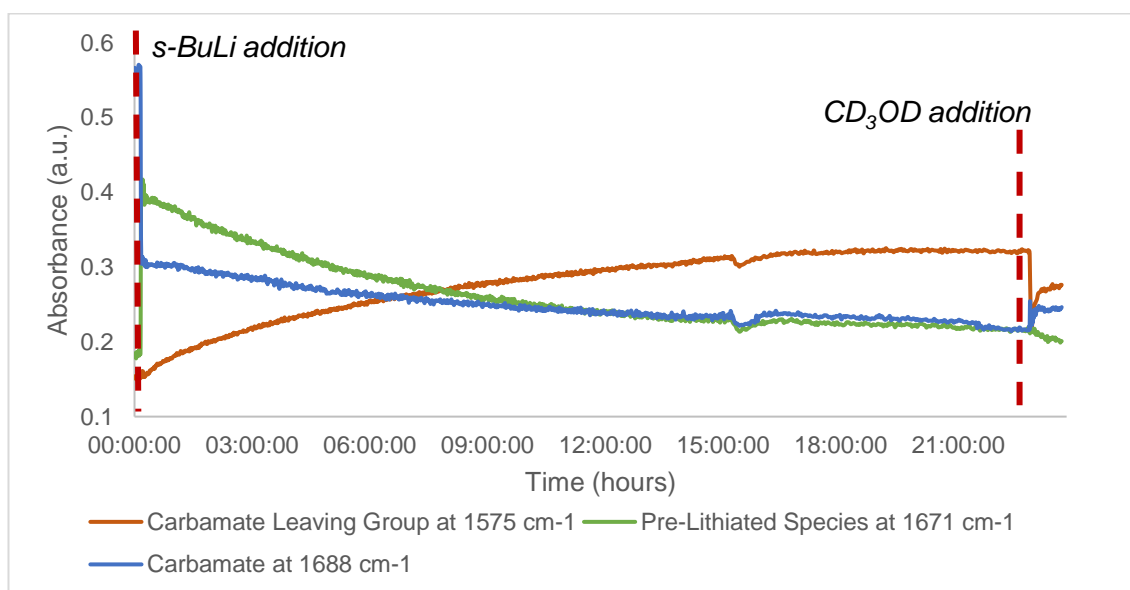
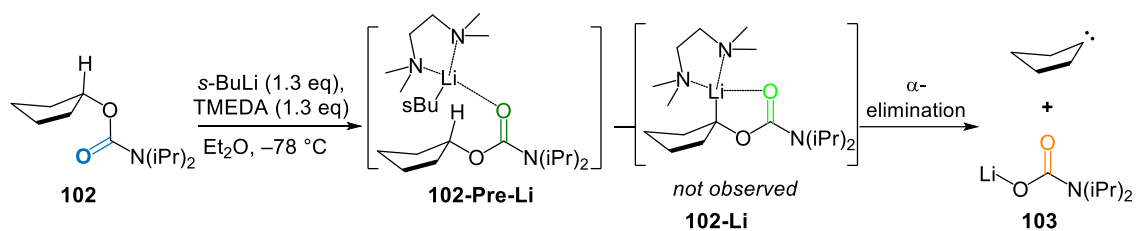


Figure 15: *In situ* IR spectroscopy trace of the lithiation and borylation of cyclopentyl carbamate **102**. Like the corresponding benzoate, no lithiated species is observed. The “pre-lithiated” complex is observed, typical of alkyl carbamates.

and carbamyl chloride) was tested. The in situ IR spectroscopy trace again did not show the lithiated carbamate (Figure 15). As expected, upon addition of *s*-BuLi to the carbamate (1688 cm⁻¹) the transient “pre-lithiated” complex is seen (1671 cm⁻¹). Both the carbamate and the “pre-lithiated” complex decrease with time however a broad signal for the carbamate anion **103** (1575 cm⁻¹) was observed. Clearly there is a high instability for the five membered lithiated compounds. Computational methods were used to try and rationalise the trends but the transition state for α -elimination was not found.

The final compound in the series was cyclohexyl benzoate **104**. Again, under our standard protocol, the benzoate ester can be observed at 1724 cm⁻¹ in solution (Et₂O). Upon addition of *s*-BuLi at -78 °C we observed a slow lithiation (~22 h, lithiated species **104-Li** at 1635 cm⁻¹) that did not go to completion (as monitored by in situ IR spectroscopy). Once the peaks had plateaued, addition of *d*₄-methanol afforded 93% recovery of material with 26% D-incorporation (**104-D**). This procedure was clearly impractical for a lithiation–borylation process. Even if the lithiation could be pushed with a large excess

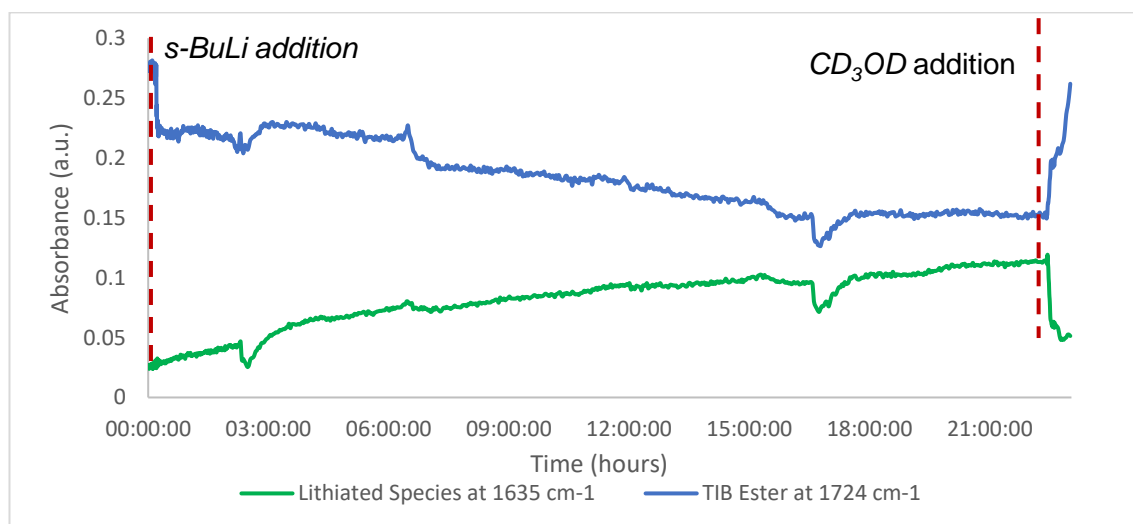
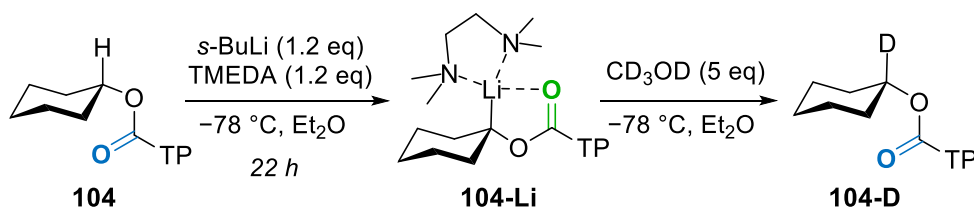


Figure 16: In situ IR spectroscopy trace of the attempted lithiation of cyclohexyl TIB ester **104**. After 22 h the lithiation slows and CD₃OD is added to give 93% recovery with 26% D-incorporation.

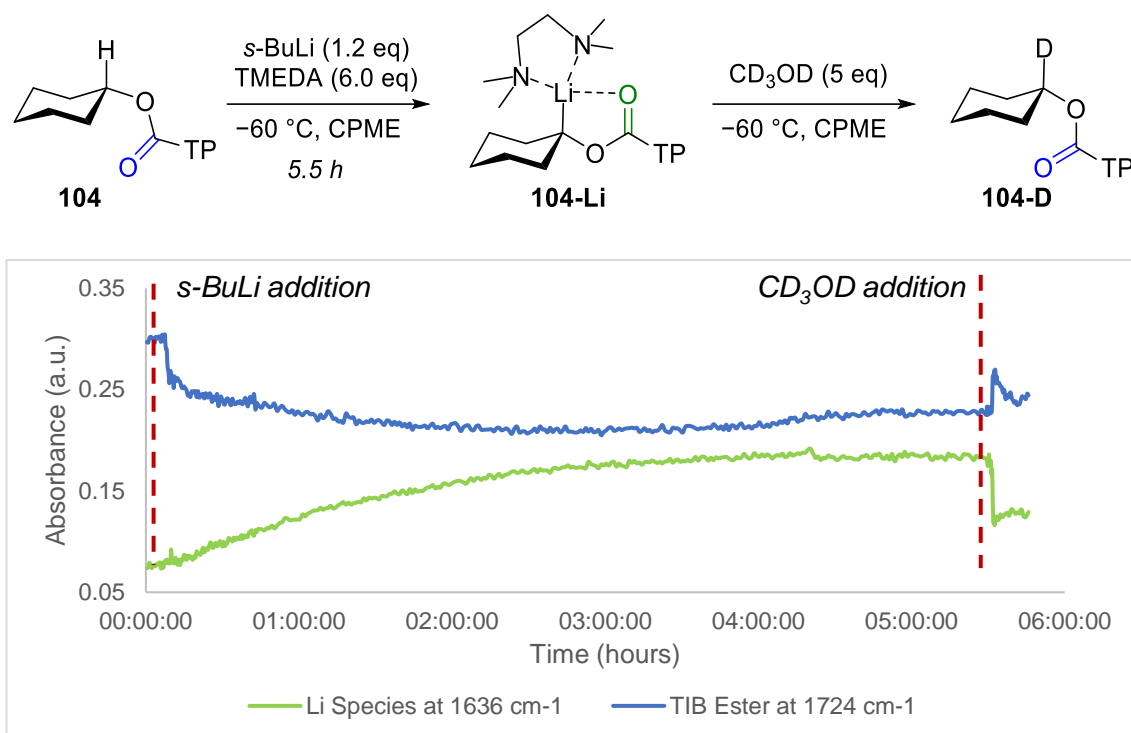


Figure 17: In situ IR spectroscopy trace of the attempted lithiation of cyclohexyl benzoate under more forcing conditions. Unfortunately, 95% material was recovered with only 21% D-incorporation.

of *s*-BuLi, that would then require a large excess of boronic ester for the borylation step. We attempted to use conditions used by Aggarwal and co-workers⁴³ for dialkyl benzoates (CPME, $-60\text{ }^{\circ}\text{C}$, TMEDA (6 equiv)) and while the lithiation time was reduced to 5 h, it still did not go to completion (monitoring again by in situ IR spectroscopy, figure 17). Addition of *d*₄-methanol led to 95% recovery of material with 21% D-incorporation. Interestingly, Aggarwal and co-workers have previously shown that use of *s*-butyl TIB ester in a lithiation–borylation process gave 35% yield with only a 2 h lithiation time (CPME, $-60\text{ }^{\circ}\text{C}$, TMEDA (6 equiv)).⁴³ Therefore, assuming full borylation and 1,2-migration, it seems cyclohexyl TIB ester **104** is lithiated even more slowly and to less completion than an acyclic dialkyl TIB ester.

2.8.3 Summary

In situ IR spectroscopy was used to study the lithiation–borylation process of small to medium sized *O*-cycloalkyl benzoates (cyclopropyl through to cyclohexyl). The lithiation was expected to be most facile for the cyclopropyl example and least for the cyclohexyl and indeed this was observed experimentally (cyclopropyl undergoing instantaneous lithiation while cyclohexyl did not undergo acceptable levels of lithiation after 22 h). However, a key factor was also uncovered: the stability of the lithiated species. The three and six membered lithiated species were stable under the reaction conditions and while

lithiated cyclobutyl benzoate **95** did show minor decomposition at $-78\text{ }^{\circ}\text{C}$ it could still be trapped with boronic esters. Lithiated cyclopentyl benzoate **101-Li** (and its corresponding carbamate **102-Li**) underwent decomposition rapidly at $-78\text{ }^{\circ}\text{C}$ and could not be observed. An α -elimination pathway is assumed for the decomposition of these substrates. Borylation of the three and four membered systems afforded the corresponding boronate complexes, but only the four membered example was large enough to permit 1,2-migration.

This careful balance of factors across the lithiation–borylation process leads us to describe the cyclobutyl benzoate as occupying a “Goldilocks zone”, where the ring size is small enough to permit lithiation and large enough to allow 1,2-migration. Due to the interest of cyclobutane substrates in medicinal chemistry, a substrate scope of boronic esters was presented.⁸⁰

3 Conclusions

The use of in situ IR spectroscopy has been demonstrated as an efficient tool for monitoring the lithiation of Hoppe-type carbamates and Beak-type TIB esters, and subsequent trapping with organoboron partners (borylation). A much better idea of the times taken for these processes, which are difficult to study conventionally as they are both carried out at low temperature and in the absence of air, has been determined for a variety of differentially sterically hindered substrates.

Lithiation times seem to be dependent on not only the steric bulk of the substrate, but also the many equilibria of the alkyllithium/sparteine complexes in solution. In Et₂O, alkyl carbamates undergo lithiation more slowly than the corresponding benzoates. Toluene increases the rate of lithiation of TIB esters however carbamates are slowed. We believe these factors are due to the small size of the carbamate group allowing it to form stable “parasitic complexes” which do not undergo lithiation. These complexes can be observed at a lower wavenumber to the main signal of the carbamates (but typically not benzoates). Further evidence for this was obtained when ethyl, propyl and isobutyl carbamate were found not to undergo lithiation under Beak’s pseudo 1st order conditions (28 equiv *s*-BuLi/sparteine) unlike ethyl benzoate.

Borylation times seem to be primarily dependent on sterics around the lithium carbenoid. To this end, benzoates borylate more slowly than carbamates. We believe borylation occurs through disassociation of the diamine or carbonyl oxygen from the lithium atom of the carbenoid. Replacement of the bulky diamine sparteine on lithium with small THF ligands (which occurs readily at -78 °C) allows a more facile coordination of lithium to the pinacol oxygen of the boronic ester, leading to a more rapid borylation. This is especially useful for hindered benzoates, where borylation can be extremely slow at -78 °C.

Further evidence for a lithium–oxygen pre-complexation event was provided by comparing the rates of borylation of lithium carbenoids with boranes, boronic esters, and borates. As Lewis acidity decreases, the number of Lewis basic oxygens for pre-complexation increases. Boronic esters and boranes react at a similar rate in Et₂O, as the lithium–oxygen pre-complexation is only possible for the less Lewis acidic but pinacol oxygen bearing boronic ester. In a similar manner, borate esters react at a similar rate to boronic esters. A through space cation– π interaction is a plausible mechanism for

the faster lithiation–borylation reactions of substrates with a proximal aromatic group. By generating the lithiated carbenoid under diamine-free conditions, we have shown how various coordinating amines interact with lithium and, as a result, strengthen/weaken the carbonyl bond.

These techniques were further applied in the studies on the lithiation–borylation of three to six membered *O*-cycloalkyl benzoates. We found that only the cyclobutyl benzoate could undergo the full process: it occupies a “Goldilocks zone”. It was acidic enough to undergo lithiation and the lithiated species is stable enough to be borylated at $-78\text{ }^{\circ}\text{C}$. The cyclobutane ring is then large enough to allow the formed boronate complexes to undergo 1,2-migration, after a solvent swap to CHCl_3 .

3.1 Outlook

It has been demonstrated that in situ IR spectroscopy is a powerful technique for studying lithiation–borylation chemistry. Evidence has been provided for the difference in lithiation half-lives between alkyl carbamates and benzoates. Further studies on the structure of the “pre-lithiation” complexes are warranted as this will provide future evidence for the hypothesis presented. The solution-state structure of the complex (or complexes) generated under pseudo 1st order conditions (section 2.4) could be studied by NMR (^1H , ^{13}C and ^6Li) at $-78\text{ }^{\circ}\text{C}$. Use of ^6Li NMR could identify the number of lithium environments and provide evidence for/against the dimeric nature of the “pre-lithiation” complex. The same study could be applied to neopentyl carbamate at $-78\text{ }^{\circ}\text{C}$ (as it does not undergo lithiation at this temperature) or other carbamates/benzoates at lower temperatures. Neopentyl substrates may have reduced aggregates due to their large size. Being able to follow a lithiation reaction by ^6Li NMR could then help identify other complexes on the pathway to the lithiated species. Performing several pseudo 1st order reactions of alkyl benzoates at different starting concentrations could allow the calculation of the overall apparent rate constant, and the determination of the overall apparent reaction order with respect to the benzoate.

Sulfoxide–metal exchange is also an area that will benefit from an in situ IR spectroscopy study as little is currently known about reaction times. A study of magnesium carbenoids in such processes (generated either by sulfoxide-magnesium exchange or transmetallation of the lithium carbenoid) is also under-explored. Useful information such as the reactivity and chemical/configurational stability of magnesium carbenoids could be determined. To

this end, additional studies on zinc carbenoids could be performed (generated by zinc–lithium exchange), as these are known to be more stable (therefore less reactive) and even configurationally stable at room temperature.⁵⁶

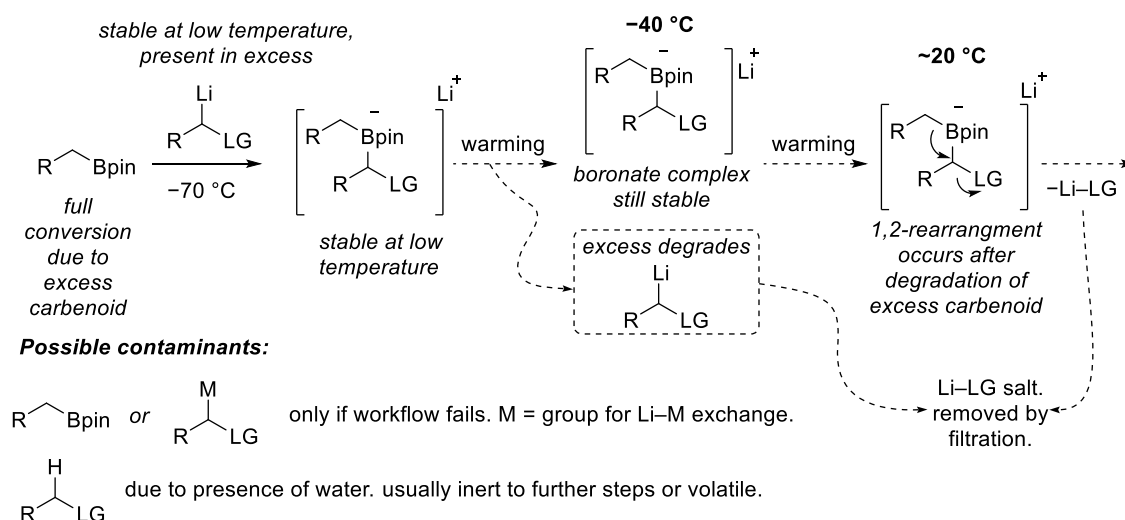
The high instability of both lithiated cyclopentyl carbamate and benzoate was presented, which undergoes decomposition presumably by α -elimination at -78 °C. The decomposition happens more quickly than the lithiation of the starting materials. Minor decomposition was noted for the cyclobutyl system, while high stability (typical of other lithiated benzoates) was observed for the cyclopropyl and cyclohexyl system. A full computational analysis on the stability and decomposition pathways of such a series could provide useful information concerning the effect of bond angle at the carbenoid centre on carbenoid stability.

4 Automated synthesis

4.1 Introduction

4.1.1 Factors required for iterative synthesis

As discussed in section 1.2.3, assembly–line synthesis represents a unique way to construct carbon–carbon bonds with excellent levels of stereocontrol. The synthetic process makes use of similar lithium carbenoids for each building block, and the product boronic ester is resubmitted into the cycle without chromatographic purification. This means that only a simple filtration through silica gel is required to provide sufficiently clean crude material for the next iteration. No chromatographic purification is needed between homologations because the lithium carbenoid degrades at temperatures below the temperatures required for 1,2-rearrangement (Scheme 29). Therefore, the product should never be formed in the presence of the lithium carbenoid, and so over-homologation is not usually observed. In addition, the degradation side-products do not interfere with subsequent iterations or they are removed by filtration. This means that full conversion of the starting boronic ester can be achieved simply by adding an excess of lithium carbenoid so that no under-homologated product is observed. The product of 1,2-rearrangement is the lithium salt of the leaving group which is easily removed in the filtration step. In the synthesis of (+)-kalkitoxin, the Aggarwal group were able to perform six iterations and three further steps with only one purification.⁸¹ Due to the factors described above, the assembly–line workflow is well suited for automation: a series of manually similar iterative steps with only a simple filtration between them. While an



Scheme 29: Characteristics of iterative synthesis, with possible contaminants that mean no chromatographic purification is needed.

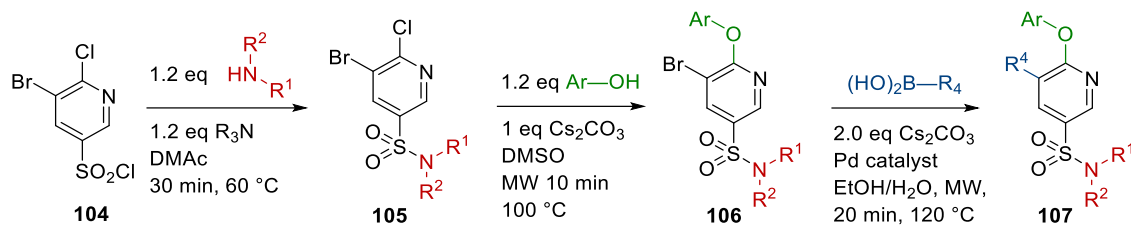
automated synthesis of complex natural products would be a significant challenge, it would represent a milestone in automation chemistry. Some similar reports do exist (see section 4.1.2) but there are few reports in automation of the use of cryogenic temperatures and air sensitive alkyl lithium chemistry, which are required for assembly-line synthesis.

The benefits of automation largely centre on an increase in work output for the same sized workforce.⁸² Robots can repeat simple manual tasks with high accuracy, and do not need to stop work to rest. Opportunities also lie in library synthesis, as a robot should be able to carry out many parallel reactions with ease. By relieving chemists of the laborious task of lab work, perhaps more time can be allowed for studying reactions, leading to new and interesting transformations. The effect of automation has most strongly been felt in the world of peptide synthesis, where synthesisers now routinely allow the automated preparation of otherwise hard to produce oligopeptides.⁸³ In other areas of organic synthesis this effect has not been felt so strongly, however the attractiveness of automating chemistry remains. To this end, the University of Bristol acquired a Chemspeed automated synthesis platform in late 2018. This type of platform can perform many of the steps a chemist is used to performing, for instance, transferring both liquids and solids, heating/cooling reactions with agitation, sampling reactions, and performing solid phase extractions (SPE, or filtrations). There are examples of both Chemspeed platforms and other automated platforms being used in the literature, which are discussed below.

4.1.2 Automation in synthesis: literature examples

4.1.2.1 Chemspeed examples

In 2016, Sarris *et al* from AbbVie demonstrated the use of a Chemspeed synthesis platform for the rapid generation of compound libraries.⁸⁴ The library synthesis consists of three steps starting with sulfonyl chloride **104** (Scheme 30): 1) addition of an amine to make sulphonamide **105**; 2) S_NAr on the chloro-substituted C₂ position of the pyridine with a phenol to give product **106**; and 3) Suzuki reaction between the bromo-substituted C₃ position and a boronic acid to give final product **107**. They use three amines, three phenols and four boronic acids, leading to a possible 36 final compounds. In total 29 compounds **107** were isolated with yields ranging from 22–39%. This example demonstrates the platform's ability to handle liquid and solid reagents, along with its ability to perform a filtration. The authors also demonstrate the platform's capability to perform reactions in a microwave reactor, as well as online, fully automated, high



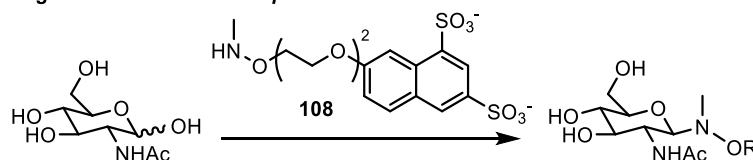
Scheme 30: AbbVie's 3 step library synthesis - each step is fully automated, including the capping of the microwave vials and transfer to the reactor.

performance liquid chromatography (HPLC) analysis (which the authors design and build themselves). Using the Chemspeed platform, AbbVie also performed a selection of Buchwald-Hartwig amination reactions, using one “core” and 10 different amines. All ten reactions were successful with yields between 39–66%. While this does not demonstrate any new robotic operations, the authors state that a common issue with the Buchwald-Hartwig amination is its sensitivity to an oxygen atmosphere. To avoid this problem, the Chemspeed platform was flushed with inert gas prior to the workflow. The platform has inlets on either side of the box to allow for inert gas distribution around the lower levels of the platform, filling the box with inert gas. The reactors themselves can also be flushed with inert gas, therefore providing an inert atmosphere for both the reactor space and material transfer. The authors state several benefits of this system, not only was all synthesis performed without any human intervention (including purification by HPLC) but also excellent cycle times were observed for each reaction – the platform can perform filtrations of reactions while one is being heated in the microwave. AbbVie have since expanded on their automated synthesis approach, which now includes biological testing.⁸⁵ This system can provide a 33-member library in only 30 hours, a process that would otherwise take several days to perform manually.

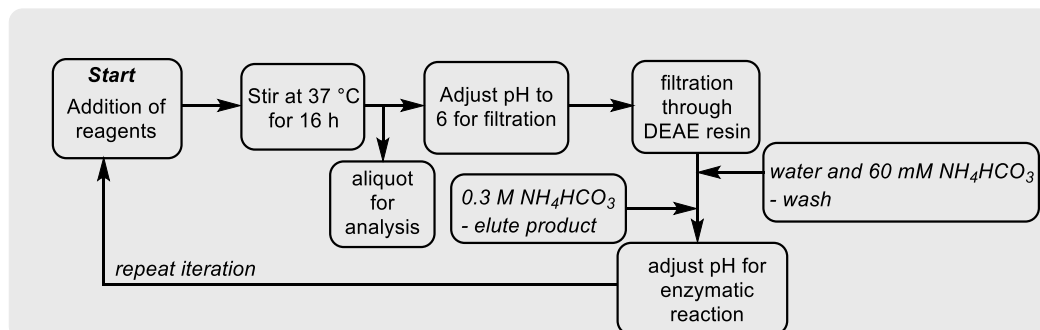
Another example of automated library synthesis using a Chemspeed platform is from Boons and co-workers in 2019, and describes the enzymatic library synthesis of a variety of complex oligosaccharides.⁸⁶ The chemical automated library synthesis of oligosaccharides has already been described, however this chemical process is limited by large excesses of reagents, and some steps have to be performed manually.⁸⁷ Boons states that enzymatic oligosaccharide synthesis has advantages over chemical synthesis, namely, there is no need for harsh conditions and excellent stereocontrol is achieved. However, no automated version exists due to difficulties with purification. To facilitate automated enzymatic synthesis, a “catch-and-release” purification system was developed, whereby the product has a ‘tag’ present on the growing oligosaccharide that adheres to a

resin used during purification. This method allows for complete removal of any leftover reagents or side products, and then the product can be selectively eluted and carried forward (Scheme 31). With this system, it is important that any starting saccharides with a tag are fully converted to products, otherwise they will remain on the solid phase and elute with the products. Sulfonate tag **108** was found to be effective at providing the catch and release system required. Once the contaminants are eluted to waste, using water and 60 mM NH_4HCO_3 on a diethylaminoethyl (DEAE) resin, the product is eluted into a vial using 0.3 M NH_4HCO_3 . This means the product is in a constant volume of aqueous solution and so can be used in subsequent enzymatic steps (using organic solvents leads to incompatibility with enzymes). The system used by Boons and co-workers also has another interesting feature: the platform can measure and adjust the pH of a solution to a desired value. This means the basic filtrate can be neutralised to pH = 7 to allow for further enzymatic steps. Many different oligosaccharides are made of varying complexity, one example features nine alternating transformations to give a decamer in 15% overall yield (average yield of 81% per step). The sulfonate tag is easily cleaved using a mild TFA/ H_2O mixture over 3 hours. This literature example again shows the Chemspeed platforms capability at handling chemical reagents and performing more complex solid phase extraction (SPE) techniques.

Sulfonate tag for catch and release purification:



Workflow:



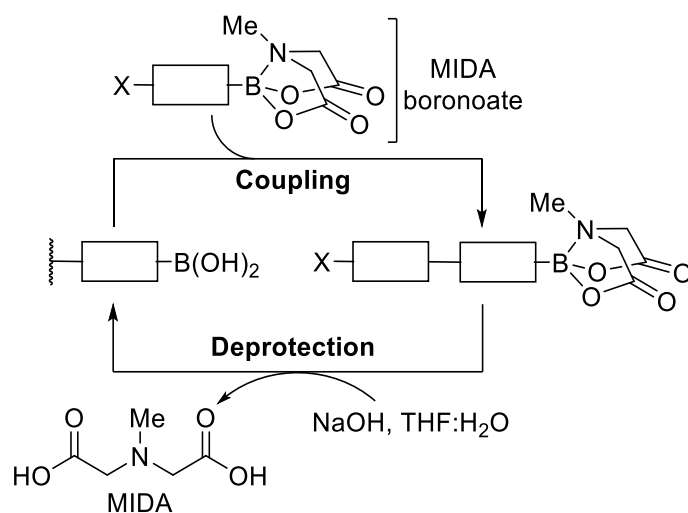
Scheme 31: Boons' catch and release system for purification, and workflow for the iterative enzymatic assembly of complex oligosaccharides.

Pohl and co-workers have developed an automated iterative oligosaccharide synthesis paradigm which utilises fluorous-tag solid phase extraction (FSPE) as a “catch-and-release” variant.^{88,89} The substrate has a fluorous tag (typically a long perfluorinated alkyl chain) which binds to the solid phase and is only eluted under certain conditions (after all by-products have been eluted to waste). There are other examples of Chemspeed platforms being used in, for example, copper-catalysed click reactions⁹⁰ but also in reaction discovery. In 2011 MacMillan *et al* used the liquid handling capabilities of a Chemspeed platform to assemble 171 reactions to search for new chemical reactivity, which led to the discovery of a new α -amino arylation strategy.⁹¹ Another recent example uses a Chemspeed platform to screen over 190 ligands for a cerium catalysed photochemical process.⁹² This example uses automated solid dispensing to dispense ligands and catalysts, demonstrating the platform’s aptitude for what is typically seen as a difficult process.

4.1.2.2 Other examples of automation platforms

There are many examples of automated synthesis platforms that are not built by Chemspeed.⁹³ Discussion will now be of some not yet commercialised platforms.

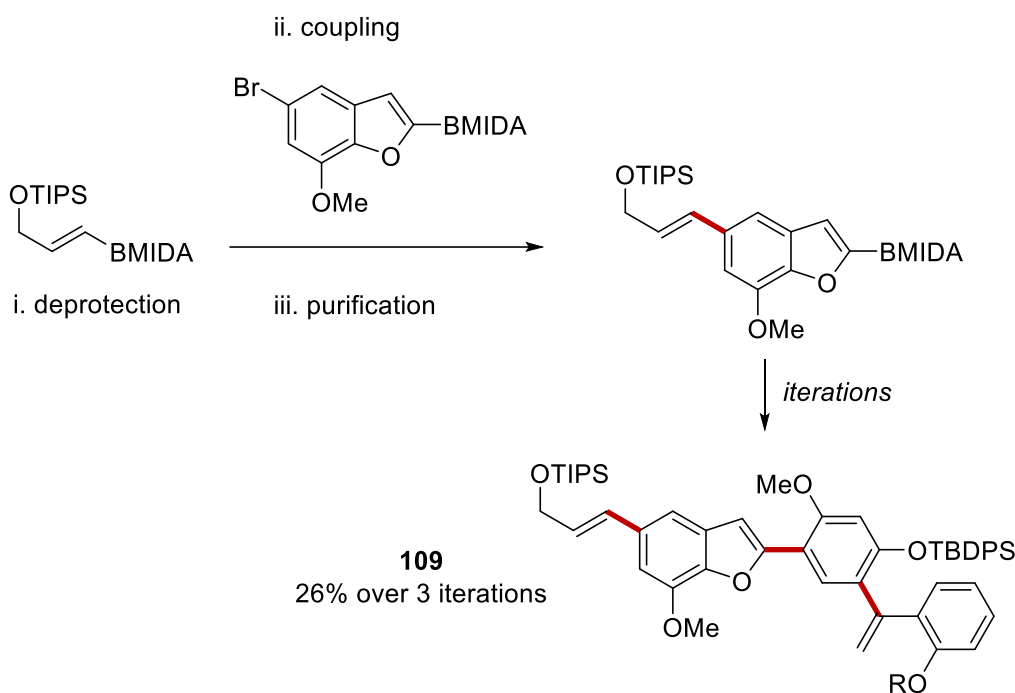
In 2015, Burke and co-workers reported a custom built automated platform for the synthesis of complex biologically active compounds.⁹⁴ Based around the idea of a peptide coupling module, the process consists of only three steps; coupling, purification and deprotection. The coupling step is a Suzuki reaction, performed between a sp^2 -boronic acid and a sp^2 -aryl bromide. To facilitate an iterative process, Burke makes use of N-methyliminodiacetic acid (MIDA) boronates (Scheme 32). The MIDA ligand acts as protecting group for boron: the nitrogen on the ligand coordinates to the boron centre making it far less Lewis acidic. Starting with a MIDA boronate, the group can be cleaved under basic conditions to afford the free boronic acid. Any aryl bromide that is introduced subsequently for coupling has a MIDA boronate also attached, which does not undergo coupling as the boron is deactivated. After successful coupling between the boronic acid and aryl bromide, product purification is facilitated by the presence of the introduced MIDA boronate in a catch and release fashion. The MIDA boronate catches on silica gel, and any contaminants are eluted with an Et₂O/MeOH mixture – note here the starting material will also elute as the MIDA boronate was cleaved in a previous step.



Scheme 32: Burke's workflow for the iterative coupling of boronic acids and deprotection of MIDA boronates.

The product is then eluted selectively with THF. One iteration has then been completed and the product is transferred to the deprotection module for MIDA cleavage. Each module is connected by tubing, with computer operated pumps attached to syringes to move solutions from one module to the other. The use of 8-way valves allows for solvent to be drawn into one syringe, and then pumped into a different module. The modules themselves are simple consisting of cartridges which have reagents added to them automatically or have silica already in them to be used for purification. The coupling module sits on a hotplate which allows for heating and agitation of the reaction.

Burke applies the automated synthesiser towards the synthesis of natural products or cores of natural products. First, the feasibility of the system is established by performing several iterations using commercially available MIDA boronates. In one example (Scheme 33), three iterations are performed to provide compound **109** in 26% yield. All products are produced on milligram scale which is enough for biological testing. The system is then applied in the synthesis of some natural product cores and full natural products. In each example, two iterations provide a “linear compound” which is then removed from the platform and standard deprotection reactions are performed. A cyclisation cascade is then also performed which again is performed manually outside of the automation platform, providing the core structure or natural product. These examples demonstrate that the platform can be used to provide intermediates for natural products. While the Suzuki reaction is well known for being one of the most widely used reactions in medicinal chemistry, a limitation of this system is that it can only perform this one type of reaction. This limitation also means that any further transformations have been undertaken off the



Scheme 33: An example from Burke and co-workers demonstrating the coupling procedure.

platform. Presumably, this platform could perform the mixing of reagents for other simple reactions, and then purification using the MIDA boronates “catch and release” protocol. Furthermore, any coupling step performed in this procedure only introduces $C_{sp^2}-C_{sp^2}$ bonds, and so the steps themselves do not introduce molecular complexity. There are however large numbers of complex MIDA boronate building blocks which are commercially available.

Another notable automation platform has been developed and reported by Cronin and co-workers in 2019.⁹⁵ This system is based around the use of laboratory glassware and machinery, thus reducing upfront costs, and increasing familiarity with chemists and therefore ease of use. To run the platform, the Cronin group develop their own software, labelling the whole system a ‘Chemputer’. This open-source software should allow for easy coding by any chemist to perform simple tasks based around the modules they have to hand. The report discusses the use of four modules: a reactor, a filter, a separator for liquid-liquid extractions (which are typically hard to automate) and a rotary evaporator. Each module is designed around common labware (Figure 18).

The reactor is a simple two necked round bottom flask attached to a condenser and situated in a computer controlled hot plate. The second neck allows for tubing to enter. This tubing travels to what is described as the ‘backbone’ of the system. This comprises

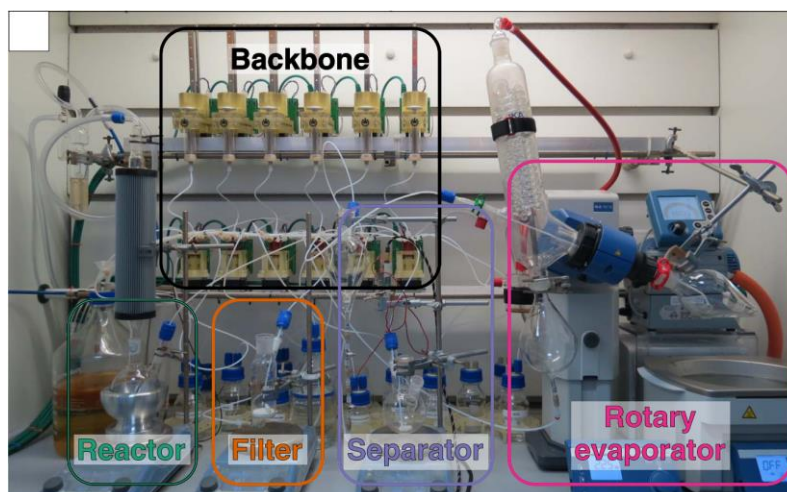
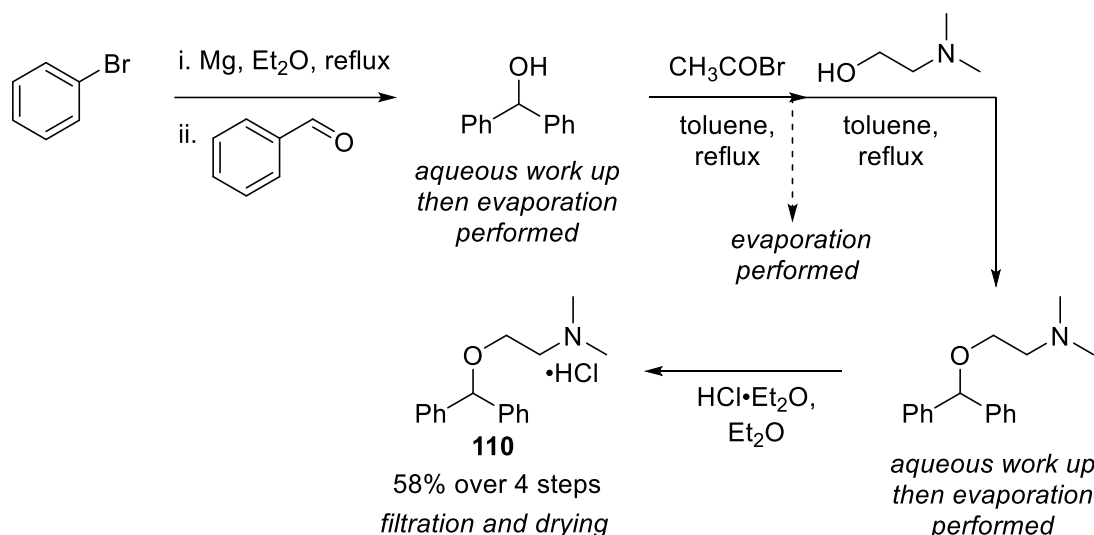


Figure 18: Cronin's Chemputer, which comprises four modules connected by a system of tubing and syringe pumps, called the 'backbone'. Taken from Cronin and co-workers.⁹⁵

of several syringes attached to pumps, all served by 6-way valves. As before, solutions can be aspirated into one syringe, and then pumped into another. From the new syringe, the solution can be pumped into a different module or another syringe. Importantly, the syringes can wash themselves with a house solvent, allowing for reuse in the same workflow. The group circumvent some unique challenges to allow for filtration and separation, which are not discussed here. The applicability is demonstrated in the synthesis of three medicinal products, all using similar well-known chemical reactions.

One example is diphenhydramine hydrochloride **110** (Scheme 34). The Chemputer performs a Grignard formation and addition reaction using bromobenzene and benzaldehyde, although the large amount of magnesium is weighed by hand into the reactor module. The reaction is then quenched with an aqueous solution of HCl and an aqueous extraction performed; the aqueous layer is sent to waste and the organic layer sent to the rotary evaporator for solvent removal. Once this is performed, the crude product is diluted in new solvent and taken to the washed reactor module for the next step (Scheme 34). The entire synthesis (four steps) required only 77 hours of Chemputer time, with no human intervention, whereas the authors state the manual synthesis took four days. The yield over four steps was 58%, compared to 68% overall for the manual synthesis, which is highly comparable – especially for the average yield per step (87% versus 91%). An updated version of Cronin's platform has been described, which includes the use of Burke's MIDA boronates in an iterative fashion and diazirine synthesis.⁹⁶



Scheme 34: Cronin's 77-hour automated synthesis of diphenhydramine hydrochloride **110**.

It is impressive how reliably Cronin and co-workers seem to have automated standard chemistry performed day to day in the lab, using common labware. In fact, they state the entire cost of the system they use, including glassware, was less than \$30,000. One can easily imagine using such a system for cryogenic reactions or air sensitive chemistry, as it is designed to work around standard labware. In addition, the entire software is completely open source so the more people that adopt, use, and contribute towards Chemputer systems, the more it will expand.

However, the Chemputer has not been used for any synthetic steps that are difficult to perform by an experienced chemist, although making chemistry more accessible to non-specialists is always beneficial. In addition, it is hard to imagine a Chemputer being used for a parallel or library synthesis based on the current report. The backbone design means that each different reaction on a library synthesis would have to be transported one at a time unless multiple backbones were used. The backbone itself needs to be washed with house solvent between each transfer, which would lead to a time-consuming process to avoid mixing different or similar reactions. Of course, as the software and hardware are completely open source, perhaps the system will evolve to one that allows parallel synthesis in the near future.

Flow chemistry is another popular area of automation. Such systems promise to be far safer and more scalable than traditional batch chemistry, as they allow extremely precise control over reaction parameters (reaction time, for example).⁹⁷ Large scale synthesis is well suited to continuous flow reactors, however, library synthesis is harder to design

although there are some examples of library synthesis using flow chemistry.^{98,99} Perhaps the differences between batch and flow chemistry, coupled with a potentially longer build time for flow systems and difficulty handling heterogeneous mixtures, have led chemists to continue to seek automated batch synthesis.

4.1.3 Description of the UOB Chemspeed platform

The University of Bristol have acquired a Chemspeed platform for automating chemical synthesis (Figure 19). The system is comparable in size to a glovebox and comprises of different areas on the 'deck' where modules, such as tools, reactors or vial racks, can be placed. The tools are picked up by a robotic arm that is suspended from the ceiling of the platform. The arm can move in three dimensions, and can also rotate, allowing it to reach any area on the platform. The platform can be connected to an inert gas supply. There is also an oil supply, which can be attached a cryostat for heating/cooling of vessels. The University of Bristol have a powerful Huber cryostat that allows for cooling to $-70\text{ }^{\circ}\text{C}$ within 15 minutes and minimum temperatures of $-90\text{ }^{\circ}\text{C}$.

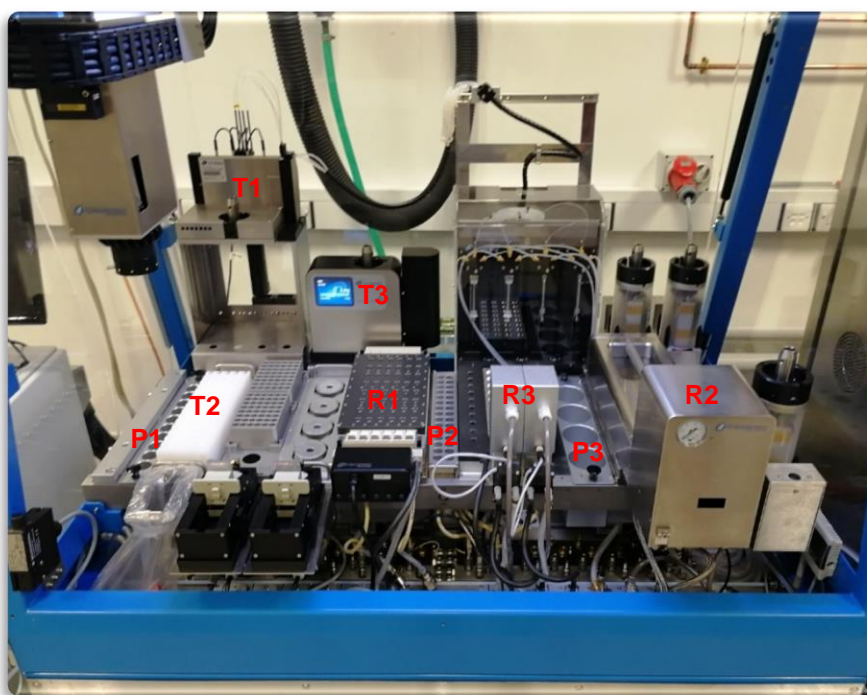


Figure 19: The 'deck' of the University of Bristol's Chemspeed platform.

4.1.3.1 Reactors

The platform has three different reactors. The first is called the ISYNTH (**R1**, figure 19) and consists of 48 positions that can take 8 mL vials, or inserts can be used to allow for the use of 2 mL vials. On top of the vials sits a plate that seals the vials and can also be

removed. This allows for each row of 8 vials to be placed under vacuum, inert gas, or sealed, independently of the other rows. This reactor can be shaken up to 600 rpm with temperatures from $-20\text{ }^{\circ}\text{C}$ to $120\text{ }^{\circ}\text{C}$. Chemspeed do provide a photochemistry plate that sits on top of the ISYNTH, projecting light into each reaction, however, in a test we found that the light sources were not powerful enough to allow for efficient reactivity. The second reactor is the high-pressure reactor (**R2**), called the microtitre plate (MTP) block, which takes the standard size MTP plates ($48 \times 2\text{ mL}$ vials). This reactor is built to work between 5–80 bar pressure, and so is much bigger in size than the other reactors. The platform has a reactive gas line with a rupture line to allow for safe use of reactive gases. It has the same shaking speed (up to 600 rpm) and temperature range (-20 to $120\text{ }^{\circ}\text{C}$) as the ISYNTH. However, the larger reactor will take longer to heat up/cool down and care should be taking when shaking at high speeds for long periods of time. The third and final reactor, of which Bristol have two sets, are the double jacketed glass arrays (**R3**), consisting of $16 \times 13\text{ mL}$ vessels which are surrounded by the cryostat oil. The double jacket only reaches to the height that $\sim 7\text{ mL}$ solvent will fill. These vessels can be cooled to $-90\text{ }^{\circ}\text{C}$, allowing for reactions that require cryogenic temperatures to be performed. Each lot of 16 vessels can be placed under vacuum or inert gas as desired.

4.1.3.2 Tools

The primary tool is the four-needle head (**T1**), which is for transferring liquids and solutions. Each needle is attached to a syringe that operates through a 6-way valve. As before (with Burke's and Cronin's systems) the use of a 6-way valve means solutions can be aspirated from solvent bottles connected directly to the syringe and then dispensed through the needles into a reaction. Alternatively, solutions can be aspirated through the needles and transferred to other reactions. The four-needle head is used to filter reactions through the solid phase extraction (SPE) rack (**T2**), which consists of 60 positions for 3 mL cartridges, with 8 mL vials beneath. A 3 mL cartridge is quite small for a filtration, especially compared to a sintered funnel one would typically use in the lab. The positions of the vials are fixed, but the cartridge rack above the vials can be moved, placing the filter cartridge over the top of the vials or over a waste position. For gravimetric dispensing (weighing and dispensing of solids), the system used is called the SWILE (**T3**). This uses small capillaries to pick up and transfer solids, with an internal balance for accurate weighing. This system is designed for weighing $<20\text{ mg}$ of material at a time.

In addition, the platform has several grippers which can move MTP plates or vials around the deck.

4.1.3.3 Reagents

The deck has positions for 60 mL (**P1**), 8 mL (**P2**) and 2 mL vials, and 250 mL Schott bottles (**P3**), allowing for great flexibility across different chemical reactions.

4.2 Results and discussion

4.2.1 Early modifications

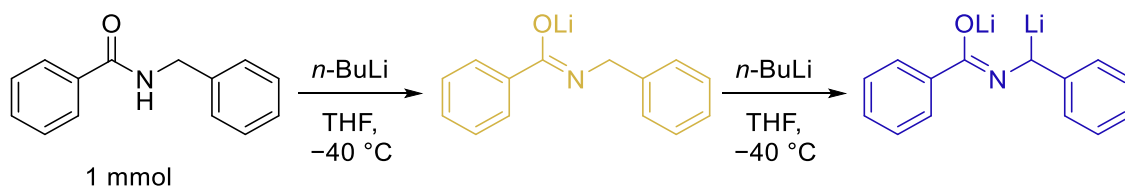
In order to perform air sensitive alkyllithium chemistry in the lab, chemists usually flame dry glassware and purge with vacuum/nitrogen cycles. To perform air sensitive chemistry on the Chemspeed platform, a suitable drying procedure was necessary. While the platform can be flushed with nitrogen gas, which lowers the O₂/H₂O reading to both less than 10 ppm within 2 hours, the glass vessels themselves need drying. As the glass arrays are surrounded by cooling oil, they are not suitable for flame drying. When the vessels were not anhydrous, any parallel reactions would be completely inconsistent with each other.

Two successful techniques for drying the reactors have been established. The first method is to add 5 mL of *n*-BuLi (1.6 M in hexanes) to the vessels. This is stirred for 5 minutes then removed to a waste position inside the platform. Dry solvent is then added to the vessels, which is then stirred and removed to the same waste. This provides sufficiently anhydrous conditions to give reproducible results. Using a lower volume of *n*-BuLi (1 mL) but diluted to the same total volume (5 mL) with dry solvent was not sufficient. The second method is to heat the vessels to 100 °C for 2 hours under vacuum (~12 mbar). This procedure could be useful as it does not generate large volumes of *n*-BuLi waste and takes the same time to dry one vessel as it does to dry all of them. However, for two to four reactions in parallel, which were commonly performed, the *n*-BuLi wash was found to be quicker, and so was primarily used. Constantly heating and cooling the glass arrays quickly could be damaging.

The solvent commonly used in the lab for lithiation–borylation reactions is diethyl ether.¹⁰⁰ THF is not normally used as the solvent can lead to non-enantioselective lithiations.⁶⁰ However, diethyl ether is a volatile solvent with a low boiling point of 35 °C. This volatility can lead to inaccurate dispenses with sealed syringes, as any vacuum generated during an aspiration will lead to solvent evaporation in the lines and therefore

bubbles in the solvent. Extremely slow aspiration rates can be used, but this is inefficient. Instead, the solvent was swapped to *tert*-butyl methyl ether (TBME), a higher boiling point (55 °C) ethereal solvent, which should not affect the chemistry performed and lead to more accurate solvent dispensing.

To ensure the concentration of alkyllithiums dispensed by the platform was as expected, a method for titration was developed. Indeed, during early testing of the platform we had observed incomplete conversions. Although the box was flushed with N₂ gas for 2 h before any chemistry was performed, there seemed to be quenching of alkyllithiums within the platform. To test this theory, we performed a titration on the platform, using *N*-benzylbenzamide, which turns a dark blue upon reaching the endpoint.¹⁰¹ Unlike a typical titration, we did not dispense a volume of *n*-BuLi dropwise and record the volume at which the end point was reached. Instead, a constant amount (1 mmol) of *N*-benzylbenzamide was added to each reactor, then an increasing volume of *n*-BuLi was added to each reactor. We hoped to have one reactor where the endpoint was not reached and the next where the endpoint was reached, thus the titre would be the middle point of these two titrations. This method was successful and provided us with a clear endpoint (table 8).



mmol	vol @ 1.6 M	C eff	Colour ?
1	0.625	1.60	N
1.05	0.656	1.52	N
1.1	0.688	1.45	N
1.15	0.719	1.39	Y
1.2	0.750	1.33	Y
1.25	0.781	1.28	Y



Table 8: Titration of the *n*-BuLi (1.6 M) on the platform with *N*-benzylbenzamide. giving a lower concentration on the platform, around 1.42 m. This demonstrates some alkyllithium is quenched on the platform.

Increasing amounts of *n*-BuLi (titrated by hand to be 1.6 M) were added from left to right in the above picture (1.05 to 1.20 mmol are shown). The endpoint is clearly not reached even adding what should be 1.1 mmol of *n*-BuLi to the 1 mmol of *N*-benzylbenzamide. Taking the midpoint of the results shown gives a new concentration (C_{eff}) of 1.42 M. To ensure reproducibility we were keen to reduce the level of moisture in the platform. First, a dummy volume of *n*-BuLi was aspirated and sent to waste before performing the titration, which only provided the same results as above. Next, the “system solvent” in the platform was considered. The tubing inside the platform that connects the needles to the syringes is filled with “system solvent” – typically the same solvent as one would use in the chemistry being run (to prevent cross contamination). We were using reagent grade (non-anhydrous) TBME as system solvent up to this point, and so decided to swap and use anhydrous TBME. Flushing the system with anhydrous TBME (after flushing the platform with N₂ for 2 h) before the titration resulted in an immediate and reproducible increase in the titre to 1.6 M. We were now confident that the conditions on the platform were anhydrous and suitable for use of moisture sensitive reagents.

4.2.2 Filtration and Evaporation

When performing lithiation–borylation chemistry, specifically assembly–line synthesis, after the chemistry is complete a filtration is required to remove any salts formed. In the lab, this provides sufficiently clean crude material for subsequent iterations. The filtration is performed through a silica plug, typically with a large excess of silica. Automated SPE is typically performing using a “catch-and-release” system. The substrate is typically tagged in such a way that when it interacts with the solid phase, one mobile phase will elute every by-product but not the tagged substrate which enables the use of large excesses of reagents. Once all the by-products are filtered to waste, a different (usually specific) mobile phase elutes the product which can then be taken forward. A catch and release system for the lithiation–borylation process was not designed, instead the filtration was performed as it is in the lab. On the platform, however, we are restricted to a 3 mL syringe to filter through. It was found that 400 mg of SiO₂ with 5% Et₃N was a suitable stationary phase while filtering 0.8 mL of reaction solution at a time. If volumes higher than 0.8 mL were filtered in one go, the syringes could explode, either halting the filtration or resulting in loss of material. For all the reaction material to pass through the filter, an air push was designed where the platform aspirates 2 mL of air before taking the reaction mixture. This air is then dispensed immediately following the dispense of the

reaction mixture. This procedure prevents the solution passing backwards out of the filter from leftover back pressure. Another 9 mL of air is then pushed through after the 2 mL air push. This air push was found to be essential to the success of the filtration.

Evaporation of any solvent under reduced pressure was performed slowly, to try and avoid any solvent bumping (Figure 20). The vacuum pump can be controlled precisely in the software, and loops were used to lower the vacuum slowly. Starting at ~1000 mbar, the vacuum was lowered by 50 mbar every 30 seconds until 200 mbar was reached. At the point, solvent loss (TBME) starts to occur, as observed by cooling of the solvent. The vacuum was then dropped by 20 mbar every 8 minutes until 120 mbar is reached (40 mins total time). At this point, by repeated observation, the TBME had all evaporated. The vacuum is then lowered to 12 mbar for 5 minutes to ensure dryness. This evaporation procedure is performed several times (2 – 4 times depending on the total volume of the reaction) and the very last time in a workflow we incorporated a 1 h drying at 12 mbar (the minimum the pump could reliably achieve) to try and ensure full dryness.

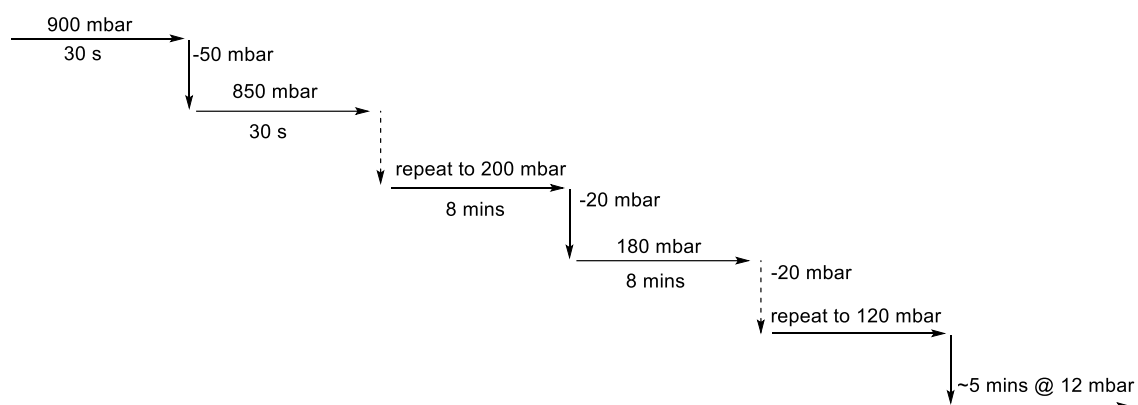


Figure 20: The solvent evaporation procedure.

4.2.3 Matteson homologation

Once all general considerations had been taken into account, and a suitable filtration and evaporation procedure identified, the Matteson homologation was explored. This transformation inserts a methylene group into the growing boronic ester chain and the reaction is performed under in situ conditions (the boronic ester and carbenoid precursor are premixed before addition of alkyllithium). The drying procedure was discussed above (5 mL *n*-BuLi rinse with 2 h N₂ flush of the box). Workflows are represented here for simplicity, as opposed to drawn out in the Autosuite software that runs the platform (see the supporting information for specifications). Setting the Huber cryostat to $-78\text{ }^{\circ}\text{C}$ gave a temperature of $-70\text{ }^{\circ}\text{C}$ in the reactor, which was not expected to affect the chemistry.

Typically, in the lab, BrCH_2Cl (2 eq.) and $n\text{-BuLi}$ (1.9 eq) would be used, with high yields (~90%) normally observed. Four reactions were performed using phenethyl boronic acid pinacol ester **111** as a model substrate (table 9). These were carried out in parallel to evaluate reproducibility, using the workflow shown in figure 21 and conditions shown in table 9. At this stage, we did not perform filtration and evaporation on the platform. While the conversions (2% SM left) and yields (68%) were good, normally higher yields are observed in the lab (~90%). The cause of the loss of material was not apparent at this stage in the optimisation.

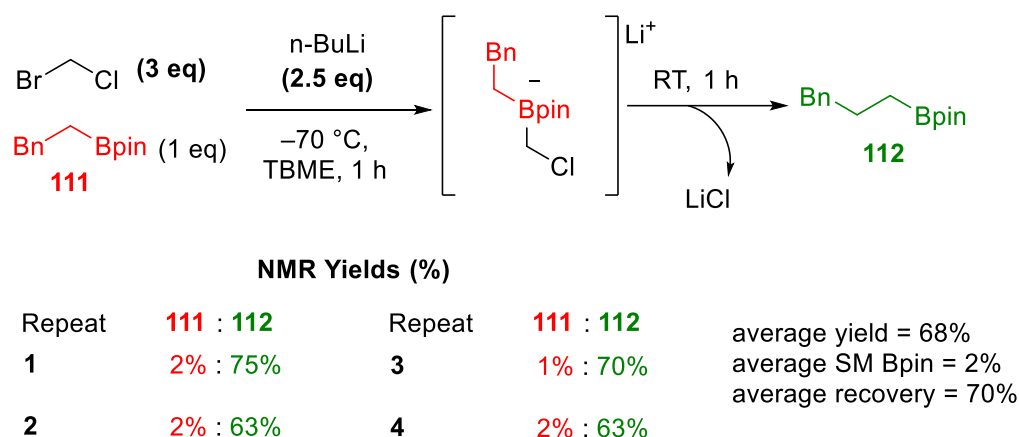


Table 9: Results from performing the Matteson homologation (4 reactions in parallel) with BrCH_2Cl , without filtration and evaporation.

Wary of the instability of the lithium carbenoid, the rate of addition of $n\text{-BuLi}$ was reduced from 0.8 mL min^{-1} to 0.1 mL min^{-1} to try and avoid any large temperature increase in the reaction. Lowering the reactor temperature from $-70 \text{ }^\circ\text{C}$ to $-78 \text{ }^\circ\text{C}$ made no difference to the yields. A large difference was observed when swapping to a different carbenoid precursor: iodochloromethane, ICH_2Cl (table 10). The yields increased from good (68%) to excellent (87%) using this carbenoid precursor. Potentially, as the lithium–iodine exchange should be faster than lithium–bromine exchange, the $n\text{-BuLi}$ has less chance of adding into the boronic ester instead. This non-productive pathway would form a boronate complex which cannot undergo 1,2-migration. If formed, such a boronate complex could degrade upon warming, or instead could be lost as a salt during filtration, leading to the reduced recoveries seen in table 9. In the lab, lithium–bromine exchange is quick enough to avoid this, however, perhaps as the reactions are shaken in the platform instead of magnetically stirred, the lithium–bromine exchange is slower.

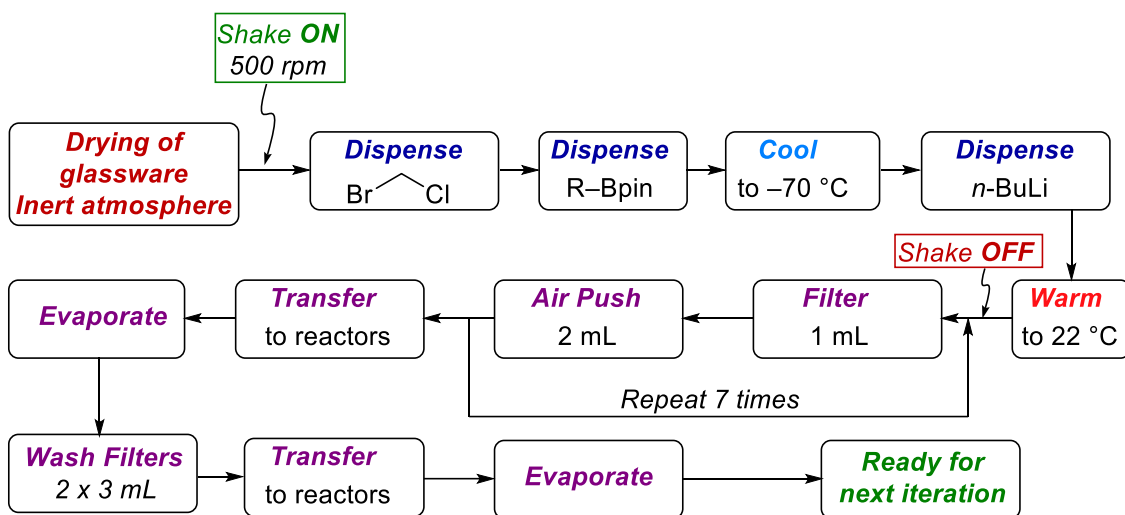
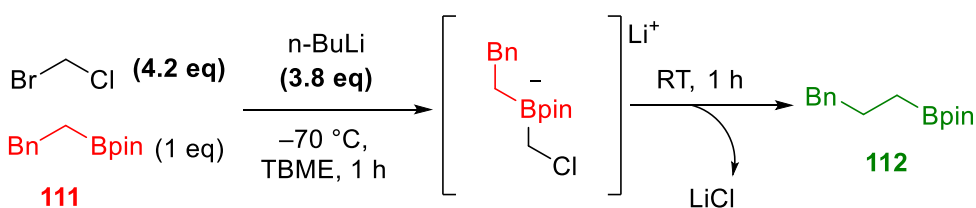


Figure 21: Workflow for the Matteson homologation. Drying the glassware takes ~40 minutes and reaction time is 2 hours. The filtration takes ~15 hours due to the 3 mL filter cartridges and slow evaporation to avoid bumping.



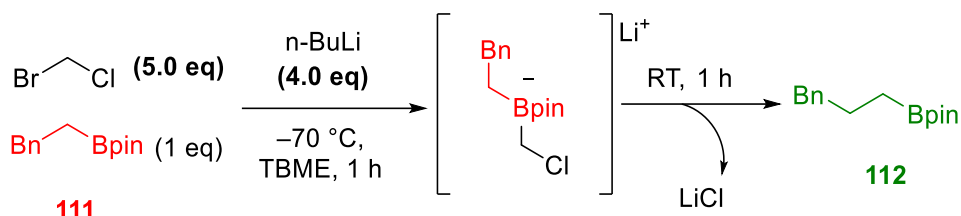
NMR Yields (%)

Repeat	111 : 112	Repeat	111 : 112	
1	<1% : 87%	3	<1% : 86%	average yield = 85% average SM Bpin = 1% average recovery = 86%
2	<1% : 81%			

Table 10: Results after swapping to ICH_2Cl as the carbenoid precursor, without filtration and evaporation.

Unfortunately, it was quickly realised that ICH_2Cl is light sensitive and cannot be kept out of the dark for more than a few hours without the solution turning pink. Indeed, poor conversions were noted for subsequent Matteson homologations performed without preparing a freshly distilled ICH_2Cl stock solution. This would hinder subsequent work if several Matteson homologations were to be performed in a row without replacing the ICH_2Cl solution. Bromochloromethane (BrCH_2Cl) was used instead, and we hoped to increase the conversion by increasing the equivalents of reagents. Previous results had shown that using a large excess of $n\text{-BuLi}$ gave poor recoveries, presumably due to undesired addition of $n\text{-BuLi}$ to the boronic ester. To try and avoid this, the ratio of carbenoid precursor to $n\text{-BuLi}$ was increased from 1.11 to 1.25 (table 11) and the equivalents of $n\text{-BuLi}$ were increased to 4 to consume the rest of the starting boronic ester.

This strategy was an improvement, affording high yields after filtration and evaporation on the platform, with little starting boronic ester remaining. Unfortunately, the conversion was never as high as when using iodochloromethane. However, ~2% remaining starting material was deemed acceptable as it could be removed by preparative-HPLC at the end of the synthesis, a technique commonplace in other iterative automated synthesis.



NMR Yields (%)

Repeat	111 : 112	Repeat	111 : 112	
1	2% : 78%	3	1% : 79%	average yield = 80%
2	2% : 82%	4	2% : 81%	average SM Bpin = 2%
				average recovery = 82%

Table 11: Results from performing the Matteson homologation with BrCH_2Cl , with filtration and evaporation, using an increased carbenoid precursor to $n\text{-BuLi}$ ratio and higher equivalents.

With the conversions now good, and a full workflow in place, attention was focused again on the yield: why was the recovery lower than expected with full conversion? As stated previously, yields of ~90% are typically observed in the lab for a Matteson homologation. While an average yield of 80% is not too far off this, when performing an iterative sequence with many steps, 80% per step will decrease the amount of material much faster than 90% per step.

4.2.4 Dispensing Tests and Transfer Optimisation

To determine where the cause of material loss, several dispense tests were performed by moving phenethylboronic acid pinacol ester **111** (SM) and 1,3,5-trimethoxybenzene (**IS**) through the workflow without performing any chemistry (Figure 22). First, the materials are transferred from stock solutions to the glass array vessels (reactor vessels), then are filtered through basic silica into 8 mL vials, and finally transferred to the ISYNTH 8 mL vessels for evaporation under reduced pressure.

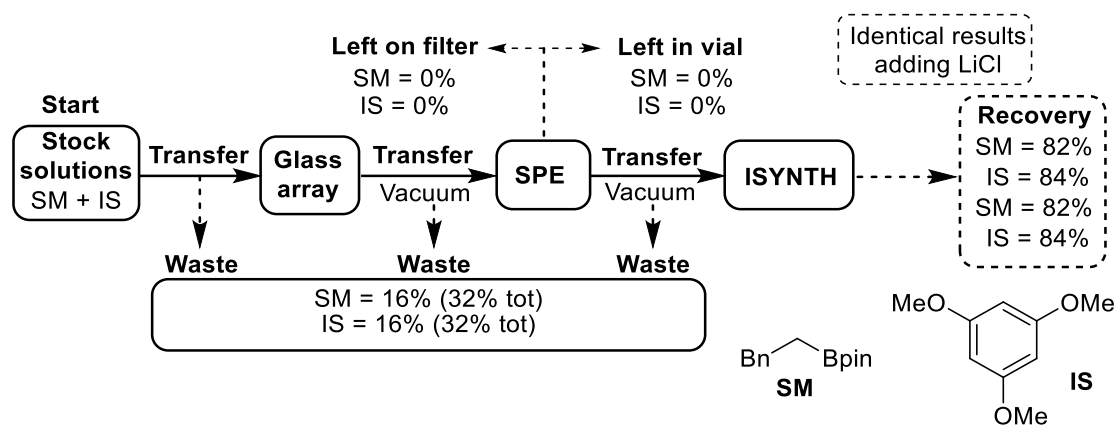


Figure 22: Dispensing test manipulating phenethylboronic acid pinacol ester (SM) and trimethoxybenzene (IS) through the Matteson workflow without performing any chemistry.

From figure 22 the final recoveries from two parallel dummy “reactions” match well with the yields from table 11. Each position where the materials had been was then washed and analysed by ^1H NMR with comparison to an added external standard (CH_2Br_2), but no material was found at each location. This indicates that the transfers used in the workflow can remove all the material from the vessels used. Surprisingly, the rest of the material was found in the waste position at the back of the platform. Potentially, the solvent containing the material was mixing with the system solvent during transfers. This material is then rinsed to waste at the end of a transfer.

To avoid this process, a 0.2 mL addition of system solvent was added directly after each dispense (Figure 23). It was anticipated that this 0.2 mL would contain all the mixed solvents and therefore the rest of the material. The use of crystalline trimethoxybenzene had led to the observation of white solid outside the 8 mL vial on the ISYNTH plate, presumably from solvent bumping. Even though the vacuum pump was controlled precisely, the 8 mL vials did not seem an appropriate location for solvent evaporation. To try and avoid solvent bumping, only 1 mL at a time was transferred to the ISYNTH for solvent removal. As can be seen in figure 23, recovery was found to be improved to 93%, and only small amounts of material were going to the waste. The filtration and vacuum sections of the workflow involve the most transfers, and this is where most material loss to waste was observed. This is in line with the solvent mixing hypothesis outlined above.

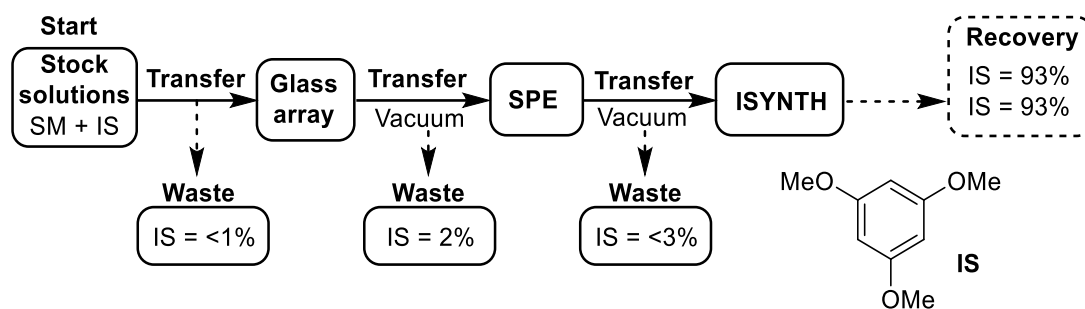


Figure 23: Performing a 0.2 mL needle rinse avoids material going to the waste, and evaporating solvent 1 mL at a time prevents bumping in the ISYNTH.

Unfortunately, taking the changes — a 0.2 mL rinse and 1 mL evaporation at a time — over to the Matteson workflow did not increase recovery. Having noticed the crystalline solid on the ISYNTH plate after the dispensing test, it was decided to move the location of the evaporation from the 8 mL ISYNTH vial into the 13 mL glass array vessels. Thankfully, this did have a large impact on recovery which jumped to 94% (table 12). Presumably during solvent evaporation in the ISYNTH, the reaction mixture was continuously bumping, leading to a reproducible loss of material.

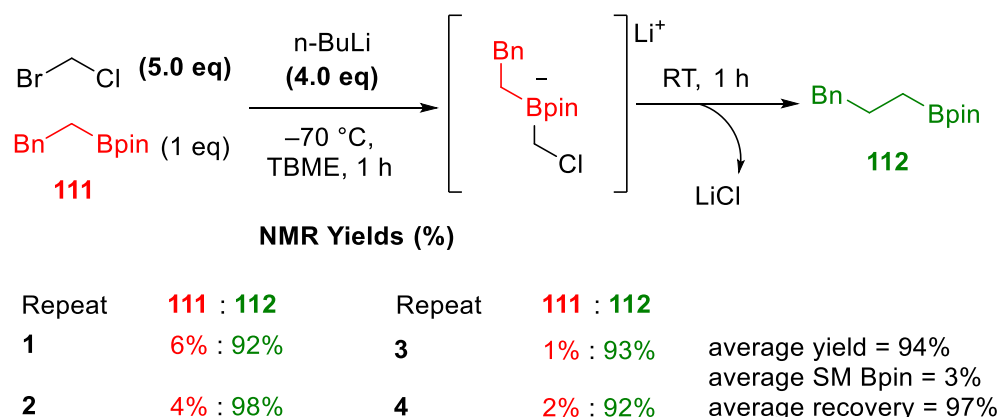


Table 12: Results from performing the Matteson homologation with $BrCH_2Cl$, with filtration, and evaporation in the 13 mL glass array vessels.

4.2.5 Iterative Matteson Reactions

Filtered boronic ester product **112** was then redissolved in anhydrous TBME and then transferred to a dried glass array vessel for another Matteson homologation. To ensure the process was not disrupted by removing the samples and performing 1H NMR analysis, the reactions were sampled automatically by the platform and transferred manually to a GC-MS machine to check the conversion (offline analysis). For the first single step, the conversion was routinely $<5:95$ **111:112**. However, as shown in table 13, when a second Matteson homologation was performed the conversion dropped to $34:66$ **112:114**, the

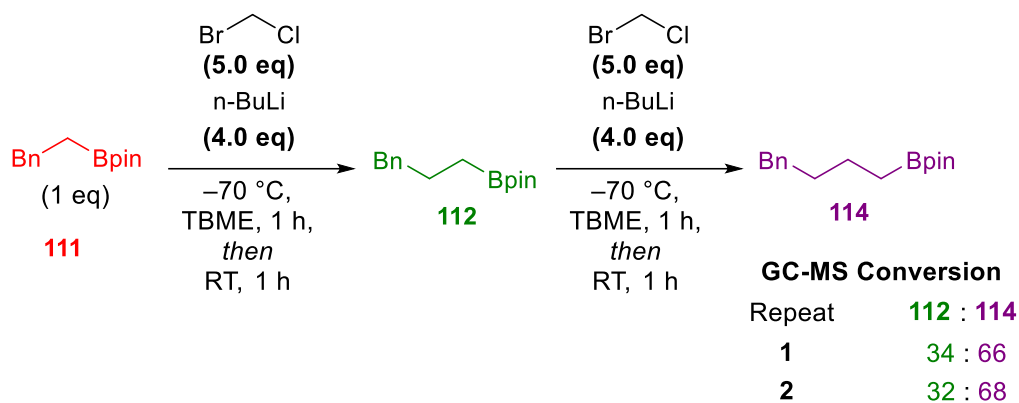


Table 13: First attempt at two iterative Matteson homologations, showing poor conversions and recoveries for the second step.

recovery was poor (~50%) and ^1H NMR analysis was difficult due to many overlapping peaks.

On closer inspection of the ^1H NMR spectrum from the first Matteson step, a triplet at $\delta = 3.5$ ppm led to the identification of 1-bromobutane in the reaction mixture. Due to the large number of equivalents of *n*-BuLi and BrCH_2Cl the generation of a large amount of 1-bromobutane (~1 eq relative to the starting boronic ester) was occurring. The exact deleterious pathway with 1-bromobutane was not determined as no other by-products were identified. With a boiling point of ~102 °C at atmospheric pressure, the length of the evaporation at the end of the workflow was increased to 3 hours to remove as much

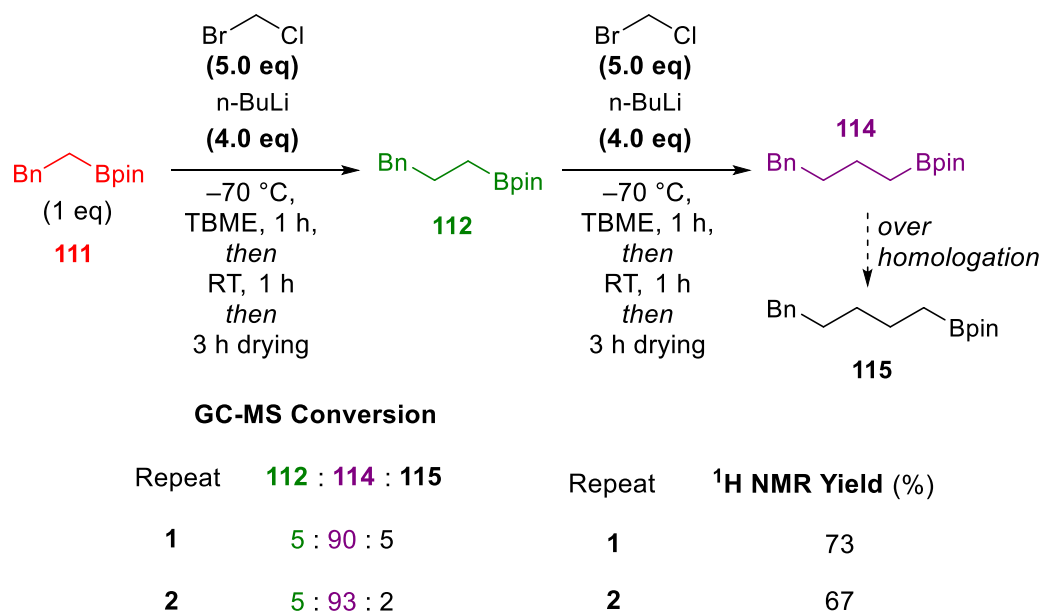
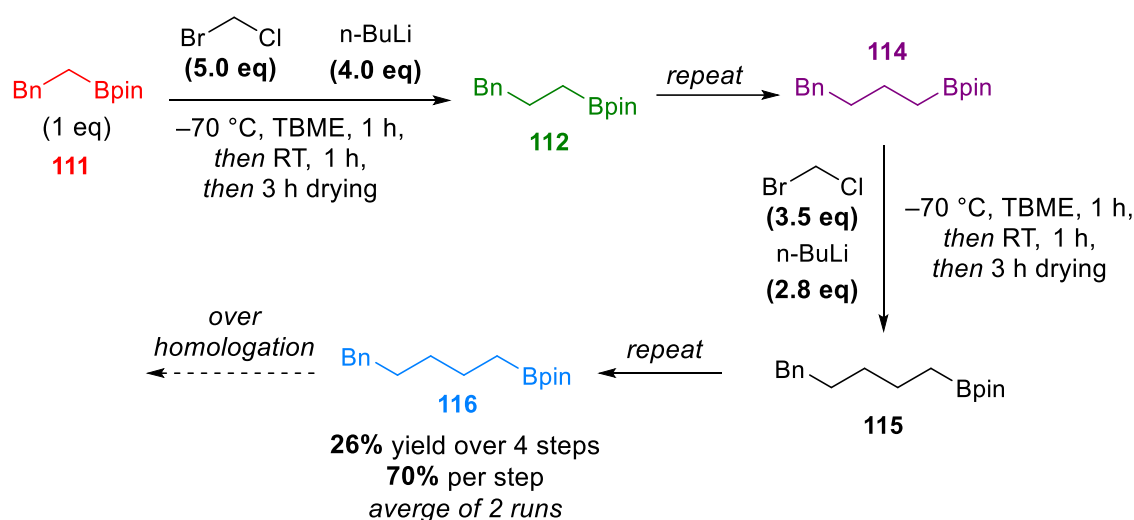


Table 14: Two iterative Matteson homologations, with a 3-hour evaporation sequence in the middle, proceeding with good recoveries (112/114/115 not separable by ^1H NMR) and good conversions. ^1H NMR yield by comparison to CH_2Br_2 as an internal standard (added to the crude reaction).

1-bromobutane as possible. Indeed, the yield over 2 steps was increased to ~70% with good conversions (table 14). GC-MS analysis showed good conversions for the second step, in contrast with the previous result without a longer evaporation (table 14). A small amount of over homologation can be observed to give boronic ester **115**. Presumably a small amount of boronate complex migrates at $-78\text{ }^{\circ}\text{C}$, which is then homologated again under the reaction conditions. This can also be observed when performing Matteson reactions manually in the lab.

Despite the improvements, the new workflow was still not perfect. A yield of ~70% over two steps with an assumed average 94% for the first step indicates a 74% yield for the second step. Perhaps 1-bromobutane still persisted even with a 3-hour drying procedure, or there was water in the present in the crude material after filtration, as non-anhydrous TBME is used for the filtration. As a proof of concept, the above conditions were applied in four iterative Matteson homologations (table 15) where the only human intervention was the replacement of stock solutions after the second homologation. Mindful of the



		GC-MS Conversions					
Iteration	Repeat	111	112	114	115	116	over
1	1	-	97	3	-	-	-
	2	-	100	-	-	-	-
2	1	-	1	96	3	-	-
	2	-	2	98	0	-	-
3	1	-	-	3	95	3	-
	2	-	-	6	94	0	-
4	1	-	-	-	5	92	5
	2	-	-	-	8	90	2

Table 15: Four iterative Matteson homologations, showing good conversions and final recovery. Both parallel reactions recorded a final yield of 26%.

reduction in yield to ~70% over two steps, the number of equivalents of reagents were reduced by 70% after the second step.

As can be seen from table 15, each step proceeds with good conversion (GC-MS). Over 4 steps, the total yield was 26%, which corresponds to 70% per step. This four-step sequence demonstrates that iterative synthesis, using complex organoboron/alkyllithium chemistry, is possible on an automated system. It was reasoned that 1-bromobutane could persist after the 3-hour drying procedure, which turned out to be correct (~15% relative to the starting boronic ester). However, while heating the crude material at 60 °C under vacuum did remove the bromobutane (~2%) the yield of product was reduced to ~84% (from a typical 94%). Potentially, the product was not stable at 60 °C under reduced pressure. A second homologation then proceeded with a 76% yield, affording a yield of 64% over two steps. From these results, it was apparent that removing the 1-bromobutane by heating did not improve the process.

It was decided to revisit the optimisation of the one-step Matteson reaction. Why were such high equivalents of BrCH_2Cl and $n\text{-BuLi}$ required for higher yields on the platform? As well as this, higher yields still are observed in the lab (~90% for simple substrates).

One theory was that the mixing of the reaction was worse on the platform than in the lab. The reactions are shaken not stirred, and potentially this could lead to inefficient mixing and therefore poor reactivity. The mixing of an aqueous copper sulphate solution (blue) and ferrocene in CH_2Cl_2 (yellow) in the glass array reactors was looked at (Figure 24). Of course, these two phases are extremely resistant to mixing and so this is a stringent test of mixing on the platform. As can be seen at 500 rpm, the mixing is minimal as the two

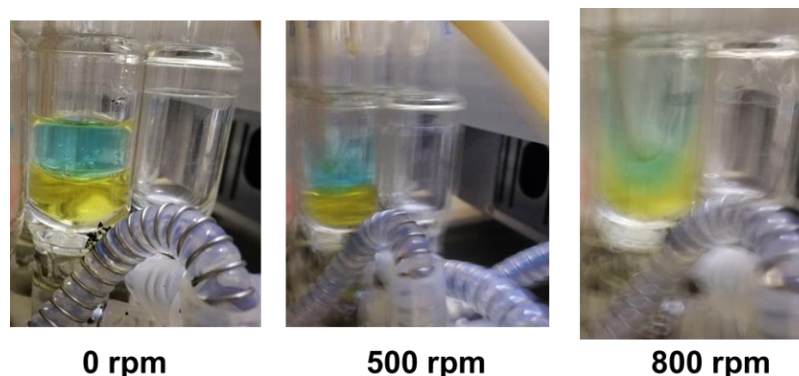


Figure 24: Mixing of aqueous copper sulphate (blue) and ferrocene in CH_2Cl_2 (yellow) the glass array reactors at the rpm specified. Mixing is poor at 500 rpm but better at 800 rpm, although still not excellent.

phases can be seen clearly. Unfortunately, this meant all our previous optimisation had been done with poor mixing. Increasing the speed to 800 rpm resulted in much better mixing although still not perfect (a factor to consider when working on the Chemspeed platform). Some green colour can be observed between the two phases and there is a definite vortex in the middle of the solution. Importantly, the level of the solvent does not go above the height of the cooling jacket on the reactors. The theoretical maximum speed of the mixing on the platform for the glass array reactors is 1000 rpm, however we were hesitant to try this as the reactors will be at $-70\text{ }^{\circ}\text{C}$ and therefore have a greater of breaking. Another way to increase mixing further would be to generate turbulence inside the reactor, using baffles or particles. Other users of the platform at the University of Bristol have used glass beads in standard reaction vials, leading to more efficient mixing.

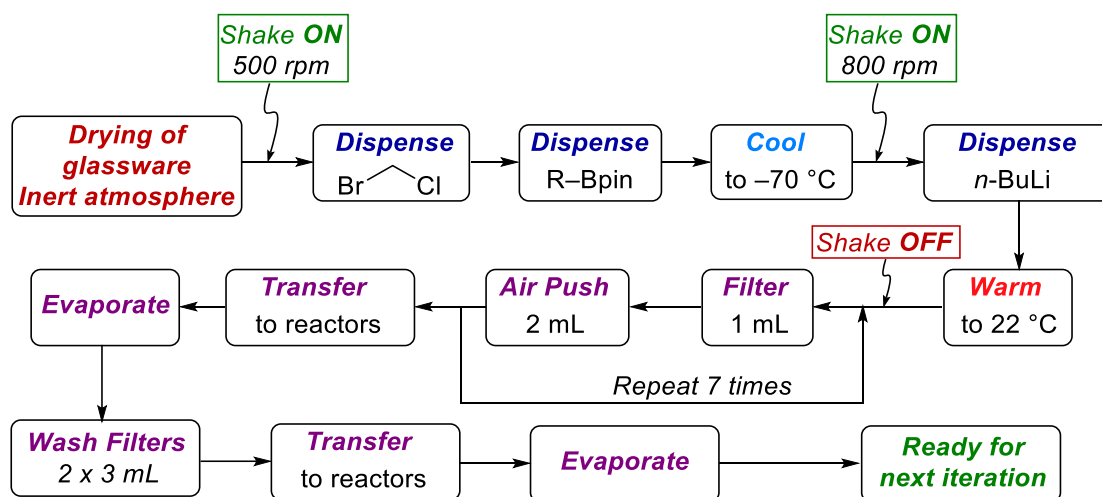


Figure 25: New Matteson workflow with increased mixing speed (800 rpm) during *n*-butyllithium addition. Drying glassware takes ~40 minutes and reaction time is 3 hours. Filtration takes ~15 hours due to small 3 mL cartridges and slow evaporation to avoid bumping.

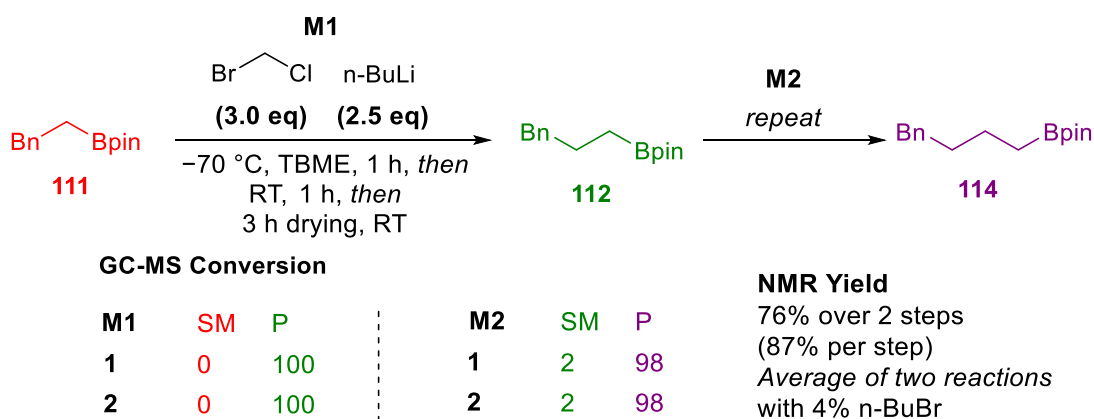


Table 16: Performing the Matteson homologation over 2 steps with increased mixing rate (800 rpm vs 500 rpm) leads to improved yields (87% per step) with only trace 1-bromobutane remaining. No heating during the 3 h drying is required.

However, we did not try this in the glass array reactor vessels as it would lead to a higher surface area to wash for good recovery and there is a potential for breakages if a needle collided with a bead.

Increasing the mixing speed during the addition of the *n*-BuLi with no heating during the 3 h drying (Figure 25) led to an immediate improvement in the results (table 16). On model substrate **111**, a 76% ¹H NMR yield was obtained (87% per step) with little 1-bromobutane present (4%, average of two runs in parallel). These results gave high confidence in multiple, selective, and high yielding Matteson homologations on the platform. The optimisation of another type of homologation reaction was now performed.

4.2.6 Homologation with stannane **41**

The homologation of boronic esters with stannane **41** (discussed in section 1.2.3) on the Chemspeed platform was then explored, to allow for the stereospecific installation of methyl groups on a growing carbon chain. If successful, this would be another step towards the automated synthesis of natural products.

The workflow performed is shown in figure 26. The only difference in the workflow at this point to that of the Matteson workflow was that tin–lithium exchange is performed before addition of the boronic ester (ex situ conditions). The stannane was first cooled to –70 °C and then *n*-BuLi added. After 1 h, when tin–lithium exchange is complete, the boronic ester is added. As there is no bulky diamine on the lithiated species, borylation is assumed to be rapid and the reaction is stirred for 1 h. It was observed that the boronate complex can precipitate at low temperatures, leading to a heterogeneous gum that was resistant to mixing. This led to the formation of layers and failed reactions. The rapid shaking (800 rpm) helped with this somewhat, as did keeping the scale (per reaction) under 0.7 mmol. Performing reactions at 1 mmol was attempted, however poor mixing and exploded filters were commonly seen so this scale was abandoned. We also found that it was necessary to rewash the reactors with TBME and filter again, presumably due to the sticky benzoate salts instead of the LiCl by-product (in the Matteson process). This simple rewash procedure was included in future Matteson processes, to ensure full recovery.

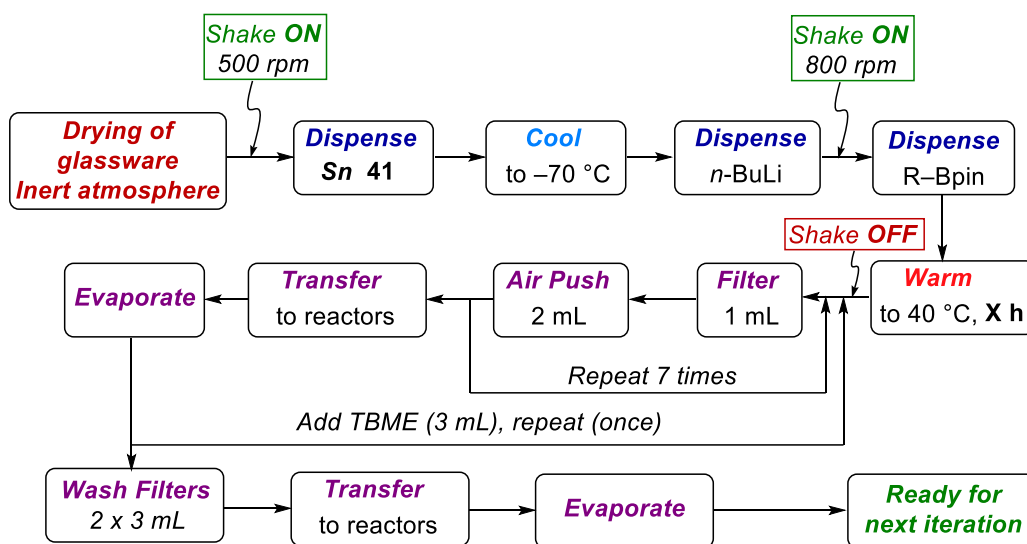
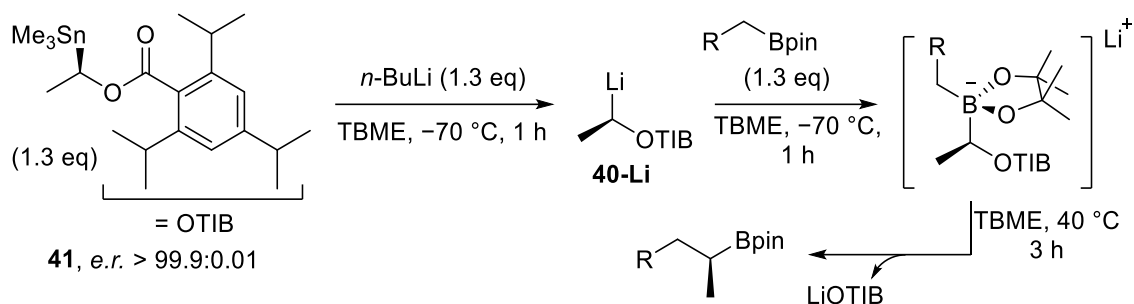
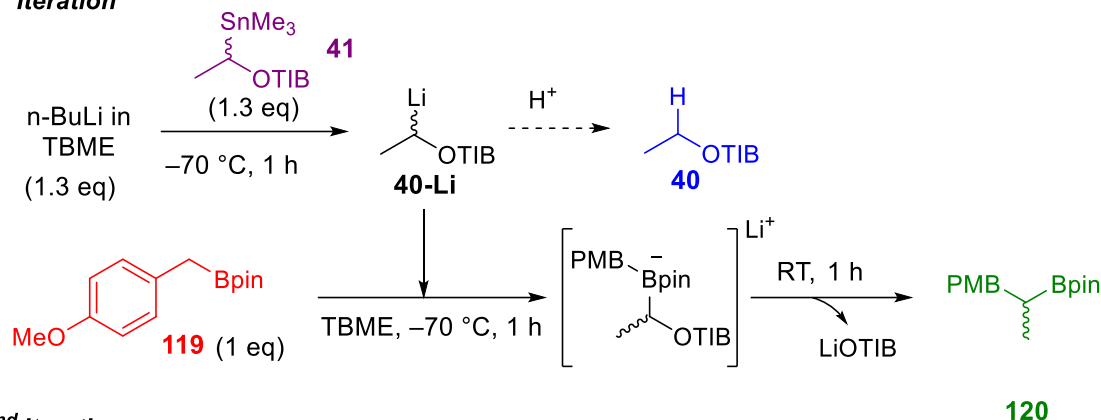
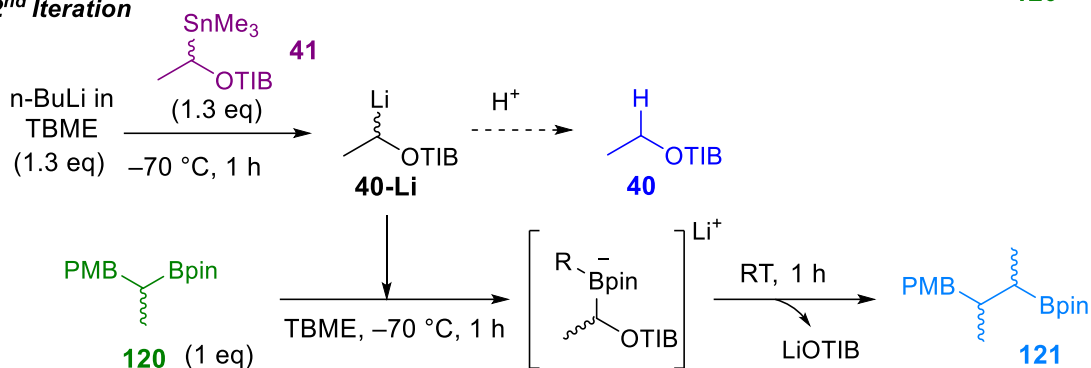


Figure 26: Scheme and workflow for the homologation of a boronic ester with organostannane **41**.

Table 17 shows the results after performing the modifications described above. Three reactions were run in parallel to check for reproducibility, which, given the low ranges of values, was found to be high. A minor amount of benzoate **40** was observed, which means that water is entering the vessels at some point during the workflow. This would typically be observed in the manual procedure as well (<10%). Similar to the Matteson process, excellent conversions were observed accompanied by low yields. Our attention turned to the filtration: unlike the Matteson process, a sticky gum was left at the end of the reaction due to the presence of the benzoate salt by-products (LiOTIB). There was concern that the platform was unable to properly mix the crude reaction. Indeed, manually dissolving all the benzoate salts in THF, removing the solution from the platform, and performing ^1H NMR analysis with an internal standard (CH_2Br_2) showed 15–20% remaining product in the reaction flask after the filtration process. Interestingly, CDCl_3 , which does not dissolve all the benzoate salts, was used first to analyse the leftover crude mixture and no product was observed. We therefore believed that the entire mixture needed to be dissolved and filtered to allow for increased recoveries and so decided to change the workflow (Figure 27).

1st Iteration**2nd Iteration****1st Iteration:** ¹H NMR Yield (%)Repeat **119** : **120** : **40** : **41****1** 0% : 68% : 11% : 0%**2** 0% : 73% : 9% : 0%**3** 0% : 69% : 10% : 0%

average yield = 70%

2nd Iteration: ¹H NMR Yield (%)Repeat **120** : **121** : **40** : **41****1** 0% : 63% : 18% : 0%**2** 0% : 74% : 27% : 0%**3** 0% : 74% : 12% : 0%average yield = 70%
(49% over 2 steps)

Table 17: First round of results for the homologation of **119** with stannane **41** after early experiments and including modifications.

At the end of the reaction, the TBME was removed under reduced pressure (12 mbar) and THF (3 mL) added to dissolve the entire crude mixture. This homogenous solution was taken to be filtered. Thankfully, this modification resulted in an improved ¹H NMR yield of 85% however, unfortunately, the benzoate salts eluted with the product leading to very impure material that would not undergo another homologation. Trying smaller volumes of THF (0.8 mL vs 3 mL) led to reduced recoveries (~70%) and similarly impure material (Figure 28).

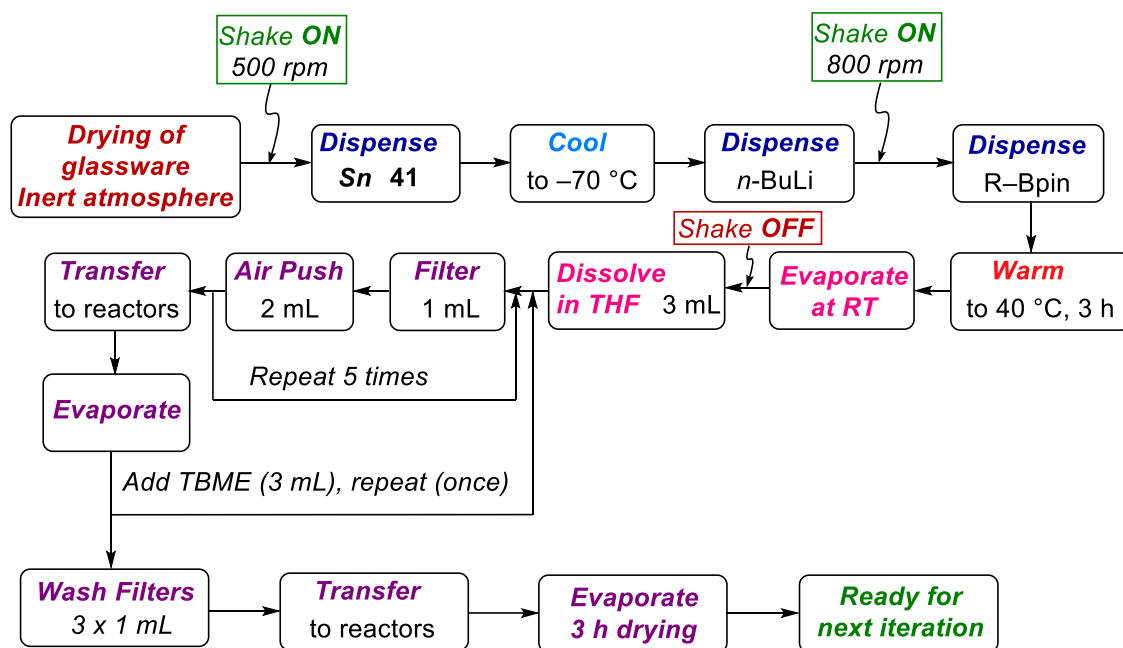


Figure 27: New workflow for the homologation of **119** with organostannane **41** to ensure full transfer of product from the reactors to filters. After the chemistry is finished, the TBME is removed under vacuum and THF added to dissolve all benzoate salts. The entire mixture is now homogenous and transferred to be filtered. Shaking is also used intermittently during filtration. Drying glassware takes ~40 minutes and reaction time is 3 hours. Filtration takes ~20 hours due to small 3 mL cartridges, slow evaporation to avoid bumping, and repeated washing.

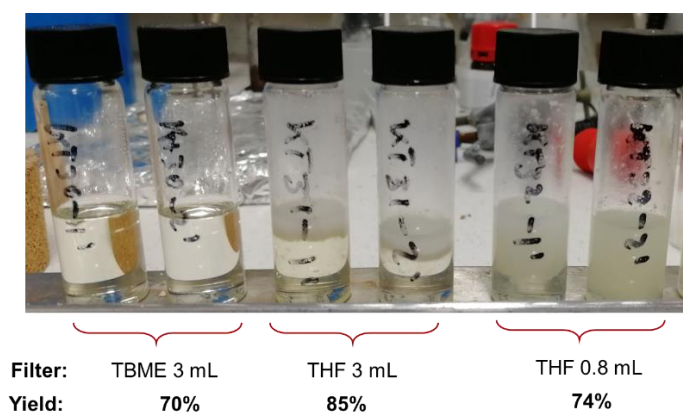
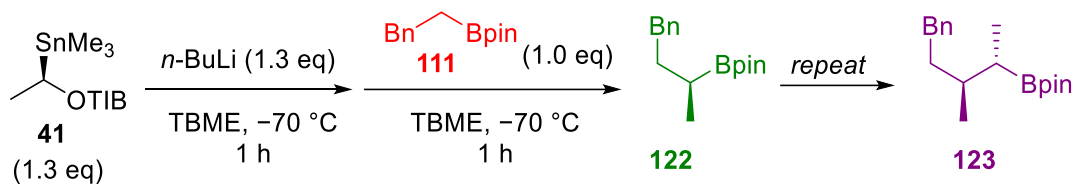


Figure 28: Filtered crude reactions. Left: Filtration using TBME. The material is homogenous, but the yield is low. Middle: Filtration using THF (3 mL). The material is heterogenous and not suitable for further reactions however the yield is high. Right: Filtration using THF (0.8 mL). The material is heterogenous and the yield is low.

The use of EtOAc and 1,2-dichloroethane (DCE) (in parallel experiments) was then tried as they have polarities between TBME and THF. The use of EtOAc led to impure material, however DCE worked well, providing a ^1H NMR yield of 90% for one step and clean crude product (Table 18). This was confirmed by performing a second homologation, which gave an ^1H NMR yield of 86% over 2-steps, demonstrating that the

~90% yield was maintained for the second homology. Fortuitously, DCE appears to be completely dissolve the product while leaving behind the majority of the benzoate salt.



Iteration 1			Iteration 2		
Entry	NMR Yield (%)	GC-MS 111 : 122	Entry	NMR Yield (%)	GC-MS 122 : 123
1	91	0 : 100	1	88 (over two steps)	2 : 98
2	93	0 : 100	2	84 (over two steps)	2 : 98

Table 18: Optimised process for 2-step homology with stannane **41**. High yields are observed over 2 steps using DCE to wash out the reactors.

4.3 Summary of optimisation

The optimisation of both the Matteson homology and homology with stannane **41** has been presented. These reactions have been improved from ¹H NMR yields of ~70% to ~90%. While 20% may not be a massive boost for a 1-step procedure, when performing multiple iterations a 20% per step leads to a large yield increase at the end of the entire process. For example, 5 iterations at 70% yield leads to an overall yield of 17%. However, five iterations at 90% yield leads to a much improved 59% yield. Optimisation of these conditions has not been trivial, where factors such as shaking speed and washing solvent (factors that would not normally be considered in a typical optimisation of a manual process) have been key to success. Early modifications, such as a proper drying procedure, were essential for reproducibility of results. With our optimised workflows in place, their application in synthesis was then explored.

4.4 Applications in the synthesis of kalkitoxin

4.4.1 Reactions in parallel

As discussed in section 1.2, the Aggarwal group, and others, have successfully used the homologation of boronic esters with metal carbenoids in total synthesis. This process has been fully automated for carbenoids LiCH_2Cl and benzoate **40-Li** with phenethyl boronic acid pinacol ester **111**. To further demonstrate the applicability of this methodology, its extension towards more complex boronic esters was sought, with an aim towards natural product synthesis. However, the synthesis of one natural product in a linear fashion using assembly–line synthesis would most likely be quicker and easier manually, though only for an experienced chemist. The automation platform’s advantage comes into play when performing multiple parallel reactions. By hand, performing two parallel reactions is not too difficult, however consider that the reactions will most likely be set-up/quenched/filtered at slightly different times, potentially leading to inconsistencies. Performing four reactions in parallel by hand is far more difficult. Keeping track of additions or even taking aliquots requires a large amount of the chemist’s time. However, it takes the same amount of time to set up one reaction in the Chemspeed platform as it does any multiple of them (within reason). The platform then easily keeps track of where reactions are being filtered, for example, and where they are being subsequently taken on further. Couple this with the fact that the robot can work 24 hours a day and vast amounts of time can be saved.

4.4.2 (+)-Kalkitoxin

The strategy of automated assembly–line synthesis will be applied to kalkitoxin, a natural product which has been synthesised previously by other groups, and in the Aggarwal group in 2015.⁸¹ When isolated in 1999, the naturally occurring (+)-kalkitoxin was shown to have potent neurotoxic properties ($\text{LC}_{50} = 3.86 \pm 1.91 \text{ nM}$) on primary rat cerebellar granule neurons (CGNs, a model for in vitro neurotoxicity).¹⁰² However, a more recent report by Nagle and co-workers suggests a higher value (less potent) for this neurotoxicity and indicates the previous value might be inflated due to experiment design.¹⁰³ Nagle also reports that (+)-kalkitoxin is a potent and selective inhibitor of hypoxia induced factor 1 (HIF-1) for various cancer cell lines. The inhibition of HIF-1 has been widely demonstrated to impede cancer cell proliferation. Crich and co-workers have shown that (+)-kalkitoxin displays potent and selective cytotoxicity ($\text{IC}_{50} 3.2 \text{ ng mL}^{-1}$) against the human hepato-carcinoma cell line HepG2 over other human cell lines.¹⁰⁴ In fact, Crich

and co-workers develop a hydroxylamine analogue of (+)-kalkitoxin for testing which is not discussed here. The varied and potent biological activity of (+)-kalkitoxin warrants further investigation.

Synthetic groups have looked at making non-natural stereoisomers of (+)-kalkitoxin for many years to explore chemical properties, discussed below. (+)-Kalkitoxin itself possesses an interesting methylated chain, flanked by a thiazoline heterocycle and an amide with a short aliphatic chain (Figure 29). A synthesis from the group of Shioiri used total synthesis to evaluate the correct structure of (+)-kalkitoxin.¹⁰⁵ In this report they succeeded in synthesising 7 different isomers out of a total possible 32, however their main aim was to establish the correct stereochemistry of (+)-kalkitoxin and so they do not synthesise some stereoisomers based on NMR studies of the natural product. However, the synthesis used by Shioiri, while elegant, is not practical for the synthesis of many stereoisomers, and involves repeating many steps from the beginning on the synthesis. Any deviation from the stereochemistry of the naturally occurring (+)-kalkitoxin resulted in a reduction in activity (3–10 times less potent to no activity) in a toxicity assay using brine shrimp (Figure 29). In 2012 Matsuda and co-workers synthesised some remaining isomers of (+)-kalkitoxin, using a similar strategy to Shioiri for the methylated chain, however a different method to construct the thiazoline, which will be discussed later.¹⁰⁶ Overall 6 more isomers were synthesised, including *nor*-isomers where a carbon with a methyl group off the chain has been replaced with a methylene. Matsuda and co-workers used the same brine shrimp assay as Shioiri and concludes the *epi*-isomers to be 3.8–80

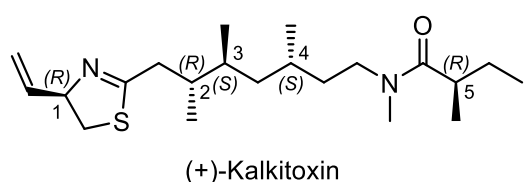
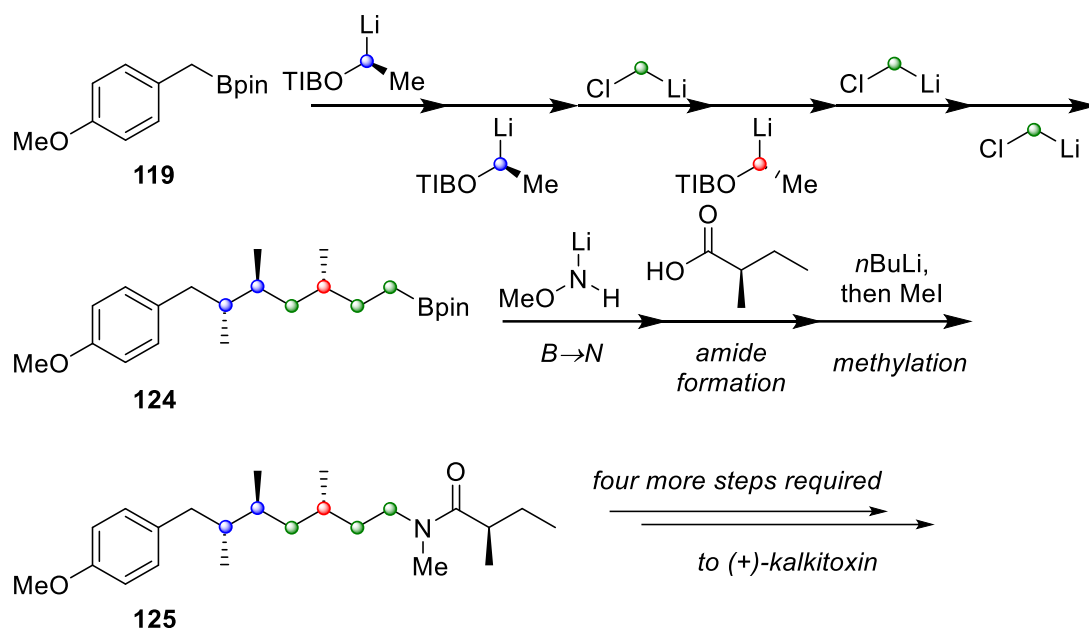
		Stereochemistry						
		Stereocentre	1	2	3	4	5	Activity (μM)
 <p>(+)-Kalkitoxin</p>	Natural	R	R	S	S	R	0.17	
		R	R	S	R	S	1.10	
		R	S	S	R	S	inactive	
	Shioiri ¹⁰⁴	R	R	S	S	S	0.55	
		S	R	S	S	S	1.70	
		R	S	R	R	S	inactive	
		S	S	R	R	S	9.30	
	Matsuda ¹⁰⁵	S	R	S	S	R	15.0	
		S	S	S	S	R	3.60	
		R	R	R	S	R	1.70	
		R	R	S	R	R	0.62	
		R	R	S	-	R	1.80	

Figure 29: Both Shioiri and Matsuda's data for toxicity of stereoisomers of (+)-kalkitoxin against brine shrimp. The final example by Matsuda is an example of a "nor-isomer", where a methyl stereocenter has been replaced by a methylene centre.

times less effective than natural (+)-kalkitoxin, and the *nor*-isomers to be much less effective or ineffective. While the synthesis is elegant, for the library synthesis of many (stereo)isomers, it required tedious manual repetition of steps, so taking a large total time. Clearly there is an interest in synthesising stereoisomers of (+)-kalkitoxin. However, repetition of either Shioiri/Matsuda's syntheses is not appealing. A parallel process, accessing all stereoisomers rapidly without repeating many synthetic steps by hand, is needed. Finally, Matsuda's idea of removing methyl groups to create *nor*-isomers is interesting, and a synthesis that allows the easy inclusion of such a technique would be desirable.

Aggarwal and co-worker's previous synthesis of (+)-kalkitoxin utilises assembly-line synthesis to construct the methylated chain (see section 1.2 for discussion related to the homologation of boronic esters). Starting from *para*-methoxybenzyl boronic acid pinacol ester **119**, six homologations are performed to arrive at boronic ester **124** (Scheme 35). It is important to note here the homologations are under strict reagent control, meaning that regardless of the diastereomer to be homologated, use of either enantiomer of stannane **41** will provide complete control over the stereocentre introduced. After the six homologations the boronic ester **124** undergoes a boron to nitrogen transformation. The resulting amine is then coupled to a carboxylic acid to form the amide and the amide is then methylated, which gives intermediate **125** and completes the right-hand side of (+)-kalkitoxin. It is important to note no column chromatography is required until this stage. The electron rich aromatic group then undergoes oxidative cleavage to the carboxylic acid (not shown), and three further steps convert the carboxylic acid into the thiazoline ring (using a similar process to Matsuda), completing (+)-kalkitoxin. For the synthesis of the several unnatural isomers, Aggarwal's synthesis is superior to the previous examples. The lack of any substrate effects (matched/mismatched) when inserting the methyl stereocentres means any isomer can be made without the potential need for separation of diastereoisomers. While installing the central chain of kalkitoxin, different lithium carbenoids can be substituted at will. This is a similar idea to Matsuda's *nor*-isomers, but now the potential for addition of more or removal of all methyl groups (impossible with previous syntheses), and potentially inclusion of other functional groups (such as hydroxyl).¹⁰⁷ This synthesis could be performed manually, but given that, even if using a different carbenoid, each homologation uses a very similar workflow, the synthesis of each isomer could be performed in parallel on an automated platform, leading

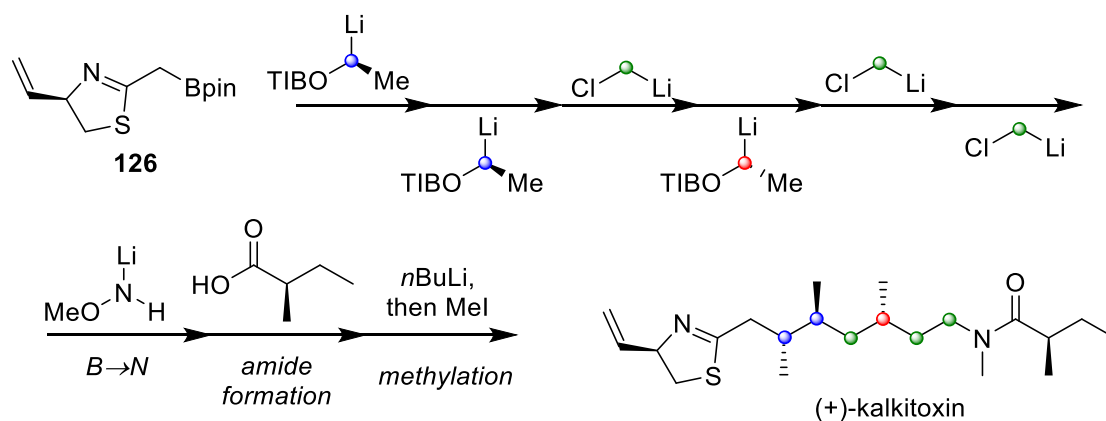


Scheme 35: Aggarwal's previous synthesis of (+)-kalkitoxin, which requires seven steps after creating several stereoisomers.

to rapid construction of many isomers.

Unfortunately automating the previous Aggarwal synthesis would lead to issues. For instance, if the complete variation of the middle three stereocentres was completed, this would lead to eight different stereoisomers. Each of these would need to undergo eight more steps to install the functionality required for kalkitoxin. This is a large number of total steps, and also there is a large amount of complex chemistry that would need to be automated, and the translation from manual to automation can be time consuming. For example, the oxidation of the aromatic ring to carboxylic acid uses quite harsh conditions, potentially not compatible with the hardware of the platform.

Instead, starting with the heterocycle already installed on boronic ester **126** (Scheme 36), which will be made in the laboratory, just three steps are needed after the six homologations: 1) boron to nitrogen transformation; 2) amide coupling; and 3) methylation of the amide. This is crucial, as it is the homologations where most of the isomers will be generated. As mentioned, there is the potential to remove or include methyl groups along the central chain of kalkitoxin, as desired. Out of the three final steps, both the amination of boron and methylation involve lithiation of a substrate, then addition of an electrophile, which is the same workflow as the lithiation–borylation chemistry and therefore should be easy to automate.



Scheme 36: New synthesis towards (+)-kalkitoxin, with only three steps after the generation of many isomers.

Amide formation should be trivial to automate, but potentially purification could complicate matters. Using this strategy, libraries based on (+)-kalkitoxin will be created, hopefully towards structure activity relationships, and potentially revealing new biological activity. Although Shiori and Matsuda have already synthesised and examined stereoisomers of kalkitoxin, this was only in a toxicity assay using brine shrimp. Potentially looking at inhibition of HIF-1, as in Nagle's report, or cytotoxicity towards HepG2, as in Crich's report, will reveal interesting biological activity of different stereoisomers of kalkitoxin.

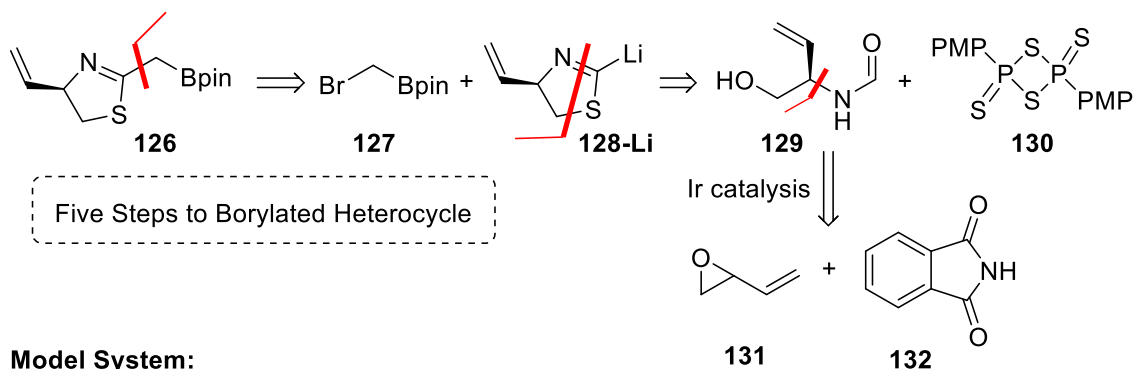
4.4.3 Synthesis of boronic ester **126**

4.4.3.1 Version 1

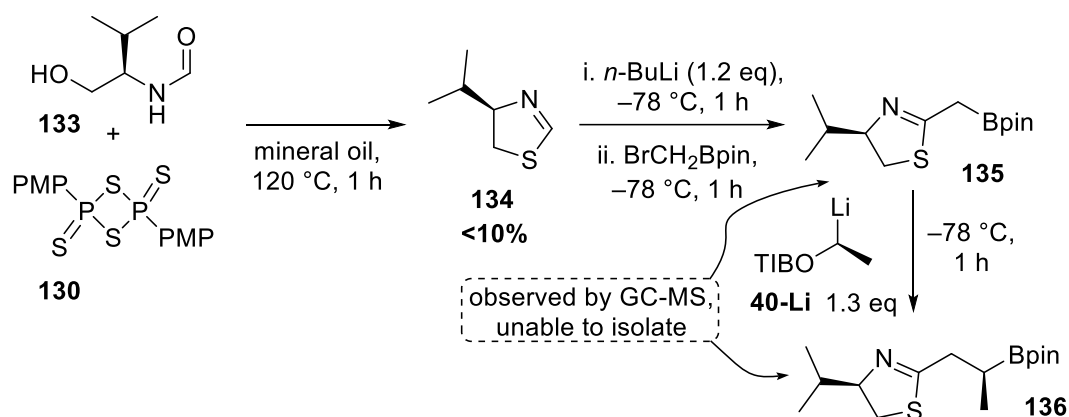
The first route (Scheme 37) attempted was based off work by Medici and co-workers, where they demonstrated that unsubstituted thiazolines can be lithiated and trapped with a variety of simple electrophiles (R_3SiCl/R_3SnCl /aldehydes) in good yields.¹⁰⁸ For the introduction of the boronic ester, commercially available bromomethylboronic acid pinacol ester **127** could be used. The thiazoline **128** could then be made by cyclisation of the corresponding *N*-formyl amino alcohol **129** with Lawesson's reagent **130**.¹⁰⁹ The amino alcohol **129** is known, and could be made through a Tsuji–Trost type displacement of butadiene monoepoxide **131** with phthalimide **132**. The phthalimide can be cleaved to reveal the amine, which could then be formylated readily.

L-Valinol was used as a model system (Scheme 37). The formylation proceeded in quantitative yields by heating the amino alcohol with ethyl formate overnight to give formamide **133**. Treating the obtained *N*-formylvalinol with Lawesson's reagent and

Version 1 Retrosynthesis:



Model System:



Scheme 37: First retrosynthetic analysis and studies with a model system. While this is the shortest route considered, ultimately poor yields and apparent instability of intermediates meant this route was discarded. PMP = *para*-methoxyphenyl.

heating unfortunately only led to low yields of thiazoline **134**, which was obtained after two distillations of the reaction mixture.

Potentially the quality of Lawesson's reagent **130** was low, and purification of the reagent by recrystallisation could have helped boost yields. Enough thiazoline **134** was made to test the subsequent lithiation and trapping on a 0.1 mmol scale.

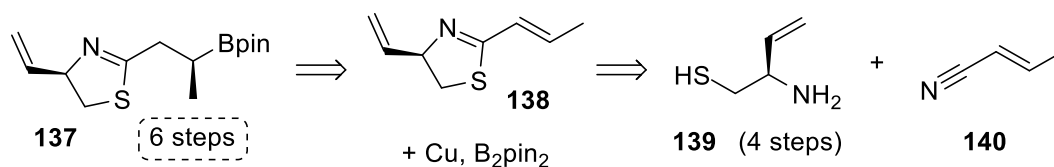
Performing the reaction under the conditions developed by Medici and co-workers, with filtration of the crude mixture through Celite did not provide any obvious product **135** by ^1H NMR or TLC analysis. The correct mass with plausible fragmentation pattern was obtained by GC-MS. In the boronic ester product **135** there is potential for nitrogen to boron coordination. This could render the boronic ester labile under a variety of conditions, most importantly silica purification. Attempting to avoid purification of the crude boronic ester **135** and instead homologating further with lithium carbenoid **40-Li** again did not provide any obvious product **136** by ^1H NMR or TLC analysis, however GC-MS did again show the correct mass. Varying the conditions for lithiating and

trapping the thiazoline **134**, either solvent or equivalents, did not improve the results in any way. During this time, it was also noted that synthesis of thiazoline **134** with Lawesson's reagent **130** was particularly difficult. Due to only slight evidence of product and difficulty with the first step, this route was discarded.

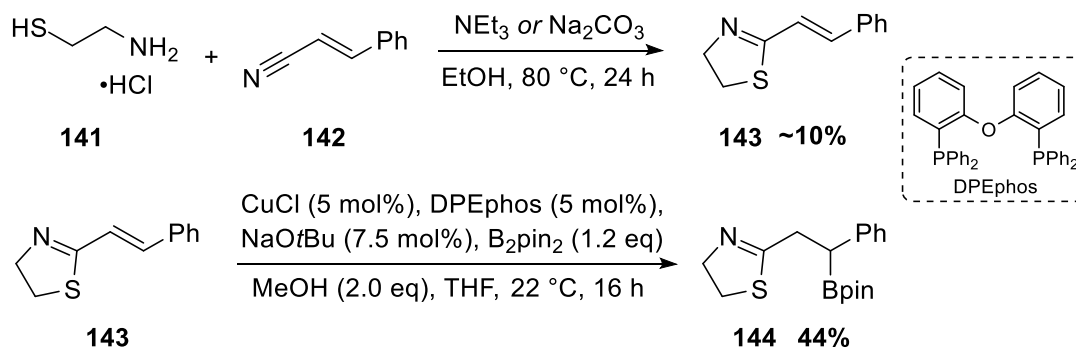
4.4.3.2 Version 2, towards boronic ester **137**

Due to potential instability of the boronic ester **126**, a route towards the homologated boronic ester **137** was sought (Scheme 38). Conjugate addition of a copper–boryl species to the electron-poor alkene present on thiazoline **138** should provide the desired product. 1,4-Conjugate borylation under copper catalysis is a well explored area, and so if successful there would be many ligands to screen to hopefully achieve good enantioselectivity.^{110,111} To build up the thiazoline ring in compound **138**, a different method from scheme 38 was required (as the previous method was low yielding). An attractive process was the double 1,2-addition of a cystamine derivative **139** to the nitrile **140** with loss of ammonia as driving force, which is known in the literature on similar substrates (including model substrate **143**, scheme 38).¹¹² There are many syntheses of 2-aryl thiazolines but only few of other 2-substituted thiazolines.¹¹³ The synthesis of the cystamine derivative **139** was not undertaken at this time and is discussed in the next section 4.4.3.3.

Retrosynthesis for version 2:



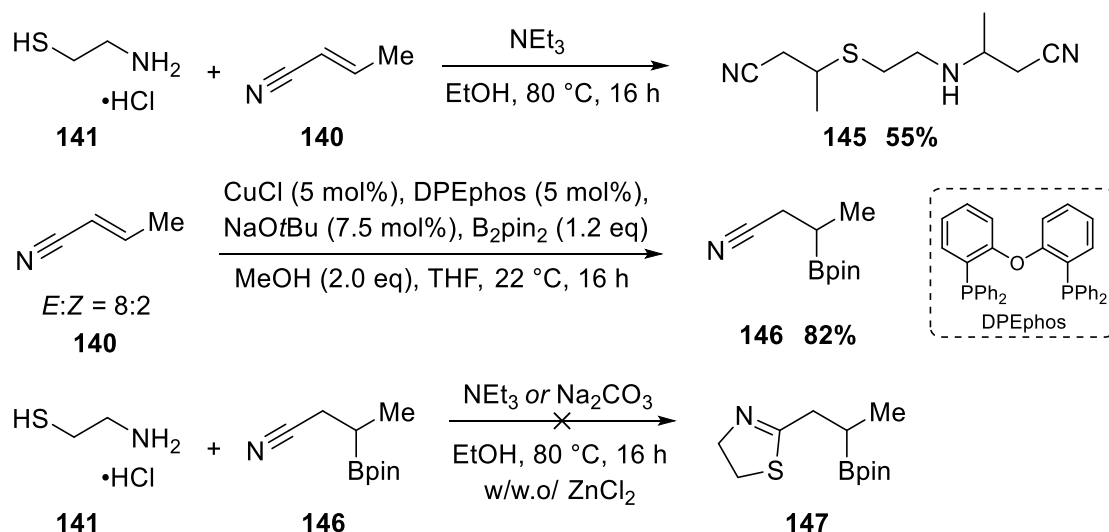
Model System:



Scheme 38: Second retrosynthetic analysis and model system. The yield of the first step was never optimised, and the boronic ester **145** is benzylic and therefore losses during purification are probably the reasons for the reduced yield.

First, taking readily available cystamine **141** and crotonitrile **142** and heating them in the presence of weak bases afforded desired thiazoline **143** in poor yield (10%). The literature yield for this step is 40%, and there was potential the yield obtained could have been improved with repetition, optimisation and/or purification of reagents. The next step was the conjugate borylation of the Michael acceptor **143**. Meng and co-workers have reported the conjugate borylation of a 2-alkenyl thiazole, which proceeds in 90% yield and with an *e.r.* value of 98:2 when using a chiral and non-racemic ligand.¹¹⁴ However, Meng does not report conditions for racemic borylation and therefore similar conditions described by Yun and co-workers were used, with DPEphos as ligand (**143** to **144**).¹¹⁵ Full conversion to boronic ester **144** was observed by GC-MS, however the product was clearly not stable on TLC, which was assumed to be because the boronic ester is benzylic and therefore labile on silica (see section 4.4.3.3 for further discussion). Nonetheless, a quick and unoptimised purification on silica gel afforded product **144** in an acceptable 44% yield. As a model system this was a positive result for this route as it demonstrates the borylation can proceed with full conversion and in the actual system, the boronic ester product **137** is not benzylic so was not expected to be labile (further discussion below).

Unfortunately, moving to crotonitrile **140**, still with just cystamine, did not reflect the success of the model system: any attempt to perform the double 1,2-addition with cystamine resulted in double 1,4-addition to give compound **145** (Scheme 39). Presumably, the lack of phenyl group on crotonitrile results in a much better Michael

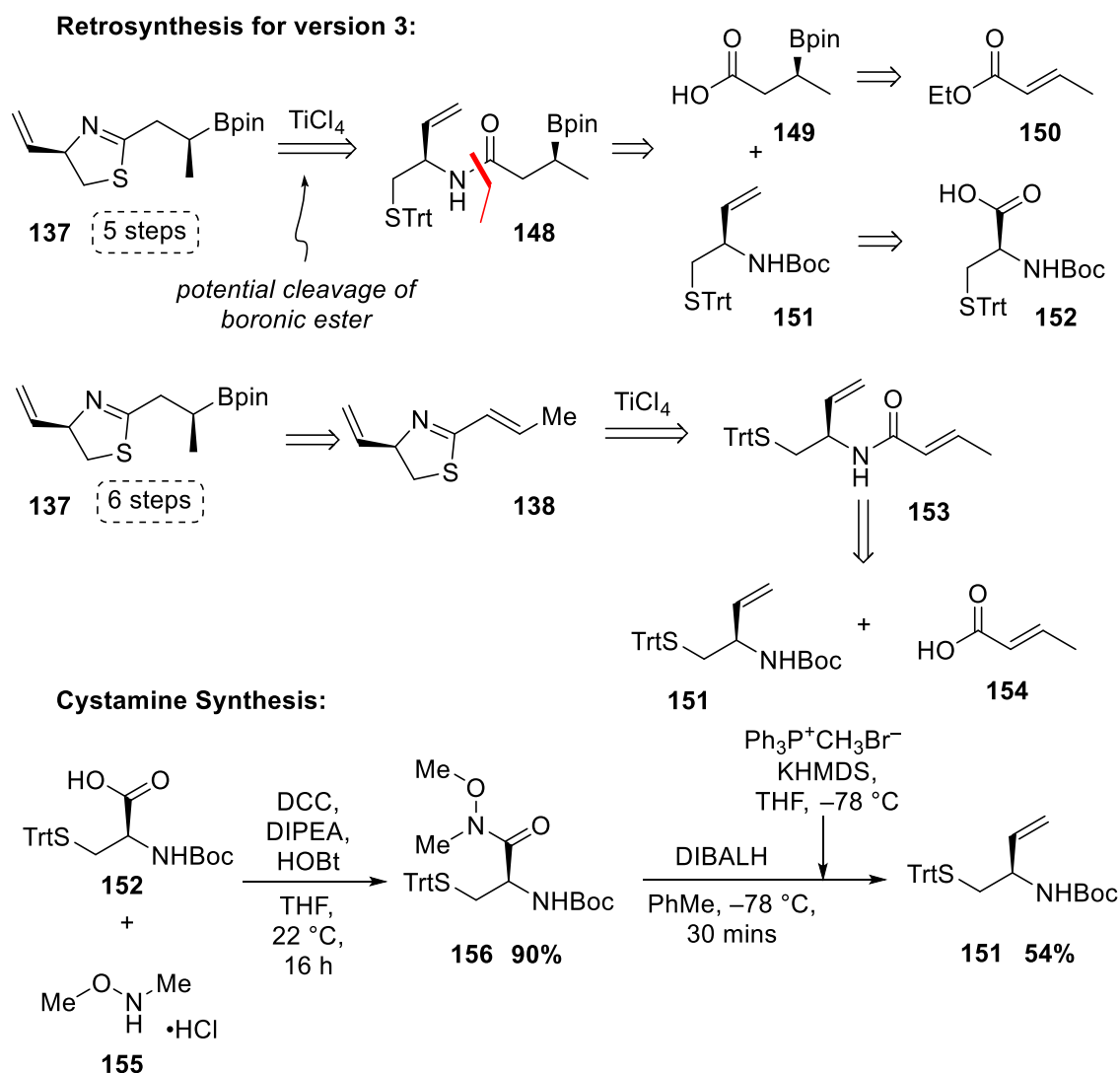


Scheme 39: Attempting the double 1,2-addition with crotonitrile gave only undesired 1,4-addition product **145**. As a good Michael acceptor, crotonitrile **140** underwent conjugate borylation readily, but boronic ester **146** was not stable under conditions required for thiazoline synthesis. w/w.o./ = with or without.

acceptor and attack at the nitrile is less favoured. Use of a Lewis acid (ZnCl_2) did not help to favour 1,2-addition and the same result was obtained.¹¹⁶ Indeed, Busacca and co-workers had difficulties preparing 2-alkenyl thiazolines from α,β -unsaturated carbonyls, which they ascribed to competing 1,4-addition.¹¹⁷ This also likely explains the poor yields observed in the model system (**143**, scheme 38). However, as crotonitrile is clearly a good Michael acceptor, it was decided to first try the conjugate borylation and then double 1,2-addition. Crotonitrile and other α,β -unsaturated nitriles have been used in conjugate borylation reactions previously.^{115,118} As such, the same conditions as above were used to give the borylated product **146** in high yield (82%). Unfortunately, any attempts to perform the double 1,2-addition with cystamine **141** in the presence of the boronic acid pinacol ester **146** did not yield any desired product or obvious by-products. Pinacol could be observed by GC-MS, so potentially the high temperatures and basic conditions were hydrolysing the boronic ester to the boronic acid which was then degrading under the reaction conditions. It was not clear whether protection of the boron atom as an *N*-methylimidodiacetic boronic acid ester (MIDA boronate) would be successful as these groups can be hydrolysed under mildly basic conditions at high temperatures.¹¹⁹ As well as this, crotonitrile is only commercially available as an 8:2 *E:Z* mixture which could potentially complicate an enantioselective conjugate borylation. Due to the above reasons, this route was discarded.

4.4.3.3 Version 3

The third retrosynthetic analysis is similar in terms of steps and relies on more literature precedent (Scheme 40). First, the desired boronic ester containing thiazoline **137** is disconnected back to the amide **148**. This can be closed and dehydrated in a Lewis acid (TiCl_4) mediated process, which is well documented in the literature.^{106,120,121} Disconnecting the amide reveals a simple borylated carboxylic acid **149**, which can be made from ethyl crotonate **150** by conjugate borylation and ester hydrolysis,¹²² and the required cystamine derivative **151**, which has been made in the literature with *S*-trityl and *N*-Boc protecting groups from commercially available cysteine derivative **152**.^{106,123} Boronic esters can be cleaved under Lewis acidic conditions and so potentially using TiCl_4 would cleave the boronic ester in amide **148**, leading to undesired reactivity.^{124,125} If this was the case, the boronic ester could be introduced at the end, by conjugate borylation of the thiazoline **138**. α,β -Unsaturated amide **153** is then made from crotonic acid **154** and cysteine derivative **151**.

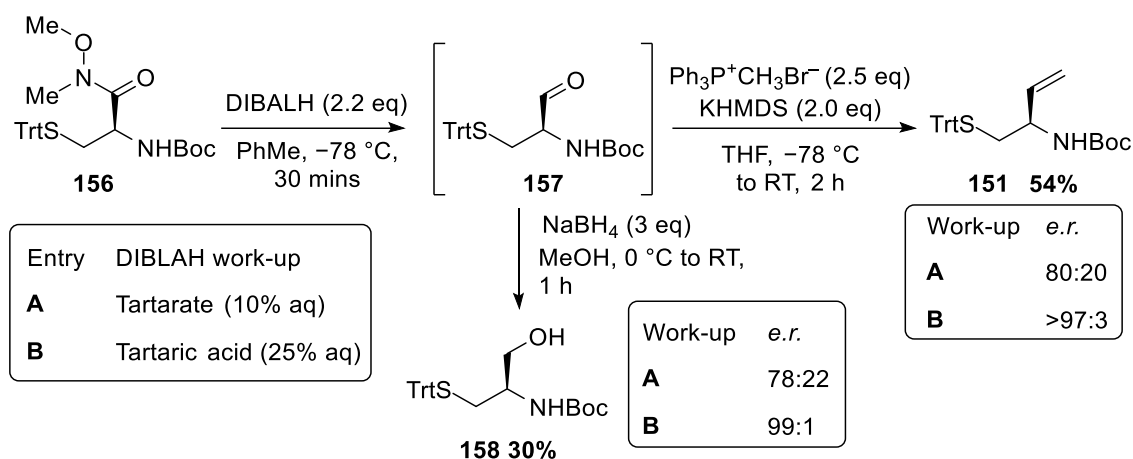


Scheme 40: Version 3 of the retrosynthetic analysis, either with the boronic ester present for the TiCl_4 mediated cyclisation (from **148**), or without in which case the boronic ester is introduced by conjugate borylation of **138**. Cystamine **150** is made in a literature known, simple and scalable, 3-step procedure.

The cystamine derivative **151** is made in 3-steps from commercially available *N*-(*tert*-butoxycarbonyl)-*S*-trityl-L-cysteine **152** (Boc-Cys(Trt)-OH) based on literature procedure from White and co-workers in their synthesis of (+)-kalkitoxin (although White and co-workers used the *S*-benzyl substrate).¹²¹ First, Boc-Cys(Trt)-OH **152** was converted into Weinreb amide **156** under the modified conditions reported in the literature with a similar yield of 90%, where we used *N,N*-Dicyclohexylcarbodiimide (DCC) instead of 1-ethyl-3-(3-dimethylaminopropyl)carbodiimide (EDCI) due to cost. THF was used in this step due to the poor solubility of by-product 1,3-dicyclohexylurea (DCU), which facilitated work-up and therefore purification. Weinreb amide **156** was then reduced to the aldehyde using diisobutylaluminium hydride (DIBALH), the crude of which then underwent a Wittig reaction to install the terminal alkene required for

kalkitoxin. The yield of 54% is literature reported and using potassium hexamethyldisilazane (KHMDs) as base rather than *n*-BuLi for the formation of the ylide was essential for this yield. The rest of the mass balance from this reaction seemed to be removal of the trityl protecting group in the Wittig step (not the reduction) as observed by triphenylmethanol at the end of the reaction. Cystamine derivative **151** could be accessed in *S*-benzyl protected form (as in White and co-worker's synthesis, mentioned above), however the major method for removal of this protecting group is Li/NH₃, which could be difficult when working on large scale. Use of *S*-trityl derivatives is well documented in the literature and the thiazoline formation by cyclisation with TiCl₄ works with removal of the *S*-trityl protecting group in the same pot, saving a step.^{106,120}

Typically, all the intermediates in this route containing an *S*-Trt moiety (for example, compounds **156**, **151** & **153**) were incredibly difficult to handle, as after purification by column chromatography and solvent evaporation they were isolated as sticky oils. To circumvent this, the materials were precipitated from Et₂O/hexane mixtures or just Et₂O, which gave easy to handle amorphous white powders. Unfortunately, in the case of Wittig product **151**, this led to a racemic solid, presumably due to a rapid crystallisation with small crystals. Samples were analysed by chiral HPLC before and after precipitation which clearly showed racemisation of the material (see supporting information for HPLC traces). Without performing the precipitation, the *e.r.* value of Wittig product **151** was typically 80:20 (Scheme 41). This relied on a medium scale reaction (<10 mmol, where 15 mmol gave racemic product) and use of 10% Rochelle salt aqueous solution (not saturated) in the workup. Taking a small sample of aldehyde intermediate **157** and reducing it to the amino alcohol **158** gave material with a similar *e.r.* value of 78:22, demonstrating the partial racemisation occurred during the DIBALH reduction or workup of the aldehyde. In 2020, Brienbauer reported the DIBALH reduction of a similar amide, generated in-situ by reaction of carboxylic acid **152** and carbonyldiimidazole (CDI).¹²⁶ Not only is this an elegant 1-step process to access aldehyde **157**, the authors also state their method did not lead to any racemization. Key to avoiding racemisation is the use of tartaric acid (25% w/w in water) in the work-up instead of tartrate salts.¹²⁷ Indeed, the aqueous layer of the work-up when using tartrate salts was pH = 9–10, however when using tartaric acid the aqueous layer was pH = 1. The work-up was also much faster and easier, in that stirring with tartaric acid solution for 20–30 mins led to two easily separable layers (versus tartrate ~1 h). After performing the tartaric acid work-up and subsequent

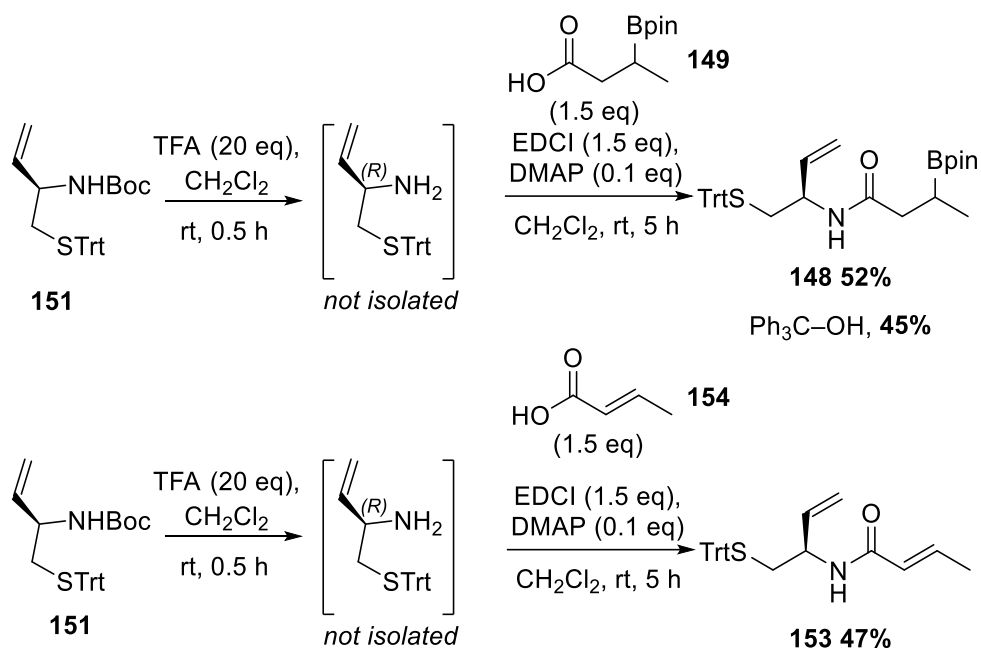


Scheme 41: Performing the DIBALH work-up with tartaric acid instead of tartarate salts leads to an improvement in the *e.r.* of the product. Reducing the amino aldehyde to the amino alcohol helped to confirm this.

Wittig reaction, olefin **151** was accessed with an *e.r.* value of >97:3. A minimum value is quoted due overlapping peaks around the minor signal in the HPLC trace. Again, a sample of aldehyde **157** was reduced with NaBH₄ and an *e.r.* of 99:1 was observed by chiral HPLC analysis for amino alcohol **158**.

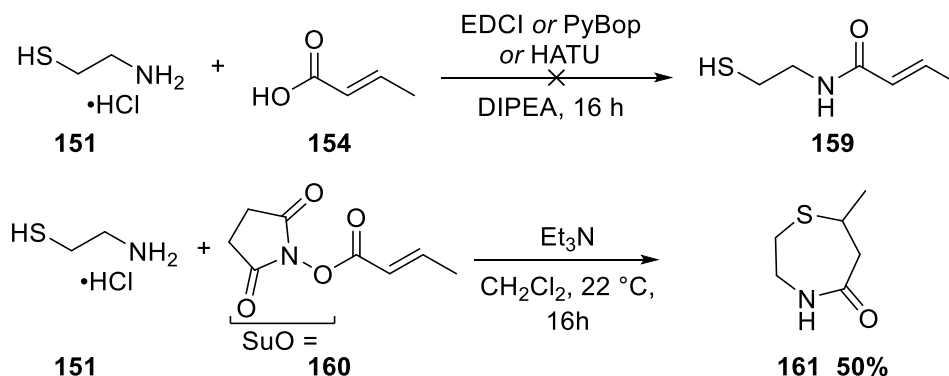
With the protected and enantioenriched cystamine derivative **151** available, the next steps were amide coupling with either crotonic acid **154** or boronic ester containing carboxylic acid **149**. Matsuda and co-workers performed a similar amide coupling with the same cystamine derivative **151**, however the coupling was performed much later in their synthesis of (+)-kalkitoxin so the carboxylic acid is more advanced and therefore is used as the limiting reagent, with the cystamine derivative **151** at 1.5 equivalents.¹⁰⁶ We wanted to swap the limiting reagent round and use our more advanced intermediate **151** as the limiting reagent. Key to Matsuda's amide coupling is removal of the *N*-Boc protecting group in the presence of the *S*-trityl protecting group as these protecting groups are not orthogonal. Having said this, Matsuda performs the deprotection under standard conditions, with a large excess of TFA (34 equivalents) and then removal of solvents and excess TFA under vacuum. This provides them with 68–90% yields over two steps (deprotection and amide formation) for their several stereoisomers of (+)-kalkitoxin.

The deprotection was performed with 20 equivalents of TFA, then neutralisation with NaOH and aqueous extraction to avoid concentration in the presence of TFA (Scheme 42). The amide coupling was then performed using Matsuda's conditions with EDCI and catalytic DMAP but afforded only ~50% yield in either case. The rest of the

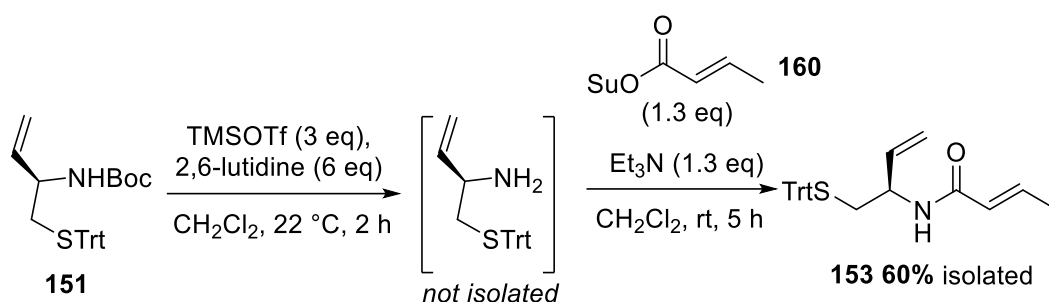


Scheme 42: Attempted amide coupling reactions. Using TFE to deprotect nitrogen also leads to unwanted sulphur deprotection.

mass balance isolated was triphenylmethanol (Ph_3COH), which must have come from the deprotection using TFA. An acidic workup (1 M HCl) is performed to remove the EDCI, however this was also performed after the Weinreb amide synthesis, which gave high yields (90%) and so acidic work-up was unlikely to be the cause of the deprotection. The amide formation was then optimised with a view to fully deprotect both the nitrogen and sulphur, which should be facile with triethylsilane (Et_3SiH) and TFA, before performing the coupling. Using cystamine **151** in amide couplings reactions with crotonic acid **154** did not yield any obvious product **159** formation by TLC or GC-MS (Scheme 43). Swapping instead to the *N*-hydroxysuccinimide (NHS, Su) activated ester of crotonic acid **160** showed the formation of lactam **161** in 50% yield, where the thiol has undergone a 1,4-addition to the unsaturated ester. This demonstrated that sulphur needed to be



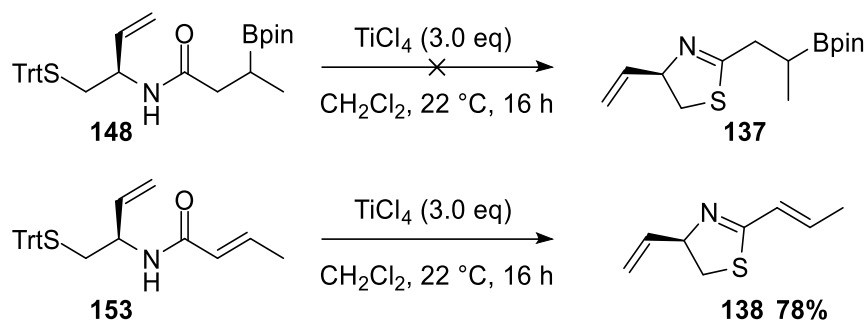
Scheme 43: Attempting to perform amide formation in the presence of the unprotected thiol either led to no reactivity or undesired side products. This demonstrated that sulphur needed to be protected for this amide coupling.



Scheme 44: Using TMSOTf and 2,6-lutidine results in an efficient nitrogen deprotection with no observable sulphur deprotection. The resulting amine can then be combined with the succinimide activated ester of crotonic acid to give the desired product in ~80% yield. On scale, 60% of this could be isolated cleanly, with ~20% eluting with impurities.

protected for the amide formation. Pomerantz and co-workers have since used this reaction in the synthesis of “3D fragments for screening libraries”.¹²⁸ Going back to the literature we then considered removal of the *N*-Boc group under Lewis acidic conditions, as Doi and co-workers have pioneered the selective deprotection of similar *N*-Boc, *S*-trityl cysteine derivatives using TMSOTf and 2,6-lutidine in high yields (Scheme 44).¹²³ Thankfully this worked well, and on smaller scale (<1 mmol), after amide coupling with activated ester **159**, the desired amide **153** could be isolated in 80% yield. Unfortunately, upon scaling up (~10 mmol) the separation of both crotonic acid **154** and activated ester **159** from the desired product was more difficult. The activated ester could be removed by stirring in MeOH with Et₃N, however still purification was challenging, leading to 60% isolated of the pure product with another mixed fraction, typically containing ~20% of product **153**. This impure fraction was usually recombined with crude material from later reactions for re-purification. Reaction set-up and separation were marginally easier with activated ester **159** versus crotonic acid **154**, and so this was taken forward as optimal conditions. We did consider use of the acid chloride of crotonic acid, but unfortunately it is only available as a 9:1 *E:Z* mixture.

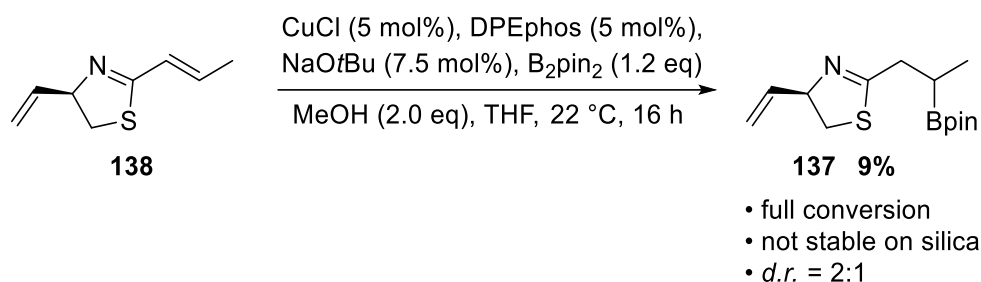
The deprotection, cyclisation and dehydration sequence was evaluated next. Attempting the cyclisation using Matsuda’s conditions with the boronic ester containing amide **148** did not afford any product, although full consumption of the starting material and formation of triphenylmethanol were observed (Scheme 45). Trying shorter reaction times or lower number of equivalents of TiCl₄ did not show any product formation either, by TLC or GC-MS. Potentially, removal of the *S*-trityl protecting group and then cyclisation with a different Lewis acid or dehydrating agent in a two-step process may have been successful, but due to the existence of literature on the TiCl₄ mediated process



Scheme 45: Unsuccessful cyclisation of boronic ester **148** to thiazoline **137**. Removing the boronic ester and using amide **153** however resulted in a practical process.

this was not explored. The use of α,β -unsaturated amide **153** thankfully did afford the desired product in 63% yield (<1 mmol scale). Interestingly, the R_f of the thiazoline product was higher (less polar) than the starting material and it was quite volatile. Upon increasing scale to >1 mmol, higher yields were obtained (78%) presumably due to smaller product losses when removing solvent under reduced pressure. Thiazoline **138** was not particularly stable if stored for greater than 1 week at $-20\text{ }^\circ\text{C}$. Decomposition products were not identified however no oxidization to the thiazole was observed by ^1H NMR analysis.

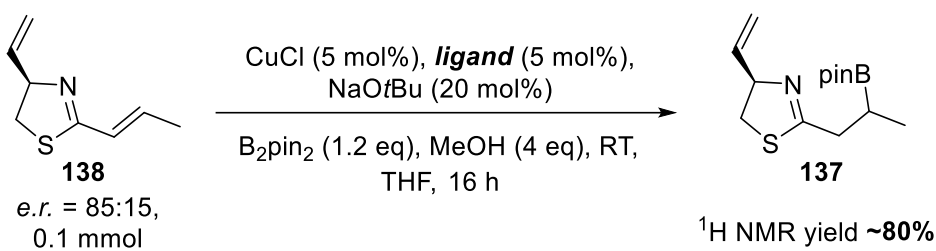
The conjugate borylation was attempted next using achiral DPEphos as ligand (Scheme 46). After stirring for 16 h, analysis by GC-MS showed full conversion of starting materials to products, and an almost clean crude mixture by ^1H NMR. However, most of the material was lost when trying to purify the product on silica gel, to give only a 9% yield. Secondary sp^3 boronic acid pinacol esters are usually stable to silica gel purification, so in this case there must have been some level of nitrogen to boron coordination, increasing the lability of the boronic ester, although ^{11}B NMR analysis only showed a signal at $\delta = 32$ ppm (typical of a 3-coordinate boronic ester). Meng and co-workers (discussed in section 4.4.3.2) state that their similar products were not stable to isolate and so the boronic esters were oxidised to alcohols for that reason. They do isolate one boronic ester product where nitrogen coordination is provided by an adjacent oxazole, seemingly with no careful purification.¹¹⁴ Another interesting point is that the benzylic boronic ester **144** was isolated in 49% yield, so it is less labile than product **137**. The steric presence of the phenyl ring must be enough to disrupt the nitrogen to boron coordination therefore increasing stability. The ^1H NMR of thiazoline **137** indicated a *d.r.* value of roughly 2:1, which demonstrates the distal alkene has little effect on the selectivity of the borylation. No signals for either diastereomer were separable by ^1H



*Scheme 46: Racemic conjugate borylation gave full conversion by GC-MS and crude ¹H NMR, however attempted purification of thiazoline **137** resulted in loss of material, presumably due to nitrogen to boron coordination.*

NMR analysis in different solvents (CDCl₃, C₆D₆, CD₃CN, DMSO-*d*₆), and the diastereomers could not be separated on TLC. Using a chiral and non-racemic phosphine ligand was then attempted in the conjugate borylation. The conditions developed by Meng and co-workers were used due to similarity of the substrate, particularly focussing on Meng's ligand screen, to avoid performing a time-consuming ligand screen ourselves (table 19). Unfortunately trying JosiPhos first (which gave Meng 90:10 *e.r.* on pyridyl substrate) gave no improvement in *d.r.* value of the product by crude ¹H NMR analysis. Using instead the (+)-enantiomer of Meng's optimised ligand Ph-BPE gave an improved 4:1 *d.r.* value. Attempts to improve this by increasing ligand loading (5 to 15 mol%) or reducing temperature (RT to -10 °C) were not successful, however the crude ¹H NMR yields remained encouragingly high at ~80%. A boost to 6:1 *d.r.* came upon increasing the scale of the reaction, potentially as now thiazoline **138** could be added neat as per Meng's protocol (in previous reactions the substrate was added in solution). This 6:1 *d.r.*, while approximate from ¹H NMR, demonstrated that the borylation must be occurring in high *e.r.* as we were starting from material with *e.r.* = 85:15, and so we took these conditions as optimised. We tried to ascertain the *d.r.* with higher confidence, however the boronic ester **137** was not stable to silica and therefore chiral HPLC was not an option. Oxidation with NaBO₃·4H₂O in THF/H₂O, which was used by Meng and is known to be more mild than typical H₂O₂/NaOH, only gave decomposition. If the precise *d.r.* value is desired in the future, then a Matteson homologation, with subsequent purification and HPLC analysis, could be performed.

Using (+) or (-) ligand gives the opposite diastereoselectivity with no matched/mismatched effects. This means we can generate either epimer at that position for generating kalkitoxin analogues. The lack of matched/mismatched effects indicates the distal olefin is not interacting with the copper-boryl species, it is therefore assumed



entry	ligand	conditions	d.r.
1	DPEphos	no change	2:1
2	<i>R</i> -[S _P -Josiphos]	no change	2:1
3	(+)-(S,S)-Ph-BPE	no change	4:1
4	(+)-(S,S)-Ph-BPE	15 mol% ligand	4:1
5	(+)-(S,S)-Ph-BPE	-10 °C o/n	4:1
6	(-)-(R,R)-Ph-BPE	no change	1:4
7	(+)-(S,S)-Ph-BPE	2 mmol scale	6:1

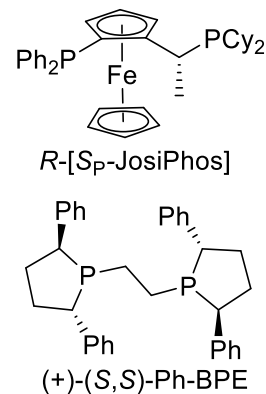
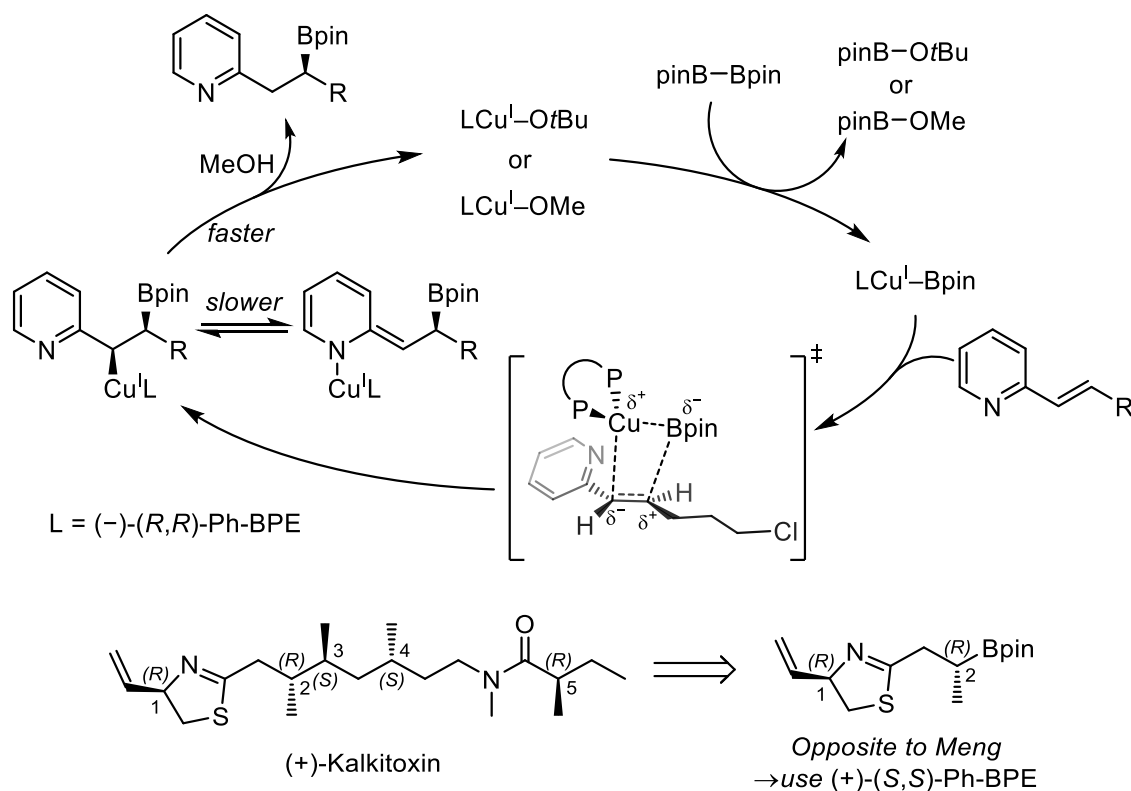


Table 19: Enantioselective conjugate borylation of thiazole **138**, using Ph-BPE as the optimal ligand. Starting from material with *e.r.* = 85:15, to achieve a d.r. of 6:1 shows the borylation must be occurring with high selectivity.



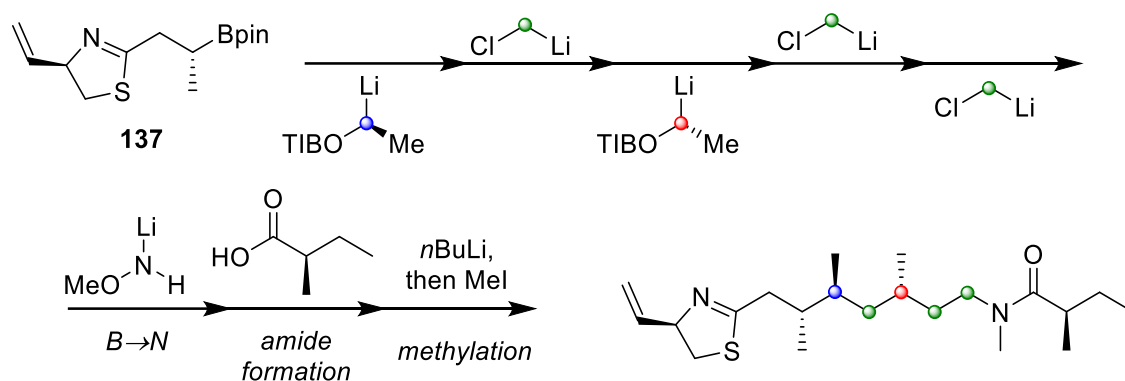
Scheme 47: Top: Meng's catalytic cycle for conjugate borylation using (-)-(R,R)-Ph-BPE to give the stereochemistry drawn. Bottom: We require the other epimer at the pertinent position for (+)-kalkitoxin, and so used the other enantiomer of ligand.

the ligand was promoting addition from the same as Meng reports, that is, (-)-(R,R)-Ph-BPE gives the *S* product (Scheme 48, top). Meng proved their absolute stereochemistry by comparison of an optical rotation value to a known literature example for one molecule, and X-ray analysis of a crystal structure of another molecule. We require the other epimer for the synthesis of naturally occurring (+)-kalkitoxin, so we used (+)-(S,S)-Ph-BPE instead (Scheme 48, bottom).

Purification of boronic ester **137** was then studied. Attempts to use SiO₂ (rapid column), SiO₂/Et₃N, SiO₂/AcOH, neutral alumina, basic alumina, or reverse phase prep-HPLC (MeCN/H₂O/1% HCO₂H) all failed. It was attempted to perform a homologation using stannane **41** on the crude material (as the ¹H NMR spectrum looked moderately clean) which gave observable product by GC-MS but poor recovery (<10%). Finally, distillation using a Kugelrohr (150 °C, <1 mbar) worked reasonably well, providing typically 60% yields of the desired product. Unfortunately, either pinBOH or pinBOBpin was difficult to remove, frequently coming over with the desired material. However, it was hypothesised that any borate would not cause any issues with the first step (homologation with stannane **41**) and just simply consume some lithiated carbenoid, which we could consider during reaction preparation.

The *d.r.* of the conjugate borylation then dropped to 1:1, with no change in reaction procedure. It was at this point we discovered we were racemising Wittig product **151** by precipitating it (discussed in section 4.4.3.3, scheme 41). Using racemic thiazoline **138** in a conjugate borylation will give a 1:1 mixture of diastereomers, regardless of the selectivity of the borylation. Ongoing in the project is bringing through thiazoline **138** in high *e.r.* to undergo conjugate borylation. If the borylation is proceeding with high selectivity this should provide >95:5 *d.r.*, which will be obvious from crude ¹H NMR analysis. Looking at our synthesis of (+)-kalkitoxin (Scheme 48), we decided to use this mixture of diastereomers to study the final three steps of the synthesis with a model substrate containing the thiazoline ring.

Automated synthesis of (+)-kalkitoxin:

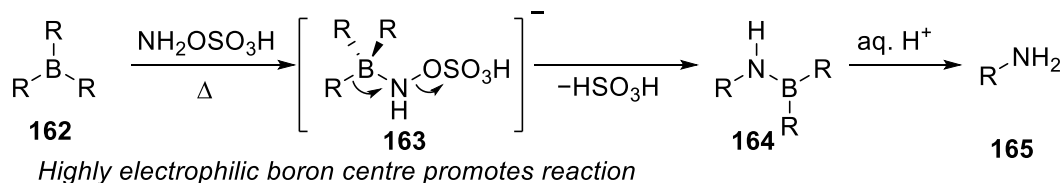


Scheme 48: Updated synthesis of (+)-kalkitoxin, using boronic ester **137** as starting material.

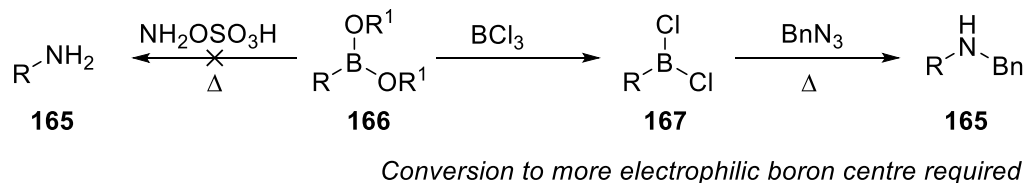
4.5 Final Three Steps

The first step after the assembly-line is boron to nitrogen transformation, also called boron amination. Brown and co-workers published a method for the stereospecific conversion of boranes **162** to amines **165** in 1964, using hydroxylamine-*O*-sulfonic acid (HOSA, (Scheme 49a)).^{129,130} This reaction works by first coordination of amination reagent to boron, forming boronate complex **163**. 1,2-Migration then ensues, expelling the leaving group and affording the intermediate **164**, which is hydrolysed under acidic conditions to generate the desired product **165**. However, Brown and co-workers note in their 1964 publication the transformation of monoalkylboronic acids to the desired alkylamine is “very slow”.¹²⁹ The equivalent oxidation of boronic acids/esters to alcohols is typically favourable and fast, demonstrating the level of nitrogen coordination to boron to be lower than that of oxygen to boron. When combined with the reduced electrophilicity of the boron atom in boronic esters versus boranes (due to donation of electron density by the adjacent oxygen atoms), a much-reduced rate of boronate complex formation is encountered. Indeed, transformation into a more electrophilic boron centre (RB(OR)₂ to RBCl₂, for example) has historically been used to allow boron amination to proceed (**166** to **167**, scheme 49b).^{131,132} This reduced rate of boronic ester ate complex formation typically leads to either no reaction at room temperature, or decomposition of the amination reagent (before amination can occur) at elevated temperatures. In 2012 Morken and co-workers presented a solution to this issue, not by increasing electrophilicity of boron but by increasing the nucleophilicity of the amination reagent, therefore increasing the rate of boronate complex **168** formation (Scheme 49c).¹³³ To increase the nucleophilicity of the amination reagent, they used lithiated methoxyamine (MeONHLi) generated from *n*-BuLi and methoxyamine. The reaction proceeds in high yields for

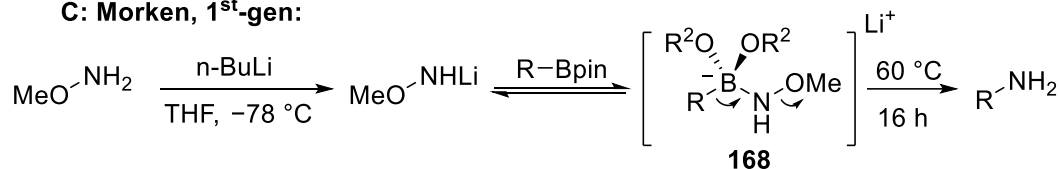
A: Boranes (Brown)



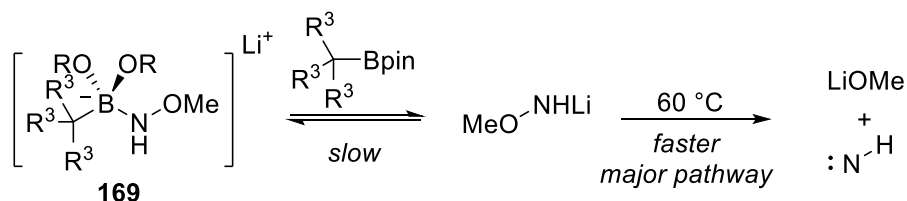
B: Boronic esters



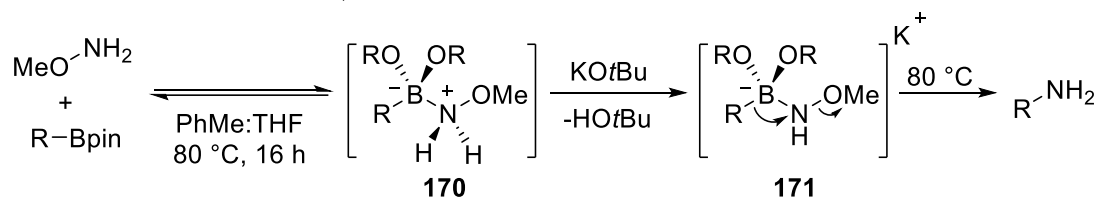
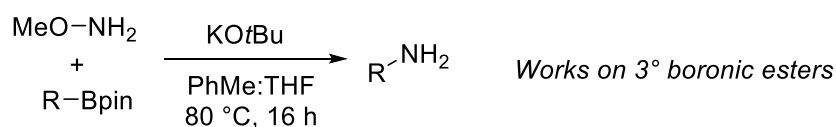
C: Morken, 1st-gen:



Not prefunctionalisation required, but doesn't work on 3° boronic esters



D: Morken, 2nd-gen:



No free metalated amine at high T therefore no degradation

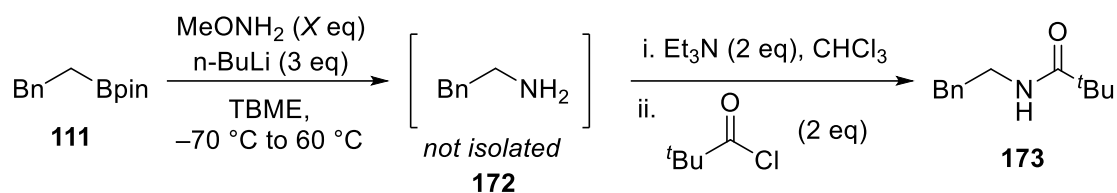
Scheme 49: Amination of boranes/boronic esters. For the conversion of boronic esters to more electrophilic boron species, many methods exist (BCl₃ shown).

primary and secondary boronic esters, however, does not proceed for tertiary boronic esters. In these cases, the rate of boronate complex **169** formation is reduced, such that the metalated amine decomposes before productive reaction can occur. A second-generation procedure was published by Morken in 2018, which allows the conversion of

tertiary boronic esters to tertiary amines (Scheme 49d).¹³⁴ This procedure uses KO t Bu as base, which Morken states does not deprotonate methoxyamine until coordination to boron has occurred (**170** to **171**). This therefore avoids the generation of free metalated methoxyamine at high temperature, precluding its decomposition.

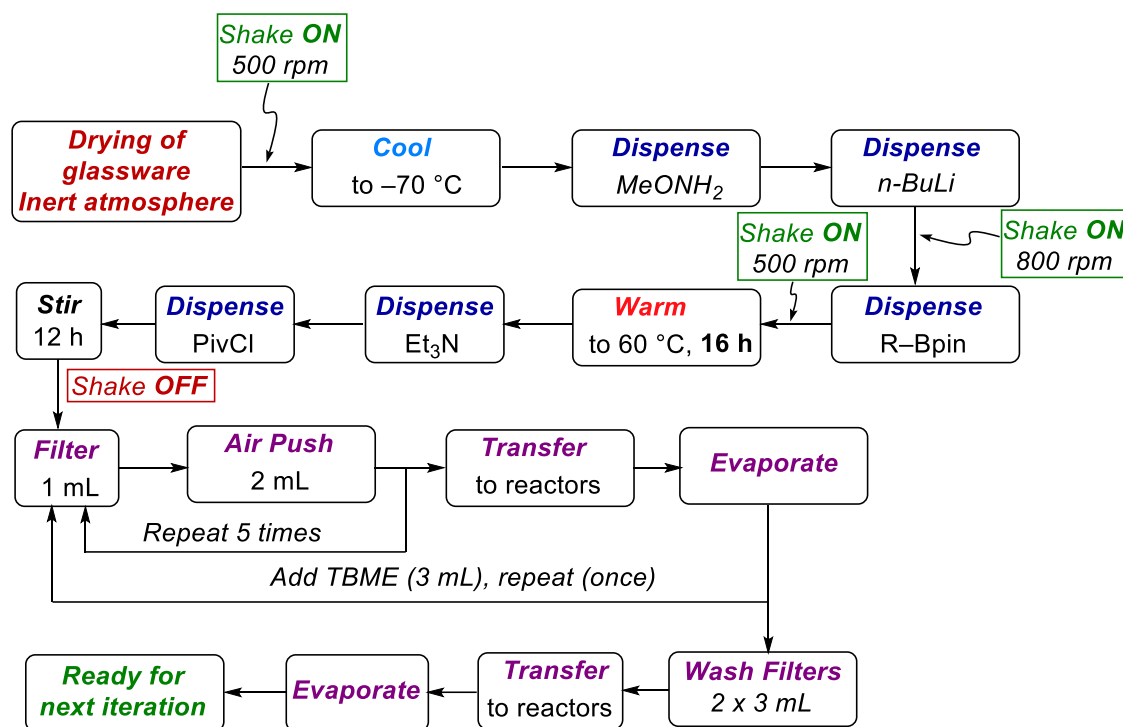
The second step of the final sequence towards (+)-kalkitoxin is amide bond formation between the formed primary amine and (*R*)-2-methylbutanoic acid. In Aggarwal's previous synthesis of (+)-kalkitoxin, an aqueous work-up of the formed primary amine (from boron amination) must be performed before amide bond formation.⁸¹ Aqueous work-ups on automated systems are possible, however on our platform (which is designed for filtration through a solid-phase) this would require laborious optimisation of needle height and aspiration amounts to ensure clean removal of one phase. Instead, an alternative approach involving addition of the corresponding acyl chloride ((*R*)-2-methylbutanoyl chloride) was used. If added in excess, the acyl chloride would hopefully react rapidly and cleanly in the presence of the crude amine. The amide could then be filtered through silica more easily than the primary amine before the next step. For the methylation we planned to use the conditions developed and used in Aggarwal's previous synthesis (*n*-BuLi, MeI, -78 °C).

First, the amination of a simple model substrate, phenethyl boronic acid pinacol ester **111**, was attempted using Morken's first generation conditions. There was concern from an early stage about the volatility of methoxyamine (b.p. = 48 °C)¹³² and it was believed Morken's second generation procedure (typically always used in the lab due to ease of set-up) would only result in evaporation of methoxyamine. Slow aspirations and dispenses (1 mL min⁻¹) of the methoxyamine stock solution were used to ensure accuracy and precision. Some reactions were trialled, using differing amounts of MeONH₂ and found a larger excess was needed versus what one would typically use in the lab (6 vs. 3 eq, table 20). Primary amine **172** was not visible by GC-MS, so we instead decided to obtain the conversion and yield of amide **173** over two steps. Pivaloyl chloride (PivCl) was used as a model acyl chloride, due to availability and as a more hindered system it was hoped to ensure success when switching to the isobutyl substrate required for kalkitoxin analogues.



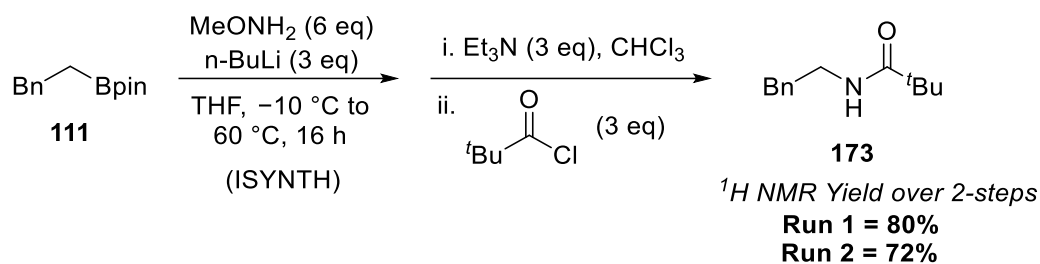
MeONH ₂ equiv.	GC-MS 111 : 173	¹ H NMR 111 : 173	¹ H NMR Yield 111	¹ H NMR Yield 173
3.0	74:26			
3.9	76:24			
5.2	17:83			
6.0	22:78			
7.8	28:72	17:83	13%	62%
8.7	21:79	16:84	9%	49%

Table 20: Initial optimisation of Morcken amination and subsequent acylation with pivaloyl chloride on the automation platform.

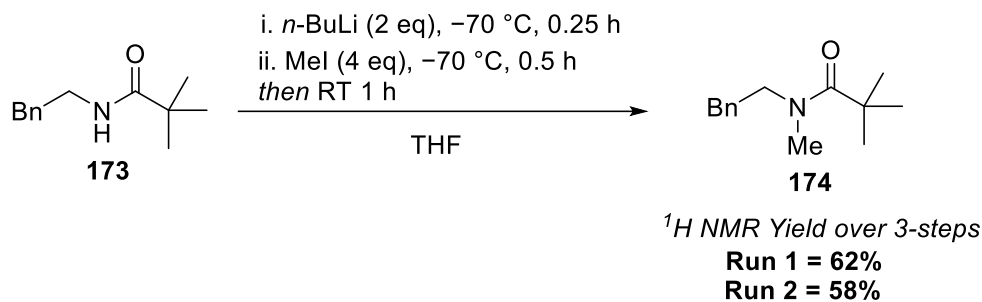


Scheme 50: Workflow of the two-step 1st gen Morcken amination and amidation with PivCl.

Unfortunately, only modest yields were obtained over 2-steps for this process (table 20). It was decided to swap to the ISYNTH reactor block, which uses standard 8 mL vials for reactors. This would hopefully allow easier small-scale reactions, and we hoped the seal around the top of the vials would be improved over the glass array vessels. The ISYNTH block cannot be cooled to $-78\text{ }^\circ\text{C}$, so we changed to $-10\text{ }^\circ\text{C}$ for the metalation of methoxyamine and boronate complex formation. Morcken and co-workers use THF for their optimised process and so we changed our solvent to anhydrous THF (from TBME).



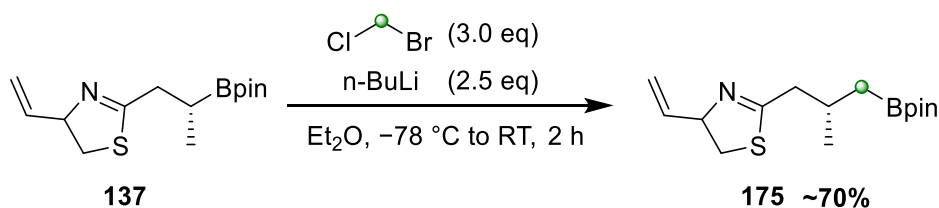
Scheme 51: Improved amination and acylation in the ISYNTH reactor block. GC-MS over 2-steps showed full conversion.



Scheme 52: Methylation of the model amide **173** worked well using *n*-BuLi and MeI.

Finally, the equivalents of acyl chloride were increased to three, as with 3 equiv. of *n*-BuLi in the first step, there should be 3 equiv. of nucleophile (amine or methoxide, for example) to react with the acyl chloride. This gave an improved average of 76% $^1\text{H NMR}$ yield for two reactions in parallel with full GC-MS conversion for both (Scheme 51). On this same material **173**, we then attempted the methylation of the amide using the conditions from Aggarwal's 2015 report (Scheme 52). Lithation of the amide is accomplished with *n*-BuLi in 15 minutes at $-78\text{ }^\circ\text{C}$, then MeI is added as electrophile. Performing this procedure on amide **173** (prepared and filtered in the automation platform) encouragingly gave full conversion by GC-MS and an average $^1\text{H NMR}$ yield of 60% for methylated amide **174** over 3-steps for the entire process. This positive result also demonstrates that chemistry can be directly transferred from manually performed literature to the automation platform without optimisation. The workflow was essentially identical to the Morcken amination and amidation provided (Scheme 50), with the desired reagents swapped out.

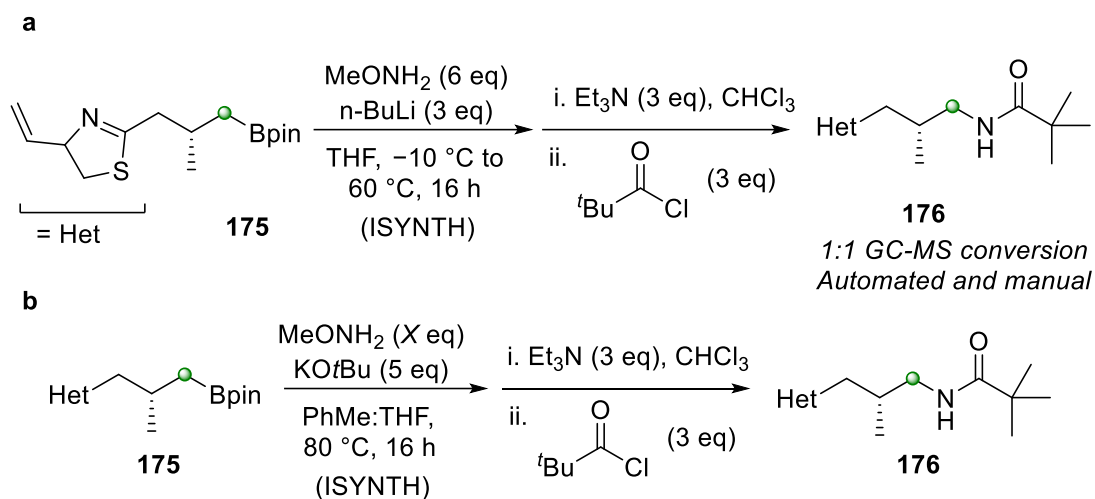
Confident in the dispense of reagents and workflows on the automation platform, we then attempted to use a model substrate containing the thiazoline ring. We used the primary boronic ester **175**, which is simply made from a Matteson reaction on secondary boronic ester **137** (Scheme 53). The material was a 1:1 *d.r.* mixture, due to racemisation of the stereocentre derived from cysteine in the unoptimised Wittig process. The $^1\text{H NMR}$ yield



Scheme 53: Matteson reaction to prepare a model substrate (primary boronic ester containing the thiazoline ring) for testing the Morcken amination, amidation and methylation.

(obtained by integrating the olefin signals) of the Matteson reaction was highly dependent on the purity of the starting boronic ester **137**, with impurities assumed to be borate esters from the conjugate borylation. Product **175** was not purified at this stage as we wanted to use crude material in the Morcken amination to better reflect the expected purity after the assembly-line synthesis on the platform when making kalkitoxin analogues.

Transferring the optimised amination conditions (Scheme 51) to model substrate **175** only gave poor conversion (~1:1) by GC-MS (Scheme 54a). Trying the same conditions manually in the lab also gave poor conversion (1:1) by GC-MS. It was reasoned there must be a slower addition of MeONHLi to the boronic ester in substrate **175** versus phenethyl boronic acid pinacol ester. This would then lead to degradation of the lithiated species instead of productive reaction (as in scheme 49c). We opted to try Morcken's second generation conditions, which use 5.0 eq of KO t Bu as base and 3.0 eq of MeONH₂. Wary of the volatility of MeONH₂, we doubled the amount used to 6.0 eq (Scheme 54b). This thankfully provided full conversion when performed manually in the lab. Unfortunately performing the reaction on the automation platform only provided low conversion (65:35 by GC-MS) even with 20 eq of MeONH₂.



Manual:

GC-MS Conversion

175	176	
1	99	6 eq MeONH ₂

In lab vials capped and parafilmed.

Volatility of MeONH₂ main issue:

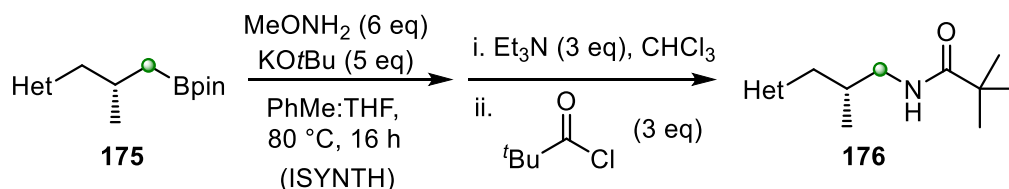
ISYNTH lid not properly sealed

Automation:

GC-MS Conversion

Run	175	176	
1	89	11	} 10 eq MeONH ₂
2	75	25	
3	66	34	} 20 eq MeONH ₂
4	65	35	

Scheme 54: Optimisation of the amination of model substrate 175. The 1st generation procedure only provided poor conversion. Switching to the 2nd generation procedure in the lab was successful, but the results did not carry over to the automation platform due to losses of volatile MeONH₂.



Automation:

GC-MS Conversion

Run	175	176
1	5	95
2	3	97

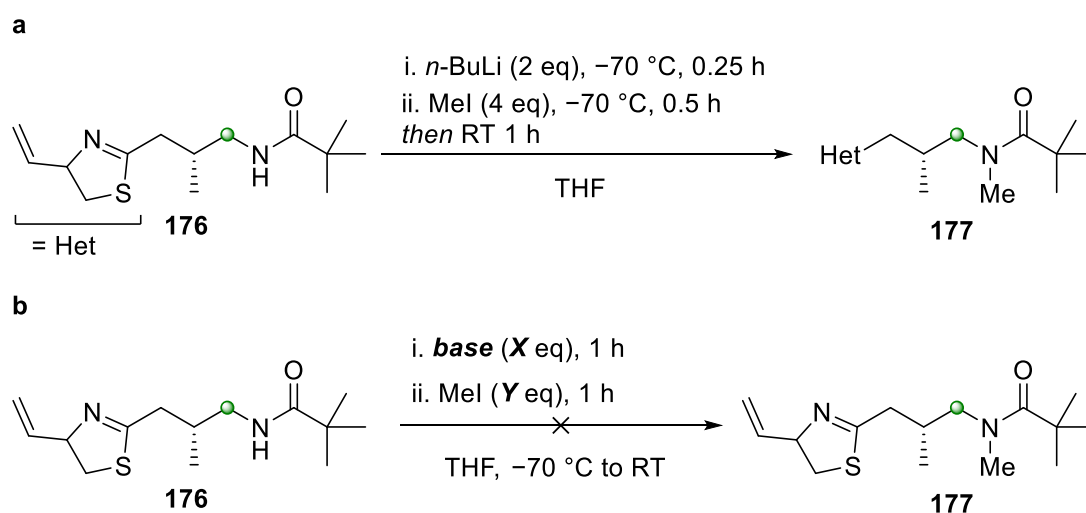
Manually capped vials in ISYNTH

Scheme 55: Successful 2nd generation Morken amination on the platform, using manually capped vials in the ISYNTH block.

The position of the vials on the platform were set to “sealed” on the workflow (as opposed to under inert gas) which demonstrated the seal was not good enough to hold MeONH₂ at 80 °C. The manual procedure in the lab uses 8 mL vials which are capped and sealed with parafilm. We decided to remove the lid of the IYNSTH reactor and cap each vial

separately by hand (Scheme 55). Thankfully, this gave full conversion (>95:5 **176**:**175** by GC-MS), demonstrating issues were with MeONH₂ volatility. Discussions about improving the seal around the ISYNTH are ongoing, however we hope to use small inserts under the vials to push them up against the seal, and Chemspeed have designed special O-rings to go round the top of the vials. However, MeONH₂ is a volatile liquid (b.p. = 48 °C) so stopping its evaporation at 80 °C is a tall order.

Amide **176** was not isolated at this point. Instead, we wanted to test the methylation of the amide immediately on the crude material. For the synthesis of kalkitoxin analogues, we did not want to remove the material from the platform to purify manually at any point. The methylation conditions described above (Scheme 52) were attempted first (Scheme 56a). Addition of *n*-BuLi at -70 °C for 15 minutes to amide **176**, then addition of MeI and warming led only to observation of complete decomposition by GC-MS. No decomposition products could be identified – the trace was essentially blank and ¹H NMR analysis only gave many peaks. Clearly, the substrate (presumably the thiazoline ring)



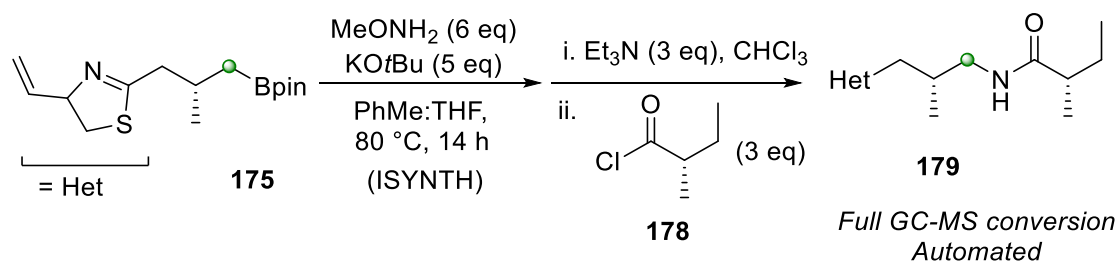
entry	base	X	Y	GC-MS Conversion		
				176	177	
1	LDA	3	4	100	0	Manual
2	KHMDS	3	4	100	0	
3	KOtBu	3	4	50	50	
4	KOtBu	6	6	28	72	Automated
5	KOtBu	6	10	25	75	
6	KOtBu	10	14	32	68	

Scheme 56: Optimisation of methylation of amide **176**.

was not stable to unhindered strong bases/nucleophiles. The vast majority of the literature shows NaH to be the typical base for methylation of secondary amides however this would not be suitable on the platform due to inability to make a stock solution.

Some hindered nitrogen bases (LDA and KHMDS) were trialled (manually), but these were unable to deprotonate the amide (no conversion by GC-MS, entry 1 & 2, scheme 56b). Using KO t Bu as base did show an improvement (entries 3 & 4), and by increasing the equivalents of base and electrophile we were able to increase the GC-MS conversion even further (25:75 **176:177**) but not to completion (entries 5 & 6). The steric hindrance was considered around the amide on the model substrate containing a t Bu group. It was reasoned that pushing this substrate to completion would require harsher conditions than for the actual substrate which will be the less hindered isobutyl amide. As such the model was changed to include the correct amide group.

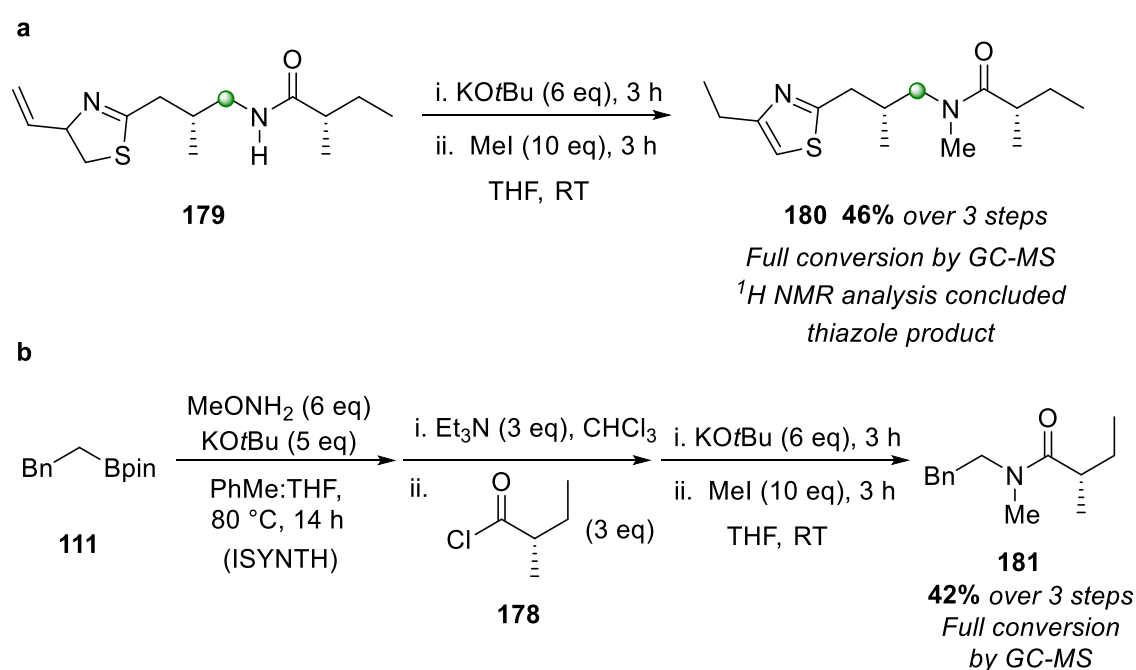
The amination and amidation was repeated on the Chemspeed platform using our optimised conditions with the correct acyl chloride **178** (albeit the incorrect enantiomer for (+)-kalkitoxin due to cost) and full conversion by GC-MS was observed, as expected (Scheme 57). This material was filtered on the platform and then was subjected to the best methylation conditions from above (entry 5, scheme 56b). Thankfully, with the less sterically hindered amide the methylation proceeded to full conversion by GC-MS (Scheme 58a). We then proceeded to determine the ^1H NMR yield for the reaction but unfortunately, the ^1H NMR spectrum showed an essentially blank olefin region, with 2 singlets close together at $\delta = \sim 6.7$ ppm. After isolation by column chromatography and characterisation it was clear we had made the thiazole containing product **180** (46% over 3 steps) instead of the desired thiazoline. Boronic ester **111** was also brought through the 3-step process in parallel, which also demonstrated 2 rotamers (at room temperature after



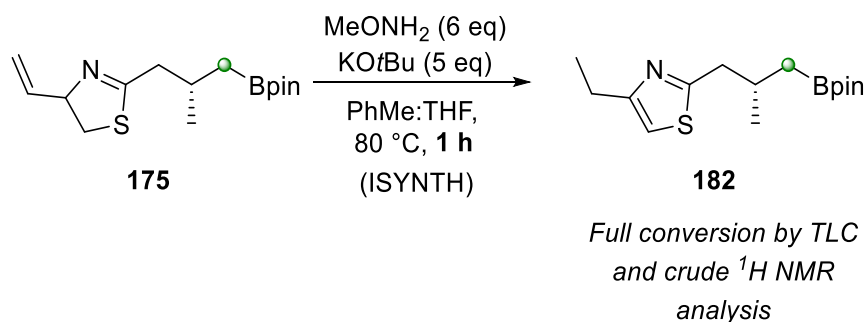
Scheme 57: Use of the less hindered isobutyl acyl chloride **178** gave the same results as our model (PivCl). We used the incorrect enantiomer of the acyl chloride (for (+)-kalkitoxin) due its lower cost.

^1H NMR analysis) for the isolated product **181** (42% over 3 steps, scheme 58b). There were some minor diastereomers present in isolated thiazole **180** (<10%), however this demonstrated the acyl chloride was not racemising to a large extent under the reaction conditions.

Unfortunately, conversion had only been checked by GC-MS up to this point and so it was not obvious at which stage aromatization was occurring. It was assumed base-catalysed isomerisation was the pathway, and out of the two base-mediated processes in the 3-step sequence the Morcken amination with heating to 80 °C seemed more likely.



Scheme 58: a) Methylation of amide **179** gave full conversion by GC-MS but unfortunately the thiazole was isolated instead. We were not sure if the aromatisation had already occurred in a previous step at this point; b) performing the same 3-step sequence on phenethyl boronic acid pinacol ester **111** gave a similar yield.



Scheme 59: The 2nd generation Morcken amination conditions gave full conversion to the thiazole product after 1 h.

Indeed, following the reaction in the lab by TLC, after 1 h heating to 80 °C, under our standard Morcken amination conditions gave full conversion to a spot with slightly higher R_f value and with same mass (TLC-MS) as the starting material. Crude ^1H NMR analysis quickly showed the lack of olefin signals and new thiazole signal (Scheme 59). This clearly demonstrated that the 2nd generation amination conditions were incompatible with the thiazoline ring. Future work will be attempting to push the amination with Morcken's 1st generation conditions to completion (1:1 conversion was seen previously) while avoided isomerization, or using a different aminating agent such as $\text{H}_2\text{N-DABCO}$ developed by Liu and co-workers.¹³⁵ This procedure still uses $\text{KO}t\text{Bu}$ but employs shorter reaction times than Morcken's 2nd generation conditions (1 h versus 16 h) and a lower number of equivalents of base (2.4 eq versus 5 eq). Alternatively, Chan-Evans-Lam couplings of amides and alkyl boronic esters are known, however these conditions typically require an oxidant which may be incompatible with the thiazoline ring.¹³⁶

4.6 Conclusions

The optimisation of lithiation–borylation chemistry (the Matteson homologation with LiCH_2Cl and homologation with **40-Li**) on a Chemspeed automation platform has been presented. To the best of our knowledge, this is the first example of complex organoboron chemistry and low temperature alkyllithium chemistry on an automated batch platform. At the outset of this project, the reactions did not proceed due to improper drying of the vessels. Once a *n*-BuLi rinse of the reactors was performed, the chemistry proceeded in good yields of ~70%, however this is a drop of 20% on expected yields when this chemistry is performed manually. Through careful observation and optimisation these yields were improved to ~90% per step over two iterative steps. For the Matteson chemistry, increased shaking (800 rpm) was found to give the main increase in yield. For the stannane chemistry, the main increase was found to be from using 1,2-DCE to rinse the reactors for filtration, as it allows full transfer of product with little to no benzoate salts transferred. Other parameters, such as where the solvent was evaporated (the ISYTH 8 mL vials gave poor recovery while the glass array gave high recovery) and using 400 mg of SiO_2 (with 5% Et_3N) were also essential to obtain high recoveries. Further details of changes made to the automated workflow are given in the supporting information.

The Chemspeed platform now affords the same yields as seen when performing the chemistry manually. Prepping the platform, including making stock solutions and calculating reagent amounts, can take ~2 h if performing a workflow for the very first time or the first time in a sequence. If the stock solution volumes are already known or the chemist is already accustomed to the workflow preparation, then setting up the Chemspeed can take <30 minutes of manual time. The run of the platform can then take 18–24 h depending on the number of reactors to be dried and the total volume to be filtered (essentially one run per day for up to four reactions). This is a large improvement in manual time spent on the reactions although the number of reactions per day equals that done manually (importantly doing four reactions manually will take up the entire day). As well as this, there is the potential for someone with no experience in assembly–line synthesis to be able to design molecules and then have a technician synthesise them on the Chemspeed platform, opening avenues for chemists with little wet lab experience.

With our optimised process in hand, we have then looked to apply it in the synthesis of (+)-kalkitoxin analogues. A scalable route towards the starting boronic ester **138** was

designed and carried out. Racemisation of α -amino aldehyde **158** was observed in the Wittig reaction however this was solved by using Breinbauer and co-workers' conditions for the work up (tartaric acid solution instead of tartrate). As well as this, a novel conjugate borylation of α - β unsaturated thiazoline **137** based on conditions by Meng and co-workers was found to proceed in good yields and with high selectivity. Better purification (distillation) of the boronic ester product is still required and is ongoing.

The final three steps of the automated synthesis have also been evaluated: Morcken amination, amidation and methylation of the formed amide. Careful optimisation of the reaction conditions (such as using capped vials in the platform) allowed the chemistry to proceed, however unfortunately it was found that the thiazoline isomerises to the thiazole under the conditions for the Morcken amination. Future work will be to avoid this isomerisation using different amination conditions.

4.6.1 Outlook

The optimisation of two different carbenoids, LiCH_2Cl and lithiated benzoate **40-Li**, on the Chemspeed automation platform has been presented. The amount of knowledge built up during this time will allow for the rapid optimisation of other types of carbenoids on the platform. α -Sulfinyl benzoates are an efficient way to generate a larger variety (than the equivalent α -stannyl benzoates) of α -metalated benzoates with high *e.r.* values. Sulfoxide-metal exchange has been shown to occur either with *t*-BuLi or *i*PrMg•LiCl, however perhaps *t*-BuLi is too dangerous to use as a stock solution. Use of *i*PrMg•LiCl will allow access to α -Mg benzoates which are useful in all but the most hindered situations. Filtration is more difficult as the sulfoxide by-product can interfere with subsequent homologations and it can coelute with the product boronic ester. Use of a less polar solvent mixture which elutes the less polar product but leaves the polar sulfoxide by-product on silica may be helpful here.

Another avenue for potential exploration is the use of a "catch and release" system. Burke and co-workers demonstrated an excellent version of a catch-and-release system with the discovery that their MIDA boronates do not elute on silica until a small amount of THF is added. This means every other by-product/impurity can be eluted to waste and then the product collected upon addition of THF. MIDA boronates are not compatible with assembly-line synthesis due to the need for strictly aprotic conditions (for this reason, Boons and co-workers sulfonate tag would not be compatible either). The boronic ester

motif needs to be tagged in such a way that does not interfere with the chemistry. Full conversion can then be achieved with higher excesses of metal carbenoid (if required) and all by-products eluted to waste. One potential method is Fluorous Solid-Phase Extraction (FSPE), of which automated studies have been performed.¹³⁷ This method requires a fluoro-tag (typically a perfluoroalkyl chain) on the molecule of interest, which then does not elute from fluorinated silica (commercially available and reusable) until certain conditions are applied (100% MeOH, for example). Normal phase silica can be used with fluorinated solvents.¹³⁸ The diol ligand on boron would then be swapped to a variant with a perfluoroalkyl chain appended (presumably at a distance to avoid interfering with the chelation strength of the diol on boron), which would hopefully not affect the chemistry. If such a catch-and-release system was effective, this could (for example): 1) reduce filtration time and increase productivity; 2) allow the automation of many iterative steps without build-up of side products; and 3) allow the automation of different carbenoid precursors with polar/apolar by-products. Other SPE methods exist, however FPSE is well documented in the literature.

Preliminary results towards the automated synthesis of (+)-kalkitoxin analogues was described. The Aggarwal group will synthesise many analogues of (+)-kalkitoxin to probe structure activity relationships (SARs). Importantly, the use of assembly-line synthesis will allow the incorporation of methyl groups anywhere along the central chain with any stereochemistry. This is not possible using previous syntheses. It is hoped to use the group's knowledge of the effect of *syn*-pentane interactions to allow the development of a SAR study concerning molecular shape along the central chain of (+)-kalkitoxin, which can be helical, linear or not controlled (depending on the methyl substitution pattern).¹³⁹

5 Experimental Section

5.1 General information

All reagents were purchased from commercial suppliers and used without further purification unless otherwise stated. All reactions were performed in flame dried glassware under nitrogen unless otherwise stated. TMEDA was distilled under nitrogen over CaH_2 prior to use. (+)-Sparteine was distilled under reduced pressure over CaH_2 and stored at $-20\text{ }^\circ\text{C}$ under nitrogen prior to use. Borate esters were distilled before use and stored under argon. Starting diisopropyl carbamates and TIB esters were synthesised according to literature procedures in identical fashion, see references for further details. Organostannes should be treated as extremely toxic and handled carefully: any contaminated weighing paper, glassware or spatulas should be washed into a labelled container which is disposed separately from standard waste. Anhydrous solvents were obtained using Anhydrous Engineering Ltd. double alumina and alumina-copper catalysed drying columns. Melting points were measured on a digital Stuart SMP30 apparatus.

Thin layer chromatography was carried out on Polygram 0.2 mm silica gel TLC plates visualising with 254 nm UV light and developed with KMnO_4 dip, unless otherwise stated. Flash column chromatography was performed on silica gel (Merck Kieselgel 60, 230-400 mesh) or Biotage Isolera One automated system.

Nuclear Magnetic Resonance (NMR) spectra were measured on a Varian 400/Bruker 400 /JEOL 400 Spectrometer (^1H : 400MHz, ^{11}B : 128 MHz, ^{13}C : 101 MHz, ^{19}F : 377 MHz) or Bruker CryoCarbon (^1H 500 MHz, ^{13}C 126 MHz) with all spectra referenced to residual NMR solvent resonances (CDCl_3 : $\delta = 7.26$ (^1H NMR), $\delta = 77.16$ (^{13}C NMR)) and processed in MestReNova 11.0. ^{11}B NMR spectra were measured using boron-free quartz NMR tubes and were recorded with complete proton decoupling using $\text{BF}_3 \cdot \text{Et}_2\text{O}$ ($\delta = 0.0$ ppm) as an external standard. Chemical shifts (δ) are quoted in ppm and coupling constants (J) in Hz. Coupling constants are left as measured with an experimental error of ± 0.5 Hz. Multiplicities are referred to as singlet (s), broad singlet (brs), doublet (d), triplet (t), quartet (q), quintet (quin), sextet (sext), septet (sept), multiplet (m) and combinations thereof. ^1H NMR yields of materials in crude mixtures were determined by addition of a suitable external standard (CH_2Br_2 or 1,3,5-trimethoxybenzene) after

work-up of the reaction. A one scan ^1H experiment was used with a 45 second relaxation delay.

Infra-red (IR) spectra for compound analysis were recorded on a Perkin Elmer FTIR spectrometer and are quoted as ν in cm^{-1} , with the abbreviations (s, strong), (m, medium) and (w, weak) standing for relative intensities.

Mass Spectra were recorded by the University of Bristol Mass Spectrometry service on a VG Analytical Quattro (ESI) spectrometer. High resolution MS spectra were recorded on the following spectrometers (ionization mode): Esquire 6000 micrOTOF FTICR (ESI) and Autospec (CI).

Chiral HPLC was performed using Daicel Chiralpak IB columns ($4.6 \text{ mm} \times 250 \text{ mm} \times 5 \mu\text{m}$)/OD column ($4.6 \text{ mm} \times 250 \text{ mm} \times 10 \mu\text{m}$)/AD-H ($4.6 \text{ mm} \times 250 \text{ mm} \times 5 \mu\text{m}$) column on an Agilent system and monitored by diode array detector (DAD).

In Situ IR spectroscopy (React-IR): The reactions were monitored using Mettler Toledo React-IR 15 mid-infrared spectrometer equipped with a Silver Halide (AgX) FiberConduit with integrated DiComp probe, using the iC IR Reaction Analysis software (version 4.3). Prior to the use of the in situ IR spectroscopy machine for data collection, the contrast and align, performance (5 runs) and stability (duration 5 minutes) were tested and saved. Lithiation/borylation (with *sec*-BuLi and boronic esters/trialkylboranes/borate esters) did not corrode the gold seal of the probe.

Unless otherwise noted, half-lives ($t_{1/2}$) for lithiation ($t_{1/2} \text{Li}$) and borylation ($t_{1/2} \text{B}$) are stated in minutes. Half-lives were determined as the time between complete addition of a reagent (*sec*-BuLi or boronic ester/trialkylborane, which were added dropwise over 3 – 5 minutes) and completion. The expression ‘completion’ refers to the curve representing the lithiated species reaching a plateau. $t_{1/2} < 15 \text{ s}$ indicates an instant reaction, as the instrument scans once every 15 s in normal mode. For every chart the y-axis is absorbance and the x-axis is time (typically the format is hh:mm:ss). In situ IR spectra are provided without baseline correction.

In situ IR spectroscopy (React-IR) setup standard procedure

To set up a reaction with the in situ IR spectroscopy probe, a 3 necked 25 mL flask was used. The recently cleaned probe was then inserted into the top of the flask using a Teflon adaptor (supplied with the instrument) inside a glass adaptor, secured with a clip, and

placed at a height where it would be immersed in the reaction mixture, but did not touch the stirring bar. The contrast and align, performance (5 runs) and stability (duration of 5 minutes) tests were then performed and saved. After the tests, the flask was placed under vacuum and dried with a heat gun. A new experiment could then be started. A background could be taken in the solvent to remove any solvent peaks, however this could also be achieved using the software's solvent subtraction once a solvent reference spectrum had been taken. Once set up, before clicking the 'start experiment button' all starting materials were added, and the reaction cooled to the desired temperature for 30 minutes. The expression 'reaction temperature' refers to temperatures of cooling bath mixtures which result in temperatures of either $-65\text{ }^{\circ}\text{C}$, $-78\text{ }^{\circ}\text{C}$ or $-95\text{ }^{\circ}\text{C}$. The resistance temperature detector (RTD) on the probe was not used.

Note: It is important to turn the instrument on 1 – 3 hours before an experiment is started. Once ready the 'TEMP OK' display under the 'contrast and align' test will change from 'false' to 'okay'. This could take anywhere from 1 – 3 hours.

5.2 In Situ IR Spectroscopy

5.2.1 General Procedures

1. Lithiation-Borylation with in situ IR spectroscopy to prepare secondary alcohols:

The TIB ester or *N,N*-diisopropylcarbamate (1 equiv.) and diamine (1.2 equiv.) was added to Et₂O (0.3 M) and cooled to -78 °C in an acetone/dry ice bath. This was left to cool for 30 minutes, to allow the in situ IR spectroscopy to stabilise. A solution of *sec*-butyllithium (1.2 equiv., 1.3 M in cyclohexane) was then added dropwise, which gave a brown/orange solution. This was then stirred at -78 °C until complete lithiation. The boronic ester (1.2 equiv.) was then added dropwise as a solution in Et₂O (1.0 M) and the reaction was stirred at -78 °C until complete borylation. The in situ IR spectroscopy probe was removed from the reaction at this point. The reaction was then heated to reflux until full 1,2-migration had occurred, as determined from ¹¹B NMR spectroscopy. Carbamates could be solvent swapped to CHCl₃ and heated to reflux to allow a more facile 1,2-migration. The reaction was then filtered through a silica plug and the solvents removed under reduced pressure to leave a crude oil. To recover the diamine, the organic layer was then washed with a 2.0 M solution of HCl three times. The acidic aqueous layer could then be extracted further with Et₂O. After removal of solvents, the crude oil was then dissolved in THF (3 mL) and cooled to 0 °C. A mixture of H₂O₂ (33% in H₂O, 1 mL) and NaOH (2 M, 2 mL) was prepared at 0 °C and added dropwise to the crude material, which was left until full oxidation of the boronic ester had occurred by TLC analysis. The mixture was then separated, and the aqueous layer extracted with Et₂O. The solvents were then removed under reduced pressure to leave a crude oil which was purified by flash column chromatography with a suitable eluent to afford the desired product.

2. Synthesis of carbamates:

To a solution of *N,N*-diisopropylcarbamoyl chloride (1.2 equiv.) and triethylamine (1.2 equiv.) in toluene (1 M) was added the selected primary alcohol (1 equiv.). The reaction mixture was then heated to 150 °C in a microwave reactor for 2 hours, to give a brown solution with a white precipitate. This was then filtered through a silica plug and washed with Et₂O to give a brown oil after solvent evaporation. This was then purified by flash column chromatography with a suitable eluent to afford the desired product.

3. Synthesis of triisopropylbenzoate esters:

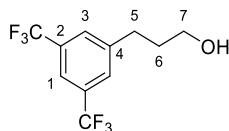
Triphenylphosphine (PPh₃, 1.1 equiv.) and 2,4,6-triisopropylbenzoic acid (TIBOH, 1 equiv.) were combined in a suitable flask, which was then flushed/evacuated with dry N₂ three times. To this was added the selected primary alcohol (1.1 equiv.) and THF (0.5 M). The reaction vessel was then cooled to 0 °C and diisopropyl azodicarboxylate (DIAD) (1.1 equiv.) was added dropwise at 0 °C. The resulting solution was then warmed to room temperature and stirred for 16 hours, until complete disappearance of the TIBOH by TLC. The solvent was then removed under reduced pressure to leave a crude oil, which was triturated with pentane, leaving a crude oil after removal of solvent. This was then purified by flash column chromatography with a suitable eluent to afford the desired product.

5.2.2 Experimental: Mechanistic Studies

5.2.2.1 Starting Materials

S1. 3-(3,5-bis(trifluoromethyl)phenyl)propan-1-ol:

Prepared following literature procedure.¹⁴⁰



Bis(dibenzylideneacetone)palladium (Pd(dba)₂, 0.02 equiv., 0.08 g, 0.14 mmol) and 2-(di-*tert*-butylphosphino)-1-phenylindole (0.06 equiv., 0.14 g, 0.41 mmol) were combined in a reaction vessel, which was then evacuated and refilled with nitrogen three times. 1,3-Bis(trifluoromethyl)-5-bromobenzene (1.0 equiv., 1.18 mL, 6.83 mmol) allyl alcohol, (1.1 equiv., 0.51 mL, 7.51 mmol), *N*-methyldicyclohexylamine (1.1 equiv., 1.60 mL, 7.51 mmol) and anhydrous *N,N*-dimethylformamide (DMF, 20 mL) were then added sequentially, and the mixture was stirred at 100 °C for 2 hours. After cooling, 50 mL EtOAc was added to the dark brown solution and it was then washed with H₂O (15 mL x 3), dried over MgSO₄ and filtered. The solvents were removed under reduced pressure to leave a crude brown oil. This was then dissolved in EtOH (20 mL) and cooled to 0 °C. Sodium borohydride (NaBH₄, 1.1 equiv. based on 100% yield of aldehyde, 0.280 g, 7.51 mmol) was then added portion wise and the reaction mixture stirred at 0 °C for 1 hour, until complete by TLC analysis. Any excess NaBH₄ was then quenched by addition of 1 M HCl. The reaction mixture was then separated, the aqueous layer extracted with Et₂O (x 3), and the solvents removed under reduced pressure to leave a crude oil. This was then purified by flash column chromatography (20% to 40% ethyl acetate (EtOAc) in hexanes (hex)) which gave the title compound as a colourless oil (1.38 g, 54%).

TLC: $R_f = 0.25$ (20% EtOAc in hexane).

¹H NMR (400 MHz, CDCl₃): $\delta = 7.71$ (s, 1H, **1**), 7.66 (s, 2H, **3**), 3.70 (t, $J = 6.2$ Hz, 2H, **7**), 2.87 (t, $J = 7.8$ Hz, 2H, **5**), 2.00 – 1.86 (m, 2H, **6**), 1.54 (brs, 1H, **-OH**).

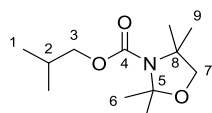
¹³C NMR (101 MHz, CDCl₃): $\delta = 144.5$ (C4), 131.8 (q, $J = 33.2$ Hz, C2), 128.7 (brs, C3), 123.6 (q, $J = 272.6$ Hz, -CF₃), 120.2 (quin, $J = 3.9$ Hz, **1**), 61.7 (C7), 33.8 (C6), 31.9 (C5).

¹⁹F NMR (377 MHz, CDCl₃): $\delta = -62.79$ (s, -CF₃).

HRMS-ESI: No mass ion found.

FT-IR (film): ν_{\max} (cm⁻¹) = 3337 (broad, m), 2943 (m), 2880 (m), 1623 (w), 1466 (w), 1379 (m), 1274 (w).

71. Isobutyl 2,2,4,4-tetramethyloxazolidine-3-carboxylate:



To a flame dried flask was added Na₂CO₃ (1.5 equiv., 0.615 g, 5.81 mmol) which was then stirred under vacuum for 15 minutes. This was then suspended in CH₂Cl₂ (5 mL) and 2,2,4,4-tetramethyloxazolidine (1 equiv., 0.500 g, 3.87 mmol) added. Isobutyl chloroformate (1.5 equiv., 0.75 mL, 5.81 mmol) was then added dropwise and the

resulting mixture stirred vigorously for 5 hours, until complete by TLC analysis. The reaction was then quenched with 2M NaOH (0.5 mL) and stirred for 30 minutes. After drying with MgSO₄ the reaction was filtered through Celite and washed with CH₂Cl₂. After removal of solvents, the crude oil recovered was purified by flash column chromatography (5 – 20% EtOAc in petrol) which gave the title product as a colourless oil (0.56 g, 62%).

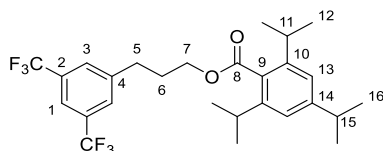
TLC: $R_f = 0.40$ (20% EtOAc in petrol). Visualised with anisaldehyde dip.

¹H NMR (500 MHz, CDCl₃): $\delta = 3.88$ (t, $J = 6.0$ Hz, 2H, **3**), 3.73 (s, 2H, **7**), 2.05 – 1.88 (m, 1H, **2**), 1.56 & 1.54 (rotamers, 2 x s, 6H, **6**), 1.42 & 1.38 (rotamers, 2 x s, 6H, **9**), 0.97 & 0.96 (rotamers, 2 x d, $J = 6.8$ Hz, 6H, **1**).

¹³C NMR (126 MHz, CDCl₃): $\delta = 153.0$ & 152.3 (rotamers, C4), 95.8 & 94.8 (rotamers, C5), 76.7 & 76.1 (rotamers, C7), 71.0 & 70.9 (rotamers, C3), 60.6 & 59.6 (rotamers, C8), 28.0 (C2), 26.6 (C6), 25.3 (C6 & C9), 24.2 (C9), 19.4 & 19.4 (rotamers, C1).

Spectral data in agreement with literature.¹⁴¹

S2. 3-(3,5-bis(trifluoromethyl)phenyl)propyl 2,4,6-triisopropylbenzoate:



Following general procedure **3** using 3-(3,5-bis(trifluoromethyl)phenyl)propan-1-ol **S1** (1.1 equiv., 0.47 g, 1.74 mmol), 2,4,6-triisopropylbenzoic acid (1 equiv., 0.39 g, 1.58 mmol), PPh₃ (1.1 equiv., 0.50 g, 1.91 mmol), THF (10 mL) and DIAD (1.1 equiv., 0.38 mL, 1.91 mmol). The crude oil was purified by flash column chromatography (5% EtOAc in petrol) to afford the title compound as a white solid (0.72 g, 82%).

Melting point: 70 – 71 °C.

TLC: $R_f = 0.62$ (20% EtOAc in petrol).

¹H NMR (400 MHz, CDCl₃): $\delta = 7.74$ (s, 1H, **1**), 7.64 (brs, 2H, **3**), 7.03 (s, 2H, **13**), 4.35 (t, $J = 6.2$ Hz, 2H, **7**), 3.07 – 2.77 (m, 5H, **5**, **11** & **15**), 2.22 – 2.08 (m, 2H, **6**), 1.27 (d, $J = 6.8$ Hz, 9H, **12/16**), 1.26 (d, $J = 6.9$ Hz, 9H, **12/16**).

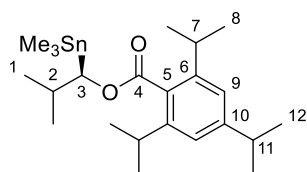
¹³C NMR (101 MHz, CDCl₃): $\delta = 170.9$ (C8), 150.4 (C9), 144.8 (C10), 143.6 (C4), 131.9 (q, $J = 33.1$ Hz, C2), 130.3 (C14), 128.6 (brs, C3), 123.4 (q, $J = 272.7$ Hz, -CF₃), 121.0 (C13), 120.4 (quin, $J = 3.8$ Hz, C1), 63.6 (C7), 34.5 (C11/15), 32.2 (C5), 31.7 (C11/15), 30.2 (C6), 24.2 (C12), 24.0 (C16).

¹⁹F NMR (377 MHz, CDCl₃): $\delta = -62.89$.

HRMS-ESI (m/z): $[M + Na]^+$ calcd for C₂₇H₃₂F₆NaO₂, 525.2204; found, 525.2194.

FT-IR (film): ν_{\max} (cm⁻¹) = 2964 (m), 2932 (m), 1727 (s), 1379 (m), 1278 (w), 1251 (w), 1174 (m), 1135 (m).

92. (*R*)-2-Methyl-1-(trimethylstannyl)propyl 2,4,6-triisopropylbenzoate:



A solution of isobutyl 2,4,6-triisopropylbenzoate⁴² (1 equiv., 2.12 g, 6.96 mmol) and (+)-sparteine (1.5 equiv., 2.40 mL, 10.44 mmol) in Et₂O (20 mL, 0.3 M with respect to benzoate) was cooled to -78 °C. After 5 minutes, *sec*-BuLi (1.6 M in cyclohexane, 1.5 equiv., 8.00 mL, 10.44 mmol) was added dropwise, and the mixture stirred at -78 °C for 5 hours. At this time, trimethyltinchloride (1.0 M in hexanes, 1.5 equiv., 10.44 mL, 10.44 mmol) was added dropwise. The solution was stirred at -78 °C for another hour. After warming, the mixture was diluted (Et₂O) and washed 2M HCl to recover the diamine. After removal of solvents under reduced pressure, the yellow crude oil was purified on a Biotage system using a 10 g UltraSnap column (5 – 20% toluene in petrol [1-10-5 CVs] λ_{all} , λ_{max} = 220 nm) to afford the title compound as a colourless oil (2.34 g, 71%).

TLC: R_f = 0.29 (20% toluene in petrol).

¹H NMR (400 MHz, CDCl₃): δ = 7.00 (s, 2H, **9**), 4.98 (d, J = 4.6 Hz, 1H, **3**), 2.97 – 2.77 (m, 3H, **7 & 11**), 2.25 (sextd, J = 6.8, 4.5 Hz, 1H, **2**), 1.27 – 1.21 (m, 18H, **8 & 12**), 1.04 (d, J = 6.7 Hz, 3H, **1**), 1.01 (d, J = 6.8 Hz, 3H, **1**), 0.22 (s, 9H, **-SnMe₃**), 0.22 (d, J = 52.5 Hz, 9H, **-^{119/117}SnMe₃**).

¹³C NMR (101 MHz, CDCl₃): δ = 171.4 (C4), 149.7 (C10), 144.9 (C6), 130.8 (C5), 120.8 (C9), 79.4 (C3), 34.3 (C11), 32.6 (C2), 31.4 (C7), 24.4 (C8/12), 24.2 (C8/12), 23.9 (C8/12), 21.3 (C1), 19.8 (C1), -8.0 (**-Me₃Sn**).

HRMS-ESI (m/z): [M + Na]⁺ calcd for C₂₃H₄₀O₂¹²⁰SnNa, 491.1948; found, 491.1937.

FT-IR (film): ν_{max} (cm⁻¹) = 2960 (s), 2978 (s), 2870 (s), 1704 (s), 1607 (m), 1574 (m), 1460 (m), 1250 (m).

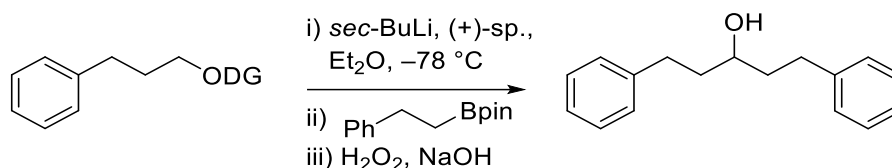
HPLC: IB column, hexane, 0.7 mL min⁻¹, T_R = 5.9 (minor), 7.4 (major).

$[\alpha]_D^{22.1}$ -27 (*c* 1.07, CHCl₃).

Spectral data in agreement with literature report.¹⁴²

5.2.2.2 In situ IR spectroscopy procedures

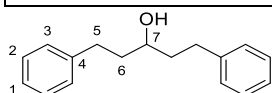
S3. 1,5-Diphenylpentan-3-ol: (from 3-phenylpropyl substrates **88/89**)



Prepared following general procedure **1** using 3-phenylpropyl diisopropylcarbamate³⁵ (1 equiv., 0.263 g, 1 mmol), *sec*-BuLi (1.2 equiv., 0.92 mL, 1.2 mmol), (+)-sparteine (1.2 equiv., 0.28 mL, 1.2 mmol) with Et₂O (3 mL), and phenylethylboronic acid pinacol ester (1.2 equiv., 0.279 g, 1.2 mmol) which was added in Et₂O (1 mL). The crude oil was purified by flash column chromatography (10 – 20% EtOAc in petrol) to afford the title compound as a colourless oil (0.140 g, 58%).

Prepared following general procedure **1** using 3-phenylpropyl 2,4,6-triisopropylbenzoate⁴² (1 equiv., 0.367 g, 1 mmol), *sec*-BuLi (1.2 equiv., 0.92 mL, 1.2 mmol), (+)-sparteine (1.2 equiv., 0.28 mL, 1.2 mmol) with Et₂O (3 mL), and phenylethylboronic acid pinacol ester (1.2 equiv., 0.279 g, 1.2 mmol) which was added in Et₂O (1 mL). The crude oil was purified by flash column chromatography (10 – 20% EtOAc in petrol) to afford the title compound as a colourless oil (0.161 g, 67%).

Entry	DG	t _{1/2} Li	t _{1/2} B
1	TIB	1	4
2	Cb	5	< 15 s



TLC: $R_f = 0.55$ (20% EtOAc in petrol).

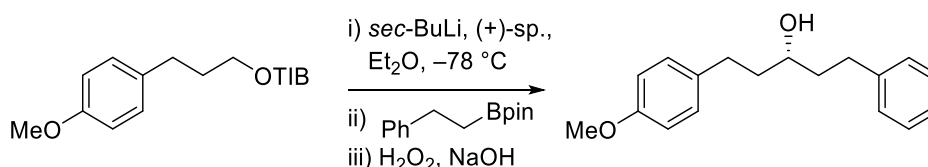
Melting point = 38 - 40 °C.

¹H NMR (400 MHz, CDCl₃): $\delta = 7.35 - 7.29$ (m, 4H, **2**), 7.26 – 7.20 (m, 6H, **1 & 3**), 3.70 (tt, $J = 8.1, 4.6$ Hz, 1H, **7**), 2.83 (ddd, $J = 13.7, 9.4, 6.1$ Hz, 2H, **5**), 2.71 (ddd, $J = 13.7, 9.4, 6.8$ Hz, 2H, **5**), 1.94 – 1.76 (m, 4H, **6**), 1.60 (s, 1H, **-OH**).

¹³C NMR (101 MHz, CDCl₃): $\delta = 142.1$ (C4), 128.4 (C2), 128.4 (C3), 125.9 (C1), 70.8 (C7), 39.2 (C6), 32.1 (C5).

Spectral data in agreement with literature.¹⁴³

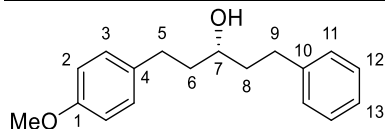
S4. (*R*)-1-(4-methoxyphenyl)-5-phenylpentan-3-ol: (from **69**)



Prepared following general procedure **1** using 3-(*para*-methoxy)phenylpropyl 2,4,6-triisopropyl TIB ester¹⁴⁴ (1 equiv., 0.396 g, 1 mmol), *sec*-BuLi (1.2 equiv., 0.92 mL, 1.2 mmol), (+)-sparteine (1.2 equiv., 0.28 mL, 1.2 mmol) with Et₂O (3 mL), and phenylethylboronic acid pinacol ester (1.2 equiv., 0.279 g, 1.2 mmol) which was added

in Et₂O (1 mL). After heating, oxidation, and work up, the crude oil was purified by flash column chromatography (10 – 20% EtOAc in petrol) to afford the title compound as a colourless oil (0.157 g, 58%).

Entry	DG	t _{1/2} Li	t _{1/2} B
1	TIB	2	5



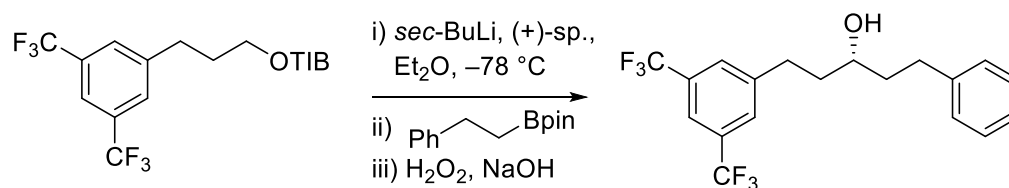
TLC: $R_f = 0.50$ (20% EtOAc in petrol).

¹H NMR (400 MHz, CDCl₃): $\delta = 7.32 - 7.27$ (m, 2H, **12**), 7.24 – 7.15 (m, 3H, **11 & 13**), 7.11 (d, $J = 8.6$ Hz, 2H, **3**), 6.84 (d, $J = 8.6$ Hz, 2H, **2**), 3.80 (s, 3H, **-OMe**), 3.67 (brs, 1H, **7**), 2.85 – 2.58 (m, 4H, **5 & 9**), 1.89 – 1.70 (m, 4H, **6 & 8**), 1.46 (brs, 1H, **-OH**).

¹³C NMR (101 MHz, CDCl₃): $\delta = 158.0$ (C1), 142.2 (C10), 134.2 (C4), 129.4 (C3), 128.6 (C11), 128.5 (C12), 126.0 (C13), 114.0 (C2), 70.9 (C7), 55.4 (-OMe), 39.6 (C6/8), 39.3 (C6/8), 32.2 (C9), 31.3 (C5).

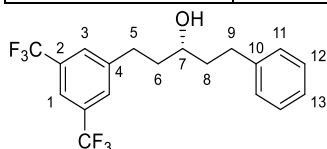
Spectral data in agreement with literature.¹⁴⁵

S5. (*R*)-1-(3,5-bis(trifluoromethyl)phenyl)-5-phenylpentan-3-ol: (from **70**)



Prepared following general procedure **1** using benzoate **70** (1 equiv., 0.502 g, 1 mmol), *sec*-BuLi (1.2 equiv., 0.92 mL, 1.2 mmol), (+)-sparteine (1.2 equiv., 0.28 mL, 1.2 mmol) with Et₂O (3 mL), and phenylethylboronic acid pinacol ester (1.2 equiv., 0.279 g, 1.2 mmol) which was added in Et₂O (1 mL). After heating, oxidation and work up the crude oil was purified by flash column chromatography (10 – 20% EtOAc in petrol) to afford the title compound as a colourless oil (0.291 g, 77%).

Entry	DG	t _{1/2} Li	t _{1/2} B	e.r.
1	TIB	<15 s	12 min	92:8



TLC: $R_f = 0.60$ (20% EtOAc in petrol).

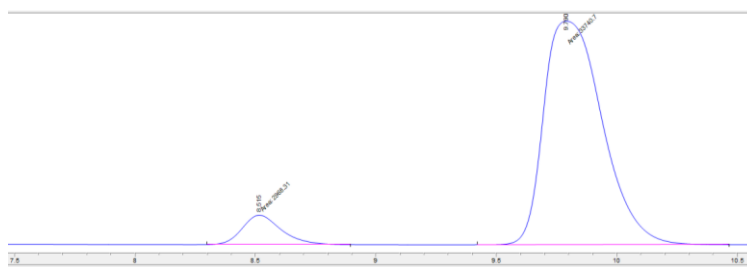
¹H NMR (400 MHz, CDCl₃): $\delta = 7.70$ (s, 1H, **1**), 7.63 (s, 2H, **3**), 7.34 – 7.26 (m, 2H, **12**), 7.23 – 7.17 (m, 3H, **11 & 13**), 3.70 – 3.63 (m, 1H, **7**), 2.94 (ddd, $J = 15.1, 9.6, 5.9$ Hz, 1H, **5**), 2.84 – 2.74 (m, 2H, **5 & 9**), 2.70 (ddd, $J = 13.8, 8.8, 7.1$ Hz, 1H, **9**), 1.90 – 1.76 (m, 4H, **6 & 8**), 1.52 (s, **-OH**).

^{13}C NMR (101 MHz, CDCl_3): δ = 144.67 (C4), 141.66 (C10), 131.68 (q, J = 32.9 Hz, C2), 128.68 (C3), 128.61 (C12), 128.44 (C11), 126.12 (C13), 123.51 (q, J = 272.6 Hz, - CF_3), 120.05 (quin, J = 3.9 Hz, C1), 70.47 (C7), 39.30 (C6/8), 38.76 (C6/8), 32.08 (C5/9), 31.80 (C5/9).

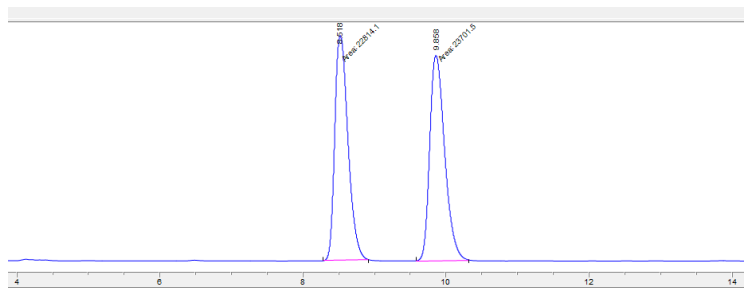
^{19}F NMR (377 MHz, CDCl_3): δ = -62.73.

HRMS-ESI: $[\text{M} + \text{Na}]^+$ calcd for $\text{C}_{19}\text{H}_{18}\text{F}_6\text{NaO}$, 399.1160; found, 399.1156.

HPLC: IB column, 95:5 hex:IPA, 1 mL min^{-1} , T_R = 8.52 (minor), 9.79 (major).



#	Time	Type	Area	Height	Width	Area%	Symmetry
1	8.515	MM	2968.3	264.3	0.1872	8.086	0.722
2	9.79	MM	33740.7	2000.1	0.2812	91.914	0.634

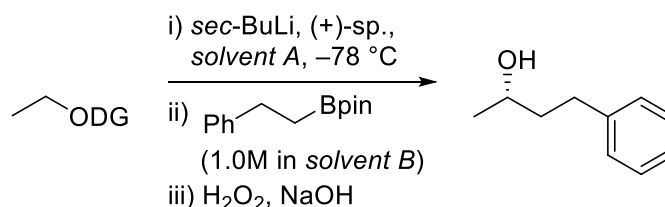


#	Time	Type	Area	Height	Width	Area%	Symmetry
1	8.518	MM	22814.1	1778	0.2139	49.046	0.614
2	9.858	MM	23701.5	1624.4	0.2432	50.954	0.71

$[\alpha]_D^{23.9} -6$ (c 1.00, CHCl_3).

The racemic alcohol was prepared following general procedure **1** using benzoate **70** (1 equiv., 0.100 g, 0.20 mmol), *sec*-BuLi (1.3 equiv., 0.20 mL, 0.26 mmol), TMEDA (1.3 equiv., 0.038 mL, 0.26 mmol) with Et_2O (0.70 mL) and phenylethylboronic acid pinacol ester (1.3 equiv., 0.060 g, 0.26 mmol) which was added in Et_2O (0.21 mL).

S6. (S)-4-phenylbutan-2-ol: (from ethyl substrates **68/40**)

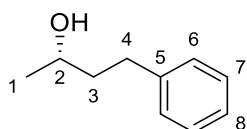


Prepared following general procedure **1** using ethyl diisopropylcarbamate³⁵ (1.0 equiv., 0.173 g, 1.00 mmol), (+)-sparteine (1.2 eq 0.28 mL, 1.20 mmol) in *solvent A* (3.33 mL) and phenylethyl boronic acid pinacol ester (1.2 equiv., 1.0 M in *solvent B*, 0.279 g, 1.20

mmol). After heating, oxidation, and work up, purification by column chromatography (petrol:EtOAc:NEt₃ 9:1:0.1) gave the title product as a colourless oil.

Prepared following general procedure **1** using ethyl 2,4,6-triisopropylbenzoate⁵⁰ (1.0 equiv., 0.276 g, 1.00 mmol), (+)-sparteine (1.2 equiv., 0.28 mL, 1.20 mmol) in *solvent A* (3.33 mL) and phenylethyl boronic acid pinacol ester (1.2 equiv., 1.0 M in *solvent B*, 0.279 g, 1.20 mmol). After heating, oxidation, and work up, purification by column chromatography (petrol:Et₂O:NEt₃ 19:1:0.1) gave the title product as a colourless oil.

Entry	DG	Solvent A	Solvent B	t _½ Li	t _½ B	e.r.	Yield
2	Cb	PhMe	PhMe	46	10	98:2	57%
3	Cb	Et ₂ O	Et ₂ O	30	<15 s	98:2	44%
5	TIB	Et ₂ O	Et ₂ O	8	2	95:5	45%
6	TIB	TBME	TBME	14	5	94:6	41%
7	TIB	PhMe	PhMe	7	165 ^c	94:6	41%
8	TIB	PhMe	THF	7	5	95:5	48%



TLC: $R_f = 0.45$ (20% EtOAc in petrol).

¹H NMR (400 MHz, CDCl₃): $\delta = 7.29$ (t, $J = 7.4$ Hz, 2H, **7**), 7.23 – 7.16 (m, 3H, **6 & 8**), 3.83 (h, $J = 6.3$ Hz, 1H, **2**), 2.83 – 2.61 (m, 2H, **4**), 1.90 – 1.70 (m, 2H, **3**), 1.23 (d, $J = 6.3$ Hz, 3H, **1**).

¹³C NMR (101 MHz, CDCl₃): $\delta = 142.03$ (C5), 128.38 (C7 & C6), 125.80 (C8), 67.51 (C2), 40.84 (C3), 32.13 (C4), 23.63 (C1).

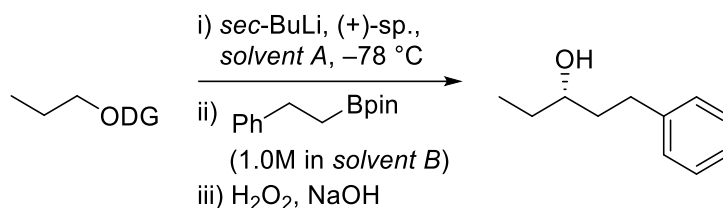
HPLC: IB column, 90:10 hex:IPA, 1 mL min⁻¹. $T_R = 5.64$ (minor), 6.63 (major).

IB column, 96:4 hex:IPA, 0.7 mL min⁻¹. $T_R = 12.69$ min (minor), 17.18 min (major).

$[\alpha]_D^{23.6} +17$ (c 0.91, CHCl₃).

Spectral data and retention times in agreement with literature.¹⁴⁶

S7. (S)-1-Phenylpentan-3-ol: (from propyl substrates **69/73**)

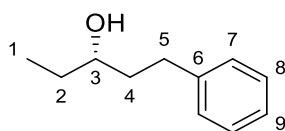


Prepared following general procedure **1** using propyl diisopropylcarbamate¹⁴⁷ (1.0 equiv., 0.187 g, 1.00 mmol), (+)-sparteine (1.2 equiv., 0.28 mL, 1.20 mmol) in *solvent A* (3.33

mL) and phenylethyl boronic acid pinacol ester (1.0 M in *solvent B*, 1.2 equiv., 0.279 g, 1.20 mmol). After heating, oxidation, and work up, purification by column chromatography (petrol:EtOAc:NEt₃ 19:1:0.1) gave the title compound as a waxy white solid.

Prepared following general procedure **1** using propyl 2,4,6-triisopropylbenzoate⁴⁴ (1.0 equiv., 0.291 g, 1.00 mmol), (+)-sparteine (1.2 equiv., 0.28 mL, 1.20 mmol) in *solvent A* (3.33 mL) with phenylethyl boronic acid pinacol ester (1.0 M in *solvent B*, 1.2 equiv., 0.279 g, 1.20 mmol). After heating, oxidation, and work up, purification by column chromatography (petrol:Et₂O:NEt₃ 19:1:0.1) gave the title compound as a waxy white solid.

Entry	DG	Solvent A	Solvent B	t _½ Li	t _½ B	e.r.	Yield
1	Cb	Et ₂ O	Et ₂ O	33	<15 s	98:2	60%
2	Cb	TBME	TBME	43	<15 s	97:3	59%
3	Cb	PhMe	PhMe	66	42	98:2	45%
4	TIB	Et ₂ O	Et ₂ O	16	8	97:3	77%
5	TIB	TBME	TBME	26	13	94:6	76%
6	TIB	PhMe	PhMe	9	501	94:6	55%
7	TIB	PhMe	THF	9	2	95:5	68%



TLC: R_f = 0.21 (10% Et₂O in petrol).

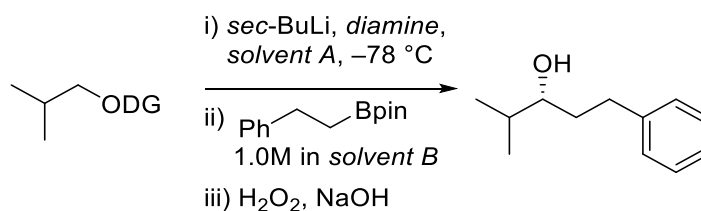
¹H NMR (400 MHz, CDCl₃): δ = 7.32 – 7.26 (m, 2H, **8**), 7.23 – 7.16 (m, 3H, **7 & 9**), 3.57 (tt, J = 7.7, 4.5 Hz, 1H, **3**), 2.80 (ddd, J = 13.8, 9.7, 6.7 Hz, 1H, **5**), 2.68 (ddd, J = 13.8, 9.7, 6.7 Hz, 1H, **5**), 1.86 – 1.68 (m, 2H, **4**), 1.62 – 1.41 (m, 2H, **2**), 0.95 (t, J = 7.5 Hz, 3H, **1**).

¹³C NMR (101 MHz, CDCl₃): δ = 142.4 (C6), 128.6 (C8), 128.5 (C7), 125.9 (C9), 72.8 (C3), 38.8 (C4), 32.2 (C5), 30.5 (C2), 10.0 (C1).

HPLC: OD column, 95:5 hex:IPA, 1.0 mL/min. T_R = 9.37 min (minor), 14.18 min (major).

Spectral data in agreement with literature.¹⁴⁸

S8. (*R*)-4-Methyl-1-phenylpentan-3-ol: (from isobutyl substrates **70/71/74** and stannane **92**)

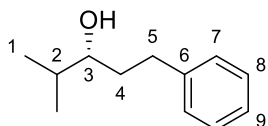


Prepared following general procedure **1** using isobutyl 2,4,6-triisopropylbenzoate⁴² (1.0 equiv., 0.31 g, 1.00 mmol) in *solvent A* (3.33 mL), either (+)-sparteine (1.2 equiv., 0.28 mL, 1.20 mmol) or (+) sparteine surrogate (1.2 equiv., 0.23 mL, 1.20 mmol) with phenylethyl boronic acid pinacol ester (1.0 M in *solvent B*, 1.2 equiv., 0.28 g, 1.20 mmol). After heating, oxidation, and work up, purification by column chromatography (petrol:Et₂O:NEt₃ 19:1:0.1) gave the title compound as a white waxy solid.

Entry	DG	Diamine	Solvent A	Solvent B	t _{1/2} Li	t _{1/2} B	e.r.	Yield
1	Cby	(+)-sp	Et ₂ O	Et ₂ O	145	3.5	98:2	28%
2	Cb	(+)-sp	Et ₂ O	Et ₂ O	81	3	98:2	67%
5	TIB	(+)-sp	Et ₂ O	Et ₂ O	31	35	97:3	66%
8	Cb	(+)-sp	PhMe	PhMe	195	ND ^a	n.d.	31%
9	TIB	(+)-sp	TBME	TBME	52	45	97:3	72%
10	TIB	(+)-sps	TBME	TBME	2	111	96:4	86%
11	TIB	(+)-sp	PhMe	PhMe	15	ND ^b	ND ^b	ND ^b
12	TIB	(+)-sp	PhMe	THF	15	11	97:3	54%

^a An accurate value was not determined to the long reaction time required.

^b Not determined due to slow formation of boronate complex



TLC: $R_f = 0.35$ (10% EtOAc in petrol).

Melting point < 30 °C

¹H NMR (400 MHz, CDCl₃): $\delta = 7.31 - 7.25$ (m, 2H, **8**), $7.23 - 7.16$ (m, 3H, **7 & 9**), $3.44 - 3.36$ (m, 1H, **3**), 2.84 (ddd, $J = 15.0, 10.0, 5.4$ Hz, 1H, **5**), 2.65 (ddd, $J = 13.7, 9.7, 6.7$ Hz, 1H, **5**), $1.86 - 1.72$ (m, 1H, **4**), $1.73 - 1.63$ (m, 2H, **2 & 4**), 1.32 (d, $J = 5.3$ Hz, 1H, -OH), 0.92 (d, $J = 6.8$, 6H, **1**).

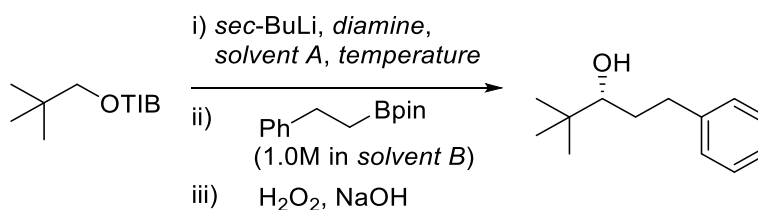
¹³C NMR (101 MHz, CDCl₃): $\delta = 142.3$ (C6), 128.4 (C8), 128.4 (C7), 125.8 (C9), 76.1 (C3), 36.0 (C4), 33.7 (C2), 32.5 (C5), 18.8 (C1), 17.1 (C1).

HPLC: IB column, 97:3 hex:IPA, 1 mL min⁻¹. $T_R = 8.08$ min (minor), 12.92 min (major).

$[\alpha]_D^{22.9} +31$ (c 1.15, CHCl₃).

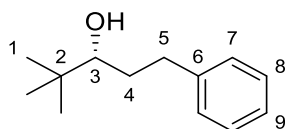
Spectral data in agreement with literature.³⁵

S9. (*R*)-4,4-Dimethyl-1-phenylpentan-3-ol: (from neopentyl TIB ester **75**)



Prepared following general procedure **1** using neopentyl 2,4,6-triisopropylbenzoate⁵³ (1.0 equiv., 0.32 g, 1.00 mmol), with either (+) sparteine (1.2 equiv., 0.28 mL, 1.20 mmol), (+) sparteine surrogate (1.2 equiv., 0.23 mL, 1.20 mmol) or TMEDA (1.2 equiv., 0.18 mL, 1.20 mmol), in *solvent A* (3.33 mL) at *temperature (T)*, and phenylethyl boronic acid pinacol ester (1.0 M in *solvent B*, 1.2 equiv., 0.28 g, 1.20 mmol). After heating, oxidation, and work up, purification by column chromatography (petrol:Et₂O:NEt₃ 19:1:0.1) gave the title compound as a colourless oil.

Entry	Diamine	T (°C)	Solvent A	Solvent B	t _{1/2} Li	t _{1/2} B	e.r.	Yield
2	(+)-sp	-78	Et ₂ O	Et ₂ O	94	296	98:2	27%
3	(+)-sp	-78	Et ₂ O	THF	94	15	98:2	54%



TLC: $R_f = 0.43$ (10% EtOAc in petrol)

¹H NMR (400 MHz, CDCl₃): $\delta = 7.33 - 7.27$ (m, 2H, **8**), $7.24 - 7.17$ (m, 3H, **7 & 9**), 3.23 (brd, $J = 10.7$ Hz, 1H, **3**), 2.93 (ddd, $J = 13.7, 9.6, 6.9$ Hz, 1H, **5**), 2.63 (ddd, $J = 13.7, 9.6, 6.9$ Hz, 1H, **5**), 1.65 - 1.53 (m, 1H, **4**), 0.89 (s, 9H, **1**).

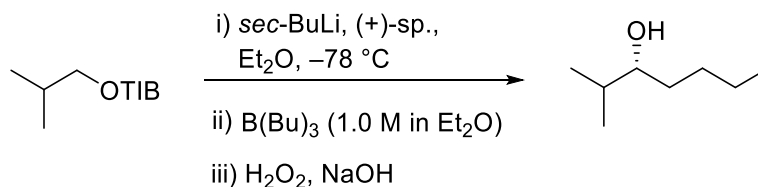
¹³C NMR (101 MHz, CDCl₃): $\delta = 142.6$ (C6), 128.6 (C8), 128.5 (C7), 125.9 (C9), 79.5 (C3), 35.1 (C2), 33.6 (C5), 33.5 (C4), 25.8 (C1).

HPLC: AD-H column, 95:5 IPA:Hex, 0.5 mL min⁻¹. $T_R = 12.68$ min (minor), 15.87 min (major).

$[\alpha]_D^{24.0} +91$ (c 1.0, CHCl₃).

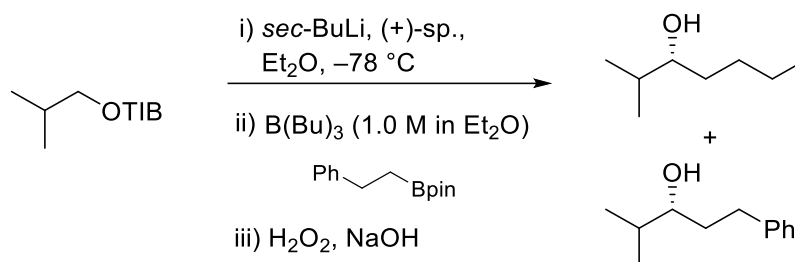
Spectral data and retention times in agreement with literature.¹⁴⁹

85. (*R*)-2-methylheptan-3-ol: (from isobutyl 2,4,6-triisopropylbenzoate **74**)

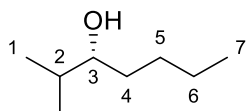


Prepared following general procedure **1**, using isobutyl 2,4,6-triisopropylbenzoate⁴² **60** (1 equiv., 0.30 g, 1 mmol), *sec*-BuLi (1.2 equiv., 0.92 mL, 1.2 mmol), (+)-sparteine (1.2 equiv., 0.28 mL, 1.2 mmol) in Et₂O (3 mL) with *n*-butyl boronic acid pinacol ester (1.2 equiv., 0.25 mL, 1.2 mmol) or tributylborane solution (1.0M in Et₂O, 1.2 equiv., 1.2 mL, 1.2 mmol). The crude oil was purified on by flash column chromatography (15 - 20% Et₂O in pentane) to afford the title compound as a volatile colourless oil (0.11 g, 81%).

Competition experiment:



Prepared following general procedure **1**, using isobutyl 2,4,6-triisopropylbenzoate⁴² (1 equiv., 0.20 g, 0.66 mmol), *sec*-BuLi (1.2 equiv., 0.61 mL, 0.79 mmol), (+)-spartiene (1.2 equiv., 0.18 mL, 0.79 mmol) in TBME (2 mL) followed by addition of a solution of phenethyl boronic acid pinacol ester (1.2 equiv., 0.79 mmol, 0.18 g) in tributylborane solution (1.0M in Et₂O, 1.2 equiv., 0.79 mL, 0.79 mmol). The crude oil was purified on a biotage system using a 10 g Ultra Column 5 to 40% Et₂O in pentane [1-10-2] CVs, λ_{all} , $\lambda_{\text{max}} = 210$ nm, to give (R)-2-methylheptan-3-ol as a colourless oil (0.02 g, 22%) and (R)-4-Methyl-1-phenylpentan-3-ol as a white waxy solid (0.05 g, 40%).

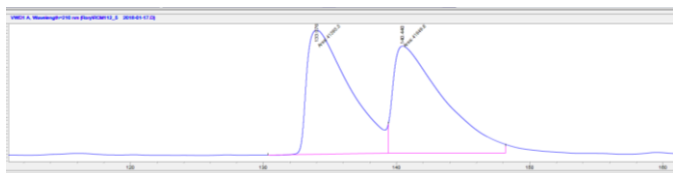


TLC: $R_f = 0.34$ (15% Et₂O in pentane, visualised as a blue spot in anisaldehyde).

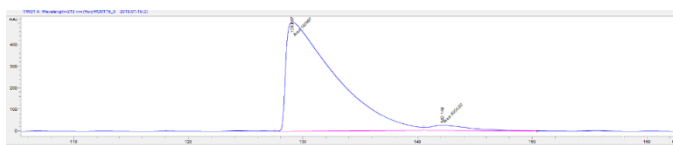
¹H NMR (400 MHz, CDCl₃): $\delta = 3.29$ (td, $J = 5.9, 5.0, 2.6$ Hz, 1H, **3**), 1.59 (septd, $J = 6.8, 5.1$ Hz, 1H, **2**), 1.47 – 1.13 (m, 7H, **4 5 6 & O-H**), 0.88 – 0.78 (m, 9H, **1 & 7**).

¹³C NMR (101 MHz, CDCl₃): $\delta = 76.9, 34.0, 33.6, 28.4, 23.0, 19.0, 17.2, 14.3$.

HPLC: 2 x IA columns, 100:0 hexane:IPA, 0.2 mL min⁻¹, $T = 0$ °C. $T_R = 130$ (major), 142 (minor).



#	Time	Type	Area	Height	Width	Area%	Symmetry
1	133.976	MM	41393.3	184.6	3.7362	49.666	0.285
2	140.44	MM	41949.8	159.6	4.381	50.334	0.224



#	Time	Type	Area	Height	Width	Area%	Symmetry
1	129.067	MM	150997	503.6	4.9969	95.964	0.146
2	142.146	MM	6350.9	25.4	4.1734	4.036	0.437

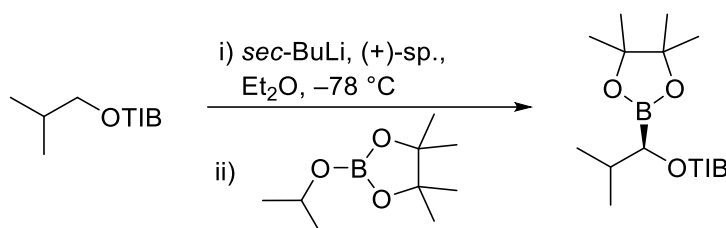
HPLC analysis performed on the corresponding phenyl ester. Either trapping with *n*-butyl boronic acid pinacol ester or tributylborane solution proceeded with 95:5 e.r. with the same sense of enantioenrichment.

Spectral data in agreement with literature.¹⁵⁰

$\nu_{C=O}$ Lithiated species	$\nu_{C=O}$ Boronate	$t_{1/2}$ 1,2-migration at $-78\text{ }^{\circ}\text{C}$
1633 cm^{-1}	1633 cm^{-1}	90 mins ^a

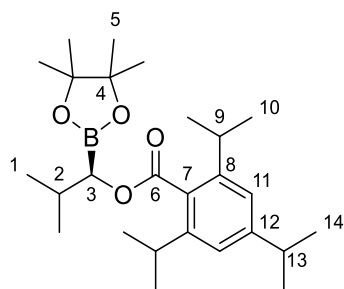
^a Approximate value due to overlapping peaks at 1592 cm^{-1} .

87. (*R*)-2-methyl-1-(4,4,5,5-tetramethyl-1,3,2-dioxaborolan-2-yl)propyl 2,4,6-triisopropylbenzoate



Prepared following general procedure **1** without oxidation:

Isobutyl 2,4,6-triisopropylbenzoate⁴² (1 equiv., 0.1 g, 0.33 mmol) and (+)-sparteine (1.2 equiv, 0.09 mL, 0.09 g, 0.4 mmol) were combined in a flask and Et₂O (1 mL) was added. This was cooled to $-78\text{ }^{\circ}\text{C}$ and then *sec*-BuLi (1.2 equiv, 0.30 mL, 0.40 mmol) was added dropwise. After stirring for 5 hours at $-78\text{ }^{\circ}\text{C}$ isopropoxy boronic acid pinacol ester (1.2 equiv, 0.08 mL, 0.07 g, 0.4 mmol) was added as a solution in Et₂O (1 M, 0.4 mL) and the mixture was stirring for a further 5 hours. The reaction was then warmed to room temperature and diluted with Et₂O and washed with 2 M HCl (2 x 5 mL). After removal of solvents, the crude oil was purified by flash column chromatography (5 – 10% Et₂O in pentane) to afford the title compound as a colourless oil (0.10 g, 69%).



TLC: $R_f = 0.28$ (5% Et₂O in pentane).

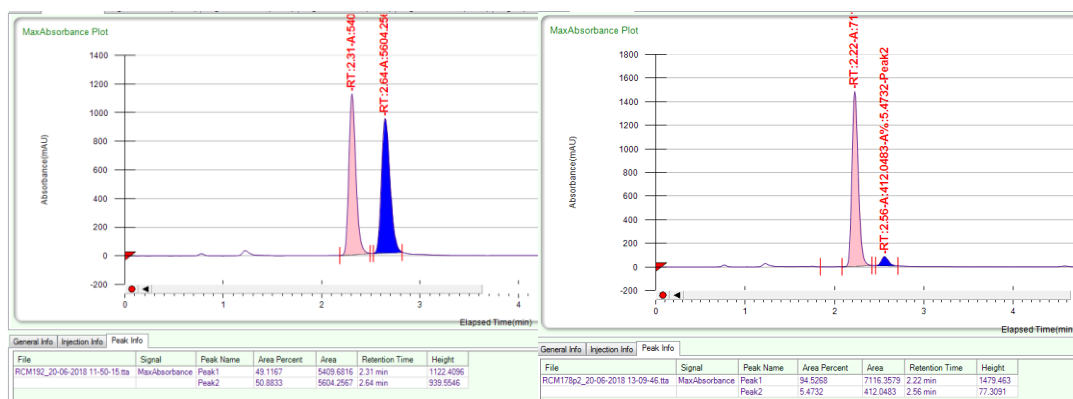
¹H NMR (500 MHz, CDCl₃): $\delta = 6.99$ (s, 2H, **11**), 3.99 (d, $J = 6.3$ Hz, 1H, **3**), 3.05 (sept, $J = 6.8$ Hz, 2H, **9**), 2.88 (sept, $J = 6.9$ Hz, 1H, **13**), 2.17 – 2.02 (m, 1H, **2**), 1.31 (s, 6H, **5**), 1.28 (s, 6H, **5'**), 1.26 – 1.21 (m, 18H, **10 & 14**), 1.03 (d, $J = 5.3$ Hz, 2H, **1**), 1.01 (d, $J = 5.3$ Hz, 2H, **1'**).

¹³C NMR (126 MHz, CDCl₃): $\delta = 172.25$ (C6), 149.82 (C7), 145.21 (C12), 130.40 (C6), 120.74 (C11), 83.79 (C4), 34.41 (C13), 30.85 (C9), 29.20 (C2), 24.99 (C14), 24.77 (C14/C10), 24.33 (C5), 24.26 (C5'), 23.97 (C10), 19.69 (C1), 19.62 (C1').

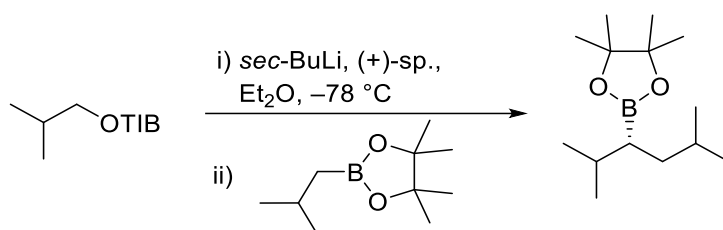
HRMS-ESI (m/z): $[M + Na]^+$ calcd for $C_{26}H_{43}^{11}BO_4$, 431.3327; found, 431.3329.

FT-IR (film): ν_{max} (cm^{-1}) = 2960 (m), 2870 (w), 1709 (s), 1607 (w), 1575 (w), 1462 (w).

SFC (method: 10% isocratic flow, 4 mL min^{-1} , 125 bar; solvent: 10% isopropanol in hexane; column: Whelk-O1, 40 °C): T_R = 2.3 (major), 2.5 (minor).
e.r. = 95:5

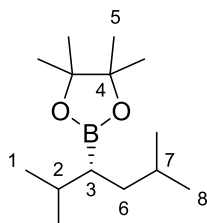


86. (R)-2-(2,5-dimethylhexan-3-yl)-4,4,5,5-tetramethyl-1,3,2-dioxaborolane:



Prepared following general procedure **1** without oxidation:

Isobutyl 2,4,6-triisopropylbenzoate⁴² ester (1 equiv., 0.08 g, 0.25 mmol) and (+)-sparteine (1.2 equiv, 0.07 mL, 0.07 g, 0.3 mmol) were combined in a flask and Et_2O (0.78 mL) was added. This was cooled to -78 °C and then *sec*-BuLi (1.2 equiv, 0.23 mL, 0.3 mmol) was added dropwise. After stirring for 5 hours at -78 °C isobutyl boronic acid pinacol ester (1.2 equiv, 0.06 g, 0.3 mmol) was added as a solution in Et_2O (1 M, 0.3 mL) and the mixture was stirring for a further 6 hours. The reaction was then warmed to room temperature and stirred overnight. The reaction was then diluted with Et_2O and washed with 2 M HCl (2 x 5 mL) and 2 M NaOH (1 x 5 mL). After removal of solvents, the crude oil was purified by flash column chromatography (10% CH_2Cl_2 in pentane) to afford the title compounds as a colourless oil (0.02 g, 25%).



TLC: R_f = 0.2 (10% CH_2Cl_2 in pentane).

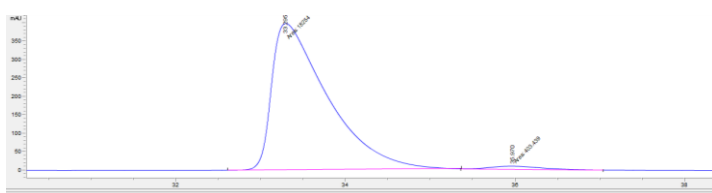
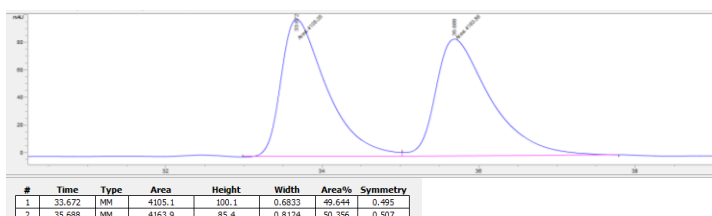
1H NMR (500 MHz, $CDCl_3$): δ = 1.73 – 1.60 (m, 1H, **2/3/7**), 1.54 – 1.44 (m, 1H, **2/3/7**), 1.38 (ddd, J = 13.3, 10.9, 5.3 Hz, 1H, **6**), 1.24 (s, 12H, **5**), 1.14 (ddd, J = 13.3, 8.8, 5.1 Hz, 1H, **6'**), 0.92 (t, J = 6.7 Hz, 6H, **1/8**), 0.86 (dd, J = 9.9, 6.6 Hz, 6H, **1/8**).

^{13}C NMR (126 MHz, CDCl_3): δ = 82.76 (C4), 38.61, 30.02, 27.86, 24.95, 24.90, 23.71, 22.49, 22.15, 21.61.

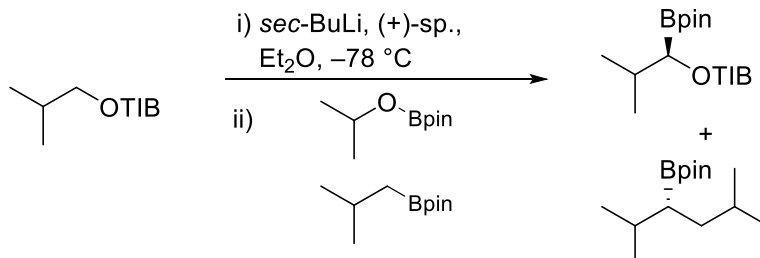
FT-IR (film): ν_{max} (cm^{-1}) = 2954 (m), 2869 (m), 1467 (w), 1379 (m), 1371 (m), 1142 (s).

HRMS-ESI (m/z): $[\text{M} + \text{Na}]^+$ calcd for $\text{C}_{14}\text{H}_{29}^{11}\text{BNaO}_2$, 263.2158, found, 263.2164.

HPLC: 2 x IA columns, 100:0 hexane:IPA, 0.5 mL min^{-1} , $T = 22 \text{ }^\circ\text{C}$. $T_R = 33.5$ (major), 35.5 (minor). HPLC analysis performed after oxidation and esterification to the corresponding phenyl ester.

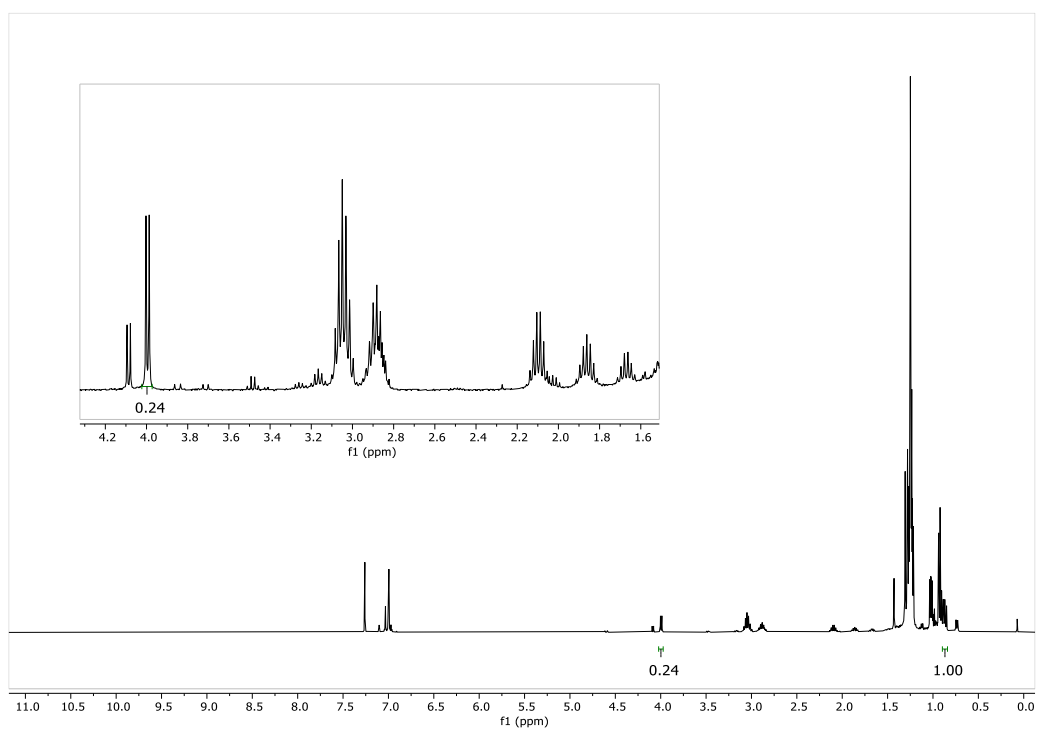


Competition experiment:



Isobutyl 2,4,6-triisopropylbenzoate⁴² (1 equiv., 0.08 g, 0.25 mmol) and (+)-sparteine (1.2 equiv, 0.07 mL, 0.07 g, 0.3 mmol) were combined in a flask and Et_2O (0.8 mL) was added. This was cooled to $-78 \text{ }^\circ\text{C}$ and then sec-BuLi (1.2 equiv, 0.23 mL, 0.3 mmol) was added dropwise. After stirring for 5 hours at $-78 \text{ }^\circ\text{C}$ a mixture of isopropoxy boronic acid pinacol ester (1.2 equiv, 0.06 mL, 0.06 g, 0.3 mmol) and isobutyl boronic acid pinacol ester (1.2 equiv, 0.3 mmol, 0.05 g) were added as a solution in Et_2O (2 M w.r.t organoboron partner, 0.3 mL) and the mixture was stirred for a further 5 hours. The reaction was then warmed to room temperature and diluted with Et_2O and washed with 2 M HCl (2 x 5 mL). After removal of solvents, the crude oil was analysed by ^1H NMR, integrating the signals at 3.99 ppm for the borate ester derived product and 0.86 ppm for the boronic ester derived product, ratio 1:1.7 in favour of the borate ester product.

Crude ^1H NMR:

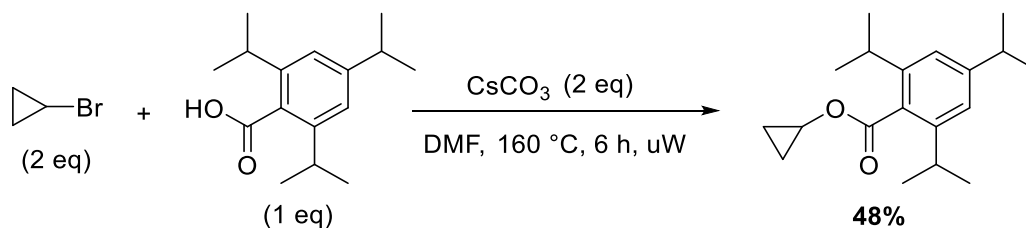


Signal at $\delta = 0.86$ is equivalent to 6 protons. $6 \times 0.24 = 1.44$

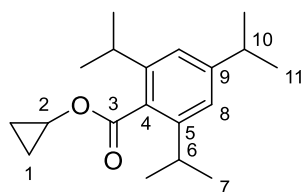
5.2.3 Experimental: O-cycloalkyl benzoate/carbamate studies

5.2.3.1 Starting Materials

93. Cyclopropyl 2,4,6-triisopropylbenzoate



In a 5.0 mL microwave vial were combined 2,4,6-triisopropylbenzoic acid (0.497 g, 2 mmol, 1.0 eq) and DMF (1.0 mL, not anhydrous). CsCO_3 (1.30 g, 4 mmol, 2.0 eq) was added and the mixture stirred for 10 minutes. Bromocyclopropane (0.32 mL, 0.434 g, 4 mmol, 2.0 eq) was added in a single portion and the reaction heated to 160 °C for 6 h with rapid stirring. The brown mixture was then filtered through a plug of SiO_2 (washing with Et_2O) and the DMF removed under reduced pressure (toluene (3 mL x 3) was added and removed to aid DMF removal) to give a crude oil. This was then purified twice on a Biotage system using a 50 g Ultra column, 1 to 8% Et_2O in pentane [1-11-2] CVs, to give the desired product (0.279 g, 48%) as a clear oil.



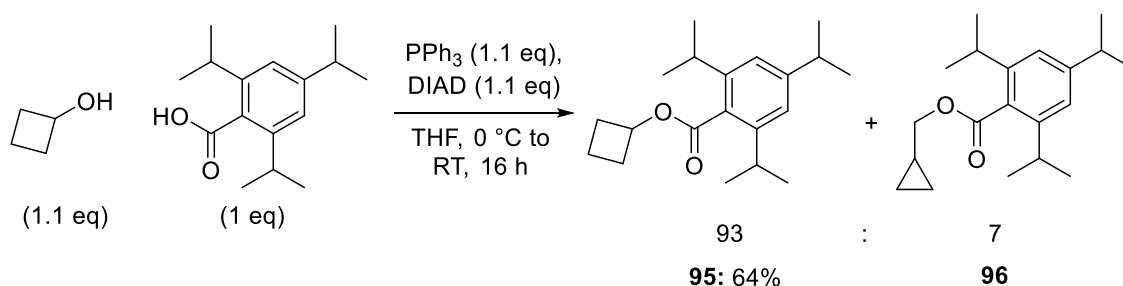
$R_f = 0.32$ (4% Et_2O in pentane, UV/anisaldehyde).

$^1\text{H NMR}$ (400 MHz, CDCl_3): $\delta = 6.99$ (s, 2H, **8**), 4.43 – 4.37 (m, 1H, **2**), 2.94 – 2.80 (m, 3H, **6 & 10**), 1.24 & 1.23 (2 x d, $J = 6.9$ Hz, 18H, **7 & 11**), 0.83 – 0.77 (m, 4H, **1**).

$^{13}\text{C NMR}$ (101 MHz, CDCl_3): $\delta = 171.8$ (**3**), 150.4 (**5/9**), 144.9 (**5/9**), 130.3 (**4**), 121.0 (**8**), 49.4 (**2**), 34.6 (**6/10**), 31.5 (**6/10**), 24.2 (**7/11**), 24.1 (**7/11**), 5.2 (**1**).

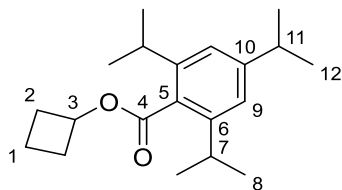
All data agree with a previous report.¹⁵¹

95. Cyclobutyl 2,4,6-triisopropylbenzoate



Benzoate **95** was made following general procedure **3** using 2,4,6-triisopropylbenzoic acid (TIBOH, 6.26 g, 25.2 mmol, 1.00 eq), PPh_3 (7.26 g, 27.7 mmol, 1.10 eq), THF (25.2 mL, 1 M), cyclobutanol (2.17 mL, 27.7 mmol, 1.10 equiv.) and DIAD (5.44 mL, 27.7 mmol, 1.10 eq). The crude material was purified by column chromatography (3% to 6%

Et₂O/petrol) to afford the mixture of products **95** & **96** (5.26 g, 93:7 ratio of desired benzoate **95** to inseparable cyclopropylmethyl benzoate **96**, 64% desired product).



$R_f = 0.57$ (10% Et₂O/petrol, *p*-anisaldehyde);

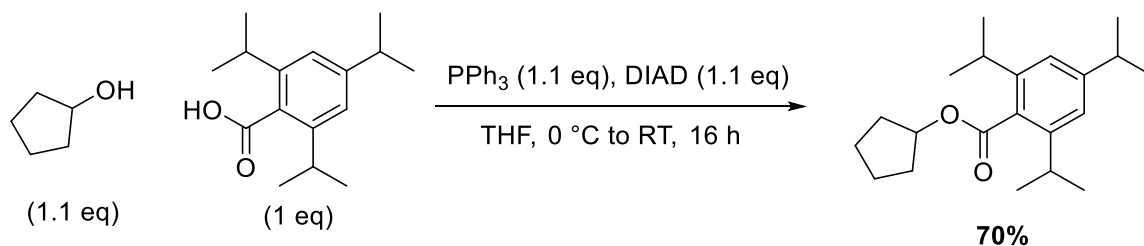
¹H NMR (400 MHz, CDCl₃): $\delta = 7.00$ (s, 2H, **9**), 5.25 (quin, $J = 7.5$ Hz, 1H, **3**), 2.94 – 2.82 (m, 3H, **7/11**), 2.51 – 2.40 (m, 2H, **2**), 2.23 – 2.11 (m, 2H, **2**), 1.91 – 1.80 (m, 1H, **1**), 1.77 – 1.64 (m, 1H, **1**), 1.25 (d, $J = 6.8$ Hz, 12H, **8**), 1.24 (d, $J = 6.8$ Hz, 6H, **12**).

¹³C NMR (101 MHz, CDCl₃): $\delta = 170.3$ (**4**), 150.2 (**6/10**), 144.9 (**6/10**), 130.7 (**5**), 121.0 (**9**), 69.4 (**3**), 34.6 (**7/11**), 31.5 (**7/11**), 30.5 (**2**), 24.3 (**9/13**), 24.1 (**9/13**), 14.1 (**1**).

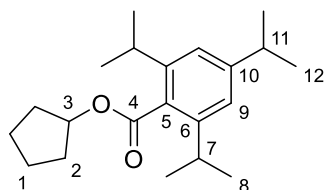
HRMS-ESI⁺ (m/z): [M + Na]⁺ calculated for C₂₀H₃₀O₂Na, 325.2143; found, 325.2140;

IR ($\nu_{\max}/\text{cm}^{-1}$, neat): 2959, 2869, 1721 (C=O), 1606, 1463, 1248, 1136, 1080, 937, 879, 755, 612.

101. Cyclopentyl 2,4,6-triisopropylbenzoate



Following general procedure **3** using TIBOH (1.24 g, 5 mmol, 1.0 eq), cyclopentanol (0.5 mL, 0.474 g, 5.5 mmol, 1.1 eq), PPh₃ (1.44 g, 5.5 mmol, 1.1 eq), DIAD (1.1 mL, 1.11 g, 5.5 mmol, 1.1 eq) and THF (25 mL) to give the desired product (1.10 g, 70%) as a white solid.



$R_f = 0.31$ (4% Et₂O in pentane, KMnO₄)

¹H NMR (400 MHz, CDCl₃): $\delta = 7.01$ (s, 2H, **9**), 5.47 (tt, $J = 5.9, 2.9$ Hz, 1H, **3**), 2.90 (sept, $J = 6.8$ Hz, 3H, **7 & 11**), 2.02 – 1.90 (m, 2H, **2**), 1.90 – 1.81 (m, 2H, **2**), 1.80 – 1.70 (m, 2H, **1**), 1.70 – 1.56 (m, 2H, **1**), 1.26 (d, $J = 6.9$ Hz, 12H, **8**), 1.25 (d, $J = 7.0$ Hz, 6H, **12**).

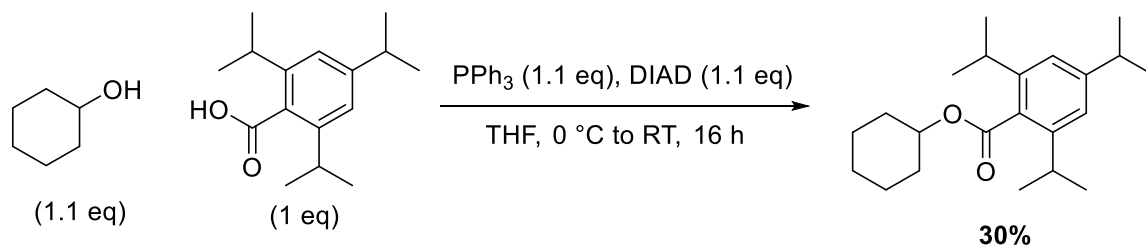
¹³C NMR (101 MHz, CDCl₃): $\delta = 170.7$ (**4**), 150.1 (**6/10**), 144.8 (**6/10**), 131.0 (**5**), 120.9 (**9**), 77.9 (**3**), 34.6 (**7/11**), 32.8 (**2**), 31.4 (**7/11**), 24.3 (**8/12**), 24.10 (**8/12**), 23.8 (**1**).

HRMS-ESI⁺ (*m/z*): [M + H]⁺ calculated for C₂₁H₃₃O₂, 317.2475; found, 317.2466.

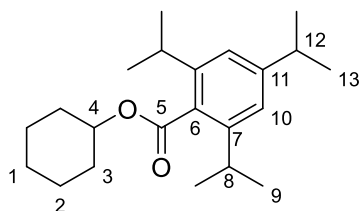
IR (ν_{max} /cm⁻¹, neat): 2959.2, 2869.9, 1708.6, 1606.7, 1461.0, 1253.8, 1078.3.

Melting point: 51 – 52 °C (pentane).

104. Cyclohexyl 2,4,6-triisopropylbenzoate



Following general procedure **3** using TIBOH (1.24 g, 5 mmol, 1.0 eq), cyclohexanol (0.58 mL, 0.474 g, 5.5 mmol, 1.1 eq), PPh₃ (1.44 g, 5.5 mmol, 1.1 eq), DIAD (1.1 mL, 1.11 g, 5.5 mmol, 1.1 eq) and THF (25 mL) gave the desired product (0.494 g, 30%) as a white solid.



R_f = 0.34 (4% Et₂O in pentane, KMnO₄)

¹H NMR (400 MHz, CDCl₃): δ = 7.01 (s, 2H, **10**), 5.13 – 5.02 (m, 1H, **4**), 2.91 (sept, *J* = 6.8 Hz, 2H, **8**), 2.89 (sept, *J* = 6.9 Hz, 1H, **12**), 2.06 – 1.96 (m, 2H, **3**), 1.84 – 1.72 (m, 2H, **2**), 1.64 – 1.55 (m, 1H, **1**), 1.55 – 1.46 (m, 2H, **3**), 1.46 – 1.37 (m, 2H, **2**), 1.32 – 1.29 (m, 1H, **1**), 1.26 (d, *J* = 6.8 Hz, 12H, **9**), 1.25 (d, *J* = 6.9 Hz, 6H, **13**).

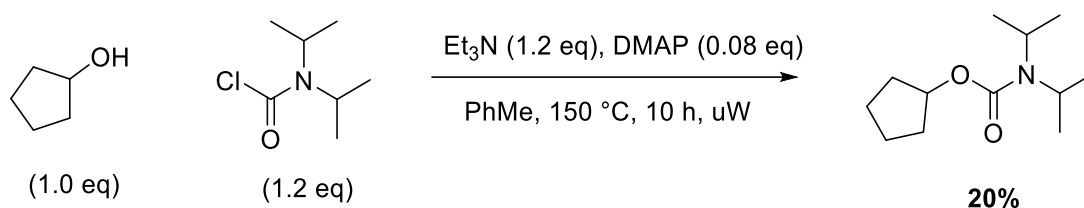
¹³C NMR (101 MHz, CDCl₃): δ = 170.3 (**5**), 149.9 (**7/11**), 144.6 (**7/11**), 131.0 (**6**), 120.8 (**10**), 73.5 (**4**), 34.5 (**12**), 31.8 (**3**), 31.3 (**8**), 25.4 (**1**), 24.1 (**9/13**), 24.0 (**9/13/2**), 23.9 (**9/13/2**).

HRMS-ESI⁺ (*m/z*): [M + H]⁺ calculated for C₂₂H₃₅O₂, 331.2632; found, 331.2632.

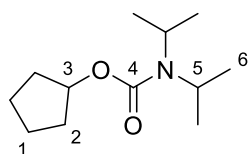
IR (ν_{max} /cm⁻¹, neat): 2957.5, 2932.6, 2863.8, 1714.9, 1608.5, 1250.9, 1077.2.

Melting point: 50 – 51 °C (pentane).

102. Cyclopentyl diisopropylcarbamate



Following general procedure **2** using carbonyl chloride (1.57 g, 9.6 mmol, 1.2 eq), cyclopentanol (0.73 mL, 0.689 g, 8.0 mmol, 1.0 eq), Et₃N (1.34 mL, 0.971 g, 9.6 mmol, 1.2 eq), DMAP (0.078 g, 0.64 mmol, 0.08 eq) and toluene (8 mL), with heating for 10 h, gave the desired product (0.656 g, 20%) as a colourless oil.



R_f = 0.4 (10% Et₂O in pentane, PMA)

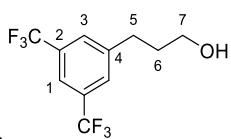
¹H NMR (400 MHz, CDCl₃): δ = 5.14 (tt, J = 5.6, 2.5 Hz, 1H, **3**), 4.59 – 3.17 (br, 2H, **5**), 1.87 – 1.77 (m, 2H, **2**), 1.77 – 1.67 (m, 4H, **2 & 1**), 1.64 – 1.54 (m, 2H, **1**), 1.17 (d, J = 6.9 Hz, 12H, **6**).

¹³C NMR (101 MHz, CDCl₃): δ = 155.9 (**4**), 77.2 (**3**), 45.5 (**5**, br), 33.0 (**2**), 23.9 (**1**), 21.2 (**6**, br).

HRMS-ESI⁺ (m/z): [M + H]⁺ calculated for C₁₂H₂₄NO₂, 214.1802; found, 214.1807.

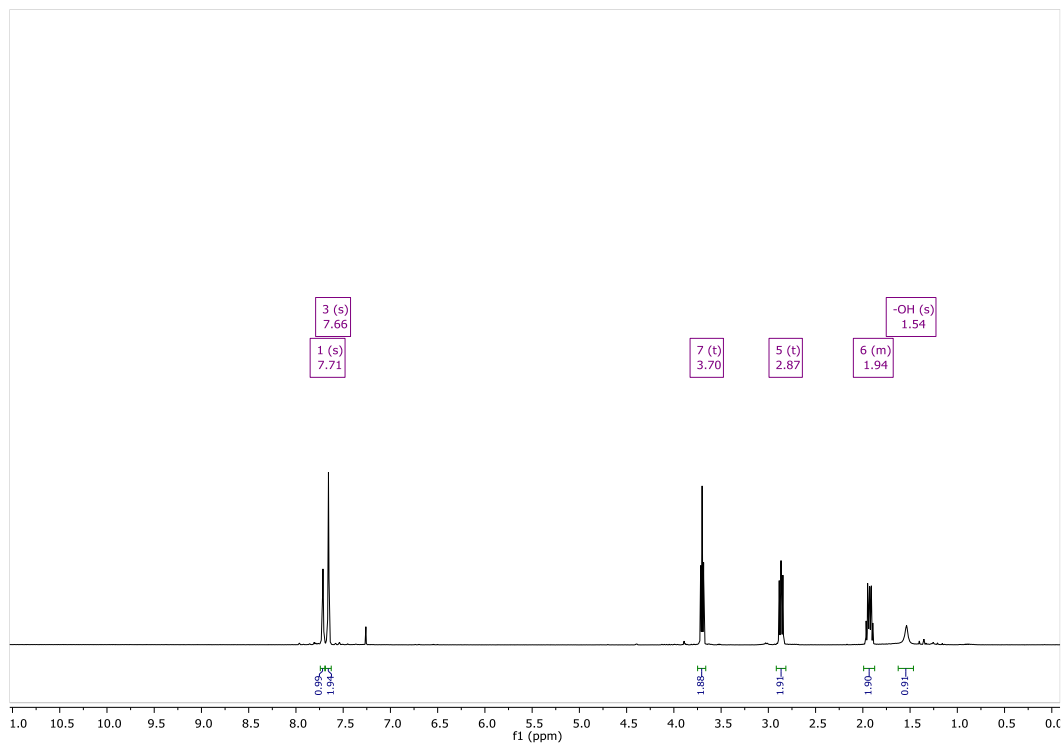
IR (ν_{max} /cm⁻¹, neat): 2966.1, 2873.4, 1683.0, 1287.4, 1049.1, 772.2.

5.2.4 NMR spectra

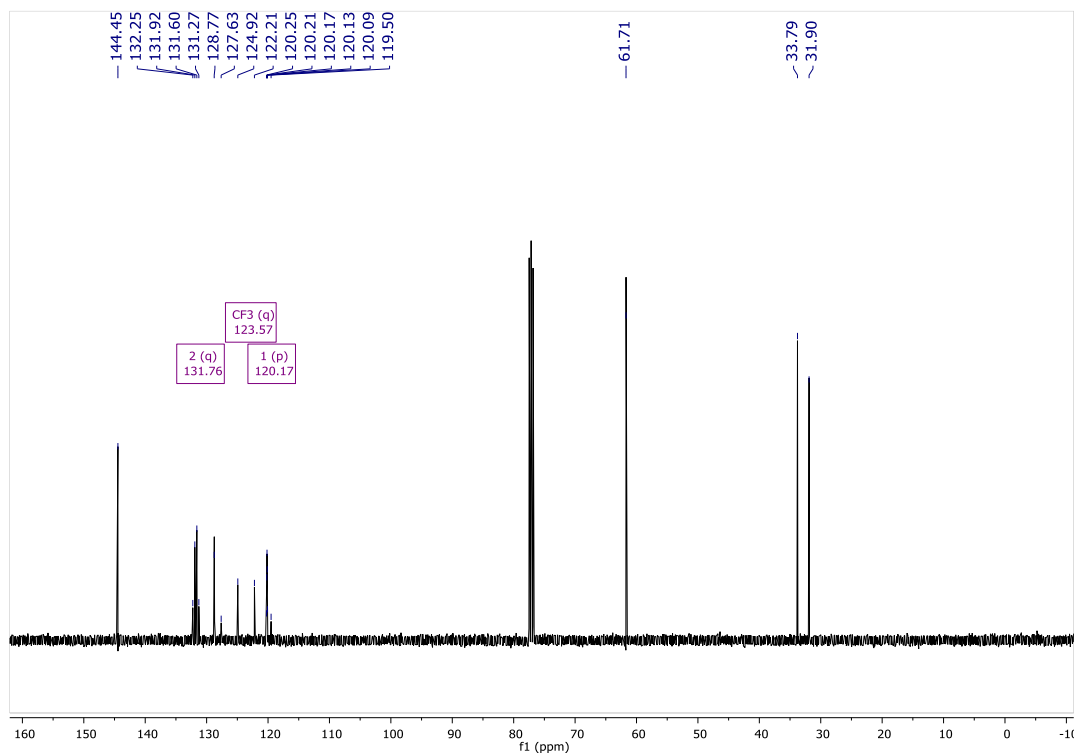


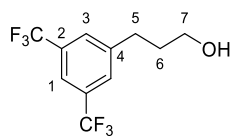
S1.

^1H NMR, 400 MHz, CDCl_3



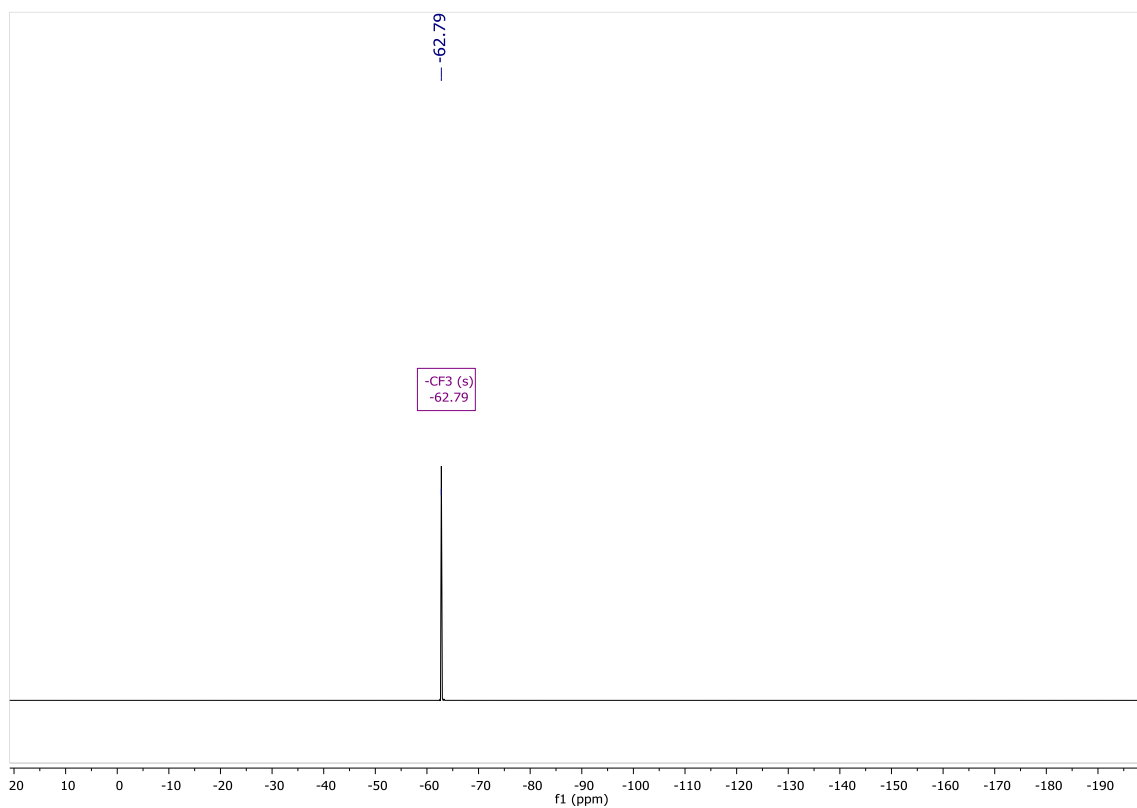
S1. ^{13}C NMR, 101 MHz, CDCl_3



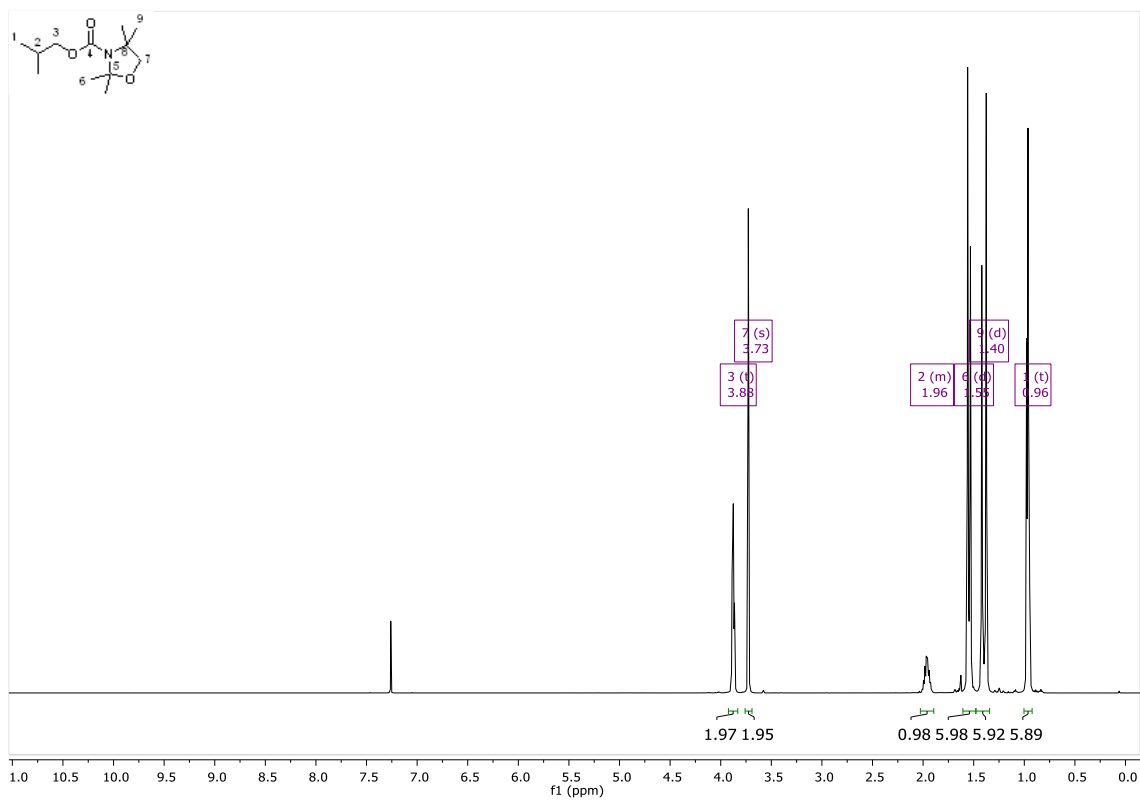


S1.

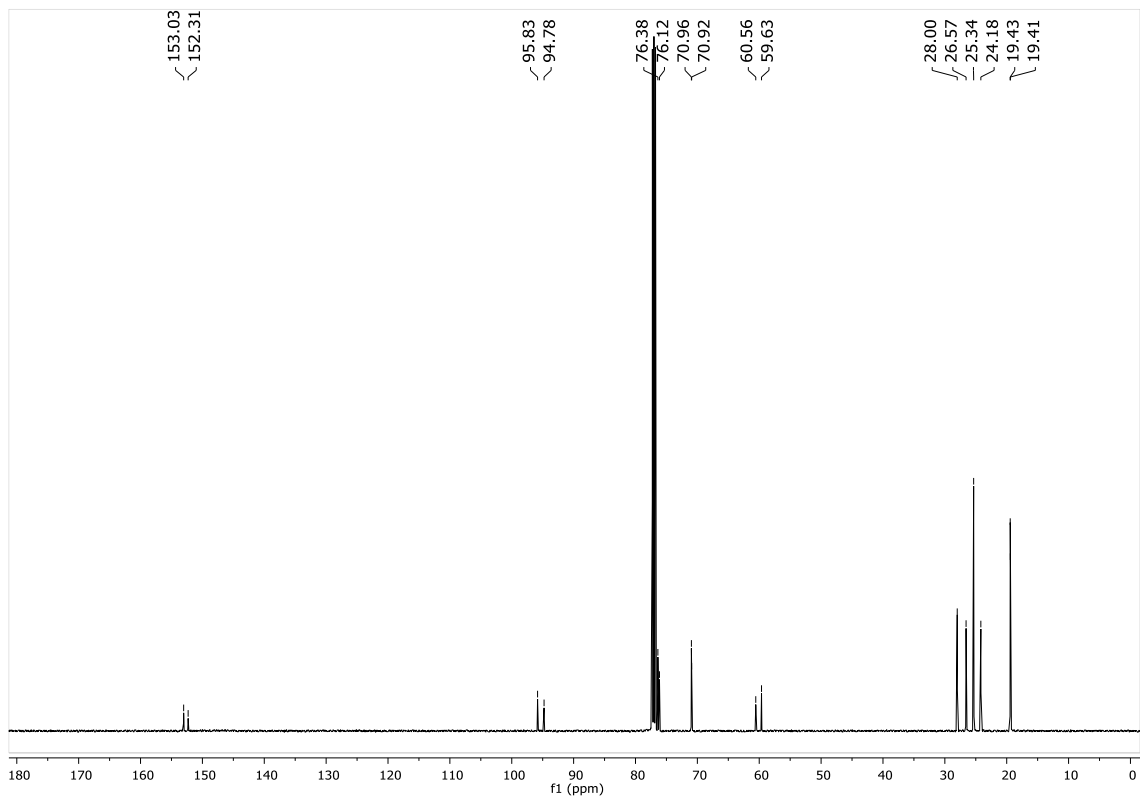
^{19}F , 377 MHz, CDCl_3

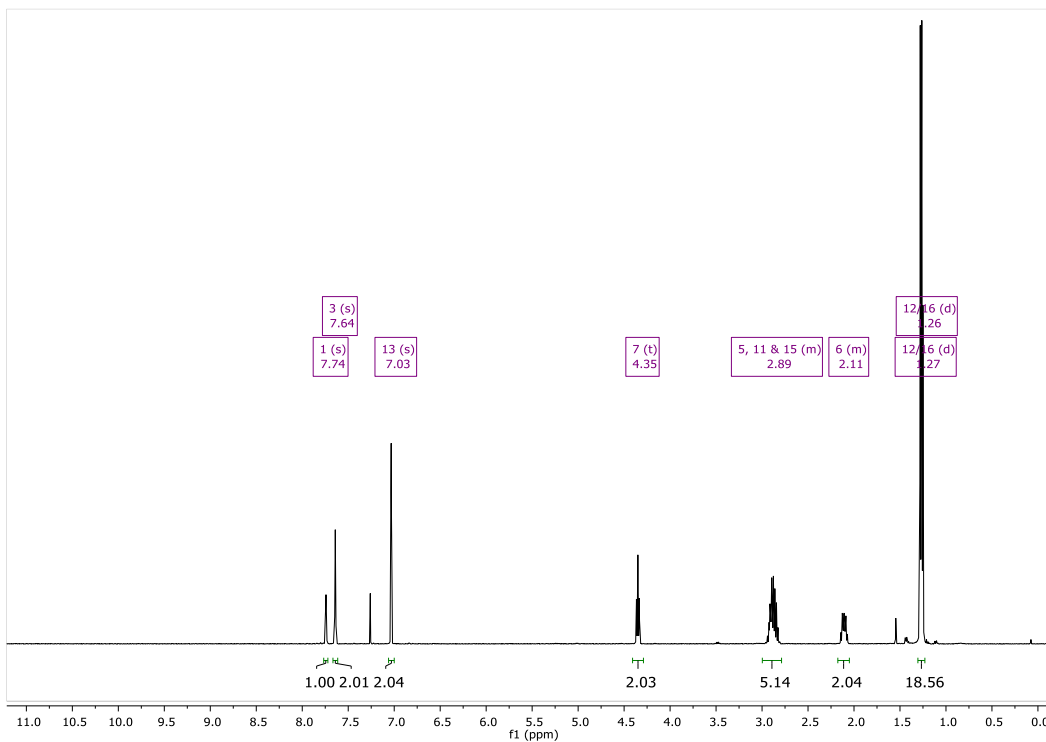
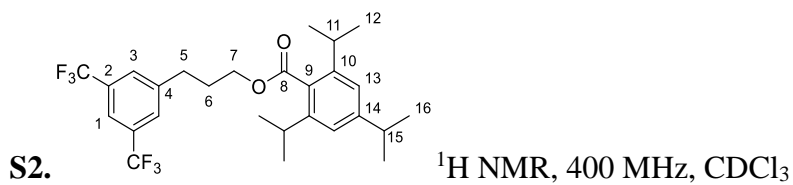


71. ^1H NMR, 500 MHz, CDCl_3

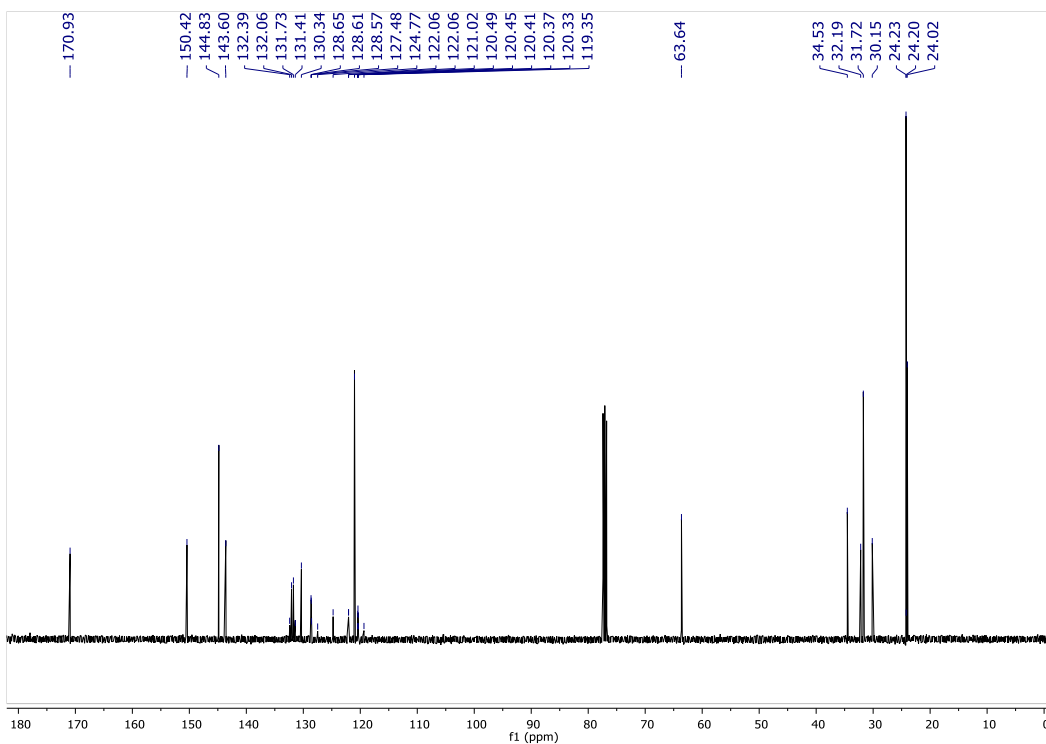


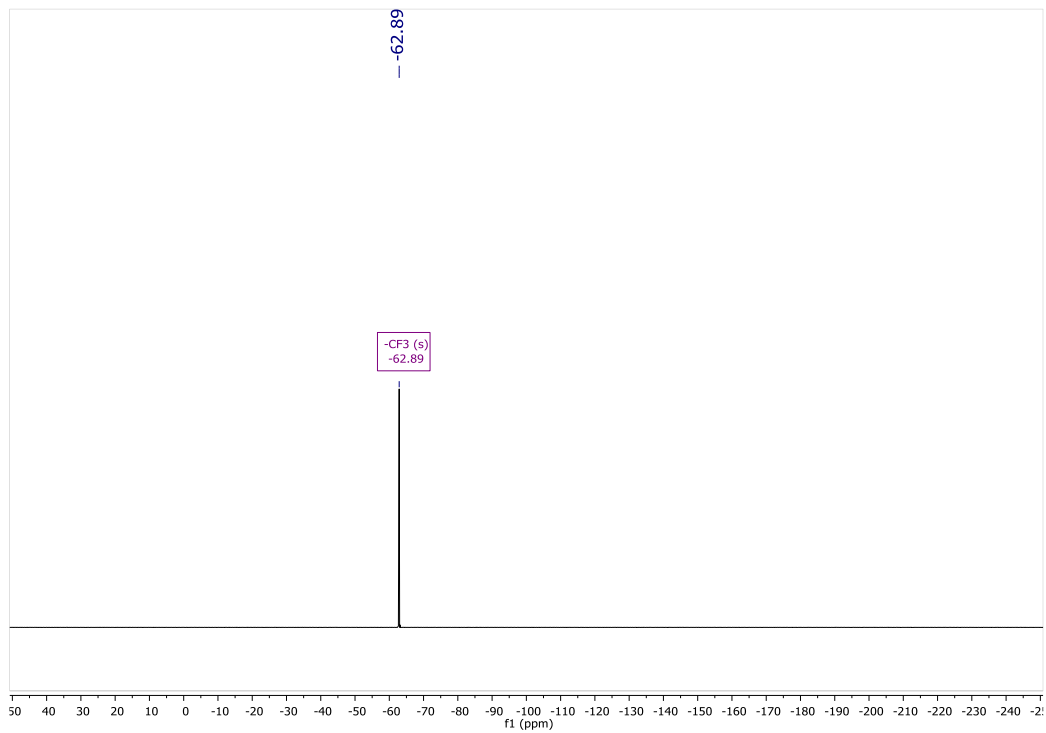
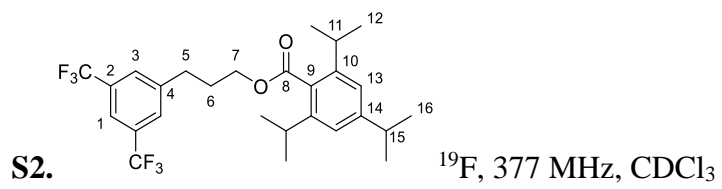
71. ^{13}C NMR, 126 MHz, CDCl_3



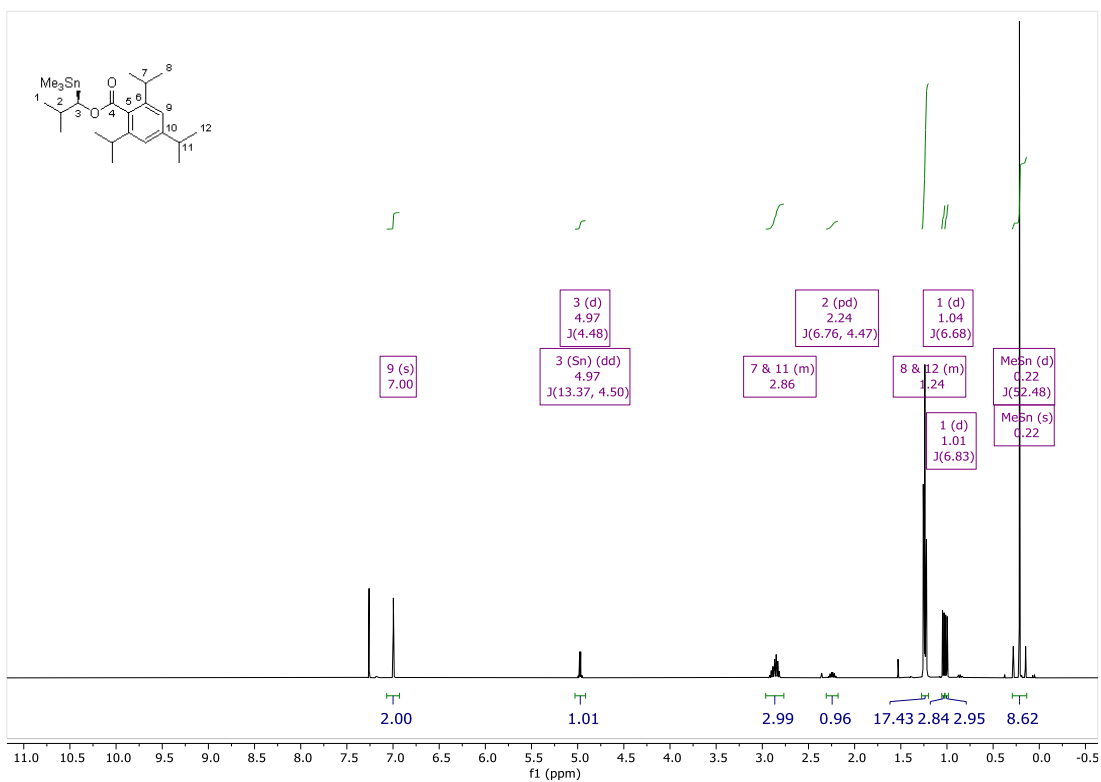


S2. $^{13}\text{C NMR}$, 101 MHz, CDCl_3

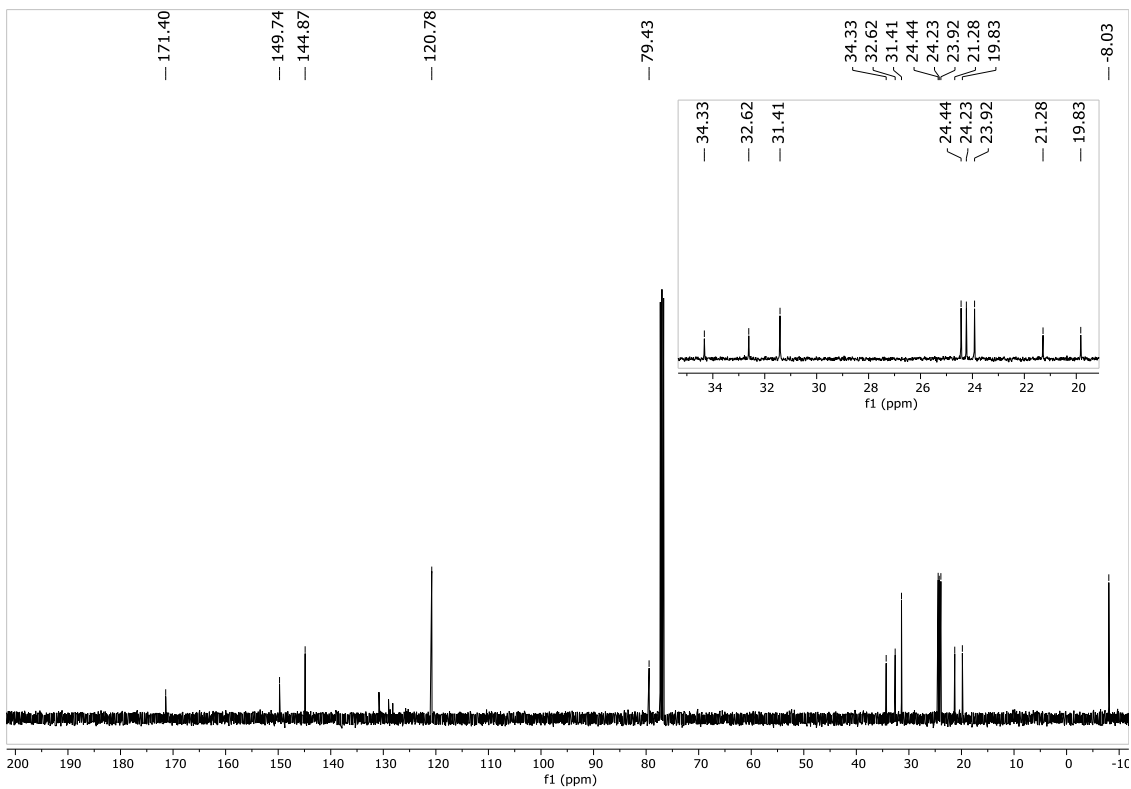




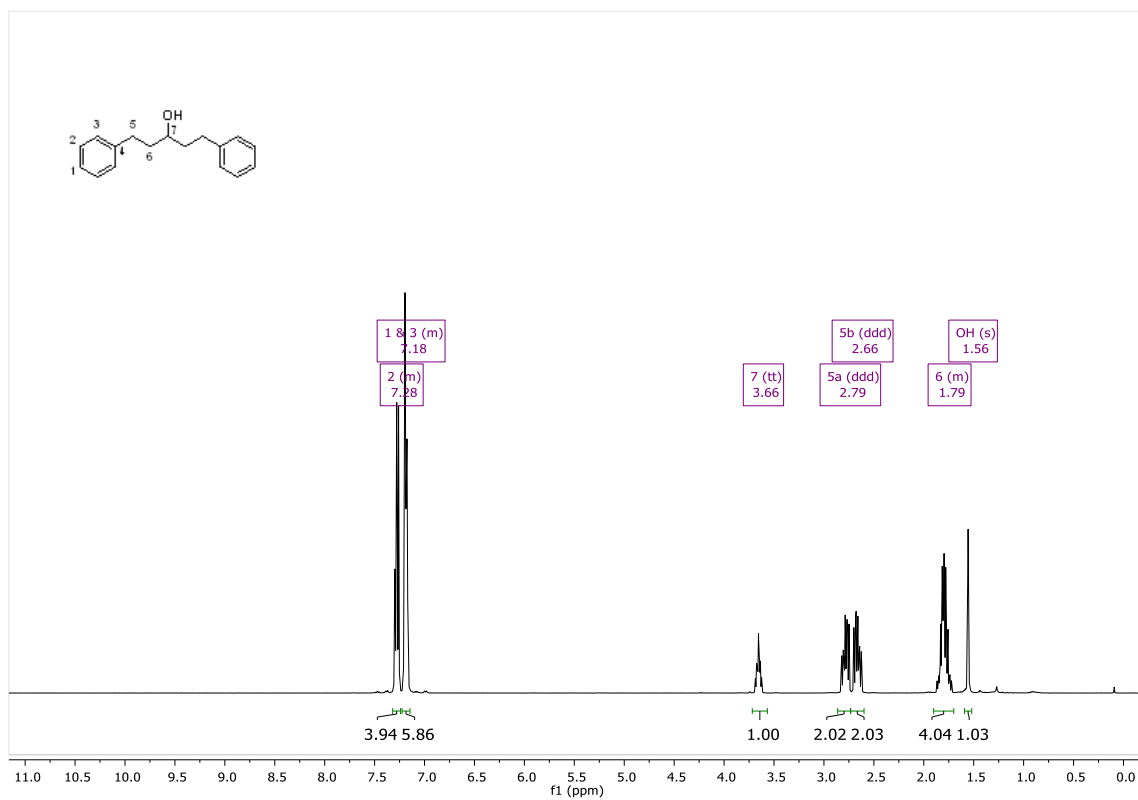
92. ^1H NMR, 400 MHz, CDCl_3



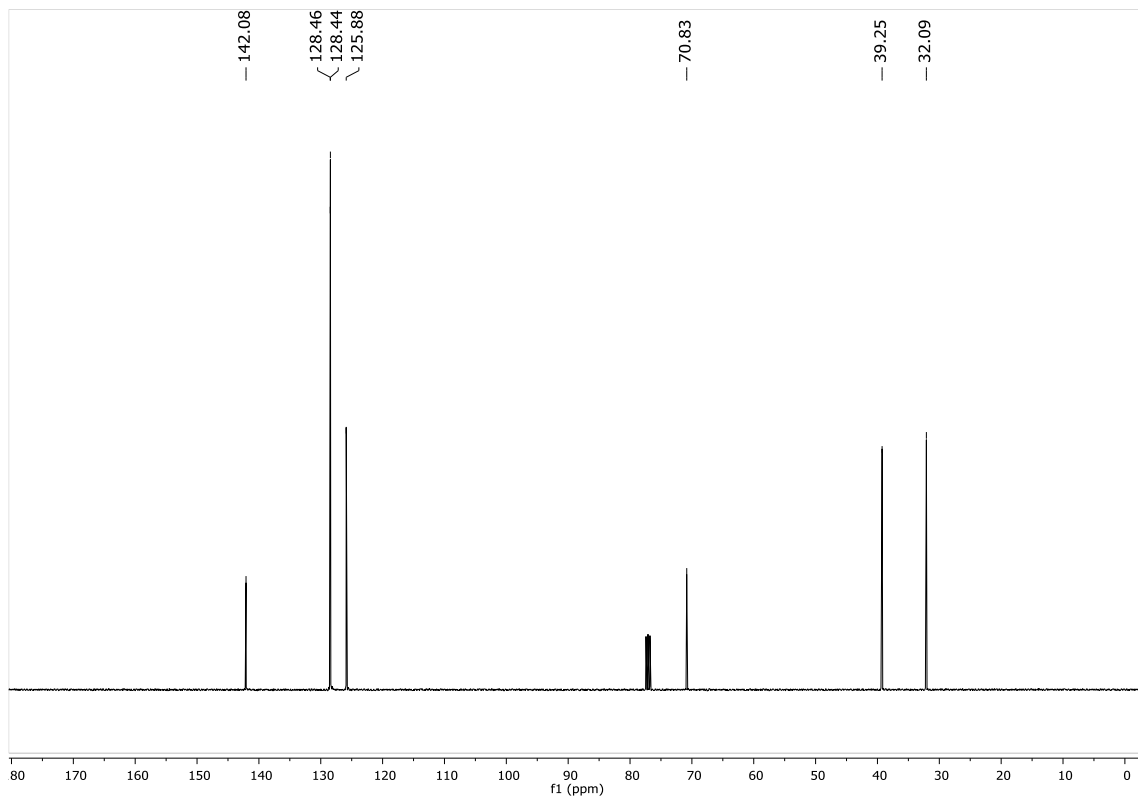
92. ^{13}C NMR, 101 MHz, CDCl_3



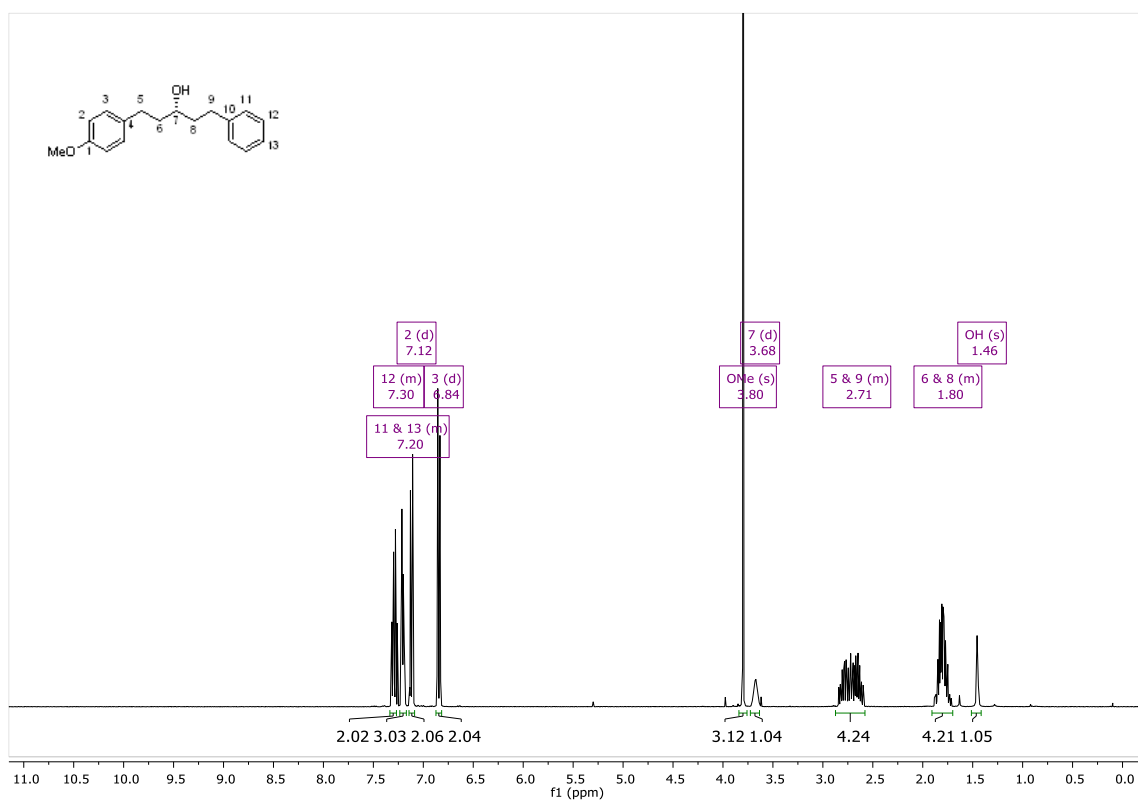
S3. ^1H NMR, 400 MHz, CDCl_3



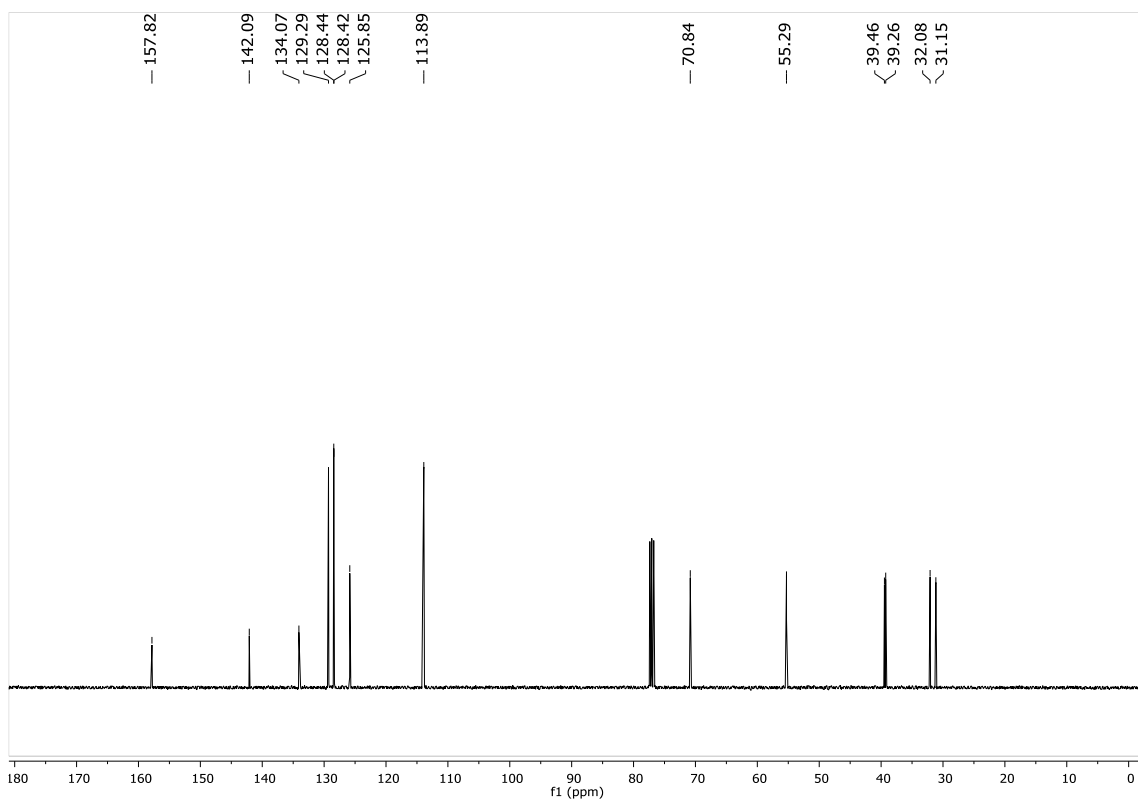
S3. ^{13}C NMR, 101 MHz, CDCl_3

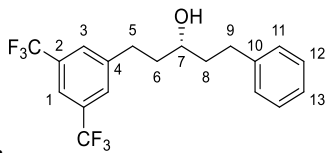


S4. ^1H NMR, 400 MHz, CDCl_3



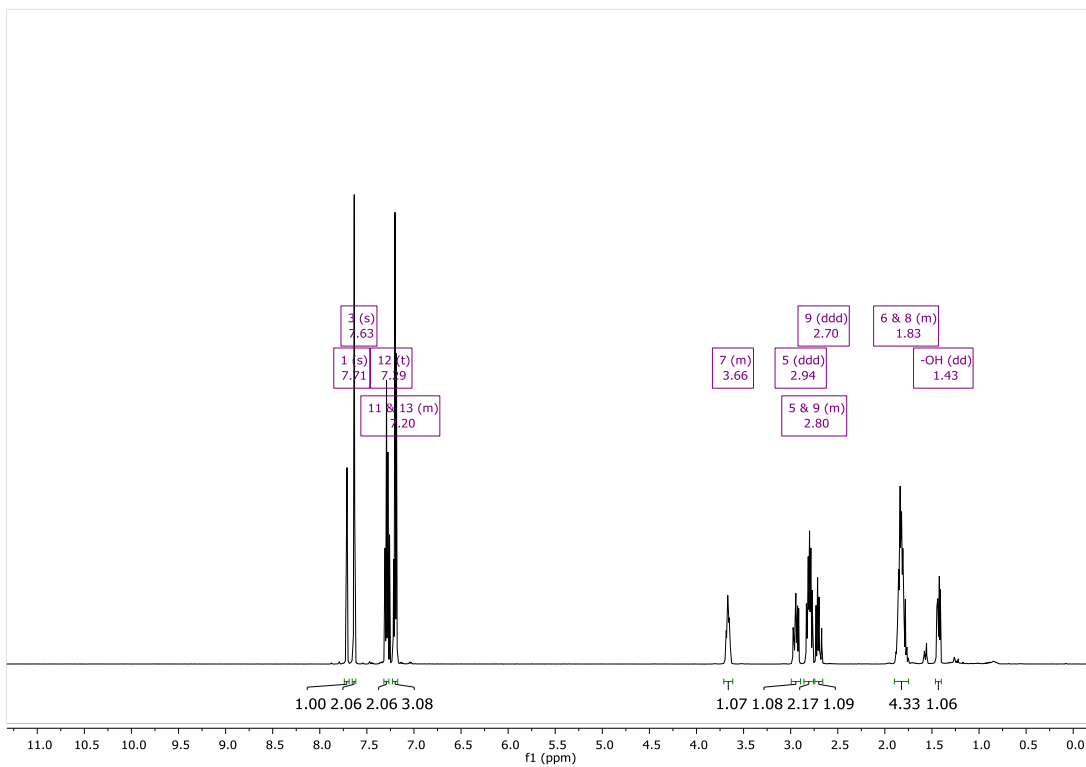
S4. ^{13}C NMR, 101 MHz, CDCl_3



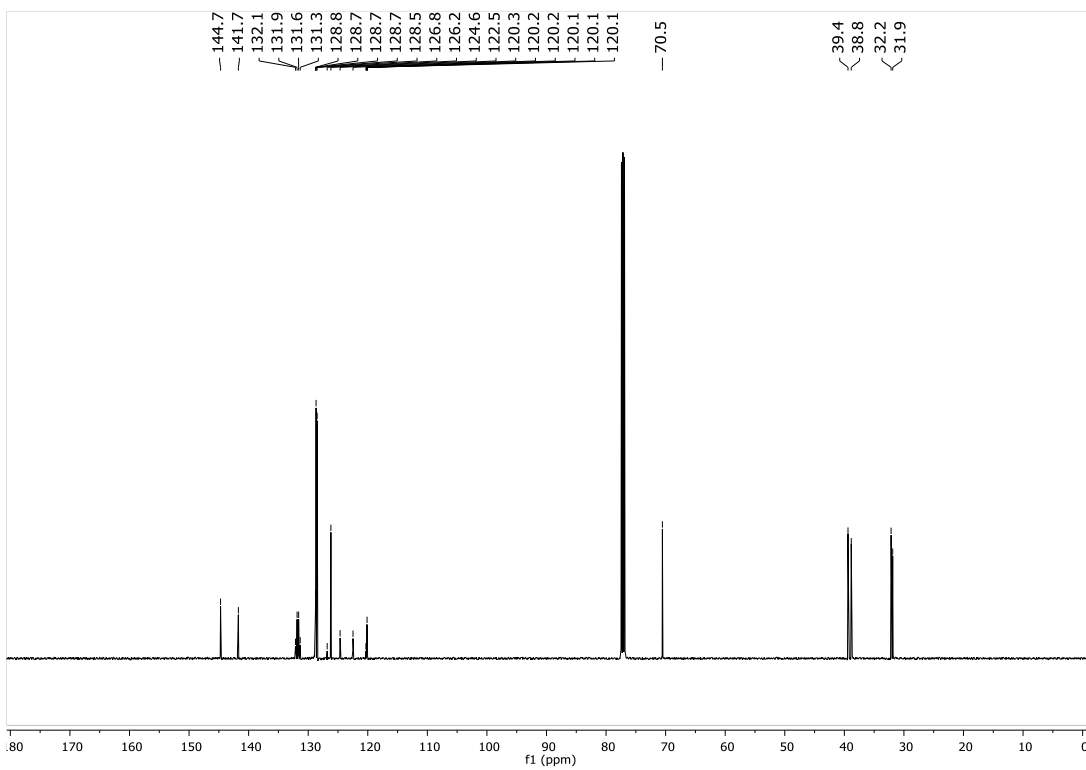


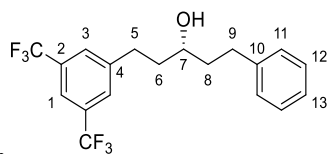
S5.

^1H NMR, 400 MHz, CDCl_3



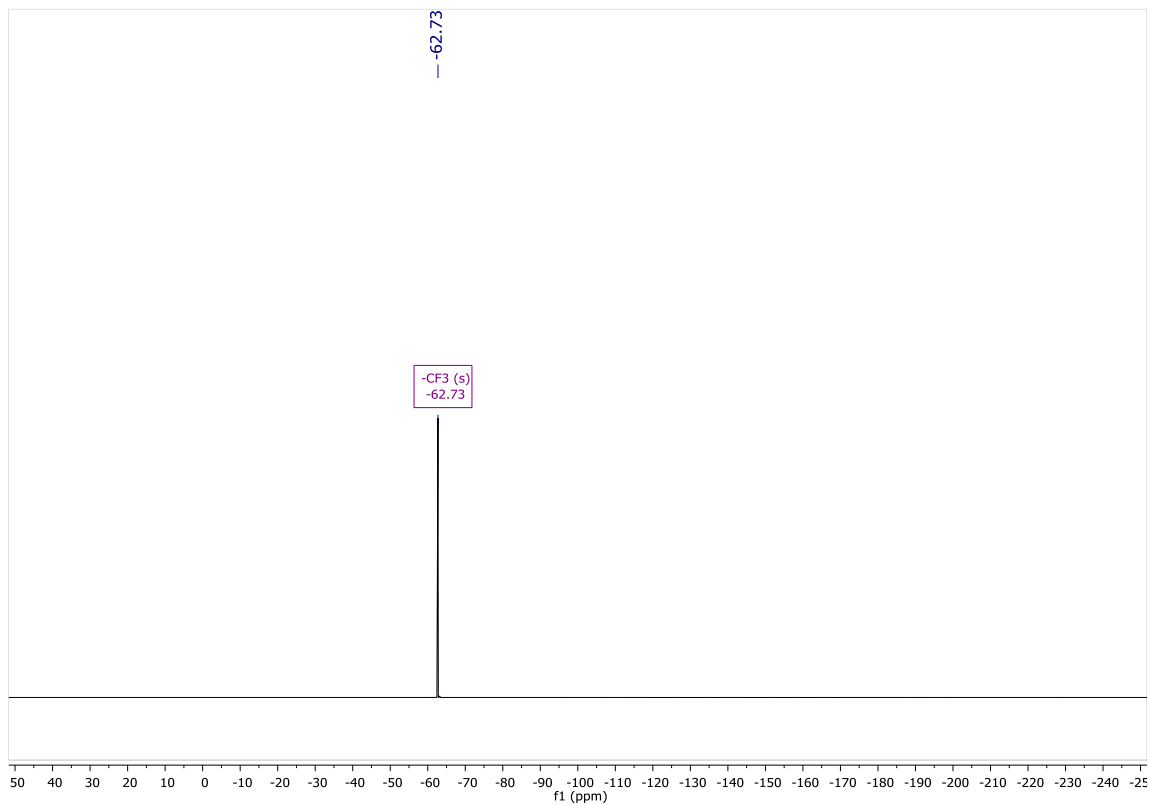
S5. ^{13}C NMR, 101 MHz, CDCl_3



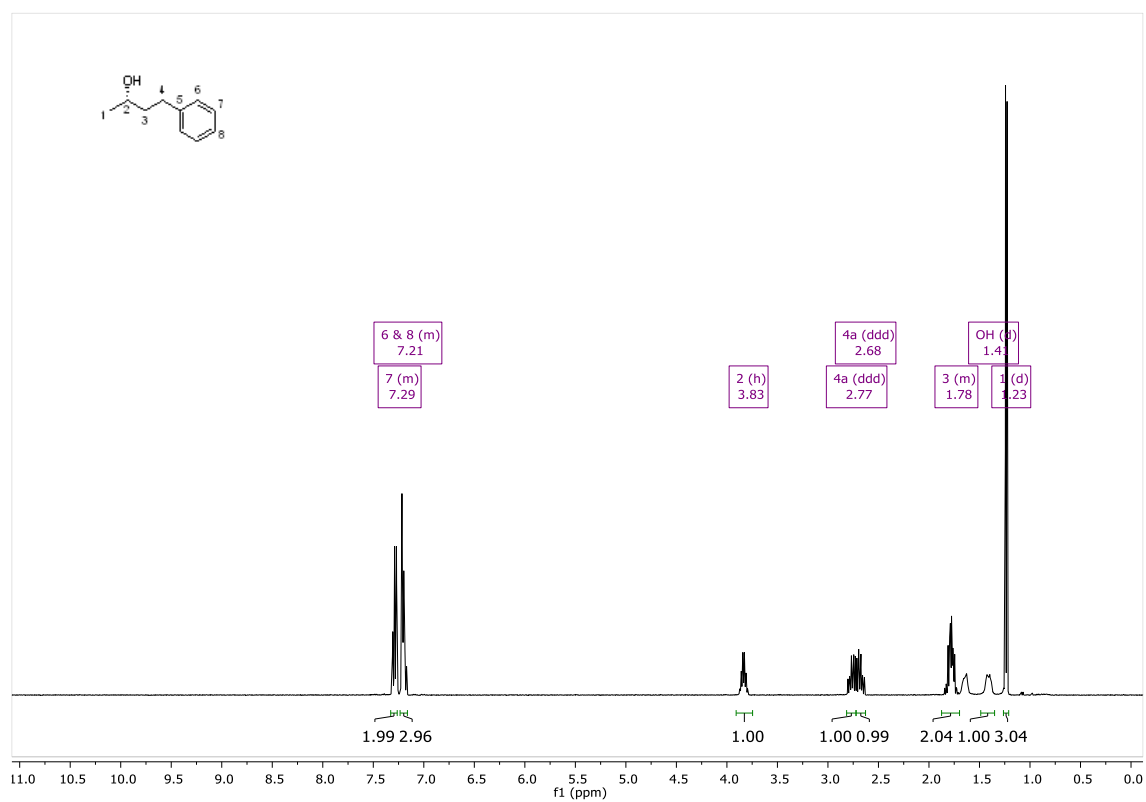


S5.

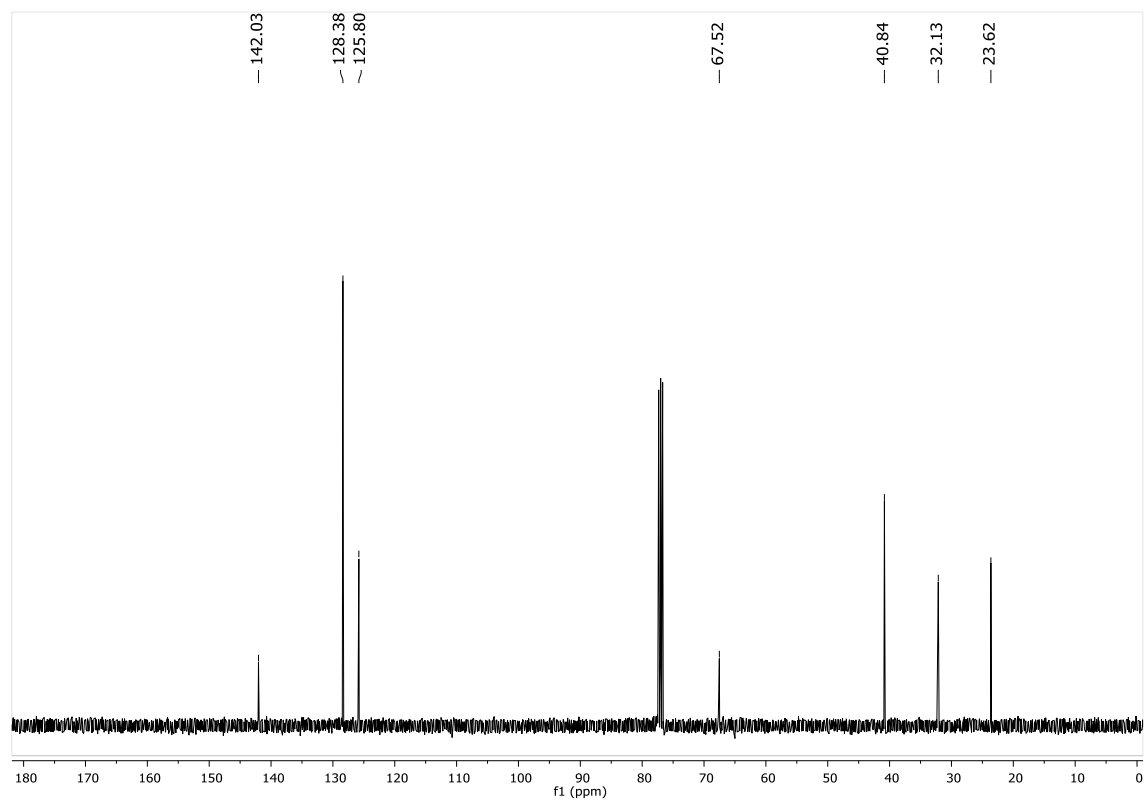
^{19}F NMR, 377 MHz, CDCl_3



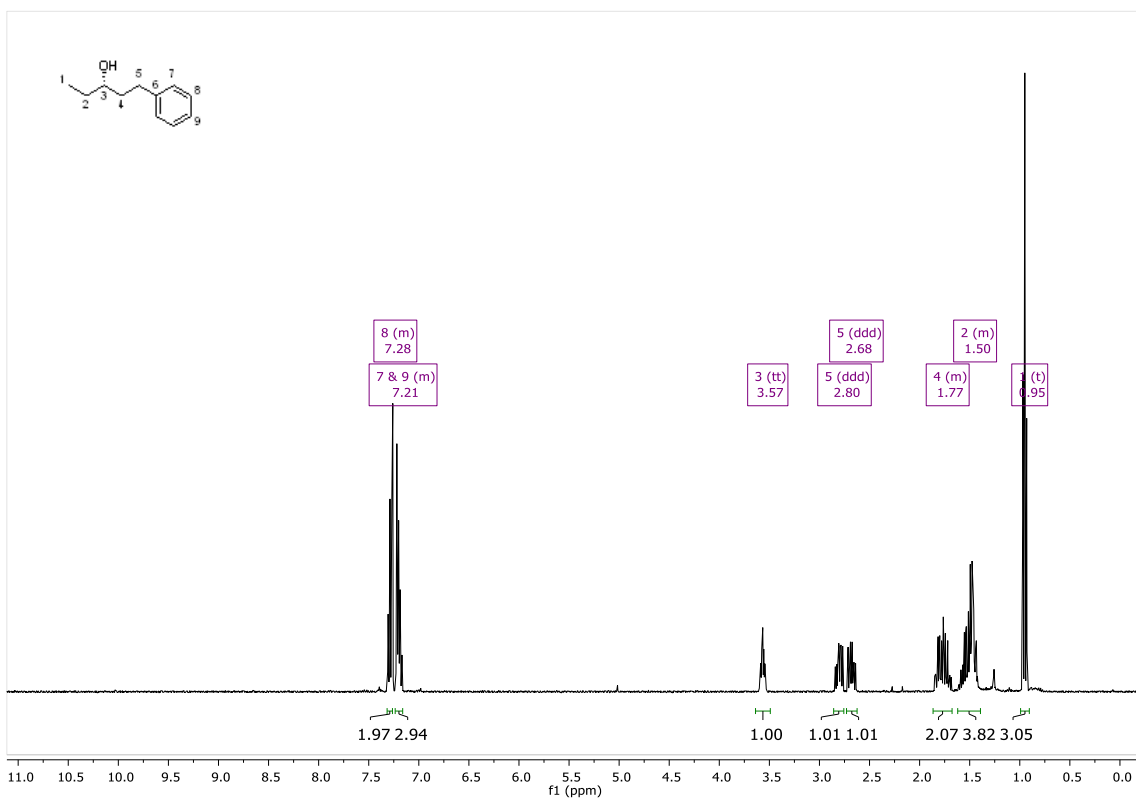
S6. ^1H NMR, 400 MHz, CDCl_3



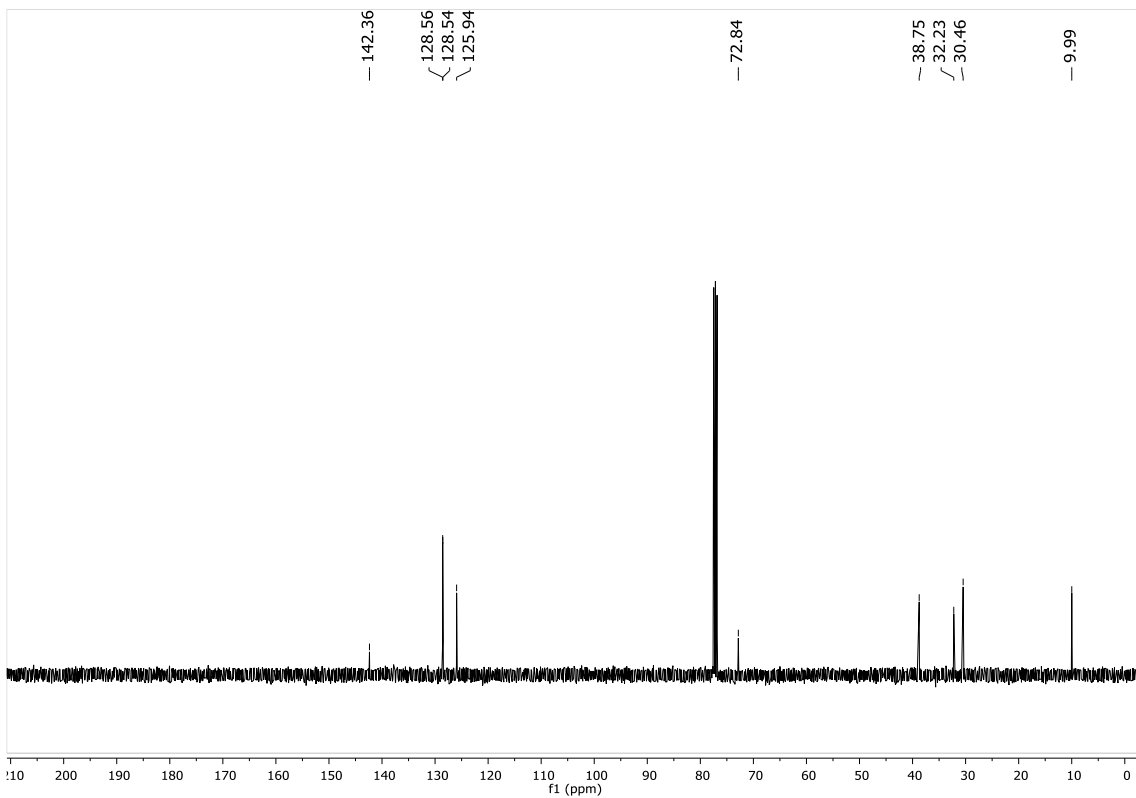
S6. ^{13}C NMR, 101 MHz, CDCl_3



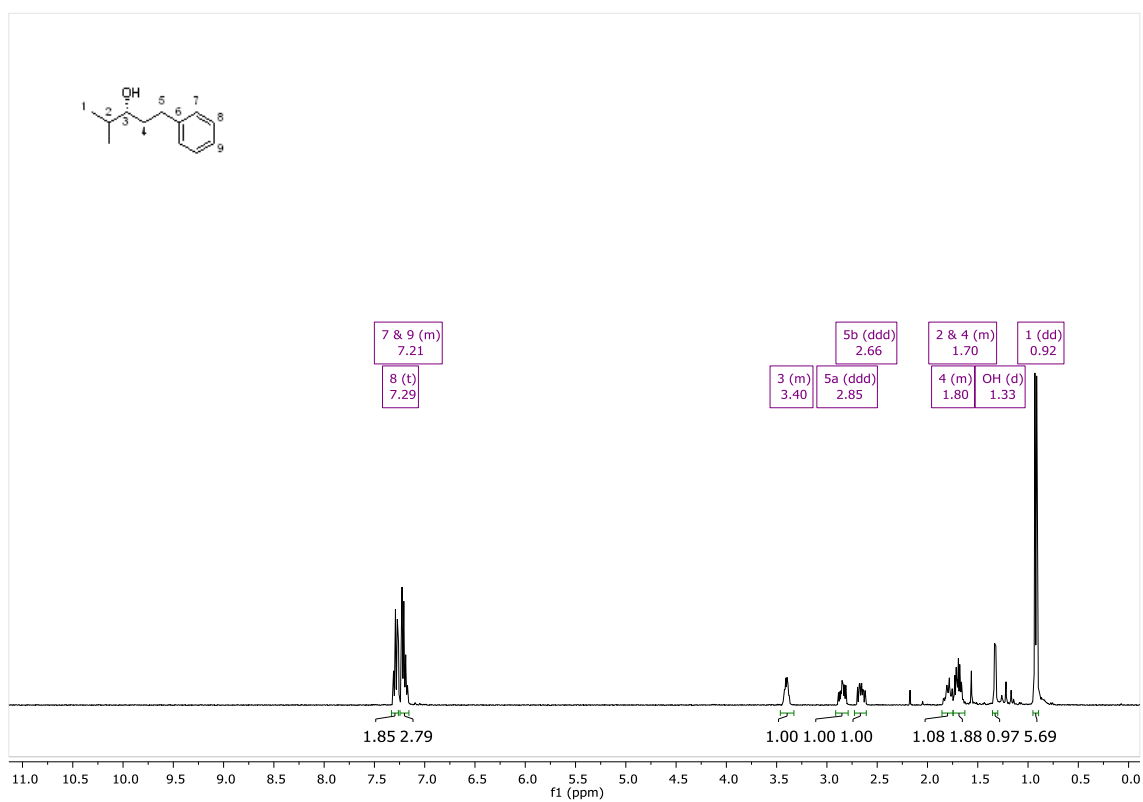
S7. ^1H NMR, 400 MHz, CDCl_3



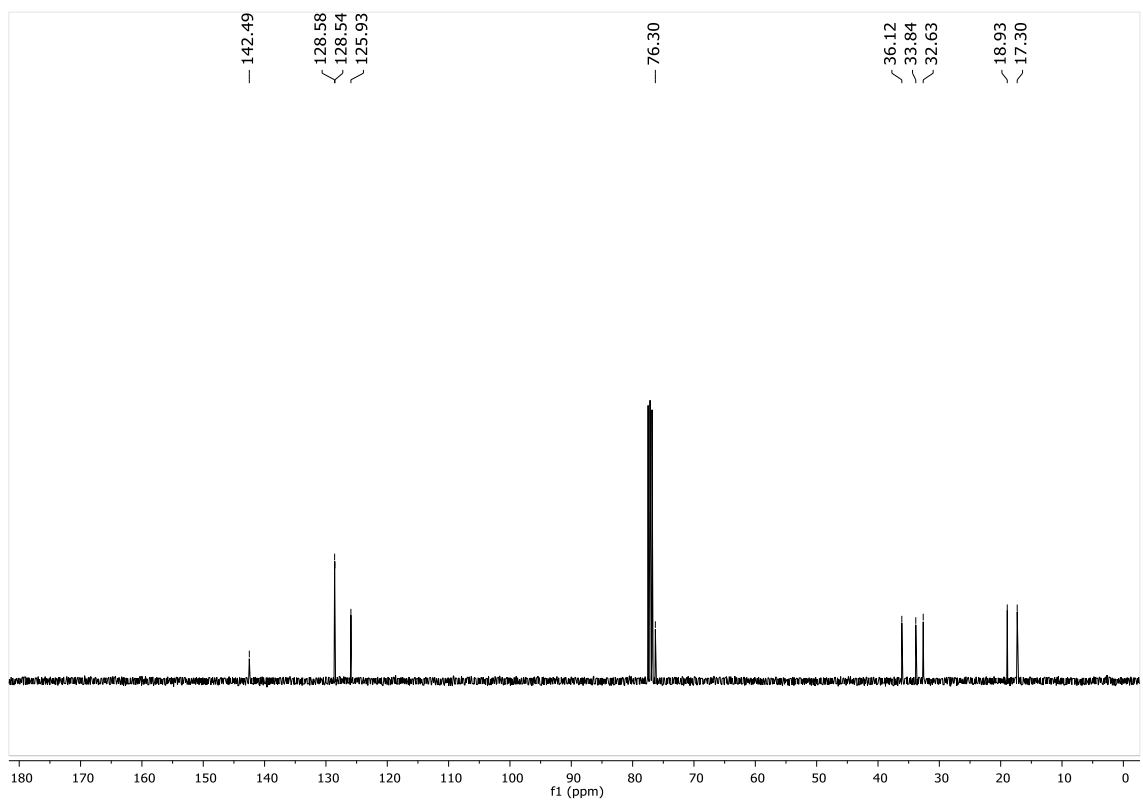
S7. ^{13}C NMR, 101 MHz, CDCl_3



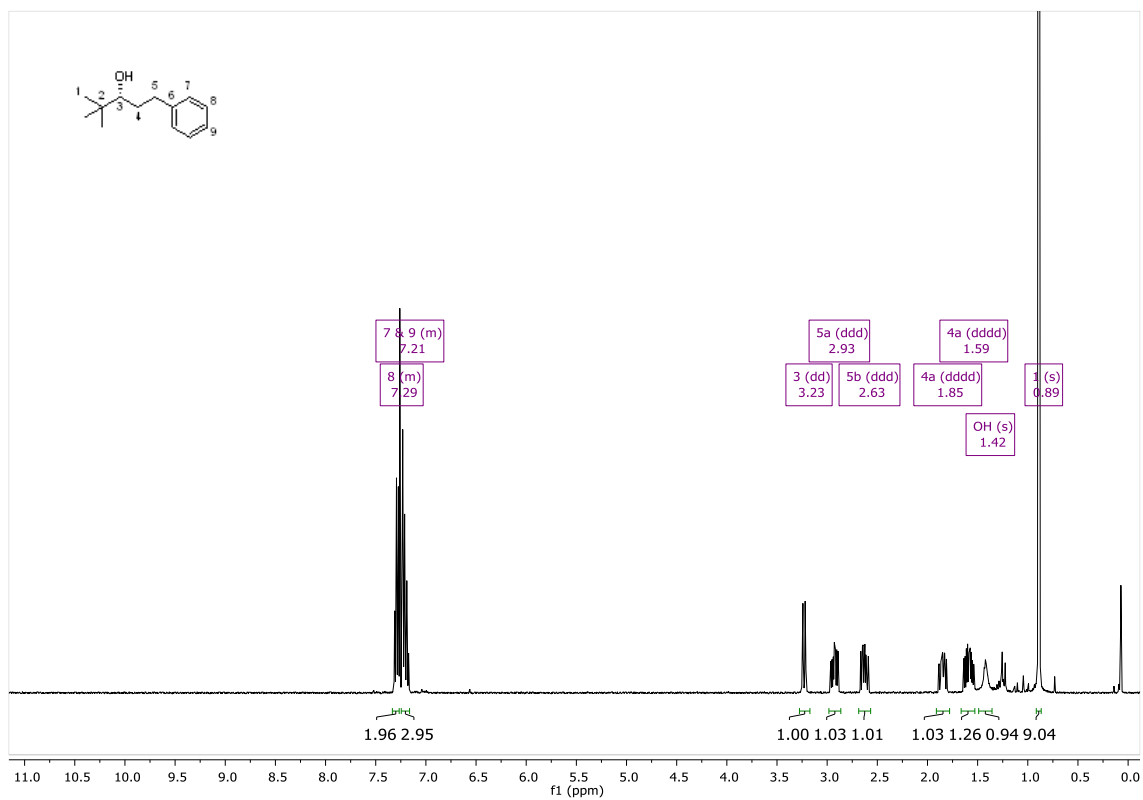
S8. ^1H NMR, 400 MHz, CDCl_3



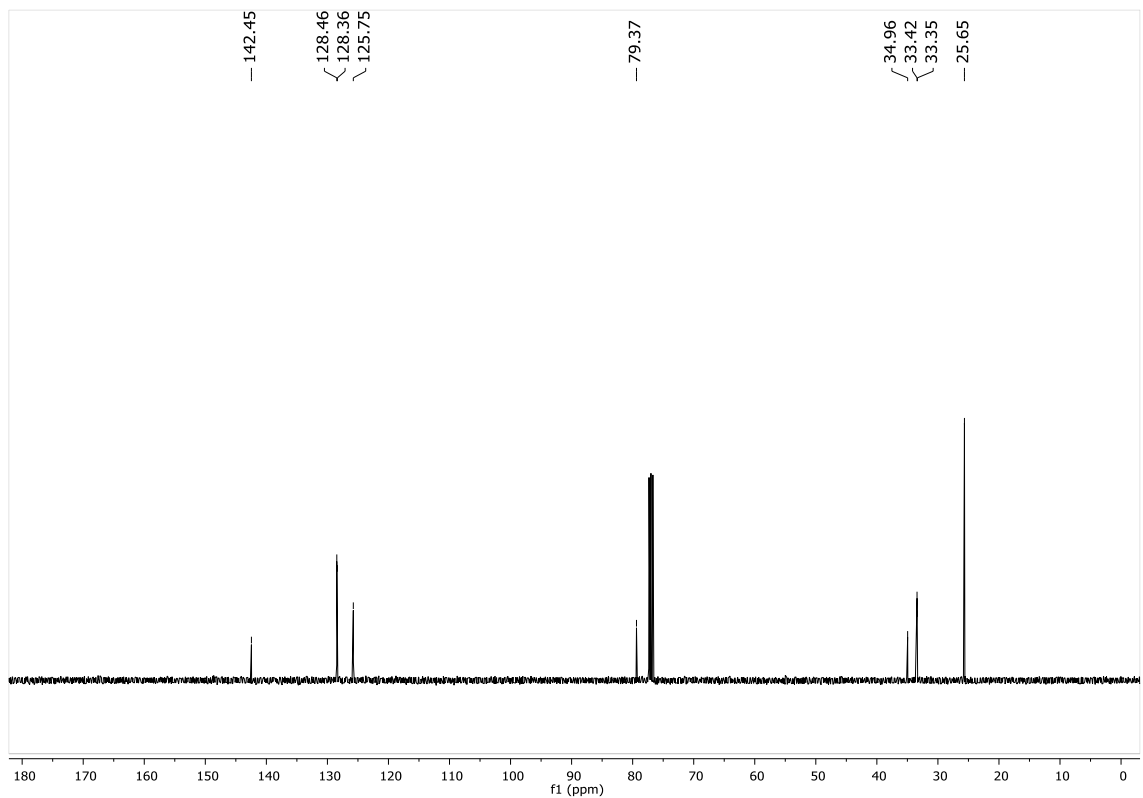
S8. ^{13}C NMR, 101 MHz, CDCl_3



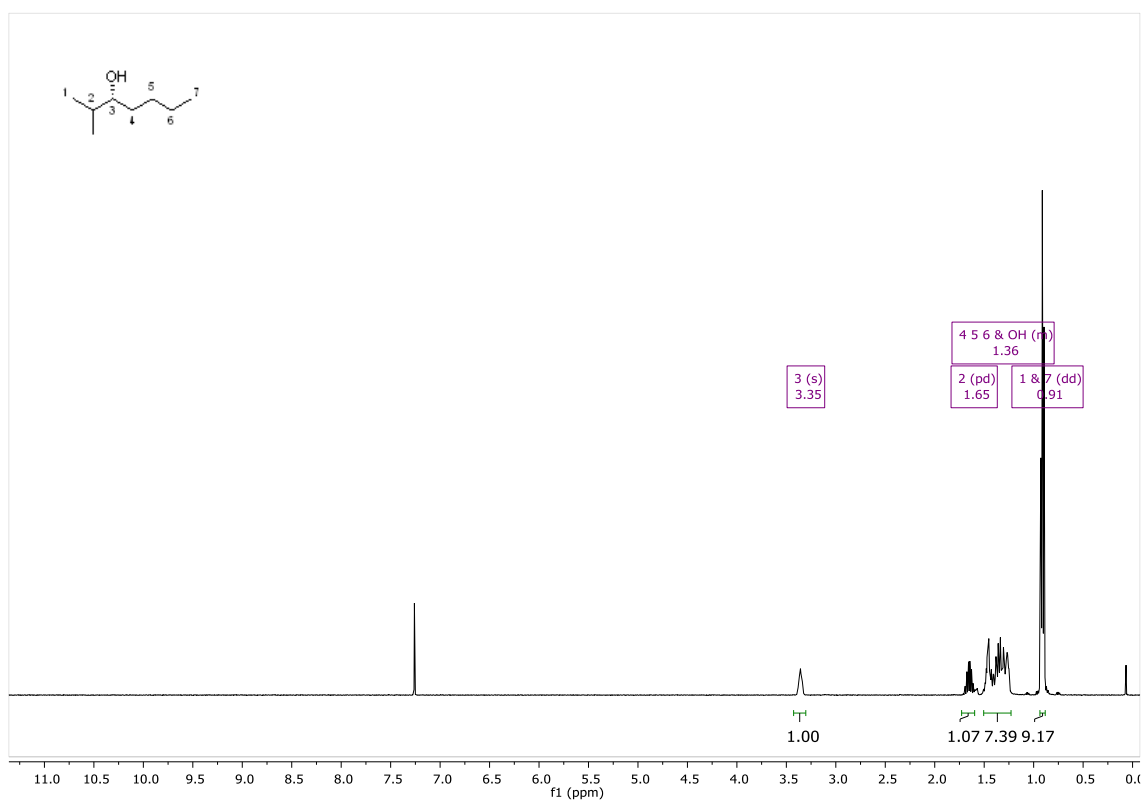
S9. ¹H NMR, 400 MHz, CDCl₃



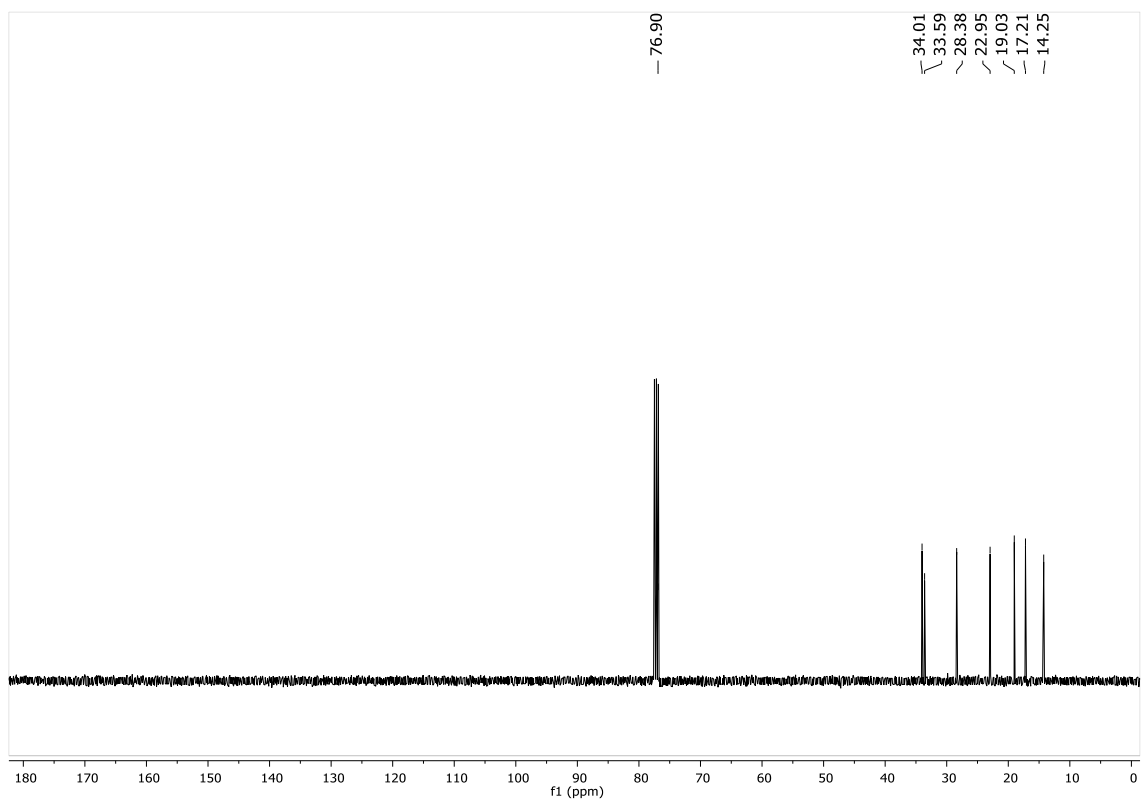
S9. ¹³C NMR, 101 MHz, CDCl₃



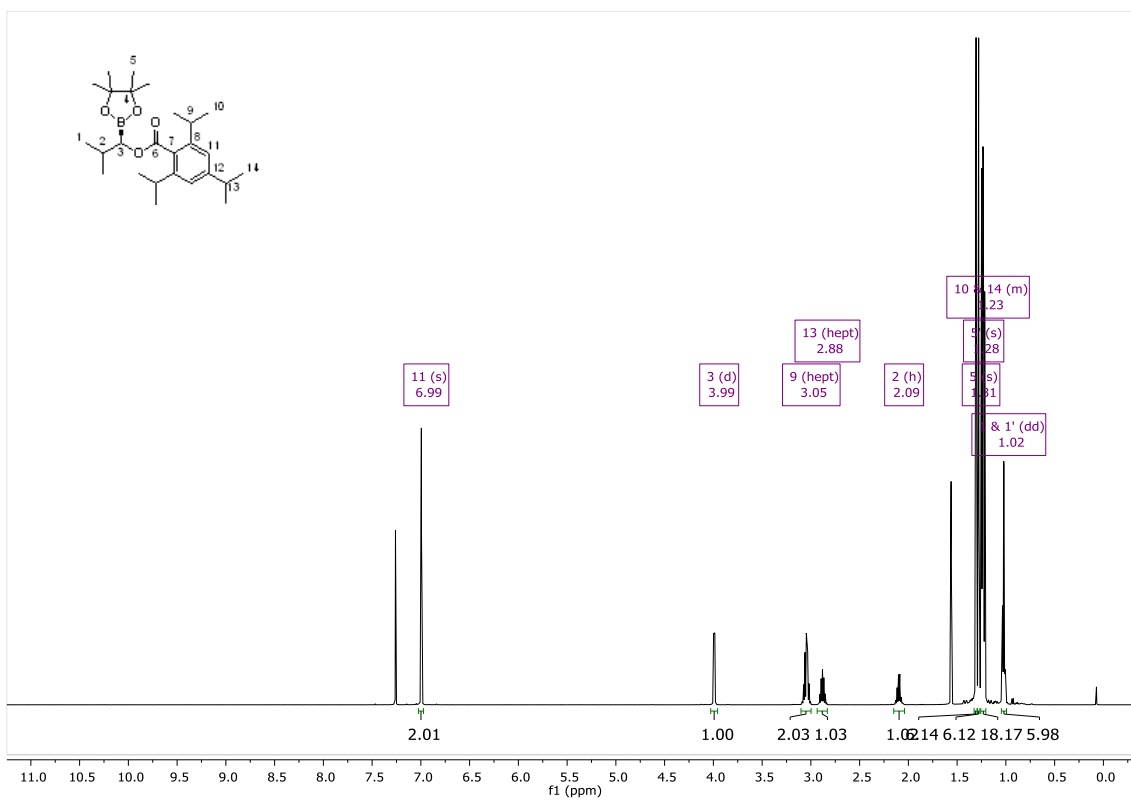
85. ^1H NMR, 400 MHz, CDCl_3



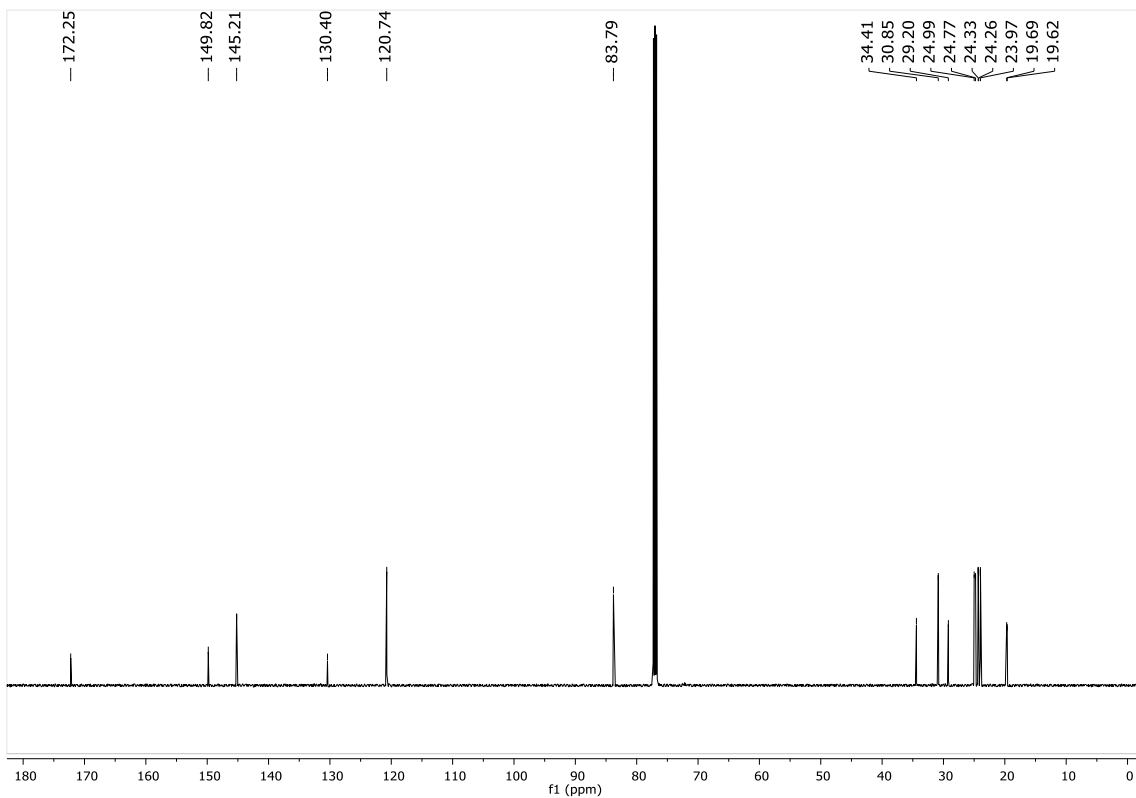
85. ^{13}C NMR, 101 MHz, CDCl_3



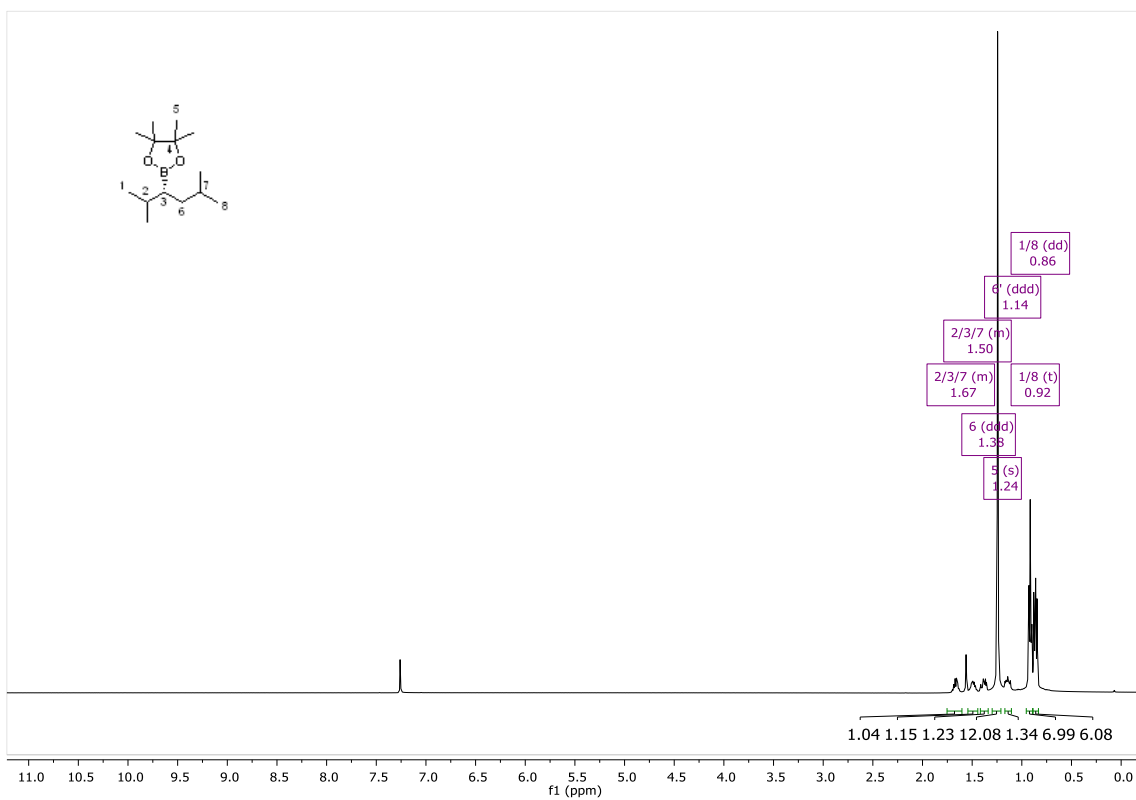
87. ^1H NMR, 500 MHz, CDCl_3



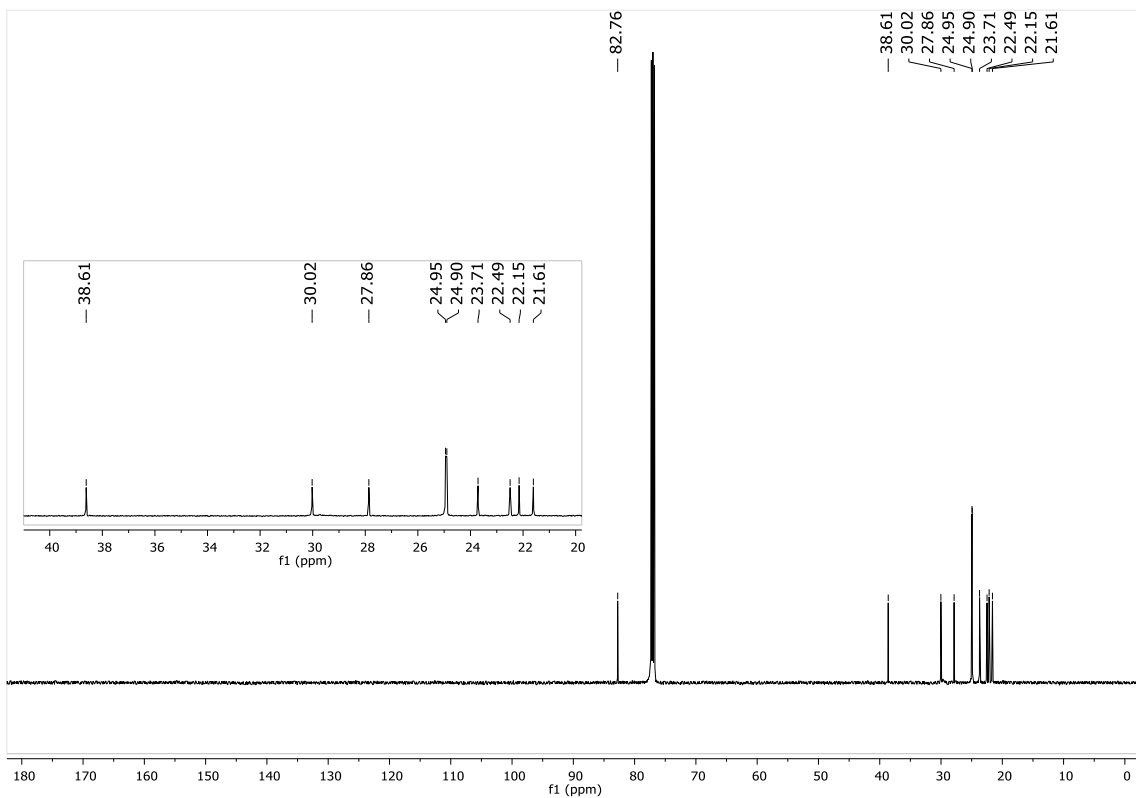
87. ^{13}C NMR, 126 MHz, CDCl_3



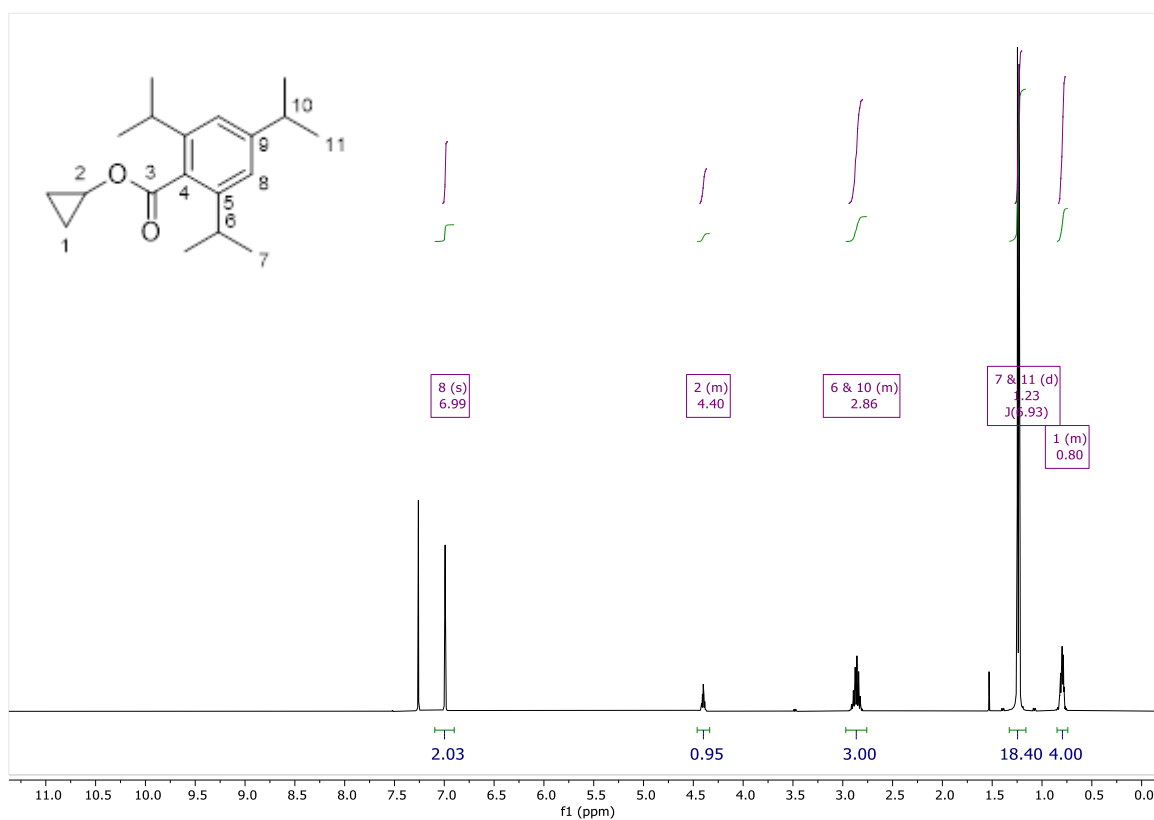
86. ^1H NMR, 500 MHz, CDCl_3



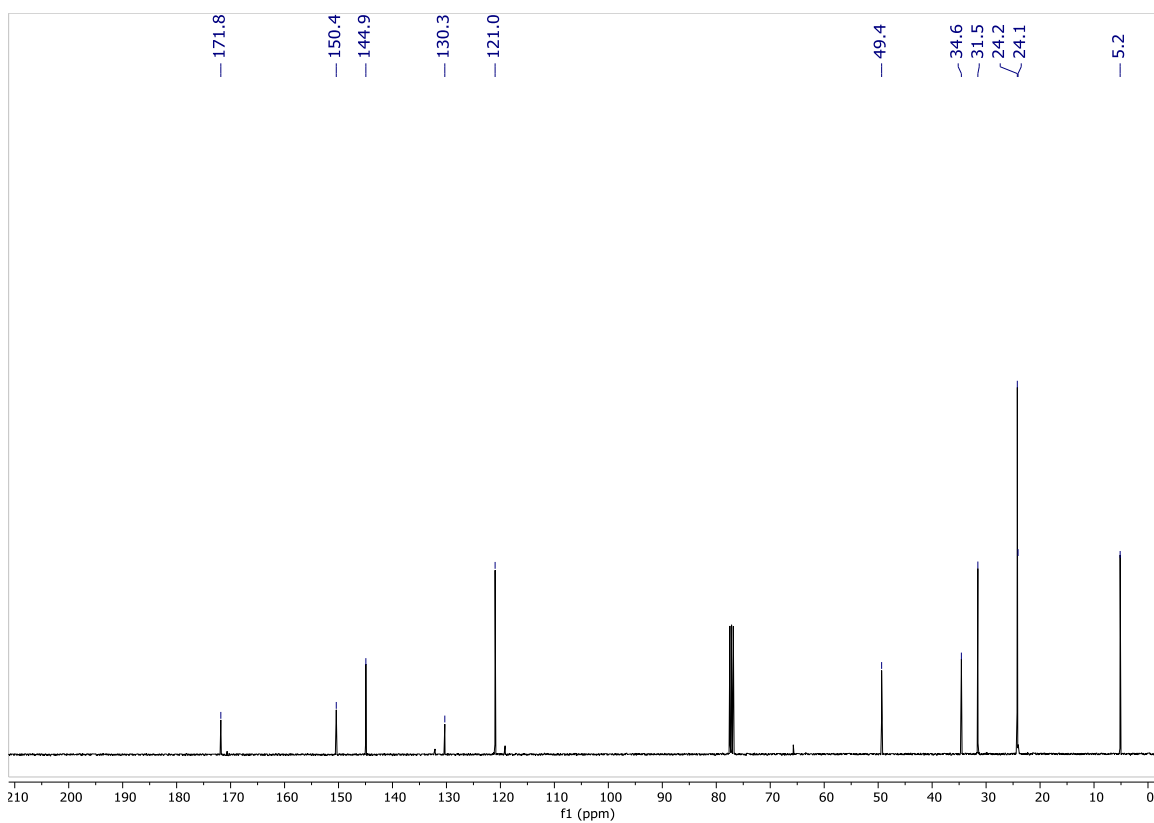
86. ^{13}C NMR, 126 MHz, CDCl_3



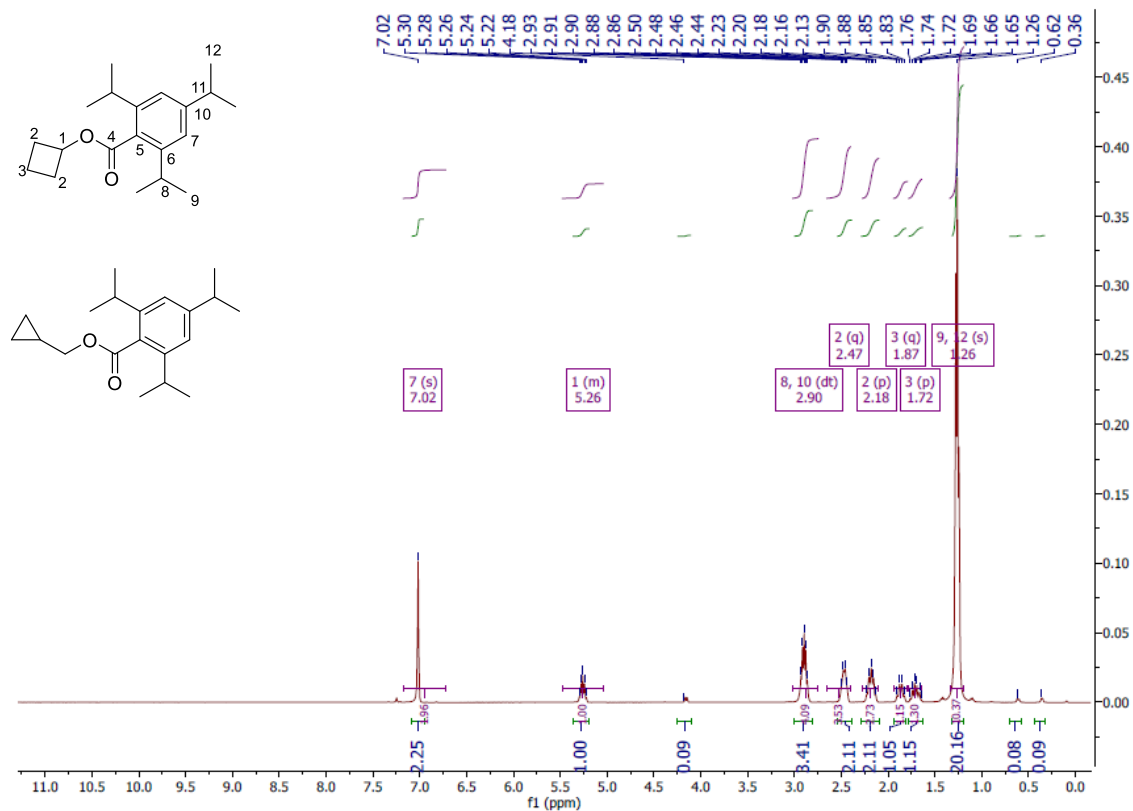
93. ^1H , 400 MHz, CDCl_3



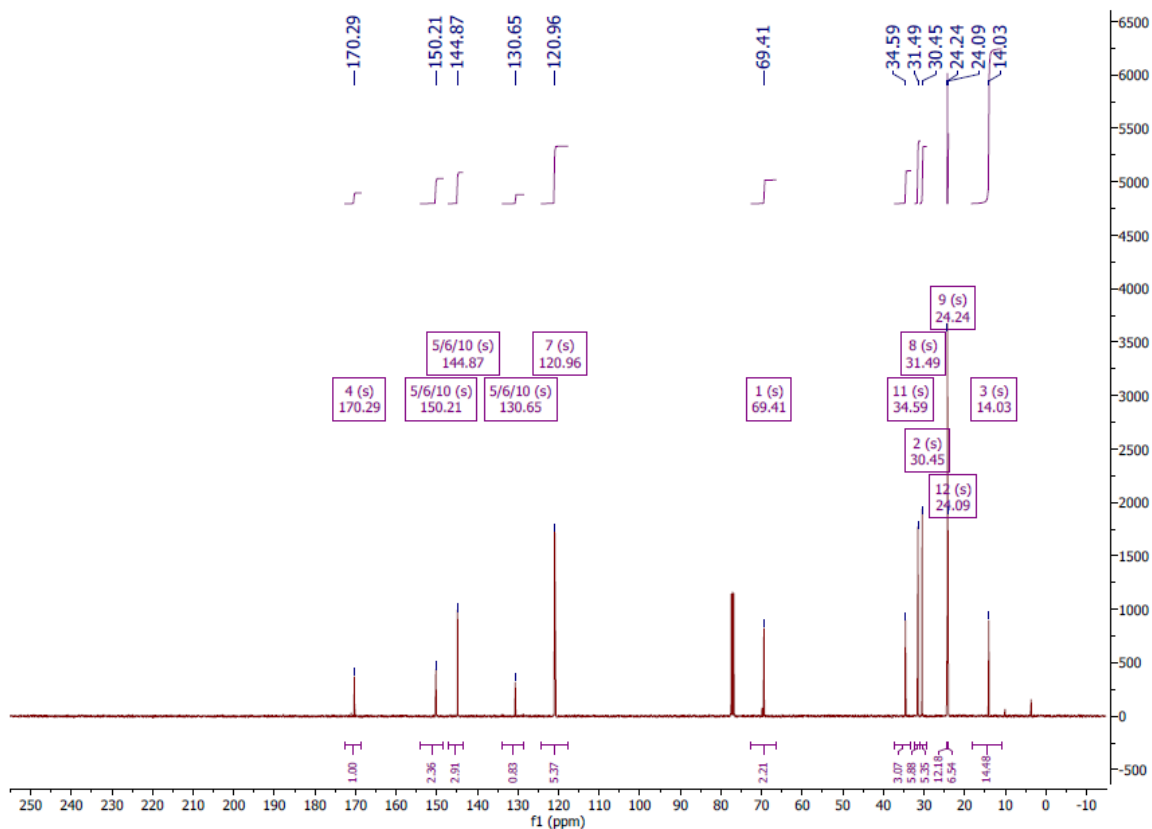
93. ^{13}C , 101 MHz, CDCl_3



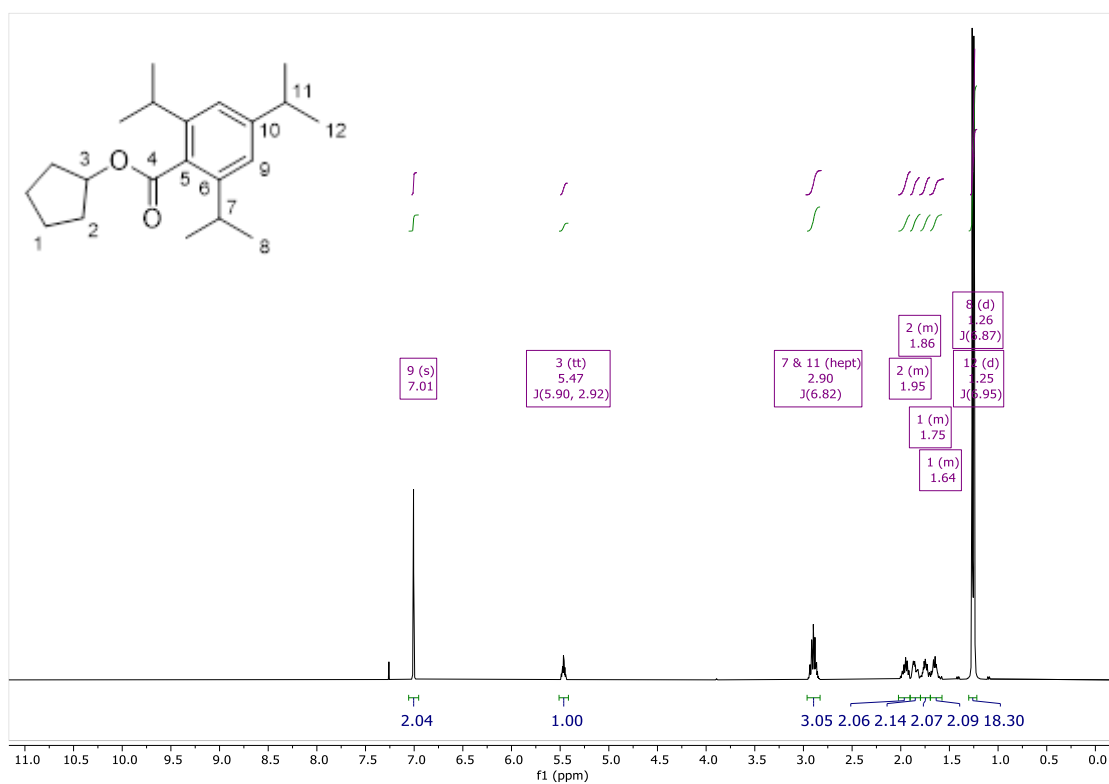
95. ¹H, 400 MHz, CDCl₃



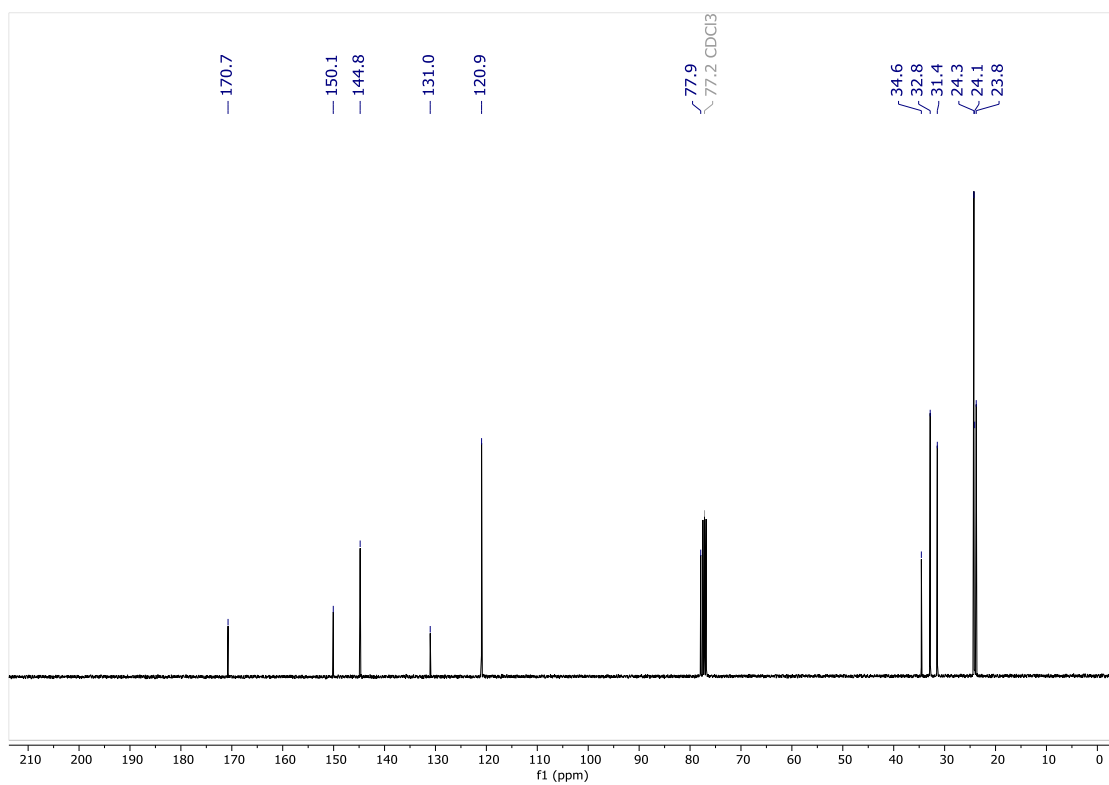
95. ¹³C, 101 MHz, CDCl₃



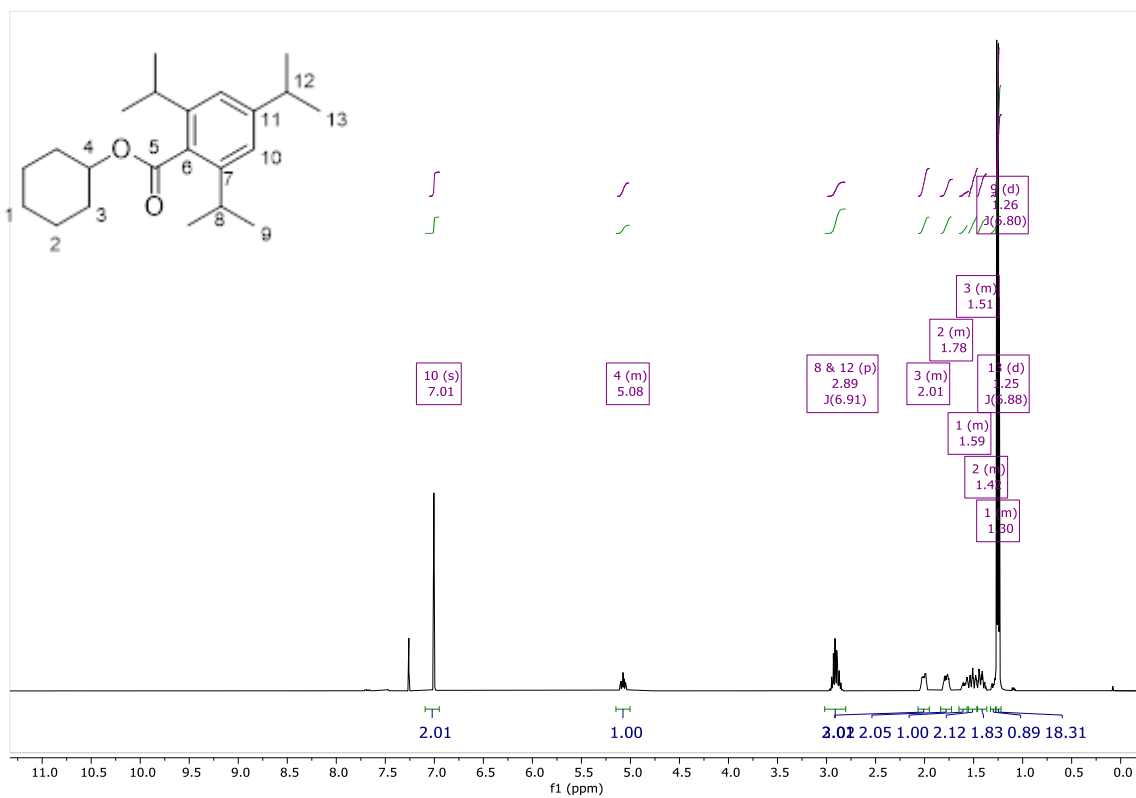
101. ^1H , 400 MHz, CDCl_3



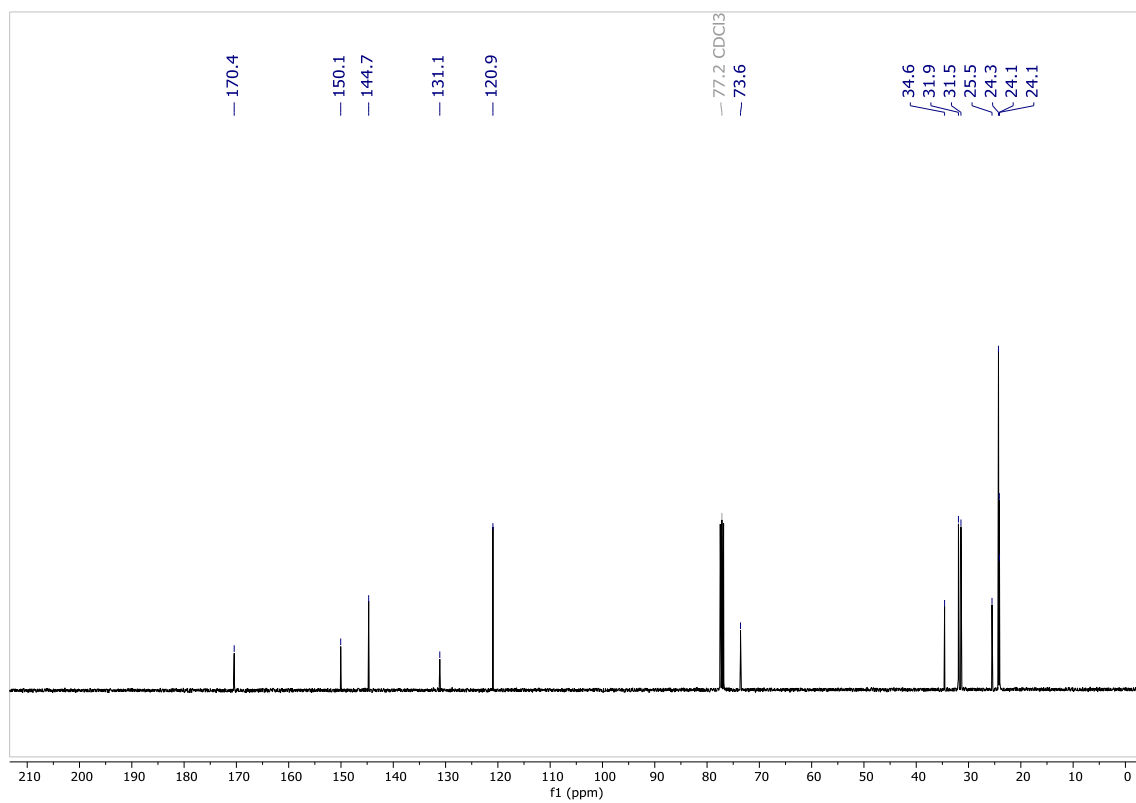
101. ^{13}C , 101 MHz, CDCl_3



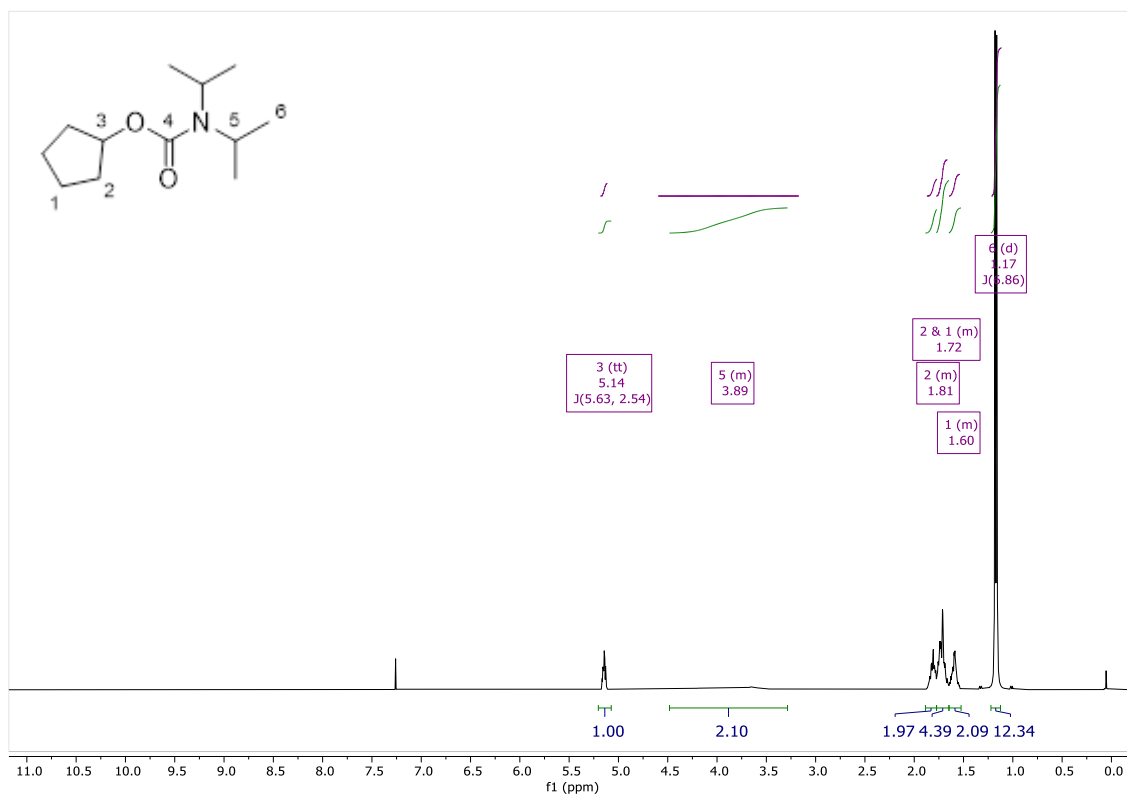
104. ^1H , 400 MHz, CDCl_3



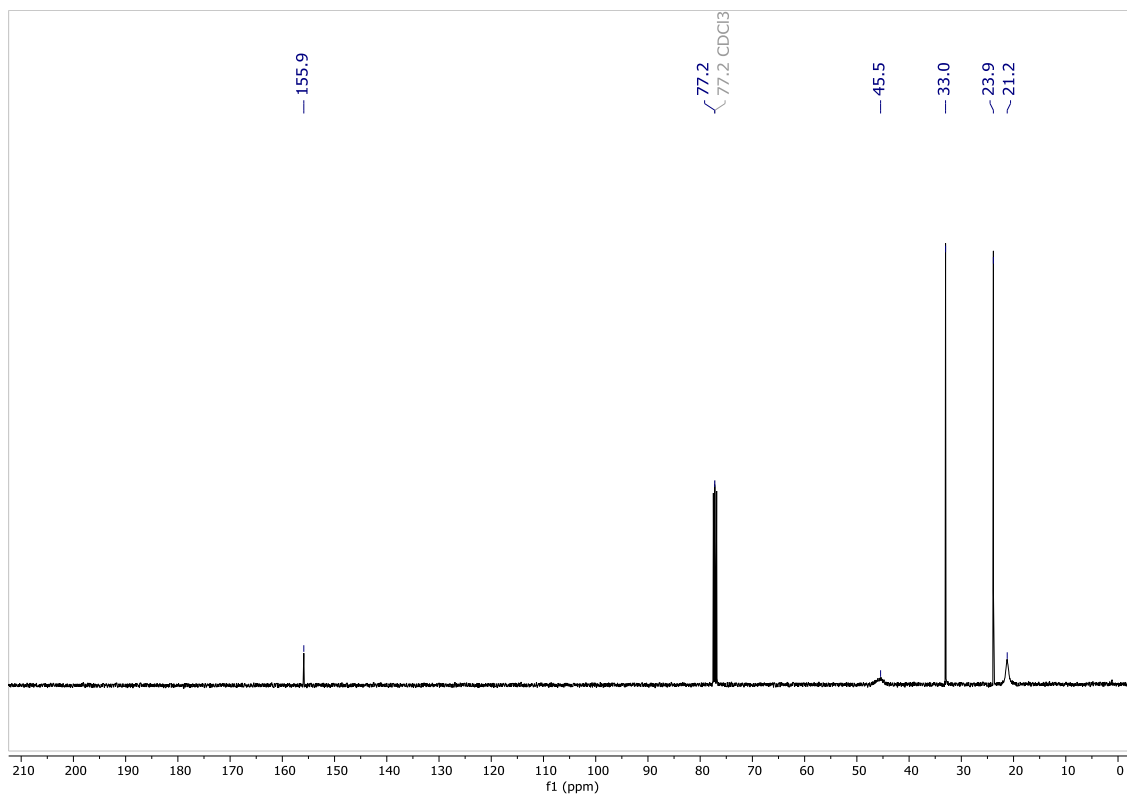
104. ^{13}C , 101 MHz, CDCl_3



102. ^1H , 400 MHz, CDCl_3



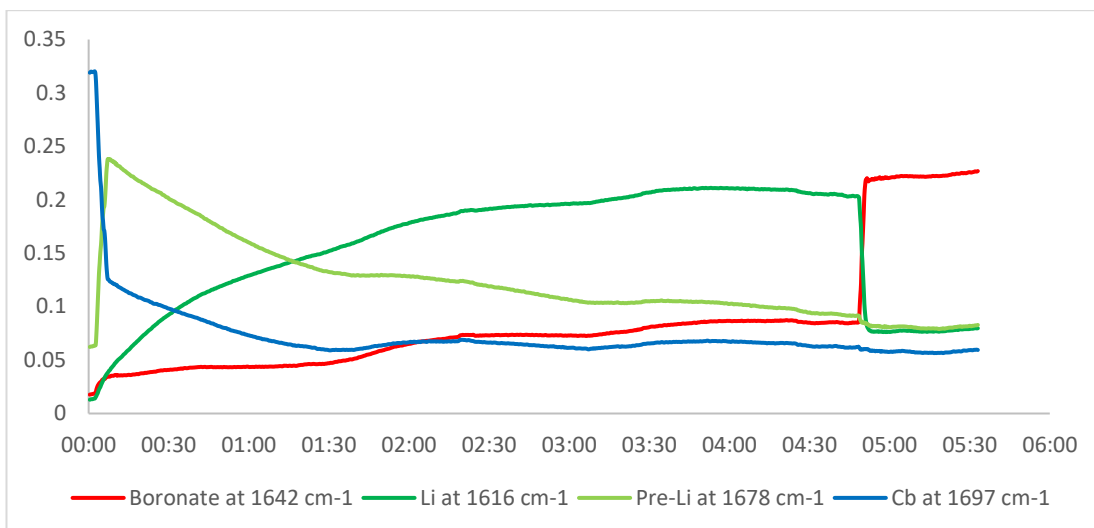
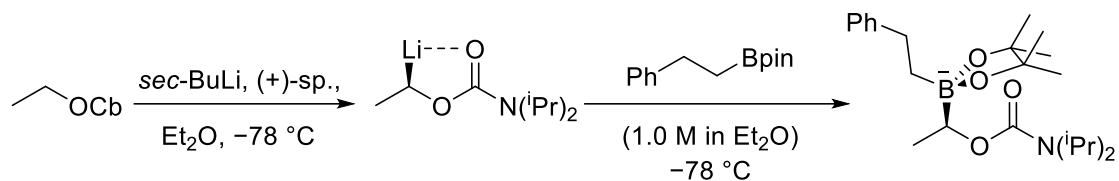
102. ^{13}C , 101 MHz, CDCl_3



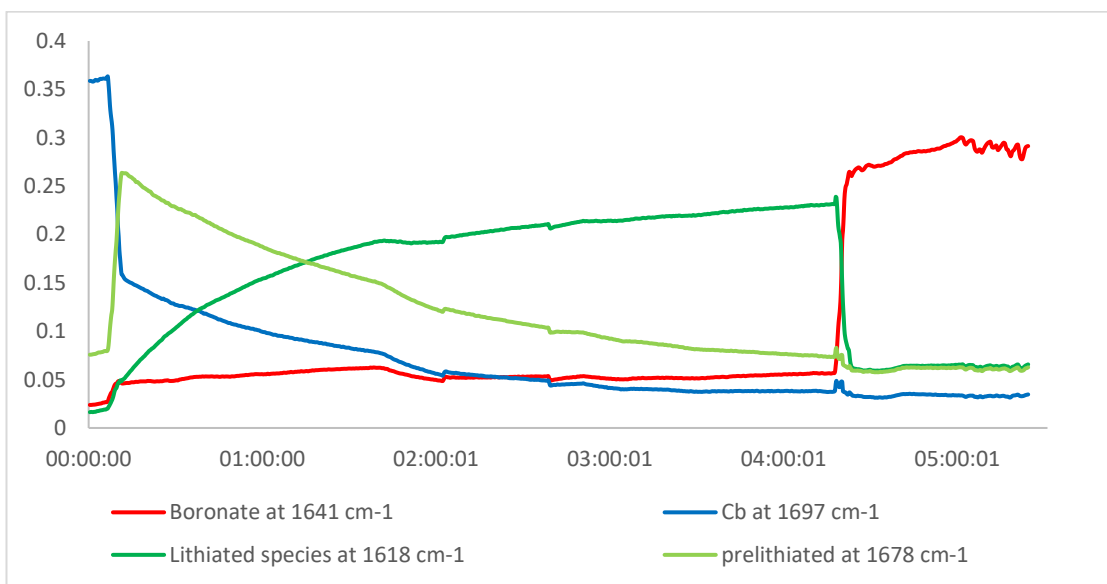
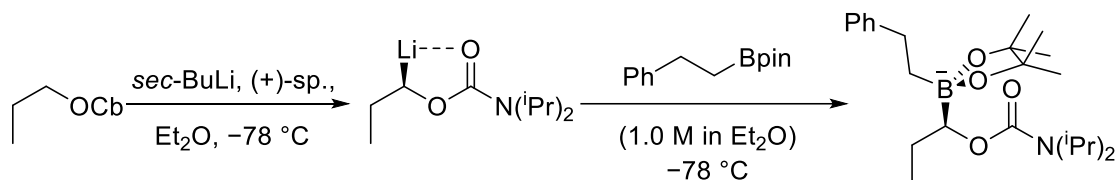
5.2.5 In Situ IR Traces

5.2.5.1 Table 1: Effect of steric hindrance at the β position

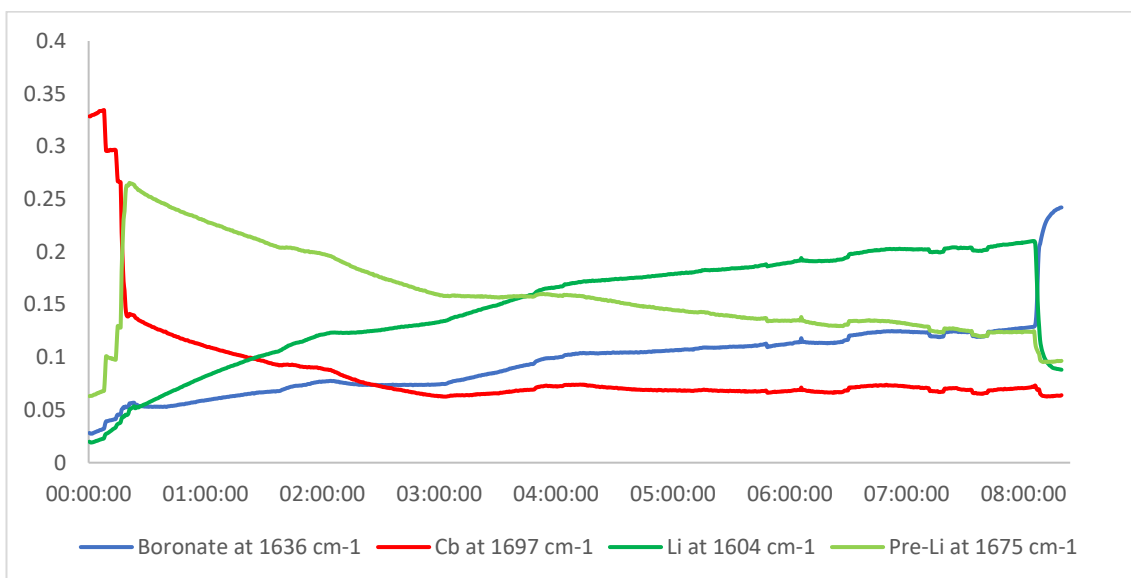
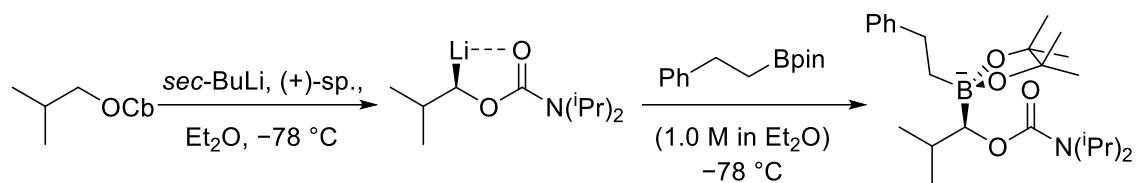
Entry 1 – Ethyl carbamate



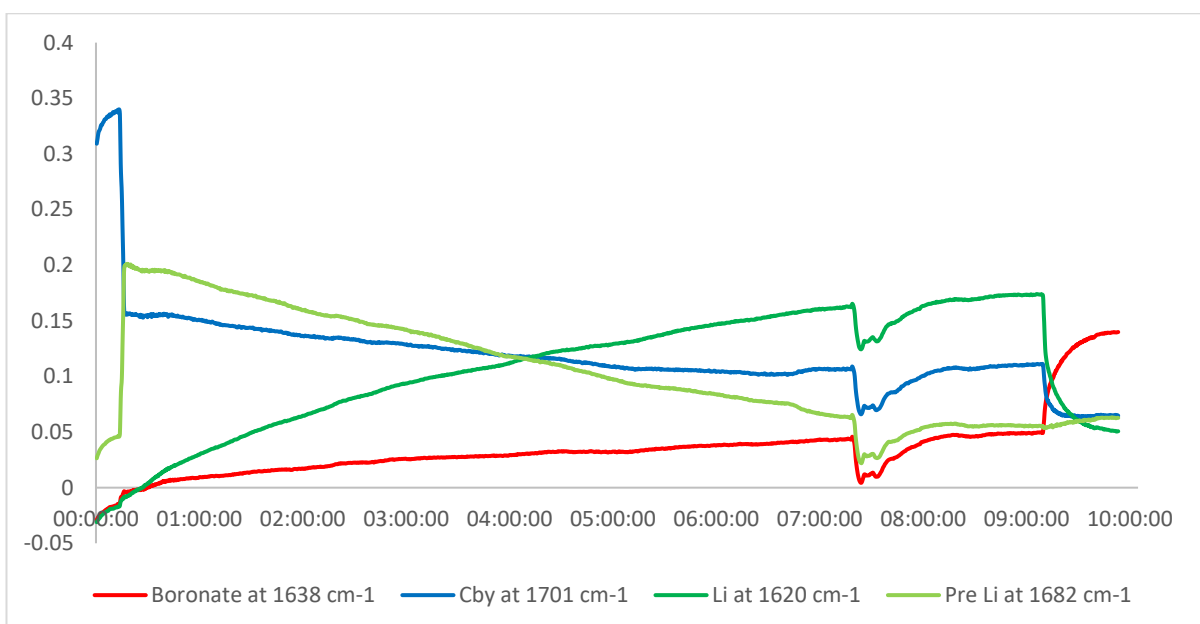
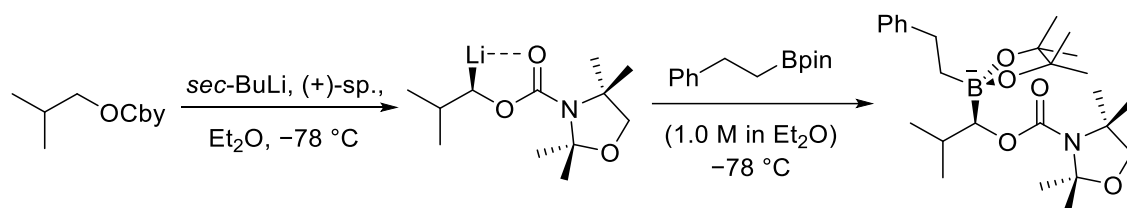
Entry 2 – Propyl carbamate



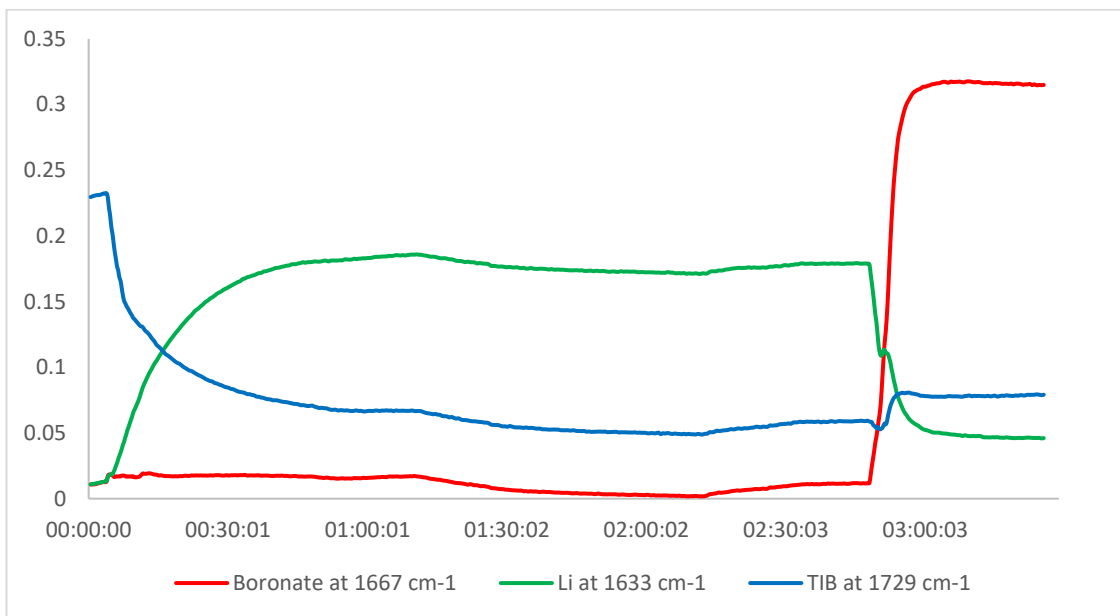
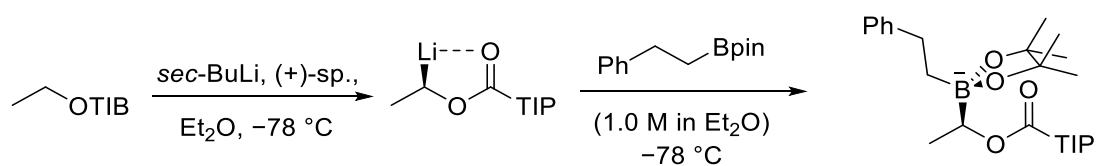
Entry 3 – Isobutyl carbamate



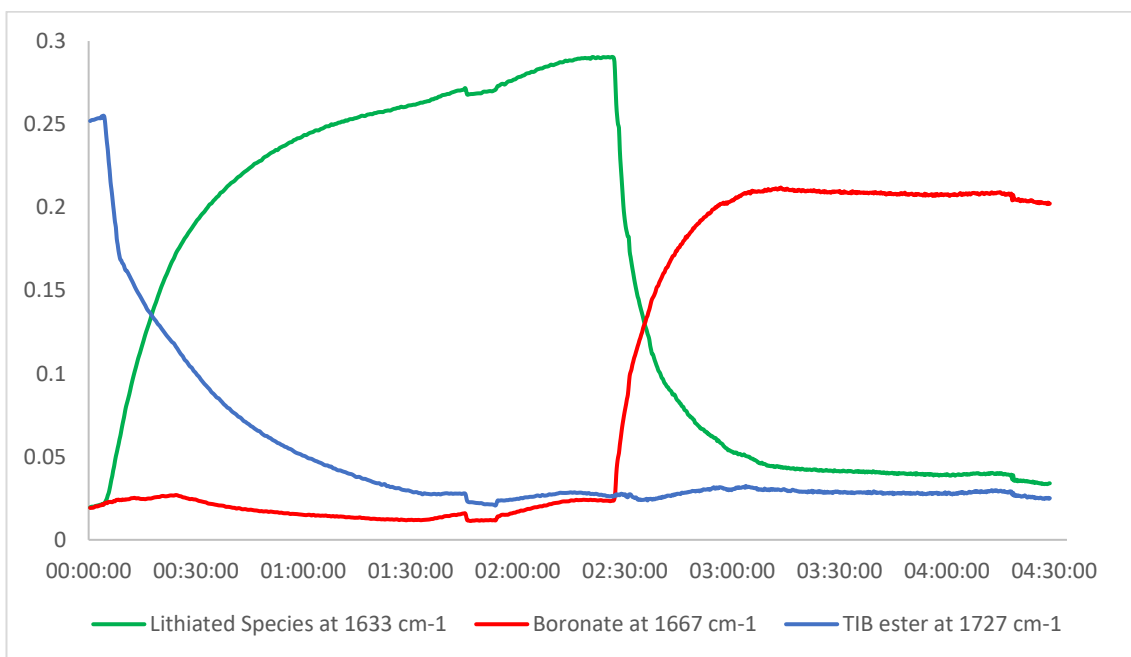
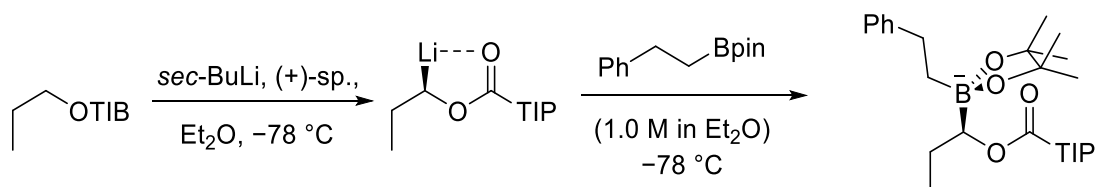
Entry 4 - Isobutyl 2,2,4,4-tetramethyloxazolidine-3-carboxylate (Cby)



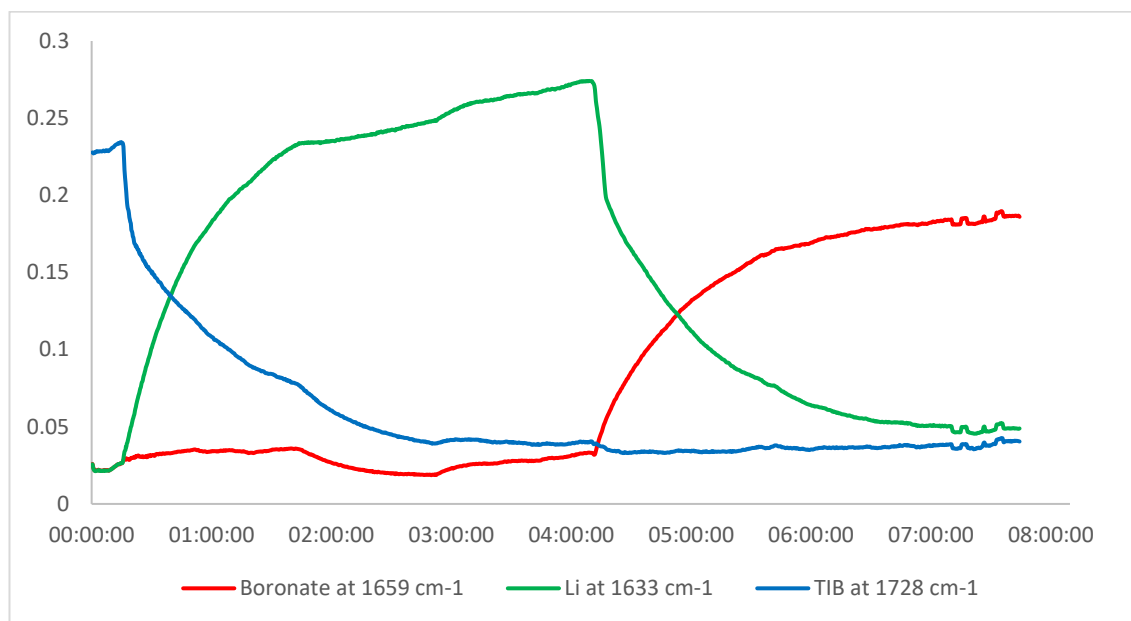
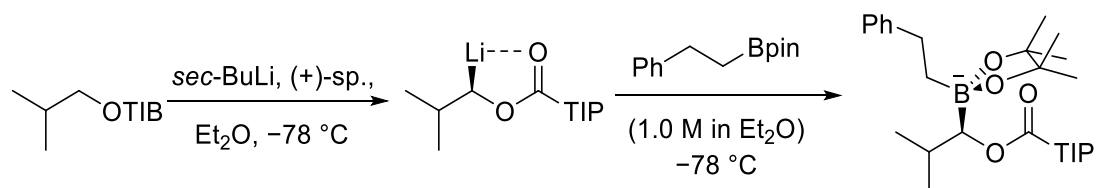
Entry 6 – Ethyl TIB ester



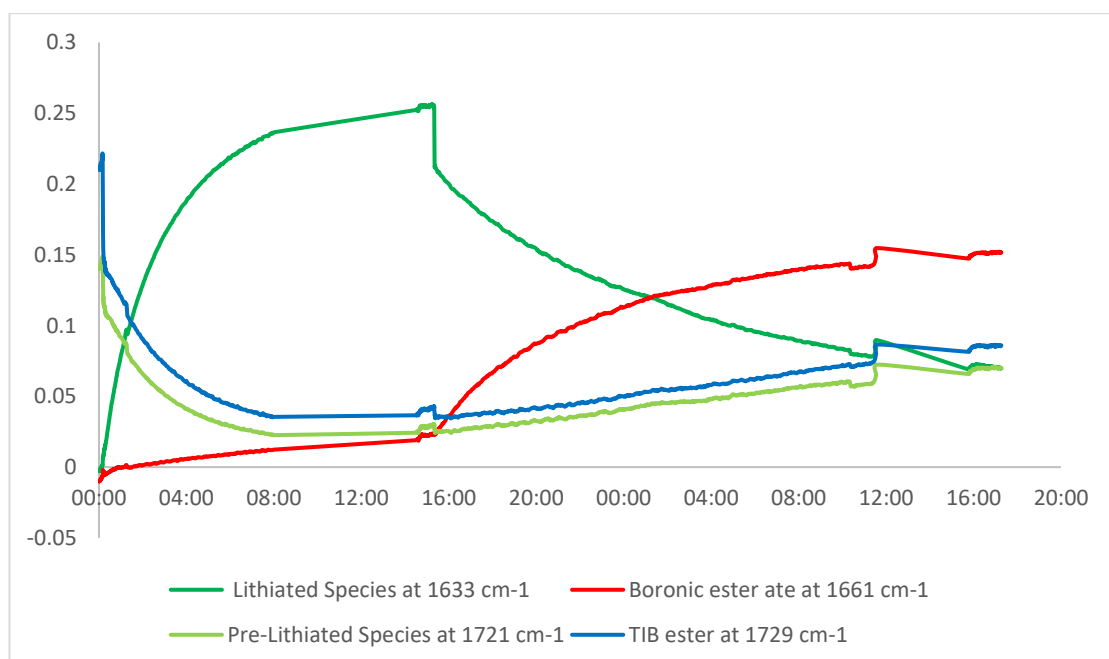
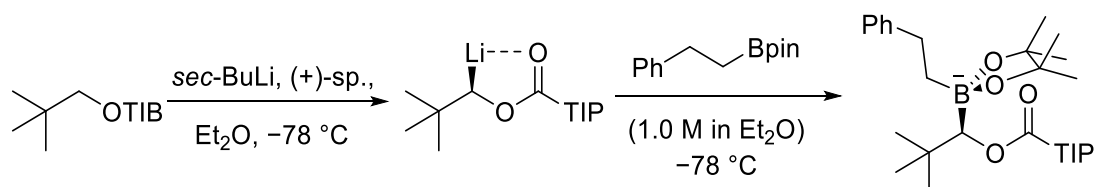
Entry 7 – Propyl TIB ester



Entry 8 – Isobutyl TIB ester

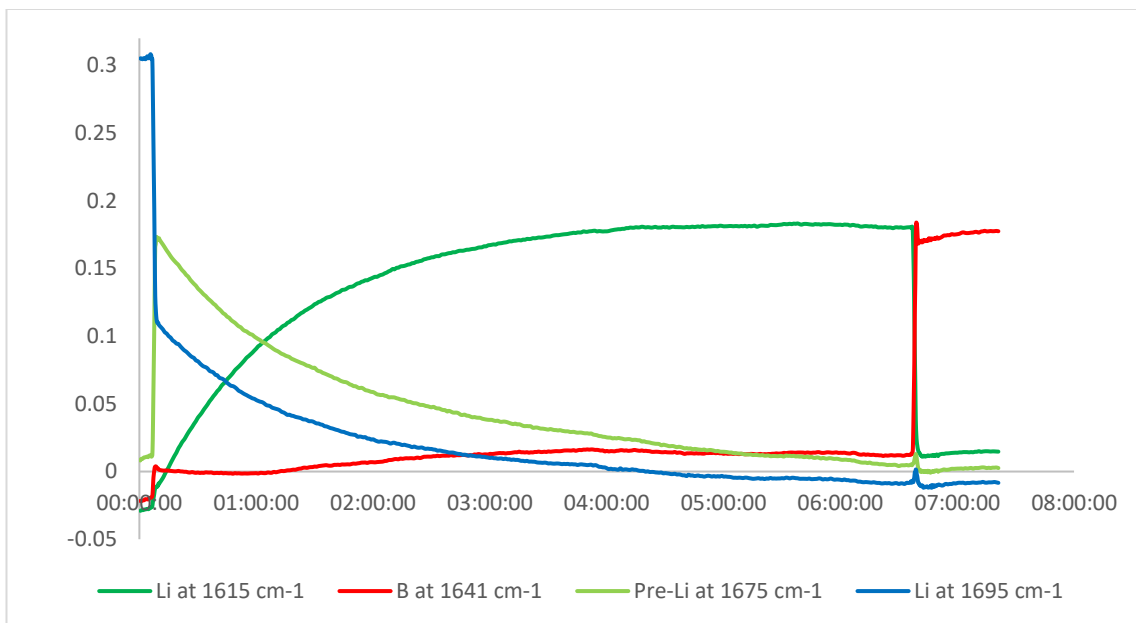
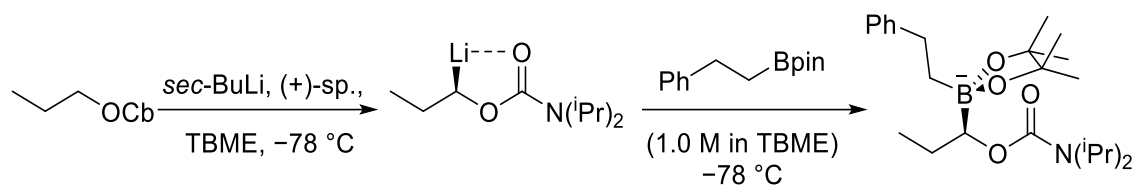


Entry 9 – Neo-pentyl TIB ester

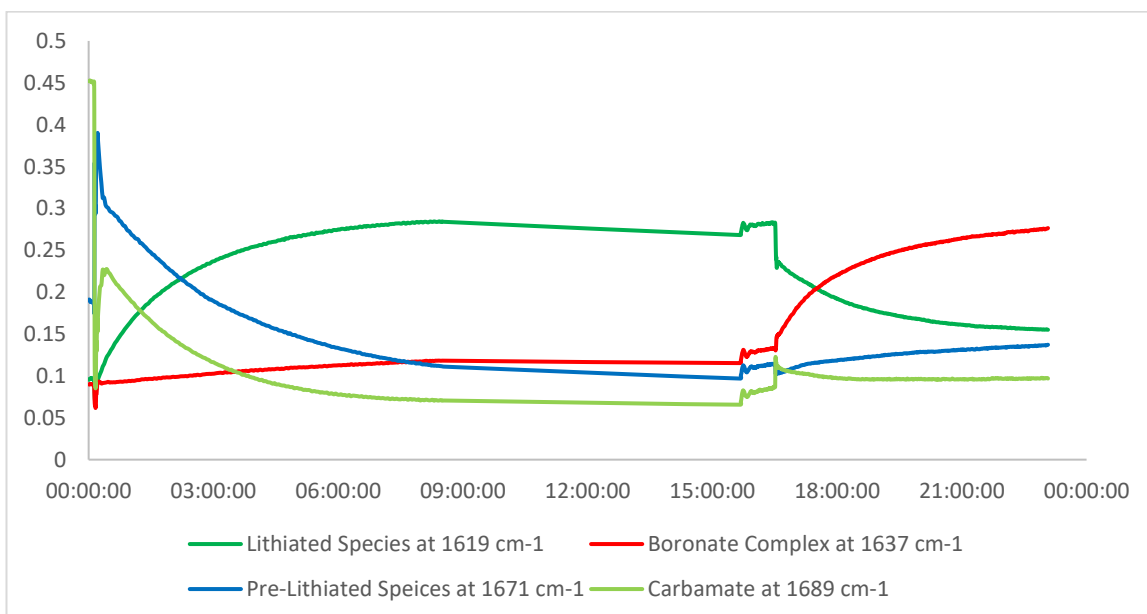
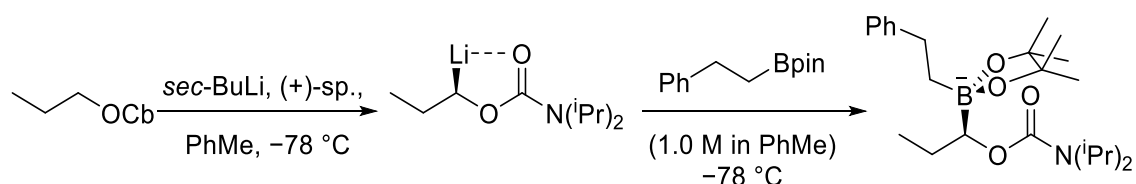


5.2.5.2 Table 2 – Effect of solvent

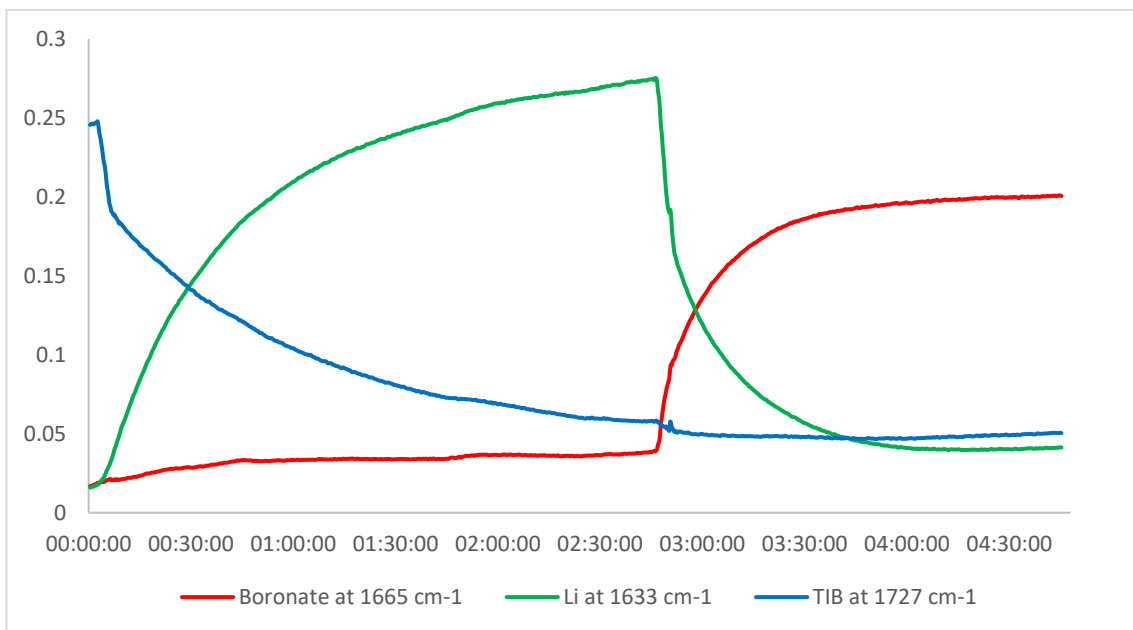
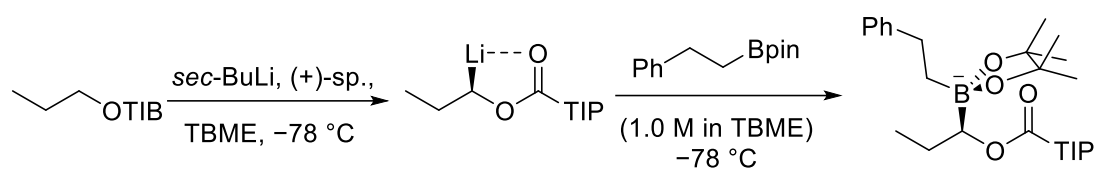
Entry 2 – Propyl carbamate in TBME



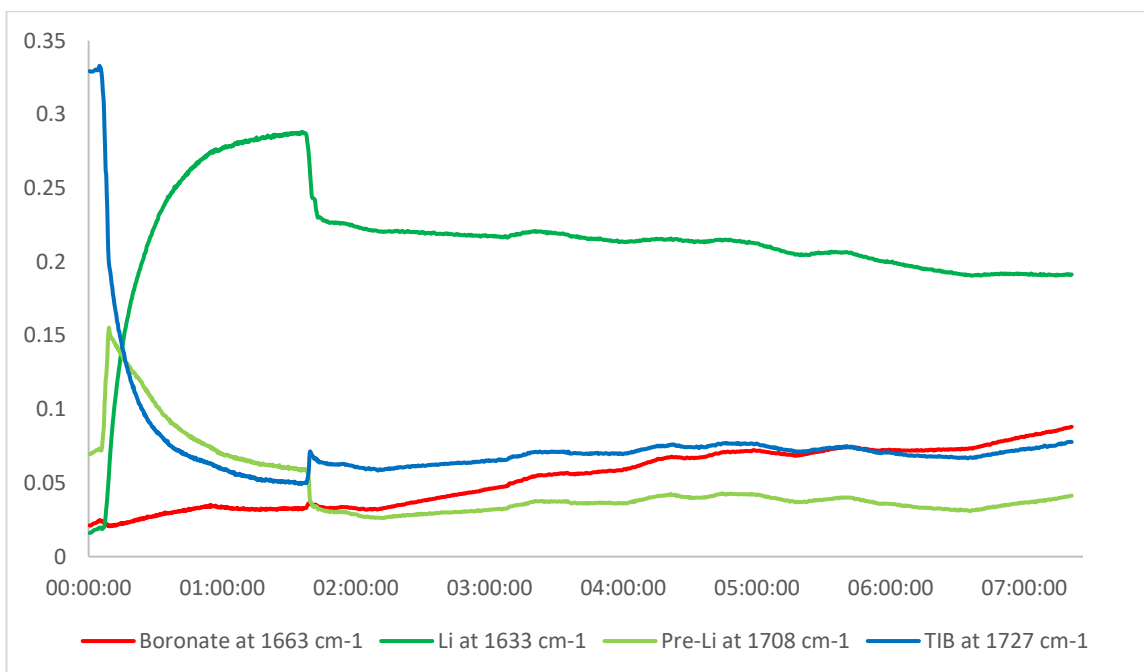
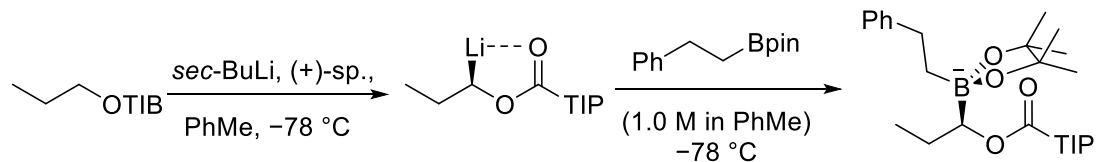
Entry 3 – Propyl carbamate in toluene



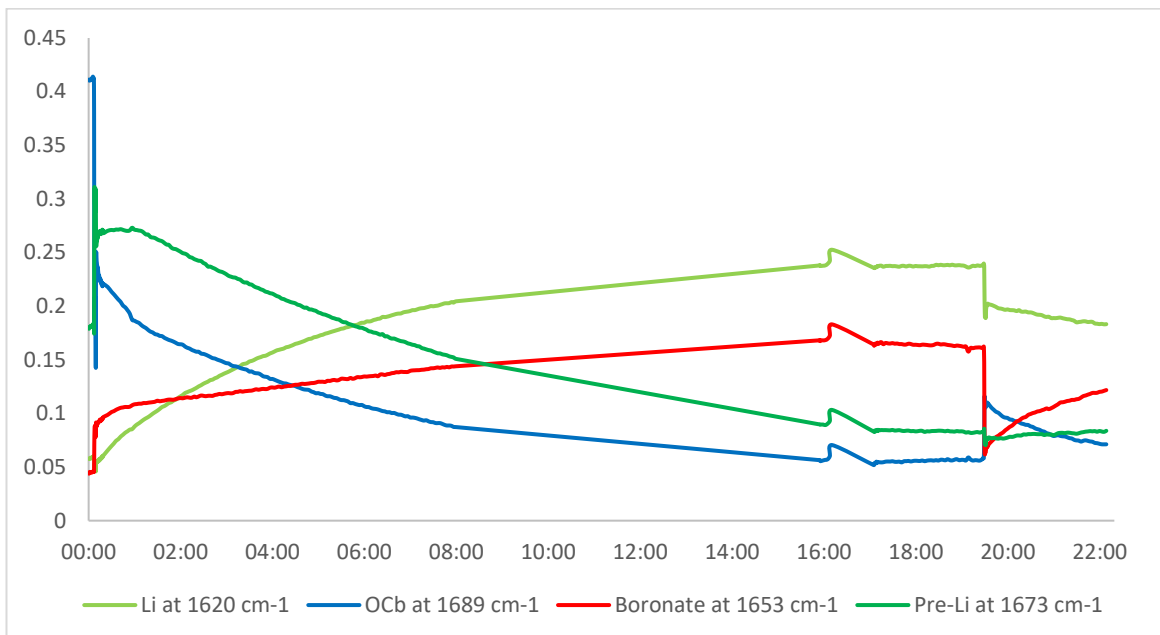
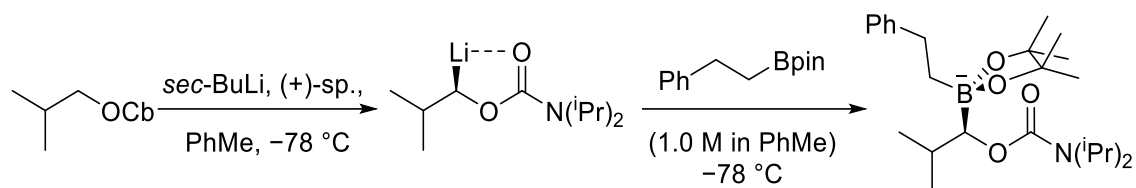
Entry 5 – Propyl TIB ester in TBME



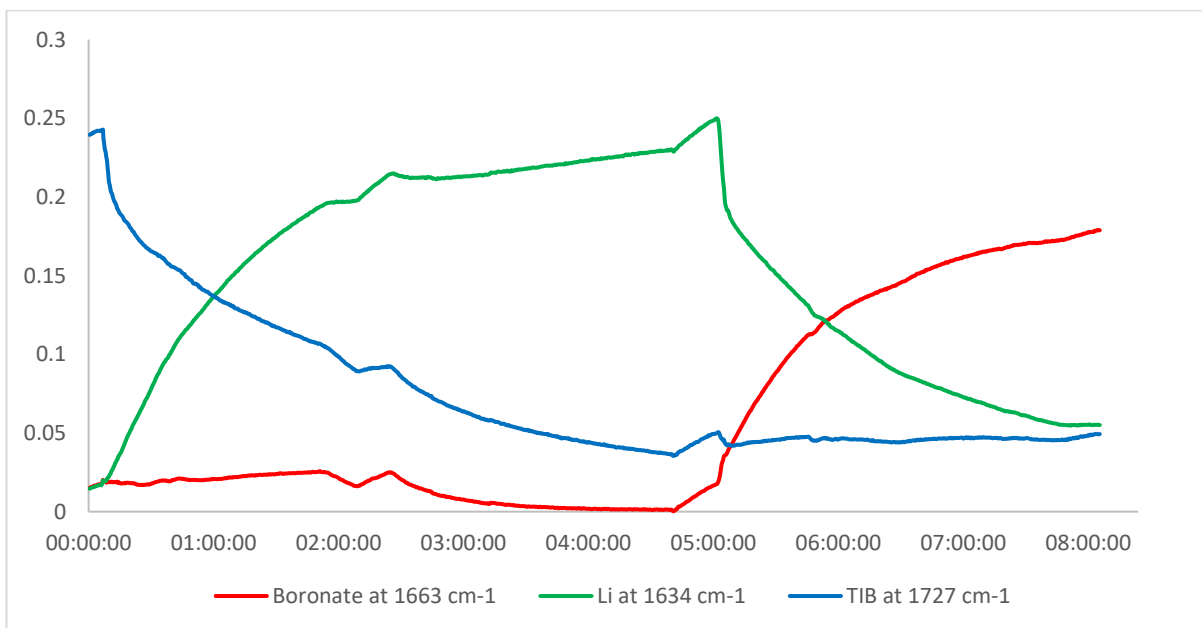
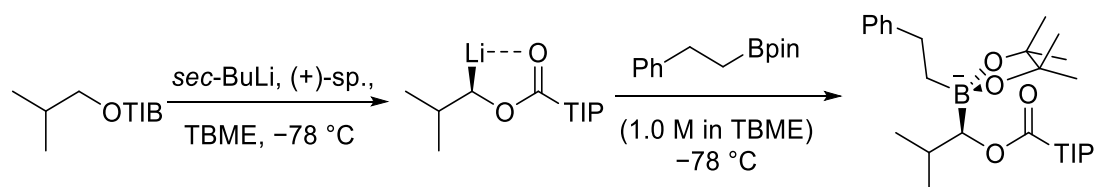
Entry 6 – Propyl TIB ester in toluene



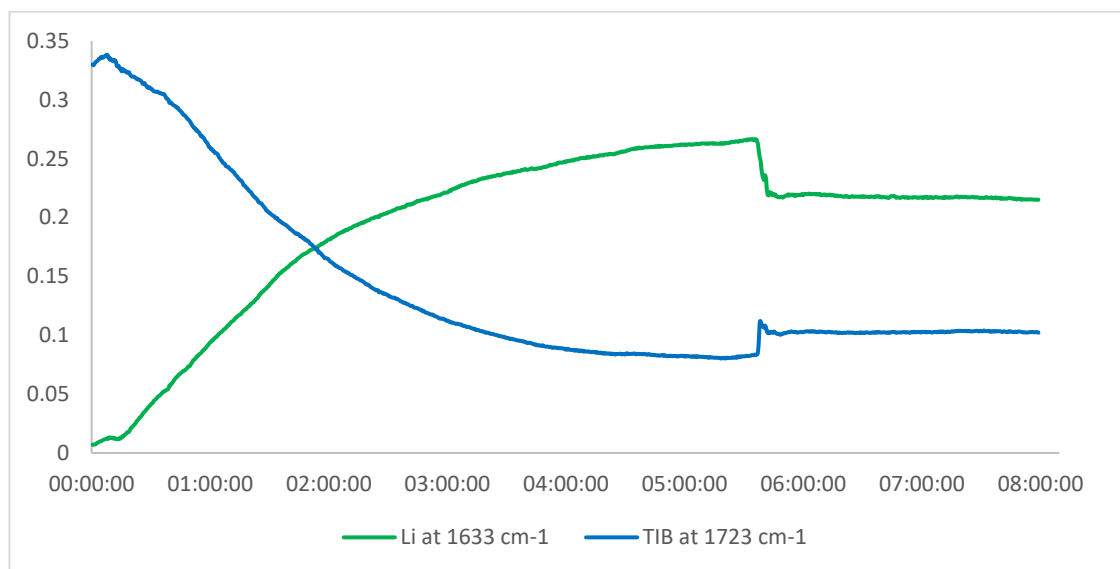
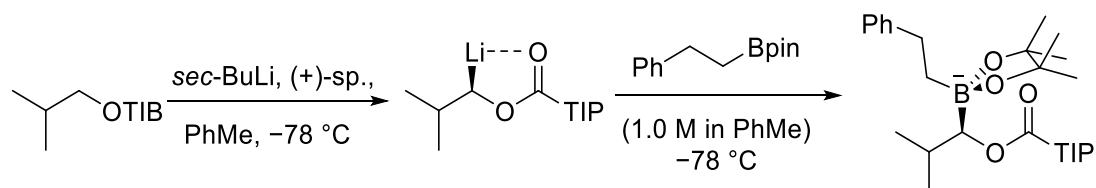
Entry 8 – Isobutyl carbamate in toluene



Entry 10 – Isobutyl TIB ester in TBME

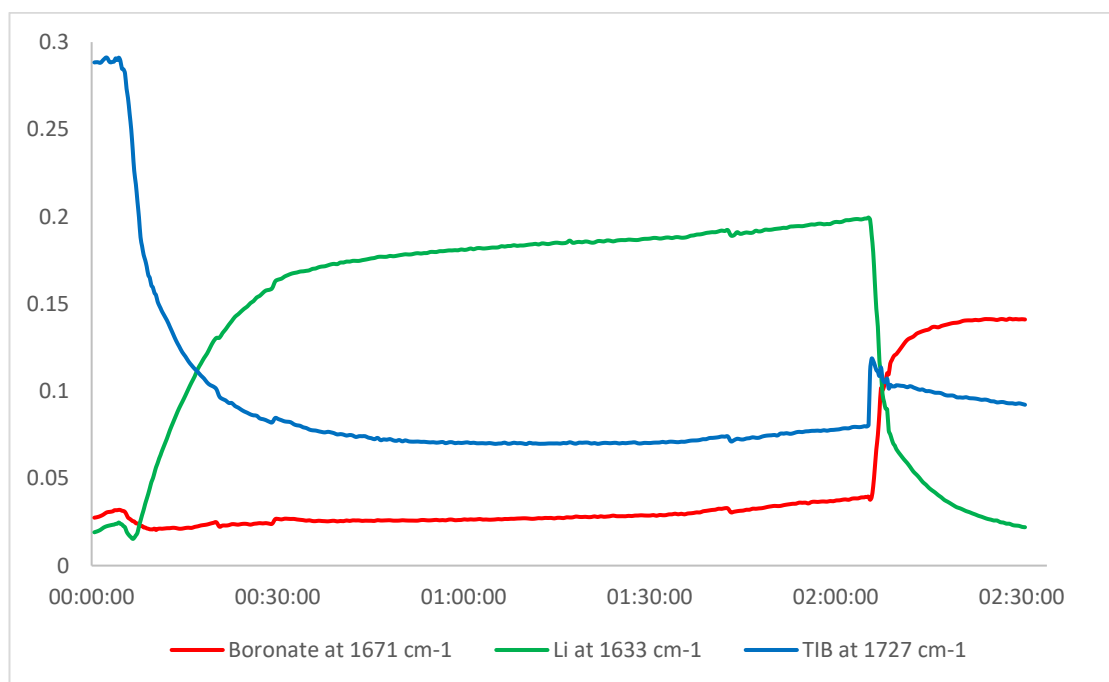
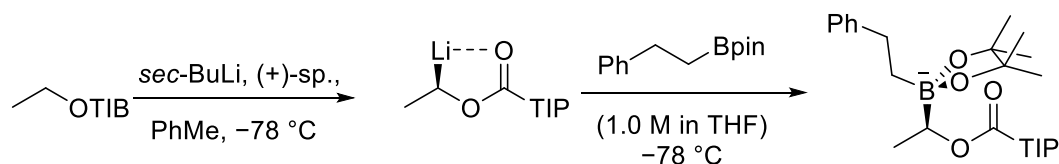


Entry 11 – Isobutyl TIB ester in toluene

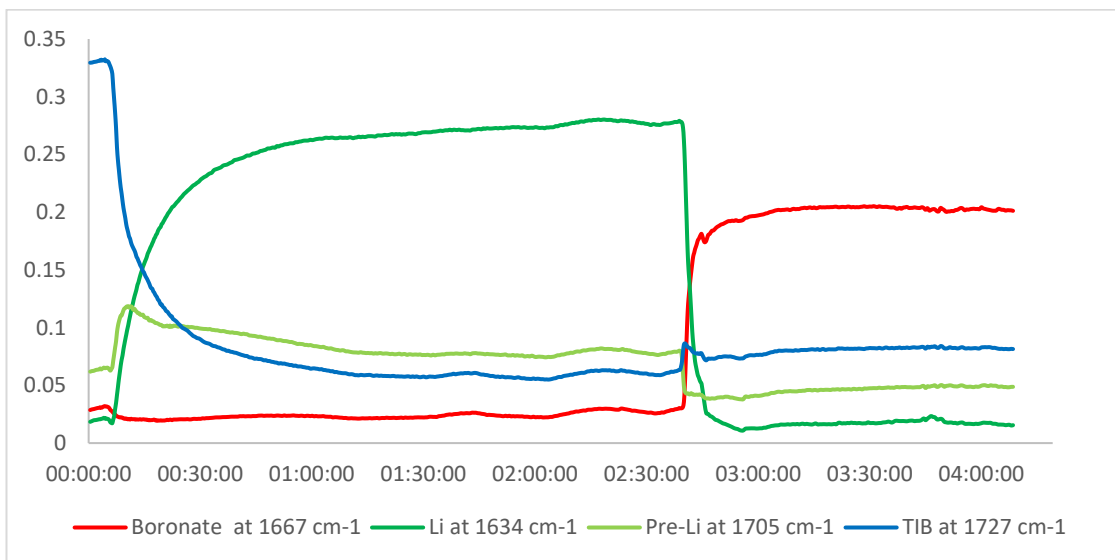
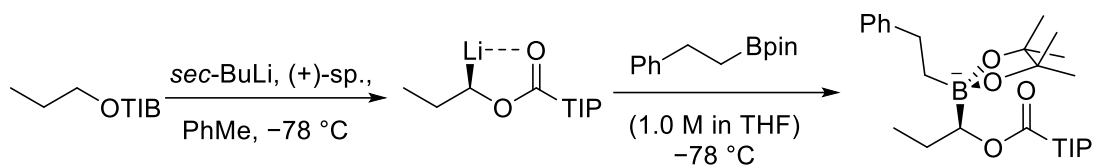


5.2.5.3 Table 3: Effect of THF on the rate of borylation

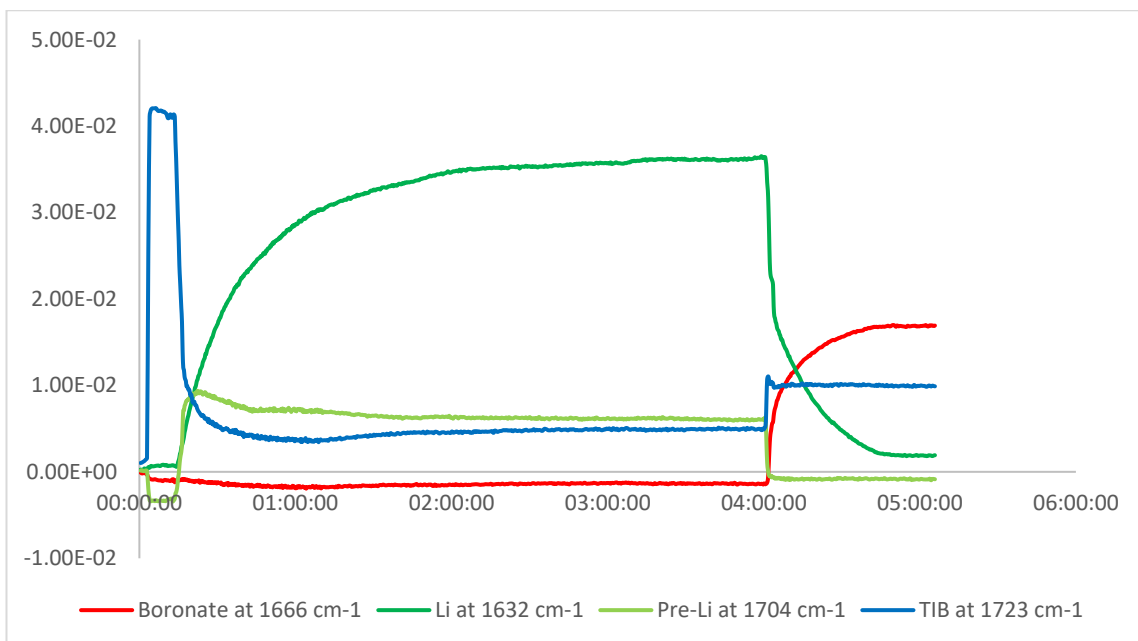
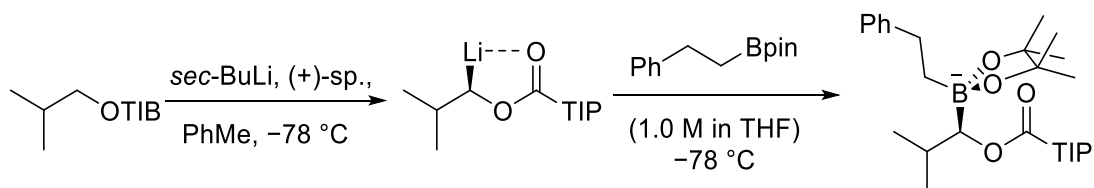
Entry 1 – Ethyl TIB ester “toluene/THF” conditions



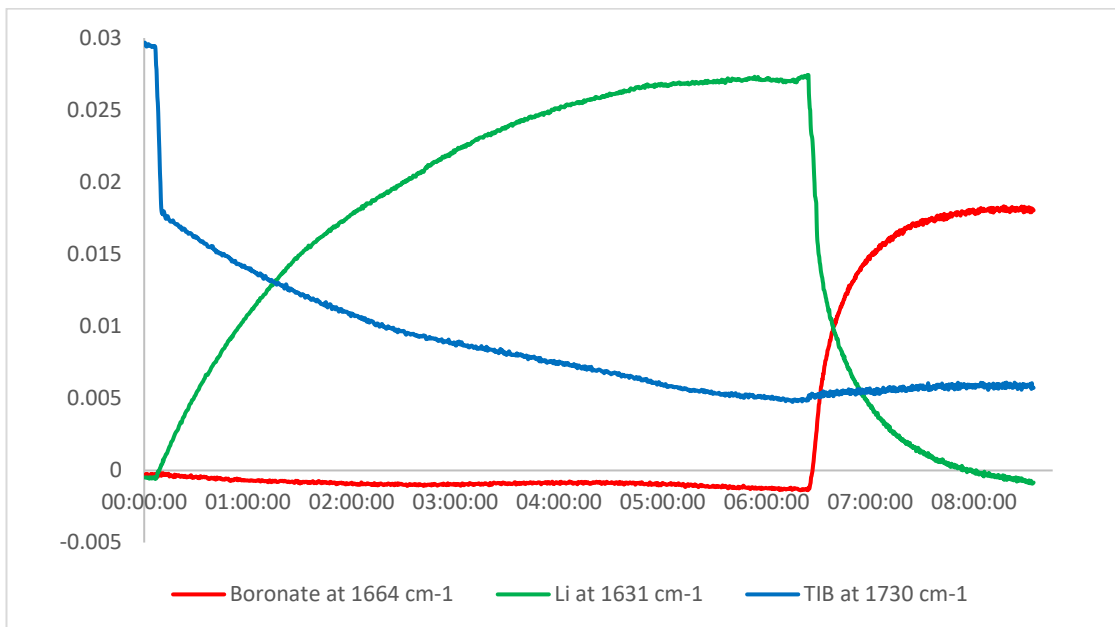
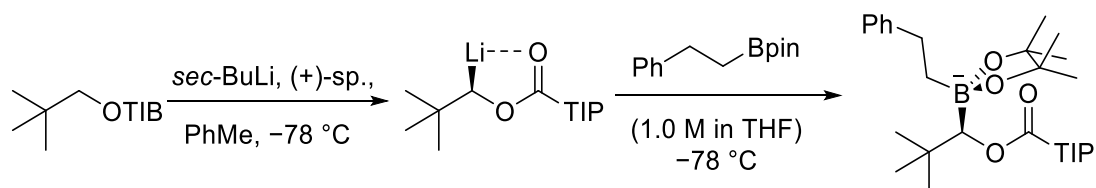
Entry 2 – Propyl TIB ester “toluene/THF” conditions



Entry 3 – Isobutyl TIB ester “toluene/THF” conditions

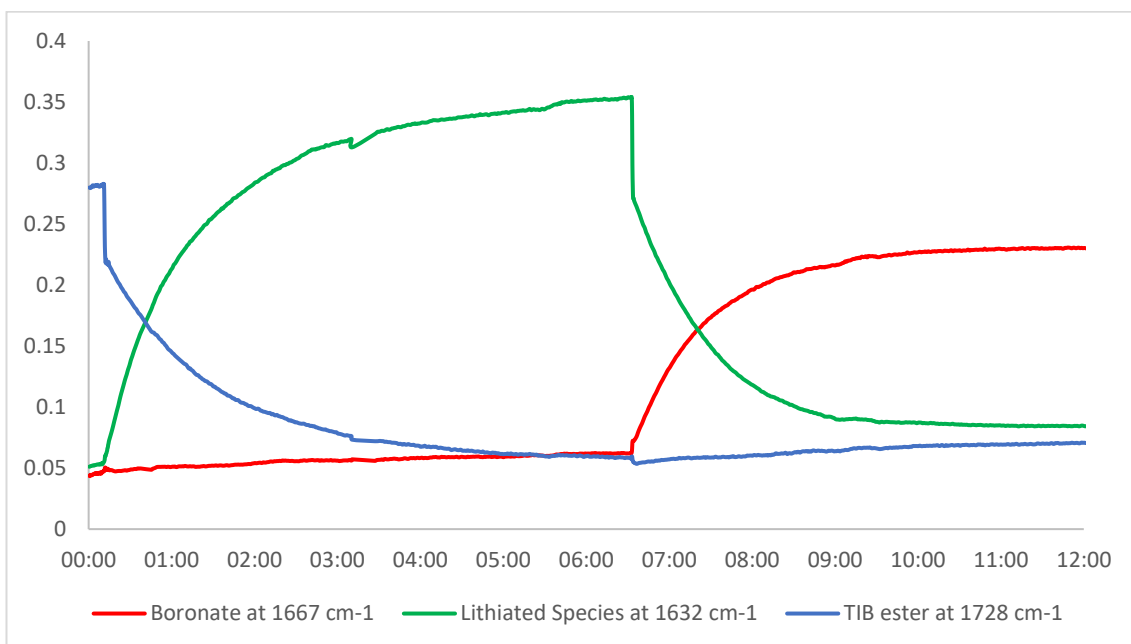
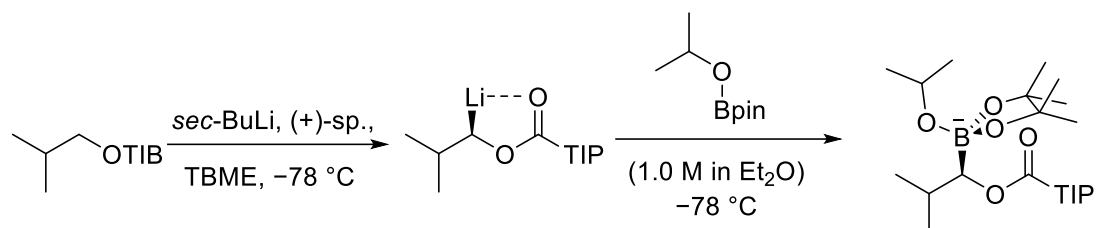


Entry 4 – Neopentyl TIB ester “toluene/THF” conditions



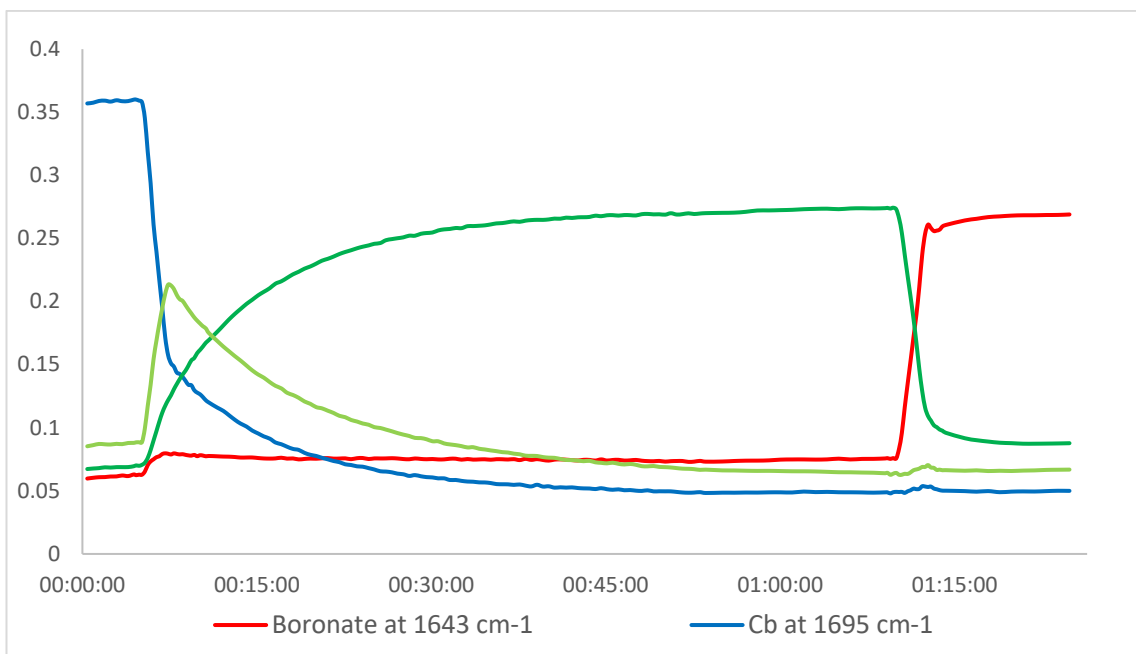
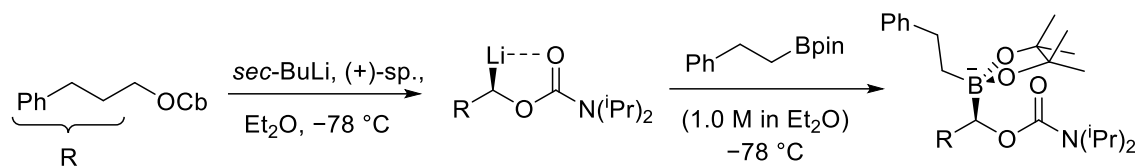
5.2.5.4 Effect of organoboron partner

Isobutyl TIB ester with isopropoxy boronic acid pinacol ester

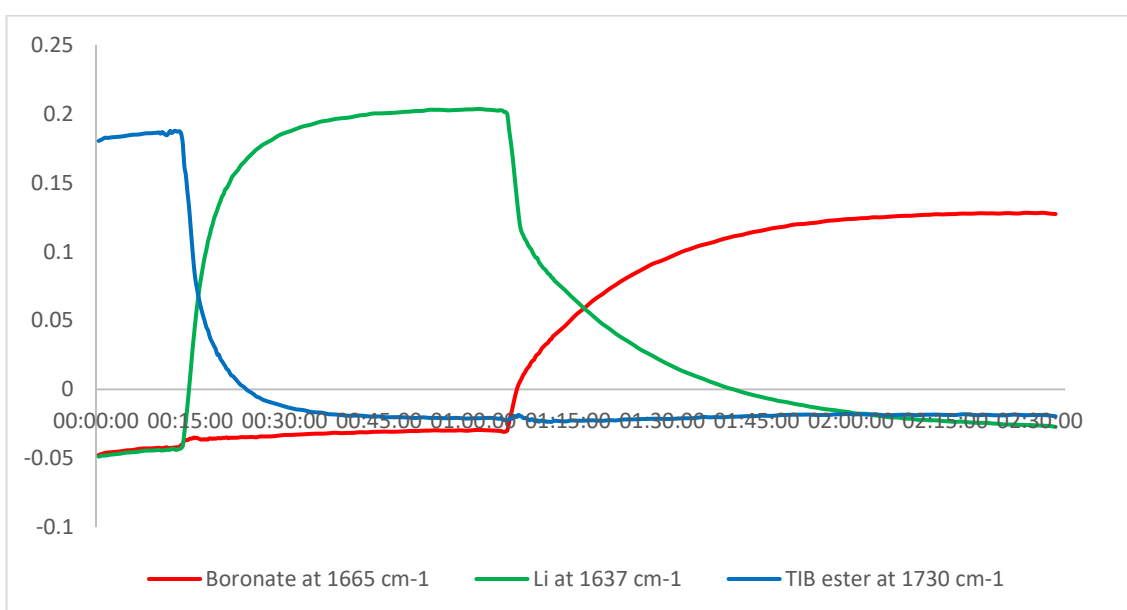
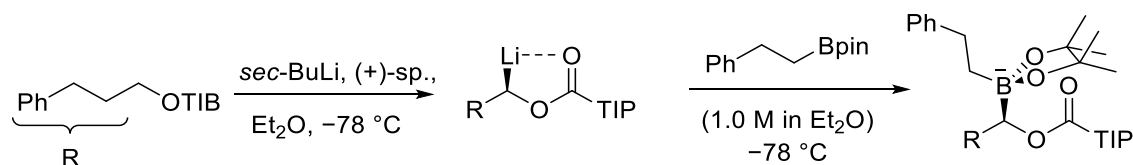


5.2.5.5 Table 4: Effect of a proximal aromatic group

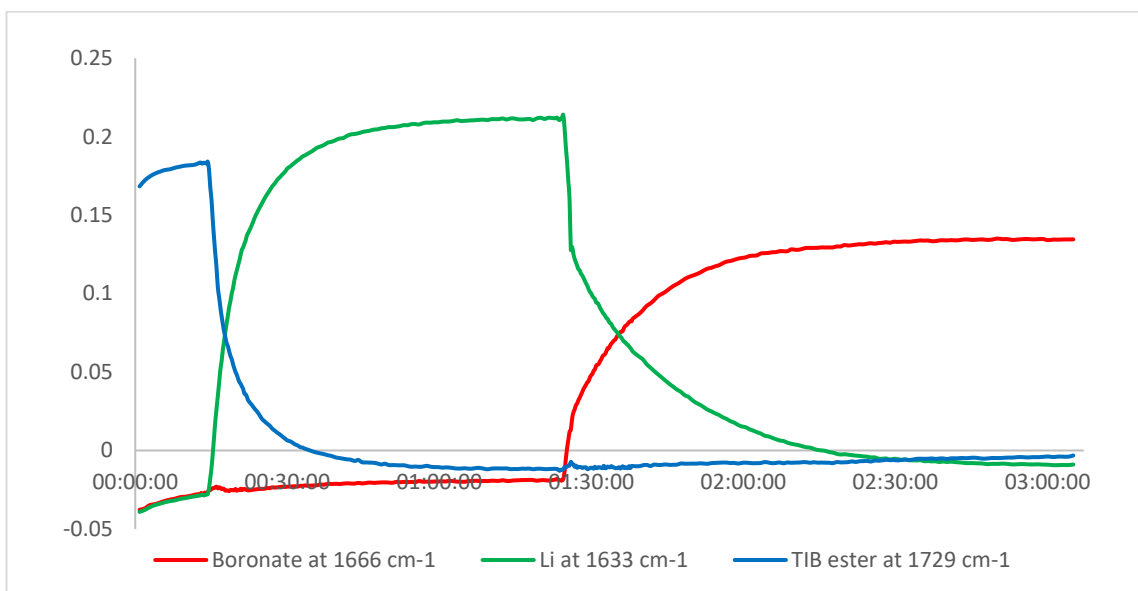
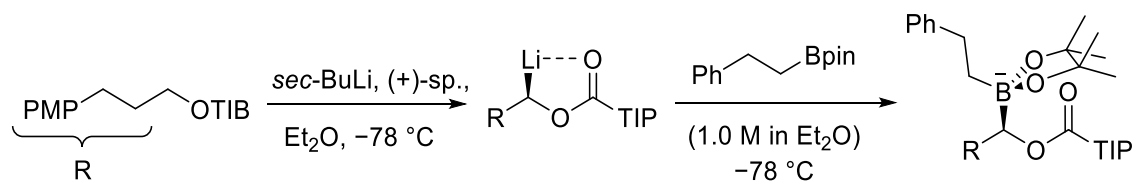
Entry 1 – 3-phenylpropyl carbamate



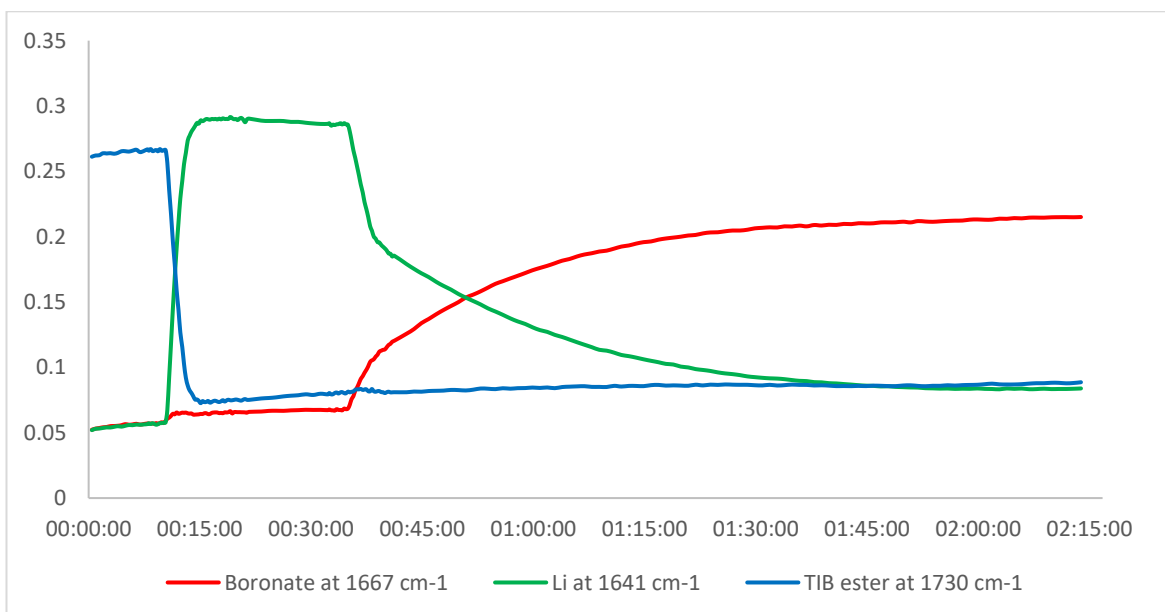
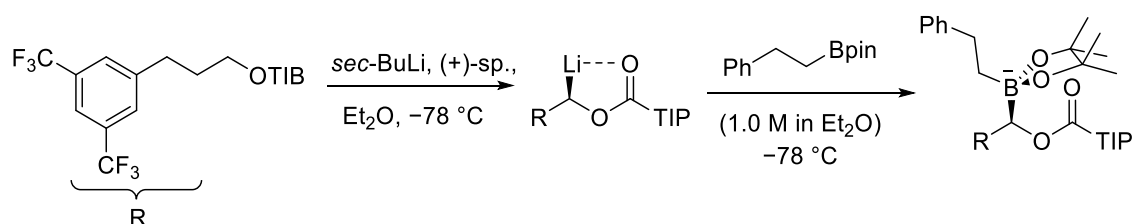
Entry 2 – 3-phenylpropyl TIB ester



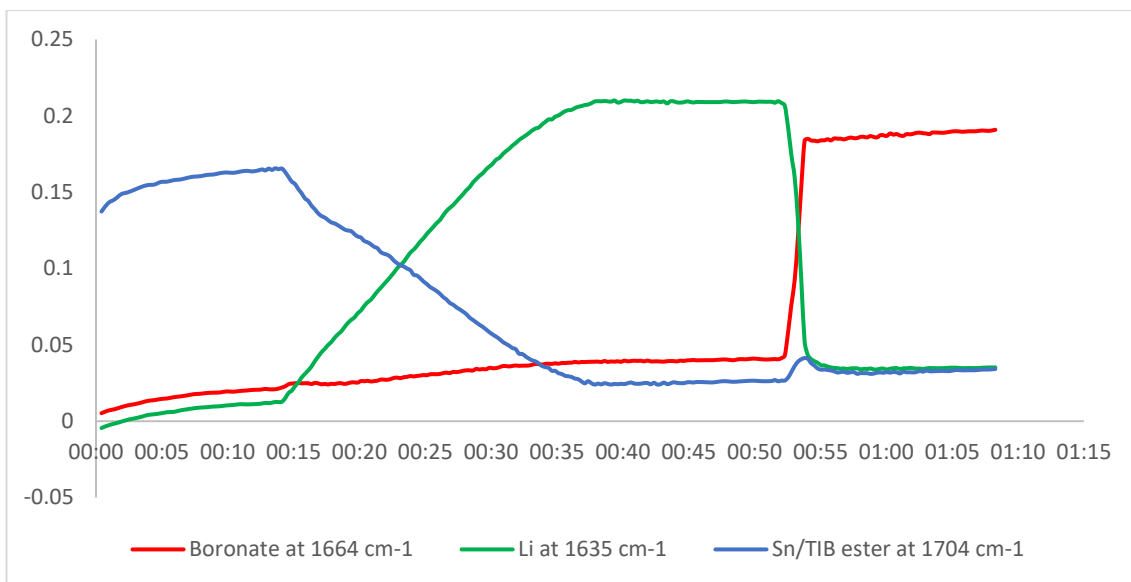
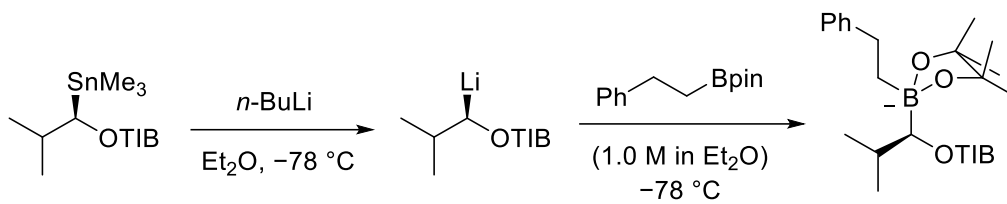
Entry 3 – 3-(*para*-methoxy)phenylpropyl TIB ester



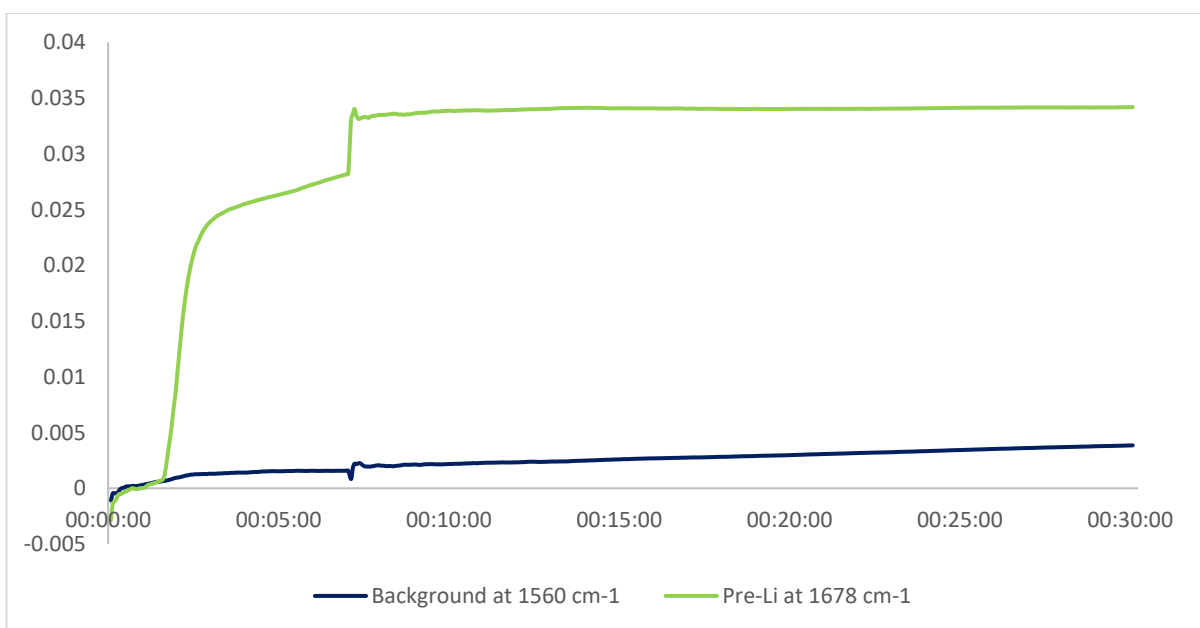
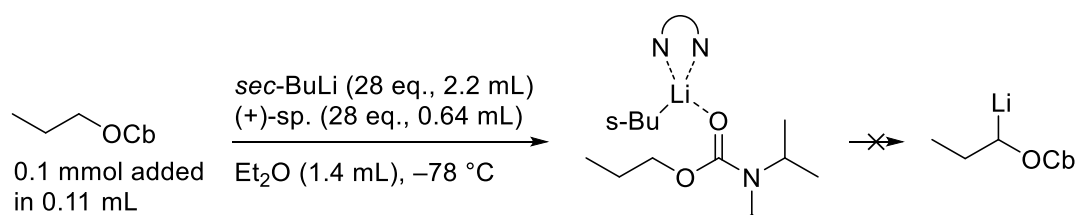
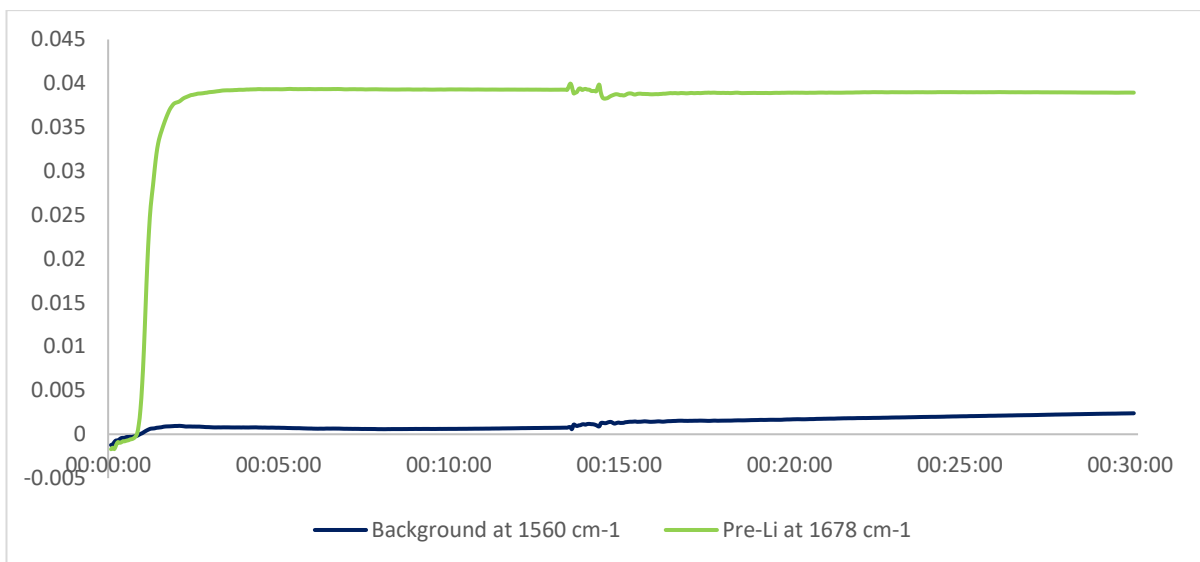
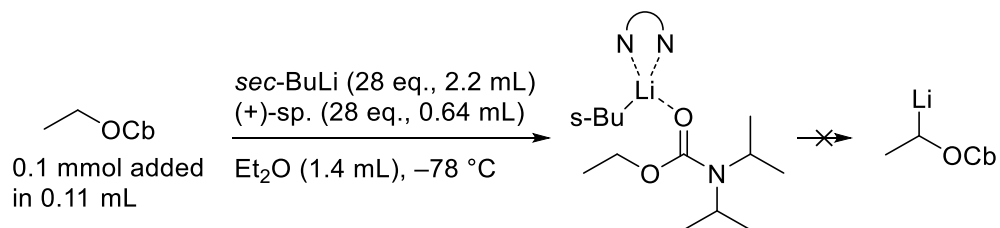
Entry 4 – 3-(3,5-bis(trifluoromethyl)phenyl)propyl TIB ester

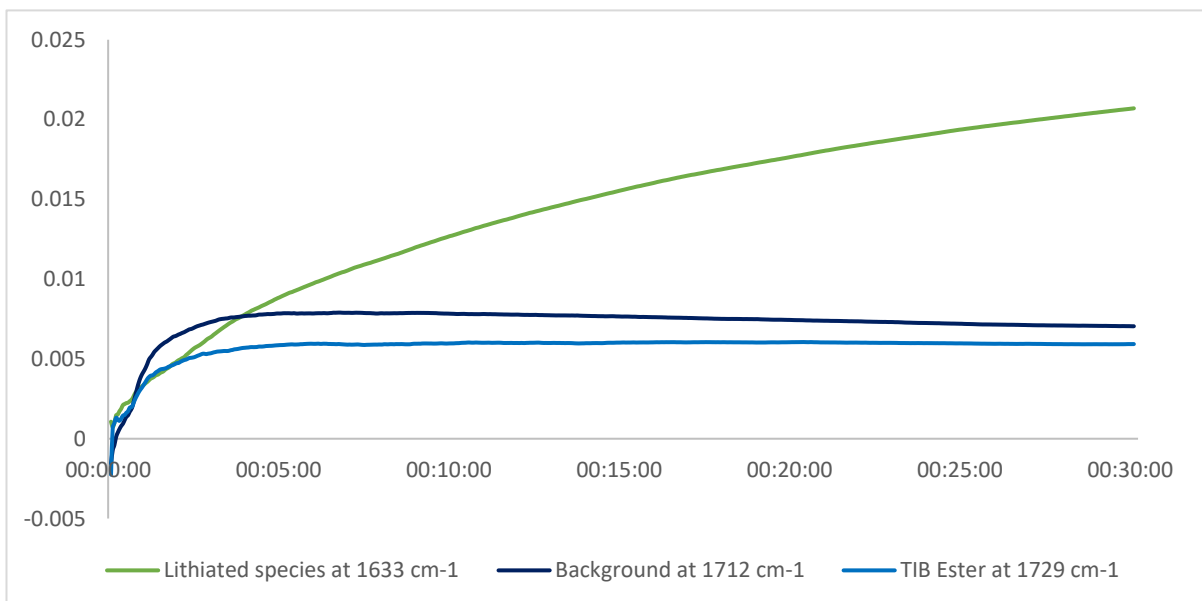
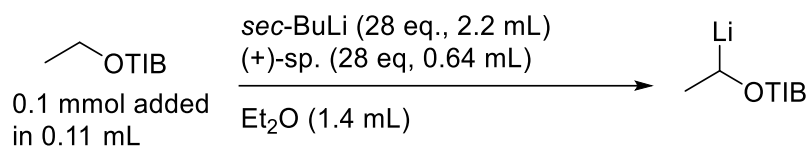
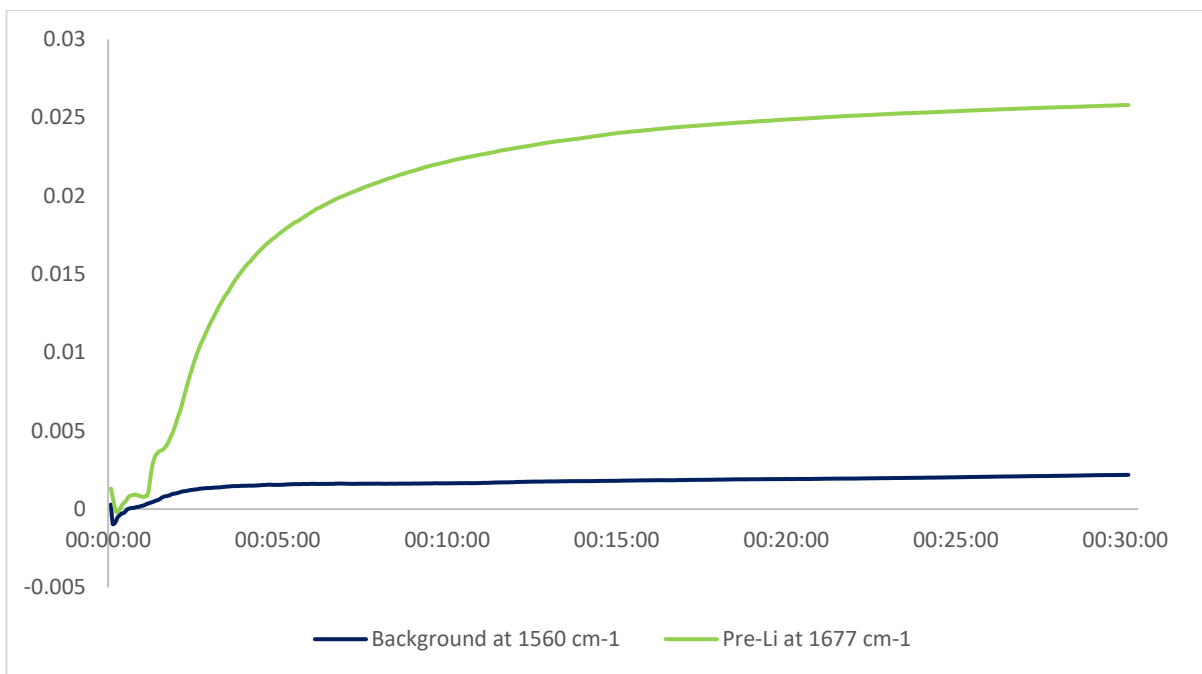
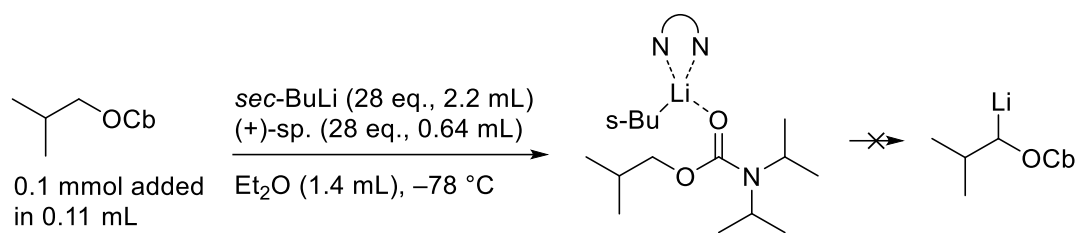


5.2.5.6 Study on tin–lithium exchange and effect of additives on borylation



5.2.5.7 Pseudo 1st Order





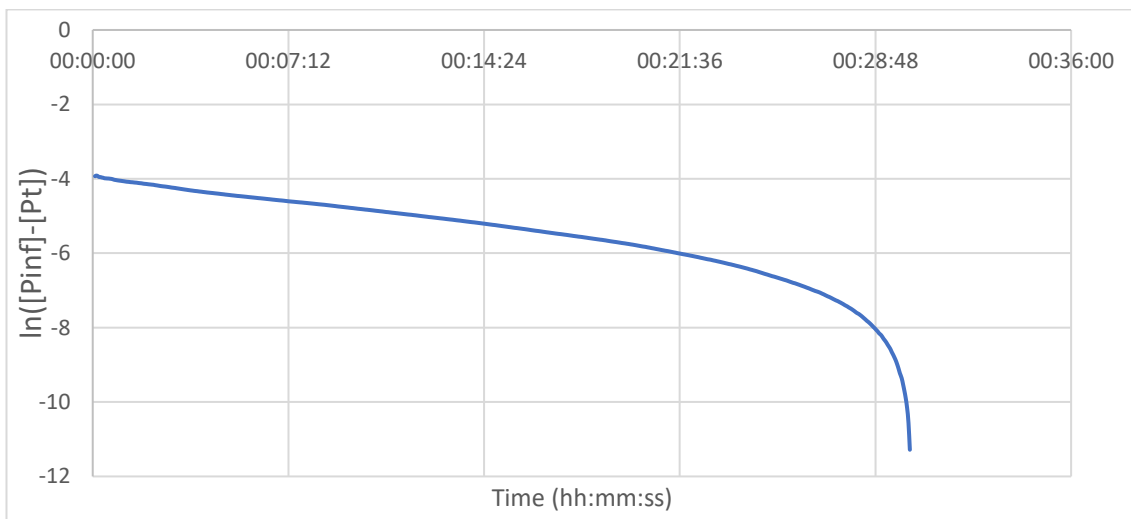
Final absorbance 0.030172

Plotting $\ln([P]_t)$ versus time (or similar) did not give a straight line ($[P]_t$ is concentration of product at time = t).

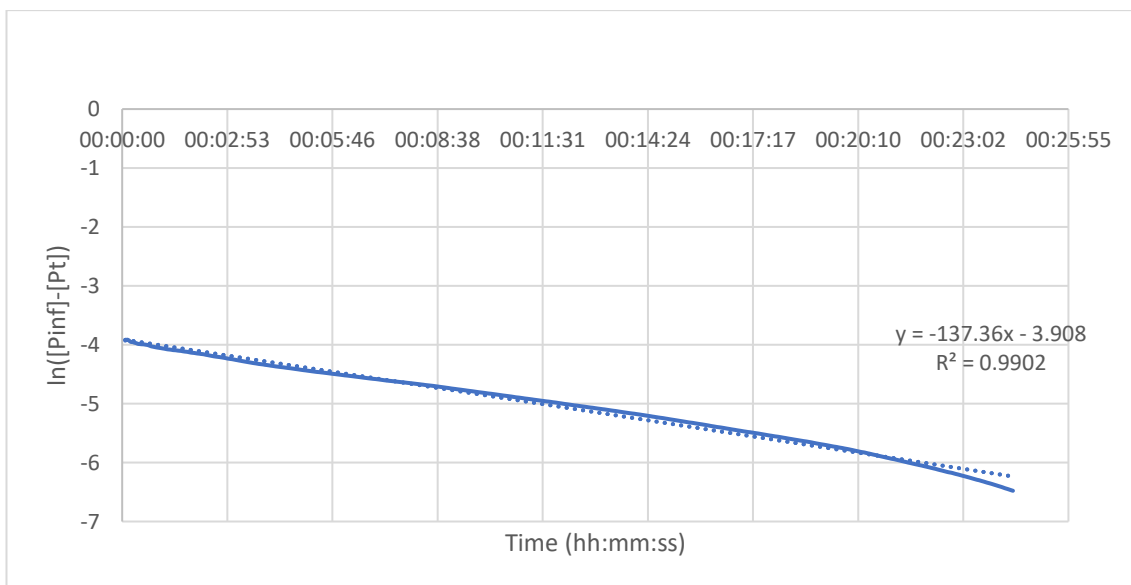
Clayden and co-workers have reported the first order kinetics of a reaction by following the product peak in an in situ IR spectroscopy experiment plotting $\ln([P]_\infty - [P]_t)$ versus time.^{152,153}

Using this method did give a section of straight line indicating the reaction is under pseudo first order kinetics:

Whole reaction:



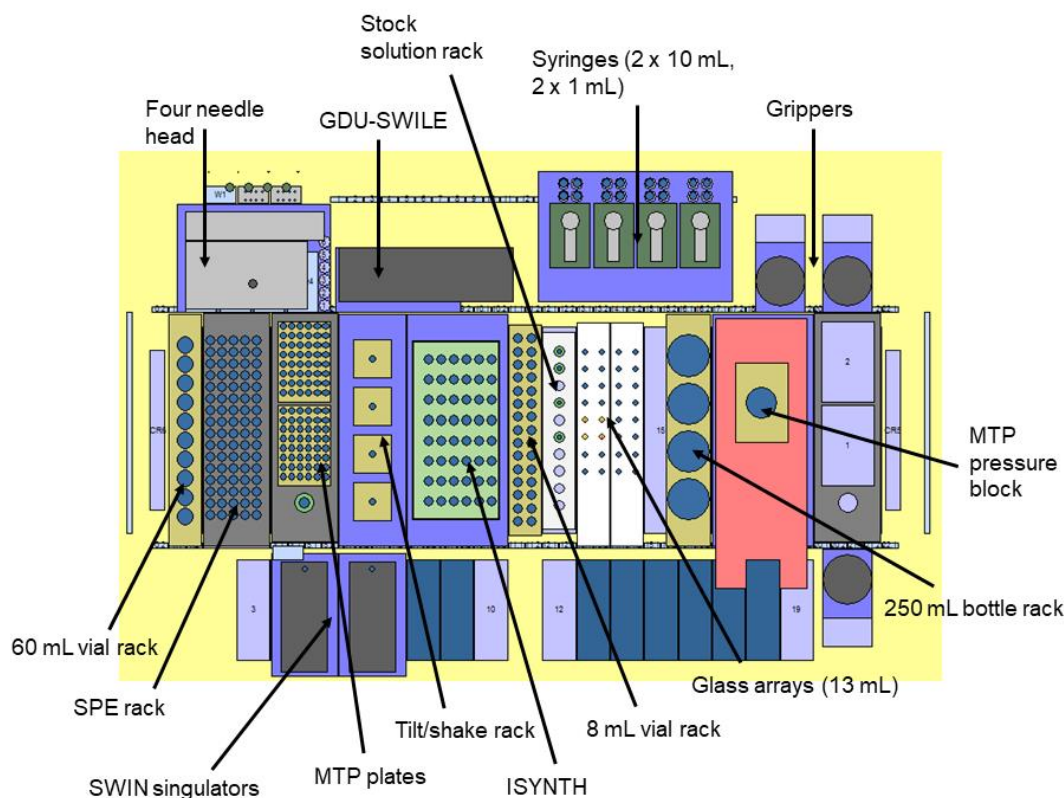
Straight section:



Attempts to plot $\frac{1}{[P]_\infty - [P]_t}$ versus time (or similar) did not give straight lines.

5.3 Automation

5.3.1 Chemspeed Platform



For complete and up to date workflows/functions in AutoSuite format please contact chem-basf@bristol.ac.uk with your enquiry.

System solvents: Reagent grade hexane was connected at valve port B and reagent grade THF was connected at valve port E, both were stored behind the platform. Anhydrous TBME was stored in the platform in a capped bottle. Once the platform was flushed with N₂ (2 h) the cap was removed and lines to valve port C placed in the bottle.

BuLi waste: A 250 mL Schott bottle was kept in the platform where waste n-BuLi from dispenses (extra volumes) or from the drying process was placed. This was then taken and quenched by the chemist manually.

Needle wash: The needles were washed with 0.2 mL of anhydrous TBME directly after dispenses to ensure full dispense of any material. This was implemented using sequential zones.

SPE filter cartridges: 400 ± 10 mg of 5% Et₃N treated silica¹⁵⁴ was used in 3 mL filter cartridges. For the stannane workflow only the cartridge was sealed with PTFE round the top of the cap.

Vacuum Procedure: See figure 20 for the stepwise vacuum procedure. This method was always used to avoid bumping of solvent. Solvent evaporation in the ISYNTH led to loss of material and so was performed in the glass array.

Primes. To remove other solvents and introduce a new one, or clean the lines, we used 19 mL solvent for the 10 mL syringes (source speed 30 mL min⁻¹, destination speed 70 mL min⁻¹, extra volume 0 mL, airgap 0 mL) and 13 mL for the 1 mL syringes (source speed 3 mL min⁻¹, destination speed 7 mL min⁻¹, extra volume 0 mL, airgap 0 mL). This was aspirated from the solvent lines and dispensed to waste. If we were worried about cross contamination (from say a protic solvent), we would use 2 or 3 times this amount. During the workflow, if the needles were unused for an hour or 2 incompatible reagents were used sequentially, we would use a “mini” prime, which was 9 mL for the 10 mL syringes and 3 mL for the 1 mL syringes (same specifics as above).

Stock solutions. We used stock solutions to dispense all reagents. The platform cannot dispense the last 2 mL from a 60 mL vial and the last ~0.8 mL from an 8 mL vial therefore stock solutions must be made in excess. Otherwise, pointed 8 mL vials were used.

Dialog Boxes. To ensure smooth running of the system, we used dialog boxes (a checklist) at the beginning of the workflow to ensure everything was included. An example from a lithiation–borylation workflow:

Task	Name	Parameter	Desc
1	Dialog Boxes	Execute Once	
2	Show Dialog	OK-Dialog: 'This workflow has N1 and N4 set up as 10 mL!'	
3	Show Dialog	OK-Dialog: 'Check the vortex.cfg file in C:\ProgramData\ChemSpeed\AutoSuite\Configurations\T101\Drivers which should match vortex.cfg on the Desktop!'	
4	Show Dialog	OK-Dialog: 'Place the nBuLi in this position'	
5	Show Dialog	OK-Dialog: 'Place the stannane in this position'	
6	Show Dialog	OK-Dialog: 'Place GC-MS vials here!'	
7	Macro Task	OK-Dialog: 'Place the filters in this position'	
8	Macro Task	Execute If 'ZoneSize(Starting_Bpin)=1'	
9	Show Dialog	Execute If 'ZoneSize(Starting_Bpin)>1'	
10	Show Dialog	OK-Dialog: 'Place the boronic ester in this position'	
11	Show Dialog	OK-Dialog: 'Place the DCE in this position'	
12	Show Dialog	OK-Dialog: 'Is your next step Matteson? Do you need to dry Product Zone as well? The zones highlighted are product and reactor zone!'	
13	Show Dialog	OK-Dialog: 'Is there enough system solvent?'	
14	Show Dialog	OK-Dialog: 'Have you put the BuLi waste in?'	
15	Show Dialog	OK-Dialog: 'Is the correct oil attached? NOT ISYNTH. If second run only 1 GA should be attached!'	
16	Show Dialog	OK-Dialog: 'Water on?'	
17	Show Dialog	OK-Dialog: 'Check all product / SM / filter / BuLi zones are correct!'	
18	Show Dialog	OK-Dialog: 'Is your math for SM and reagents correct?'	
19	Show Dialog	OK-Dialog: 'Check 180 any on 60 mL rack!'	
20	Show Dialog	OK-Dialog: 'Have you attached the dry TBME?'	
21	Show Dialog	OK-Dialog: 'Switch N2 on. Check N2 Time.'	
22	Show Dialog	OK-Dialog: 'Do you need a pause before reagent addition? (After drying).'	
23	Show Dialog	OK-Dialog: 'Have you parafilmed all vials?'	
24	Wait	OK-Dialog: 'Check your 1,2-migration time!'	
		Waiting for 2:00:00 hours	

Cleaning workflow. Performed when all glass array vessels were dirty.

The glass array vessels were cleaned (solvent was added, shaken at 600 rpm for 10 minutes, then solvent dispensed to waste) with H₂O:THF (1:1, 13 mL), then THF (8 mL), then hexane (4 mL). The vessels were then heated to 100 °C under vacuum (12 mbar) for 1 h. During this the needles aspirated and dispensed (to the same position) 1 M HCl (aq, 1 mL) 20 times, then H₂O (1 mL) 20 times and then were rinsed with THF primes (19 mL x 3).

Workflows consisted of 3 main parts: Drying, Reaction, Filtration

Before drying the reactors were placed under vacuum (as low as possible, set to 0 mbar) for 2 minutes and then back to inert gas (15 s) to properly flush them with inert gas. This was done 3 times.

Drying. The drying procedure was the same regardless of workflow. Dispense volumes did not need to be incredibly accurate in this section so rapid aspiration volumes were used. A large air gap (1 mL) was used to prevent n-BuLi mixing with the system solvent.

n-BuLi (4 mL, aspiration = 20 mL min⁻¹, dispense = 20 mL min⁻¹, extra volume = 0 mL, air gap = 1 mL) was added to each vessel with a 10 mL syringe, which was then stirred for 10 minutes. TBME (1 mL, aspiration = 20 mL min⁻¹, dispense = 20 mL min⁻¹, extra volume = 0 mL, air gap = 1 mL) was then added and the mixture removed to a waste 250 mL bottle inside the platform. Anhydrous TBME (4 mL, aspiration = 20 mL min⁻¹, dispense = 20 mL min⁻¹, extra volume = 0 mL, air gap = 1 mL) was then added from line C, stirred for 5 minutes then removed to the same waste.

Reaction. Transfers of reagents: aspiration = 2 mL min⁻¹, dispense = 2 mL min⁻¹, extra volume = 0.1 mL, air gap = 100 µL. **These were our default transfer parameters and are used unless stated otherwise.** We found the parameters shown gave high accuracy in volumetric dispenses of 100 µL of TBME from 10 mL syringes and 40 µL with 1 mL syringes. For small dispenses (<200 µL) the needle tip should be in the solution at the end of the dispense. A needle wash was always used. It is convenient to parafilm the tops of reagents inside the platform: this keeps them sealed to avoid solvent evaporation however the needle can easily pierce the parafilm. The extra volume was dispensed to the source zone and the air gap to the destination zone. See specific reactions below for full procedures.

Filtration. SPE “Sampling” Function. We found with 400 mg of SiO₂ in a 3 mL cartridge 0.8 mL to be a safe quantity to filter per time. Source speed 20 mL min⁻¹, destination speed 1 mL min⁻¹, extra volume 0 mL, airgap volume 2 mL. The airgap was immediately dispensed to the destination zone following a “sample” to ensure full elution. The air gap speed was set to 2 mL min⁻¹ in the configuration. 10 s equilibration was used after each stroke. The 0.2 mL needle wash was also used post each “sample”.

Air Push Function. Quantity 9 mL, source speed 20 mL min⁻¹, destination speed 2 mL min⁻¹, extra volume & air gap volume both 0 mL. “Air” was aspirated from above the

SPE filters and dispensed into them to ensure full elution of filtered material therefore preventing solvent spills. This filled the lines with bubbles and so “mini primes” (9 mL solvent) were always used after air pushes.

The filtration was performed using non-anhydrous solvent, with hexane as the system solvent.

Stannane homologation only: After the reaction sequence had finished the solvent (TBME) was removed as per the vacuum procedure (Figure 20 main text). The crude material was then redissolved in 1,2-DCE (3 mL). The SPE cartridges were already sealed with PTFE tape around the top (not covering the hole).

Cartridge wetting. 0.8 mL TBME was dispensed to the SPE cartridges over the waste position then an air push performed.

First filtration. The number of “samples” to be performed was calculated by the reaction total volume (the sum of *n*-BuLi, carbenoid precursor and boronic ester dispenses) divided by the sampling volume (0.8 mL) with 2 added on (to make sure the full volume was taken. For the stannane workflow the total volume is 3 mL (DCE added). This was then performed with a loop over [stir 30 s, sample, needle wash, air push, prime]. Once all material had been filtered this was then taken from the SPE vials to the glass array using a 60 μ L extra volume dispensed to a 2 mL vial for offline GC-MS analysis. Importantly the vials under the SPE rack are 8 mL total volume so if this amount is ever exceeded then 2 transfer and vac down procedures are required.

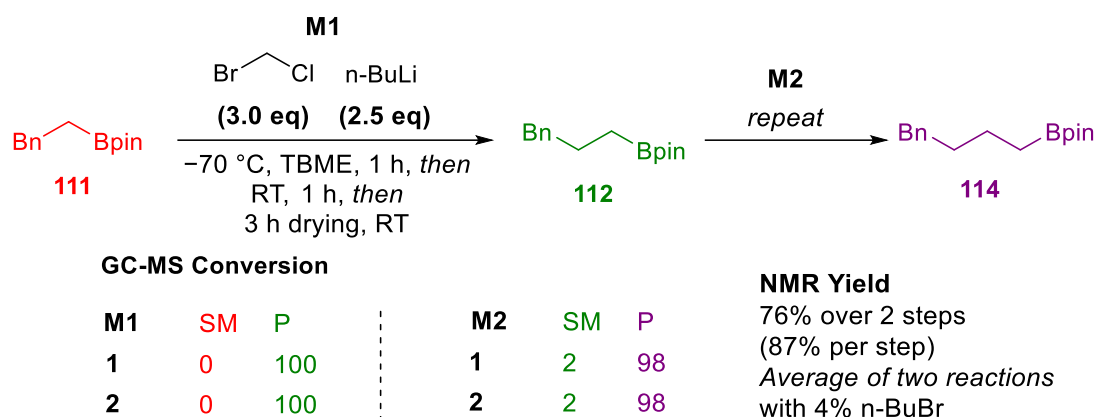
Second and third filtration. Same as above using 3 mL TBME (Matteson) or DCE (stannane) to rinse with no GC-MS sample taken. This was repeated twice to give 3 filtrations in total.

Filter rinse. The filters were then rinsed with 5 x samples of TBME (both Matteson and stannane). This was then taken to the glass array and solvent removed.

Vial rinse. The vials beneath the SPE rack were then rinsed with 7 mL TBME which was then taken to the glass array and the solvent removed.

Final drying. The product was then dried for 3 h at 12 mbar (the lowest our glass arrays would go without overworking the vacuum pump) to ensure dryness for the next step.

Matteson



Iteration 1 and 2 (**M1** & **M2**) stock solutions:

We prepared the stock solutions fresh before each step.

BrCH₂Cl: (0.402 mL, 6.2 mmol) in 4.8 mL TBME. Total volume (V_{tot}) = 5.2 mL

$$c = \frac{n}{v} = \frac{6.2}{5.2} = 1.19 \text{ mmol mL}^{-1}$$

BnCH₂Bpin: (0.348 g, 1.5 mmol) in 3.8 mL TBME. V_{tot} = 3.8 mL

$$c = \frac{n}{v} = \frac{1.5}{3.8} = 0.39 \text{ mmol mL}^{-1}$$

n-BuLi: (24 mL). 4 x 5 mL for reactor drying (reactor and product zones) + 2 mL for reactions + 2 mL spare.

Iteration 1 (**M1**) reaction volumes: (0.25 mmol scale)

BrCH₂Cl: (3 eq = 0.75 mmol); $V = \frac{n}{c} = \frac{0.75}{1.19} = 0.630 \text{ mL}$.

BnCH₂Bpin: (1 eq = 0.25 mmol); $V = \frac{n}{c} = \frac{0.25}{0.39} = 0.641 \text{ mL}$.

n-BuLi: (2.5 eq = 0.625 mmol); $V = \frac{n}{c} = \frac{0.625}{1.6} = 0.391 \text{ mL}$.

Concentration of boronic ester is $\frac{0.25}{0.63+0.641} = 0.2 \text{ M}$ upon addition of n-BuLi, as per the manual procedure.

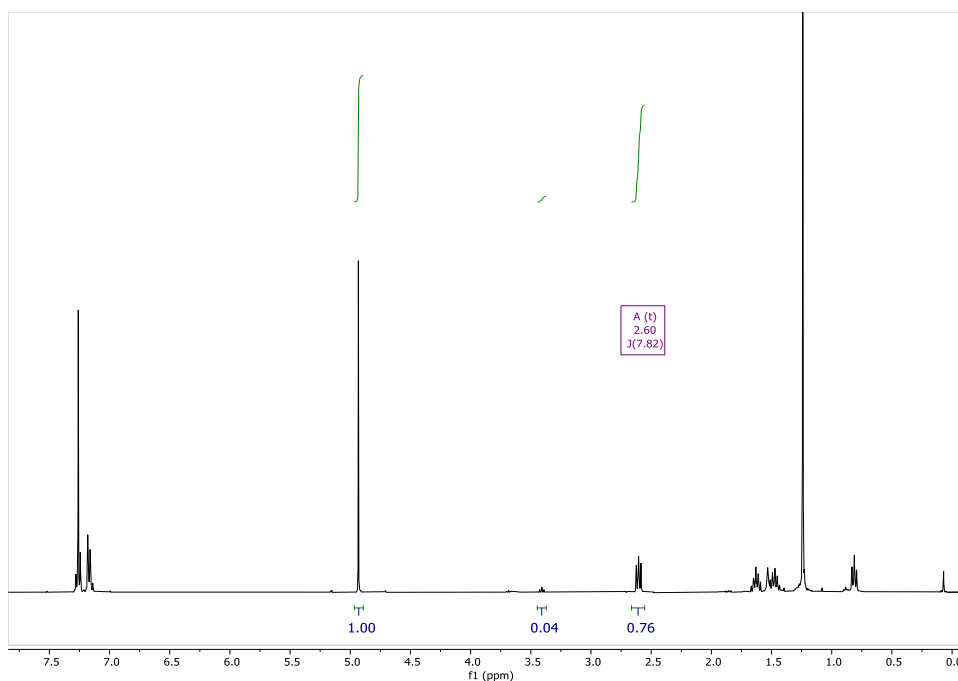
For iteration 2 (**M2**) we assumed a 90% yield for the first step and so reduced the amounts above by 90%, the same as doing the reaction on a 0.225 mmol scale. For the second step the boronic ester is not dispensed as a stock solution (see procedure) and so instead the equivalent volume of TBME is dispensed onto the boronic ester to achieve the correct concentration.

Procedure:

First the reactor and product zones are dried as the drying procedure. We dry the product zones now (where the product goes after filtration) as then the next Matteson step can be performed directly in the same zone, therefore saving reactor vessels, and preventing losses of material in an unnecessary transfer. BnCH_2Bpin and BrCH_2Cl were dispensed using default parameters and the volumes above. The reactors were then cooled to $-70\text{ }^\circ\text{C}$ ($-78\text{ }^\circ\text{C}$ internal setting on the cryostat, $10\text{ }^\circ\text{C min}^{-1}$) and stirred (600 rpm) at this temperature for 30 mins to equilibrate. The stirring rate was increased to 800 rpm and $n\text{-BuLi}$ was then dispensed (volume above, 0.1 mL min^{-1} dispense speed) and the reactors further stirred (600 rpm) for 1 h. The reactors were then warmed to $22\text{ }^\circ\text{C}$ (RT, $10\text{ }^\circ\text{C min}^{-1}$) and stirred (600 rpm) for 1 h. The reactors were then filtered as per the filtration process.

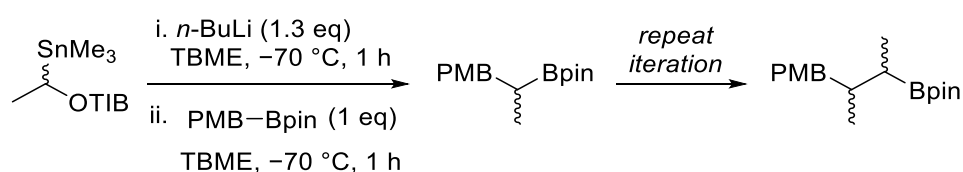
The second iteration was then performed in the same fashion except there was no drying performed, and the addition of TBME directly to the boronic ester starting material.

^1H NMR analysis we compared against known signals at $\delta = 2.60\text{ ppm}$.^{155,156} Example:



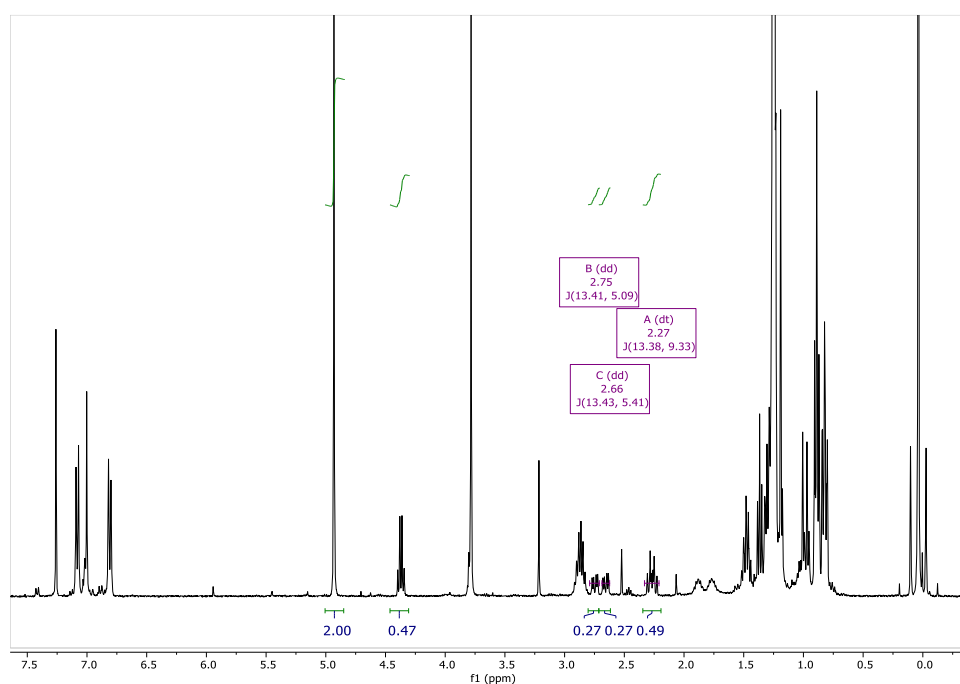
CH_2Br_2 (0.25 mmol, 1 eq) was added manually at the end of **M2** and the analysis conducted straightaway. Integrating the peak for CH_2Br_2 ($\delta = 4.93\text{ ppm}$) as 1H gives a 76% yield over 2 steps with 4% remaining 1-bromobutane.

Homologation with stannane 41

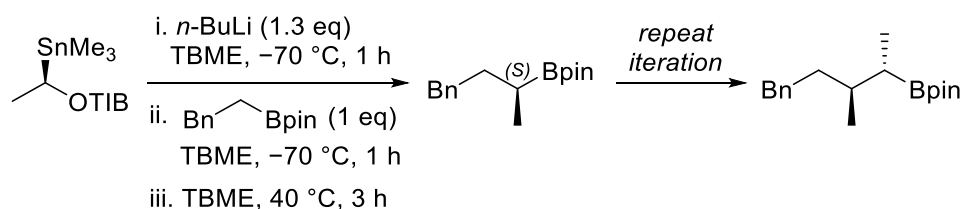


See below for procedure.

^1H NMR analysis we compared to known signals at $\delta = 2.75/2.26$ ppm.⁸¹ Example:



CH_2Br_2 (0.25 mmol, 1 eq) was added manually at the end of the second iteration and the analysis conducted straightaway. Integrating the peak for CH_2Br_2 ($\delta = 4.93$ ppm) as 2H gives a 49% yield over 2 steps (using the peak at $\delta = 2.27$ ppm which is the two diastereomers together). The other two signals are each diastereomer in a 1:1 ratio.



Iterations 1 and 2 stock solutions:

We prepared the stock solutions fresh before each step.

Sn 41: (0.439 mg, 1 mmol) in 4.6 mL TBME. Total volume (V_{tot}) = 4.8 mL

$$c = \frac{n}{v} = \frac{1}{4.8} = 0.208 \text{ mmol mL}^{-1}$$

BnCH₂Bpin: (0.464 g, 2 mmol) in 1.5 mL TBME. V_{tot} = 1.9 mL

$$c = \frac{n}{v} = \frac{2}{1.9} = 1.05 \text{ mmol mL}^{-1}$$

n-BuLi: (14 mL). 2 x 5 mL for reactor drying + 2 mL for reactions + 2 mL spare.

Iteration 1 reaction volumes: (0.25 mmol scale)

Sn **41**: (1.3 eq = 0.325 mmol); $V = \frac{n}{c} = \frac{0.325}{0.208} = 1.563$ mL.

BnCH₂Bpin: (1 eq = 0.25 mmol); $V = \frac{n}{c} = \frac{0.25}{1.05} = 0.238$ mL.

n-BuLi: (1.3 eq = 0.325 mmol); $V = \frac{n}{c} = \frac{0.325}{1.6} = 0.203$ mL.

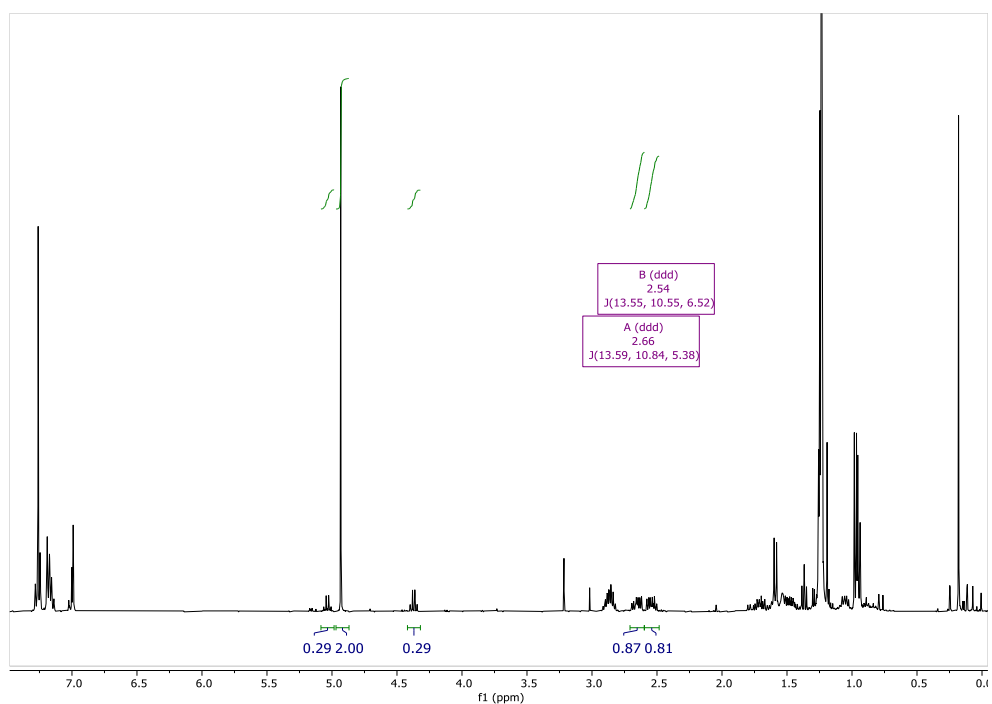
Concentration of Sn **41** is ~0.2 M upon addition of n-BuLi and the boronic ester is added as a ~0.1 M solution, as per the manual procedure.

Procedure:

First the reactor zones are dried as per the drying procedure. The product zones were not dried as the boronic ester is to be transferred to another zone, however this could be done if desired or if the next step is a Matteson reaction. Sn **41** was then dispensed to the glass array using the default parameters above. The reactors were then cooled to -70 °C (-78 °C internal setting on the cryostat, 10 °C min⁻¹) and stirred (600 rpm) at this temperature for 30 mins to equilibrate. *n*-BuLi was then dispensed using the default parameters and volumes above at the reactions stirred at 600 rpm for 1 h. The stirring was then increased to 800 rpm and the boronic ester transferred using default parameters (except 1 mL min⁻¹ dispense). The stirring was slowed to 600 rpm and stirred for 1 h. The reactors were then warmed to a suitable 1,2-migration temperature for a suitable time (40 °C for 3 h for this boronate complex) to give full 1,2-migration. The reactors were then cooled to 18 °C and stirred for 10 mins to ensure removal of heat. The reactions were then filtered as per the filtration process.

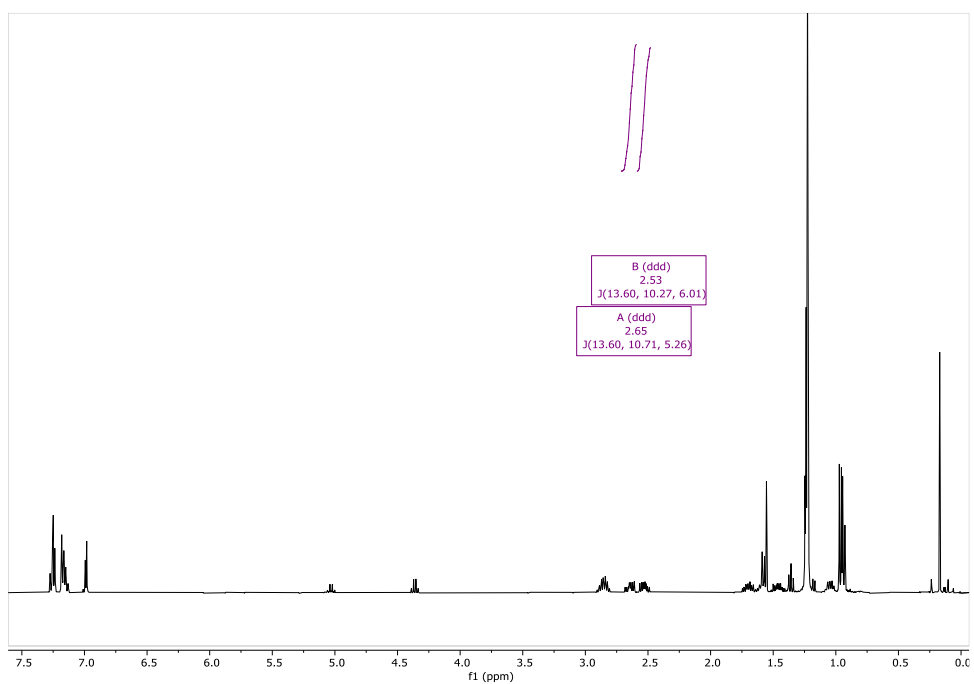
For iteration 2 we assumed a 90% yield for the first step and so reduced the amounts above by 90%, the same as doing the reaction on a 0.225 mmol scale. For the second step the boronic ester is dissolved in 0.5 mL and then 1 mL aspirated and dispensed to the reaction. This is repeated once more to ensure full transfer of the boronic ester (which was confirmed several times by checking the zones by ¹H NMR analysis with an internal standard).

^1H NMR analysis. The benzylic signals from the boronic ester were used:



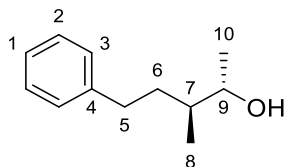
CH_2Br_2 (0.25 mmol, 1 eq) was added manually at the end of iteration 2 and the analysis conducted straightaway. Integrating the peak for CH_2Br_2 ($\delta = 4.93$ ppm) as 2H gives an 84% yield over 2 steps.

We attempted to purify the boronic for full characterisation:



Unfortunately, the boronic ester could not be isolated cleanly (stannane **41** and EtOTIB **40** impurities) so it was oxidised (NaOH, H₂O₂) following a literature procedure¹⁵⁷ to the corresponding alcohol for full characterisation:

S11. (2*S*,3*S*)-3-methyl-5-phenylpentan-2-ol.



$R_f = 0.10$ (10% EtOAc in pentane, KMnO₄)

¹H NMR (500 MHz, CDCl₃): $\delta = 7.29$ (dd, $J = 8.1, 6.8$ Hz, 2H, **2**), 7.22 – 7.16 (m, 3H, **1 & 3**), 3.76 (qd, $J = 6.4, 4.1$ Hz, 1H, **9**), 2.73 (ddd, $J = 13.6, 10.3, 4.9$ Hz, 1H, **5'**), 2.59 (ddd, $J = 13.6, 9.7, 6.5$ Hz, 1H, **5''**), 1.89 – 1.74 (m, 1H, **6'**), 1.58 – 1.41 (m, 2H, **6'' & 7**), 1.33 (brs, 1H, **OH**), 1.16 (d, $J = 6.4$ Hz, 3H, **10**), 0.97 (d, $J = 6.5$ Hz, 3H, **8**).

¹³C NMR (126 MHz, CDCl₃): $\delta = 142.8$ (**4**), 128.5 (**2/3**), 128.4 (**2/3**), 125.8 (**1**), 71.4 (**9**), 39.4 (**7**), 34.6 (**6**), 33.8 (**5**), 20.3 (**10**), 14.3 (**8**).

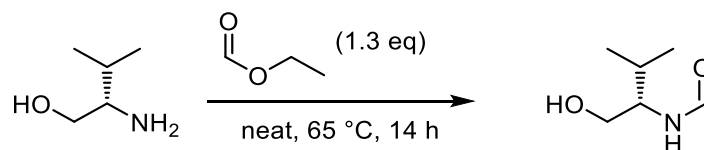
HRMS-EI (m/z): [M + Na]⁺ calcd for C₁₂H₁₈NaO, 201.1250; found, 201.1260.

FT-IR (film): ν_{\max} (cm⁻¹) = 3366, 3026, 2966, 2927, 1495, 1453, 746, 696.

5.3.2 Experimental

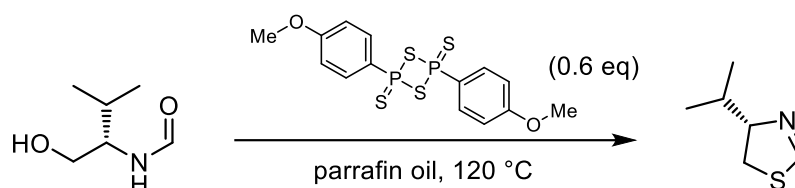
5.3.2.1 Boronic ester synthesis

129. (*S*)-4-isopropyl-4,5-dihydrothiazole



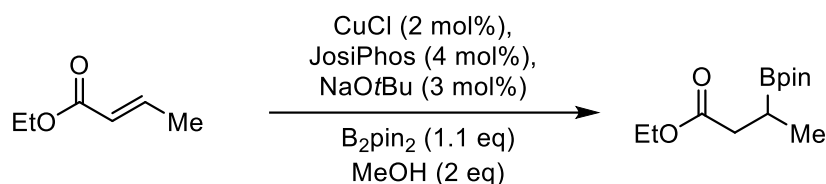
Prepared following a literature procedure on 40 mmol scale with 98% yield.¹⁰⁹

128. (*S*)-4-isopropyl-4,5-dihydrothiazole



Prepared following a literature procedure on 14 mmol scale with 8% yield.¹⁰⁹

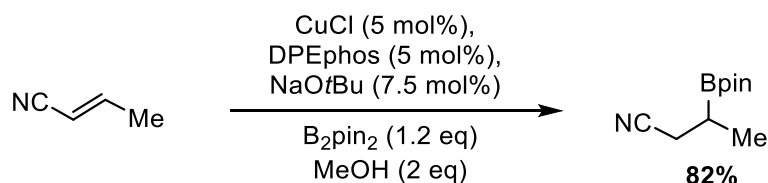
S10. Ethyl 3-(4,4,5,5-tetramethyl-1,3,2-dioxaborolan-2-yl)butanoate



Prepared following a literature procedure on 5 mmol scale with 84% yield.¹²²

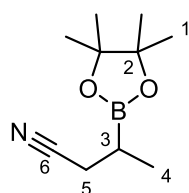
Hydrolyzed to the corresponding carboxylic acid (**149**) following a literature procedure in quantitative yield.¹⁵⁸

146. 3-(4,4,5,5-tetramethyl-1,3,2-dioxaborolan-2-yl)butanenitrile



Prepared following a modified literature procedure.¹²² To a flame-dried Schlenk tube was added DPEphos (0.135 g, 0.25 mmol, 5 mol%). This was then taken into a glovebox and CuCl (0.025 g, 0.25 mmol, 5 mol%) was added. Once removed from the glovebox THF (5 mL) and NaOtBu (2 M in THF, 0.38 mL, 0.38 mmol, 7.5 mol%) were added. The resulting white suspension was stirred for 0.5 h, during which time the solution became

almost clear and light brown. B₂pin₂ (1.52 g, 6 mmol, 1.2 eq) was then added as a solution in THF (1 mL) and the solution turned immediately black. After stirring for 10 minutes, the reaction was cooled to 0 °C and crotonitrile (mixture of *cis* and *trans*, 0.40 mL, 0.335 g, 5 mmol, 1.0 eq) was added as a solution in THF (1 mL). MeOH (0.41 mL, 0.320 g, 10 mmol, 2.0 eq) was then added. The reaction was left to stir and warm up in the ice bath overnight. After this time GC-MS showed full conversion to product. The crude mixture was filtered through a small pad of silica (EtOAc) and solvents removed under reduced pressure. The crude mixture was then purified on a Biotage isolera flash column chromatography machine (wet loading, minimal CH₂Cl₂) using a 100 g, 60 mM column with a gradient of 7% EtOAc in petrol to 80% EtOAc, [1-10-2] CVs, λ_{all}. This gave the title compound (0.799 g, 4.09 mmol, 82%) as a colourless oil.

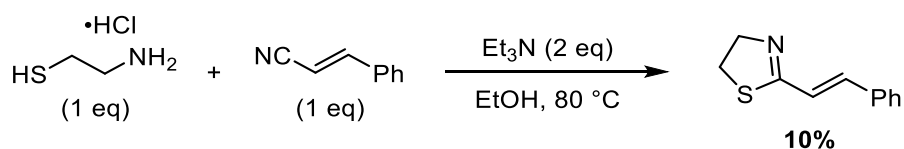


¹H NMR (400 MHz, CDCl₃): δ = 2.45 (dd, *J* = 16.8, 5.9 Hz, 1H, **5'**), 2.31 (dd, *J* = 16.8, 8.4 Hz, 1H, **5''**), 1.39 (sept, *J* = 7.5 Hz, 1H, **3**), 1.24 (s, 12H, **1**), 1.14 (d, *J* = 7.6 Hz, 3H, **4**).

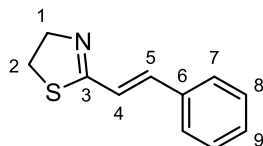
¹³C NMR (101 MHz, CDCl₃): δ = 120.0 (**6**), 84.0 (**2**), 24.82 (**1**), 24.76 (**1**), 20.5 (**5**), 15.0 (**4**).

Spectroscopic data matched with the literature.¹¹⁸

143. (*E*)-2-styryl-4,5-dihydrothiazole



Cystamine hydrochloride (1.79 g, 15 mmol, 1 eq) was added to EtOH (7.5 mL). Triethylamine (4.18 mL, 3.04 g, 30 mmol, 2 eq) was then added dropwise. After 5 minutes stirring at room temperature, cinnamitrile (1.88 mL, 1.94 g, 15 mmol, 1 eq) was added as a solution in EtOH (3.8 mL) dropwise. The mixture was heating to 80 °C and stirred at this temperature for 24 h. After cooling, the reaction mixture was filtered through a thin pad of silica, eluting with MeCN. After removal of solvents under reduced pressure, the crude mixture was purified on a Biotage isolera flash column chromatography machine (wet loading, minimal CH₂Cl₂) using a 25 g, 20 μM column with a gradient of 12% EtOAc in pentane to 100% EtOAc, [1-10-2] CVs, λ_{all}. This gave impure product which was partially recrystallized from heptane (heating/cooling) to give white crystals which were scratched away from the side product (red gum). After drying under high vacuum, this gave the title compound (0.29 g, 10%) as white crystals.

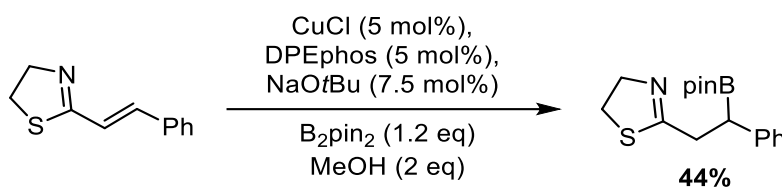


¹H NMR (500 MHz, CDCl₃): δ = 7.51 – 7.47 (m, 2H, **7**), 7.39 – 7.31 (m, 3H, **8 & 9**), 7.11 (d, J = 16.2 Hz, 1H, **5**), 7.04 (d, J = 16.2 Hz, 1H, **4**), 4.38 (t, J = 8.2 Hz, 2H, **1**), 3.34 (t, J = 8.2 Hz, 1H, **2**).

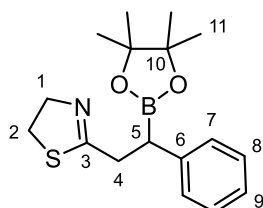
¹³C NMR (126 MHz, CDCl₃): δ = 168.0 (**3**), 141.2 (**5**), 135.4 (**6**), 129.5 (**9**), 128.9 (**8**), 127.5 (**7**), 122.7 (**4**), 64.7 (**1**), 33.1 (**2**).

Spectroscopic data matches literature example.¹⁵⁹

144. 2-(2-phenyl-2-(4,4,5,5-tetramethyl-1,3,2-dioxaborolan-2-yl)ethyl)-4,5-dihydrothiazole



Prepared following a modified literature procedure.¹²² To a flame-dried Schlenk tube was added DPEphos (14 mg, 0.025 mmol, 10 mol%). This was then taken into a glovebox and CuCl (3 mg, 0.025 mmol, 10 mol%) was added. Once removed from the glovebox THF (0.70 mL) and NaOtBu (2 M in THF, 0.02 mL, 0.038 mmol, 15 mol%) were added. The resulting white suspension was stirred for 0.5 h, during which time the solution became almost clear and light brown. B₂pin₂ (0.76 g, 0.3 mmol, 1.2 eq) was then added as a solution in THF (0.21 mL) and the solution turned immediately black. After stirring for 10 minutes, the reaction was cooled to 0 °C and (*E*)-2-styryl-4,5-dihydrothiazole (0.047 g, 0.25 mmol, 1.0 eq) was added as a solution in THF (0.20 mL). MeOH (0.02 mL, 0.016 g, 0.5 mmol, 2.0 eq) was then added. The reaction was left to stir and warm up in the ice bath overnight. After this time GC-MS showed full conversion to product. The crude mixture was filtered rapidly through a small pad of silica (MeCN) and solvents removed under reduced pressure. The crude mixture (yellow oil) was then purified on a Biotage isolera flash column chromatography machine (wet loading, minimal CH₂Cl₂) using a 5 g, 20 μ M, pH = 7, 60 mL min⁻¹ column with a gradient of 15% EtOAc in pentane to 100% EtOAc, [1-8-4] CVs, λ_{all} . After removal of solvents this gave the desired product as a yellow oil (35 mg, 44%).



R_f = 0.23, 60:40 EtOAc:Pentane (KMnO₄, product is not silica stable)

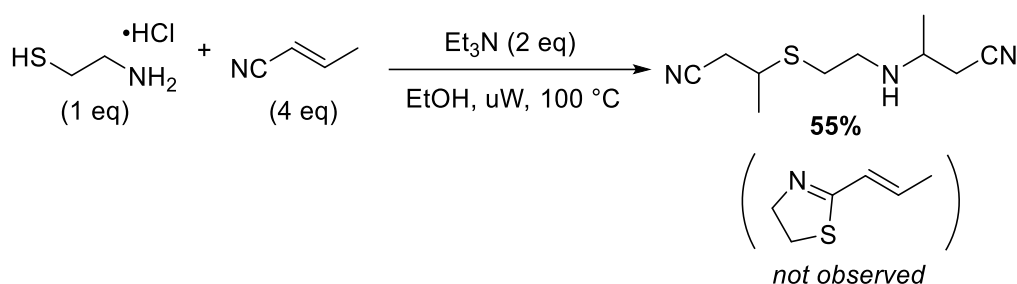
¹H NMR (500 MHz, CDCl₃): δ = 7.25 – 7.20 (m, 3H, **7 & 8**), 7.14 – 7.10 (m, 1H, **9**), 4.21 (dtt, J = 14.8, 8.4, 1.9 Hz, 1H, **1'**), 4.18 – 4.07 (m, 1H, **1''**), 3.37 (br t, J = 8.4 Hz, 1H, **2**), 2.97 (ddt, J = 16.8, 9.8, 2.0 Hz, 1H, **4'**), 2.87 (ddt, J = 16.8, 6.7, 1.7 Hz, 1H, **4''**), 2.75 (dd, J = 9.8, 6.7 Hz, 1H, **5**), 1.11 (s, 12H, **11**).

¹³C NMR (126 MHz, CDCl₃): δ = 175.9 (**3**), 142.8 (**6**), 128.22 (**7/8**), 128.21 (**7/8**), 125.2 (**9**), 82.41 (**11**), 82.39 (**11**), 61.42 (**1**), 61.37 (**1**), 37.5 (**4**), 34.4 (**2**), 32.9 (**5**), 24.9 (**11**), 24.7 (**11**).

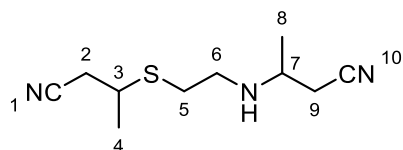
HRMS-ESI (m/z): [M + H]⁺ calcd for C₁₇H₂₅BNO₂S, 318.1697; found, 318.1700.

FT-IR (film): ν_{max} (cm⁻¹) = 2978, 1629, 1492, 1361, 1319, 1140, 966.

145. 3-((2-((1-cyanopropan-2-yl)amino)ethyl)thio)butanenitrile



Adapted from a literature procedure.¹¹² Cystamine hydrochloride (0.170 g, 1.5 mmol, 1.0 eq) was added to a 2 mL microwave vial and EtOH (1 mL) was added. Triethylamine (0.42 mL, 0.303 g, 3 mmol, 2 eq) was then added and the mixture stirred for 5 minutes. (*E*)-But-2-enenitrile (crotononitrile, 0.48 mL, 0.402 g, 6 mmol, 4 eq) was then added in one portion. The vial was sealed and heated to 100 °C in a microwave reactor for 4 h. After cooling, the brown crude mixture was filtered through a silica plug (acetone) and the solvents removed under reduced pressure to give a crude oil. The crude oil was then purified on a Biotage isolera flash column chromatography machine (wet loading, minimal CH₂Cl₂) using a 10 g, 60 μ M column with a gradient of 18% acetone in pentane to 100% acetone, [1-10-2] CVs, λ_{all} . This gave the title product (0.175 g, 55%) and none of the desired thiazoline product.



R_f = 0.20 1:1 acetone:pentane, KMnO₄

¹H NMR (500 MHz, CDCl₃): δ = 3.10 (quin, J = 6.5 Hz, 1H, **3**), 3.04 (quin, J = 6.5 Hz, 1H, **7**), 2.84 (m, 2H, **6**), 2.74 (m, 2H, **5**), 2.67 (dd, J = 16.9, 5.7 Hz, 1H, **2'**), 2.58 (dd, J = 16.9, 7.2 Hz, 1H, **2''**, diastereomers) & 2.57 (dd, J = 16.9, 7.1 Hz, 1H, **2''**, diastereomers), 2.44 (m, 2H, **9**), 1.42 (d, J = 6.9 Hz, 3H, **4**), 1.24 (d, J = 6.4 Hz, 3H, **8**).

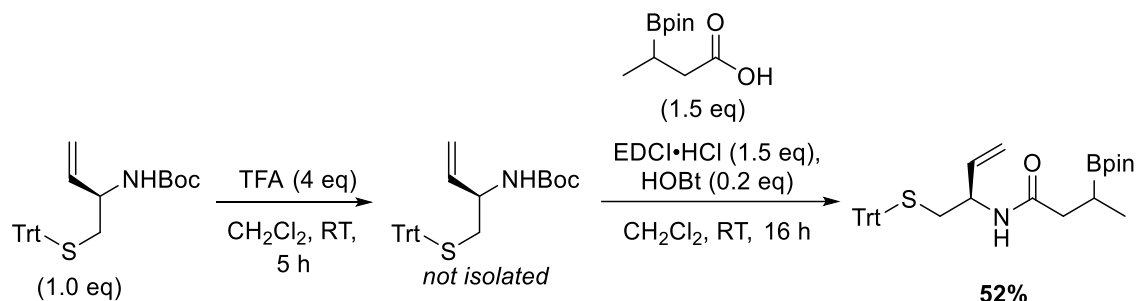
¹³C NMR (126 MHz, CDCl₃): δ = 118.04 & 118.02 (**2**), 117.7 (**1**), 50.06 & 50.04 (**7**), 46.26 & 46.22 (**6**), 36.59 & 36.58 (**3**), 31.87 & 31.84 (**5**), 26.31 & 26.30 (**2**), 25.30 & 25.27 (**9**), 21.2 (**4**), 20.73 & 20.72 (**8**).

Presence of two diastereomers leads to doubling of some peaks.

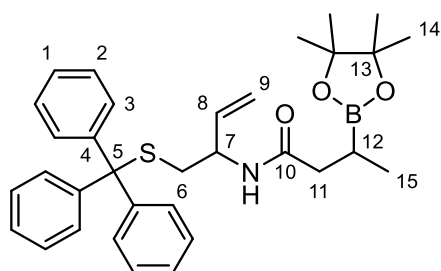
HRMS-ESI (m/z): $[M + Na]^+$ calcd for $C_{10}H_{17}N_3NaS$, 234.1035; found, 234.1037.

FT-IR (film): ν_{max} (cm^{-1}) = 3317, 2967, 2929, 2247, 1595, 1454, 1420, 1382, 1146, 757.

148. 3-(4,4,5,5-tetramethyl-1,3,2-dioxaborolan-2-yl)-N-((R)-1-(tritylthio)but-3-en-2-yl)butanamide



To a solution of *tert*-butyl (R)-1-(tritylthio)but-3-en-2-ylcarbamate **151** (52 mg, 0.15 mmol, 1.0 eq) in CH_2Cl_2 (1.5 mL) was added TFA (46 μ L, 68 mg, 0.6 mmol, 4.0 eq) dropwise at 0 °C. The reaction was allowed to warm to RT and stirred for 5 h. After this time, the reaction was cooled again to 0 °C and $NaOH_{aq}$ (1.5 mL, 1 M) added dropwise. The layers were separated, and the aqueous layer extracted with CH_2Cl_2 (3 x 3 mL). The combined organic layers were dried over $MgSO_4$ and the solvents removed under reduced pressure to leave a crude oil. The oil was redissolved in CH_2Cl_2 (1.5 mL), then 3-(4,4,5,5-tetramethyl-1,3,2-dioxaborolan-2-yl)butanoic acid **149** (48 mg, 0.23 mmol, 1.5 eq) and HOBt (4 mg, 0.03 mmol, 0.2 eq) were added. After stirring for ~5 minutes, EDCI·HCl (43 mg, 0.23 mmol, 1.5 eq) was added and the resulting mixture stirred for 16 h. After this time, the reaction was cooled again to 0 °C and HCl_{aq} (1.5 mL, 1 M) added dropwise. The layers were separated, and the aqueous layer extracted with CH_2Cl_2 (3 x 3 mL). The combined organic layers were washed with Na_2CO_3 (5 mL, sat), dried over $MgSO_4$ and the solvents removed under reduced pressure to leave a crude oil. The crude oil was then purified on a Biotage isolera flash column chromatography machine (wet loading, minimal 7% EtOAc in pentane) using a 10 g, 20 μ M, column with a gradient of 7% EtOAc in pentane to 60% EtOAc, [1-10-2] CVs, λ_{all} . After removal of solvents this gave the desired product as a yellow oil (40 mg, 52%, *d.r.* not determined).



R_f = 0.33 (1:1 EtOAc:pentane, $KMnO_4$).

1H NMR (500 MHz, $CDCl_3$): δ = 7.22 (m, 6H, **3**), 7.11 (m, 6H, **2**), 7.04 (m, 3H, **1**), 5.48 (m, 2H, **8** & **NH**), 4.90 (m, 2H, **9**), 4.46 – 4.35 (m, 1H, **7**), 2.31 (m, 1H, **6'**), 2.20 – 2.07 (m, 2H, **6''** & **11'**), 2.00 (dd, J = 14.8, 6.3 Hz, 1H, **11''**), 1.27 – 1.13 (m, 1H, **12**), 1.04 (s, 12H, **14**), 0.83 (d, J = 7.5 Hz, 3H, **15**).

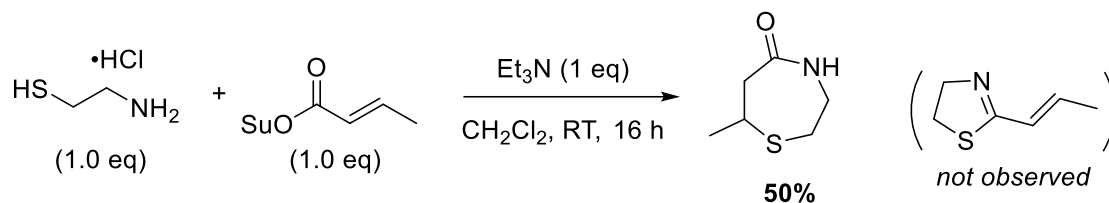
¹³C NMR (126 MHz, CDCl₃): δ = 172.3 (**10**), 144.6 (**4**), 136.8 (**8**), 129.7 & 129.6 (**3**), 128.0 (**2**), 126.8 (**1**), 115.6 (**9**), 83.23 & 83.22 (**13**), 66.7 (**5**), 49.8 (**7**), 40.0 & 39.9 (**11**), 36.7 (**6**), 24.79 & 24.74 (**14**), 15.4 & 15.2 (**15**).

Presence of two diastereomers leads to doubling of some peaks.

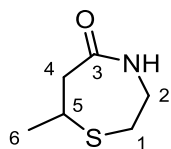
HRMS-ESI (m/z): [M + Na]⁺ calcd for C₃₀H₄₀BNNaO₃S, 564.2720; found, 564.2700.

FT-IR (film): ν_{\max} (cm⁻¹) = 2979, 1651, 1490, 1315, 1142, 742, 698.

161. 7-methyl-1,4-thiazepan-5-one



To a suspension of cystamine hydrogen chloride (0.114 g, 1 mmol, 1 eq) in CH₂Cl₂ (5.0 mL) was added Et₃N (0.14 mL, 0.101 g, 1 mmol, 1.0 eq) and the resulting mixture stirred for ~5 minutes. After this time 2,5-dioxopyrrolidin-1-yl (*E*)-but-2-enoate **160** (0.183 g, 1 mmol, 1 eq) was added in one portion and the mixture was stirred for a further 16 h. After this time the reaction was concentrated under reduced pressure and the resulting crude mixture purified on a Biotage isolera flash column chromatography machine (wet loading, minimal CH₂Cl₂) 10 g, 60 μ M, 17% acetone in petrol to 100% acetone, [1-7-5] CVs, λ_{all} . This gave the title product as a white solid (0.073 g, 50%) and none of the desired thiazoline.



R_f = 0.30 (60:40 acetone:petane, KMnO₄).

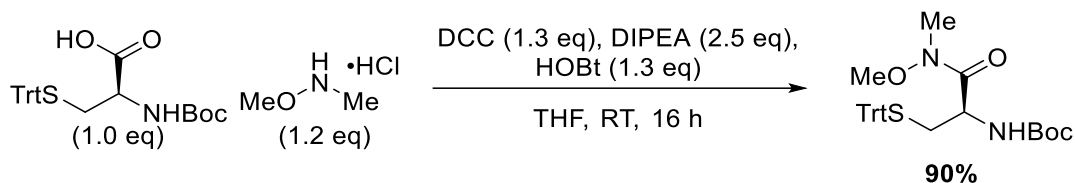
¹H NMR (500 MHz, CDCl₃): δ = 7.21 (br s, 1H, NH), 3.58 (m, 2H, **2**), 3.07 (m, 1H, **5**), 2.92 (dd, J = 14.0, 9.1 Hz, 1H, **4'**), 2.83 (m, 1H, **4''**), 2.74 (m, 2H, **1**), 1.33 (d, J = 7.0 Hz, 3H, **6**).

¹³C NMR (126 MHz, CDCl₃): δ = 176.56 & 176.52 (**3**), 48.3 (**3**), 45.75 & 45.74 (**2**), 32.83 & 32.82 (**5**), 30.71 & 30.70 (**1**), 21.8 (**6**).

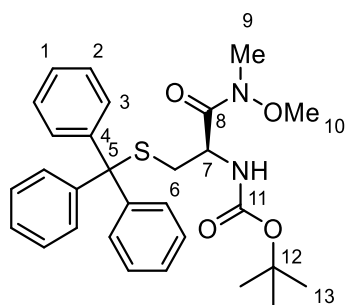
HRMS-ESI (m/z): [M + H]⁺ calcd for C₆H₁₂NOS, 146.0634; found, 146.0640.

FT-IR (film): ν_{\max} (cm⁻¹) = 3186, 3076, 2970, 2905, 2864, 1660, 1616, 1408, 1300, 946, 786.

156. *tert*-butyl (*R*)-(1-(methoxy(methyl)amino)-1-oxo-3-(tritylthio)propan-2-yl)carbamate



To a solution of *N*-Boc-(*S*-Trt)-*L*-Cys-OH (**152**) (13.91 g, 30.0 mmol, 1.00 eq) and *N,O*-dimethylhydroxylamine hydrochloride (3.51 g, 36 mmol, 1.2 eq) in THF (75 mL, ~0.4 M) was added *N,N*-diisopropylethylamine (13.0 mL, 9.69 g, 75.0 mmol, 2.50 eq) and HOBT (20 wt% H₂O, 4.86 g, 36.0 mmol, 1.2 eq). The mixture was stirred together for 10 minutes until all the HOBT had dissolved. A solution of DCC (8.05 g, 39.0 mmol, 1.3 eq) in THF (8 mL, 1 g mL⁻¹) was then added quickly dropwise. After being stirred at the same temperature for 16 h, or until full consumption of starting material by LC-MS, the reaction mixture was cooled to 0 °C and filtered through a sinter frit, washing with minimal cold (0 °C) THF. The THF was then removed under reduced pressure and the residue taken into Et₂O (150 mL) and washed with HCl (0.13 M, ~800 mL) and then Na₂CO₃ (sat, 600 mL). The organic layer was dried over MgSO₄ and concentrated under reduced pressure. The residue was then loaded onto Celite® (1.5 x crude weight, typically 18 g crude weight + 27 g Celite) using CH₂Cl₂ ensuring full solvent removal. The crude mixture was then purified on a Biotage isolera flash column chromatography machine using a 350 g column (refilled with 60 μM silica), 7% EtOAc in petrol to 80% EtOAc, [1-10-2] CVs, λ_{all}. The gave a sticky oil which was dissolved in minimal Et₂O (if not all solids dissolve even when heating, then cool and filter to remove DCU) and precipitated by addition of hexane. After cooling to 0 °C and filtering (washing with cold (0 °C) hexane), *tert*-butyl (*R*)-(1-(methoxy(methyl)amino)-1-oxo-3-(tritylthio)propan-2-yl)carbamate was obtained (13.5 g, 26.6 mmol, 90%) as a white and amorphous powder.

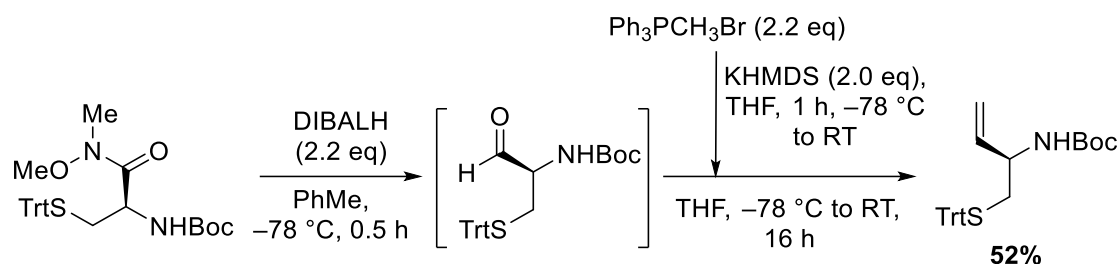


¹H NMR (500 MHz, CDCl₃): δ = 7.42 (m, 6H, **3**), 7.29 (m, 6H, **2**), 7.23 (m, 3H, **1**), 5.14 (br d, *J* = 9.0 Hz, 1H, **NH**), 4.77 (br s, 1H, **7**), 3.66 (s, 3H, **10**), 3.17 (s, 3H, **9**), 2.57 (dd, *J* = 12.2, 4.7 Hz, 1H, **6'**), 2.40 (dd, *J* = 12.2, 7.8 Hz, 1H, **6''**), 1.46 (s, 9H, **13**).

¹³C NMR (126 MHz, CDCl₃): δ = 171.1 (**8**), 155.2 (**11**), 144.5 (**4**), 129.6 (**3**), 127.9 (**2**), 126.8 (**1**), 79.7 (**12**), 66.7 (**5**), 61.6 (**10**), 49.8 (**7**), 34.2 (**6**), 32.2 (**9**), 28.4 (**13**).

Spectroscopic data matched with the literature.¹⁶⁰

151. *tert*-butyl (*R*)-(1-(tritylthio)but-3-en-2-yl)carbamate

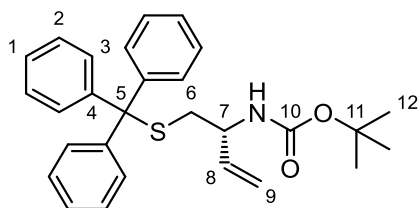


To a solution of Weinreb amide **156** (5.07 g, 10 mmol, 1.00 eq) in toluene (100 mL, ~0.1 M) was added dropwise DIBALH (1.0 M in PhMe, 0.7 mL min⁻¹, 22.2 mL, 22.22 mmol, 2.22 eq) at -78 °C. After the addition, the reaction was stirred at -78 °C for 0.5 h – until complete by TLC (30% EtOAc in pentane, anisaldehyde). At -78 °C, EtOAc (20 mL) was added, dropwise at first. The acetone/dry ice bath was removed, and a 25% solution (25 g in 75 mL H₂O) of tartaric acid was then added, dropwise at first, while the mixture warmed to RT. It was then stirred rapidly for 1 h.

During this time, the Wittig ylide was prepared. To a solution of methyltriphenylphosphonium bromide (8.21 g, 23 mmol, 2.3 eq) in THF (80 mL, ~0.3 M) at -78 °C was added KHMDS (1.0 M in THF, 1.0 mL min⁻¹, 18 mL, 1.8 eq). After the addition, the yellow/orange solution was immediately warmed to RT and stirred at this temperature for minimum 1 h.

The layers from the DIBALH reduction were separated, and the aqueous layer extracted with Et₂O (3 x 75 mL). The combined organic layers were dried over MgSO₄, concentrated under reduced pressure and dried under high vacuum. The Wittig ylide was then cooled to -78 °C and the crude aldehyde dissolved in THF (10 mL, ~1 M), added dropwise (0.7 mL min⁻¹). Once the addition was finished the dry ice/acetone bath was removed and the mixture stirred for 1 h, until complete by TLC (20% EtOAc in pentane, anisaldehyde). The reaction was then cooled to 0 °C and filtered through a short plug of silica, washing with Et₂O (~200 mL). The solvent was then removed under reduced pressure and typically the crude was stored at -20 °C overnight. The residue was then loaded onto Celite® (CH₂Cl₂, 1.5 x crude weight, typical crude weight ~ 9 g), ensuring full solvent removal. The crude mixture was then purified on a Biotage isolera flash column chromatography machine (350 g column, refilled with 60 μM SiO₂), using the step gradient 8% EtOAc in pentane [1.5 CVs] to 13% EtOAc in pentane [2.2 CVs] to 25% EtOAc in pentane [2.0 CVs], λ_{all}, to give *tert*-butyl (*R*)-(1-(tritylthio)but-3-en-2-yl)carbamate (1.77 g, 3.90 mmol, 39%) as a sticky and white/yellow gum.

Note: precipitation of this compound with Et₂O/hexane leads to a white powder which is racemic.



¹H NMR (500 MHz, CDCl₃): δ = 7.42 (m, 6H, **3**), 7.29 (m, 6H, **2**), 7.23 (m, 3H, **1**), 5.65 (ddd, J = 17.1, 10.4, 5.2 Hz, 1H, **8**), 5.10 (dt, J = 17.1, 1.4 Hz, 1H, **9'**), 5.08 (dt, J = 10.5, 1.4 Hz, 1H, **9''**), 4.62 (br s, 1H, **NH**), 4.19 (br s, 1H, **7**), 2.52 – 2.26 (m, 2H, **6**), 1.45 (s, 9H, **12**).

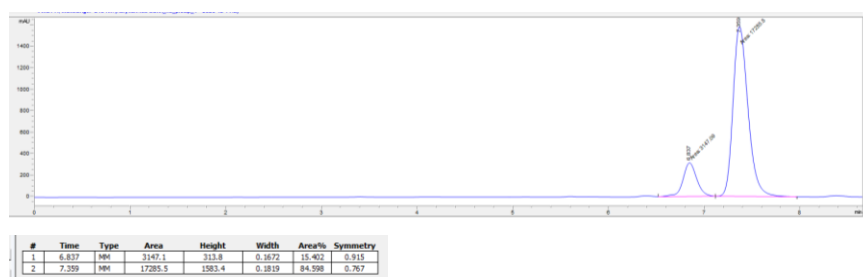
¹³C NMR (126 MHz, CDCl₃): δ = 155.0 (**10**), 144.6 (**4**), 137.3 (**8**), 129.6 (**3**), 128.0 (**2**), 126.8 (**1**), 115.4 (**9**), 79.5 (**11**), 66.7 (**5**), 51.6 (**7**), 37.0 (**6**), 28.4 (**12**).

Spectroscopic data matched with the literature.¹

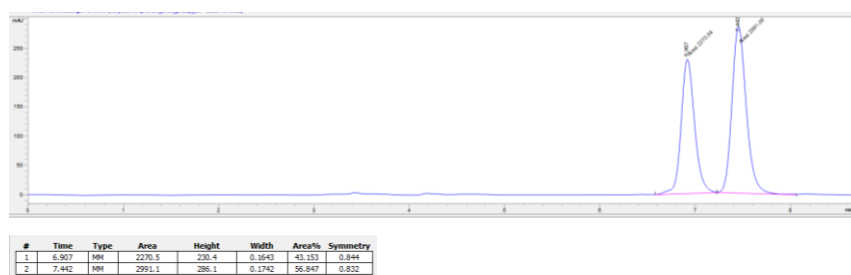
$[\alpha]_D^{25}$ +16 (c 1.00, CHCl₃)

HPLC: conditions = IB column, 99:1 hexane:IPA, 1 mL min⁻¹, 210 nm.

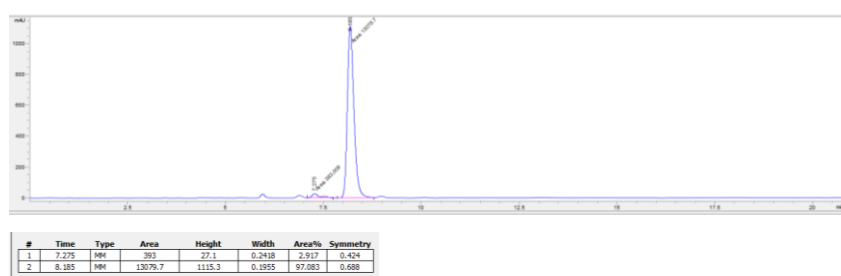
Tartrate work-up:



After dissolution in Et₂O and precipitation with hexane:

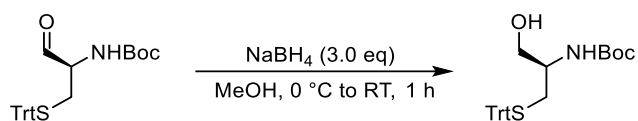


Tartaric acid work-up and no precipitation:

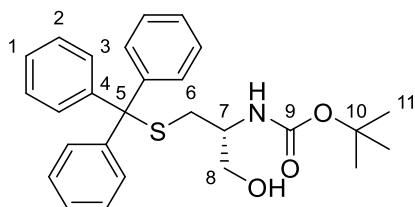


e.r. is given as >97:3 due to overlapping minor peaks.

158. *tert*-Butyl (*R*)-(1-hydroxy-3-(tritylthio)propan-2-yl)carbamate



To a solution of aldehyde **157** (from DIBALH reduction of Weinreb **156** with no chromatographic purification, 45 mg, assumed 0.1 mmol, 1 eq) in MeOH (1 mL) was added NaBH₄ (12 mg, 0.3 mmol, 3 eq) in one portion at 0 °C. The reaction was warmed to RT and stirred for 1 h (until complete by TLC, 30% EtOAc in pentane). The solvent was removed under reduced pressure and then the solids redissolved in H₂O (2 mL) and the aqueous layer extracted with EtOAc (4 x 2 mL). The combined organics were washed with brine (6 mL), dried (MgSO₄), filtered and concentrated under reduced pressure. The crude oil was purified by flash column chromatography (10 to 70% EtOAc in pentane) which gave *tert*-butyl (1-hydroxy-3-(tritylthio)propan-2-yl)carbamate as a colourless oil (13 mg, 30%).



R_f = 0.31 (30% EtOAc in pentane, anisaldehyde).

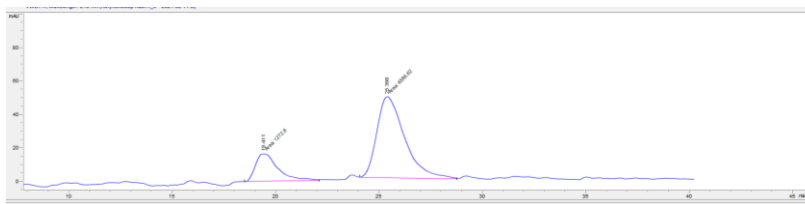
¹H NMR (500 MHz, CDCl₃): δ = 7.43 (m, 6H, **3**), 7.30 (m, 6H, **2**), 7.23 (m, 3H, **1**), 4.67 (s, 1H, NH), 3.49 (m, 3H, **7 & 8**), 2.41 (m, 2H, **6**), 1.43 (s, 9H, **11**).

¹³C NMR (126 MHz, CDCl₃): δ = 155.9 (**9**), 144.5 (**4**), 129.6 (**3**), 128.0 (**2**), 126.9 (**1**), 79.8 (**10**), 67.0 (**5**), 64.6 (**8**), 51.8 (**7**), 33.2 (**6**), 28.4 (**11**).

Spectroscopic data matched with the literature.¹⁶¹

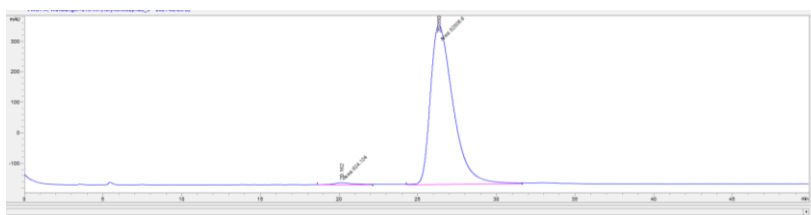
HPLC: Conditions = IA column, 90:10 hexane:IPA, 1 mL min⁻¹, 210 nm.

Tartrate work-up:



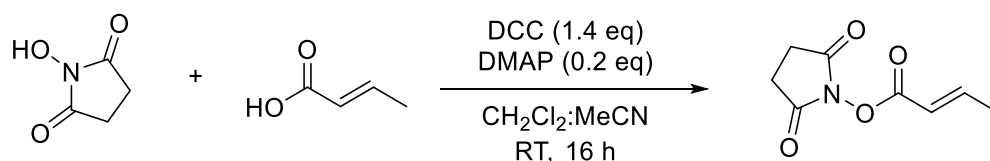
#	Time	Type	Area	Height	Width	Area%	Symmetry
1	19.411	MM	1272.6	16.5	1.2821	21.720	0.524
2	25.398	MM	4586.6	48.9	1.564	78.280	0.575

Tartaric acid work-up:



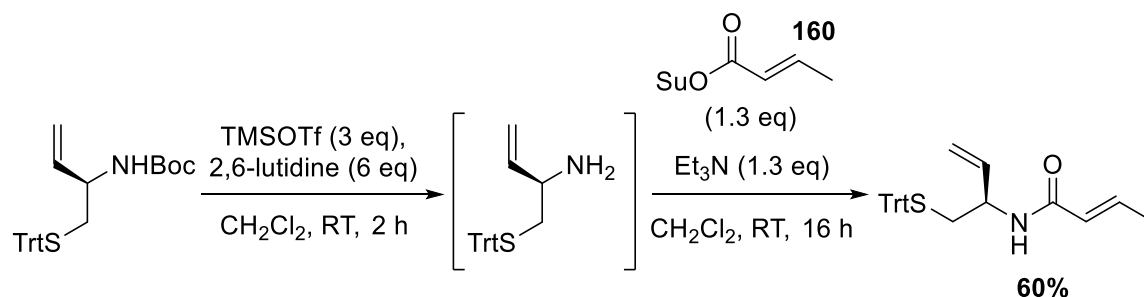
#	Time	Type	Area	Height	Width	Area%	Symmetry
1	20.162	MM	624.1	6.9	1.5124	1.175	0.666
2	26.35	MM	52508.8	525	1.6668	98.825	0.578

160. 2,5-dioxopyrrolidin-1-yl (*E*)-but-2-enoate



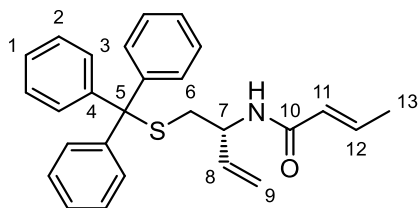
Prepared following a literature procedure on 35 mmol scale with 49% yield.¹⁶²

153. (*R,E*)-*N*-(1-(tritylthio)but-3-en-2-yl)but-2-enamide



To a solution of *tert*-butyl (*R*)-(1-(tritylthio)but-3-en-2-yl)carbamate **151** (2.00 g, 4.5 mmol, 1.00 eq) and 2,6-lutidine (3.14 mL, 2.89 g, 27 mmol, 6 eq) in CH₂Cl₂ (23 mL, ~0.20 M) at 0 °C (ice/water bath) was added dropwise TMSOTf (2.44 mL, 3.00 g, 13.5 mmol, 3.00 eq) over 5 mins. The reaction was warmed to RT and stirred for 2 h (until complete by TLC, 20% EtOAc in pentane, anisaldehyde). Once complete, the reaction was cooled to 0 °C (ice/water bath) and MeOH (1 mL) was added dropwise and then H₂O (35 mL, dropwise at first) and the reaction stirred for 5 minutes. The layers were then separated, and the aqueous layer extracted with CH₂Cl₂ (3 x 30 mL). The combined organic layers were then dried over MgSO₄ and the solvent removed under reduced pressure. At this point the purity of the crude amine can be checked by ¹H NMR, if required. Otherwise, the amine was re-dissolved in CHCl₂ (15 mL) and added quickly dropwise to a solution of 2,5-dioxopyrrolidin-1-yl (*E*)-but-2-enoate **160** (1.07 g, 5.85 mmol, 1.30 eq) and Et₃N (0.82 mL, 0.591 g, 5.85 mmol, 1.30 eq) in CH₂Cl₂ (8 mL). The reaction was then stirred at RT for 16 h. The crude was then redissolved in MeOH (23 mL, ~0.20 M) and Et₃N (0.63 mL, 0.455 g, 4.50 mmol, 1.00 eq) was added, and the mixture stirred for 3 h (to remove any leftover activated ester, until complete by TLC, 30% EtOAc in pentane, KMnO₄). The solvents were again removed under reduced pressure and the residue was then loaded onto Celite® (CH₂Cl₂, 1.5 x crude weight),

ensuring full solvent removal. The crude mixture was then purified on a Biotage isolera flash column chromatography machine (350 g column, refilled with 60 μM SiO_2) using a gradient of 7% EtOAc in pentane to 80% EtOAc, [1-10-2] CVs, λ_{all} , to give *tert*-butyl (*R,E*)-*N*-(1-(tritylthio)but-3-en-2-yl)but-2-enamide (1.10 g, 59%) as a sticky gum.



$R_f = 0.29$ (10% EtOAc in pentane, anisaldehyde).

$^1\text{H NMR}$ (500 MHz, CDCl_3): $\delta = 7.43$ (m, 6H, **3**), 7.31 (t, $J = 7.6$ Hz, 6H, **2**), 7.24 (t, $J = 7.3$ Hz, 2H), 6.84 (dq, $J = 13.9, 6.8$ Hz, 1H, **12**), 5.76 (dt, $J = 13.9, 1.5$ Hz, 1H, **11**), 5.70 (ddd, $J = 16.4, 10.3, 5.1$ Hz, 1H, **8**), 5.50 (br d, $J = 8.4$ Hz, 1H, **NH**), 5.11 (m, 2H, **9**), 4.65 (m, 1H, **7**), 2.57 (dd, $J = 12.3, 5.9$ Hz, 1H, **6'**), 2.44 (dd, $J = 12.3, 5.1$ Hz, 1H, **6''**), 1.88 (dt, $J = 6.8, 1.5$ Hz, 3H, **13**).

$^{13}\text{C NMR}$ (126 MHz, CDCl_3): $\delta = 165.0$ (**10**), 144.6 (**4**), 140.2 (**12**), 136.6 (**8**), 129.6 (**3**), 128.0 (**2**), 126.8 (**1**), 125.0 (**11**), 115.8 (**9**), 66.8 (**5**), 49.9 (**7**), 36.6 (**2**), 17.8 (**13**).

HRMS-ESI (m/z): $[\text{M} + \text{Na}]^+$ calcd for $\text{C}_{27}\text{H}_{27}\text{NNaOS}$, 436.1706; found, 436.1697.

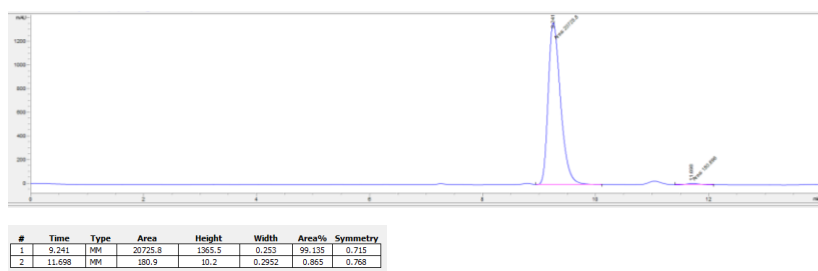
FT-IR (neat): ν_{max} (cm^{-1}) = 3279, 3053, 1675, 1627, 1541, 1444, 965, 702.

Melting Point = 137 – 139 $^{\circ}\text{C}$ (amorphous, precipitated from Et_2O).

$[\alpha]_D^{24} +20$ (c 1.00, CHCl_3) (*e.r.* = 97:3)

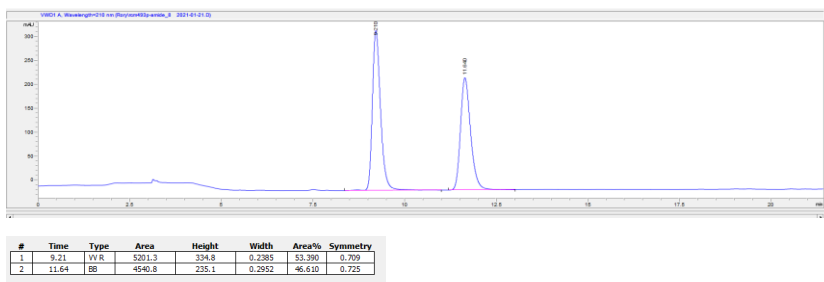
HPLC: Conditions = IA column, 90:10 hexane:IPA, 1 mL min^{-1} , 210 nm.

Before precipitation with Et_2O :

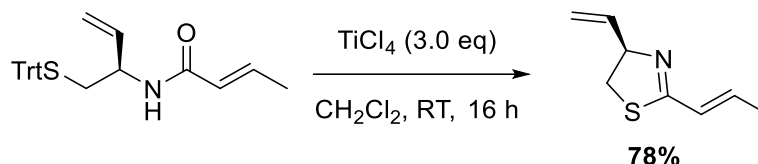


Integrating the peak at 11 minutes as the minor peak gives 97:3 *e.r.*

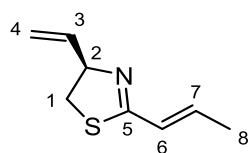
After precipitation with Et_2O with then analysing the solid:



138. (*R,E*)-2-(prop-1-en-1-yl)-4-vinyl-4,5-dihydrothiazole



To a solution of *tert*-butyl (*R,E*)-*N*-(1-(tritylthio)but-3-en-2-yl)but-2-enamide **153** (1.683 g, 4.07 mmol, 1.00 eq) in CH₂Cl₂ (41 mL, ~0.1 M) at 0 °C was added neat TiCl₄ (pale yellow, distilled from Cu filings, stored under N₂ at RT, 1.34 mL, 2.316 g, 12.21 mmol, 3.00 eq) dropwise. The yellow/red reaction was then warmed to RT and stirred for 14 h. The reaction was then cooled to 0 °C and MeOH (0.99 mL, 0.782 g, 24.42 mmol, 6.00 eq) was added dropwise (this generates Ph₃COMe for easier separation), then a saturated aqueous solution of Na₂CO₃ (~12 mL) was added dropwise at first, then finally a 10% solution of Rochelle's salt (sodium potassium tartarate, 1.2 g in 12 mL) was added and the white mixture stirred rapidly for 1 h. After this time, the layers were separated, and the organic layer removed carefully. The aqueous layer was then extracted with Et₂O (3 x 50 mL), and the combined organic layers washed with brine and dried over MgSO₄. The solvent was then removed carefully under reduced pressure (volatile product) to leave a thick red oil. This was purified on a Biotage isolera flash column chromatography machine (wet loading, minimal CH₂Cl₂), on a 100 g column (refilled with 60 μM SiO₂), 20% Et₂O in petrol to 100% Et₂O, [1-10-2] CVs, λ_{all}, to give (*R,E*)-2-(prop-1-en-1-yl)-4-vinyl-4,5-dihydrothiazole (0.486 g, 3.17 mmol, 78%) as a volatile oil.



R_f = 0.17 (30% Et₂O in pentane, KMnO₄ (bright)).

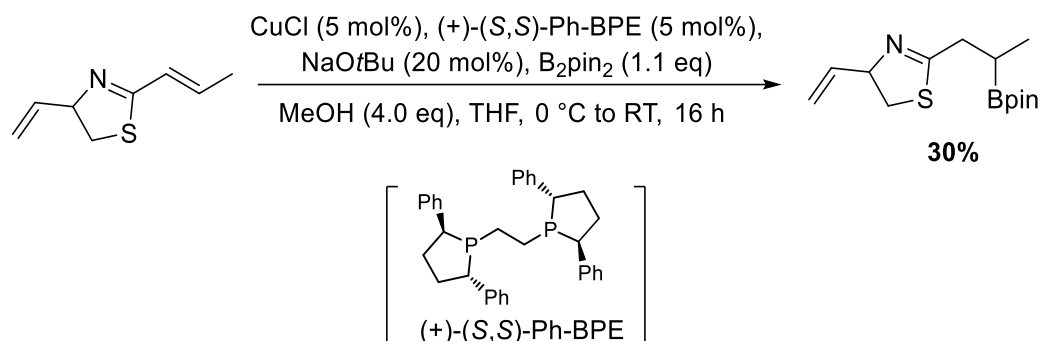
¹H NMR (500 MHz, CDCl₃): δ = 6.40 (m, 1H, **6 & 7**, ABX₃), 5.96 (ddd, *J* = 17.1, 10.3, 6.8 Hz, 1H, **3**), 5.30 (dt, *J* = 17.1, 1.2 Hz, 1H, **4'**), 5.18 (dt, *J* = 10.3, 1.2 Hz, 1H, **4''**), 4.98 (m, 1H, **2**), 3.41 (dd, *J* = 10.9, 8.3 Hz, 1H, **1'**), 3.04 (dd, *J* = 10.9, 8.2 Hz, 1H, **1''**), 1.90 (m, 3H, **8**, ABX₃).

¹³C NMR (126 MHz, CDCl₃): δ = 167.4 (**5**), 140.5 (**6/7**), 137.1 (**3**), 126.6 (**6/7**), 116.3 (**4**), 78.5 (**2**), 37.6 (**1**), 18.5 (**8**).

HRMS-EI (m/z): [M + H]⁺ calcd for C₈H₁₁NS, 152.0528; found, 152.0528.

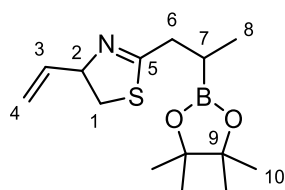
FT-IR (film): ν_{max} (cm⁻¹) = 2972, 2930, 2219, 1582, 921, 909, 728.

137. 2-(2-(4,4,5,5-tetramethyl-1,3,2-dioxaborolan-2-yl)propyl)-4-vinyl-4,5-dihydrothiazole



Based on a modified literature procedure.¹¹⁴

CuCl (12 mg, 0.125 mmol, 5 mol%) and Ph-BPE ligand (63 mg, 0.125 mmol, 5 mol%) were placed in an oven-dried Schlenk tube and THF (8 mL) was added. NaOtBu (2 M in THF, 0.25 mL, 0.5 mmol, 20 mol%) was then added and the reaction mixture was stirred rapidly for 0.5 – 1 h at room temperature, to give a brown homogenous mixture. Bis(pinacolato)diboron (B₂pin₂, 0.698 g, 2.75 mmol, 1.1 eq) dissolved in THF (2 mL) was added and the solution turned immediately black. The reaction mixture was stirred for 10 min, then cooled to 0 °C, and (*R,E*)-2-(prop-1-en-1-yl)-4-vinyl-4,5-dihydrothiazole (0.383 g, 2.5 mmol, 1.0 eq) was added, followed by anhydrous MeOH (0.41 mL, 0.320 g, 10 mmol, 4.0 eq). The reaction was left to warm up slowly and stirred for 16 h, after which time GC-MS showed full conversion. The mixture was filtered through a thin pad of silica (Et₂O) as quickly as possible. After removal of solvents, this gave a crude brown oil which was purified by Kugelrohr distillation [4 bulbs (including crude), <1 mbar, collecting at 0 °C, starting at 100 °C to 120 °C to remove B₂pin₂/pinacol/pinBOMe, then switch collecting bulb along, heat up to 160/180 °C, collecting a clear oil (product)]. This gave the title product (0.208 g, 0.74 mmol, 30%) as a clear oil with other impure fractions (B₂pin₂/pinacol/pinBOMe) which could be redistilled.



R_f = Not silica stable

¹H NMR (500 MHz, CDCl₃): δ = 5.95 (ddt, *J* = 17.2, 9.9, 6.8 Hz, 1H, **3**), 5.30 (dm, *J* = 17.2 Hz, 1H, **4'**), 5.15 (dm, *J* = 10.3, 1H, **4''**), 4.96 – 4.86 (m, 1H, **2**), 3.43 (ddd, *J* = 10.5, 8.5, 3.7 Hz, 1H, **1'**), 3.06 (ddd, *J* = 10.6, 8.0, 2.3 Hz, 1H, **1''**), 2.66 (ddt, *J* = 15.4, 7.2, 1.4 Hz, 1H, **6'**), 2.52 (ddt, *J* = 15.4, 7.6, 1.3 Hz, 1H, **6''**), 1.45 (h, *J* = 7.4 Hz, 1H, **7**), 1.26 – 1.23 (m, 12H, **10**), 1.04 (dd, *J* = 7.5 Hz, 3H, **8**).

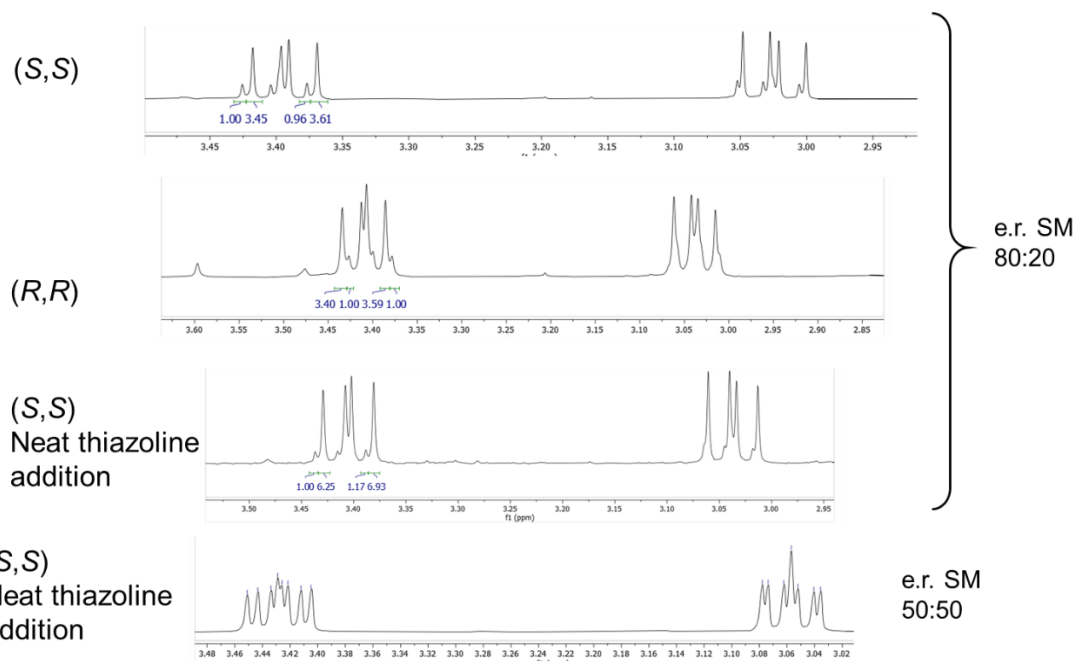
¹³C NMR (126 MHz, CDCl₃): δ = 171.7 & 171.6 (**5**), 137.52 & 137.48 (**3**), 115.9 & 115.8 (**4**), 83.12 & 83.10 (**9**), 78.5 & 78.4 (**2**), 38.9 & 38.8 (**1**), 37.60 & 37.59 (**6**), 24.80 & 24.79 & 24.73 & 24.67 (**10**), 16.1 (**7**), 15.2 & 15.1 (**8**).

Some peaks doubled/extra splitting due to two diastereomers present at 1:1 ratio.

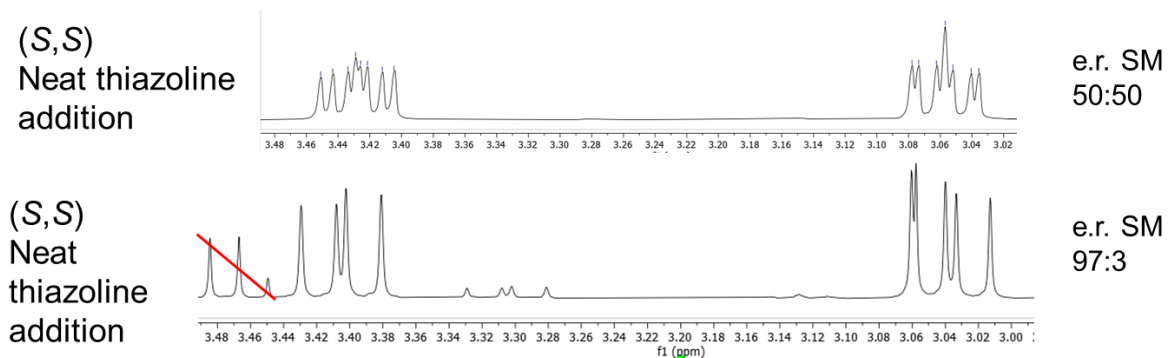
HRMS-EI (m/z): $[M + H]^+$ calcd for $C_{14}H_{24}NO_2BS$, 281.1615; found, 281.1616.

FT-IR (film): ν_{max} (cm^{-1}) = 2976, 2929, 2901, 1369, 1317, 1143, 851, 674.

The *d.r.* of boronic ester **137** was determined by looking at the protons adjacent to sulphur (on carbon **1**). These were the only separable proton signals in the spectrum. The enantiomer of ligand is indicated on the left and the *e.r.* of starting α - β unsaturated thiazoline **138** on the right.

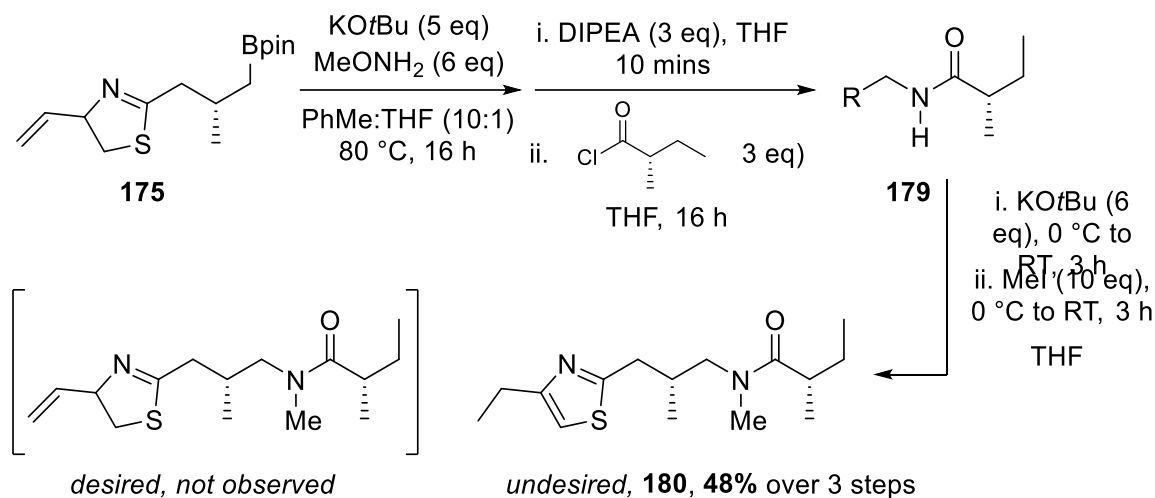


Recently, starting material **138** was brought through in high *e.r.* 97:3. Unfortunately the material was not fully purified due to time constraints. However, the protons of interest show that product **137** has a *d.r.* value $\geq 95:5$, therefore the borylation proceeded with high selectivity.



5.3.2.2 Final Three Steps

180. (*S*)-*N*-((*R*)-3-(4-ethylthiazol-2-yl)-2-methylpropyl)-*N*,2-dimethylbutanamide



Morken Amination & Amidation:

Stock solutions:

Bpin 175: (29.5 mg, 0.1 mmol) in a pointed 8 mL vial.

MeONH₂: (0.15 mL, 2.75 mmol) in 1.25 mL THF. Total volume (V_{tot}) = 1.4 mL

$$c = \frac{n}{v} = \frac{2.75}{1.4} = 1.96 \text{ mmol mL}^{-1}.$$

We calculated the density of MeONH₂ as 0.867 g mL⁻¹ at 24 °C.

KOtBu: (3 mL). 1.6 M in THF. Commercial.

PhMe: (3 mL). Anhydrous

DIPEA: (0.35 mL, 2 mmol) in 2.6 mL non-anhydrous THF. V_{tot} = 3 mL.

$$c = \frac{n}{v} = \frac{2}{3} = 0.67 \text{ mmol mL}^{-1}.$$

Acid Chloride: (0.12 mL, 1 mmol) in 1.3 mL non-anhydrous THF. V_{tot} = 1.4 mL.

$$c = \frac{n}{v} = \frac{1}{1.4} = 0.71 \text{ mmol mL}^{-1}.$$

Reaction volumes: (0.1 mmol scale)

Bpin 175: (1 eq = 0.1 mmol); a 0.2 M solution in PhMe (0.5 mL) is required.

MeONH₂: (6 eq = 0.6 mmol); $V = \frac{n}{c} = \frac{0.6}{1.96} = 0.306 \text{ mL}$.

KOtBu: (5 eq = 0.5 mmol); $V = \frac{n}{c} = \frac{0.5}{1.6} = 0.313 \text{ mL}$.

DIPEA: (3 eq = 0.3 mmol); $V = \frac{n}{c} = \frac{0.3}{0.67} = 0.448$ mL.

Acid Chloride: (3 eq = 0.3 mmol); $V = \frac{n}{c} = \frac{0.3}{0.71} = 0.422$ mL.

Procedure:

The reactions were performed in the ISYNTH reactor block. Once the platform was flushed with N₂ (2 h) oven dried vials were placed to cool in the ISYNTH block along with the starting boronic esters. Reagents were placed in the vial racks. The boronic ester was dissolved in 0.25 mL of PhMe (with shaking) and dispensed. This was repeated to ensure full transfer of the boronic ester. Pointed 8 mL vials were essential for full transfer. MeONH₂ was dispensed (1 mL min⁻¹ source and dispense speeds) followed by KO^tBu. The lid of the ISYNTH was then removed manually and the vials manually capped and sealed with parafilm. We used a “dummy workflow” where the ISYNTH block had been removed from the configuration (leaving the shaker) to heat to 80 °C and stir at 500 rpm overnight (~14 h). Once complete, the vials were cooled to 22 °C, the caps removed and the ISYNTH lid replaced. Back to the standard workflow, the DIPEA was dispensed, the reactions stirred (500 rpm) for 5 minutes, and then the acid chloride was dispensed. The ISYNTH was set to sealed independent and stirred for 14 h (this step was assumed to not be air sensitive). The product zone (glass array) was then dried with n-BuLi (5 mL per reaction) as per the drying procedure so the next step (methylation) could occur directly in there. We could not observe the intermediate amine by GC-MS, only the amide product after acylation.

Methylation:

Stock solutions:

MeI: (0.29 mL, 4.66 mmol) in 3 mL THF. Total volume (V_{tot}) = 3.3 mL

$$c = \frac{n}{v} = \frac{4.66}{3.3} = 1.41 \text{ mmol mL}^{-1}.$$

THF: (5 mL). Anhydrous.

KO^tBu: (4 mL). 1.6 M in THF. Commercial.

Reaction volumes: (0.1 mmol scale). Assumed from last reaction.

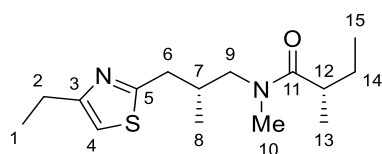
SM: (1 eq = 0.1 mmol); a 0.2 M solution in THF (0.5 mL) is required.

MeI: (10 eq = 1 mmol); $V = \frac{n}{c} = \frac{1}{1.41} = 0.709$ mL.

KO^tBu: (6 eq = 0.6 mmol); $V = \frac{n}{c} = \frac{0.6}{1.6} = 0.375$ mL.

Procedure:

The drying procedure had already been performed on the zone (glass array) where the starting material is for this step. THF was dispensed onto the starting material and the reactions were stirred at 600 rpm. The vessels were cooled to 0 °C (internal temperature on the cryostat) and KO^tBu was dispensed (destination speed 0.7 mL min⁻¹). The reactors were warmed to 22 °C and stirred for 5 h 10 mins (5 h including equilibration time). The reactors were then cooled again to 0 °C (internal temperature on the cryostat) and MeI was dispensed (destination speed 0.7 mL min⁻¹). The reactors were warmed to 22 °C and stirred for another 5 h 10 mins (5 h including equilibration time). After this time the filtration was performed as per the filtration workflow. GC-MS analysis of the reaction showed 7:93 **179:180**. Unfortunately, ¹H NMR analysis demonstrated the thiazole below.



$R_f = 0.13$ (60% EtOAc in pentane, KMnO₄)

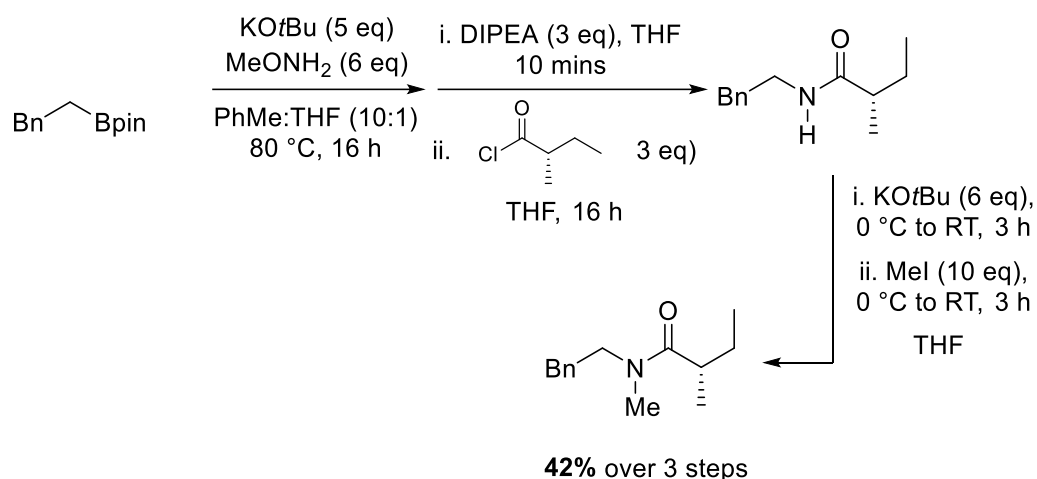
¹H NMR (500 MHz, CDCl₃): $\delta = 6.75$ (s, 1H, **4'**), 6.71 (s, 1H, **4''**), 3.50 (dd, $J = 13.3, 8.2$ Hz, 1H, **9A'**), 3.42 – 3.33 (m, 2H, **9**), 3.25 (dd, $J = 13.2, 6.4$ Hz, 1H, **9B'**), 3.17 (dd, $J = 14.6, 9.1$ Hz, 1H, **9**), 3.03 (s, 3H, **10'**), 2.99 – 2.95 (m, 1H, **6A'**), 2.94 (s, 3H, **10''**), 2.89 – 2.82 (m, 1H, **6B'**), 2.82 – 2.74 (m, 3H, **2 & 6''**), 2.59 (sext, $J = 6.8$ Hz, 1H, **12'**), 2.58 (sext, $J = 6.8$ Hz, 1H, **12''**), 2.41 – 2.28 (m, 1H, **7**), 1.69 (m, 1H, **14A**), 1.38 (dsext, $J = 13.6, 7.0$ Hz, 1H, **14B**), 1.28 (d, $J = 7.6$ Hz, 3H, **1'**), 1.27 (d, $J = 7.5$ Hz, 3H, **1''**), 1.09 (d, $J = 6.7$ Hz, 3H, **13'**), 1.07 (d, $J = 6.7$ Hz, 3H, **13''**), 1.00 (d, $J = 6.6$ Hz, 3H, **8'**), 0.92 (d, $J = 6.7$ Hz, 3H, **8''**), 0.88 (t, $J = 7.4$ Hz, 1H **15'**), 0.83 (t, $J = 7.4$ Hz, 3H, **15''**). Presence of two rotamers (around 4:6) denoted with n' and n'' . Presence of two diastereomers (major/minor not assigned, around 9:1) denoted with n_A and n_B . Signals which cannot be assigned to either rotamer/diastereomer are denoted with just the number of the environment.

¹³C NMR (126 MHz, CDCl₃): $\delta = 177.1$ & 176.9 (**11**), 168.8 & 167.8 (**5**), 159.0 & 158.8 (**3**), 111.5 & 111.2 (**4**), 55.0 & 53.2 (**9**), 38.2 & 38.0 (**6**), 37.6 & 37.1 (**12**), 35.9 & 34.5 (**10**), 34.3 & 33.0 (**7**), 27.4 & 26.7 (**14**), 24.82 (**2**), 17.7 (**13/8**), 17.4 (**13/8**), 17.3 (**13/8**), 17.2 (**13/8**), 13.52 & 13.50 (**1**), 12.09 & 12.07 (**15**).

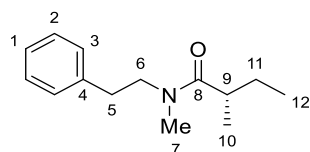
HRMS-EI (m/z): [M + H]⁺ calcd for C₁₅H₂₇N₂OS, 283.1839; found, 283.1833.

FT-IR (film): ν_{\max} (cm⁻¹) = 3675, 2967, 2928, 2901, 1640, 1407, 1076, 1066, 1056.

181. (*S*)-*N*,2-dimethyl-*N*-phenethylbutanamide



Performed in parallel with **180** on the same scale (23.2 mg, 0.1 mmol).



$R_f = 0.20$ (30% EtOAc in pentane, KMnO_4)

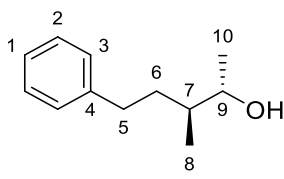
^1H NMR (500 MHz, CDCl_3): $\delta = 7.34 - 7.26$ (m, 2H, **2**), $7.25 - 7.13$ (m, 3H, **1 & 3**), $3.68 - 3.51$ (m, 2H, **6**), 2.95 (s, 1H, **7'**), 2.91 (s, 1H, **7''**), 2.85 (m, 2H, **5**), 2.56 (sext, $J = 6.8$ Hz, 1H, **9'**), 2.40 (sext, $J = 6.8$ Hz, 1H, **9''**), 1.68 (m, 1H, **11A'**), 1.58 (m, 1H, **11B''**), 1.36 (m, 1H, **11A'' & 11B'**), 1.07 (d, $J = 6.8$ Hz, 3H, **10'**), 0.98 (d, $J = 6.7$ Hz, 3H, **10''**), 0.86 (t, $J = 7.4$ Hz, 3H, **12'**), 0.79 (t, $J = 7.4$ Hz, 3H, **12''**). Presence of two rotamers denoted with n' and n'' . Presence of two diastereomers denoted protons with nA and nB .

^{13}C NMR (126 MHz, CDCl_3): $\delta = 176.8$ & 176.4 (**8**), 139.3 & 138.2 (**4**), 128.9 & 128.8 (**1/2/3**), 128.78 , & 128.4 (**1/2/3**), 126.7 & 126.3 (**1/2/3**), 51.5 & 50.1 (**6**), 37.4 & 37.2 (**9**), 36.0 (**7'**), 35.4 (**5'**), 33.8 (**5''/7''**), 33.8 (**5''/7''**), 27.3 & 27.0 (**11**), 17.5 & 17.1 (**10**), 12.03 & 11.99 (**11**).

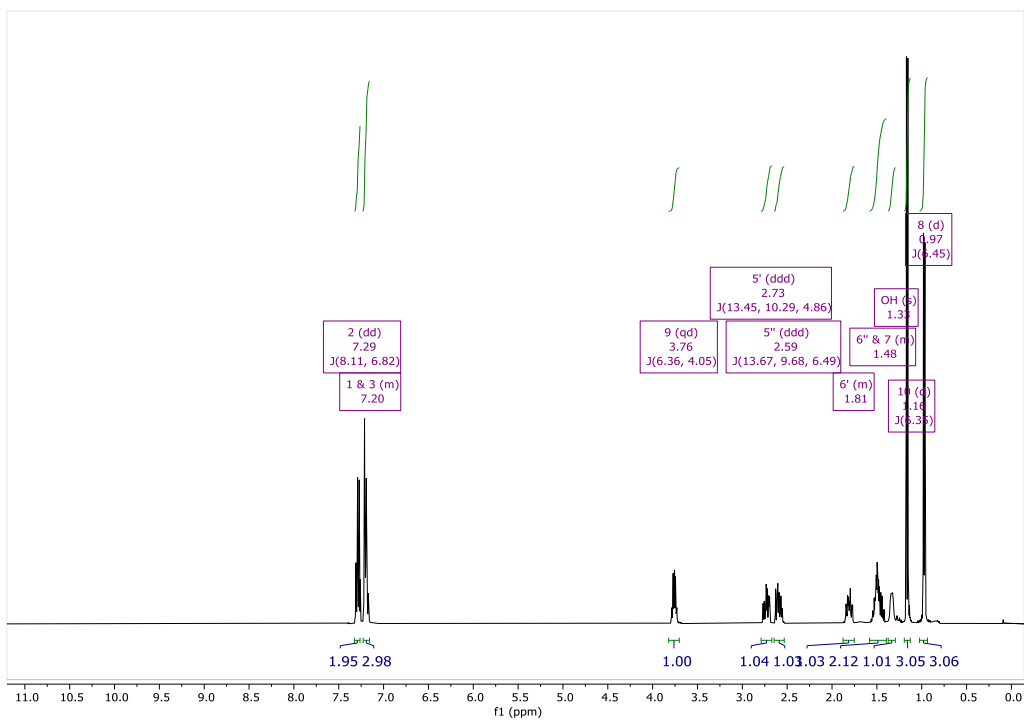
HRMS-EI (m/z): $[\text{M} + \text{H}]^+$ calcd for $\text{C}_{14}\text{H}_{22}\text{NO}$, 220.1696; found, 220.1697.

FT-IR (film): ν_{max} (cm^{-1}) = 3674, 2966, 2929, 2901, 1638, 1453, 1408, 1075, 1066, 700.

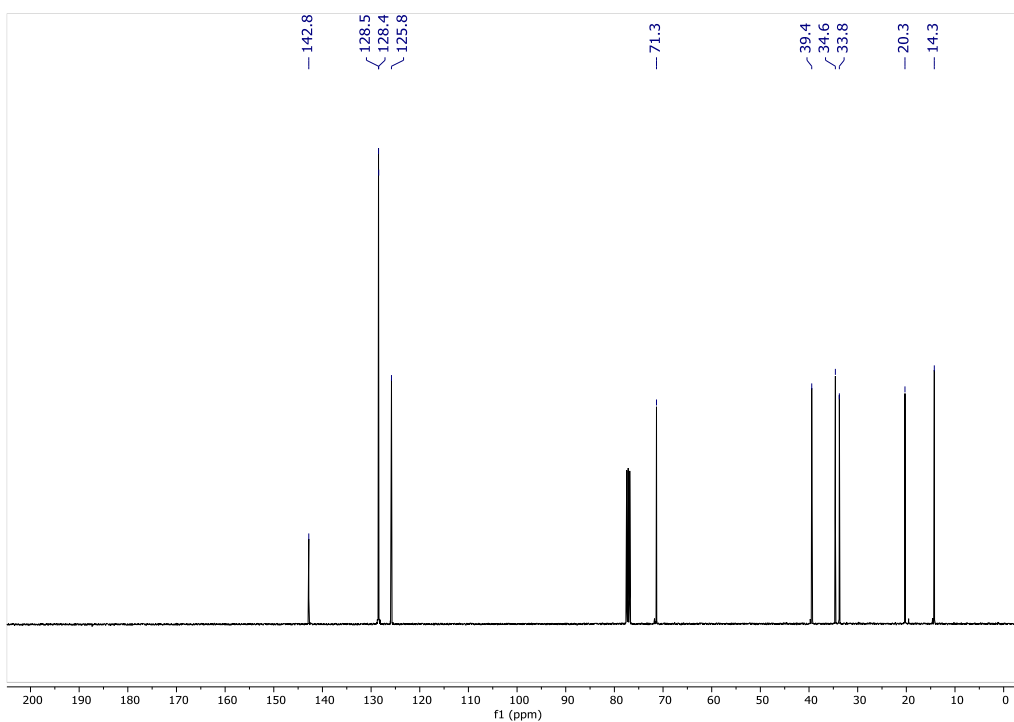
5.3.3 NMR Spectra

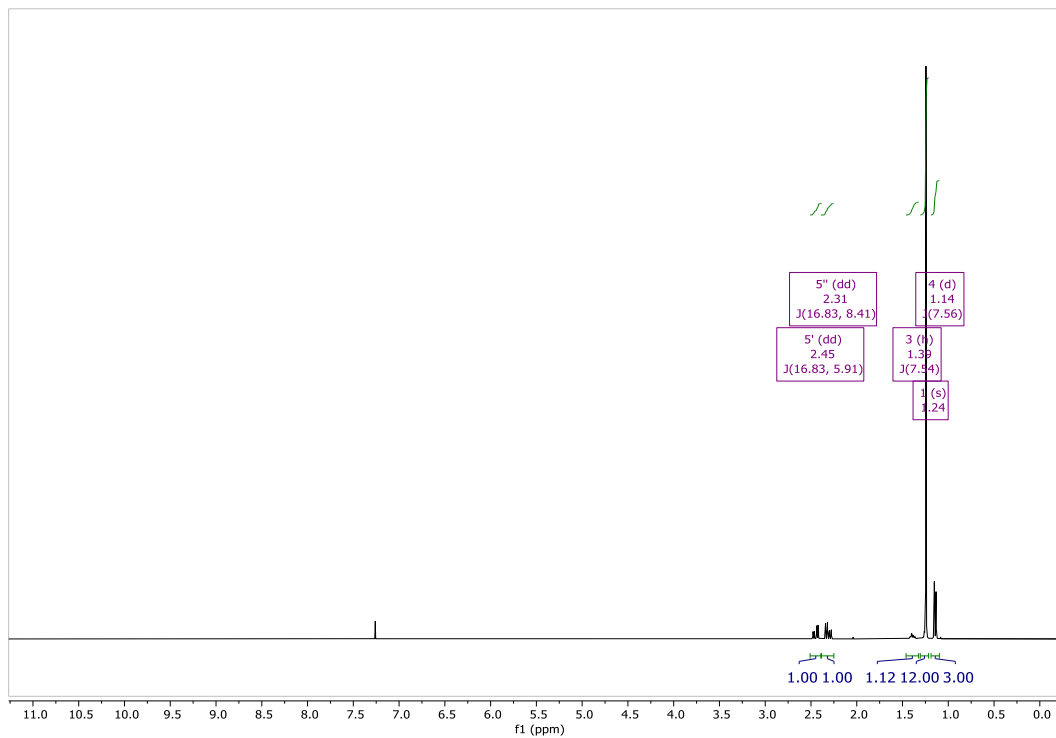
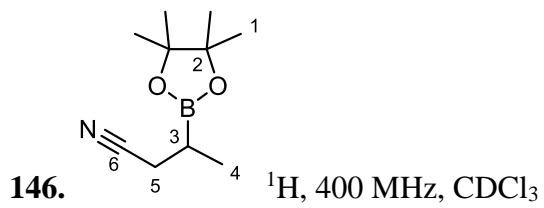


S11. ^1H , 500 MHz, CDCl_3

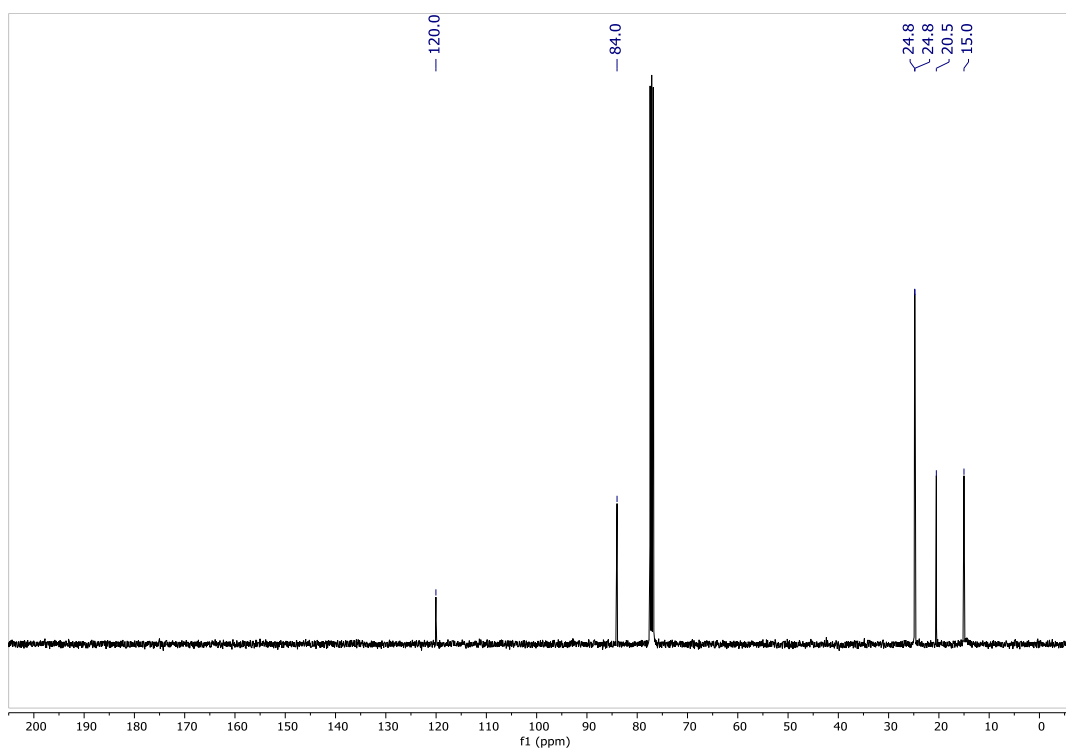


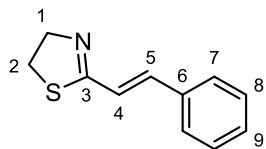
S11. ^{13}C , 126 MHz, CDCl_3



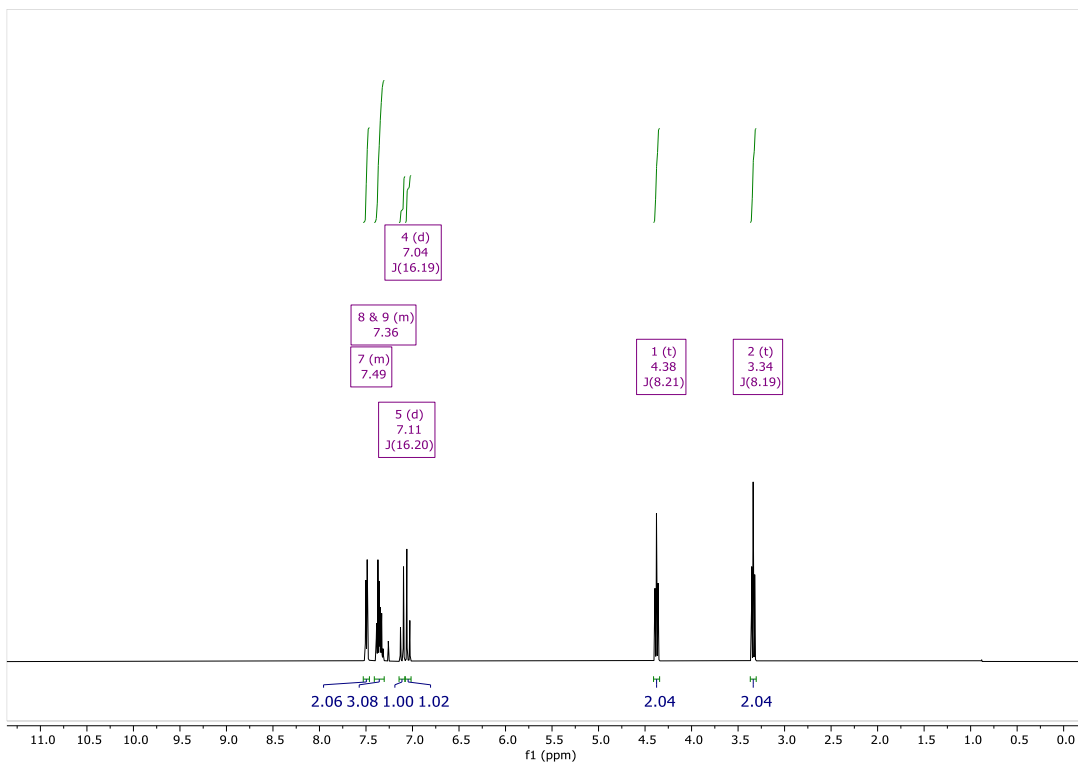


146. ^{13}C , 101 MHz, CDCl_3

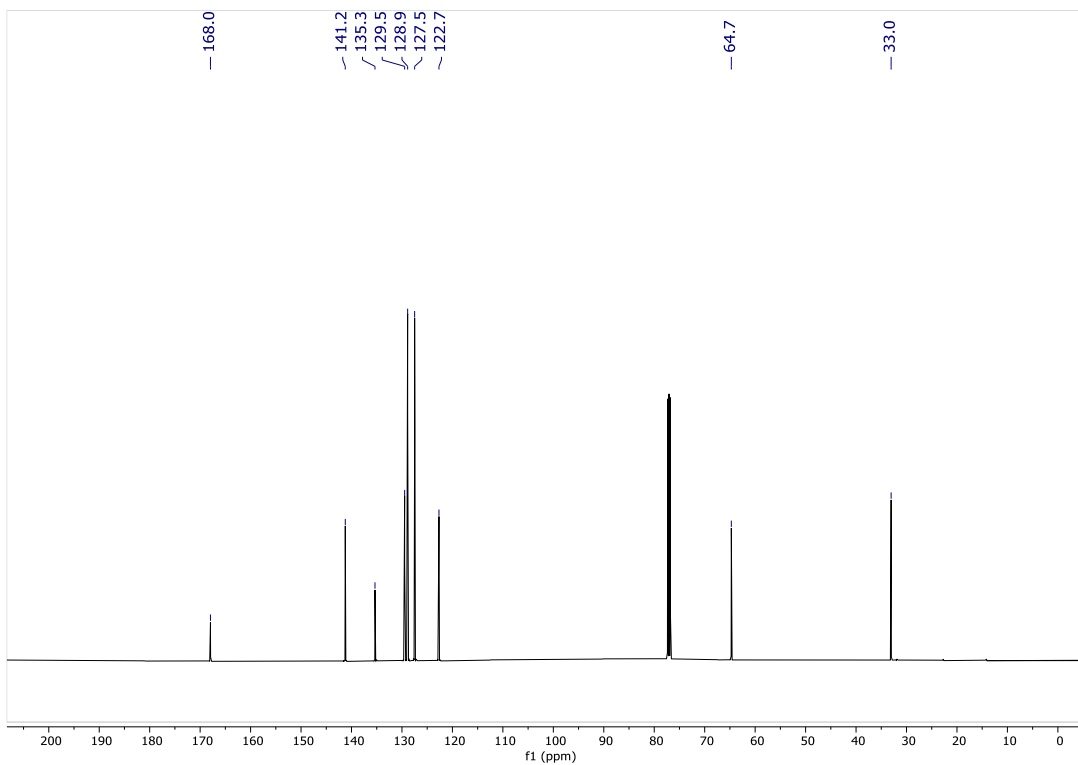


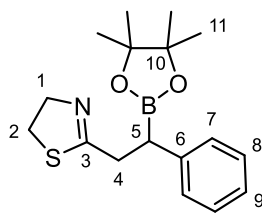


143. ^1H , 500 MHz, CDCl_3

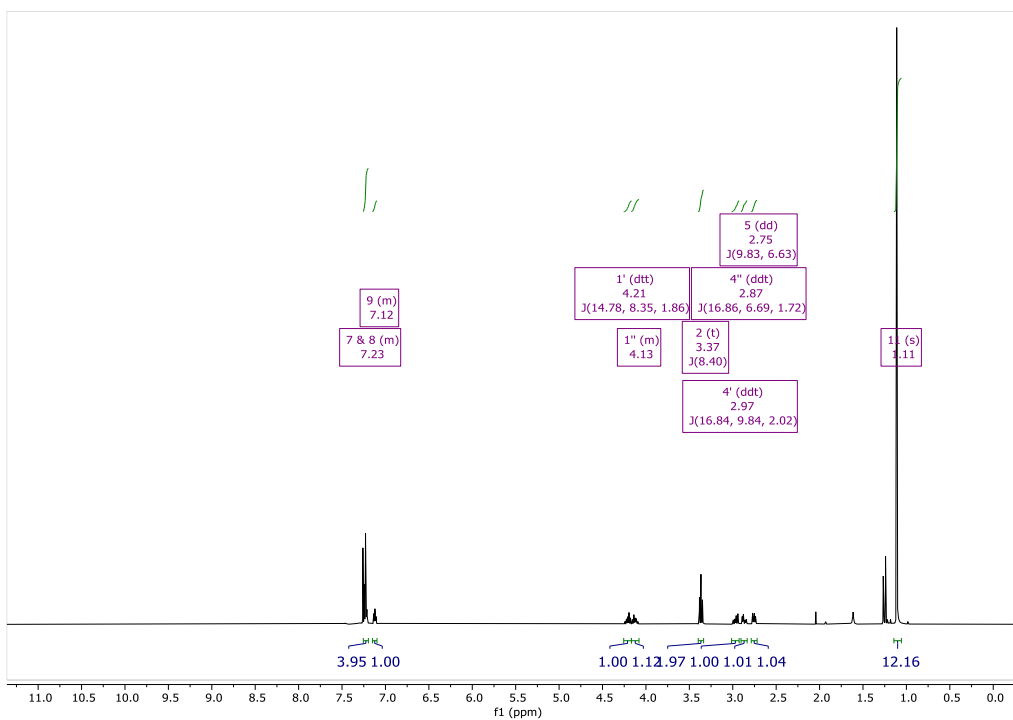


143. ^{13}C , 126 MHz, CDCl_3

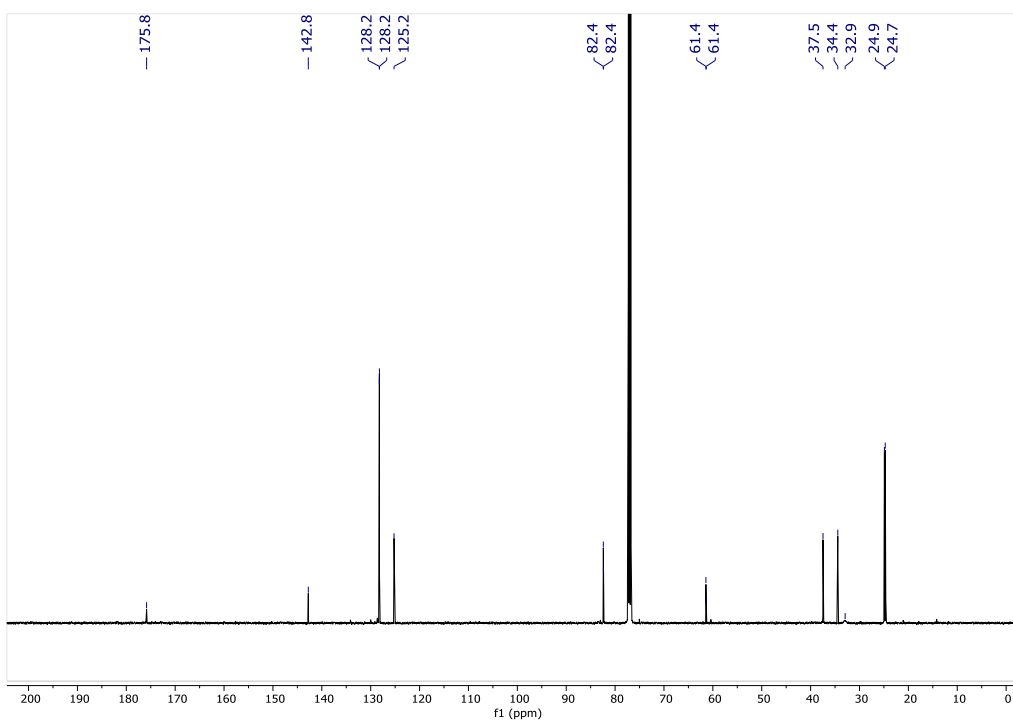


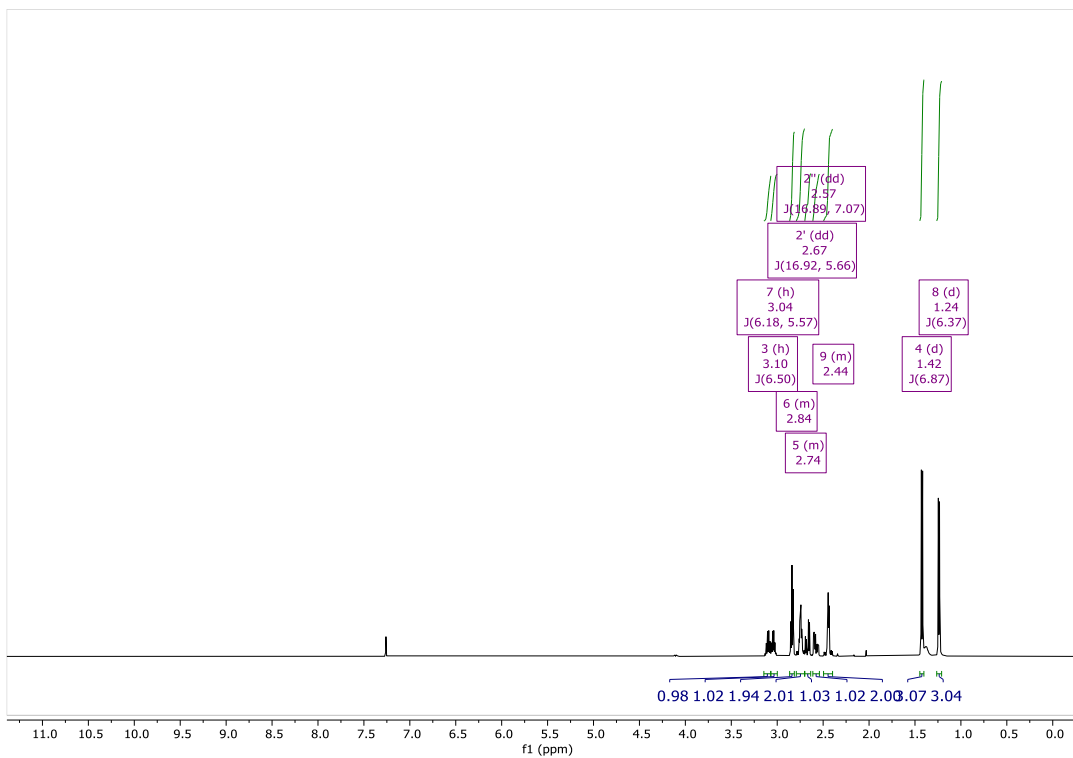
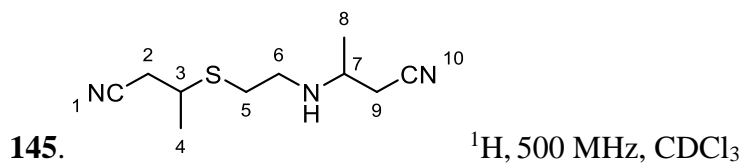


144. ^1H , 500 MHz, CDCl_3

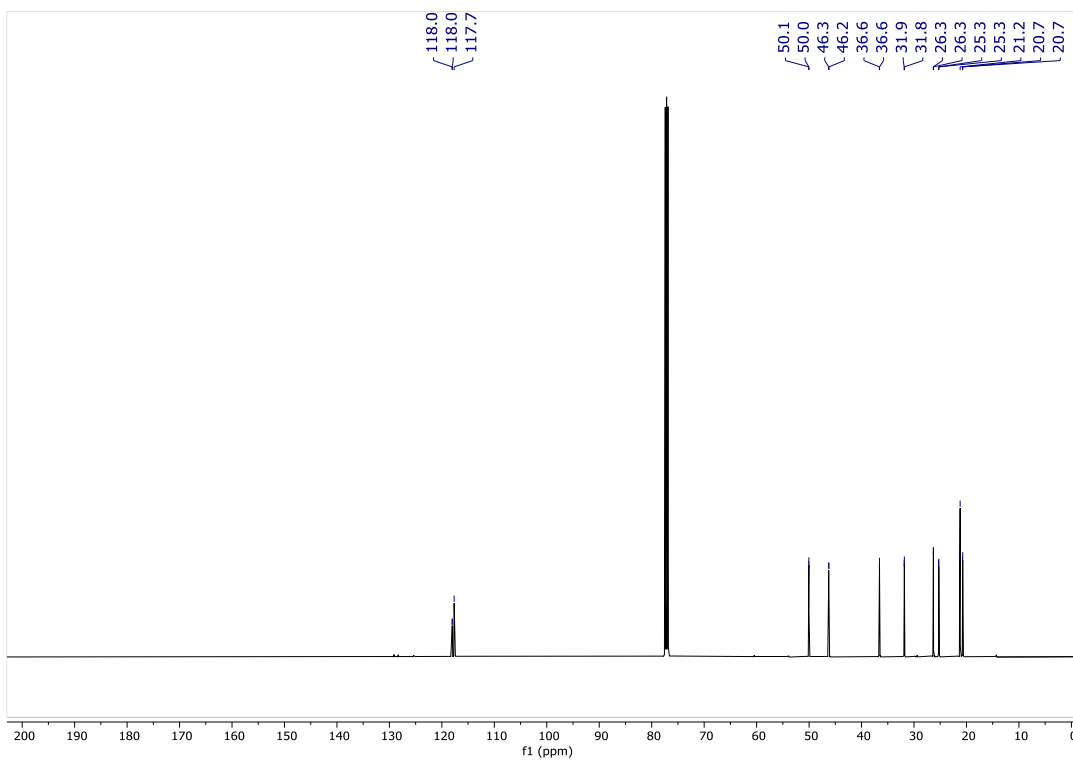


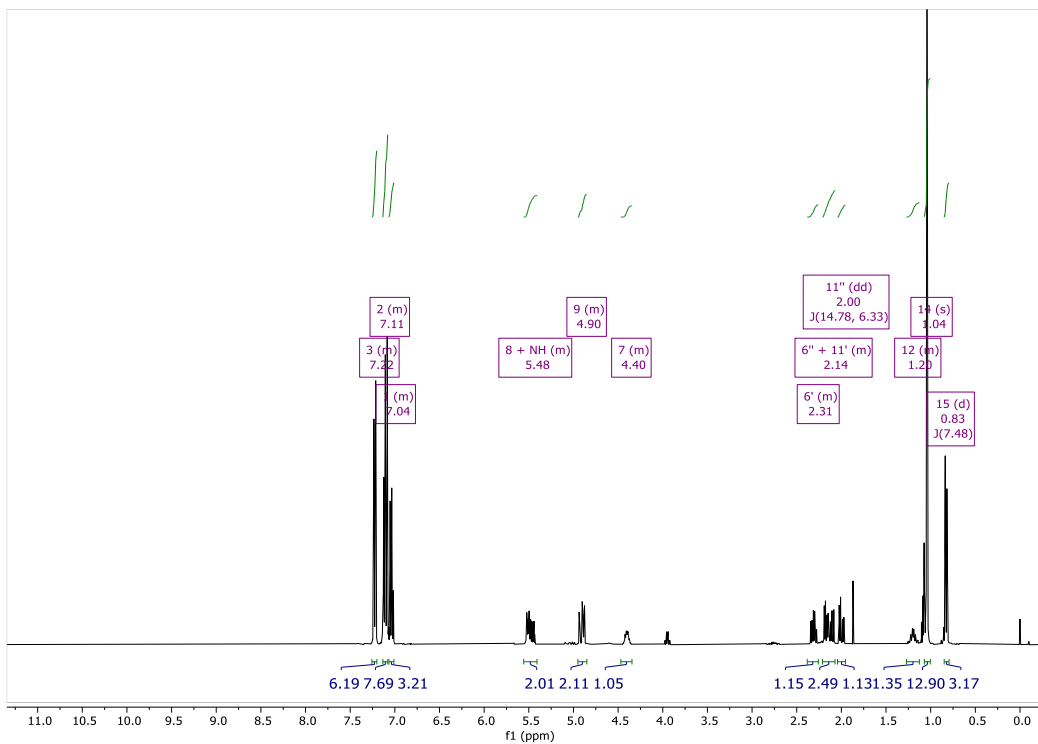
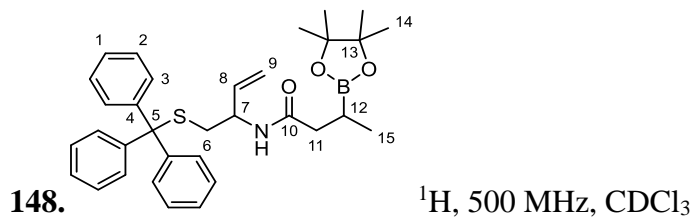
144. ^{13}C , 126 MHz, CDCl_3



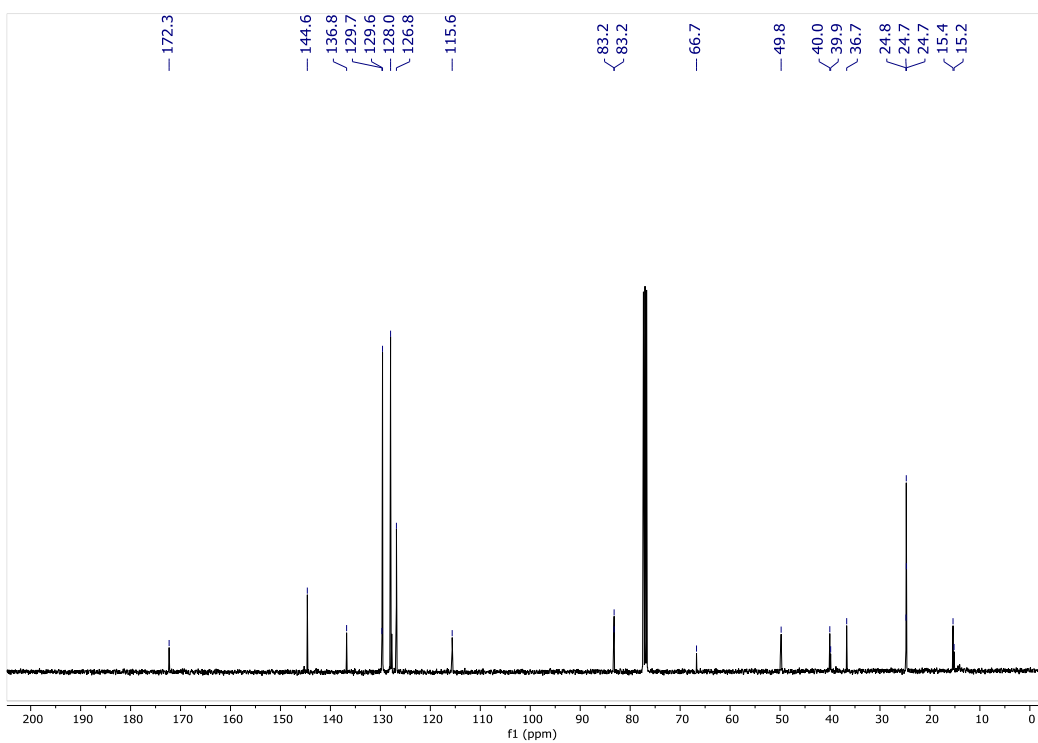


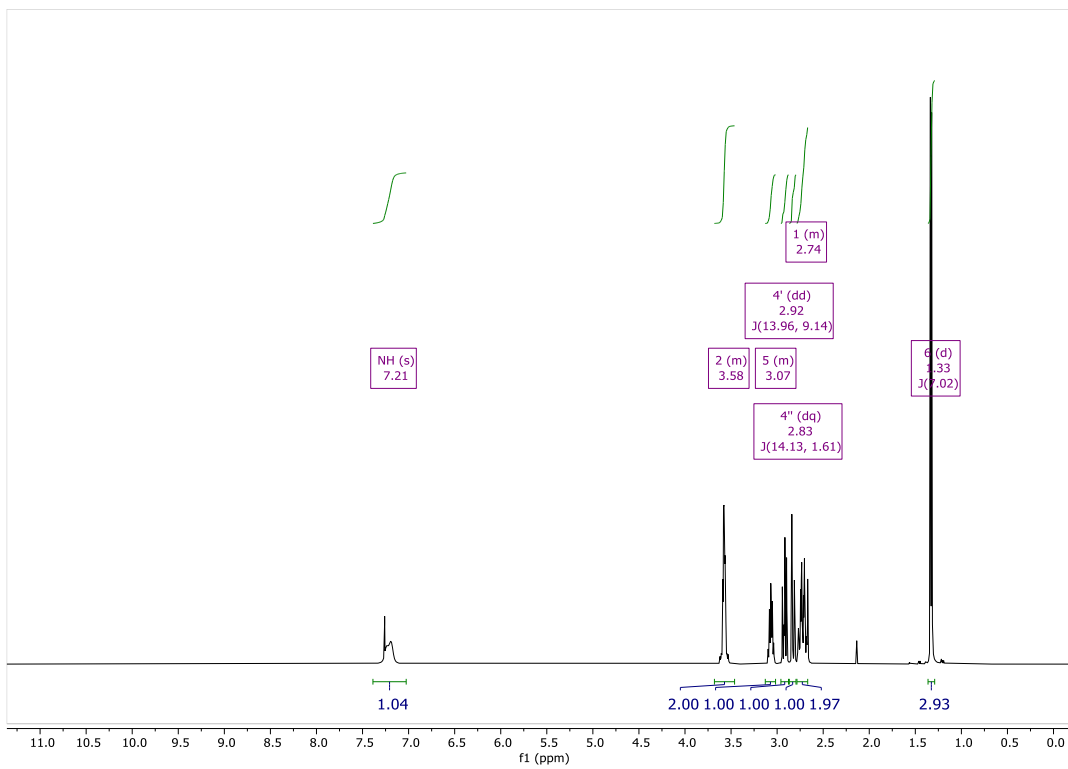
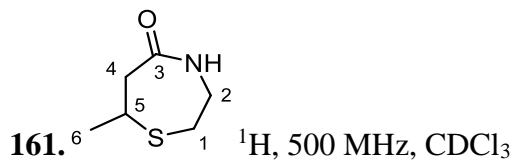
145. ^{13}C , 126 MHz, CDCl_3



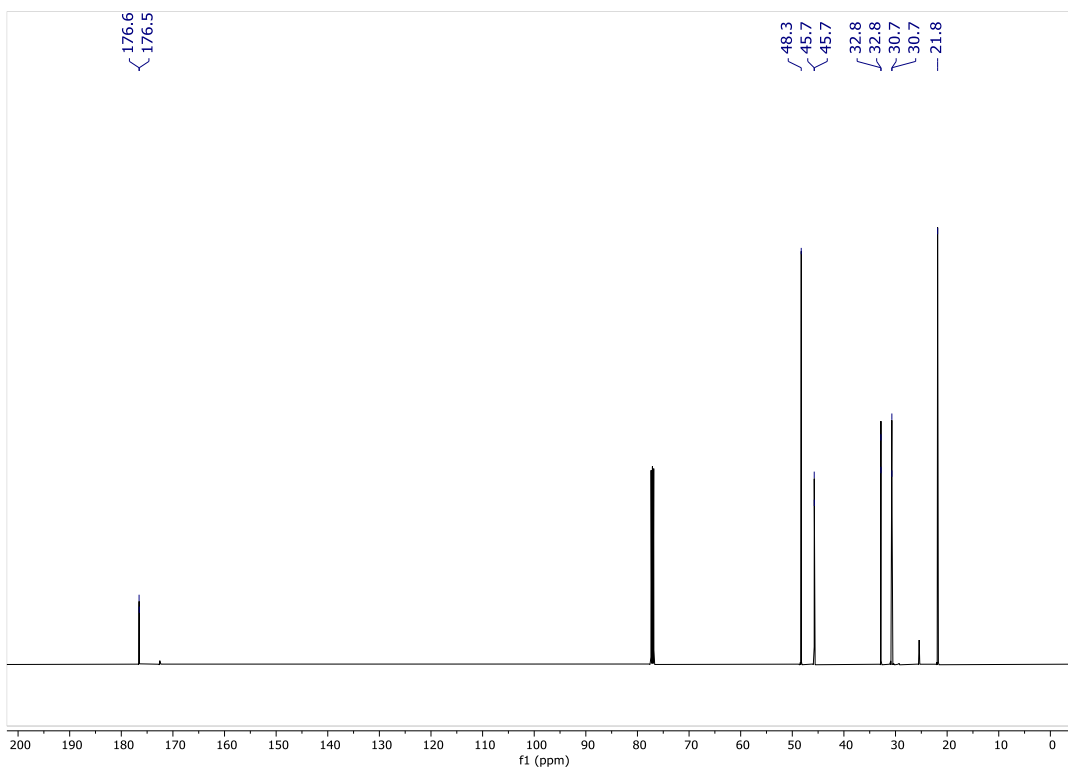


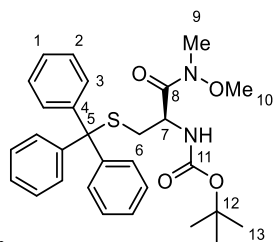
148. ^{13}C , 126 MHz, CDCl_3



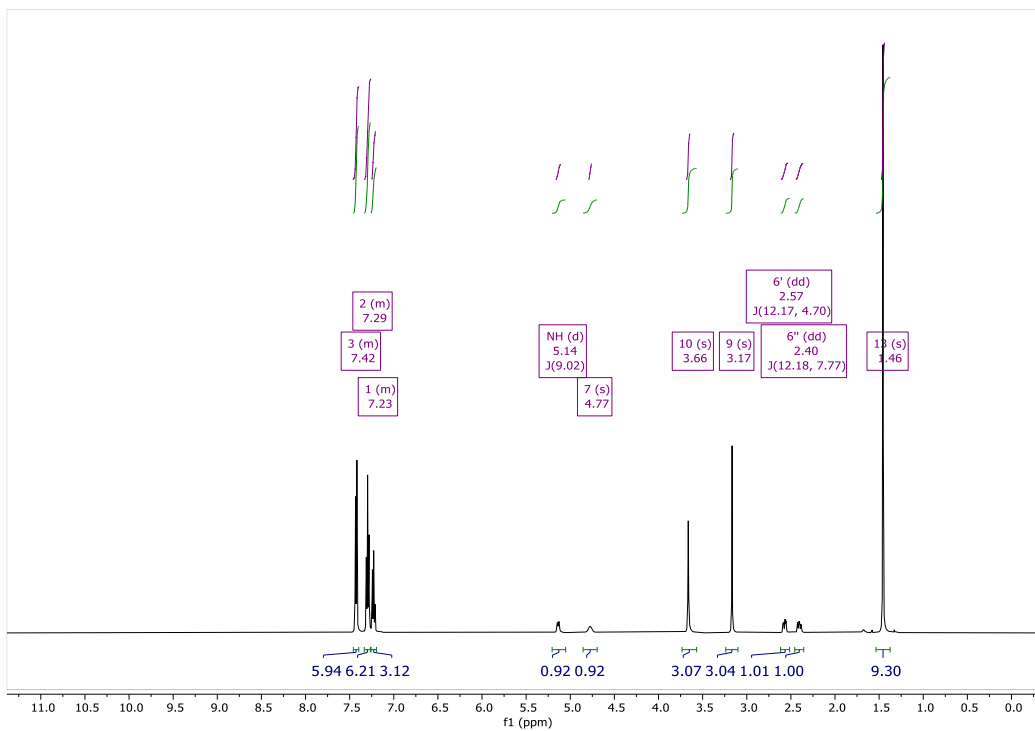


161. ¹³C, 126 MHz, CDCl₃

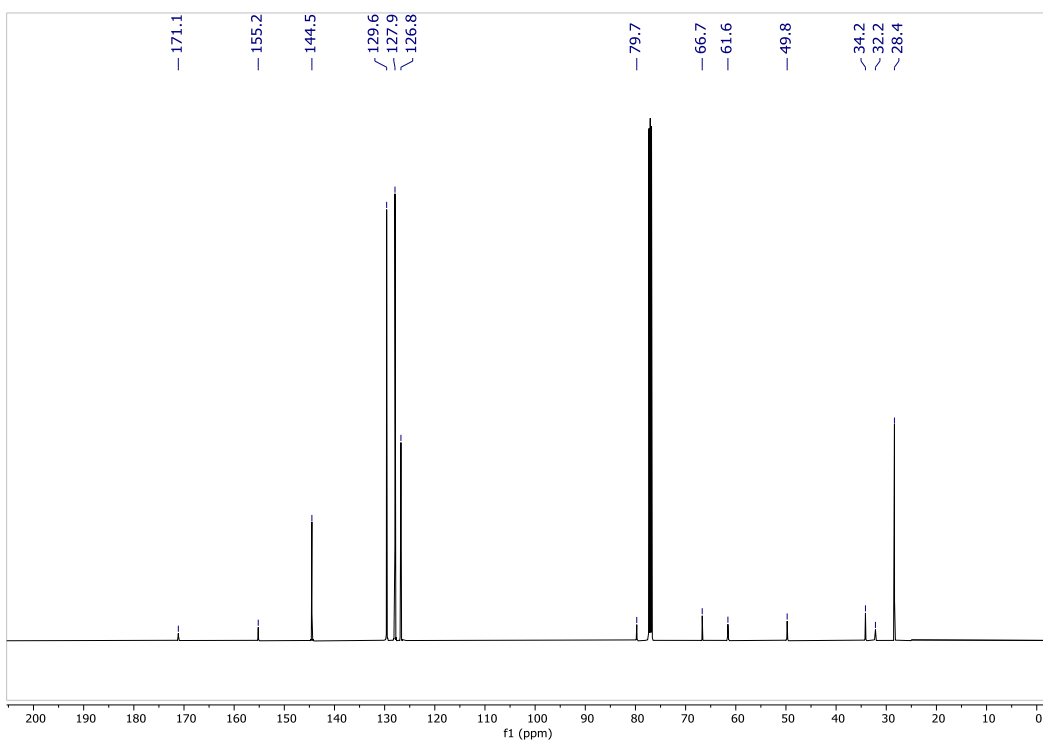


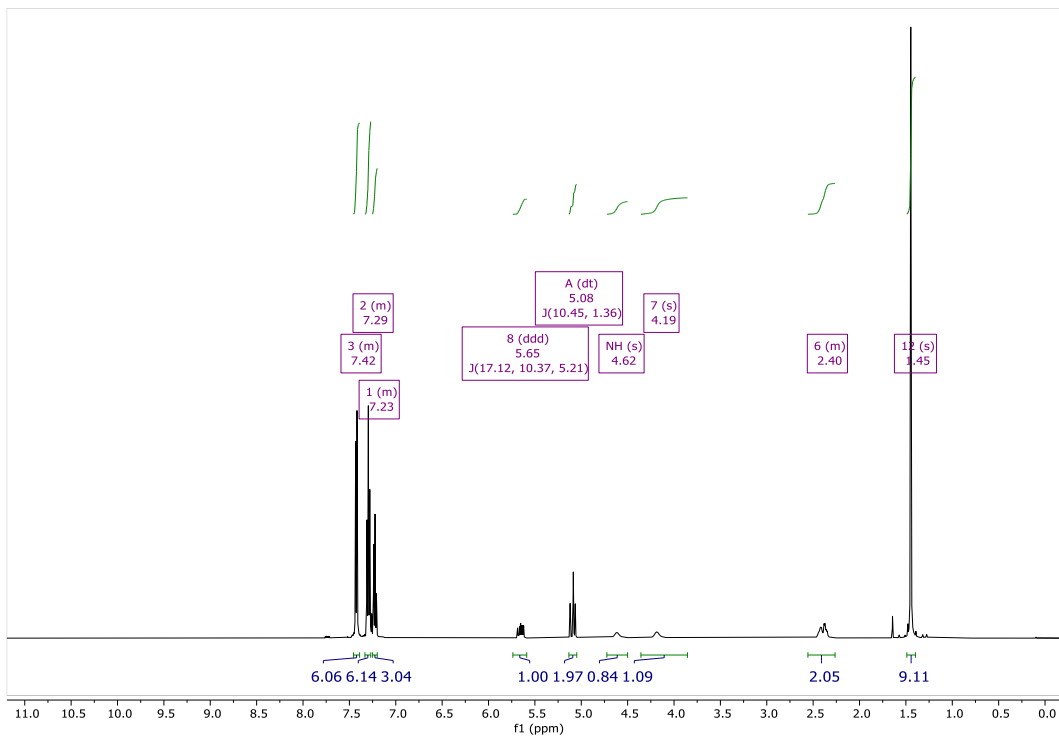
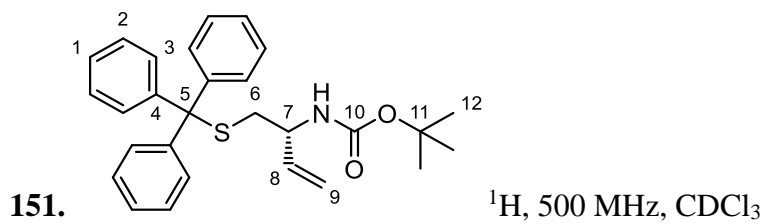


156. ^1H , 500 MHz, CDCl_3

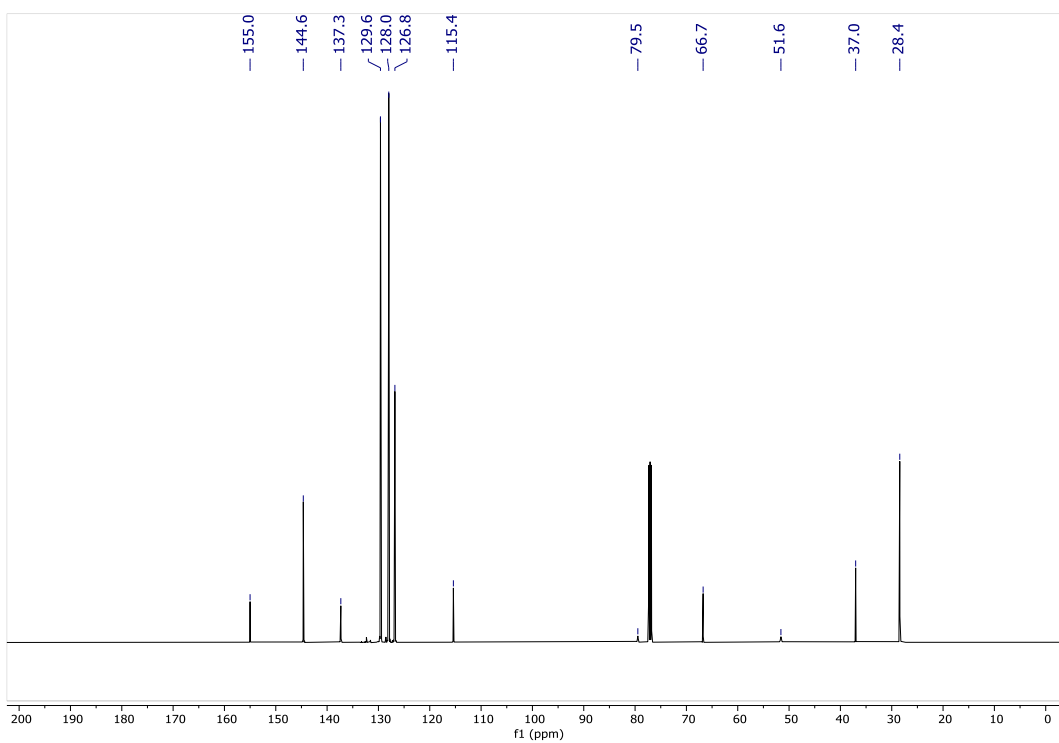


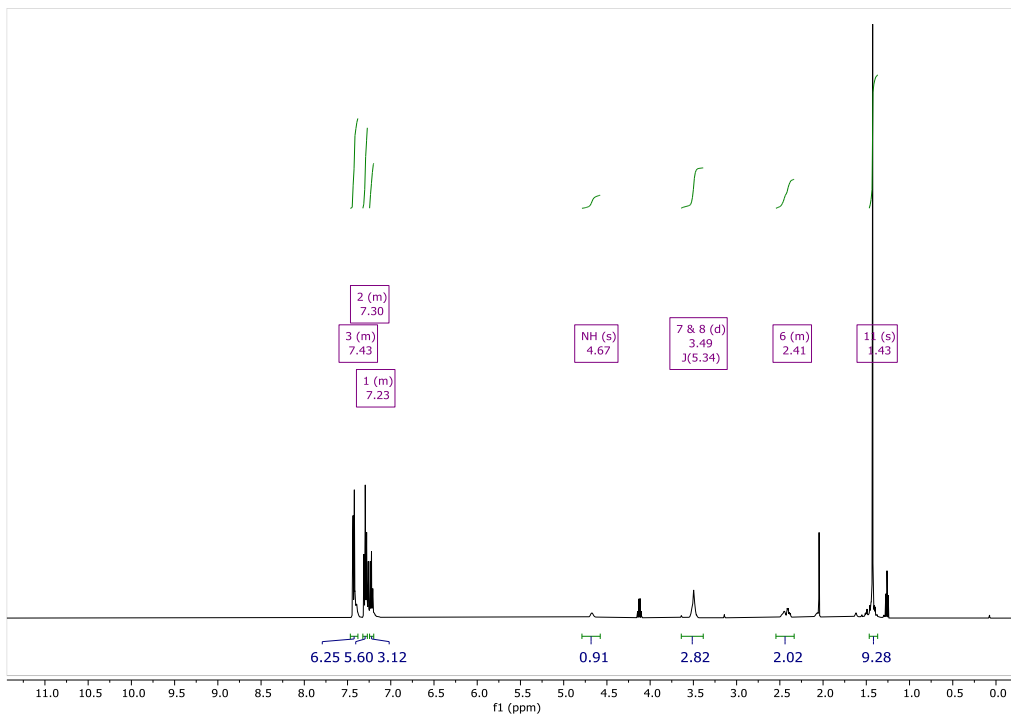
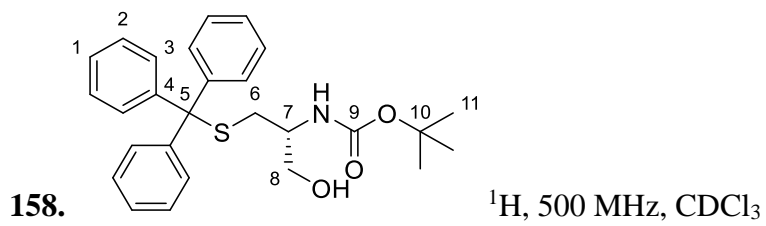
156. ^{13}C , 126 MHz, CDCl_3



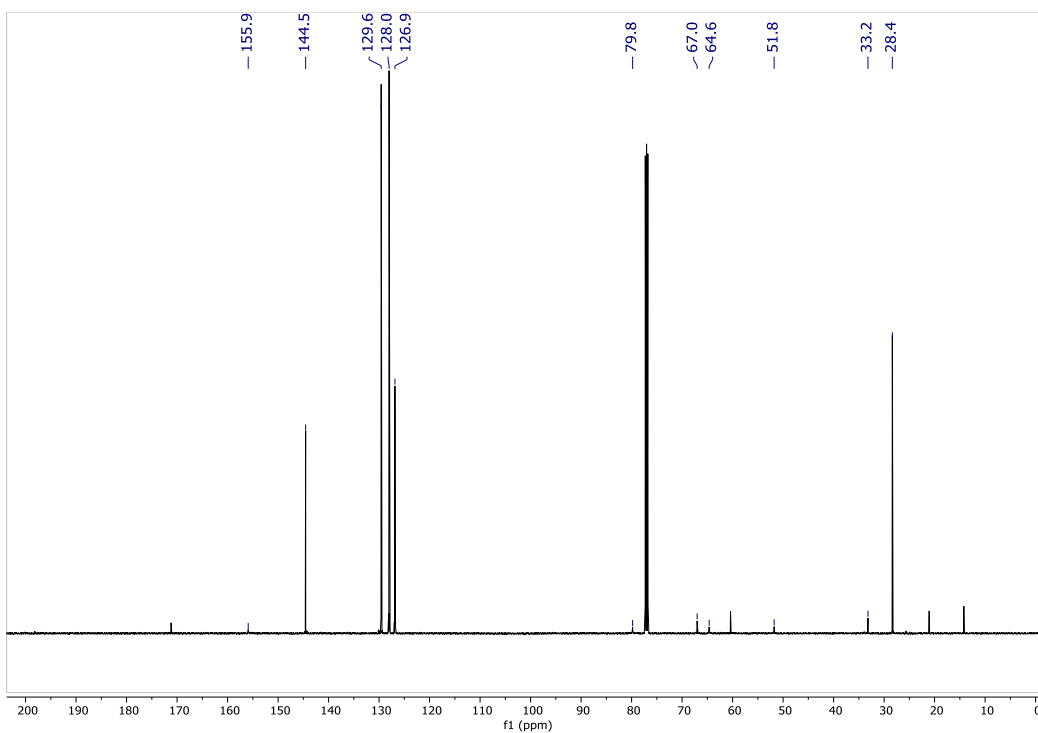


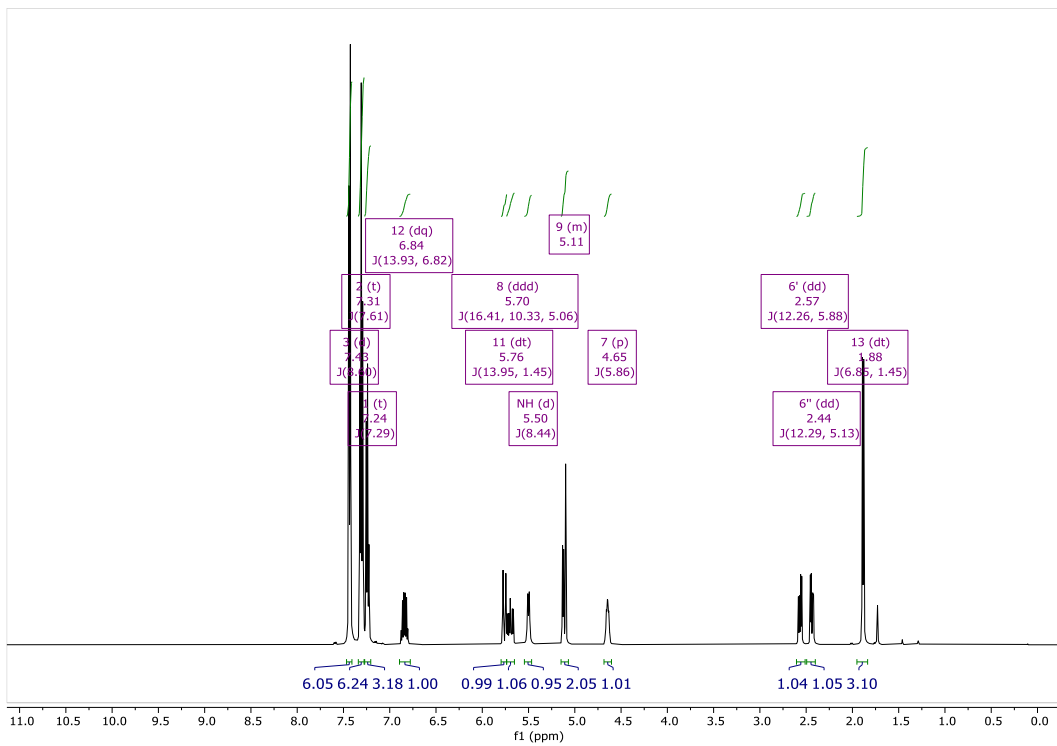
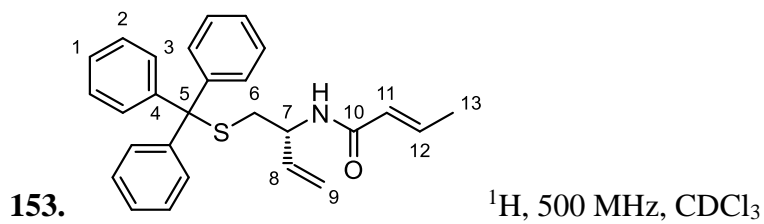
151. ^{13}C , 126 MHz, CDCl_3



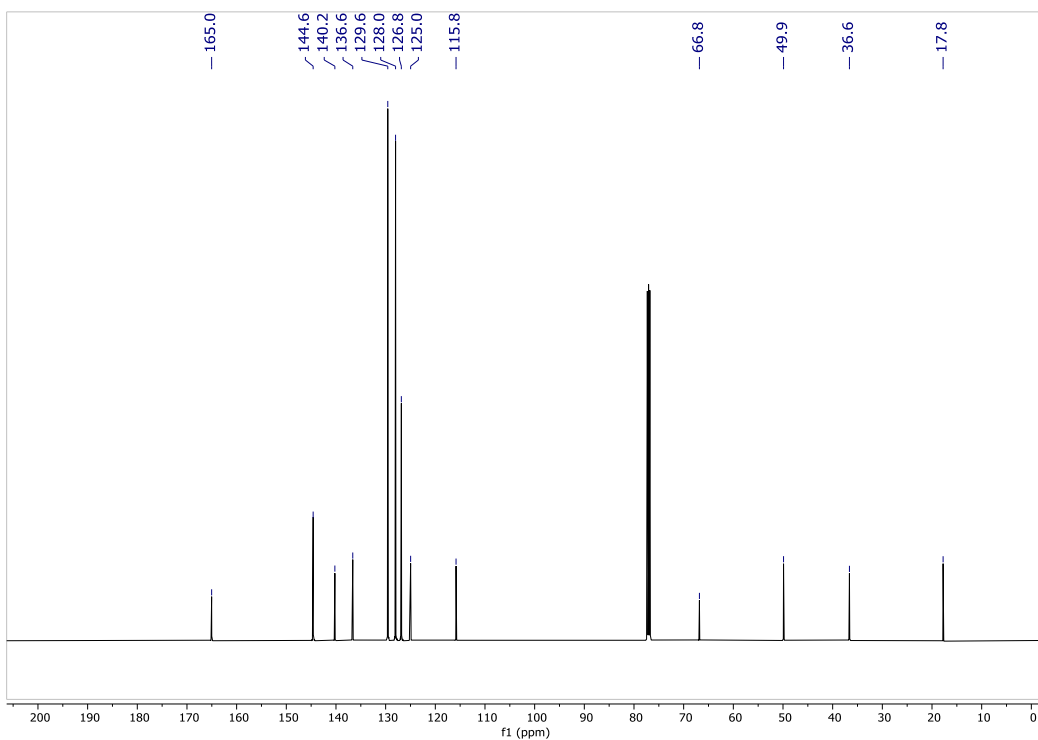


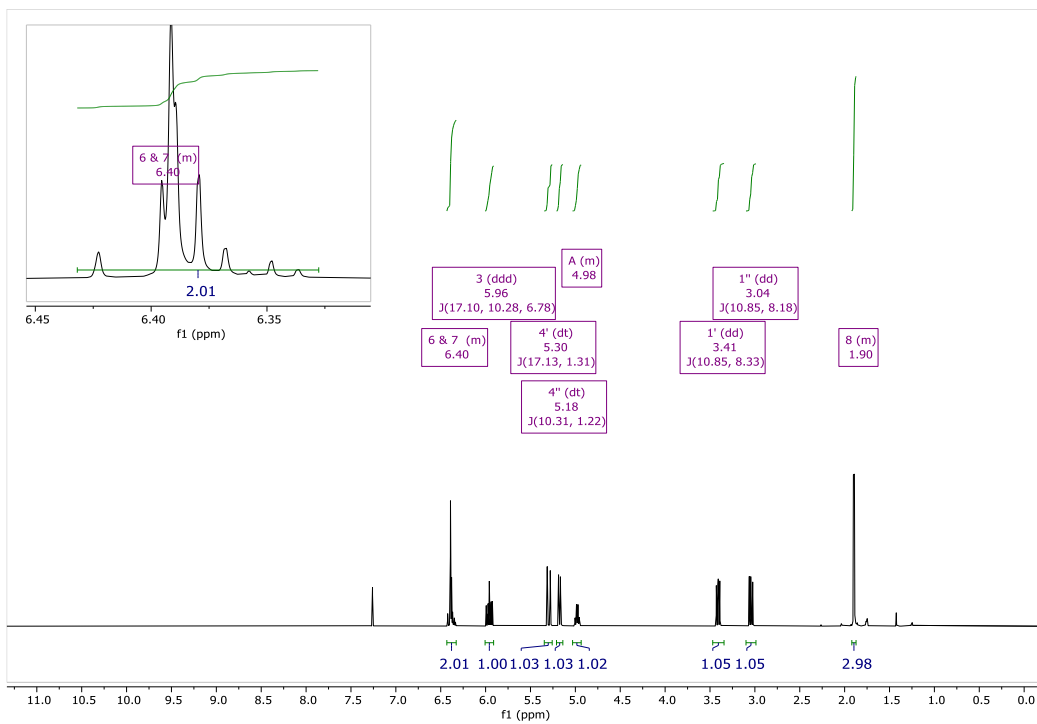
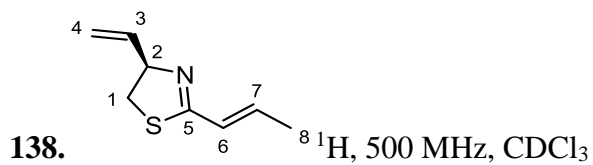
158. ^{13}C , 126 MHz, CDCl_3



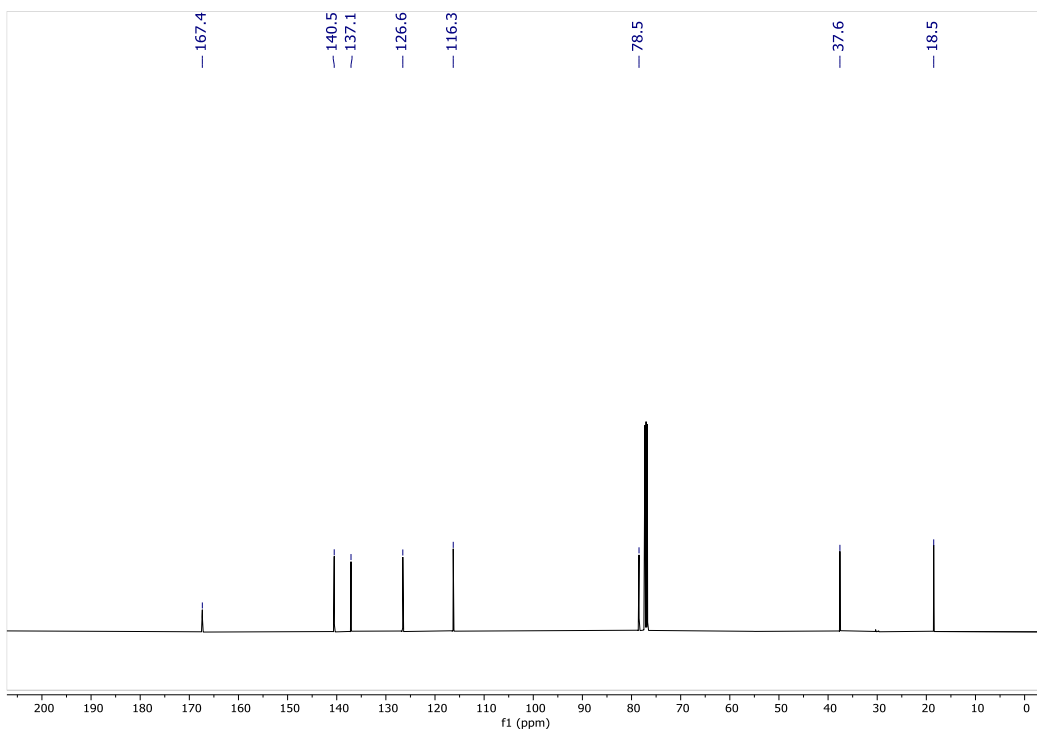


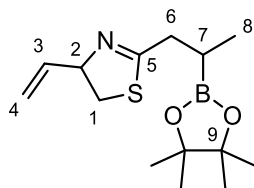
153. ^{13}C , 126 MHz, CDCl_3



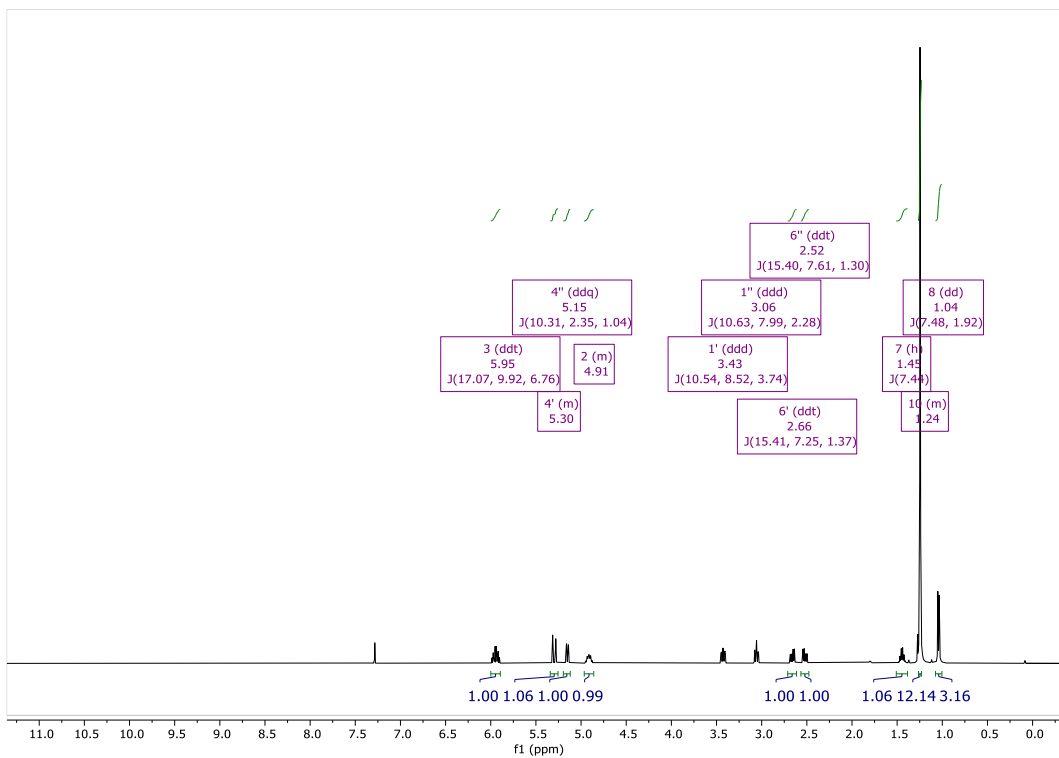


138. ¹³C, 126 MHz, CDCl₃

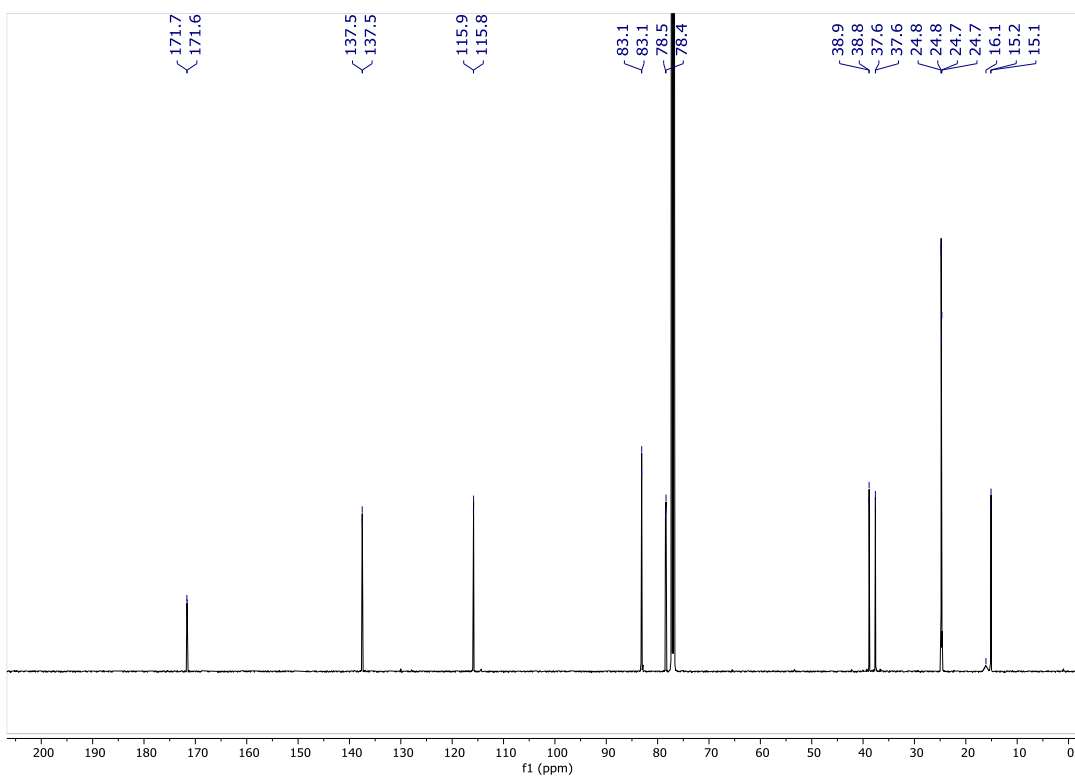


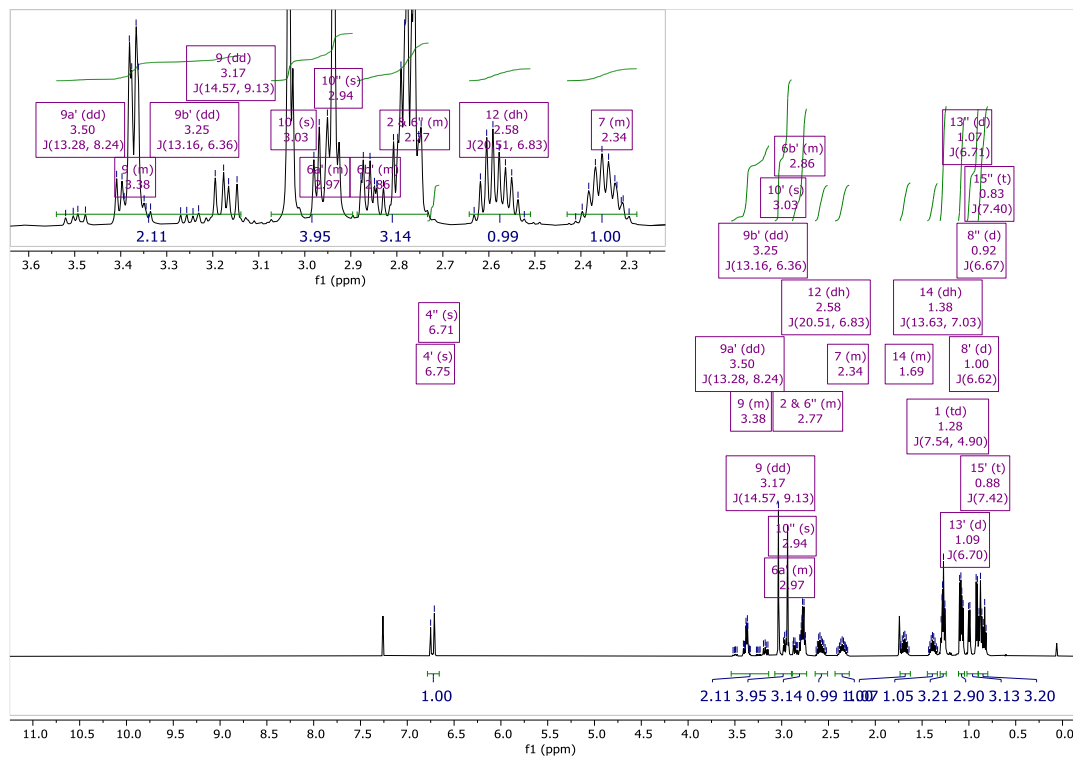
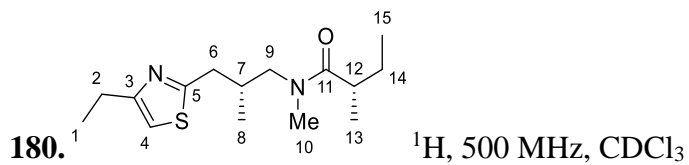


137. $^{10} \text{H}$, 500 MHz, CDCl_3

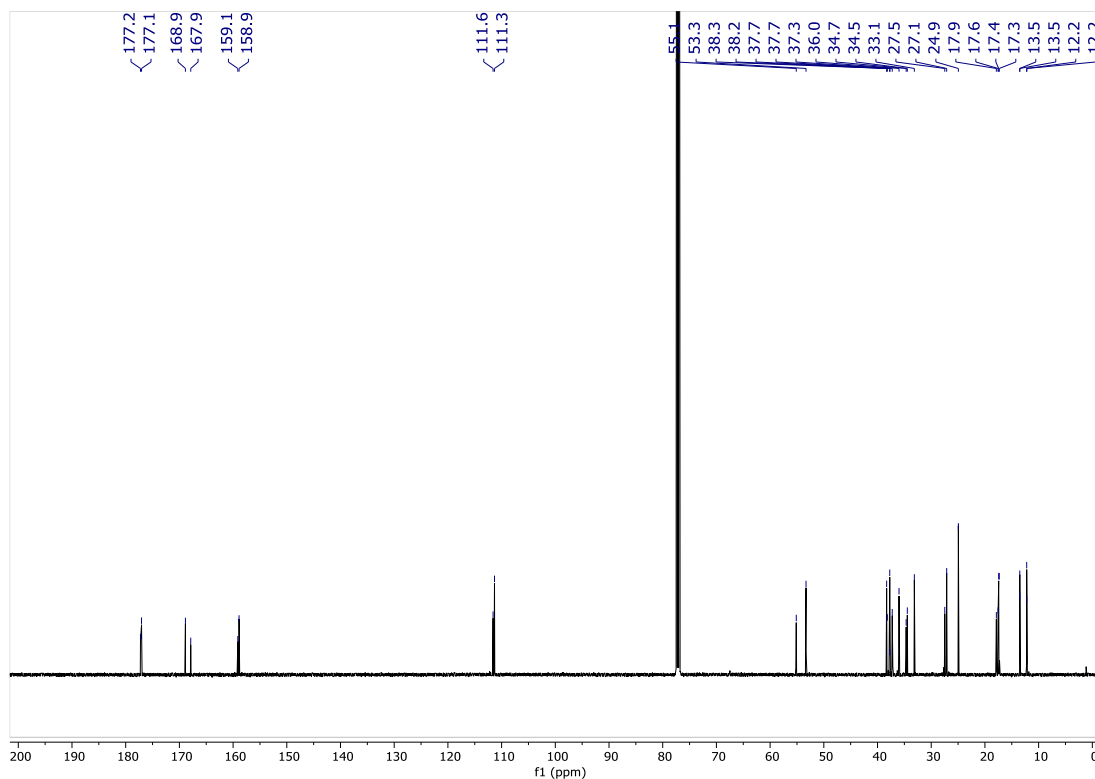


137. ^{13}C , 126 MHz, CDCl_3

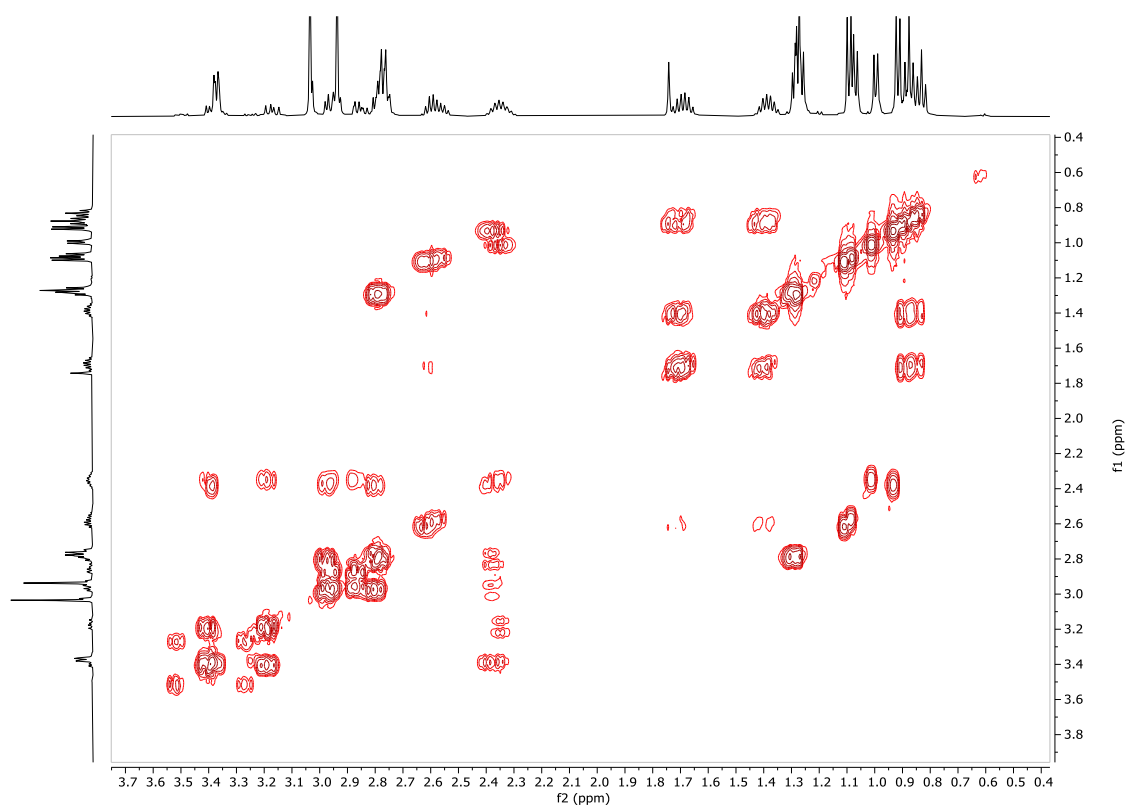




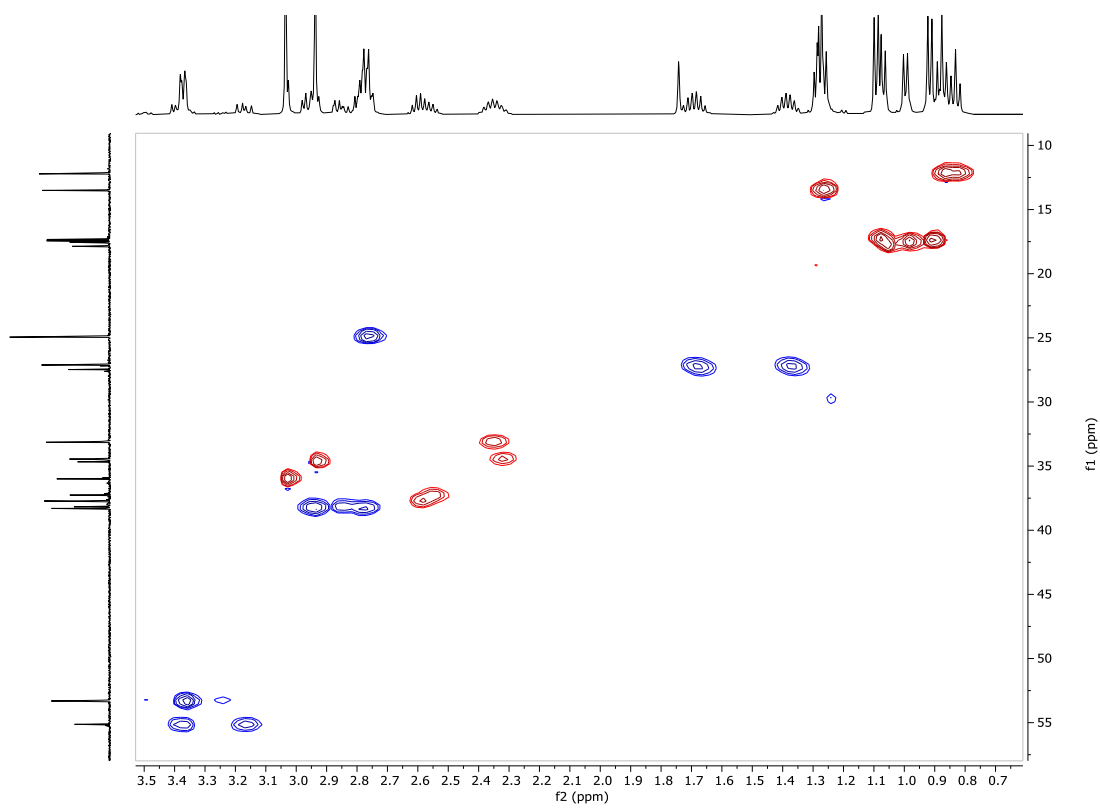
180. ^{13}C , 126 MHz, CDCl_3



180. ^1H - ^1H COSY, 500 MHz, CDCl_3

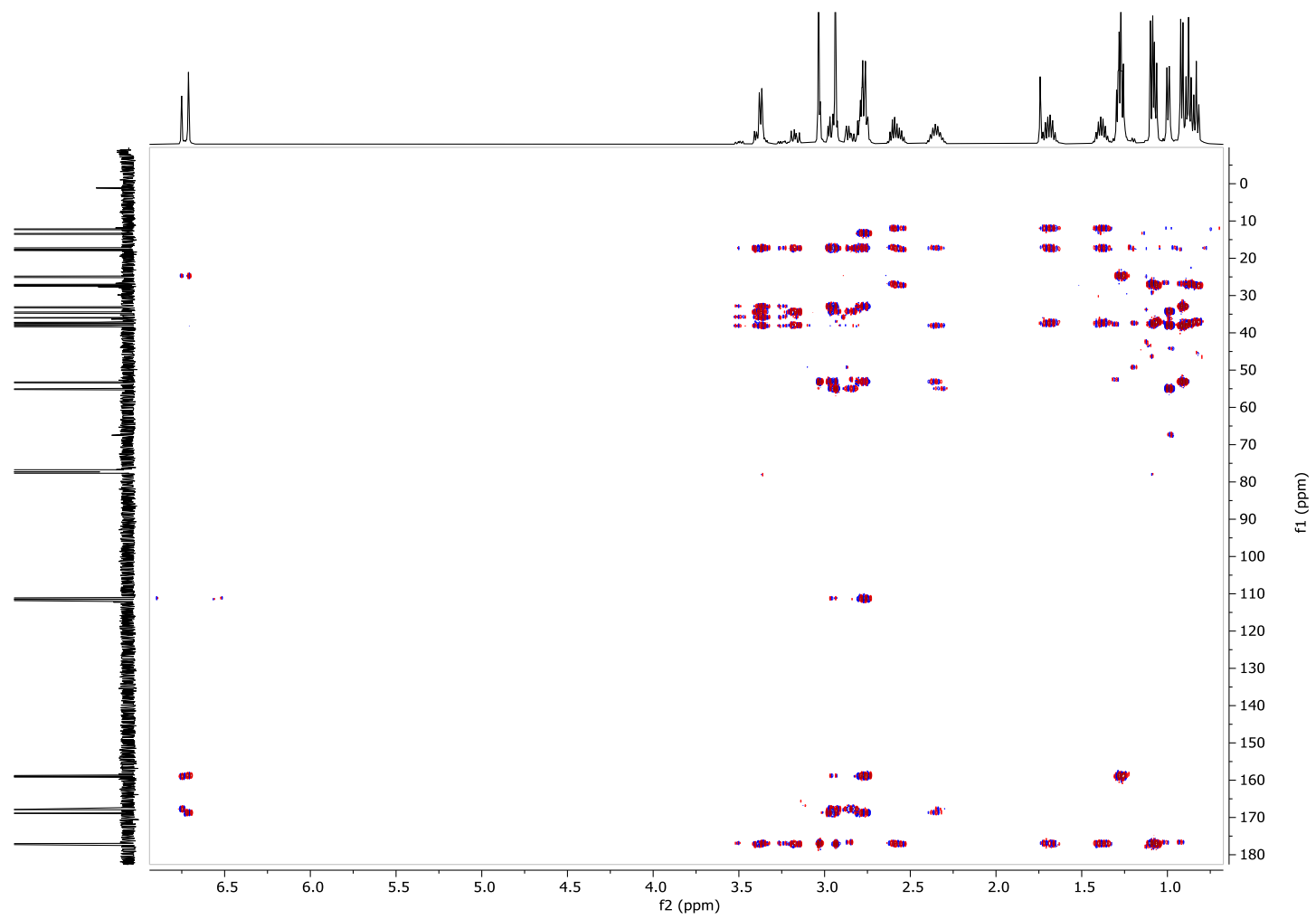


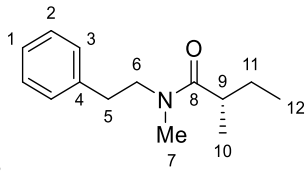
180. ^1H - ^{13}C HSQC, 500 MHz, CDCl_3



Red = CH and CH₃; Blue = CH₂

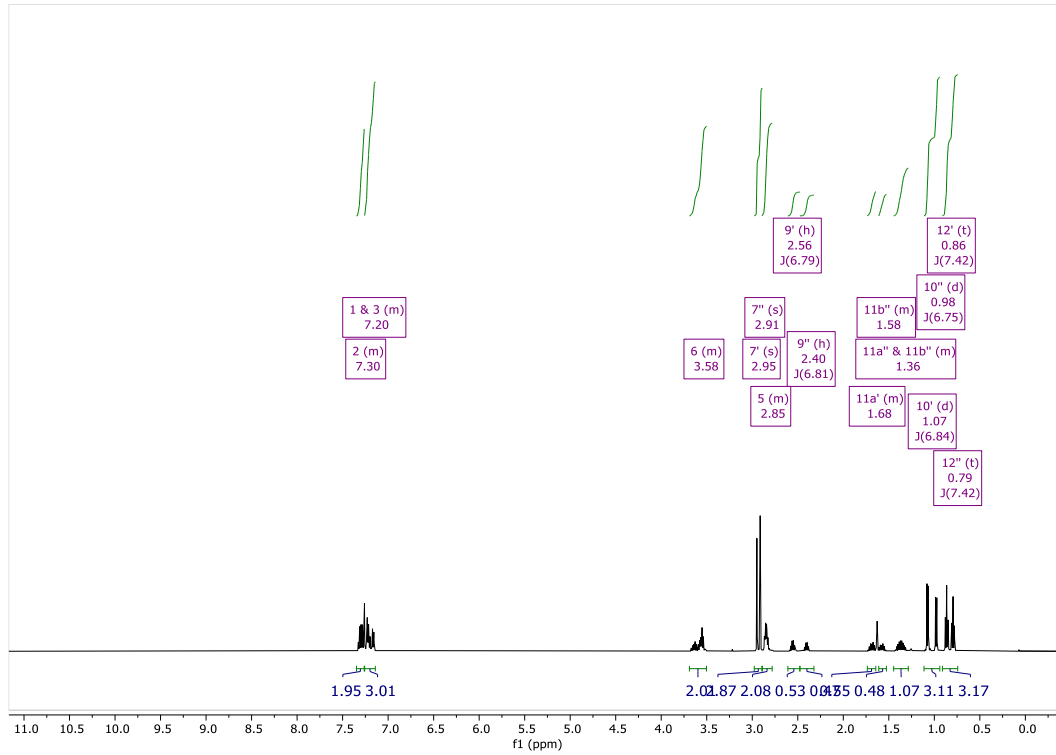
180. ^1H - ^{13}C HMBC, 500 MHz, CDCl_3



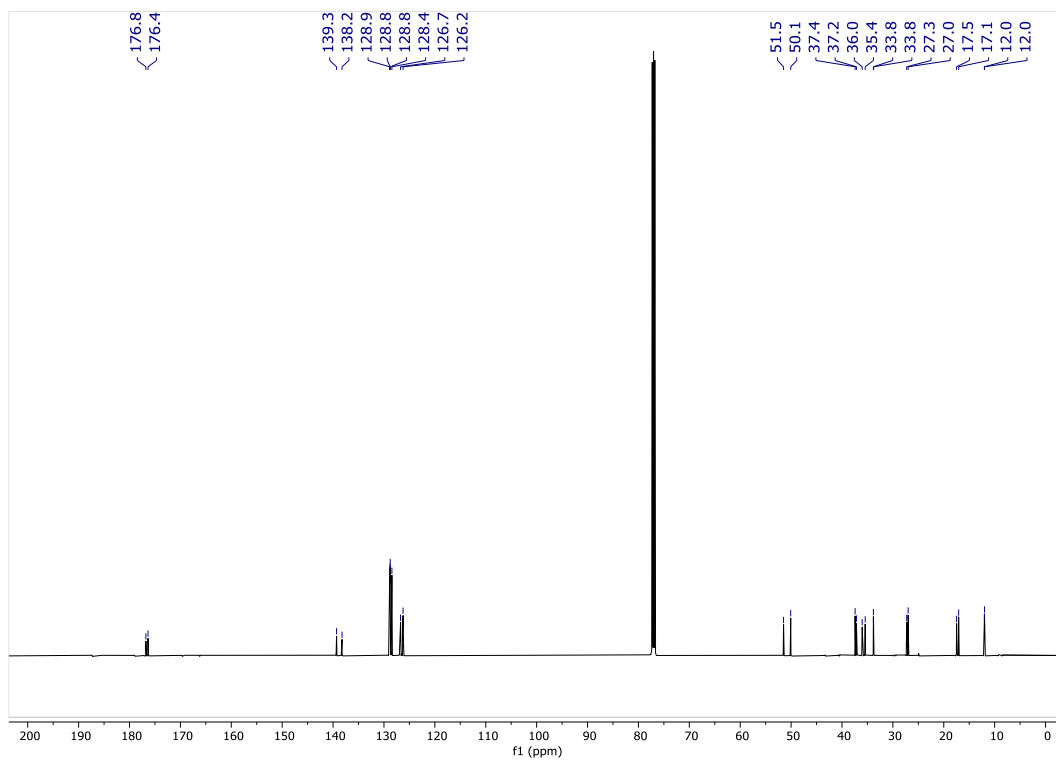


181.

^1H , 500 MHz, CDCl_3



181. ^{13}C , 126 MHz, CDCl_3



6 References

- (1) Beak, P.; Bonham, J. The Deuteration of Some N-Methyl-4-Pyridones. *J. Am. Chem. Soc.* **1965**, *87*, 3365–3371.
- (2) Abramovitch, R. A.; Coutts, R. T.; Smith, E. M. The Direct Acylation of Pyridine 1-Oxides. *J. Org. Chem.* **1972**, *37*, 3584–3587.
- (3) Beak, P.; Farney, R.; Doonan, D. J.; Balch, A. L. Dipole-Stabilized Carbanions from a Methyl Thio Ester and a Methylamide. *J. Am. Chem. Soc.* **1973**, *95*, 4771–4772.
- (4) Upton, C. J.; Beak, P. Dipole Stabilized Carbanions. Reactions of Benzoate Esters with Lithium 2,2,6,6-Tetramethylpiperidide. *J. Org. Chem.* **1975**, *40*, 1094–1098.
- (5) Beak, P.; McKinnie, B. G. Dipole-Stabilized Carbanions. Direct Lithiation of the Methyl Group of a Methyl Ester. *J. Am. Chem. Soc.* **1977**, *99*, 5213.
- (6) Beak, P.; Baillargeon, M.; Carter, L. G. Lithiation of Ethyl 2,4,6-Triisopropylbenzoate Adjacent to Oxygen: The α -Lithioalkyl Alcohol Synthone. *J. Org. Chem.* **1978**, *43*, 4255–4256.
- (7) Rondan, N. G.; Houk, K. N.; Beak, P.; Zajdel, W. J.; Chanrasekhar, J.; Schleyer, P. V. R. Dipole Stabilization of α -Heteroatom Carbanions: Theory and Experiment. *J. Org. Chem.* **1981**, *46*, 4108–4110.
- (8) Wiberg, K. B.; Bailey, W. F. Dipole-Stabilized Carbanions: A Computational Study of N-Methylformamide Anion and Methyl N-Methylcarbamate Anion. *J. Org. Chem.* **2002**, *67*, 5365–5368.
- (9) Jones, F. N.; Zinn, M. F.; Hauser, C. R. Metalations of Benzyldimethylamine and Related Amines with N-Butyllithium in Ether. Deuteration to Form Ring and Side-Chain Derivatives. *J. Org. Chem.* **1963**, *28*, 663–665.
- (10) Hoppe, D.; Hanko, R.; Brönneke, A. Lithiated Allyl N,N-Dialkylcarbamates as Homo-enolate Equivalents; Synthesis of Protected 4-Oxoalkanoates. *Angew. Chem. Int. Ed.* **1980**, *19*, 625–627.
- (11) Hoppe, D.; Brönneke, A. Highly Diastereoselective Synthesis of Di- and Trisubstituted 4-Butanolides from Aldehydes and Ketones via Three-Carbon-Extension by Allylic Homo-enolate Reagents. *Tetrahedron Lett.* **1983**, *24*, 1687–1690.
- (12) Hoppe, D.; Krämer, T. α -Deprotonation of an α -Chiral 2-Alkenylcarbamate with Retention and Lithium-Titanium Exchange with Inversion— the Homoaldol Reaction with 1,3-Chirality Transfer. *Angew. Chem. Int. Ed.* **1986**, *25*, 160–162.
- (13) Krämer, T.; Hoppe, D. Reagent-Controlled Enantioselective Homoaldol Reaction with Chiral 1-Oxyallyllithium Derivatives. Enantio-Divergent Tuning by Achiral Titanium Reagents. *Tetrahedron Lett.* **1987**, *28*, 5149–5152.
- (14) Tebben, P.; Hintze, F.; Hoppe, D. Chiral Lithium-1-oxyalkanides by Asymmetric Deprotonation; Enantioselective Synthesis of 2-Hydroxyalkanoic Acids and Secondary Alkanols. *Angew. Chem. Int. Ed.* **1990**, *29*, 1422–1424.
- (15) Hintze, F.; Hoppe, D. Enantioselective Synthesis of (S)-1-Methyldodecyl Acetate, a Pheromone of *Drosophila Mulleri*, via (-)-Sparteine-Assisted Deprotonation of 1-Dodecanol. *Synthesis (Stuttg.)* **1992**, *1992*, 1216–1218.
- (16) Kerrick, S. T.; Beak, P. Asymmetric Deprotonations: Enantioselective Syntheses of 2-Substituted (Tert-Butoxycarbonyl)Pyrrolidines. *J. Am. Chem. Soc.* **1991**, *113*, 9708–9710.
- (17) Faibish, N. C.; Park, Y. S.; Lee, S.; Beak, P. A Mechanistic and Structural Investigation of the (-)-Sparteine Mediated Asymmetric Benzylic Lithiation Substitution Reactions of N-Boc-N-(p-Methoxyphenyl)Benzylamine. *J. Am.*

- Chem. Soc.* **1997**, *119*, 11561–11570.
- (18) Jastrzebski, J. T. B. H.; van Koten, G.; Konijn, M.; Stam, C. H. Intramolecularly Chelated Di- and Tetranuclear Aryllithium Compounds: Crystal Structure of $\text{Li}_4[\text{C}_6\text{H}_4(2\text{-CH}_2\text{NMe}_2)]_4$ Containing Four-Center Two-Electron-Bonded C(Aryl) Atoms and Heptacoordinate Lithium Atoms. *J. Am. Chem. Soc.* **1982**, *104*, 5490–5492.
 - (19) Al-Aseer, M.; Beak, P.; Hay, D.; Kempf, D. J.; Mills, S.; Smith, S. G. Dipole-Stabilized Carbanions: Evidence for a Complex in the α' -Lithiation of N,N-Dimethyl-2,4,6-Triisopropylbenzamide. *J. Am. Chem. Soc.* **1983**, *105*, 2080–2082.
 - (20) Charbonneau, L. F.; Smith, S. G. Kinetics of the Reaction of n-Butyllithium with 4-Methylmercaptoacetophenone in Benzene. *J. Org. Chem.* **1976**, *41*, 808–812.
 - (21) Meyers, A. I.; Rieker, W. F.; Fuentes, L. M. Initial Complex and the Role of Solvent in Metalations Leading to Dipole-Stabilized Anions. *J. Am. Chem. Soc.* **1983**, *105*, 2082–2083.
 - (22) Beak, P.; Meyers, A. I. Stereo- and Regiocontrol by Complex Induced Proximity Effects: Reactions of Organolithium Compounds. *Acc. Chem. Res.* **1986**, *19*, 356–363.
 - (23) Hay, D. R.; Song, Z.; Smith, S. G.; Beak, P. Complex-Induced Proximity Effects and Dipole-Stabilized Carbanions: Kinetic Evidence for the Role of Complexes in the α' -Lithiations of Carboxamides. *J. Am. Chem. Soc.* **1988**, *110*, 8145–8153.
 - (24) Gallagher, D. J.; Kerrick, S. T.; Beak, P. Enantioselective Deprotonation: The Structure and Reactivity of an Unsymmetrically Complexed Isopropylithium/Sparteine/Et₂O Dimer. *J. Am. Chem. Soc.* **1992**, *114*, 5872–5873.
 - (25) Fernández-Nieto, F.; Paleo, M. R.; Colunga, R.; Raposo, M. L.; Garcia-Rio, L.; Sardina, F. J. The Two Alternative Rate-Determining Steps in Benzylic Lithiation Reactions of Esters and Carbamates. *Org. Lett.* **2016**, *18*, 5520–5523.
 - (26) Beckmann, E.; Desai, V.; Hoppe, D. Stereospecific Reaction of α -Carbamoyloxy-2-Alkenylboronates and α -Carbamoyloxy-Alkylboronates with Grignard Reagents - Synthesis of Highly Enantioenriched Secondary Alcohols. *Synlett* **2004**, *13*, 2275–2280.
 - (27) Matteson, D. S.; Mah, R. W. H. Neighboring Boron in Nucleophilic Displacement. *J. Am. Chem. Soc.* **1963**, *85*, 2599–2603.
 - (28) Matteson, D. S. Boronic Ester Neighboring Groups. *Acc. Chem. Res.* **1970**, *3*, 186–193.
 - (29) Matteson, D. S.; Majumdar, D. ..Alpha.-Chloro Boronic Esters from Homologation of Boronic Esters. *J. Am. Chem. Soc.* **1980**, *102*, 7588–7590.
 - (30) Matteson, D. S.; Sadhu, K. M. Boronic Ester Homologation with 99% Chiral Selectivity and Its Use in Syntheses of the Insect Pheromones (3S,4S)-4-Methyl-3-Heptanol and Exo-Brevicomine. *J. Am. Chem. Soc.* **1983**, *105*, 2077–2078.
 - (31) Sadhu, K. M.; Matteson, D. S. (Chloromethyl)Lithium: Efficient Generation and Capture by Boronic Esters and a Simple Preparation of Diisopropyl (Chloromethyl)Boronate. *Organometallics* **1985**, *4*, 1687–1689.
 - (32) Blakemore, P. R.; Marsden, S. P.; Vater, H. D. Reagent-Controlled Asymmetric Homologation of Boronic Esters by Enantioenriched Main-Group Chiral Carbenoids. *Org. Lett.* **2006**, *8*, 773–776.
 - (33) Blakemore, P. R.; Burge, M. S. Iterative Stereospecific Reagent-Controlled Homologation of Pinacol Boronates by Enantioenriched α -Chloroalkyllithium Reagents. *J. Am. Chem. Soc.* **2007**, *129*, 3068–3069.
 - (34) Besong, G.; Jarowicki, K.; Kocienski, P. J.; Sliwinski, E.; Boyle, F. T. Synthesis

- of (S)-(-)-N-Acetylcolchinol Using Intramolecular Biaryl Oxidative Coupling. *Org. Biomol. Chem.* **2006**, *4*, 2193–2207.
- (35) Stymiest, J. L. L.; Dutheuil, G.; Mahmood, A.; Aggarwal, V. K. K. Lithiated Carbamates: Chiral Carbenoids for Iterative Homologation of Boranes and Boronic Esters. *Angew. Chem. Int. Ed.* **2007**, *46*, 7491–7494.
- (36) Aggarwal, V. K.; Fang, G. Y.; Schmidt, A. T. Synthesis and Applications of Chiral Organoboranes Generated from Sulfonium Ylides. *J. Am. Chem. Soc.* **2005**, *127*, 1642–1643.
- (37) Carstens, A.; Hoppe, D. Generation of a Configurationally Stable, Enantioenriched α -Oxy- α -Methylbenzylithium: Stereodivergence of Its Electrophilic Substitution. *Tetrahedron* **1994**, *50*, 6097–6108.
- (38) Stymiest, J. L.; Bagutski, V.; French, R. M.; Aggarwal, V. K. Enantiodivergent Conversion of Chiral Secondary Alcohols into Tertiary Alcohols. *Nature* **2008**, *456*, 778–783.
- (39) Pulis, A. P.; Aggarwal, V. K. Synthesis of Enantioenriched Tertiary Boronic Esters from Secondary Allylic Carbamates. Application to the Synthesis of C30 Botryococcene. *J. Am. Chem. Soc.* **2012**, *134*, 7570–7574.
- (40) Partridge, B. M.; Chausset-Boissarie, L.; Burns, M.; Pulis, A. P.; Aggarwal, V. K. Enantioselective Synthesis and Cross-Coupling of Tertiary Propargylic Boronic Esters Using Lithiation-Borylation of Propargylic Carbamates. *Angew. Chem. Int. Ed.* **2012**, *51*, 11795–11799.
- (41) Essafi, S.; Tomasi, S.; Aggarwal, V. K.; Harvey, J. N. Homologation of Boronic Esters with Organolithium Compounds: A Computational Assessment of Mechanism. *J. Org. Chem.* **2014**, *79*, 12148–12158.
- (42) Larouche-Gauthier, R.; Fletcher, C. J.; Couto, I.; Aggarwal, V. K. Use of Alkyl 2,4,6-Triisopropylbenzoates in the Asymmetric Homologation of Challenging Boronic Esters. *Chem. Commun.* **2011**, *47*, 12592.
- (43) Pulis, A. P.; Blair, D. J.; Torres, E.; Aggarwal, V. K. Synthesis of Enantioenriched Tertiary Boronic Esters by the Lithiation/Borylation of Secondary Alkyl Benzoates. *J. Am. Chem. Soc.* **2013**, *135*, 16054–16057.
- (44) Noble, A.; Roesner, S.; Aggarwal, V. K. Short Enantioselective Total Synthesis of Tatanan A and 3-Epi-Tatanan A Using Assembly-Line Synthesis. *Angew. Chem. Int. Ed.* **2016**, *55*, 15920–15924.
- (45) Varela, A.; Garve, L. K. B.; Leonori, D.; Aggarwal, V. K. Stereocontrolled Total Synthesis of (-)-Stemaphylline. *Angew. Chem. Int. Ed.* **2017**, *56*, 2127–2131.
- (46) Fletcher, C. J.; Wheelhouse, K. M. P.; Aggarwal, V. K. Stereoselective Total Synthesis of (+)-Giganin and Its C10 Epimer by Using Late-Stage Lithiation-Borylation Methodology. *Angew. Chem. Int. Ed.* **2013**, *52*, 2503–2506.
- (47) Sandford, C.; Aggarwal, V. K. Stereospecific Functionalizations and Transformations of Secondary and Tertiary Boronic Esters. *Chem. Commun.* **2017**, *53*, 5481–5494.
- (48) Dutheuil, G.; Webster, M. P.; Worthington, P. A.; Aggarwal, V. K. Stereocontrolled Synthesis of Carbon Chains Bearing Contiguous Methyl Groups by Iterative Boronic Ester Homologations: Application to the Total Synthesis of (+)-Faranal. *Angew. Chem. Int. Ed.* **2009**, *48*, 6317–6319.
- (49) Harned, A. M. From Determination of Enantiopurity to the Construction of Complex Molecules: The Horeau Principle and Its Application in Synthesis. *Tetrahedron* **2018**, *74*, 3797–3841.
- (50) Burns, M.; Essafi, S.; Bame, J. R.; Bull, S. P.; Webster, M. P.; Balieu, S.; Dale, J. W.; Butts, C. P.; Harvey, J. N.; Aggarwal, V. K. Assembly-Line Synthesis of

- Organic Molecules with Tailored Shapes. *Nature* **2014**, *513*, 183–188.
- (51) Nath, M. Toxicity and the Cardiovascular Activity of Organotin Compounds: A Review. *Appl. Organomet. Chem.* **2008**, *22*, 598–612.
- (52) Rayner, P. J.; O'Brien, P.; Horan, R. A. J. Preparation and Reactions of Enantiomerically Pure α -Functionalized Grignard Reagents. *J. Am. Chem. Soc.* **2013**, *135*, 8071–8077.
- (53) Casoni, G.; Kucukdisli, M.; Fordham, J. M.; Burns, M.; Myers, E. L.; Aggarwal, V. K. α -Sulfinyl Benzoates as Precursors to Li and Mg Carbenoids for the Stereoselective Iterative Homologation of Boronic Esters. *J. Am. Chem. Soc.* **2017**, *139*, 11877–11886.
- (54) Pippel, D. J.; Weisenburger, G. A.; Faibish, N. C.; Beak, P. Kinetics and Mechanism of the (-)-Sparteine-Mediated Deprotonation of (E)-N-Boc-N-(p-Methoxyphenyl)-3-Cyclohexylallylamine. *J. Am. Chem. Soc.* **2001**, *123*, 4919–4927.
- (55) Stead, D.; Carbone, G.; O'Brien, P.; Campos, K. R.; Coldham, I.; Sanderson, A. Asymmetric Deprotonation of N-Boc Piperidine: React IR Monitoring and Mechanistic Aspects. *J. Am. Chem. Soc.* **2010**, *132*, 7260–7261.
- (56) Barker, G.; McGrath, J. L.; Klapars, A.; Stead, D.; Zhou, G.; Campos, K. R.; O'Brien, P. Enantioselective, Palladium-Catalyzed α -Arylation of N-Boc Pyrrolidine: In Situ React IR Spectroscopic Monitoring, Scope, and Synthetic Applications. *J. Org. Chem.* **2011**, *76*, 5936–5953.
- (57) Fina, N. J.; Edwards, J. O. The Alpha Effect. A Review. *Int. J. Chem. Kinet.* **1973**, *5*, 1–26.
- (58) Graña, P.; Paleo, M. R.; Sardina, F. J. A Relative Organolithium Stability Scale Derived from Tin-Lithium Exchange Equilibria. Substituent Effects on the Stability of α -Oxy- and α -Aminoorganolithium Compounds. *J. Am. Chem. Soc.* **2002**, *124*, 12511–12514.
- (59) Monje, P.; Graña, P.; Paleo, M. R.; Sardina, F. J. Quantitative Data on the Effects of Alkyl Substituents and Li-O and Li-N Chelation on the Stability of Secondary α -Oxy-Organolithium Compounds. *Chem. Eur. J.* **2007**, *13*, 2277–2289.
- (60) Hoppe, I.; Marsch, M.; Harms, K.; Boche, G.; Hoppe, D. Generation of Enantiomerically Enriched Lithium Indenides by Means of (-)-Sparteine: Structure, Stereoselective Substitution, and Solvent Effects. *Angew. Chem. Int. Ed.* **1995**, *34*, 2158–2160.
- (61) Carbone, G.; O'Brien, P.; Hilmersson, G. Asymmetric Deprotonation Using *s*-BuLi or *i*-PrLi and Chiral Diamines in THF: The Diamine Matters. *J. Am. Chem. Soc.* **2010**, *132*, 15445–15450.
- (62) Millán, A.; Grigol Martinez, P. D.; Aggarwal, V. K. Stereocontrolled Synthesis of Polypropionate Fragments Based on a Building Block Assembly Strategy Using Lithiation-Borylation Methodologies. *Chem. Eur. J.* **2018**, *24*, 730–735.
- (63) Rutherford, J. L.; Hoffmann, D.; Collum, D. B. Consequences of Correlated Solvation on the Structures and Reactivities of RLi-Diamine Complexes: 1,2-Addition and α -Lithiation Reactions of Imines by TMEDA-Solvated *n*-Butyllithium and Phenyllithium. *J. Am. Chem. Soc.* **2002**, *124*, 264–271.
- (64) Monje, P.; Paleo, M. R.; Garcá, L.; Sardina, F. J. Determination of the Effect of Cation- π Interactions on the Stability of Alpha-Oxy-Organolithium. *J. Org. Chem.* **2008**, *73*, 7394–7397.
- (65) Morizawa, Y.; Yasuda, A.; Uchida, K. Trifluoromethyl Group Induced Highly Stereoselective Synthesis Of Cu-Hydroxy Carbonyl Compounds. *Tetrahedron Lett.* **1986**, *27*, 1833–1836.

- (66) Beak, P.; Lee, W. K. ..Alpha.-Lithioamine Synthetic Equivalents: Syntheses of Diastereoisomers from Boc Derivatives of Cyclic Amines. *J. Org. Chem.* **1993**, *58*, 1109–1117.
- (67) Hammerschmidt, F.; Hanninger, A.; Peric Simov, B.; Völlenkle, H.; Werner, A. Chiral Carbanions, III. - Configurational Stability and Stannylation of Dipole-Stabilised Cyclic Tertiary Benzylic α -Oxycarbanions, Which Occurs with Retention or Inversion of Configuration Depending on R and X of R₃SnX Used. *Eur. J. Org. Chem.* **1999**, No. 12, 3511–3518.
- (68) Zhao, H.; Tong, M.; Wang, H.; Xu, S. Transition-Metal-Free Synthesis of 1{,}1-Diboronate Esters with a Fully Substituted Benzylic Center via Diborylation of Lithiated Carbamates. *Org. Biomol. Chem.* **2017**, *15*, 3418–3422.
- (69) Streitwieser, A.; Caldwell, R. A.; Young, W. R. Acidity of Hydrocarbons. XXXI. Kinetic Acidities of Small-Ring Cycloalkanes and Correlation with J(13C-H). *J. Am. Chem. Soc.* **1969**, *91*, 529.
- (70) Renk, E.; Roberts, J. D. Small-Ring Compounds. XXXII. The Reaction of Allylcarbinylamine- α -14C (3-Butenyl-1-14C-Amine) with Nitrous Acid_{1,2}. *J. Am. Chem. Soc.* **1961**, *83*, 878–881.
- (71) Olah, G. A.; Reddy, V. P.; Prakash, G. K. S. Long-Lived Cyclopropylcarbinyl Cations. *Chem. Rev.* **1992**, *92*, 69–95.
- (72) Bauer, A.; Di Mauro, G.; Li, J.; Maulide, N. An α -Cyclopropanation of Carbonyl Derivatives by Oxidative Umpolung. *Angew. Chem. Int. Ed.* **2020**, *59*, 18208–18212.
- (73) Luc, E. Investigating the Generation of 1,1-Disubstituted Cyclobutanes by the Lithiation–Borylation of Cyclobutyl Esters and Carbamates, University of Bristol, 2018.
- (74) Roesner, S.; Casatejada, J. M.; Elford, T. G.; Sonawane, R. P.; Aggarwal, V. K. Enantioselective Syntheses of (+)-Sertraline and (+)-Indatraline Using Lithiation/Borylation–Protodeboronation Methodology. *Org. Lett.* **2011**, *13*, 5740–5743.
- (75) Danheiser, R. L.; Savoca, A. C. Applications of Cyclopropylboranes in Organic Synthesis. 1. A Stereocontrolled Route to Substituted Cyclopropanol Derivatives. *J. Org. Chem.* **1985**, *50*, 2401–2403.
- (76) Harris, M. R.; Wisniewska, H. M.; Jiao, W.; Wang, X.; Bradow, J. N. A Modular Approach to the Synthesis of Gem-Disubstituted Cyclopropanes. *Org. Lett.* **2018**, *20*, 2867–2871.
- (77) Hari, D. P.; Abell, J. C.; Fasano, V.; Aggarwal, V. K. Ring-Expansion Induced 1,2-Metalate Rearrangements: Highly Diastereoselective Synthesis of Cyclobutyl Boronic Esters. *J. Am. Chem. Soc.* **2020**, *142*, 5515–5520.
- (78) Hammerschmidt, F.; Hanninger, A. Chiral Carbanions, I. Configurational Stability and Reactions of α -Acyloxy-Substituted α -Methylbenzyl lithium Compounds. *Chem. Ber.* **1995**, *128*, 1069–1077.
- (79) Gessner, V. H. Stability and Reactivity Control of Carbenoids: Recent Advances and Perspectives. *Chem. Commun.* **2016**, *52*, 12011–12023.
- (80) Mykura, R. C.; Songara, P.; Luc, E.; Rogers, J.; Stammers, E.; Aggarwal, V. K. Studies on the Lithiation, Borylation, and 1,2-Metalate Rearrangement of O - Cycloalkyl 2,4,6-Triisopropylbenzoates. *Angew. Chem. Int. Ed.* **2021**, *n/a*, anie.202101374.
- (81) Balieu, S.; Hallett, G. E.; Burns, M.; Bootwicha, T.; Studley, J.; Aggarwal, V. K. Toward Ideality: The Synthesis of (+)-Kalkitoxin and (+)-Hydroxyphthioceranic Acid by Assembly-Line Synthesis. *J. Am. Chem. Soc.* **2015**, *137*, 4398–4403.

- (82) Selekman, J. A.; Qiu, J.; Tran, K.; Stevens, J.; Rosso, V.; Simmons, E.; Xiao, Y.; Janey, J. High-Throughput Automation in Chemical Process Development. *Annu. Rev. Chem. Biomol. Eng.* **2017**, *8*, 525–547.
- (83) Delort, E.; Nguyen-Trung, N. Q.; Darbre, T.; Reymond, J. L. Synthesis and Activity of Histidine-Containing Catalytic Peptide Dendrimers. *J. Org. Chem.* **2006**, *71*, 4468–4480.
- (84) Tu, N. P.; Searle, P. A.; Sarris, K. An Automated Microwave-Assisted Synthesis Purification System for Rapid Generation of Compound Libraries. *J. Lab. Autom.* **2016**, *21*, 459–469.
- (85) Baranczak, A.; Tu, N. P.; Marjanovic, J.; Searle, P. A.; Vasudevan, A.; Djuric, S. W. Integrated Platform for Expedited Synthesis-Purification-Testing of Small Molecule Libraries. *ACS Med. Chem. Lett.* **2017**, *8*, 461–465.
- (86) Li, T.; Liu, L.; Wei, N.; Yang, J. Y.; Chapla, D. G.; Moremen, K. W.; Boons, G. J. An Automated Platform for the Enzyme-Mediated Assembly of Complex Oligosaccharides. *Nat. Chem.* **2019**, *11*, 229–236.
- (87) Tang, S. L.; Pohl, N. L. B. Automated Solution-Phase Synthesis of β -1,4-Mannuronate and β -1,4-Mannan. *Org. Lett.* **2015**, *17*, 2642–2646.
- (88) Jaipuri, F. A.; Pohl, N. L. Toward Solution-Phase Automated Iterative Synthesis: Fluorous-Tag Assisted Solution-Phase Synthesis of Linear and Branched Mannose Oligomers. *Org. Biomol. Chem.* **2008**, *6*, 2686–2691.
- (89) Kern, M. K.; Pohl, N. L. B. Automated Solution-Phase Synthesis of S-Glycosides for the Production of Oligomannopyranoside Derivatives. *Org. Lett.* **2020**, *22*, 4156–4159.
- (90) Jlalía, I.; Beauvineau, C.; Beauvière, S.; Önen, E.; Aufort, M.; Beauvineau, A.; Khaba, E.; Herscovici, J.; Meganem, F.; Girard, C. Automated Synthesis of a 96 Product-Sized Library of Triazole Derivatives Using a Solid Phase Supported Copper Catalyst. *Molecules* **2010**, *15*, 3087–3120.
- (91) McNally, A.; Prier, C. K.; Macmillan, D. W. C. Arylation Reaction Using the Strategy of Accelerated Serendipity. *Science* **2011**, *334*, 1114–1117.
- (92) Chen, Y.; Wang, X.; He, X.; An, Q.; Zuo, Z. Photocatalytic Dehydroxymethylative Arylation by Synergistic Cerium and Nickel Catalysis. *J. Am. Chem. Soc.* **2021**.
- (93) Trobe, M.; Burke, M. D. The Molecular Industrial Revolution: Automated Synthesis of Small Molecules. *Angew. Chem. Int. Ed.* **2018**, *57*, 4192–4214.
- (94) Li, J.; Ballmer, S. G.; Gillis, E. P.; Fujii, S.; Schmidt, M. J.; Palazzolo, A. M. E.; Lehmann, J. W.; Morehouse, G. F.; Burke, M. D. Synthesis of Many Different Types of Organic Small Molecules Using One Automated Process. *Science* **2015**, *347*, 1221–1226.
- (95) Steiner, S.; Wolf, J.; Glatzel, S.; Andreou, A.; Granda, J. M.; Keenan, G.; Hinkley, T.; Aragon-Camarasa, G.; Kitson, P. J.; Angelone, D.; Cronin, L. Organic Synthesis in a Modular Robotic System Driven by a Chemical Programming Language. *Science* **2019**, *363*, eaav2211.
- (96) Angelone, D.; Hammer, A. J. S.; Rohrbach, S.; Krambeck, S.; Granda, J. M.; Wolf, J.; Zaleskiy, S.; Chisholm, G.; Cronin, L. Convergence of Multiple Synthetic Paradigms in a Universally Programmable Chemical Synthesis Machine. *Nat. Chem.* **2021**, *13*, 63–69.
- (97) Ley, S. V.; Fitzpatrick, D. E.; Myers, R. M.; Battilocchio, C.; Ingham, R. J. Machine-Assisted Organic Synthesis. *Angew. Chem. Int. Ed.* **2015**, *54*, 10122–10136.
- (98) Lange, P. P.; James, K. Rapid Access to Compound Libraries through Flow Technology: Fully Automated Synthesis of a 3-Aminoindolizine Library via

- Orthogonal Diversification. *ACS Comb. Sci.* **2012**, *14*, 570–578.
- (99) Perera, D.; Brahmabhatt, S.; Chong, A.; Farrell, W.; Richardson, P.; Sach, N. W.; Tucker, J. W.; Helal, C. J. A Platform for Automated Nanomole-Scale Reaction Screening and Micromole-Scale Synthesis in Flow. *Science* **2018**, *359*, 429–434.
- (100) Leonori, D.; Aggarwal, V. K. Lithiation-Borylation Methodology and Its Application in Synthesis. *Acc. Chem. Res.* **2014**, *47*, 3174–3183.
- (101) Burchat, A. F.; Chong, J. M.; Nielsen, N. Titration of Alkylolithiums with a Simple Reagent to a Blue Endpoint. *J. Organomet. Chem.* **1997**, *542*, 281–283.
- (102) Berman, F. W.; Gerwick, W. H.; Murray, T. F. Antillatoxin and Kalkitoxin, Ichthyotoxins from the Tropical Cyanobacterium *Lyngbya Majuscula*, Induce Distinct Temporal Patterns of NMDA Receptor-Mediated Neurotoxicity. *Toxicon* **1999**, *37*, 1645–1648.
- (103) Morgan, J. B.; Liu, Y.; Coothankandaswamy, V.; Mahdi, F.; Jekabsons, M. B.; Gerwick, W. H.; Valeriote, F. A.; Zhou, Y. D.; Nagle, D. G. Kalkitoxin Inhibits Angiogenesis, Disrupts Cellular Hypoxic Signaling, and Blocks Mitochondrial Electron Transport in Tumor Cells. *Mar. Drugs* **2015**, *13*, 1552–1568.
- (104) Dhanju, S.; Upadhyaya, K.; Rice, C. A.; Pegan, S. D.; Media, J.; Valeriote, F. A.; Crich, D. Synthesis, Cytotoxicity, and Genotoxicity of 10-Aza-9-Oxakalkitoxin, an N, N, O -Trisubstituted Hydroxylamine Analog, or Hydroxalog, of a Marine Natural Product. *J. Am. Chem. Soc.* **2020**, *142*, 9147–9151.
- (105) Yokokawa, F.; Asano, T.; Okino, T.; Gerwick, W. H.; Shioiri, T. An Expeditious Total Synthesis of Kalkitoxins: Determination of the Absolute Stereostructure of Natural Kalkitoxin. *Tetrahedron* **2004**, *60*, 6859–6880.
- (106) Umezawa, T.; Sueda, M.; Kamura, T.; Kawahara, T.; Han, X.; Okino, T.; Matsuda, F. Synthesis and Biological Activity of Kalkitoxin and Its Analogues. *J. Org. Chem.* **2012**, *77*, 357–370.
- (107) Bootwicha, T.; Feilner, J. M.; Myers, E. L.; Aggarwal, V. K. Iterative Assembly Line Synthesis of Polypropionates with Full Stereocontrol. *Nat. Chem.* **2017**, *9*, 896–902.
- (108) Fantin, G.; Fogagnolo, M.; Medici, A.; Pedrini, P. Lithiation of Δ^2 -Thiazolines: The C2-Anion Approach to 2-Substituted Derivatives and Their Reactivity. *Heterocycles* **1993**, *36*, 473–484.
- (109) Thompson, D. K.; Suzuki, N.; Hegedus, L. S.; Satoh, Y. Optically Active Quaternary Carbon Centers from the Photoaddition of Chromium-Alkoxycarbene Complexes and Optically Active Thiazolines. *J. Org. Chem.* **1992**, *57*, 1461–1467.
- (110) Hartmann, E.; Vyas, D. J.; Oestreich, M. Enantioselective Formal Hydration of α,β -Unsaturated Acceptors: Asymmetric Conjugate Addition of Silicon and Boron Nucleophiles. *Chem. Commun.* **2011**, *47*, 7917–7932.
- (111) Hemming, D.; Fritzemeier, R.; Westcott, S. A.; Santos, W. L.; Steel, P. G. Copper-Boryl Mediated Organic Synthesis. *Chem. Soc. Rev.* **2018**, *47*, 7477–7494.
- (112) Boyce, R. J.; Mulqueen, G. C.; Pattenden, G. Total Synthesis of Thiangazole, a Novel Inhibitor of HIV-1 from *Polyangium* Sp. *Tetrahedron Lett.* **1994**, *35*, 5705–5708.
- (113) Gaumont, A.-C.; Gulea, M.; Levillain, J. Overview of the Chemistry of 2-Thiazolines. *Chem. Rev.* **2009**, *109*, 1371–1401.
- (114) Wen, L.; Yue, Z.; Zhang, H.; Chong, Q.; Meng, F. Cu-Catalyzed Enantioselective Boron Addition to N-Heteroaryl-Substituted Alkenes. *Org. Lett.* **2017**, *19*, 6610–6613.
- (115) Mun, S.; Lee, J.-E.; Yun, J. Copper-Catalyzed β -Boration of α,β -Unsaturated Carbonyl Compounds: Rate Acceleration by Alcohol Additives. *Org. Lett.* **2006**,

- 8, 4887–4889.
- (116) Yamakuchi, M.; Matsunaga, H.; Tokuda, R.; Ishizuka, T.; Nakajima, M.; Kunieda, T. Sterically Congested ‘Roofed’ 2-Thiazolines as New Chiral Ligands for Copper(II)-Catalyzed Asymmetric Diels–Alder Reactions. *Tetrahedron Lett.* **2005**, *46*, 4019–4022.
- (117) Busacca, C. A.; Dong, Y.; Spinelli, E. M. A One Step Synthesis of Thiazolines from Esters. *Tetrahedron Lett.* **1996**, *37*, 2935–2938.
- (118) Takahashi, K.; Ishiyama, T.; Miyaura, N. Addition and Coupling Reactions of Bis(Pinacolato)Diboron Mediated by CuCl in the Presence of Potassium Acetate. *Chem. Lett.* **2000**, *29*, 982–983.
- (119) Gonzalez, J. A.; Ogba, O. M.; Morehouse, G. F.; Rosson, N.; Houk, K. N.; Leach, A. G.; Cheong, P. H.-Y.; Burke, M. D.; Lloyd-Jones, G. C. MIDA Boronates Are Hydrolysed Fast and Slow by Two Different Mechanisms. *Nat. Chem.* **2016**, *8*, 1067–1075.
- (120) Raman, P.; Razavi, H.; Kelly, J. W. Titanium(IV)-Mediated Tandem Deprotection–Cyclodehydration of Protected Cysteine N-Amides: Biomimetic Syntheses of Thiazoline- and Thiazole-Containing Heterocycles. *Org. Lett.* **2000**, *2*, 3289–3292.
- (121) White, J. D.; Lee, C.-S.; Xu, Q. Total Synthesis of (+)-Kalkitoxin. *Chem. Commun.* **2003**, *3*, 2012–2013.
- (122) Lee, J.-E.; Yun, J. Catalytic Asymmetric Boration of Acyclic α,β -Unsaturated Esters and Nitriles. *Angew. Chem. Int. Ed.* **2008**, *47*, 145–147.
- (123) Doi, T.; Numajiri, Y.; Munakata, A.; Takahashi, T. Total Synthesis of Apratoxin A. *Org. Lett.* **2006**, *8*, 531–534.
- (124) Matteson, D. S.; Jesthi, P. K.; Sadhu, K. M. Synthesis and Properties of Pinanediol .Alpha.-Amido Boronic Esters. *Organometallics* **1984**, *3*, 1284–1288.
- (125) Sun, J.; Perfetti, M. T.; Santos, W. L. A Method for the Deprotection of Alkylpinacolyl Boronate Esters. *J. Org. Chem.* **2011**, *76*, 3571–3575.
- (126) Doler, C.; Friess, M.; Lackner, F.; Weber, H.; Fischer, R. C.; Breinbauer, R. Stereoselective Synthesis of Chiral Thiol-Containing 1,2-Aminoalcohols via SmI₂-Mediated Coupling. *Tetrahedron* **2020**, *76*, 131249.
- (127) Ivkovic, J.; Lembacher-Fadum, C.; Breinbauer, R. A Rapid and Efficient One-Pot Method for the Reduction of N-Protected α -Amino Acids to Chiral α -Amino Aldehydes Using CDI/DIBAL-H. *Org. Biomol. Chem.* **2015**, *13*, 10456–10460.
- (128) Pandey, A. K.; Kirberger, S. E.; Johnson, J. A.; Kimbrough, J. R.; Partridge, D. K. D.; Pomerantz, W. C. K. Efficient Synthesis of 1,4-Thiazepanones and 1,4-Thiazepanes as 3D Fragments for Screening Libraries. *Org. Lett.* **2020**, *22*, 3946–3950.
- (129) Brown, H. C.; Heydkamp, W. R.; Breuer, E.; Murphy, W. S. The Reaction of Organoboranes with Chloramine and with Hydroxylamine-O-Sulfonic Acid. A Convenient Synthesis of Amines from Olefins via Hydroboration. *J. Am. Chem. Soc.* **1964**, *86*, 3565–3566.
- (130) Rathke, M. W.; Inoue, N.; Varma, K. R.; Brown, H. C. A Stereospecific Synthesis of Alicyclic and Bicyclic Amines via Hydroboration. *J. Am. Chem. Soc.* **1966**, *88*, 2870–2871.
- (131) Bagutski, V.; Elford, T. G.; Aggarwal, V. K. Synthesis of Highly Enantioenriched C-Tertiary Amines From Boronic Esters: Application to the Synthesis of Igmesine. *Angew. Chem. Int. Ed.* **2011**, *50*, 1080–1083.
- (132) Hupe, E.; Marek, I.; Knochel, P. Diastereoselective Reduction of Alkenylboronic Esters as a New Method for Controlling the Stereochemistry of up to Three

- Adjacent Centers in Cyclic and Acyclic Molecules. *Org. Lett.* **2002**, *4*, 2861–2863.
- (133) Mlynarski, S. N.; Karns, A. S.; Morken, J. P. Direct Stereospecific Amination of Alkyl and Aryl Pinacol Boronates. *J. Am. Chem. Soc.* **2012**, *134*, 16449–16451.
- (134) Edelstein, E. K.; Grote, A. C.; Palkowitz, M. D.; Morken, J. P. A Protocol for Direct Stereospecific Amination of Primary, Secondary, and Tertiary Alkylboronic Esters. *Synlett* **2018**, *29*, 1749–1752.
- (135) Liu, X.; Zhu, Q.; Chen, D.; Wang, L.; Jin, L.; Liu, C. Aminoazanium of DABCO: An Amination Reagent for Alkyl and Aryl Pinacol Boronates. *Angew. Chem. Int. Ed.* **2020**, *59*, 2745–2749.
- (136) Mori-Quiroz, L. M.; Shimkin, K. W.; Rezazadeh, S.; Kozlowski, R. A.; Watson, D. A. Copper-Catalyzed Amidation of Primary and Secondary Alkyl Boronic Esters. *Chem. – A Eur. J.* **2016**, *22*, 15654–15658.
- (137) Zhang, W.; Lu, Y. Automation of Fluorous Solid-Phase Extraction for Parallel Synthesis. *J. Comb. Chem.* **2006**, *8*, 890–896.
- (138) Matsugi, M.; Curran, D. P. Reverse Fluorous Solid-Phase Extraction: A New Technique for Rapid Separation of Fluorous Compounds. *Org. Lett.* **2004**, *6*, 2717–2720.
- (139) Pradeilles, J. A.; Zhong, S.; Baglyas, M.; Tarczay, G.; Butts, C. P.; Myers, E. L.; Aggarwal, V. K. Odd–Even Alternations in Helical Propensity of a Homologous Series of Hydrocarbons. *Nat. Chem.* **2020**, *12*, 475–480.
- (140) Colbon, P.; Ruan, J.; Purdie, M.; Mulholland, K.; Xiao, J. Double Arylation of Allyl Alcohol via a One-Pot Heck Arylation–Isomerization–Acylation Cascade. *Org. Lett.* **2011**, *13*, 5456–5459.
- (141) Würthwein, E.-U.; Behrens, K.; Hoppe, D. Enantioselective Deprotonation of Alkyl Carbamates by Means of (R,R)-1,2-Bis(N,N-Dimethylamino)Cyclohexane/Sec-Butyllithium— Theory and Experiment. *Chem. – A Eur. J.* **1999**, *5*, 3459–3463.
- (142) Blair, D. J.; Tanini, D.; Bateman, J. M.; Scott, H. K.; Myers, E. L.; Aggarwal, V. K. Selective Uni- and Bidirectional Homologation of Diborylmethane. *Chem. Sci.* **2017**, *8*, 2898–2903.
- (143) Zhang, Q.-C.; Wu, F.-T.; Hao, H.-M.; Xu, H.; Zhao, H.-X.; Long, L.-S.; Huang, R.-B.; Zheng, L.-S. Modulating the Rotation of a Molecular Rotor through Hydrogen-Bonding Interactions between the Rotator and Stator. *Angew. Chem. Int. Ed.* **2013**, *52*, 12602–12605.
- (144) Larouche-Gauthier, R.; Elford, T. G.; Aggarwal, V. K. Ate Complexes of Secondary Boronic Esters as Chiral Organometallic-Type Nucleophiles for Asymmetric Synthesis. *J. Am. Chem. Soc.* **2011**, *133*, 16794–16797.
- (145) Alderson, J. M.; Phelps, A. M.; Scamp, R. J.; Dolan, N. S.; Schomaker, J. M. Ligand-Controlled, Tunable Silver-Catalyzed C–H Amination. *J. Am. Chem. Soc.* **2014**, *136*, 16720–16723.
- (146) Zuo, Z.; Zhang, L.; Leng, X.; Huang, Z. Iron-Catalyzed Asymmetric Hydrosilylation of Ketones. *Chem. Commun.* **2015**, *51*, 5073–5076.
- (147) Roesner, S.; Blair, D. J.; Aggarwal, V. K. Enantioselective Installation of Adjacent Tertiary Benzylic Stereocentres Using Lithiation-Borylation-Protodeboronation Methodology. Application to the Synthesis of Bifluranol and Fluorohexestrol. *Chem. Sci.* **2015**, *6*, 3718–3723.
- (148) Rosanna Bernardi, Claudio Fuganti, Piero Grasselli, G. M. Synthesis of the Enantiomeric Forms of 4-Hexanolide (γ -Caprolactone) from the Optically Active 5-Phenyl-4-Pentene-2,3-Diol Prepared from Cinnamaldehyde and Baker's Yeast. *Synthesis (Stuttg.)* **1980**, *1980*, 50–52.

- (149) Yamamura, T.; Nakatsuka, H.; Tanaka, S.; Kitamura, M. Asymmetric Hydrogenation of Tert-Alkyl Ketones: DMSO Effect in Unification of Stereoisomeric Ruthenium Complexes. *Angew. Chem. Int. Ed.* **2013**, *52*, 9313–9315.
- (150) Arvidsson, P. I.; Davidsson, Ö.; Hilmersson, G. Enantioselective Butylation of Aliphatic Aldehydes by Mixed Chiral Lithium Amide/n-BuLi Dimers. *Tetrahedron: Asymmetry* **1999**, *10*, 527–534.
- (151) Gadwood, R. C.; Rubino, M. R.; Nagarajan, S. C.; Michel, S. T. Generation of (1-Alkoxypropyl)Lithium Reagents. *J. Org. Chem.* **1985**, *50*, 3255–3260.
- (152) Leonard, D. J.; Ward, J. W.; Clayden, J. Asymmetric α -Arylation of Amino Acids. *Nature* **2018**, *562*, 105–109.
- (153) Abrams, R.; Jesani, M. H.; Browning, A.; Clayden, J. Triarylmethanes and Their Medium-Ring Analogues by Unactivated Truce–Smiles Rearrangement of Benzanilides. *Angew. Chem. Int. Ed.* **2021**, *n/a*, anie.202102192.
- (154) Fordham, J. M.; Grayson, M. N.; Aggarwal, V. K. Vinylidene Homologation of Boronic Esters and Its Application to the Synthesis of the Proposed Structure of Machillene. *Angew. Chem. Int. Ed.* **2019**, *58*, 15268–15272.
- (155) Dudnik, A. S.; Fu, G. C. Nickel-Catalyzed Coupling Reactions of Alkyl Electrophiles, Including Unactivated Tertiary Halides, To Generate Carbon–Boron Bonds. *J. Am. Chem. Soc.* **2012**, *134*, 10693–10697.
- (156) Greenhalgh, M. D.; Thomas, S. P. Chemo-, Regio-, and Stereoselective Iron-Catalysed Hydroboration of Alkenes and Alkynes. *Chem. Commun.* **2013**, *49*, 11230–11232.
- (157) Armstrong, R.; Aggarwal, V. K. Homologation of Boronic Esters with Lithiated Epoxides. *Org. Synth.* **2017**, *94*, 234–251.
- (158) Knott, K.; Fishovitz, J.; Thorpe, S. B.; Lee, I.; Santos, W. L. N-Terminal Peptidic Boronic Acids Selectively Inhibit Human ClpXP. *Org. Biomol. Chem.* **2010**, *8*, 3451–3456.
- (159) Katritzky, A. R.; Cai, C.; Suzuki, K.; Singh, S. K. Facile Syntheses of Oxazolines and Thiazolines with N-Acylbenzotriazoles under Microwave Irradiation. *J. Org. Chem.* **2004**, *69*, 811–814.
- (160) Dose, C.; Seitz, O. Convergent Synthesis of Peptide Nucleic Acids by Native Chemical Ligation. *Org. Lett.* **2005**, *7*, 4365–4368.
- (161) Jung, M. E.; Yi, S. W. Synthesis of Threo- β -Aminoalcohols from Aminoaldehydes via Chelation-Controlled Additions. Total Synthesis of l-Threo Sphingosine and Safingol. *Tetrahedron Lett.* **2012**, *53*, 4216–4220.
- (162) Gucma, M.; Gołębiewski, W. M.; Krawczyk, M. Application of Chiral Ligands: Carbohydrates, Nucleoside-Lanthanides and Other Lewis Acid Complexes to Control Regio- and Stereoselectivity of the Dipolar Cycloaddition Reactions of Nitrile Oxides and Esters. *RSC Adv.* **2015**, *5*, 13112–13124.